



UNIVERSITY OF
LEICESTER

**INVESTIGATION OF ENDOCANNABINOID
SYSTEM SIGNALLING PATHWAYS
AND THEIR REGULATIONS
IN ENDOMETRIAL CARCINOMA**

**Thesis submitted for the degree of
Doctor of Philosophy
at the University of Leicester**

By

**Thangesweran Ayakannu
MBBS, DFFP, MRCOG**

June 2016



Investigation of Endocannabinoid System Signalling Pathways and Their Regulations in Endometrial Carcinoma

Thangesweran AYAKANNU
MBBS, DFFP, MRCOG

Reproductive Sciences Section
Department of Cancer Studies and Molecular Medicine
University of Leicester
Leicester
United Kingdom.

June 2016

Investigation of endocannabinoid system signalling pathways and their regulations in endometrial carcinoma

Thangesweran Ayakannu

Abstract

In the UK, endometrial cancer (EC) is the 4th most common cancer and its incidence is rapidly rising. This study aimed to elucidate the role of the endocannabinoid system (ECS) in the pathogenesis of EC. Plasma and endometrial tissues levels of anandamide (AEA), palmitoylethanolamide (PEA) and oleoylethanolamide (OEA) quantified by UHPLC from atrophic and EC group. Using the qRT-PCR and immunohistochemistry (IHC), CB1, CB2, FAAH, NAPE-PLD, GPR55 and TRPV1, mRNAs and protein levels was evaluated, respectively. The effects of *in-vitro* exposure of Ishikawa cell-line to AEA, OEA, PEA and capsaicin were evaluated. Plasma and tissue AEA levels were significantly ($p < 0.05$) higher in EC than control, as were PEA levels. Logistic regression raised the area under the ROC curve (AUC) from 0.781 for plasma AEA, 0.857 for PEA and 0.543 for OEA to a combined AUC of 0.933 for EC diagnosis. The transcript level of FAAH was 75% lower in EC and NAPE-PLD levels were more variable. Histomorphometric analysis of FAAH and NAPE-PLD staining complements the transcript data. CB1 and CB2 mRNA were significantly decreased by 90% ($p < 0.0004$) and 80% ($p < 0.0001$), respectively, compared with control and these was supported by the IHC. In the EC, GPR55 mRNA were significantly raised ($p < 0.0020$) compared with control and its protein expressions were markedly stained in EC tissues. TRPV1 receptor transcript levels were significantly reduced ($p < 0.0054$) in EC compared with controls and markedly decreased in EC by IHC. Cancer cell growth *in-vitro* was decreased by the endocannabinoids in a pseudo dose-dependent and time-dependent manner. The endocannabinoids might prevent cancer cell growth by inhibiting cell proliferation or by activating apoptosis. This idea was tested using BAX/Bcl-2 and Ki-67 expression and found to be due to decrease cell proliferation. It is evident that there is an apparent perturbation of ECS at tissue and plasma levels and this could be used as diagnostic and prognostic markers with potential therapeutic target for the prevention EC.

Author's declaration

I state that this thesis represents my own unaided work, except where acknowledge in the text, and has not been submitted previously in consideration for a degree at this, or any other university.

.....

30/6/2016

Thangesweran Ayakannu
Reproductive Sciences Section
Department of Cancer Studies and Molecular Medicine
University of Leicester
Leicester
United Kingdom

June 2016

Acknowledgements

My most heartfelt thanks go to thank my supervisors Prof Justin Konje, Dr. Anthony Taylor, Dr Jonathon Willets and Dr. Timothy Marczylo. It is a pleasure to thank the many people who made this thesis possible.

Foremost, I would like to thank my principle supervisor, Professor Justin Konje, for giving me a very interesting and challenging project to study; thanks for your kind advice, guidance and support throughout the course of my doctorate degree and I will forever be thankful. Thank you for the many hours spent proof reading my thesis and drafts of manuscripts for publication.

I am extremely grateful to Dr Anthony Taylor for his unwavering support and continuous encouragement. Thank you for your never-ending advice, guidance and friendship throughout my thesis and I will forever be thankful. I am extremely grateful to Dr Taylor for the many hours spent on proof reading my thesis and manuscripts drafts and without his involvement; this study would not have been possible. In addition, I would like to thank Dr. Jonathan Willets and Dr. Timothy Marczylo for their support and guidance.

I wish to acknowledge funding support from the University Hospitals of Leicester NHS Trust for providing my postgraduate scholarship and to the University of Leicester for providing consumables and travel grants. I would like to thank all the women who participated in this study and the gynaecology surgeons at Leicester General Hospital. Furthermore, I would like to thank for his kind time and patience, Dr Lawrence Brown, for helping me by providing all the pathological specimens including the slides for my study.

I also have to thank my fellow researchers, especially Dr Alpha Gebeh and Dr Akwasi Amoako for their never-ending moral support, encouragement and friendship. Thank you to the staff in the Department of Cancer and Molecular Medicine for their help with technical issues and being great to work with.

Dedication

To my loving wife Nisha Nanthini and to my loving son Divyeshram for their kindness, patience and support, which made this hard work, feel easy. Thank you for your understanding and encouragement in all my endeavours.

To my father, mother, grandmother and my siblings for their enduring love and support.

Presentations and publications arising from this thesis

Publications

Peer reviewed journals

1. Ayakannu, T., Taylor, A.H., Marczylo, T.H, Brown, L., Maccarrone, M. & Konje, J.C. Plasma Anandamide: Potential Biomarker of Endometrial Cancer
Submitted: - Gynaecology Oncology
2. Ayakannu, T., Taylor, A.H. Konje, J.C. Cannabinoid Receptor Expression in Oestrogen-dependent and Oestrogen-independent Endometrial Cancer.
Submitted: - British Journal of Cancer
3. Ayakannu, T., Taylor, A.H., Bari, M., Mastrangelo, N., Maccarrone, M. & Konje, J.C. Expression and Function of the Endocannabinoid Modulating Enzymes Fatty Acid Amide Hydrolase and N-Acyl Phosphatidylethanolamine Phospholipase D in Endometrial Carcinoma
Submitted: - European Journal of Cancer
4. Ayakannu, T., Taylor, A.H., Willets, J.M., Brown, L., Lambert, D.G., McDonald, J., Davies, Q., Moss, E.C. & Konje, J.C. Validation of Endogenous Control Reference Genes for Normalising Gene Expression Studies in Endometrial Carcinoma. *Molecular Human Reproduction* (MHR-15-0005.R1), first published online: June 29, 2015. Doi: 10.1093/molehr/gav0332015
5. Ayakannu, T., Taylor, A.H., Willets, J.M., Konje, J.C. The Evolving Role of the Endocannabinoid System in Gynaecological Cancers. Review article: *Hum. Reprod. Update* (July/August 2015) 21 (4): 517-535 first published online May 9, 2015 Doi:10.1093/humupd/dmv022
6. Ayakannu, T., Taylor, A.H., Willets, J.M., Konje, J.C. The Endocannabinoid System and Sex Steroid Hormone-Dependent Cancers
Review article: *International Journal of Endocrinology*, October 2013, Article ID 259676, 14 Doi.org/10.1155/2013/259676

Published abstracts

1. T. Ayakannu, M. Bari, A.H. Taylor, T.H. Marczylo, J.M. Willets, E.C. Moss, Q. Davies, L. Brown and J.C. Konje. The activity and expression of the endocannabinoid metabolising enzyme fatty acid amide hydrolase and its relationship with AEA in endometrial carcinoma.
Poster abstract: *Reproductive Sciences*, March 2015; vol. 22, 1 suppl: pp. 1A-54A. DOI: 10.1177/1933719115579630

2. T. Ayakannu, A.H. Taylor, T.H. Marczylo, J.M. Willets, Q. Davies, L. Brown, E.C. Moss and J.C. Konje. Exploring the expression of the endovanilloid receptor TRPV1 in endometrial carcinoma. Poster abstract: Reproductive Sciences, March 2015; vol. 22, 1 suppl: pp. 54A-390A. DOI: 10.1177/1933719115579631
3. T. Ayakannu, A.H. Taylor T. H. Marczylo, J.M. Willets, Q. Davies, L. Brown, M. Maccarrone and J.C. Konje. The endocannabinoid, anandamide and its regulating enzymes in endometrial carcinoma – a potential biomarker for early diagnosis? Poster abstract: Reproductive Sciences, March 2015; vol. 22, 1 suppl: pp. 1A-54A. DOI: 0.1177/1933719115579630
4. T. Ayakannu, A.H. Taylor, T.H. Marczylo, J.M. Willets, E.C. Moss, Q. Davies, L. Brown and J.C. Konje. Modelling: The effect of endocannabinoids on endometrial carcinoma growth using the Ishikawa cell line. Poster abstract: Reproductive Sciences, March 2015; vol. 22, 1 suppl: pp. 1A-54A. DOI: 10.1177/1933719115579630
5. T. Ayakannu, A.H. Taylor, T.H. Marczylo, J.M. Willets, L. Brown, Q. Davies , E.C. Moss and J.C. Konje. Effect of anandamide on endometrial adenocarcinoma (Ishikawa) cell numbers: implications for endometrial cancer therapy. Poster abstract: THE LANCET, February 2015; Vol. 385, S20. DOI: [http://dx.doi.org/10.1016/S0140-6736\(15\)60335-X](http://dx.doi.org/10.1016/S0140-6736(15)60335-X)
6. T. Ayakannu, A.H. Taylor, J.M. Willets and J.C. Konje. Selection of suitable endogenous control reference genes for gene expression studies in endometrioid and non-endometrioid adenocarcinoma. Poster abstract: Reproductive Sciences March 2014 vol. 21 no. 3 suppl 1A-70A. DOI: 10.1177/ 1933719114528274
7. T. Ayakannu, A. H. Taylor, J.M. Willets and J.C. Konje. Profiling the endocannabinoid system in endometrial carcinoma. Poster abstract: Reproductive Sciences March 2014(21):1A. DOI: 10.1177/ 1933719114528274
8. T. Ayakannu, A.H. Taylor, T.H. Marczylo, J.M. Willets, L. Brown, Q. Davies, E. Moss, J.C. Konje. Association of cannabinoid receptor expression with anandamide concentrations in endometrial cancer. Poster abstract: THE LANCET, February 2014, Vol. 383, S23. Doi: 10.1016/S0140-6736(14)60286-5
9. T. Ayakannu, A.H. Taylor, J.M. Willets, T.M. Marczylo, Q. Davies, L. Brown, E.L. Moss, J.C. Konje. Identification of the correct endogenous reference genes for qRT-PCR analysis of normal and malignant human endometrial tissues. Poster abstract: In International Journal of Gynaecological Cancer. October 2013(23)8, suppl 1.

Presentations

Podium presentations

International

1. T. Ayakannu, A. H. Taylor, J.M. Willets and J.C. Konje. Profiling the Endocannabinoid System in Endometrial Carcinoma Society for Gynaecologic Investigation (SGI), Florence, Italy March 26-29th, 2014.

National

1. T. Ayakannu, A. H. Taylor, J.M. Willets and J.C. Konje. Endocannabinoids: Potential Diagnostic Markers for Endometrial Cancer. Blair Bell Research Society Competition RCOG, London, UK 16-17-December 2013.

Poster presentations

International

1. T. Ayakannu, A.H. Taylor, T.H. Marczylo, J.M. Willets, E.C. Moss, Q. Davies, L. Brown and J.C. Konje. Modelling, the effect of endocannabinoids on endometrial carcinoma growth using the Ishikawa cell line. SRI, San Francisco, USA. 27/3/2015
2. T. Ayakannu, A.H. Taylor, T.H. Marczylo, E.C. Moss, J.M. Willets, Q. Davies, L. Brown and J.C. Konje. Is endocannabinoid system expressed in uterine fibroids? SRI. San Francisco, USA. 27/3/2015
3. T. Ayakannu, M. Bari, A.H. Taylor, T.H. Marczylo, J.M. Willets, E.C. Moss, Q. Davies, L. Brown and J.C. Konje. The activity and expression of the endocannabinoid metabolising enzyme fatty acid amide hydrolase and its relationship with AEA in endometrial carcinoma. SRI, San Francisco, USA, 2015
4. T. Ayakannu, A.H. Taylor, T.H. Marczylo, J.M. Willets, Q. Davies, L. Brown, E.C. Moss and J.C. Konje. Exploring the expression of the endovanilloid receptor TRPV1 in endometrial carcinoma. SRI, San Francisco, USA. 27/3/2015
5. T. Ayakannu, A.H. Taylor T. H. Marczylo, J.M. Willets, Q. Davies, L. Brown, M. Maccarrone and J.C. Konje. The endocannabinoid, anandamide and its regulating enzymes in endometrial carcinoma – a potential biomarker for early diagnosis? SRI, San Francisco, USA. 27/3/2015
6. T. Ayakannu, A.H. Taylor, J.M. Willets and J.C. Konje. Selection of suitable endogenous control reference genes for gene expression studies in endometrioid and non-endometrioid adenocarcinoma. SGI, Italy. 26/3/2014.

National

1. T. Ayakannu, A.H. Taylor, T.H. Marczylo, J.M. Willets, L. Brown, Q. Davies , E.C. Moss and J.C. Konje. Effect of anandamide on endometrial adenocarcinoma (Ishikawa) cell numbers: implications for endometrial cancer therapy. Spring Meeting, London. 26/2/2015
2. T. Ayakannu, A. H. Taylor, T.H. Marczylo, E.C. Moss, J.M. Willets, Q. Davies, L. Brown and J.C. Konje. Aberrant expression of FAAH and CB1 is associated with elevated Anandamide concentrations in endometrial cancer. BGCS. 9/July/2014.
3. T. Ayakannu, A.H. Taylor, T.H. Marczylo, J.M. Willets, L. Brown, Q. Davies, E. Moss, J.C. Konje. Association of cannabinoid receptor expression with anandamide concentrations in endometrial cancer. Spring Meeting, London. 26/2/2014.
4. T. Ayakannu, A.H. Taylor, J.M. Willets, T.M. Marczylo, Q. Davies, L. Brown, E.L. Moss, J.C. Konje. Identification of the correct endogenous reference genes for qRT-PCR analysis of normal and malignant human endometrial tissues. 18th International Meeting of the European Society of Gynaecological Oncology, 2013.
5. T. Ayakannu, A.H. Taylor, J.M. Willets, T.M. Marczylo, Q. Davies, L. Brown, E.L. Moss, J.C. Konje. Expression and Distribution of Cannabinoid Receptors CB1 and CB2 in Endometrial Cancer. NCRI Cancer Conference, 2013.
6. T. Ayakannu, A.H. Taylor, J.M. Willets, T.M. Marczylo, Q. Davies, L. Brown, E.L. Moss, J.C. Konje. Plasma Endocannabinoids as Potential Biomarkers for Endometrial Cancer. 2013 NCRI, Liverpool, 3/11/13.

The List of Contents

Abstract		3
Author's declaration		4
Acknowledgements		5
Dedication		6
Presentations and publications arising from this thesis		7
The List of Contents		11
The List of Tables		19
The List of Figures		20
The List of Abbreviations		26
Chapter 1	Introduction and Background	31
1.1	Cancer	32
1.2	Gynaecological Carcinoma	32
1.2.1	Worldwide Incidence	32
1.2.2	In the United Kingdom	33
1.3	Endometrium	34
1.3.1	Histology and Function of Endometrium	34
	Hormone Receptors and their Roles in the	
1.3.2	Endometrial Changes of the Menstrual Cycle	35
1.3.3	Postmenopausal Endometrium	36
1.4	Endometrial Carcinoma	37
1.4.1	Introduction	37
1.4.2	Aetiology	37
1.4.2.1	Risk Factors for Endometrial Carcinoma	37
	Role of Molecular (Genetic) Alterations in	
1.4.2.2	Endometrial Cancer	39
1.4.3	Symptoms	42
1.4.4	Diagnosis	43
1.4.5	Histological Types of Endometrial Cancer	43
1.4.6	Hormones and Endometrial Cancer	44
1.5	The Endocannabinoid System	45
1.5.1	Endocannabinoids	46
	<i>N</i> -arachidonylethanolamide or Anandamide	
1.5.1.1	(AEA)	47
1.5.1.2	<i>N</i> -palmitoylethanolamide (PEA)	47
1.5.1.3	<i>N</i> -oleoylethanolamide (OEA)	48
1.5.1.4	2-arachidonylglycerol (2-AG)	48
1.5.2	Biosynthesis of Endocannabinoids	49
1.5.3	Degradation of AEA, OEA, PEA and 2-AG	52
1.5.4	Transport Mechanism for <i>N</i> -acylethanolamides	54
1.6	Cannabinoid Receptors	56
1.6.1	Classical Cannabinoid Receptors	57
1.6.2	Non-classical Cannabinoid Receptors	57

1.6.3	Other Receptors	58
1.7	The Endocannabinoid System and Cancer	58
1.7.1	Introduction	58
	Modes of Action of the Endocannabinoid System	
1.7.2	in Cancer	59
	Cannabinoid Receptor-Dependent Modes of	
1.7.2.1	Action	60
1.7.2.1.1	Transformation of Cell Cycle Regulation	60
1.7.2.1.2	Inhibition of Cancer Proliferation	60
1.7.2.1.3	Induction of Apoptosis	61
1.7.2.1.4	Cancer Cell Invasion	61
1.7.2.1.5	Inhibition of Cancer Angiogenesis	62
1.7.2.1.6	Cancer Cell Adhesions	62
1.7.2.1.7	Cancer Cell Migration	63
	Cannabinoid Receptor-Independent Modes of	
1.7.2.2	Action	63
	The Endocannabinoid System and Endometrial	
1.8	Cancer	65
1.9	Hypothesis	66
1.9.1	Aims	66
1.9.2	Objectives	66
	Relationship Between Tissue and Plasma <i>N</i>-	
	Acylethanolamine Concentrations in	
Chapter 2	Endometrial Carcinoma	68
2.1	Introduction	69
2.2	Hypothesis	70
2.3	Questions to Address the Hypothesis	71
2.4	Subjects	71
2.5	Methods	72
2.5.1	Chemical, Reagents and Solutions	72
2.5.2	Blood Collection	72
2.5.3	Endometrial collection	72
2.5.4	Quantification of Endocannabinoids by UHPLC	73
2.5.4.1	Preparation of Standards and Calibration Curves	73
2.5.4.2	Extraction of Endocannabinoids from Plasma	74
	Extraction of Endocannabinoids from Endometrial	
2.5.4.3	Tissue	75
2.5.4.4	Measurement of <i>N</i> -acylethanolamides	75
2.6	Statistics	76
2.7	Results	77
2.7.1	Power Calculations	77
2.7.2	Demographic Variables	77
	Detection of <i>N</i> -acylethanolamines in Plasma and	
2.7.3	Endometrial Tissues	78
2.7.4	Plasma Levels of <i>N</i> -acylethanolamines	78

2.7.5	Tissue Levels of <i>N</i> -acylethanolamines	86
2.7.6	The Relationship Between Plasma AEA, OEA and PEA Concentrations	90
2.7.7	The Relationship Between AEA, OEA and PEA Tissue Levels	92
2.7.8	The Relationship Between Plasma Concentrations and Endometrial Tissue Levels of AEA, OEA and PEA	93
2.7.9	Receiver-operator Characteristic (ROC) Analyses	95
2.7.9.1	Diagnostic Significance of Plasma AEA	95
2.7.9.2	Diagnostic Significance of Plasma OEA	96
2.7.9.3	Diagnostic Significance of Plasma PEA	98
2.7.9.4	Combining the Best Two AUC Values - Plasma AEA and PEA	100
2.7.9.5	Combining All Three Biomarkers - Plasma AEA, PEA and OEA	101
2.8	Discussion	101
2.9	Conclusions	103
Chapter 3	Activity, Expression and Location of the Endocannabinoid Regulating Enzymes FAAH and NAPE-PLD	104
3.1	Introduction	105
3.1.1	Hypothesis	106
3.1.2	Aims	107
3.2	Materials and Methods	107
3.2.1	Recruitment and Subjects	107
3.2.2	Quantification of the FAAH Enzyme Activity in Lymphocytes by Reverse Phase High Performance Liquid Chromatography (HPLC)	108
3.2.3	Identification of Endogenous Control Reference Genes for Normalizing Gene Expression Studies	109
3.2.3.1	Taqman® Chemistry	109
3.2.3.2	Taqman® Array 96-Well Fast Plates	111
3.2.3.3	Reagents, Buffers and Solutions	113
3.2.3.4	Preparation and Storage of Endometrial Tissues	114
3.2.3.5	RNA Extraction and cDNA Synthesis	114
3.2.3.6	Quantitative Real-Time PCR	115
3.2.3.7	Software Determination of Reference Gene Stability	115
3.2.3.8	Stability of the Chosen Reference Gene	116
3.2.3.9	Expression and Relative Quantification of FAAH and NAPE-PLD	116
3.2.4	Identification, Localisation and Histomorphometric Analysis of FAAH and NAPE-PLD Protein	117

	Reagents and Solutions for	
3.2.4.1	Immunohistochemistry (IHC)	117
3.2.4.2	Tissue Preparation	118
3.2.4.3	FAAH Immunohistochemistry	118
3.2.4.4	NAPE-PLD Immunohistochemistry	119
	Image Capture and Evaluation of	
3.2.4.5	Immunohistochemical Staining	120
3.2.5	Statistical Analysis	122
3.3	Results	122
	Selection of Endogenous Control Reference	
3.3.1	Genes	122
3.3.1.1	Patient Characteristics	122
3.3.1.2	RNA Concentration and Purity	123
	Analysis of Reference Gene Stabilities via the	
3.3.1.3	GeNorm PLUS Algorithm	123
	Analysis of Reference Gene Stability via the	
3.3.1.4	NormFinder Algorithm	126
	Analysis of Reference Gene Stability via the	
3.3.1.5	BestKeeper Algorithm	127
	Expression Stability of Putative Reference Genes	
3.3.1.6	Recommended by the Three Software Packages	128
	The Effect of Using Three Endogenous Reference	
	Genes (MRPL19, IPO8 and PPIA) for	
3.3.1.7	normalization	131
3.3.2	FAAH Activity and Expression	131
3.3.2.1	Patient Characteristics - FAAH Activity	131
	FAAH Enzyme Activity Measurement in	
3.3.2.2	Peripheral Lymphocytes	132
	FAAH Enzyme Activity and its Correlation with	
3.3.2.3	Plasma AEA Concentrations	134
	FAAH Enzyme Activity and its Correlation with	
3.3.2.4	Plasma PEA Concentrations	135
	FAAH Enzyme Activity and its Correlation with	
3.3.2.5	Plasma OEA Concentrations	136
3.3.3	FAAH Transcript Levels	136
3.3.3.1	Patient Characteristics - FAAH Transcript Levels	136
3.3.3.2	Relative Expression of FAAH mRNA	138
3.3.4	FAAH Protein Levels	139
3.3.4.1	Patient Characteristics - FAAH Protein Levels	139
	Optimisation and Validation of the FAAH	
3.3.4.2	Immunohistochemical Methods	140
3.3.4.3	Identification and Localisation of FAAH Protein	142
	Histomorphometric Quantification of FAAH	
3.3.4.4	Proteins	143
3.3.5	NAPE-PLD Transcript Levels	147
3.3.5.1	Patient Characteristics – NAPE-PLD Transcript	147

	Levels	
3.3.5.2	Relative Expression of NAPE-PLD mRNA	147
3.3.6	NAPE-PLD Protein Levels	147
	Patient Characteristics- NAPE-PLD Protein	
3.3.6.1	Levels	147
	Optimisation and Validation of the NAPE-PLD	
3.3.6.2	Immunohistochemical Methods	149
	Identification and Localisation of NAPE-PLD	
3.3.6.3	Protein	151
	Histomorphometric Quantification of NAPE-PLD	
3.3.6.4	Proteins	153
	The Relationship Between the NAPE-PLD and	
3.3.7	FAAH Expression Levels	157
	Examination of the Relationship Between FAAH	
3.3.7.1	Transcript and Protein Levels	157
	Examination of the Relationship Between NAPE-	
3.3.7.2	PLD Transcript and Protein Levels	158
	Correlation of NAPE-PLD and FAAH Expression	
3.3.7.3	at the Transcript Level	159
	Correlation of NAPE-PLD and FAAH Expression	
3.3.7.4	at the Protein Level	159
3.3.7.5	NAPE-PLD: FAAH Transcript Ratios	160
3.4	Discussion	161
	Identifying and Validating Endogenous Control	
3.4.1	Reference Genes for the Transcript Studies	162
	Localisation and Histomorphometric Analysis of	
3.4.2	NAPE-PLD and FAAH Expression	164
	Expression and Localisation of the Classical	
Chapter 4	and Non-Classical Endocannabinoid Receptors	166
4.1	Introduction	167
4.1.1	Aims	168
4.2	Subjects and Methods	169
4.2.1	Participants	169
	Transcripts Levels for CB1, CB2, GPR55 and	
4.2.2	TRPV1	169
	Localisation and Determination of Distribution	
	Patterns of CB1, CB2, GPR55 and TRPV1	
4.2.3	Receptor Proteins Using Immunohistochemistry	169
4.2.3.1	Immunohistochemistry for CB1	170
4.2.3.2	Immunohistochemistry for CB2	170
4.2.3.3	Immunohistochemistry for GPR55	171
4.2.3.4	Immunohistochemistry for TRPV1	171
4.3	Statistics	171
4.4	Results	172
4.4.1	Patient Characteristics	172

4.4.2	CB1 Expression	172
4.4.2.1	CB1 Transcript Levels	172
4.4.2.2	CB1 Protein Expression	174
	Optimisation and Validation of	
4.4.2.2.1	Immunohistochemical Methods for CB1	174
	Identification and Location of CB1 Protein	
4.4.2.2.2	Expression	176
4.4.2.2.3	Histomorphometric Quantification of CB1 Protein	178
4.4.3	CB2 Expression	182
4.4.3.1	CB2 Transcript Levels	182
4.4.3.2	CB2 Protein Expression	184
	Optimisation and Validation of	
4.4.3.2.1	Immunohistochemical Methods for CB2	184
4.4.3.2.2	Identification and Locations of CB2 Protein	186
4.4.3.2.3	Histomorphometric Quantification of CB2 Protein	187
4.4.4	GPR55 Expression	191
4.4.4.1	GPR55 Transcript Levels	191
4.4.4.2	GPR55 Protein Expression	193
	Optimisation and Validation of	
4.4.4.2.1	Immunohistochemical Methods for GPR55	193
4.4.4.2.2	Identification and Locations of GPR55 Protein	195
4.4.4.2.3	Histomorphometric Quantification of GPR55	196
4.4.5	TRPV1 Expression	200
4.4.5.1	TRPV1 Transcript Levels	200
4.4.5.2	TRPV1 Protein Expression	202
	Optimisation and Validation of	
4.4.5.2.1	Immunohistochemical Methods for TRPV1	202
4.4.5.2.2	Identification and Locations of TRPV1 Protein	204
4.4.5.2.3	Histomorphometric Quantification of TRPV1	205
4.5	Discussion	209
	<i>In-Vitro</i> Modelling - Effect of	
	Endocannabinoids on Endometrial Carcinoma	
Chapter 5	Cell Growth and Survival	213
5.1	Introduction	214
5.1.1	Aim	215
5.2	Materials and Methods	215
5.2.1	The Materials Used for the Cell Culture Studies	215
5.2.2	Cell Culture	216
5.2.2.1	Subculture	216
5.2.2.2	Cryopreservation and Recovery	216
5.2.2.3	Cell Count	217
5.2.3	Ishikawa Cell Dose-Response Curve Model	218
	Production of Endocannabinoids/ Endovanilloids	
5.2.4	Containing Media	219
5.2.5	Cell Proliferation (XTT) Assay	220

5.2.6	Statistical Analysis	221
5.3	Results	221
	Dose-response Curve for AEA, OEA, PEA and Capsaicin	
5.3.1		221
	Time Dependent Effect of Endocannabinoids/Endovanilloids on Cell Viability	
5.3.2		223
5.3.3	Effect of AEA on Ishikawa Cell Viability	223
5.3.4	Effect of OEA on Ishikawa Cell Viability	225
5.3.5	Effect of PEA on Ishikawa Cell Viability	227
5.3.6	Effect of Capsaicin on Ishikawa Cell Viability	229
5.4	Discussion	231
Cellular Apoptosis and Proliferation Markers in Endometrial Cancer and their Relationship with the Endocannabinoid System		
Chapter 6		234
6.1	Introduction	235
6.1.1	Hypothesis	236
6.1.2	Aims	236
6.2	Subjects and Methods	237
6.2.1	Patient Characteristics	237
	Localisation and Determination of Distribution Patterns of BAX, Bcl-2 and Ki-67 Proteins Using Immunohistochemistry	
6.2.2		237
6.2.3	Immunohistochemistry for BAX	238
6.2.4	Immunohistochemistry for Bcl-2	238
6.2.5	Immunohistochemistry for Ki-67	239
6.2.6	Statistical Analysis	239
6.3	Results	239
6.3.1	Patient Characteristics for IHC	239
6.3.2	BAX Protein Expression	239
	Optimisation of Immunohistochemical Methods for BAX	
6.3.2.1		239
6.3.2.2	Identification and Locations of BAX Proteins	241
	Histomorphometric Quantification of BAX Proteins	
6.3.2.3		243
6.3.3	Bcl-2 Protein Expression	247
	Optimisation of Immunohistochemical Methods for Bcl-2	
6.3.3.1		247
6.3.3.2	Identification and Locations of Bcl-2 Proteins	248
	Histomorphometric Quantification of Bcl-2 Proteins	
6.3.3.3		250
6.3.4	Ki-67 Protein Expression	254
	Optimisation of Immunohistochemical Methods for Ki-67	
6.3.4.1		254
6.3.4.2	Identification and Locations of Ki-67 Proteins	255
6.3.4.3	Quantification of Ki-67 Proteins	256

6.3.5	The BAX/Bcl-2 Ratio	260
	Relationship Between Proliferation and Apoptosis	
6.3.6	Markers	264
6.3.6.1	Ki-67 and BAX	264
6.3.6.2	Ki-67 and Bcl-2	265
6.3.6.3	Ki-67 and BAX/Bcl-2 Ratio	266
	Relationship Between BAX/Bcl-2 Ratio or Ki-67	
6.3.7	Expression with Components of the ECS	267
6.4	Discussion	276
Chapter 7	General Discussion and Future Directions	281
7.1	Discussion	282
7.2	Future Work	297
7.3	Conclusions	297
Chapter 8	Appendices	299
8.1	Letter of Ethical Approval	300
8.2	Published Works	301
Chapter 9	Bibliography	302
9.1	References	303

Lists of Tables

Table Number	Description	Page Number
1-1	GLOBOCAN 2012, estimated number of genital tract cancers and mortality rate.	33
1-2	Known risk factors for endometrial cancer	38
1-3	Genetic factors involved in the pathogenesis of endometrial malignancies	42
1-4	Summary of the histopathological subtypes of endometrial carcinoma	43
2-1	Serial dilutions of stock solutions of internal standards of AEA, OEA and PEA	74
3-1	Individual studies and the number of subjects/samples used	108
3-2	Advantages of TaqMan® Chemistry	109
3-3	TaqMan® Endogenous Control Genes Assay ID, gene names and accession numbers	112
3-4	The contents of the reverse transcriptase reactions, reagents and volumes needed to create cDNA from the total RNA samples	115
3-5	Chemicals used for the IHC studies and their sources	117
3-6	Patients Characteristics	123
3-7	BestKeeper output	129
3-8	Patient characteristics of blood samples sent for FAAH activity analysis	132
3-9	Patient characteristics for the expression of FAAH mRNAs in endometrial carcinoma	137
3-10	Age and BMI characteristics of the patients who provided samples for the FAAH IHC experiment	139
4-1	The antibodies used for IHC studies (with their sources and suppliers)	170
5-1	The products used in the cell culture experiments and their supplier	215
6-1	The antibodies used for BAX, Bcl-2 and Ki-67 IHC studies	237

Lists of Figures

Figure Number	Description	Page Number
1-1	Histological appearance of the endometrial compartment in proliferative and secretory phase of the menstrual cycles.	34
1-2	Histological description of a post-menopausal endometrium.	36
1-3	Molecular pathogenesis of endometrial carcinoma.	40
1-4	The various components of the ECS.	46
1-5	Pathways for the biosynthesis of the <i>N</i> -acylethanolamides (NAEs).	51
1-6	Biosynthesis pathways of 2-AG.	52
1-7	Schematic representations of the NAE degradation pathways.	54
1-8	Schematic representation of the degradation of 2AG.	55
1-9	The cannabinoid and non-cannabinoid receptors.	56
1-10	The potential mechanism of actions of the endocannabinoid system in cancer.	59
1-11	Schematic models of different signalling pathways through which endocannabinoid exert their receptor-mediated effects.	64
1-12	Schematic representation of the patient cohort used in these studies and the numbers used in the different analyses used to test the objectives.	67
2-1	BMI of women in the control and type 1 and type 2 EC groups.	77
2-2	The ages of the women in the control and type 1 and 2 endometrial cancer groups.	78
2-3A	Plasma NAEs in control (atrophic) patients and patients with endometrial cancer (EC).	80
2-3B	Plasma NAEs in control (atrophic) patients and patients with type 1 and 2 EC.	81
2-3C	Plasma NAEs in control (atrophic) and grade 1, 2 and 3 type 1 EC.	82
2-3D	A re-evaluation of plasma AEA (without one value) and PEA (without three values) in control (atrophic) patients and patients with endometrial cancer (EC).	83
2-3E	A re-evaluation of plasma AEA (without one value) and PEA (without three values) in control (atrophic) patients and patients with type 1 and 2 EC.	84
2-3F	A re-evaluation of plasma AEA (without one value) and PEA (without three values) concentrations in control (atrophic) and grade 1 and 3 type 1 EC.	85
2-4A	Tissue NAEs in control (atrophic) patients and patients with endometrial cancer (EC).	87
2-4B	Tissue NAEs in control (atrophic) patients and patients with	

	type 1 and 2 EC.	88
2-4C	Tissue NAEs in control (atrophic) and grade 1, 2 and 3 type 1 EC.	89
2-5A-F	Correlation curves showing the relationship between plasma levels of AEA, OEA and PEA.	91
2-6A-C	Correlation curves showing the relationship between tissues levels of AEA, OEA and PEA.	92
2-7A-E	Relationship between plasma and endometrial tissue concentrations of AEA, OEA or PEA in EC.	94
2-8	Diagnostic test in plasma AEA in atrophic and EC.	95
2-9	Diagnostic test in plasma AEA in atrophic and type 1 EC.	96
2-10	Diagnostic test in plasma OEA in atrophic and EC.	97
2-11	Diagnostic test in plasma OEA in atrophic and type 1 EC.	98
2-12	Diagnostic test in plasma PEA in atrophic and EC.	99
2-13	Diagnostic test in plasma PEA in atrophic and type 1 EC.	100
3-1	The steps involved in TaqMan® Chemistry.	101
3-2	Illustrations of FAAH immunohistochemical staining of atrophic tissues and how the imagescope software image analysis system was used.	121
3-3	geNorm analyses of reference genes.	124
3-4	geNorm ^{PLUS} analysis of 32 reference genes.	126
3-5	Stability values for the 32 endogenous ‘housekeeping genes’ as ranked by the NormFinder.	127
3-6	Relative CB1 expressions in endometrial carcinoma using the indicated combinations of genes for normalization from the three software packages.	130
3-7	FAAH activity in peripheral blood lymphocytes in EC.	132
3-8	FAAH activity in peripheral blood lymphocytes in different grades of type 1 EC.	133
3-9	Spearman correlation analysis of lymphocytic FAAH activity and plasma AEA concentrations.	134
3-10	Spearman correlation analysis of lymphocytic FAAH activity and plasma PEA concentrations.	135
3-11	Spearman correlation analysis of lymphocytic FAAH activity and plasma OEA concentrations (n=21).	136
3-12	Relative expression of FAAH mRNAs via qRT-PCR.	138
3-13	Staining intensities for FAAH at different antibody dilutions (S=stroma, G = glands).	140
3-14	An example of a control experiment demonstrating the specificity of the primary antibody FAAH.	141
3-15	Localisation and expression of FAAH protein in various tissues (G=glands, S=stromas and EC=endometrial carcinoma).	142
3-16A	Histomorphometric analysis (H-score) of FAAH (G+S)	

	immunoreactivity.	144
3-16B	Histomorphometric analysis of FAAH immunoreactivity (H-score) in the glandular tissue (G).	145
3-16C	Histomorphometric analysis of FAAH immunoreactivity (H-score) in stromal tissue (S).	146
3-17	Relative expression of NAPE-PLD mRNAs as determined by qRT-PCR.	148
3-18	Staining intensities for NAPE-PLD at different antibody dilutions (S=stroma, G=glands).	149
3-19	Negative control demonstrating the specificity of the primary antibody NAPE-PLD.	150
3-20	Localisation and expression of the NAPE-PLD protein in various tissues (G=gland, S= stroma and EC= endometrial carcinoma).	151
3-21A	Histomorphometric analysis (H-score) of NAPE-PLD (G+S) immunoreactivity.	154
3-21B	Histomorphometric analysis of NAPE-PLD immunoreactivity (H-score) in the glandular tissue (G).	155
3-21C	Histomorphometric analysis of NAPE-PLD immunoreactivity (H-score) in stromal tissue (S).	156
3-22	Graphs comparing FAAH transcripts and FAAH H-scores.	157
3-23	Graphs comparing NAPE-PLD transcripts and FAAH H-scores.	158
3-24	Correlation between NAPE-PLD and FAAH at the transcript level.	159
3-25	Correlation between NAPE-PLD and FAAH protein in the endometrium.	159
3-26	NAPE-PLD: FAAH transcript and protein ratios in control and EC endometria.	160
4-1	Relative expression of tissue CB1 transcript levels.	173
4-2	Staining intensities for CB1 at different antibody dilutions (S=stroma, G=glands).	174
4-3	Specificity of the primary CB1 antibody.	175
4-4	Localisation and expression of the CB1 protein in various tissues (G=glands, S=stroma and EC=endometrial carcinoma).	176
4-5A	Histomorphometric (H-score) analysis of immunoreactive CB1 (G+S) proteins.	179
4-5B	Histomorphometric (H-score) analysis of immunoreactive CB1 (G) proteins.	180
4-5C	Histomorphometric (H-score) analysis of immunoreactive CB1 (S) proteins.	181
4-6	Relative expression of tissue CB2 transcript levels.	183
4-7	Staining intensities for CB2 at different antibody dilutions (S=stroma, G=glands).	184

4-8	Negative control experiment demonstrating the specificity of the primary CB2 antibody.	185
4-9	Localisation and expression of the CB2 protein in various tissues (G=glands, S=stroma and EC=endometrial carcinoma).	186
4-10A	Histomorphometric (H-score) analysis of immunoreactive CB2 (G+S) proteins.	188
4-10B	Histomorphometric (H-score) analysis of immunoreactive CB2 (G) proteins.	189
4-10C	Histomorphometric (H-score) analysis of immunoreactive CB2 (S) proteins.	190
4-11	Relative expression of tissue GPR55 transcript levels.	192
4-12	Staining intensities for GPR55 at different antibody dilutions using human pancreas as the control tissue (S=stroma, G=glands).	193
4-13	Negative control experiment demonstrating the specificity of the primary GPR55 antibody in pancreatic tissue.	194
4-14	Localisation and expression of the GPR55 protein in various tissues (G=glands, S=stroma and EC=endometrial carcinoma).	195
4-15A	Histomorphometric (H-score) analysis of immunoreactive GPR55 (G+S) proteins.	197
4-15B	Histomorphometric (H-score) analysis of immunoreactive GPR55 (G) proteins.	198
4-15C	Histomorphometric (H-score) analysis of immunoreactive GPR55 (S) proteins.	199
4-16	Relative expression of tissue TRPV1 transcript levels.	201
4-17	Staining intensities for TRPV1 at different antibody dilutions (S=stroma, G=glands).	202
4-18	Negative control experiment demonstrating the specificity of the primary TRPV1 antibody (S=stroma, G=glands).	203
4-19	Localisation and expression of the TRPV1 protein in various tissues (G=glands, S=stroma and EC=endometrial carcinoma).	204
4-20A	Histomorphometric (H-score) analysis of immunoreactive TRPV1 (G+S) proteins.	206
4-20B	Histomorphometric (H-score) analysis of immunoreactive TRPV1 (G) proteins.	207
4-20C	Histomorphometric (H-score) analysis of immunoreactive TRPV1 (S) proteins.	208
5-1	A diagrammatic representation of a grid on the Neubauer haemocytometer.	218
5-2	A graphical representation of the Ishikawa modelling experiments.	219
5-3	Visual representation of the Ishikawa cell modelling experiment.	220
5-4	Dose-response curves for the individual endocannabinoid and	

	capsaicin ligands.	222
5-5	Effect of time on the treatment of Ishikawa cells with different AEA concentrations.	224
5-6	Effect of time on the treatment of Ishikawa cells with different OEA concentrations.	226
5-7	Effect of time on the treatment of Ishikawa cells with different PEA concentrations.	228
5-8	Effect of time on the treatment of Ishikawa cells with different Capsaicin concentrations.	230
6-1	Negative control demonstrating the specificity of the primary antibody BAX.	240
6-2	Localisation and expression of the BAX protein (G=glands, S=stroma and EC=endometrial cancers).	241
6-3A	Histomorphometric analysis of BAX (G+S) (H-score) proteins immunoreactivity.	244
6-3B	Histomorphometric analysis of BAX (G) (H-score) proteins immunoreactivity.	245
6-3C	Histomorphometric analysis of BAX (S) (H-score) proteins immunoreactivity.	246
6-4	Negative control demonstrating the specificity of the primary antibody Bcl-2.	247
6-5	Localisation and expression of the Bcl-2 protein in the indicated tissues (G=glands, S=stroma and EC=endometrial cancers).	248
6-6A	Histomorphometric analysis of Bcl-2 (G+S) (H-score) proteins immunoreactivity.	251
6-6B	Histomorphometric analysis of Bcl-2 (G) (H-score) proteins immunoreactivity.	252
6-6C	Histomorphometric analysis of Bcl-2 (S) (H-score) proteins immunoreactivity.	253
6-7	Negative control demonstrating the specificity of the primary antibody Ki-67.	254
6-8	Localisation and expression of the Ki-67 protein in the indicated tissues (G=glands, S=stroma and EC=endometrial cancers).	255
6-9A	Histomorphometric analysis of Ki-67 (G+S) (H-score) proteins immunoreactivity.	257
6-9B	Histomorphometric analysis of Ki-67 (G) (H-score) proteins immunoreactivity.	258
6-9C	Histomorphometric analysis of Bcl-2 (S) (H-score) proteins immunoreactivity.	259
6-10A	BAX/Bcl-2 ratio in the glands and stroma (G+S).	261
6-10B	BAX/Bcl-2 ratio in the glands (G).	262
6-10C	BAX/Bcl-2 ratio in the stroma (S).	263

6-11	Correlation curves showing the relationship between Ki-67 and BAX tissue protein levels.	264
6-12	Correlation curves showing the relationship between Ki-67 and Bcl-2 tissue protein levels.	265
6-13	Correlation curves showing the relationship between Ki-67 and BAX/Bcl-2 ratio tissue protein levels.	266
6-14	Analysis of the relationship between BAX/Bcl-2 ratio and endocannabinoid ligands.	268
6-15	BAX/Bcl-2 ratio and CB1 and CB2 correlation analyses.	269
6-16	BAX/Bcl-2 ratio and non-classical receptors, GPR55 and TRPV1.	270
6-17	BAX/Bcl-2 ratio and FAAH and NAPE-PLD.	271
6-18	Ki-67 and endocannabinoid ligands analysis.	272
6-19	Ki-67 and classical cannabinoid receptors (CB1 and CB2) analysis.	273
6-20	Ki-67 and non-classical receptor GPR55 and TRPV1 analysis.	274
6-21	Ki-67 and the ECS metabolizing enzymes FAAH and NAPE-PLD.	275
6-22	A hypothetical pathway of endometrial cell apoptosis and cellular proliferation.	278

List of Abbreviations

Δ^9 -THC	delta-9-tetrahydrocannabinol
μ	micro
2-AG	2-arachidonoyl-glycerol
AA	Arachidonic acid
AEA	Anandamide
ANOVA	Analysis of variance
AMT	Anandamide membrane transporter
ASR	Age-Standardised Mortality Rate
ATP	Adenosine triphosphate
AUC	Area under the curve
BAX	Bcl-2 associated X protein
Bcl-2	B cell lymphoma 2
BMI	Body mass index
BSA	Bovine serum albumin
CA-125	Cancer antigen 125
Ca ²⁺	Calcium
cAMP	Cyclic adenosine monophosphate
CAP	Capsaicin
CB1	Type 1 cannabinoid receptor
CB2	Type 2 cannabinoid receptor
cdc25A	Cell division cycle 25A
cDNA	Complementary DNA
Cdk2	Cyclin dependent kinase-2
CHK1	Cycle checkpoint kinase 1
CNS	Central nervous system
COX-2	Cyclooxygenase 2

Ct	Threshold cycle
CTNNB1	Beta-catenin
CYP19	Cytochrome P450 aromatase
DAB	3,3'-diaminobenzidine
DAGL	sn-1-diacylglycerol lipase
DNA	Deoxyribonucleic acid
ECS	Endocannabinoid system
EC	Endometrial cancer
ECM	Extra cellular matrix
EDTA	Ethylenediaminetetraacetic acid
EEC	Estrogen-related endometrioid carcinoma
EGF-R	Epidermal growth factor receptor
ER	Estrogen receptor
ERK1/2	Extracellular signal-regulated kinase 1/2
FAAH	Fatty acid amide hydrolase
FAM	Fluorogenic carboxyfluorescein
FSH	Follicle stimulating hormone
GPR119	G-protein-coupled receptor 119
GPR18	G-protein-coupled receptor 18
GPR55	G-protein-coupled receptor 55
H-score	Histomorphometric score
H&E	Haematoxylin and eosin
HE4	Human epididymis 4
HIF-1 α	Hypoxia-inducible factor-1 alpha
hr	Hours
HRT	Hormone replacement therapy
IARC	International Agency for Research on Cancer

IgG	Immunoglobulin
IHC	Immunohistochemistry
IMB	Intermenstrual bleeding
IMS	Industrial methylated spirit
IPO8	Importin 8
IQR	Interquartile range
Ki-67	Marker of proliferation Ki-67
Kg	Kilogram
K-RAS	Kirsten ras sarcoma viral oncogene homolog
L	Litre
LOH	Loss of heterozygosity
m	Metre
M	Molar
min	Minutes
MAGL	Monoacylglycerol lipase
MGP	Minor groove binder
MI/ MSI	Microsatellite instability
ml	Millilitre
MLH1	MutL Homolog 1
MMP-2	Matrix metalloproteinase-2
mRNA	Messenger RNA
miRNA	Micro RNA
MRPL19	Mitochondrial ribosomal protein L 19
MSH6	MutS Homolog 6
NAAA	<i>N</i> -acylethanolamine-hydrolysing acid amidase
NADA	<i>N</i> -arachidonoyl-dopamine
NAEs	<i>N</i> -acylethanolamides

NAPE	<i>N</i> -arachidonoyl phosphatidylethanolamine
NAPE-PLD	<i>N</i> -acyl-phosphatidyl ethanolamine-specific phospholipase D
NEEC	Non endometrioid endometrial carcinoma
ng	Nanogram
NGS	Normal goat serum
NRS	Normal rabbit serum
NTC	No template control
OD	Optical density
OEA	<i>N</i> -oleoylethanolamine
p	Probability
PBA	Phosphate buffered saline containing BSA
PBS	Phosphate buffered saline
PCOS	Polycystic ovarian syndrome
PCR	Polymerase chain reaction
PEA	<i>N</i> -palmitoylethanolamine
PIK3CA	Phosphatidylinositol-4, 5-bisphosphate 3-kinase ,catalytic subunit alpha
PKB	Protein kinase B
PLC	Phospholipase C
PMB	Postmenopausal bleeding
PPAR- α	Peroxisome proliferator activated receptor alpha
PPIA	Peptidylpropyl isomerase A (cyclophilin A)
PR	Progesterone Receptor
PTEN	Phosphatase and tensin homolog
qPCR	Quantitative PCR
RNA	Ribonucleic acid
ROC	Receiver–operator characteristics
RT	Reverse transcriptase

RT-PCR	Real time polymerase chain reaction
SD	Standard deviation
SEA	Stearoylethalamide
SEM	Standard error of the mean
SHBG	Sex hormone binding globulin
SPE	Solid-phase extraction
TAMARA	6-carboxytetramethylrhodamine
TBA	Tris-buffered saline containing BSA
TBS	Tris-buffered saline
TGF- α	Transforming growth factor alpha
TNF	Tumour necrosis factor
TRPV1	Transient receptor potential vanilloid type 1
TVS	Transvaginal ultrasound scanning
UHPLC-ESI-MS/MS	Ultra-high performance liquid chromatography- electrospray ionisation-tandem mass spectrometry
UHPLC-MS/MS	Ultra-high performance liquid chromatography-tandem mass spectrometry
VEGF	Vascular endothelial growth factor
VIC	4,7,2'-trichloro-7'-phenyl-6-carboxyfluorescein
VEGF-1	Vascular endothelial growth factor receptor 1
WFDC1	WAP four-disulphide core domain 1
Yrs	Years



Chapter 1

Introduction and Background

1.1 Cancer

Cancer is characterised by an imbalance in cell cycle regulation leading to uncontrolled cell division and abnormal cell growth with a potential to invade and spread to other parts of the body (NCI 2014, WHO February 2014).

Cancer is the number one leading cause of death in more resourced countries, and the second leading cause of death in less resourced countries (following heart disease) (GLOBOCAN 2012). According to the International Agency for Research on Cancer (IARC), GLOBOCAN (Estimated Cancer Incidence, Mortality and Prevalence Worldwide) database and the World Health Organisation (GLOBOCAN 2012, Bray et al. 2013), an estimated 14.1 million new cancer cases and 8.2 million cancer-related deaths occurred in 2012, compared with 12.7 million and 7.6 million, in 2008, respectively (Ferlay J 2008). There were an estimated 32.6 million people living with cancer within 5 years of diagnosis in 2012 (GLOBOCAN 2012). Since the world's population is growing and ageing, the burden of cancer will inevitably increase and GLOBOCAN estimates that there will be almost 21.4 million new cases diagnosed annually and there will be 13.2 million deaths from cancer worldwide by 2030, (Ferlay J 2008, Bray et al. 2012).

1.2 Gynaecological Carcinoma

1.2.1 Worldwide Incidence

Cancers of the female reproductive tract make up approximately 1 out of 6 cancers in women (Sankaranarayanan and Ferlay, 2006) and are a diverse group of malignancies with different epidemiological and pathological features, clinical presentations and treatment modalities. Gynaecological cancers include those of the ovary, Fallopian tube, uterus, cervix, vagina and vulva as well as choriocarcinoma. Table 1.1 shows the estimated total number of different cancers of the genital tract and mortality rates according to GLOBOCAN 2012.

Table 1-1: GLOBOCAN 2012, estimated number of genital tract cancers and mortality rate.

Type of genital tract cancer	Incidence	Mortality Rate
Cervix uteri	527,624	265,563
Corpus uteri	319,605	76155
Ovary	238,719	151,905

1.2.2 In the United Kingdom

Gynaecological cancers remain an important cause of morbidity and mortality in the United Kingdom (UK) with the September 2014 Cancer Research UK statistics showing there were 2,000 deaths from endometrial cancers (more than 5 every day) and 4,300 deaths from ovarian cancer (nearly 12 every day) (Cancer Research UK September 2014). Both endometrial and ovarian cancer were in the top ten most common causes of cancer death in females (Cancer Research UK September 2014). The female cancer with the second biggest increase incidence is endometrial cancer, where mortality burden has also increased by 4 per 100,000 females and the age-standardised mortality rate (ASR) has increased by 15% in the last decade (Cancer Research UK September 2014).

While significant progress has been made in reducing the incidence of some of these, especially cervical cancers, the same cannot be said of endometrial cancer. This is partly because of the lack of an appropriate early screening / diagnostic test (DeVita et al. 2012, WHO February 2014). The need for a method to improve outcomes, especially early diagnosis, and tissue-specific treatment modalities, may improve quality of life and offer substantial health benefits. A thorough understanding of the aetiopathogenesis of endometrial carcinoma could therefore lead to new and improved diagnostic tests and therapies. This chapter reviews the physiological functions of the dynamic endometrial tissue, the factors that cause it to undergo critical dysregulation of the cellular mechanisms including cell division, differentiation and death, which are thought to be involved in the development of cancer.

1.3 Endometrium

1.3.1 Histology and Function of Endometrium

The endometrium (**Figure 1-1**) is a complex dynamic mucosa consisting of two major compartments: a basal layer, adjacent to the myometrium which persists from cycle to cycle (basalis), and a transient superficial functional layer (functionalis). The tissue components of the endometrium are surface columnar epithelium and simple tubular glands with connective tissue stroma in which is embedded an elaborate vascular network (Cornillie et al. 1985).

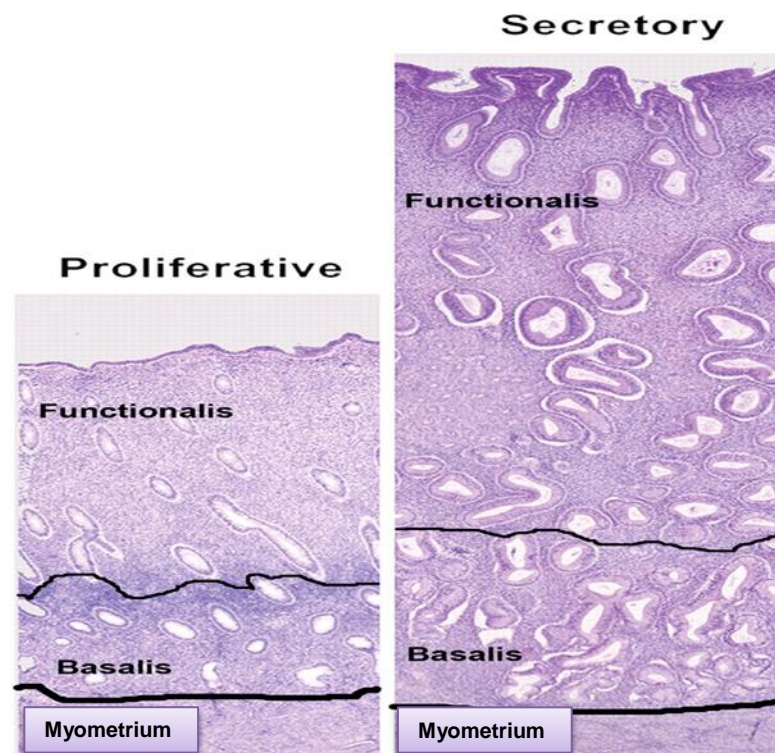


Figure 1-1: Histological appearance of the endometrial compartment in proliferative and secretory phases of the menstrual cycle.

Adapted from <http://humupd.oxfordjournals.org/content/13/6/567/F1.expansion>

The key role of the transient superficial functional layer is to accommodate the implanting blastocyst, provide the maternal component of the placenta and to nurture the fetus throughout gestation (Padykula 1989). However, in the absence of

implantation, the superficial layer is shed followed by remodelling in preparation for the next menstrual cycle, in response to cyclical changes of the ovarian steroid hormones estrogen and progesterone (Wynn 1989).

1.3.2 Hormone Receptors and their Roles in the Endometrial Changes of the Menstrual Cycle

Estrogen action is mediated by ligand-specific estrogen receptors (ER). There are two forms of the ER; α and β (Green et al. 1986). Estrogen is a steroid hormone responsible for endometrial cell proliferation (S.K. 2002). ER α is evident in the glandular epithelial cells and stromal compartments of the endometrium (Garcia et al. 1988). ER α expression increases during the proliferative phase of the menstrual cycle reaching a peak in the late proliferative phase and this is mainly in the functionalis. It is the predominant receptor for epithelial cell proliferation mediated via estrogen, (Okulicz 2002). It is down-regulated in both the glands and stroma of the functionalis during the secretory phase (Lessey et al. 1988).

ER β expression has been documented in nuclei of glandular, stromal and endothelial cells (Critchley 2000). There is no apparent decrease in ER β expression in the stromal cells of the functionalis across the menstrual cycle, but it declines in the glandular component in the late secretory phase (Matsuzaki et al. 1999, Okulicz 2002), suggesting that it may play a role in the regulation of vascular function during this phase of the menstrual cycle (Saunders 1998).

The progesterone receptor (PR) is a nuclear receptor; there are at least 3 forms, PR-A, PR-B and PR-C; however, PR-A and PR-B are the key receptors that mediate progesterone response (Jabbour et al. 2006). The concentrations of PR-A and PR-B in the glandular compartment increase during the follicular phase under the influence of estrogen and then decline under the influences of progesterone in the luteal phase (Lessey et al. 1988, Snijders et al. 1992). In endometrial stroma, PR-A is the predominant subtype during the luteal phase and is regulated by estrogen (Bethea et al. 1998, Wang et al. 1998). During the mid-late proliferative phase, the expression of receptors in the glands is at its highest level (Lessey et al. 1988). Estrogen-induced proliferation of the endometrium is antagonised by progesterone acting via these receptors (Ferenczy et al. 1979).

1.3.3 Postmenopausal Endometrium

The non-cycling peri-menopausal endometrium gradually becomes atrophic as menopause approaches. After menopause the mucosa is shallow in nature with loss of the demarcation between the basalis and the functionalis (Sivridis et al. 2004). The atrophic endometrium is composed of small tubular glands that spread widely in a dense and fibrous stroma and lined by cuboidal indeterminate epithelium. The small tubular endometrial glands may initially possess some weak proliferative functions but with further decline in estrogen secretion, the mucosa reaches a state where it becomes functionally inactive (Sivridis et al. 2004). Finally, with complete absence of ovarian function, the atrophic endometrium becomes a cystic, thin mucosa with cystically dilated endometrial glands and flattened inactive epithelium (Rance 2009) (**Figure 1-2**).

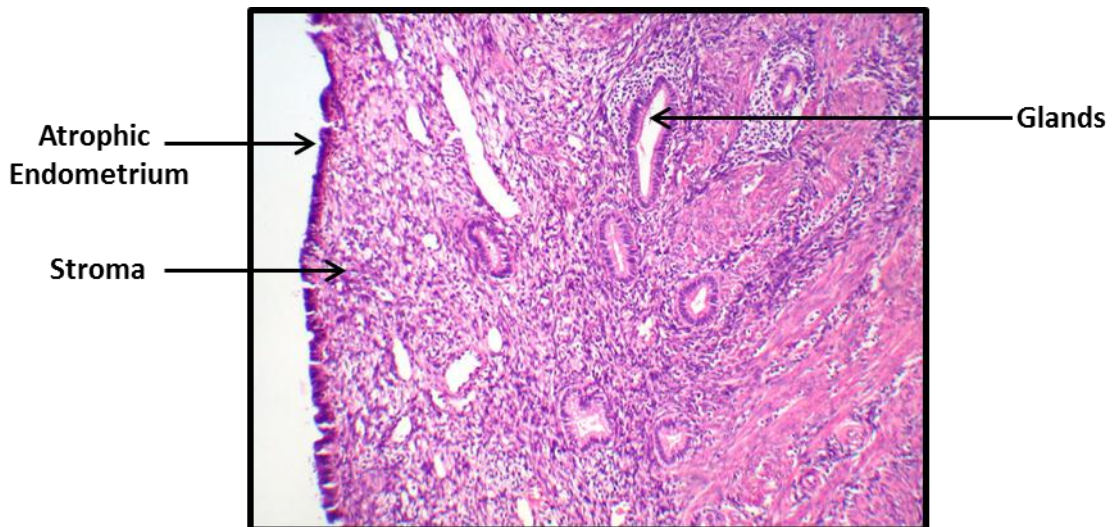


Figure 1-2: Histological description of a post-menopausal endometrium.

Atrophic endometrium is thin and smooth. The glands are a single layer of flattened cuboidal epithelial cells. The stromal cells are spindle in shape and are closely packed.

Adapted from, <http://www.hsc.stonybrook.edu/gyn-atlas/images>.

Menopause occurs naturally around the age of 51 (Wise 2005). The loss of the negative estrogen feedback on the hypothalamus causes a marked increase in serum gonadotropins; mainly pituitary-derived follicle stimulating hormone (Reyes et al. 1977). This stimulates the production of androgens, mainly androstenedione and testosterone, by the non-specialised ovarian stroma. The peripheral conversion of ovarian and adrenal androgens becomes the primary source of endogenous estrogens in

postmenopausal women and this may be sufficient to stimulate the endometrium (Kaaks et al. 2002). In the postmenopausal endometrium, ERs are localised in both the glandular and stromal compartments, making it possible for it to become proliferative when exposed to a high estrogen levels. Such proliferation then progresses to pre-malignant or malignant states.

1.4 Endometrial Carcinoma

1.4.1 Introduction

Endometrial cancer (EC) is the most common female genital tract carcinoma in more resourced countries. In the United Kingdom, despite improvement in overall survival rates, the incidence of EC has risen by 65% while mortality has risen by 20% (Wise 2005, Cancer Research UK September 2014). Although the life time risk of developing EC is around 2-3% (Engelsen et al., 2009), most cases arise after the menopause (> 80 - 90%) (Sivridis and Giatromanolaki, 2004, Saso et al., 2011), with a mean age at diagnosis of about 60 years (range 50-74 years) (Cancer Research UK, September 2014, Saso et al., 2011).

1.4.2 Aetiology

Endometrial cancer falls into two different types; they are known as type I and II. Type I cancers are low grade estrogen-related endometrioid carcinomas (EEC) that usually first appear in peri-menopausal and postmenopausal women. In contrast, type II cancers are aggressive non-endometrioid carcinomas (NEEC) that occur in older postmenopausal women and are unrelated to estrogen stimulation (Okuda et al. 2010).

1.4.2.1 Risk Factors for Endometrial Carcinoma

The precise causes of EC are still unknown; however, various associated risk factors have been identified. These can be grouped as endogenous and exogenous (Saso et al. 2011) as shown in (**Table 1-1**).

One of the main risk factors for EC is exposure to unopposed estrogen, which causes endometrial cell proliferation and predisposes the tissue to pre-malignant changes (hyperplasia) and malignancies (Jick et al. 1993). Elevated levels of estrogen may be exogenous such as from estrogen-only hormone replacement therapy (HRT) or

endogenous as in polycystic ovary syndrome, obesity or estrogen producing tumours. Indeed, the best established risk factors, such as obesity (Friberg et al. 2007), early onset of menstruation, late menopause (Brinton et al. 1992) and nulliparity (McPherson et al. 1996) all relate to chronic exposure to estrogen (Saso et al. 2011). These hormonal factors interact with various other factors including genetic/ molecular and an emerging family of compounds known as the endocannabinoids. Adipose tissue is also an important source of endogenous estrogen in postmenopausal women (Siiteri 1987), hence obesity is associated with an increased risk of EC (Calle et al. 2003).

Excess unopposed estrogen in the pre-menopausal women as in cases of chronic anovulation is also a risk factor for endometrial hyperplasia and cancer (Mills et al. 2010) (Woodruff et al. 1994). Diabetes and hypertension, conditions associated with increased estrogen levels are separate risk factors (Furberg et al. 2003, Friberg et al. 2007, Noto et al. 2010), but may not be truly independent .

Table 1-2: Known risk factors for endometrial carcinoma.

Endogenous factors	Exogenous factors
Increasing age	Unopposed estrogen or hormone replacement therapy
Obesity	Treatment with tamoxifen
Physical inactivity	Dietary habits
Early menarche	Radiotherapy therapy
Late menopause	
Low parity	
Poly cystic ovary syndrome	
Lynch Syndrome	
Estrogen secreting tumours	
Diabetes mellitus	
Hypertension	
History of breast cancer	
Immunodeficiency	

Although most EC are estrogen-dependent, a small proportion are estrogen-independent, and display negative or low estrogen receptor expression (Ryan et al. 2005), suggesting a different aetiopathology for the two forms of EC.

1.4.2.2 Role of Molecular (Genetic) Alterations in Endometrial Cancer

Molecular (genetic) alterations have been shown to be involved in the development of endometrial cancers. It has been revealed that the molecular alterations involved in the development of EEC (type I) carcinomas differ from those of NEEC (type II) carcinomas. Type I endometrial cancers shows microsatellite instability (MI or MSI), MutL Homolog 1 (MLH1), MutS Homolog 6 (MSH6), protein kinase B (PKB or Akt), B cell lymphoma 2 (Bcl-2) and mutations in phosphatase and tensin homolog (PTEN), Kirsten ras sarcoma viral oncogene homolog (K-RAS), Phosphatidylinositol-4, 5-Bisphosphate 3-Kinase, Catalytic Subunit Alpha (PIK3CA) and beta-catenin (CTNNB1) genes, whereas type II exhibits alterations of tumour protein (TP53 or p53), loss of heterozygosity (LOH) on several chromosomes, as well as other molecular alterations in calcium-dependent adhesion (E-cadherin), tumour amplified kinase (STK15), inhibitor of cyclin dependent kinase (p16), and human epidermal growth factor receptor (HER-2/neu or c-erb-B2), as shown in **(Figure 1-3)**. In addition, patients with Lynch Syndrome who have gene mutations in MLH1 and MSH2 have an increased the risk of developing EC, whilst those with MSH6 mutation have a decreased EC risk.

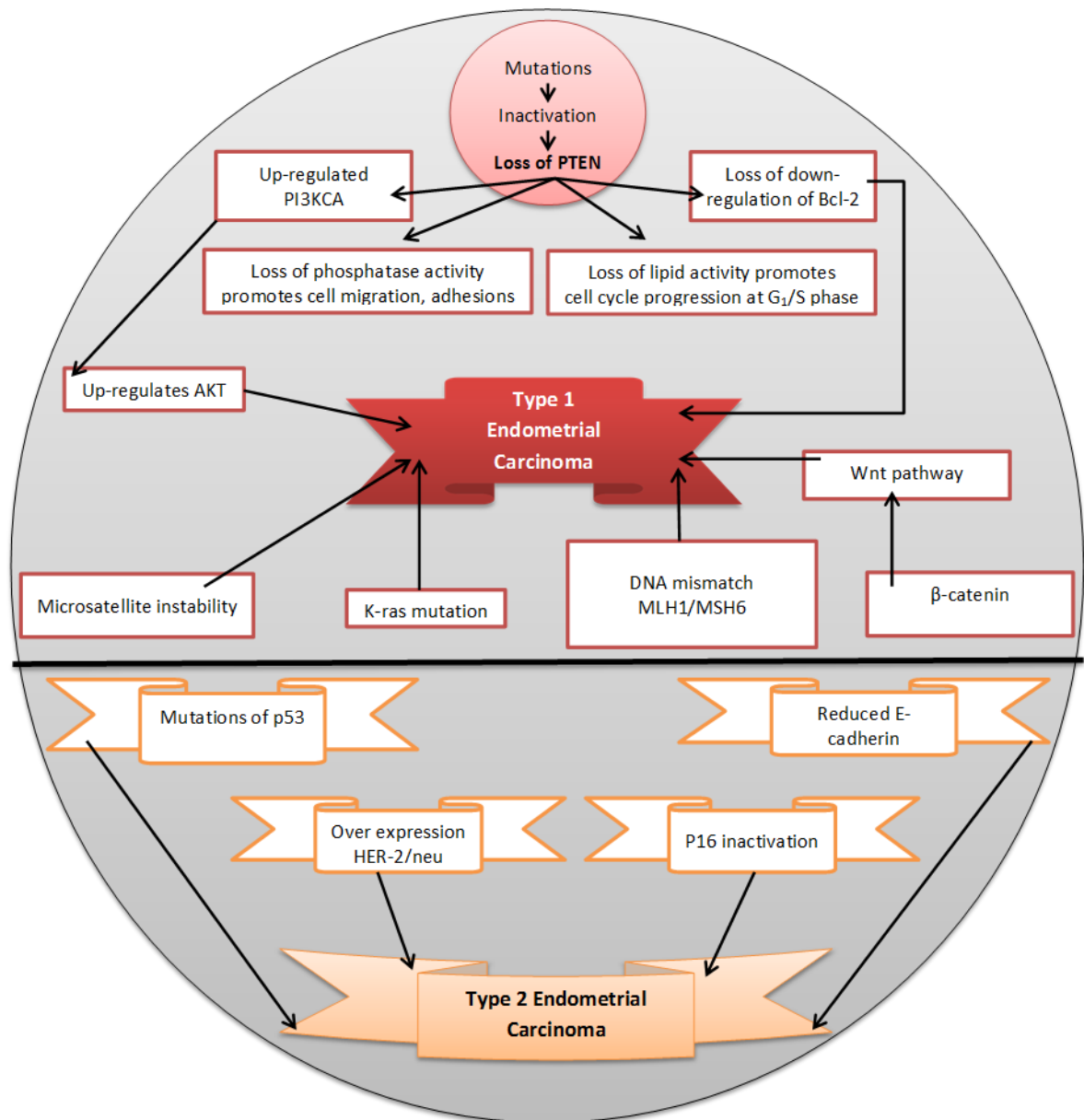


Figure 1-3: Molecular pathogenesis of endometrial carcinoma.

The top half of the figure shows the potential molecular pathways, such as PTEN, PI3KCA, Bcl-2, AKT, MLH1/ MSH6, K-ras, DNA, Wnt and β catenin involved in the initiation and development of type 1 EC (red lined boxes) and the bottom half of the circle indicates the possible mechanistic and gene pathways, such as p53, HER-2/ neu, P16 and E-cadherin involved in type 2 EC. Figure modified from Bansal et al., (Bansal et al. 2009).

Endometrioid adenocarcinoma (type 1) is characterised by a variety of genetic alterations. Although the molecular mechanism(s) leading to type 1 cancer are still not fully understood a number of factors have been studied (Clement et al. 2002). The type 1 EC is associated with a high incidence of mutations in the pathways, such as,

phosphatase and tensin homolog (*PTEN*) tumour-suppressor genes (Tashiro et al. 1997, Mutter et al. 2000), K-ras (Caduff et al. 1995, Lax et al. 2000), β -catenin (Stefansson et al. 2004), defects in DNA mismatch repair and near-diploid karyotype (Hecht et al. 2006). Of these, the most frequent alteration is in the *PTEN* gene. *PTEN* is located at the chromosome 10q23, encodes a protein and lipid phosphatase that behaves as a tumour suppressor gene. Loss of *PTEN* function by either a mutation or deletion appears to be an early phenomenon in the carcinogenesis of endometrioid endometrial adenocarcinomas and this suggests that *PTEN* plays the role of a “gatekeeper gene” for this disease. Some studies have found loss of *PTEN* protein expression in normal endometrium exposed to prolonged unopposed estrogen and in cancerous endometrium. *PTEN* has been reported to be altered in up to 83% of EC and 55% of precancerous lesions. In addition, progesterone receptors are present in type 1 cells and progestogens affect *PTEN* expression by promoting the involution of endometrial cells containing *PTEN*-mutations (Mutter et al. 2000).

Microsatellite instability (MSI) has been recorded in 20% of endometrioid EC. Inactivation of any number of components of the mismatch repair system, such as (MLH1/MSH6) can lead to MSI, which represents an early event in endometrial carcinogenesis and has been demonstrated in precancerous lesions (Basil et al. 2000).

Other genetic mutations / alterations that have been studied included functional mutations in genes such as K-ras and β -catenin. Most studies have revealed a higher incidence of K-ras mutation in MSI associated EC. Although β -catenin may play a role in the early events of EC, its exact function remains unknown.

Type 2, non-endometrioid endometrial carcinoma, is typically associated with mutations in the tumour protein p53 (TP53 or p53) (Tashiro et al. 1997, Lax et al. 2000) or the ERBB-2 (HER-2/neu) gene product (Santin 2003). Most NEEC tumours are non-diploid (Okamoto et al. 1991, Pradhan et al. 2006), with the most common genetic mutation in type 2 serous carcinoma occurring in the p53 tumour suppressor gene. The function of p53 is to prevent the survival of cells with damaged DNA. After the DNA damage, nuclear p53 accumulates and causes cell cycle arrest by inhibiting cyclin-D1 phosphorylation and promoting apoptosis (Lax et al. 2000, Doll et al. 2008). Other common genetic alterations in type 2 carcinoma are inactivation of p16 and over-

expression of HER-2/neu. Both, the p53 and HER-2/neu are found in serous cancer. Inactivation of p16 results in uncontrolled cell growth.

At the molecular level, EC resembles the proliferative rather than the secretory phase of the menstrual cycle (Mutter et al. 2000). Molecular/genetic pathogenesis studies suggest that endometrial malignancies are likely to develop as a result of a series of steps involving tumour suppressor inactivation and a multistep process of oncogenic activation (**Table 1-2**) (Berchuck et al. 1995).

Table 1-3: Genetic factors involved in the pathogenesis of endometrial malignancies.

	Type 1 EEC	Type 2 NEEC	Function
PTEN	35-50%	10%	Loss of function
P53	10-20%	90%	Loss of function
Genomic instability (microsatellite)	20-40%	0-5%	Loss of function
K-ras	15-30%	0-5%	Gain of function
Her2/ neu	10-20%	9-30%	Gain of function
B- Catenin	31-47%	0-3%	Gain of function

EEC=endometrioid endometrial carcinoma, NEEC=non-endometrioid endometrial carcinoma

1.4.3 Symptoms

The classical presentation of patients with EC are postmenopausal bleeding (PMB), with an estimated 20% of patients presenting with PMB diagnosed with carcinoma, which is mostly of endometrial origin, but it can also be from the cervix (Baekelandt et al. 2009). The documented absolute risk of EC in non-users of hormone replacement (HRT) who present with PMB ranges from 5.7% to 11.5% (Bray et al. 2005, Cancer Research UK September 2014). Younger women may present with intermenstrual bleeding (IMB), menorrhagia, dysfunctional uterine bleeding or a change in bleeding pattern (irregular). Less common symptoms include low pelvic pain, vaginal discharge and pyometra, which occasionally may be indicative of advanced disease.

1.4.4 Diagnosis

This is primarily from histological examination of endometrial tissue samples. Postmenopausal women presenting with PMB can either have a hysteroscopy and endometrial biopsy (the gold standard) or a blind biopsy without hysteroscopy. However, transvaginal ultrasound scanning (TVS) is commonly used to screen those who will benefit from a biopsy. A thickened endometrium may indicate the presence of pathology, with the United Kingdom threshold set at 5 mm; an endometrial thickness of more than 5mm gives a 7.3% likelihood of EC (Smith-Bindman et al. 2004). On the other hand, if the endometrial thickness is uniformly less than 5 mm, then the probability of cancer is less than 1% (Sahdev 2007). For an asymptomatic woman, however, an upper limit of endometrial thickness of 11 mm is used as guidance for further investigation (Smith-Bindman et al. 2004). For a cut-off of 10 mm or greater, sensitivity and specificity were 54.1% (45.3–62.8) and 97.2% (97.0–97.4) (Jacobs et al. 2011).

1.4.5 Histological Types of Endometrial Cancer

As described above, EC can be divided into two major types, namely types 1 and 2. Type 1 (EEC), accounts for 70-80% of cases, tends to present early and generally has a good prognosis. Type 2 (NEEC), presents late and behaves more aggressively. Within this category, the commonest histological types are uterine papillary serous carcinoma, clear cell carcinoma and the more uncommon uterine carcinosarcoma, which accounts for 10-20% of cases. Type 2 EC carries a poorer prognosis and the risks of relapse and metastases are high (Bokhman 1983). The histological types are summarised in **Table 1-2** as per the WHO and International Society of Gynaecological Pathology classifications.

Table 1-4: Summary of the histopathological subtypes of endometrial carcinoma.

Type 1	Type 2
Endometrioid adenocarcinoma	Papillary serous adenocarcinoma
With squamous differentiation	Clear cell adenocarcinoma
Villoglandular	Mucinous adenocarcinoma
Secretory	Undifferentiated carcinoma
With ciliated cells	Mixed carcinoma/ Uterine carcinosarcoma

1.4.6 Hormones and Endometrial Cancer

The fact that the postmenopausal women suffer from an estrogen deficiency due to ovarian function failure and have a thin atrophic endometrium may suggest that EC in this group may not be stimulated by estrogen. However, it is well established that the postmenopausal women continues to produce estrogen mostly from extra – ovarian sources, such as the adrenal and fat cells (Judd 1976, Siiteri 1978).

Estrogen is produced during the menopausal state via aromatisation of androgens produced by the adrenal glands and the non-specialised ovarian stroma (Cleland et al. 1985, Sasano et al. 1998). During this period, androstenedione and testosterone production are increased in parallel with an increased conversion of androgens to estrone (Knab 1977, Tseng et al. 1984, Nagamani et al. 1986, Mollerstrom et al. 1993). This aromatisation is through the action of the enzyme cytochrome P450 aromatase (CYP19), which has been documented to be expressed at a level 3-5 times higher than in pre-menopausal women and is further increased by obesity and advanced age (Cleland et al. 1985). Obesity, as an enhancing factor in the conversion mechanism, has been implicated in about 40% of all endometrial malignancies in postmenopausal women (Kaaks et al. 2002, Renehan et al. 2010). This is more evident only in those who have a higher efficiency in performing these conversions, as they are at a higher risk of developing endometrial cancer (Potischman et al. 1996). The bio-availabilities of free estrogens produced are increased and these can freely diffuse into the endometrium because of low levels of sex hormone binding globulin (SHBG) (Kaaks et al. 2002). The levels of SHBG are decreased in obese postmenopausal women as a consequence of hyperinsulinaemia (Khandekar et al. 2011). Furthermore, it is documented that some conversions may occur directly in the endometrium through the action of local endometrial CYP19 enzyme (Nagamani et al. 1986).

Nulliparity or low parity and chronic an ovulatory states, such as in polycystic ovary syndrome (PCOS), may enhance the possibility of developing EC by increasing exposure of the endometrium to endogenous estrogens (Fox et al. 1970). Furthermore, under the influence of relatively high levels of unopposed estrogenic stimulation, such as with estrogen only hormone replacement therapy, the atrophic endometrium may undergo mild architectural changes and develop into a disordered proliferative

endometrium. This, in turn, can lead to a more complicated form of endometrial architecture and cause atypical cytological changes, which then progress to atypical endometrial hyperplasia (endometrial intra-epithelial neoplasia) also known as endometrial intra-epithelial malignancy, and then on to endometrial malignancy (Zeleniuch-Jacquotte et al. 2001). The use of estrogen only HRT preparation has been associated with an 8- to 15-fold increase in incidence of EC (Ziel et al. 1975). It is well documented that an insufficient concentration / level of progesterone in the endometrium contributes to the tumourogenesis of EC because of progesterone's important antagonistic effect on the actions of estrogen.

1.5 The Endocannabinoid System

Despite the close relationship between estrogen and EC, whereby the hormone probably interacts with genetic / molecular factors to predispose individuals to EC, the search for other factors / mechanisms involved in the aetiopathogenesis of EC continues. More recently, an emerging group of compounds known as the endocannabinoids has been linked with other forms of cancer, suggesting that they might have a role to play in the aetiopathogenesis of EC.

The endocannabinoid system (ECS) is known to have a role in the development of some forms of cancer and to have a protective role against growth and metastasis of several types of malignancies (Ayakannu et al. 2013, Pisanti et al. 2013). Although, the relationship between endocannabinoids and cancer aetiology has recently emerged, the relationship between the ECS and endometrial cancer is relatively unexplored.

The ECS comprises of endocannabinoids (ligands), the enzymes that regulate their synthesis and degradation, the prototypical cannabinoid receptors (CB1 and CB2), some non-cannabinoid receptors, a transport system and an intracellular signalling pathways regulated by activation of the receptors (De Petrocellis et al. 2004). **Figure 1-4** shows the classical components of the ECS.

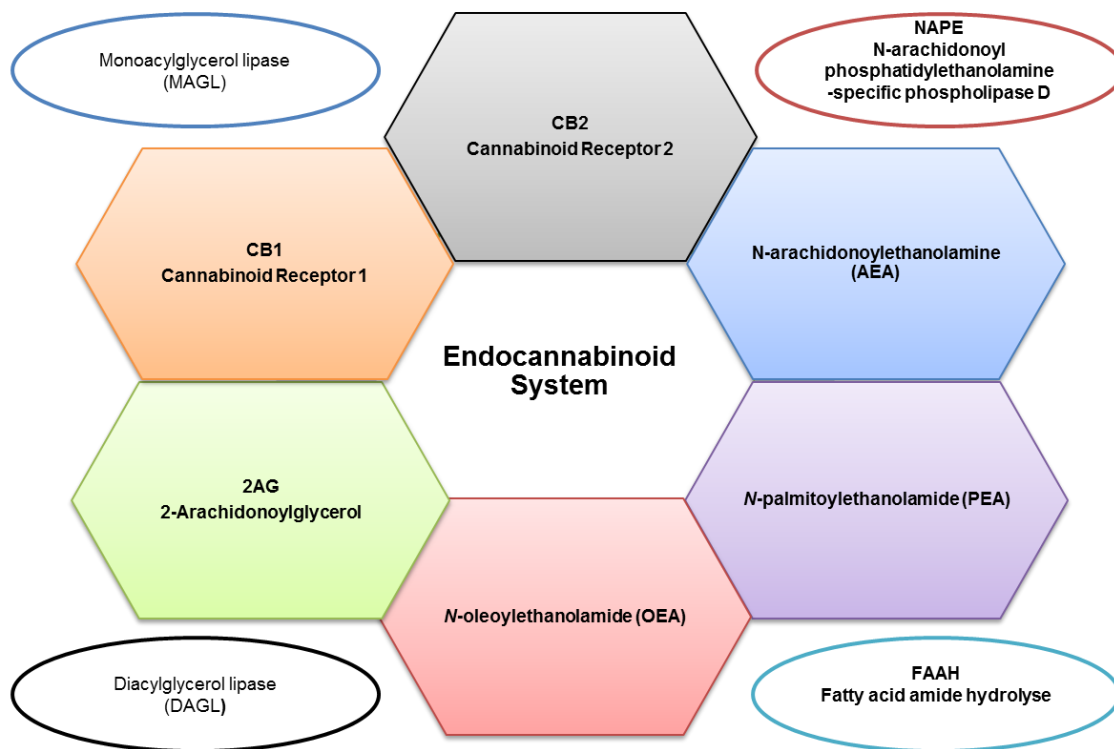


Figure 1-4: The various components of the ECS.

The endocannabinoid system (ECS) comprises the endocannabinoids ligands *N*-arachidonylethanolamide (AEA), *N*-palmitoylethanolamide (PEA) and *N*-oleoylethanolamide (OEA), 2-arachidonoylglycerol (2AG) the enzymes that regulate their synthesis, diacylglycerol lipase (DAGL), *N*- arachidonoylphosphatidylethanolamine - specific phospholipase D (NAPE-PLD) and degradation, monoacylglycerol lipase (MAGL), Fatty acid amide hydrolyase (FAAH) and the prototypical cannabinoid receptors 1 (CB1) and cannabinoid receptors (CB2).

1.5.1 Endocannabinoids

Endocannabinoids are fatty acid derivatives and include *N*-arachidonylethanolamide (AEA), *N*-palmitoylethanolamide (PEA) and *N*-oleoylethanolamide (OEA) and 2-arachidonoylglycerol (2-AG). Other less studied endocannabinoids include *N*-arachidonoyl-dopamine (NADA) (Bisogno et al 2000) nolidan ether and virodhamine (Porter et al 2002).

1.5.1.1 *N*-arachidonylethanolamide or Anandamide (AEA)

AEA, belongs to a large class of endogenous fatty acid amide molecules called the *N*-acylethanolamides (NAEs) and it is derived from arachidonic acid, a 20 carbon fatty acid with four double bonds (C20:4). The name anandamide is derived from the Sanskrit word; *Ananda* which means, ‘bliss’ and it was the first endogenous ligand (endocannabinoid) identified for the cannabinoid receptors. It was first discovered from porcine brain (Devane et al. 1992) and later found to be distributed throughout human tissues including the brain, testis, sperm, leucocytes, placenta, fetal membranes, endothelial cells, anterior eye, pituitary gland, breast and the reproductive tissues (Gerard et al. 1991, Bouaboula et al. 1993, Liu et al. 2000, Porcella et al. 2000, Pagotto et al. 2001, Pertwee 2005, Bifulco et al. 2006, El-Talatini et al. 2009).

AEA has been implicated in several pathological processes and acts as a partial cannabinoid receptor agonist (Ross et al., 1999) at the cannabinoid receptors 1 (CB1), to which it has a high affinity (Devane et al., 1992) or the cannabinoid receptor 2 (CB2), on which it has low affinity (Mechoulam et al., 1995). AEA also activates the non-cannabinoid receptors G- protein-coupled receptor 55 (GPR55) (Ryberg et al., 2007) and the transient receptor potential vanilloid subtype 1 (TRPV1) (Nilius, 2007).

1.5.1.2 *N*-palmitoylethanolamide (PEA)

N-palmitoylethanolamide (PEA) is also a bioactive fatty acid amide belonging to the family of NAEs, that does not bind to the classic CB receptors and its underlying mechanism of action is still a matter of speculation (Di Marzo 1998). PEA exerts anti-inflammatory, analgesic, anti-convulsant and anti-proliferative effects (LoVerme et al. 2005). There are several suggestions to explain its effects, especially the anti-inflammatory and analgesics effects and include: (1) direct activation of the orphan receptor GPR55 (Ryberg et al. 2007), (2) direct stimulation of an as yet uncharacterised ‘cannabinoid CB2 receptor-like’ target (Calignano et al. 1998, Conti et al. 2002), (3) an ‘entourage effect’ where it acts as a substrate to the enzyme fatty acid amide hydrolase (FAAH) thereby enhancing the action of elevated AEA via its activation of CB1 and CB2 or TRPV1, (4) direct action on the nuclear peroxisome proliferator-activated receptor- α (PPAR- α) (Costa et al. 2002) and (5) an autacoid local inflammation antagonism (ALIA) through which it acts by reducing mast cell degranulation (Aloe et al. 1993).

PEA is widely distributed in the central nervous system and periphery (LoVerme et al. 2006) and has been measured in EC (Guida et al. 2010). It enhances the anti-proliferative effects of AEA and synthetic cannabinoids, such as arvanil (a cannabinoid CB1 and TRPV1 agonist) and HU-210 (a potent central cannabinoid (CB1) and peripheral cannabinoid (CB2) receptor agonist) in a prostate cancer cell line (Di Marzo et al., 2001).

1.5.1.3 N-oleoylethanolamide (OEA)

N-oleoylethanolamide (OEA) has been measured in various bio-matrices such as human blood, seminal plasma, mid-cycle oviductal fluid, milk and fluid from malignant ovarian cysts (Schuel et al. 2002, Amoako et al. 2010, Lam et al. 2010). In human and animal studies, OEA has been shown to be involved in the regulation of satiety through a mechanism that controls food intake, feeding and body weight. OEA does not appear to activate CB1 or CB2, with most of the documented effects from therapy with OEA attributed to activation of PPAR- α (Brown 2007, Matias et al. 2007, Capasso et al. 2008), the G-protein coupled receptor 119 (GPR119) (Godlewski et al. 2009) and/or TRPV1 (Hansen 2010). OEA activates TRPV1 on perivascular sensory nerves in human cell lines expressing TRPV1 (Movahed et al. 2005). It also acts via the ‘entourage effect’, which has been postulated to occur predominantly through TRPV1. For example, OEA enhanced AEA-induced vasorelaxation is mediated through TRPV1 in the rat mesentery artery (Ho et al. 2008). Recently OEA has been studied in relation to cancer. One of the studies on the local growth of a tumour in mice showed that OEA was reduced and modulated cell migration. In addition, increased OEA concentrations correlated with the number of metastasis in a human cell line model (Sailler et al. 2014).

1.5.1.4 2-arachidonoylglycerol (2-AG)

The second most common endogenous ligand for cannabinoid receptors or endocannabinoid to be discovered was 2-AG and was shown to bind to CB1 (Sugiura et al. 1999) and CB2 receptors (Mechoulam et al. 1995). It has been found in various tissues both in human and animals, such as the central nervous system (Murataeva et al. 2014), brain tissues (mouse) (Kondo et al. 1998, Sugiura et al. 1999), maternal bovine and human milk (Fride et al. 2005), canine gut (Mechoulam et al. 1995), the uterus (Guida et al. 2010), cervix (Rudolph et al. 2008), ovaries (Nomura et al. 2010) and various cancer tissues and cell lines (Chakravarti et al. 2014). It plays a role as an

antiemetic, analgesic, appetite stimulant and tumour growth inhibitor (Devane et al. 1992, Joseph et al. 2004, Bifulco et al. 2006). 2-AG has been studied in various cancers and is associated with different signalling mechanisms, such as suppression of nerve growth factor receptor (Trk) expression and reduction of prolactin receptors in breast cancer (Melck et al. 2000), inhibition of androgen-independent prostate cancer cell invasion (Nithipatikom et al. 2004), apoptosis via TRPV2-dependent Ca^{2+} influx in glioma (Nabissi et al. 2013), inhibition of migration in cervical cancer (Rudolph et al. 2008), and causing of an imbalance in estrogen/ progesterone concentrations and an increase in CB2 receptor expression, leading to a defect in mitochondrial function, inhibition of cell growth, decrease in proliferation and cell death in endometrial cancer (Guida et al. 2010). 2-AG may also decrease cell growth through modulation of mitochondrial function, apoptosis and cell death (Guida et al. 2010) and promote cell migration, invasion, survival and tumour growth in ovarian cancer (Nomura et al. 2010).

1.5.2 Biosynthesis of Endocannabinoids

Endocannabinoids were originally thought to be synthesised ‘on demand’ from phospholipid precursors residing in the plasma membrane (Guo et al. 2005), but are now known to be synthesised and stored in intracellular lipid droplets and released from those stores under appropriate conditions, and then transported around the cell by fatty acid binding proteins (Kaczocha et al. 2009).

NAEs are produced via several pathways, but the pathway that is most active in non-neuronal cells involves the conversion of the membrane phospholipid *N*-arachidonoylphosphatidylethanolamine (NAPE) through hydrolysis by the actions of a *N*-arachidonoylphosphatidylethanolamine - specific phospholipase D (NAPE-PLD) (Di Marzo et al. 1994) in a calcium²⁺ (Ca^{2+})-dependent manner (Muccioli 2010). **Figure 1-5** shows the pathway for the biosynthesis of the endocannabinoid AEA.

Recent evidence indicates the existence of two additional, parallel paths for the biosynthesis of NAEs. These are the phospholipase C (PLC) and secreted phospholipase A2 (sPLA2)-catalysed Ca^{2+} -independent pathways.

One of these pathways involves the secretion of phospholipase A2 (sPLA2) and α / β serine hydrolase domain containing protein 4 (ABDH4). The recently identified sPLA2

can convert NAPE to 2-lyso-*N*-acylphosphatidylethanolamine (2-lyso-NAPE), which is then metabolised to AEA through a Ca²⁺-independent mechanism, by lyso-PLD. PLA2 expression in tissue is restricted; therefore, there is a possibility that additional enzymes take part in generating lyso-NAPE. One such enzyme, is ABDH4, which can act on either NAPE or lyso-NAPE, to generate the glycerophospho-arachidonoyl ethanolamide (GpAEA), which is later acted on by glycerophosphodiester phosphodiesterase 1 (GDE1) to generate AEA (Sun et al. 2004, Simon et al. 2006).

The PLC pathway involves PLC itself and two other enzymes with parallel activity: protein tyrosine phosphatase non-receptor 22 (PTPN22) and phosphatidylinositol-3, 4, 5-trisphosphate 5-phosphatase 1 (INPP5D). This pathway was identified in the RAW264.7 mouse macrophage cell line. This alternative pathway involves the hydrolysis of NAPE by phospholipase C to yield phosphoanandamide (pAEA), which is then dephosphorylated by phosphatases, such as the INPP5D, and tyrosine phosphatase PTPN22 (Liu et al. 2006, Liu et al. 2008).

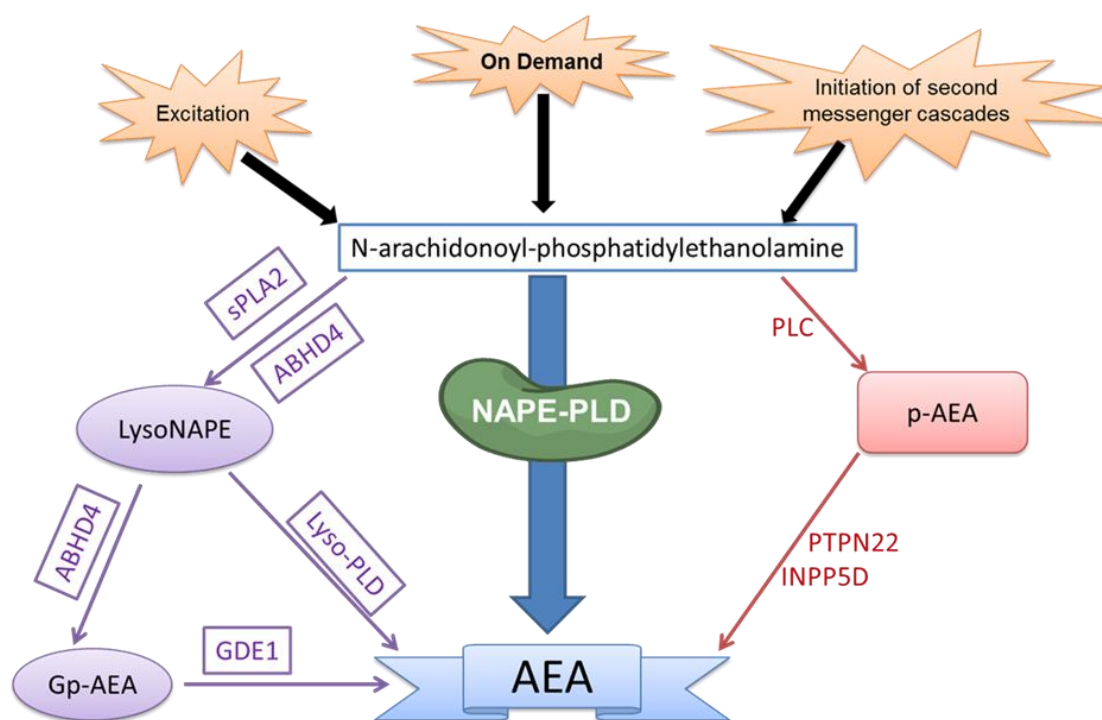


Figure 1-5: Pathways for the biosynthesis of the *N*-acylethanolamides (NAEs).

A schematic representation of the proposed pathways for the synthesis of the NAEs using AEA as the example. The thick blue arrow indicates the dominant pathway in most cells. The purple trail shows the sPLA2 pathway, which also includes ABHD4 and GDE1. The red trail shows the PLC pathway and the two enzymes that act in parallel, PTPN22 and INPP5D.

NAPE=*N*-acylphosphatidylethanolamines, NAPE-PLD=*N*-arachidonoylphosphatidylethanolamine - specific phospholipase D, PLC=phospholipase C, p-AEA=phospho-anandamide, PTPN22=protein tyrosine phosphatase non-receptor 22, INPP5D=phosphatidylinositol-3,4,5-trisphosphate 5-phosphatase 1, AEA=anandamide, sPLA2=secretory phospholipase A2, ABHD4= α/β serine hydrolase domain containing protein 4, LysoNAPE=lyso-*N*-acylphosphatidylethanolamine, Lyso-PLD=lyso-phospholipase D, GDE1=glycerophosphodiesterphosphodiesterase 1 and Gp-AEA=glycerophospho-arachidonoyl ethanolamide.

2-arachidonoylglycerol is synthesised from arachidonic acid-containing inositol phospholipids by the sequential actions of phospholipase C (PLC) and diacylglycerol lipases (DAGL) (Prescott et al. 1983). DAGL is an enzyme hydrolysing diacylglycerol (DAG) to yield 2-AG (Di Marzo 2008). When released from cells, 2-AG act in an autocrine or paracrine manner to stimulate signalling through interaction with various extracellular and intracellular receptor targets. **Figure 1-6** shows the pathway for the biosynthesis of 2-AG.

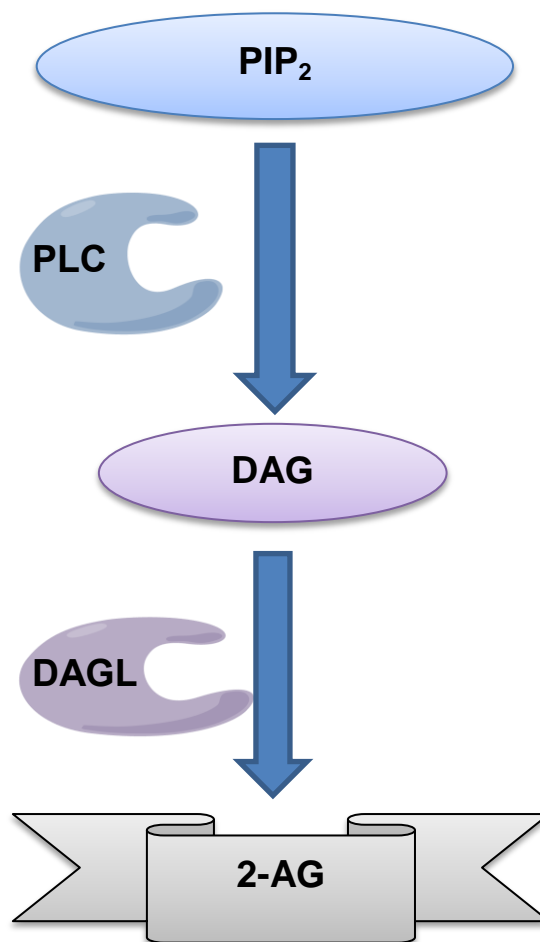


Figure 1-6: Biosynthesis pathway for 2-AG.

Phosphatidylinositol-4, 5-bisphosphate (PIP₂) is hydrolysed by phospholipase to form diacylglycerol (DAG). The DAG is then hydrolysed to 2-AG by diacylglycerol lipase (DAGL).

1.5.3 Degradation of AEA, OEA, PEA and 2-AG

Degradation of the NAEs is primarily through the actions of fatty acid amide hydrolase (FAAH), an intracellular integral membrane protein, belonging to the amidase family of enzymes. It catalyses the hydrolysis of *N*-acylethanolamides (AEA, OEA and PEA) into the respective fatty acids and ethanolamine (Cravatt et al. 1996, Giang et al. 1997). FAAH was the first enzyme identified in the hydrolysis process of NAEs and has been shown that in human lymphocytes, it is stimulated by progesterone (Maccarrone et al. 2001). FAAH was first cloned in 1996 and has been extensively studied because of its role in the regulation of NAEs, in both the CNS and the periphery and in carcinogenesis (Ahn et al. 2008, Petrosino et al. 2010, Hamtiaux et al. 2011).

Two isoforms of human FAAH, FAAH 1 and 2, have been described. AEA is predominantly metabolised to arachidonic acid and ethanolamine by FAAH-1 (Cravatt et al. 1996) and to a lesser extent by FAAH-2. FAAH-2 is found in humans, but not in rodent tissues. The two human FAAH enzymes have only limited sequence homology of around 20%. FAAH-2 is localised in cytosolic lipid droplets while FAAH-1 is found in the endoplasmic reticulum (Wei et al. 2006, Kaczocha et al. 2010).

A third NAE-hydrolysing enzyme, *N*-acylethanolamine-hydrolysing acid amidase (NAAA), is highly expressed in immune cells, specifically macrophages. It is localised in lysosomes and activated by autoproteolytic cleavage (Tsuboi et al. 2005, Tsuboi et al. 2007, Zhao et al. 2007). Studies have reported that the preferred substrate for NAAA may be PEA because of the high numbers of macrophage NAAA and PEA observed in inflammatory processes (Stella 2009).

It is generally accepted that FAAH is the principle contributor to NAE hydrolysis and the role of FAAH-2 and NAAA remains unresolved (Muccioli 2010). In addition, endocannabinoids may also undergo oxidative metabolism by a number of fatty acid oxygenases such as cytochrome P450 enzymes (CYP450) (Bornheim et al. 1993, Bornheim et al. 1995), lipoxygenases (LOX) (Edgemond et al. 1998, Kozak et al. 2002) and cyclooxygenase-2 (COX-2) (Yu et al. 1997, Kozak et al. 2000), (**Figure 1-7**).

2-AG is degraded through the action of the specific enzyme monoacylglycerol lipase (MAGL), and to a lesser extent, by FAAH (Goparaju et al. 1998, Ueda et al. 2000). MAGL converts 2-AG to arachidonic acid (AA) and glycerol as shown in **Figure 1-8** (Di Marzo et al. 1998, Goparaju et al. 1999).

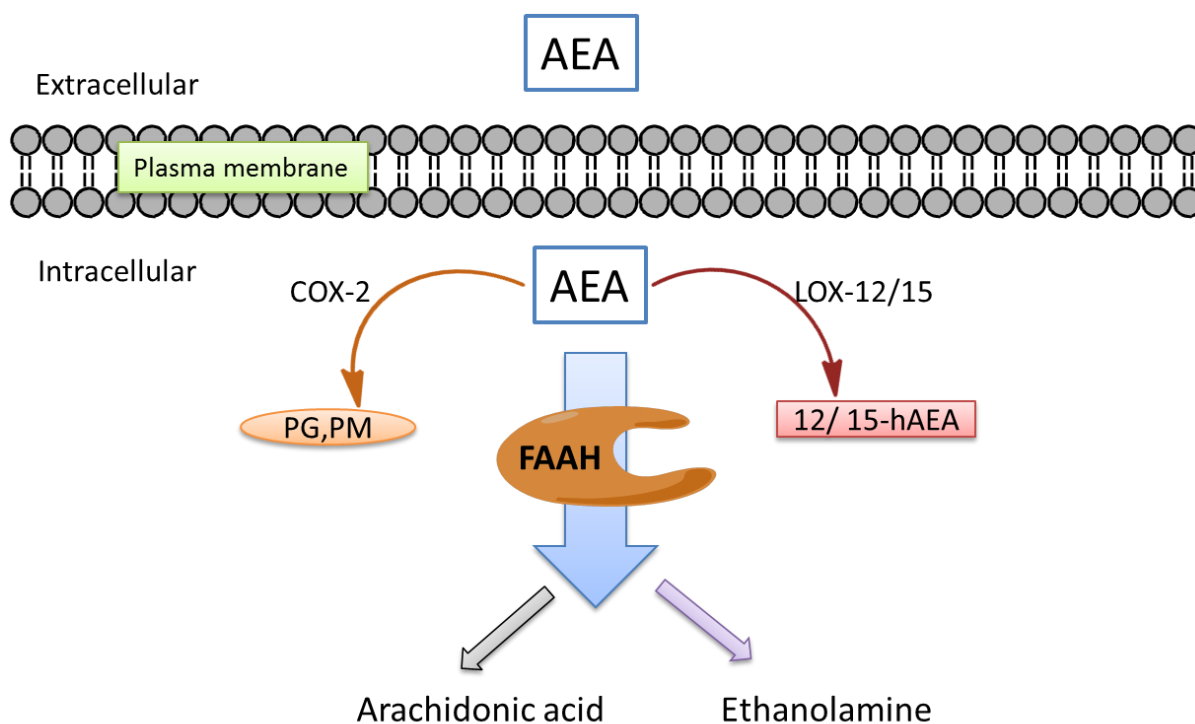


Figure 1-7: Schematic representations of the NAE degradation pathways.

The main route of AEA degradation is via hydrolysis by FAAH (shown by the thick light blue arrow). AEA=anandamide, FAAH=fatty acid amide hydrolase, COX-2=cyclooxygenase 2, PG=prostaglandins, PM=prostamides, LOX-12=arachidonate 12-lipoxygenase, LOX-15=arachidonate 15-lipoxygenase, and 12/15-hAEA=12/15-hydroxyanandamide.

1.5.4 Transport Mechanism for *N*-acylethanolamides

Endocannabinoids bind and activate receptors such as CB1 and CB2, resulting in various biological actions. Even though endocannabinoids are lipophilic in nature, they freely cross the cell membrane (Muccioli 2010). To facilitate endocannabinoid re-uptake and attenuate signalling, a diverse number of transport systems have been suggested. These include cellular endocytosis, passive diffusion, an anandamide membrane transporter' (AMT), facilitated diffusion, intracellular sequestration and movement around cells by intracellular transport proteins (McFarland et al. 2004, Kaczocha et al. 2009, Fowler 2013). None of this has, however, been proven (Maccarrone et al. 1998, Maccarrone et al. 2010).

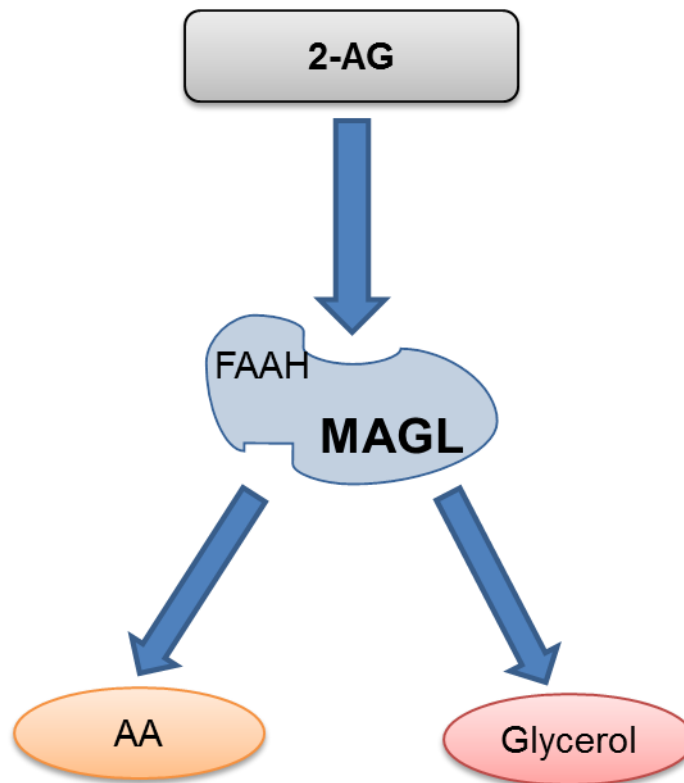


Figure 1-8: Schematic representation of the degradation of 2-AG.

2-AG is hydrolysed by FAAH and MAGL. As indicated by the size of the letters, MAGL is the major enzyme degrading 2-AG.

Several studies have been undertaken to identify and characterise some of these transport mechanisms in various cell models, both neuronal and non-neuronal in origin and have concluded for example that the AEA uptake is temperature-dependent, saturable and independent of energy in the form of ion gradients or ATP hydrolysis (Hillard et al. 1997, Maccarrone et al. 2000, Day et al. 2001, Hillard et al. 2003).

The most widely accepted mechanism for AEA transport/ uptake is via facilitated diffusion and this has been supported by a vast majority of research (Hillard et al. 2003, Fegley et al. 2004, Ligresti et al. 2004, McFarland et al. 2004, Ortega-Gutierrez et al. 2004). Extracellular AEA can cross the plasma membrane along the concentration gradient un-aided by any carrier proteins (Hillard et al. 2003).

1.6 Cannabinoid Receptors

Several receptors have been identified for endocannabinoids. These are the classical and non-classical cannabinoid type receptors as shown in **Figure 1-9**.

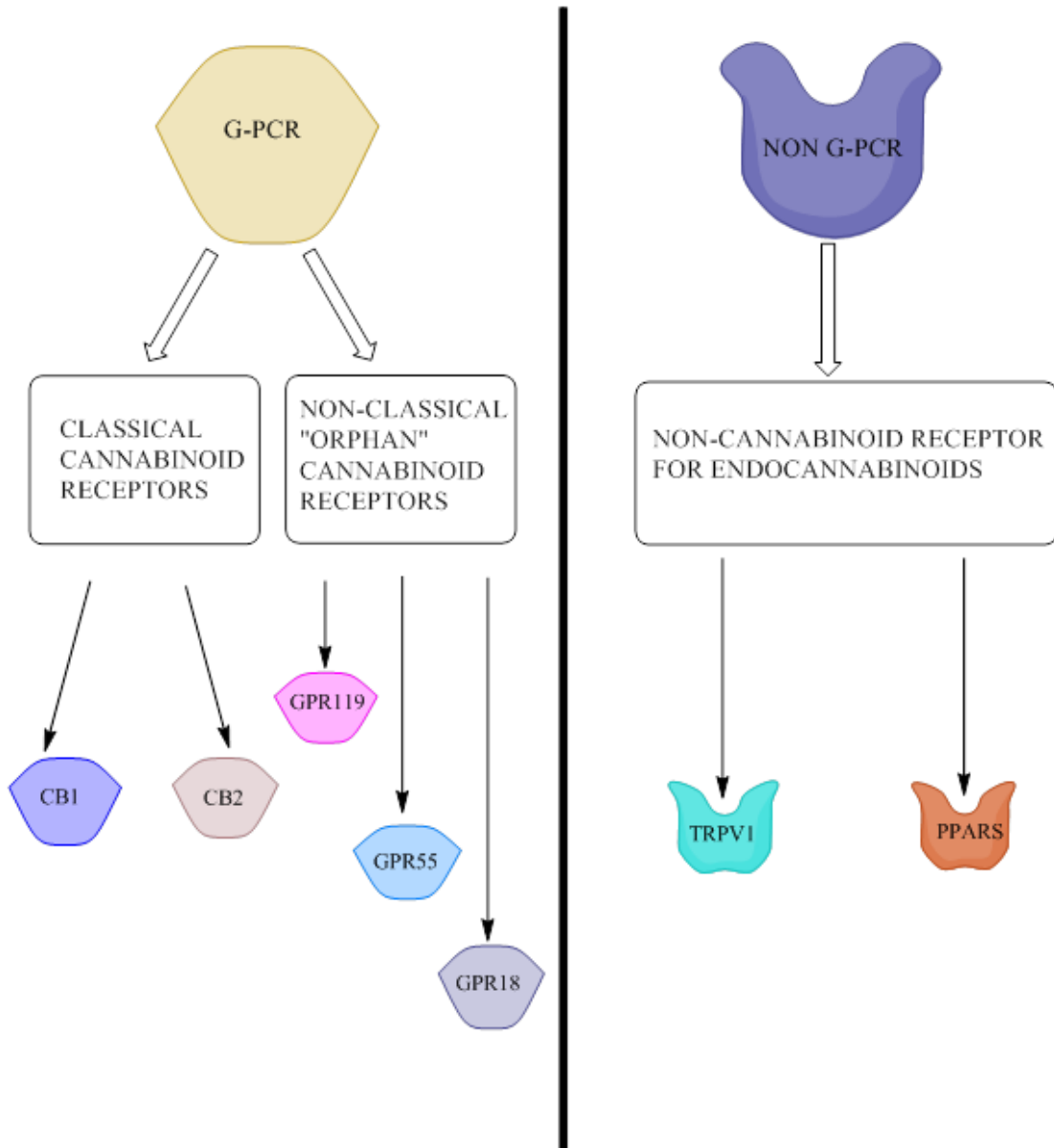


Figure 1-9: The cannabinoid and non – cannabinoid receptors.

The schematic representations of the classical cannabinoid receptors (CB1 and CB2), the non-classical orphan cannabinoid receptors-G protein coupled receptors (GPR-119, 18 and 55) and the non-cannabinoid receptor for endocannabinoids, which includes the transient receptor potential vanilloid 1 (TRPV1) and peroxisome proliferator-activated receptors (PPARS).

1.6.1 Classical Cannabinoid Receptors

The two subtypes of cannabinoid receptors belong to the Gi/o family of seven transmembrane G-protein-coupled receptors (GPCR). CB1, initially cloned from a rat cerebral cortex cDNA library (Matsuda et al. 1990), is also present in a variety of peripheral tissues at much lower levels, such as the cardiovascular, reproductive and gastro-intestinal systems (Mailleux et al. 1992, Glass et al. 1997, Pertwee 2001, Szabo et al. 2001, Wagner et al. 2001, Wang J 2008). The endocannabinoids that bind to CB1 are AEA (high affinity) and 2-AG (low affinity). In addition, *N*-arachidonoyl-dopamine (NADA) also activates CB1 (Reggio 2010).

CB2 or the splenic type receptor, first cloned from a human promyelocytic leukaemic cell HL60 cDNA library (Munro et al. 1993), is primarily expressed in immune and blood cells, although it has also been found in the brain (Gong et al. 2006, Pacher et al. 2006, Basavarajappa 2007). The CB2 receptor recognises the same structural endocannabinoid agonists as CB1 with differing affinities in some cases. It has been reported that CB2 has a higher affinity for 2-AG, and a low affinity for AEA (Song et al. 1999) and the human CB2 receptor exhibits 68% homology to human CB1 receptor within the transmembrane regions and 44% identity throughout the whole protein (Munro et al. 1993, Lutz 2002).

1.6.2 Non-classical Cannabinoid Receptors

Non-classical cannabinoid receptors can be broadly divided into orphan GPCRs or vanilloid type receptors. The first documented GPCR that binds cannabinoids is GPR55 and was originally isolated in 1999 as an orphan GPCR and documented to be highly expressed in human striatum (Sawzdargo et al. 1999). GPR55 is also known as the third endocannabinoid receptor (CB3) (McPartland et al. 2006) and has been reported to bind with endocannabinoids at an extracellular site (as per CB1 and CB2), but it shares a low amino acid identity with the classical CB1 (13.5%) and CB2 (14.4%) receptors (Sawzdargo et al. 1999, Maccarrone 2009). GPR55 has also been identified in the gut, spleen, breast adipose tissues, testis, ovary and adrenals (Sawzdargo et al. 1999, Ford et al. 2010, Pineiro et al. 2011), but very little is known about its physiological role in these or other tissues. Although AEA, 2-AG and PEA have the greatest affinity for GPR55 (Begg et al. 2005, Mackie et al. 2006), OEA also activates the receptor (Brown

2007). Recent studies suggest that lysophosphatidylinositol (LPI) may be the endogenous ligand for GPR55 (Oka et al. 2010). GPR55 has been implicated in the control of pain induced by an inflammatory process or neuropathic pain, and in the control of bone formation (Staton et al. 2008, Whyte et al. 2009). The transient vanilloid receptor (TRPV1) is a ligand-gated cation channel activated by various noxious stimuli including heat, acid, and vanilloid compounds such as capsaicin (Szallasi et al. 2007). TRPV1 is expressed in various tissues, such as, skin, fibroblast, liver, prostate and bladder smooth muscles (Messeguer et al. 2006), and it too binds NAEs.

1.6.3 Other Receptors

Other non-classical ‘orphan’ cannabinoid receptors include GPR119 and GPR18. GPR119 has the greatest affinity for OEA and has a more limited tissue distribution, being found predominantly in the pancreas and intestinal tissues (Godlewski et al. 2009). *N*-arachidonoyl glycine (NAGLy), an endogenous metabolite of AEA has been reported to be a GPR18 ligand (Kohno et al. 2006). Lately, the peroxisome proliferator-activated receptors (PPARs) have also been considered as receptors for endocannabinoid. PPARs have been shown to be stimulated by endocannabinoids under both physiological and pathological conditions and of interest is the fact that they have a higher affinity for OEA and PEA than the other endocannabinoids (Pistis et al. 2010). Whether this receptor is present in gynaecological cancers remains unknown.

1.7 The Endocannabinoid System and Cancer

1.7.1 Introduction

The anti-cancer activity of delta⁹-tetrahydrocannabinol (Δ^9 -THC) was first observed in early 1970s (Munson et al., 1975), but surprisingly these observations were not investigated in depth at that time. In contrast, the palliative effects of cannabinoids in cancer patients are well investigated, including appetite stimulation, inhibition of nausea and emesis associated with chemo- or radio-therapy, pain relief, mood elevation, and relief from insomnia (Hall et al., 2005, Walsh et al., 2003). Oral, Δ^9 -THC (Dronabinol, Marinol), and its synthetic derivative nabilone (Cesamet) have been approved by the U.S. Food and Drug Administration for the control of nausea in cancer patients particularly those undergoing chemotherapy (Hall et al., 2005). Studies in animals

found that long term administration of Δ^9 -THC possibly favours tumour growth. One study suggested that the growth of lung cancer was enhanced (Zhu et al. , 2000), whereas in a two year study of long term administration of high Δ^9 -THC doses, a reduction in the spontaneous onset of hormone-dependent tumours was reported (NIH publication, 1996).

1.7.2 Modes of Action of the Endocannabinoid System in Cancer

The role of the ECS in the modulation of tumourogenesis is currently thought to be via cannabinoid receptor-dependent and -independent mechanisms, as shown in **Figures 1-10 and 1-11**.

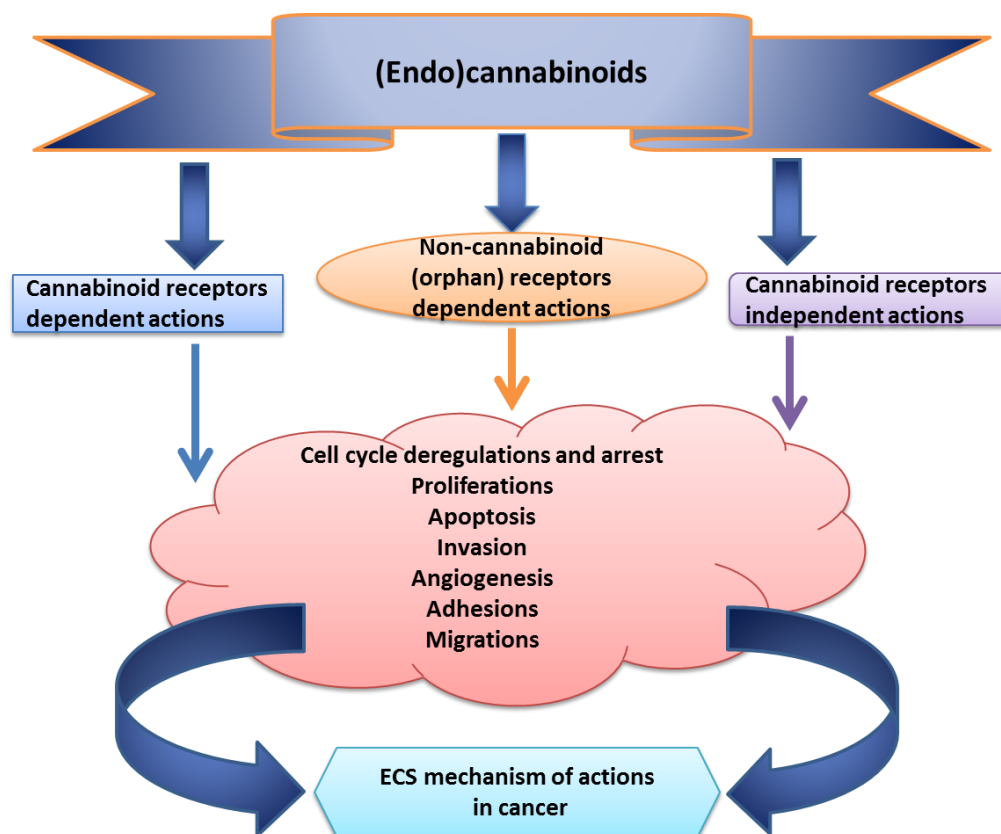


Figure 1-10: The potential mechanisms of actions of the endocannabinoid system in cancer.

The schematic illustrations describes the mechanism of actions of (endo)-cannabinoids via the cannabinoid and non-cannabinoid (orphan)-dependent; and the cannabinoid-independent receptor action. ECS affects all the hall-marks of cancer, such as the cell cycle deregulations, cell cycle arrest, proliferations, apoptosis, invasions, angiogenesis, cell adhesion and migration.

1.7.2.1 Cannabinoid Receptor Modes of Action

1.7.2.1.1 Transformation of Cell Cycle Regulation

AEA has been shown to arrest human MDA-MB-231 breast cancer cells in the S phase of the cell cycle primarily because of the loss in cyclin dependent kinase-2 (Cdk2) activity, up-regulation of cyclin-dependent kinase inhibitor 1 (p21^{waf1}) and a reduced formation of the active complex cyclin E/Cdk2 kinase (Laezza et al. 2006). In addition, AEA arrests cells in the S phase through cell cycle checkpoint kinase 1 (Chk1) activation and cell division cycle 25A (cCdc25A) proteolysis, which prevents Cdk2 activation by dephosphorylation on critical inhibitory residues phospho-cdc2(Thr14/Tyr15) (Laezza et al. 2006). In a CB2 receptor-dependent mechanism, Δ^9 -THC inhibits breast cancer cell proliferation by blocking the cell cycle at G2/M phase through the down-regulation of cyclin dependent protein kinase or cell division cycle protein 2 homolog (Cdc2) (Caffarel et al. 2006). Prostate cancer (LNCaP) cells when treated with WIN-55,212-2 (a CB1 agonist) arrest at the G0/G1 phase of the cell cycle and this arrest is sustained by the activation of extracellular signal-regulated kinase (ERK1/2), induction of cytoplasmic p27 (p27^{KIP1}) and inhibition of cyclin D (Sarfaraz et al. 2006).

1.7.2.1.2 Inhibition of Cancer Proliferation

The proliferation of various cancer cells can be inhibited by many different mechanisms, such as a decrease in the expression and/or activity of nerve growth factor, decrease in prolactin or vascular endothelial growth factor tyrosine kinase receptors (De Petrocellis et al. 1998, Melck et al. 2000, Portella et al. 2003) and a decrease in epidermal growth factor receptor (EGF-R) expression and/or attenuation of EGF-R tyrosine kinase activity (Mimeault et al. 2003) via the inhibition of adenylate cyclase activity and the cAMP/protein kinase A pathway (Melck et al. 1999). Breast cancer cell proliferation is inhibited by AEA via reduced expression of the prolactin receptor (Melck et al. 1999, Melck et al. 2000). A number of intraepithelial or invasive prostatic cancers exhibit evidence of increased expression of the EGF receptor (EGF-R), EGF and transforming growth factor α (TGF α) (Mimeault et al. 2003). Micromolar concentrations of AEA inhibit the EGF-induced proliferation of PC3, DU145 and

LNCaP prostate cancer cells through G1 arrest and down regulation of EGF-R expression. These effects are mediated via CB1 receptors (Mimeault et al. 2003).

1.7.2.1.3 Induction of Apoptosis

BAD, a pro-apoptotic member of the Bcl-2 family of signalling molecules is hypothesized to play a role in endocannabinoid-dependent apoptosis (Ellert-Miklaszewska et al. 2005). These pro-apoptotic effects may also depend on a CB1-independent stimulation of sphingomyelin breakdown (Sanchez et al. 1998). In leukaemia and lymphoma cell lines, CB agonists, such as WIN-55,212-2 and Δ^9 -THC, induce CB-dependent apoptosis via ceramide accumulation and caspase stimulation through the p38-MAPK signalling pathway, down regulation of the RAF1/MAPK pathway and translocation of BAD to mitochondria (Jia et al. 2006); depolarization of mitochondria via cytochrome c release is a common event in endocannabinoid-induced apoptosis (Jia et al. 2006). CB agonist-induced colon cancer cell death is via TNF α -stimulated ceramide synthesis; therefore, TNF α may act as a linkage between endocannabinoid receptor activation and ceramide production (Cianchi et al. 2008). It has been shown that prolonged AEA incubation (5-6 days), induces massive apoptosis in DU145 and PC3 prostate cancer cells and this was also mediated through CB1/2 via cellular ceramide accumulation, but noted to be absent in LNCaP cells (Mimeault et al. 2003).

1.7.2.1.4 Cancer Cell Invasion

Several studies have evaluated the effects of endocannabinoids on cancer cell invasion and the signalling pathways involved, such as inhibition of the endogenous tissue inhibitor of metalloproteinase TIMP-1 (Ramer et al. 2008), inhibition of FAK/Src signalling (Grimaldi et al. 2006) and inhibition of matrix metalloproteinase-2 (MMP-2) expression (Blazquez et al. 2008). In relation to the matrix metalloproteinase (MMP) system, endocannabinoids have a direct inhibitory effect that plays a key role in their anti-invasive action. MMP-2 and MMP-9 promote cancer invasion by proteolytic degradation of major basement membrane components, such as laminin, collagen and nidogens (Curran et al. 2000). Extracellular matrix components (ECM) are important in cancer angiogenesis, invasion and metastasis (Stamenkovic 2000). MMP proteolytic activity is inhibited by the tissue inhibitor of metalloproteinase (TIMP). In lung cancer cells, inhibition of invasion by AEA and Δ^9 -THC depends on the induction of TIMP-1

expression (Ramer et al. 2008). In addition, Δ^9 -THC inhibits MMP-2 expression and cell invasion in glioma cells (Blazquez et al. 2008). Down regulation of MMP-2 plays a vital role in Δ^9 -THC-mediated inhibition of cancer cell invasion (Blazquez et al. 2008). Studies in androgen-independent prostate cancer cell lines (PC3 and DU145) show that endogenous 2-AG and CB1 agonists reduced invasion through the CB1-dependent inhibition of adenylate cyclase, decreasing phosphokinase A activity (Nithipatikom et al. 2004).

1.7.2.1.5 *Inhibition of Cancer Angiogenesis*

Angiogenesis is the formation of new blood vessels. Endocannabinoids can inhibit tumour growth by reducing angiogenesis, by decreasing the production of pro-angiogenic factors and/or by direct modulation of vascular endothelial cells (Freimuth et al. 2010). The pro-angiogenic growth factor, vascular endothelial growth factor (VEGF) and its receptor VEGFR-1 are major cancer cell-released chemo-attractants in angiogenesis and several studies have reported that endocannabinoids can modulate the expression of VEGF and VEGFR-1 (Saia G 2007). Indeed, endocannabinoids inhibit angiogenesis in thyroid cancer by decreasing the levels of VEGF and VEGFR-1 (Portella et al. 2003). In addition, intra-tumoural administration of Δ^9 -THC to glioblastoma patients decreased both VEGF and VEGFR-2 expression (Blazquez et al. 2004). Endocannabinoid treatment of glioma inhibits the expression of VEGF, angiopoietin-2, matrix metalloproteinase-2 (MMP-2) and hypoxia-inducible factor-1 α (HIF-1 α), which is the major factor responsible for VEGF expression (Blazquez et al. 2004).

1.7.2.1.6 *Cancer Cell Adhesion*

Matrix proteins, such as cell adhesion molecules of the immunoglobulin superfamily (IgSF CAMs), integrins, selectins and cadherins, are integral to the adhesive property of cells to the extracellular matrix (ECM). Changes to the adhesive properties of cancer cells and their interactions with the surrounding microstructures play a vital role in cancer growth, invasion, migration and metastases. Studies of endocannabinoids have reported that they have various effects on the adhesion of cancer cells to the ECM. AEA inhibits adhesion of the highly invasive MDA-MB-231 and TSA-E1 metastatic breast cancer cell lines on type IV collagen, the major component of the basement membrane (Grimaldi et al. 2006) and of SW480 colon cancer cells via the stimulation of

endocannabinoid receptors (CB1) (Joseph et al. 2004). AEA has no effect on adhesion of these cancer cells to fibronectin and laminin (Grimaldi et al. 2006), but decreases the affinity of integrins to collagen via the suppression of the pro-oncogenic tyrosine kinase, c-Src and by the phosphorylation of focal adhesion kinase (FAK) (Grimaldi et al. 2006).

1.7.2.1.7 Cancer Cell Migration

The endocannabinoid system has shown to directly regulate cancer cell migration; in the scratch wound healing assay, cancer cell migration is reduced by 2-AG and WIN-55,212-2 in a CB1 receptor-dependent manner (Grimaldi et al. 2006). Migration of the highly invasive metastatic breast cancer cell lines MDA-MB-231 and TSA-E1 is inhibited by AEA on type IV collagen (Grimaldi et al. 2006). In SW480 colon carcinoma cells, AEA inhibited migration via activation of CB1 receptors (Joseph et al. 2004). Inhibition of migration of lung cancer cells was reported for both AEA and Δ^9 -THC (Ramer et al. 2008).

1.7.2.2 Cannabinoid Receptor-independent Modes of Action

In addition to the effects mediated via the endocannabinoid receptors, endocannabinoids, in particular AEA and cannabidiol, are known to have CB-receptor-independent effects (Begg et al. 2005). AEA, for example, induces both neuroblastoma and lymphoma cell death via vanilloid receptor-mediated mechanisms (Maccarrone et al. 2000), whilst methanandamide inhibits cancer cell invasion through TIMP-1 degradation, which is mediated via TRPV1 activation (Ramer et al. 2008). It is proposed that lipid rafts rich in sphingolipids and cholesterol, mediate AEA effects via CB1 signalling (Bari et al. 2005). Indeed, lipid raft stabilization, ceramide accumulation, recruitment of FAS and FAS ligand into lipid rafts, facilitate the anti-proliferative and pro-apoptotic action of AEA, in cholangiocarcinoma (DeMorrow et al. 2007). COX-2, another important cellular protein in CB-receptor-independent cell death induced by endocannabinoids, can metabolize the conversion of arachidonic acid to prostaglandins (PG) and in neoplastic tissues elevated levels of both COX-2 and PG have been reported. Cannabidiol, a cannabinoid with no activity on CB1 or CB2 receptors and thus lacking psychotropic effects has been reported to inhibit glioma and breast tumour growth *in vitro* and *in vivo* through the induction of apoptosis and the inhibition of angiogenesis and cell migration. These effects of cannabidiol are

independent of both CB and TRPV1 receptor activation (Vaccani et al. 2005, Ligresti et al. 2006), but since some cannabinoids, including cannabidiol, interfere with the ability of lysophosphatidylinositol (LPI) to bind to GPR55, this cannabidiol or the CB1 receptor antagonist, rimonabant, probably prevents LPI-induced cell proliferation via GPR55 (Pineiro et al. 2011).

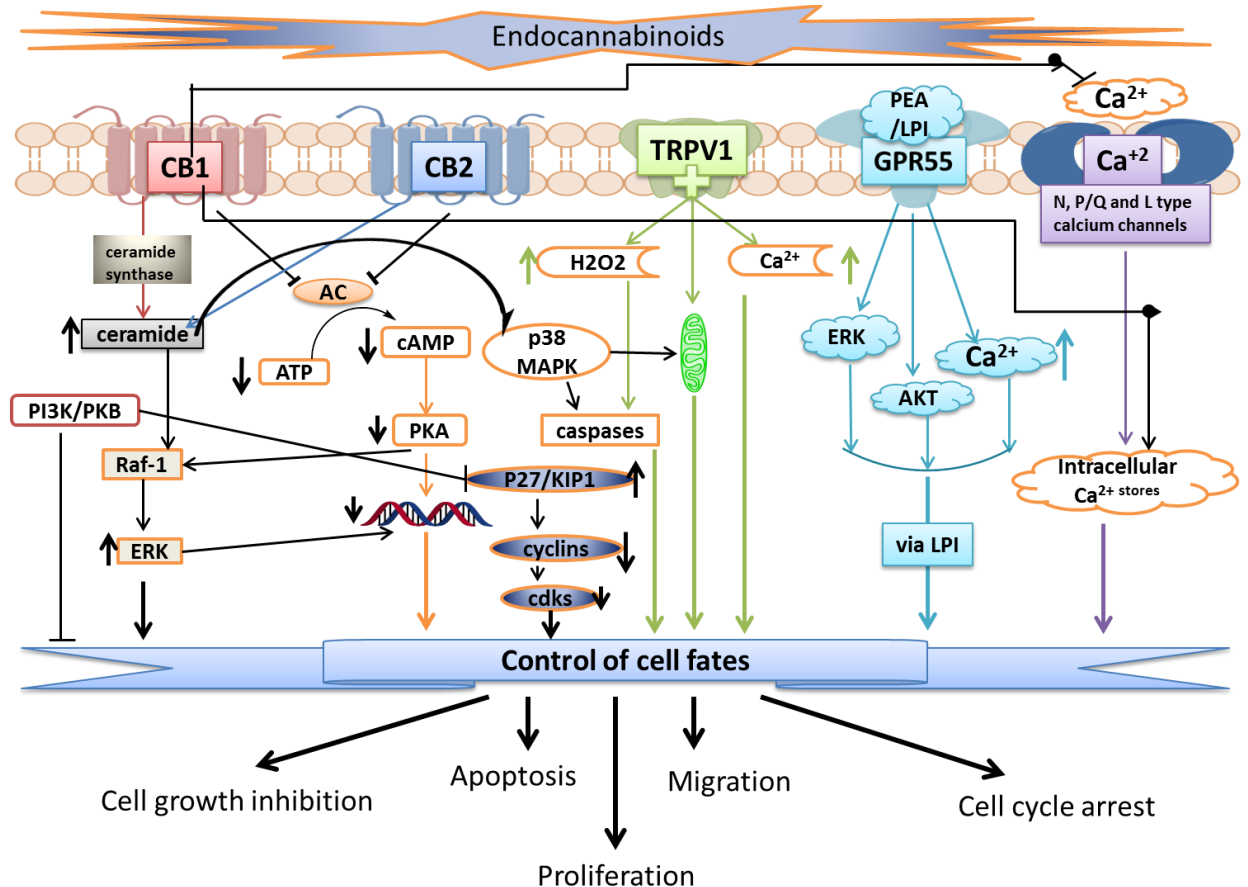


Figure 1-11: Schematic models of different signalling pathways through which endocannabinoids exert their receptor-mediated effects.

The endocannabinoid and non-endocannabinoid mediated signalling pathways acting on the receptors, such as, CB1, CB2, TRPV1 and GPR55 are shown together with activated via calcium channels. Activation of these results in numerous events that have effects on the control of the cell fates, which include, inhibition of cell growth, apoptosis, proliferation, migration and cell cycle arrest. AC=adenylyl cyclase; AKT=protein kinase B; ATP=adenosine triphosphate; cAMP=cyclic adenosine monophosphate; CB1=cannabinoid receptor 1; CB2=cannabinoid receptor 2; cdk2=cyclin-dependent kinases; GPR55=G protein-coupled receptor 55; H₂O₂=hydrogen peroxide, PKA=protein kinase A; p27/KIP1=cyclin kinase inhibitor; p21 ras=p21 ras protein; PI3K=phosphatidylinositol 3 kinase; Raf-1=protein Raf-1; TRPV1=temporary receptor potential cation channel V1; LPI=ligand lysophosphatidylinositol and Ca⁺²=calcium ion.

1.8 The Endocannabinoid System and Endometrial Cancer

The expression of endocannabinoid receptors in different endometrial cancer (EC) tissues/cell lines has been described, with CB2 selectively expressed, with a very weak expression in healthy cells in the same biopsies (Guida et al. 2010). Immunoblotting analysis showed that CB2 protein expression was significantly elevated in the EC when compared to healthy endometrial tissues (Guida et al. 2010) and no significant differences were noted in CB1 expression (Guida et al. 2010). Mass spectrometry in that study showed an increase in 2-AG in EC (n=18) compared to healthy tissues (n=16), with no significant increase in AEA or PEA levels (Guida et al. 2010). Similarly, immunoblotting revealed a selective down-regulation of MAGL expression in EC compared with healthy tissue and no significant difference in FAAH protein expression (Guida et al. 2010). Furthermore, CB2 receptor regulation was dysregulated in EC, because CB2 levels were significantly higher in the AN3CA human endometrial carcinoma cell line compared to control cells when transfected with a plasmid containing the cDNA for the endocannabinoid receptor CB2 (Guida et al. 2010). It has been postulated from these data that CB2 receptors may perhaps play a role in the growth of EC (Guzman et al. 2002).

The authors suggest that the elevation in CB2 receptor expression and higher 2-AG concentrations found in EC tissues may be due to an underlying imbalance in the estrogen/progesterone ratio, which is one of the aetiological factors for the development of EC (Guida et al. 2010). This is, however; only speculative as there is no evidence yet to support this proposition. What is known is that in transfected AN3CA cells (transfected with a plasmid containing the cDNA for the endocannabinoid receptor CB2), CB2 caused a 40% reduction in cell mitochondrial function when compared with controls (Guzman et al. 2002). This effect was not improved by addition of the CB2 receptor agonist, JWH133, but was fully prevented by the CB2 receptor antagonist SR144528.

It would seem from the literature review above that the ECS is likely to be involved not only in the aetiopathogenesis of EC but may also be involved in its progression. A better understanding of the precise role it plays in this cancer could potentially allow for the development of novel therapeutic interventions or diagnostic tools.

1.9 Hypothesis

The presence of the ECS in the endometrium, has led to speculation that the ECS may be involved in the development of endometrial carcinoma. Based on this, it was postulated that there would be an aberrant expression of the ECS in patients' endometrial cancer when compared to controls. This would be demonstrated by changes in the levels of ECS ligands in cancer patients both in the blood and tissue. These changes would be related to the proliferative and apoptotic activities of endometrial cells. Dysregulation of the ECS in the plasma and endometrial tissues may be responsible for the aetiopathogenesis of endometrial carcinoma.

1.9.1 Aims

The first aim was to measure plasma and tissues NAEs and determines the relationship between these. These data are shown in **chapter 2**. The second aim was to measure the activity, expression and location of endocannabinoid regulating enzymes FAAH and NAPE-PLD. These data are shown in **chapter 3**. The third aim was to determine the expression and location of the classical and non-classical endocannabinoid receptors in endometrial cancer. These data are shown in **chapter 4**. The fourth aim was to model the effect of endocannabinoids/endovanilloids on endometrial carcinoma cell growth and survival *in-vitro*. These data are shown in **chapter 5**. The final aim was to determine whether cellular apoptosis or proliferation in endometrial cancer is affected by the ECS.

1.9.2 Objectives

The hypothesis was tested in experiments designed to (a) determine the relationship between the plasma and endometrial tissues levels of AEA, OEA and PEA and the pattern of the ECS expression in the endometrial cancer patients and the control (atrophic) group and (b) to determine the functional response of an endometrial cancer cell line to in-vitro exposure to AEA, OEA, PEA and capsaicin and (c) evaluate the relationship between proliferative and apoptotic markers in endometrial cancer in relation to ECS. These objectives were studied using a cohort of postmenopausal women, as summarised in **Figure 1-12**. The histological diagnosis of the uteri studied were atrophic, type 1 EC (grade 1, 2 and 3) and type 2 EC (serous and carcinosarcoma).

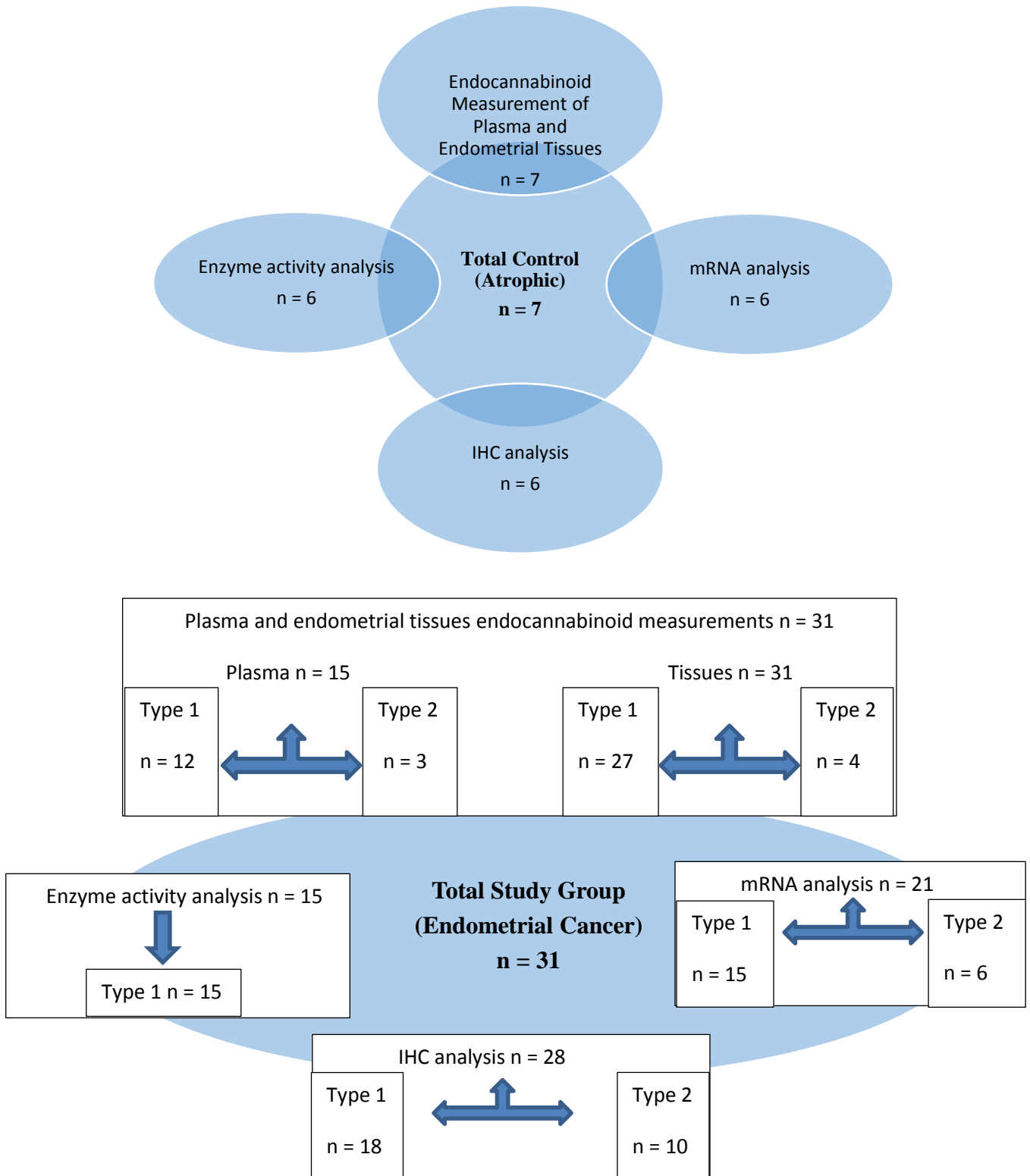


Figure 1-12: Schematic representation of the patient cohort used in these studies and the numbers used in the different analyses used to test the objectives.

All the above patients were postmenopausal. The upper panel shows the controls (atrophic) and the lower panel shows the study group (endometrial cancer). Each box describes the total number of individual within each of the studies.



Chapter 2

Relationship Between Tissue and Plasma *N*-Acylethanolamine Concentrations in Endometrial Carcinoma

2.1 Introduction

N-acylethanolamides (NAEs) are a family of naturally occurring signalling lipids and consist of several and structurally-related lipids of which AEA is the prototypical molecule. NAEs are produced by enzymatic degradation of *N* – acyl-phosphatidylethanolamines (NAPEs) through a pathway involving a specific membrane-associated phospholipase D enzyme called *N*-acylphosphatidylethanolamine specific phospholipase D (NAPE-PLD) (Schmid 2000, Okamoto et al. 2004) . The primary products of this enzyme are *N*-arachidonoylethanolamide (AEA), *N*-oleoylethanolamide (OEA) and *N*-palmitoylethanolamide (PEA), which are all enzymatically released from membrane phospholipid precursors into the extracellular environment when the cells are stimulated by hormones, neurotransmitters and several membrane-depolarising agents (Berdyshev 2000, De Petrocellis et al. 2000, Stella et al. 2001). Upon release, NAEs activate molecular targets and are then subsequently inactivated following cellular re-uptake (McFarland et al. 2004). Diverse transport systems have been proposed for NAEs, including endocytosis, passive and active diffusion and a specific carrier protein (McFarland et al. 2004). Once inside the cell, the NAEs are thought to be trafficked by an intracellular fatty acid amide hydrolase (FAAH)-like protein (FLAT-1) that is catalytically silent and delivers it to FAAH-2 on microsomal membranes (Fu et al. 2012), where they are rapidly metabolised into free fatty acids and ethanolamine (McKinney et al. 2005). In addition, although PEA is hydrolysed by FAAH, it is preferentially metabolised by the cysteine amidase *N*-acylethanolamine-hydrolysing acid amidase (NAA) (Solorzano et al. 2009, Saturnino et al. 2010). Endocannabinoids may also undergo oxidative metabolism by a different number of fatty acid oxygenases, such as cytochrome P450 enzymes (CYP450) (Bornheim et al. 1993, Bornheim et al. 1995), lipoxygenases (LOX) (Edgmond et al. 1998, Kozak et al. 2002) and cyclooxygenase-2 (COX-2) (Yu et al. 1997, Kozak et al. 2000). NAEs in peripheral and neuronal tissues have been shown to function as paracrine or autocrine mediators, involved in various physiological functions and pathological conditions, including cancer. Such functions include cell proliferation, differentiation, apoptosis, inhibition of cancer cell growth (occurring mainly through their anti-proliferative and cell cycle inhibition effects) (De Petrocellis et al. 1998, De Petrocellis et al. 2000, Galve-Roperh et al. 2000, Bifulco et al. 2008).

A recent pilot investigation on Italian women found that biopsies of endometrial carcinoma contained 2-arachidonoylglycerol (2-AG), AEA and PEA with the levels of 2-AG significantly higher in tumours compared with age-matched controls (Guida et al. 2010). 2-AG has been less widely investigated compared to AEA (Rouzer et al. 2002, Buczynski et al. 2010), but it is known to be synthesised from diacylglycerol by the sequential actions of phospholipase C and two calcium sensitive *sn*-2-selective diacylglycerol lipases (α and β DAGL) (Prescott et al. 1983). It is also catabolised by FAAH to a lesser extent, whereas the enzyme monoacylglycerol lipase (MAGL) is the enzyme predominantly involved in 2-AG degradation (Di Marzo et al. 1998, Goparaju et al. 1999). The other endocannabinoids *N*-oleoylethanolamide (OEA) and *N*-palmitoylethanolamide (PEA), also known as cannabinoid-receptor inactive molecules (Annuzzi et al. 2010, Naccarato et al. 2010), have a low affinities for the cannabinoid receptors CB1 and CB2, and are known to have an ‘entourage effect’ on endocannabinoid potency; by inhibiting the degradation of AEA through competing for FAAH and MAGL (Katayama et al. 1997, Ben-Shabat et al. 1998). The entourage endocannabinoids are also known to potentiate AEA actions at TRPV1 receptors (Lambert et al. 2005). There is increasing evidence that OEA and PEA themselves can activate other receptors that are potential targets of endocannabinoids, such as TRPV1 (Ho et al. 2008, Hansen 2010) or PPARs (Hansen 2010). Our group has established and validated a reliable method for the quantification of endocannabinoids in plasma and tissues using ultra-high-performance liquid chromatography-tandem mass spectrometry (UHPLC-MS/MS) (Lam et al. 2008, Marczylo et al. 2009, Marczylo et al. 2010), which was used for the experiments described in this Chapter.

2.2 Hypothesis

N-acylethanolamides (NAEs), such as anandamide (AEA), *N*-oleoylethanolamide (OEA) and *N*-palmitoylethanolamide (PEA) will be present and quantifiable in plasma and tissue (endometrial cancers and normal atrophic endometrium) from volunteers and that there will be differences between the levels found in cancer and normal patients. These differences will be detectable both in the plasma and tissue (cancerous and non-cancerous endometrium).

2.3 Questions to Address the Hypothesis

1. What are the plasma concentrations of *N*-acylethanolamides (NAEs) in postmenopausal women and endometrial cancer patients using the UHPLC-MS/MS method?
2. What are the tissue levels of the NAEs in atrophic endometrium and endometrial cancer tissue using the UHPLC-MS/MS method?
3. What are the relationships between plasma and tissue endocannabinoid levels in women with endometrial cancer and in normal controls?
4. How useful are these NAEs for diagnosis of endometrial cancer?

2.4 Subjects

Inclusion criteria were postmenopausal women undergoing a hysterectomy and bilateral salpingoophorectomy for either endometrial carcinomas (study group) or benign gynaecological condition, uterine prolapse (control group). They all gave written informed consent to take part in the study, which was approved and conducted according to the guidelines of Leicestershire and Rutland Research Ethics Committee (reference number 06/Q2501/49).

Exclusion criteria were those with concurrent or previous hormonal treatment, (such as hormone replacement therapy or the levonorgestrel intrauterine system) or currently on prescription or recreational drugs. Women with chronic medical conditions or any other type of cancer were also excluded. In this thesis, a pure patient group were studied to evaluate the direct effect of endocannabinoid system in EC.

Volunteers with EC diagnosis were divided into type and grade of cancer, according to the FIGO system (Pecorelli 2009). In the study group, a total of 31 endometrial carcinomas patients volunteered for endometrial cancerous tissues for evaluation: 27 were type 1 endometrioid adenocarcinoma and 4 were type 2 (serous 2, carcinosarcoma 1 and clear cell carcinoma 1). Among patients with type 1 EC, (12 had grade 1, 11 had grade 2, and 4 had grade 3 disease). From this total, 31 EC patients (study group), 15 patients volunteered for plasma sample. In control atrophic group, there were 7 patients in total and all volunteered for plasma and atrophic endometrial tissues.

2.5 Methods

2.5.1 Chemicals, Reagents and Solutions

All the chemicals, reagents and solutions used for UHPLC-MS/MS, were of HPLC or research grade. HPLC grade water was obtained using a water purification system from (Maxima ELGA, High Wycombe, UK). Oasis HLB solid phase extraction (SPE) cartridges (1cc, 30mg) were obtained from (Waters UK Ltd, Elstree, UK). Acetonitrile, chloroform, ammonium acetate, formic acid and methanol were all obtained from Fisher Scientific (Loughborough, UK). AEA, OEA and PEA and their deuterated equivalents (AEA-d8, OEA-d2 and PEA-d4) were all obtained from Cayman Chemicals (Ann Arbor, MI, USA).

2.5.2 Blood Collection

Whole venous blood samples were collected into evacuated tubes containing EDTA (Sarstedt, Leicester, United Kingdom) and centrifuged within 60 minutes of collection at 1200 x g for 30 minutes at 4°C and plasma carefully transferred into 7 mL Kimble scintillation vials (Kinesis, St. Neots, Cambridgeshire, U K). These plasma samples were then stored as 2 ml aliquots at – 80°C prior to lipid extraction.

2.5.3 Endometrial Tissue Collection

As soon as the uterus was removed at hysterectomy, it was immediately transported on ice to the Histopathology Department where the endometrial biopsies from the hysterectomies were obtained and a consultant gynaecology histopathologist divided the endometrial biopsies into two; one for this study and the other for histological confirmation of diagnosis. The endometrial biopsies (cancer and normal tissue) were washed with phosphate buffered saline (PBS) to remove excess blood and immediately placed into sterile polypropylene tubes. These were immediately transported to the laboratory in liquid nitrogen and stored at -80°C until processing for endocannabinoid measurement.

2.5.4 Quantification of Endocannabinoids by UHPLC

The methods used to extract and quantify endocannabinoids in plasma and tissue specimens were those developed and validated by Dr. Timothy Marczylo and Dr. Patricia Lam, Reproductive Sciences Section, Department of Cancer Studies and Molecular Medicine, University of Leicester. The UHPLC-ESI-MS/MS method was validated according to FDA guidelines as described (Lam et al. 2008, Marczylo et al. 2009, Lam et al. 2010).

2.5.4.1 Preparation of Standards and Calibration Curves

AEA was diluted in acetonitrile to make a stock of 5 mg/ml. AEA-d8 stock solutions were prepared by drying the supplied stocks under nitrogen and reconstituting in acetonitrile (100 µg/ml). OEA and PEA were purchased as solids and were dissolved in ethanol at 10 mg/ml and 2.5 mg/ml, respectively. OEA-d2 (1 µg/ml) and PEA-d4 (1 µg/ml) were all purchased as ethanol stocks. All the purchased and prepared stocks were stored at -20°C until used. Further dilutions were made in ice cold acetonitrile, on ice, on the day of analysis. Seven point calibration curves were prepared in triplicate prior to each experiment using serial dilutions of AEA, OEA (0.25-20 nM) and PEA (1-38 nM) in acetonitrile as shown in **Table 2-1**. These standards were spiked with 2.5 pmol/ml of deuterated standard. Standards were then thoroughly vortexed and analysed via UHPLC-ESI-MS/MS. The internal standards were prepared as follows:

- 1 in 25 dilution: 20 µl 6.272 pmol/µl AEA-d8 + 20 µl 6.6272 pmol/µl OEA-d2 + 20 µl 6.6272 pmol/µl PEA-d4 + 440 µl ACN = 500 µl 0.25 pmol/µl AEA-d8, OEA-d2 and PEA-d4 (used as internal standards in the calibration curves).
- 1 in 100 dilution: 10 µl 6.272 pmol/µl AEA-d8 + 10 µl 6.6272 pmol/µl OEA-d2 + 20 µl 6.6272 pmol/µl PEA-d4 + 960 µl ACN = 1000 µl 0.06272 pmol/µl AEA-d8, OEA-d2 and 0.125 pmol/µl PEA-d4 (used as the internal standard for samples).

Table 2-1: Serial dilutions of stock solutions of internal standards of AEA, OEA and PEA.

	AEA and OEA	PEA	Serial Dilutions
A	1 μ M	4 μ M	200 μ l MM + 200 μ l ACN
B	100nM	400nM	100 μ l of A + 900 μ l ACN
C	20nM	80nM	200 μ l of B + 800 μ l ACN
D	10nM	40nM	500 μ l of C + 500 μ l ACN
E	5nM	20nM	500 μ l of D + 500 μ l ACN
F	2nM	8nM	400 μ l of E + 600 μ l ACN
G	1nM	4nM	500 μ l of F + 500 μ l ACN
H	0.5nM	2nM	500 μ l of G + 500 μ l ACN
I	0.25nM	1nM	500 μ l of H + 500 μ l ACN

2.5.4.2 Extraction of Endocannabinoids from Plasma

Endocannabinoid extraction and purification was undertaken using a solid-phase method for plasma as described (Lam et al. 2008, Marczylo et al. 2009). Deuterated internal standard AEA-d8 (2.5 pmol/ml plasma), OEA-d2 (2.5 pmol/ml) and PEA-d4 (5 pmol/ml) was added to plasma (0.5 ml) and then diluted to 1 ml with deionized water. Samples were vortex mixed for 10-20 seconds and transferred to preconditioned Oasis HLB 1 ml cartridges (Water Ltd., Elstree, United Kingdom) for extraction of endocannabinoids. The Oasis HLB 1 ml cartridges were preconditioned and equilibrated using 1 ml of methanol and 1 ml of distilled water via a vacuum manifold (Waters, Elstree, UK). Diluted samples were introduced onto the cartridges and drawn under gentle vacuum at a flow rate of approximately ~1 ml/min. The cartridges were washed with 1 ml of 40% aqueous methanol and AEA, OEA and PEA eluted in 1 ml of acetonitrile. The eluent was dried under a gentle stream of nitrogen, reconstituted in 80 μ l of acetonitrile and transferred to a clean UHPLC sample vial for UHPLC-ESI-MS/MS analysis (Lam et al. 2008, Marczylo et al. 2009). For each volunteer, 2 x 0.5 ml aliquots of plasma were processed by solid-phase extraction analysed in triplicate.

2.5.4.3 Extraction of Endocannabinoids from Endometrial Tissue

A modification to the method described by Marczylo *et al* (Marczylo et al. 2010) was used. Briefly, endometrial tissues (approximately 100 mg) were combined with internal standard (AEA-d8 (12.5 pmol/g) OEA-d2 (12.5 pmol/g), and PEA-d4 (25pmol/g), all from Cayman Chemical, Ann Arbor, MI, USA) and 1 ml phosphoric acid (5%) added. To this mixture 1 ml of deionized water was added and the tissue homogenized using a Tissue Ruptor (Qiagen Crawley, UK). The samples were then centrifuged at 1500 x g for 30 min at 4°C. One ml of the supernatant was transferred carefully to a preconditioned cartridge as described in section 2.5.4.2 and drawn under a gentle vacuum at a flow rate of ~1 ml/min. The cartridges were washed and endocannabinoids were eluted into acetonitrile and dried under a constant stream of nitrogen before being reconstituted in 80 µl of acetonitrile as described in **section 2.5.4.2**. Each endometrial sample was homogenised in duplicate and quantified in triplicate using the UHPLC-MS/MS (Lam et al. 2008, Marczylo et al. 2009, Marczylo et al. 2010).

2.5.4.4 Measurement of *N*-acylethanolamides

Quantification of AEA, OEA, PEA and their deuterated equivalents was performed using a UHPLC ESI-MS/MS system comprising an Acquity UHPLC in line with a Quattro Premier tandem mass spectrometer (Waters Corp, USA). Separation was accomplished with an Acquity UHPLC BEH C18 column (2.1 x 50 mm) maintained at 40°C. Mobile phases consisted of A (2 mM ammonium acetate containing 5% acetonitrile and 0.1% formic acid) and B (acetonitrile containing 0.1% formic acid). Gradient conditions were as follows: 0 – 0.5 min, 80% A; 1.5 min, 0% A; 2.5 min, 80% A and then re-equilibrated at 80% A until 4 min. Samples were kept at 4°C throughout. Quantification of analytes was achieved using tandem electrospray mass spectrometry in positive ion mode (ES⁺). Source parameters included a capillary voltage of 1 kV, a cone voltage of 21 V, source temperature of 120°C, desolvation temperature of 440°C, cone gas flow of 50 L/h and desolvation gas flow of 800 L/h. MS/MS conditions for monitoring each precursor [M+H]⁺ ion comprised entry, collision and exit energies of 6, 16 and 2eV respectively.

Daughter products were monitored in multiple reactions monitoring mode. Transitions employed were as follows: AEA (*m/z* 348.25>61.9), AEA-d8 (*m/z* 356.25>62.9), OEA (*m/z* 326.5>61.9), OEA-d2 (*m/z* 328.2>61.9), PEA (*m/z* 300.5>61.9) and PEA-d4 (*m/z*

304.2>61.9). Injection volumes for samples and standards were 7 µl. Seven point calibration curves in triplicate were analysed. Quanlynx software (Waters Corp. USA) was used to calculate the concentration of endocannabinoids using the calibration curve concentration or external calibration method against the relative response of endocannabinoids. This was calculated as:

Peak area of endocannabinoid

([Peak area of internal standard/ [concentration of internal standard])

An alternate method to calculate the concentration of endocannabinoids is the single point or internal calibration method, which assumes that the deuterium incorporation on the internal standard is >99% AEA-d8.

2.6 Statistics

Statistical analysis of the data was performed using Graph-Pad Prism version 7.0 for Windows (Graph-Pad Software. San Diego, CA, USA; www.graphpad.com;(2009)). Parametric tests (Student's t-test or one-way ANOVA with an appropriate post hoc analysis) were used for Gaussian distributed data. For non-Gaussian distributed data, comparison between groups was performed using Mann-Whitney U test and where appropriate one-way analysis of variance (ANOVA) followed by an appropriate post hoc analysis (Kruskal-Wallis test). Correlations were determined using the Spearman's correlation analysis. To assess the clinical potential of each marker at a time, receiver – operator characteristics (ROC) curves were plotted and the areas under curves (AUC) calculated with their 95% confidence intervals (95% CI) using standard techniques to evaluate the sensitivity and specificity. Logistic regression analysis was run to calculate the probability of EC diagnosis using different combinations of plasma NAE (AEA, PEA and OEA) concentrations. The ROC and logistic regression statistical analyses were run on MedCalc version 15.5 (Ostend, Belgium). *P* values < 0.05 were considered statistically significant.

2.7 Results

2.7.1 Power Calculation

Power calculations for AEA, OEA and PEA measurement were performed using an alpha of 0.05 and a beta of 0.8 from plasma measurements published by the research group (Habayeb et al. 2004, Habayeb et al. 2008). The minimum number of subjects required in each of the groups (study and control) in order to detect a mean difference in each of the endocannabinoid levels of 20% with an alpha of 0.05 and a power of 80%, was 6 (Habayeb et al. 2008).

2.7.2 Demographic Variables

The mean (\pm SD) BMI of the women studied were 26.6 ± 5.9 kg/m² for the atrophic and 34.8 ± 7.8 kg/m² for the type 1 and 38.0 ± 5.8 kg/m² for type 2 endometrial cancers (**Figure 2-1**). In general comparison, the BMI was higher in type 1 and type 2 EC when compared to the control (atrophic) group ($P < 0.05$).

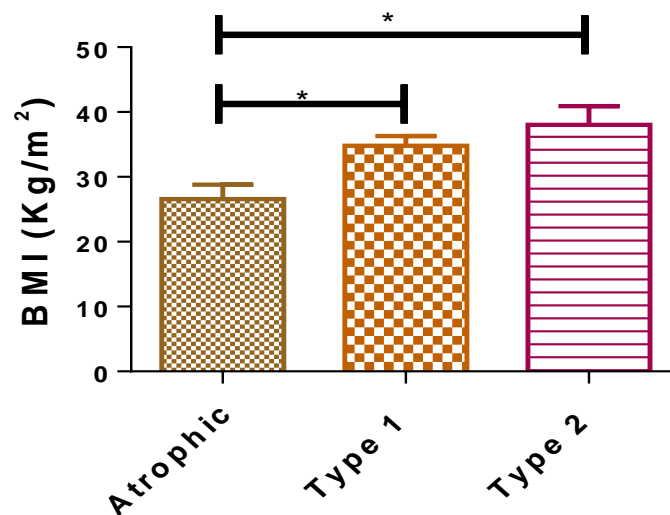


Figure 2-1: BMI of women in the control and type 1 and type 2 EC groups.

Data are presented as mean \pm SD; * $p < 0.05$; one way ANOVA with Dunnett's *ad hoc* post-test.

The mean (\pm SD) age of the women studied was 62.1 ± 5.5 years for the atrophic, 64.9 ± 10.0 years for the type 1 and 56.8 ± 7.8 for type 2 endometrial cancers. There were no significant differences in age ($p = 0.2504$, one-way ANOVA), (**Figure 2-2**).

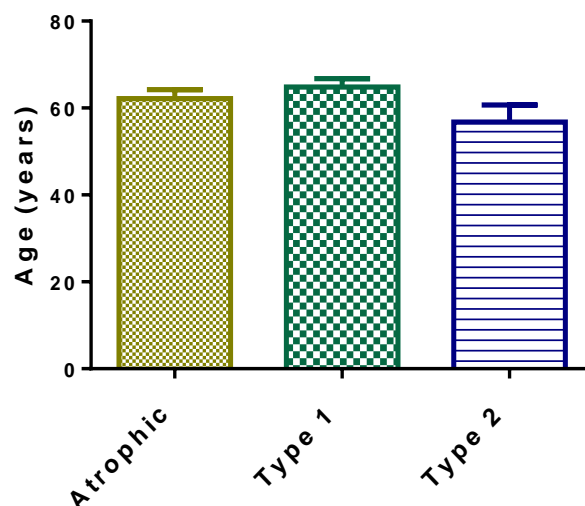


Figure 2-2: The ages of the women in the control and type 1 and 2 endometrial cancer groups. The data are presented as the mean \pm SD; $p > 0.05$; one way ANOVA with Dunnett's *ad hoc* post-test.

2.7.3 Detection of *N*-acylethanolamines in Plasma and Endometrial Tissues

AEA/AEA-d8, OEA/OEA-d2 and PEA/PEA-d4 were eluted from the UHPLC and detected by MS/MS at the following retention times; 2.27 ± 0.003 min, 2.47 ± 0.004 min and 2.42 ± 0.004 min, respectively. In all plasma and endometrial tissues samples a second peak with SRM of m/z $328.2 > 61.9$ was observed at a retention time of 2.67 min. This peak had good baseline separation from the peak representing OEA-d2. Co-evaluation studies with an authentic standard as performed by Marczylo et al. identified this peak to be representative of stearylethanolamide (SEA) and consequently did not interfere with OEA quantification (Marczylo et al. 2010).

2.7.4 Plasma Levels of *N*-acylethanolamines

Plasma AEA and PEA concentrations were significantly higher in women with EC than in controls ($p=0.037$ and $p=0.0066$, respectively) but plasma OEA concentrations were not significantly different (**Figure 2-3A**). Plasma AEA and PEA concentrations in type 1 EC patients were significantly higher than in the control (atrophic) group ($p=0.0094$ and $p=0.0001$, respectively), but plasma OEA and in type 2 EC patients the differences were not statistically different to that in atrophic patients (**Figure 2-3B**). The plasma

AEA and OEA concentrations in type 1 EC patients were not statistically different from those of the control (atrophic) group, however, plasma concentrations of PEA in grade 2 were statistically significantly higher ($p=0.0001$) (**Figure 2-3C**).

A Grubb's test for the identification of outliers was undertaken for all the plasma NAEs concentrations obtained prior to the statistical analysis. There were no outliers detected following the Grubb's test. However, when plotted as a scatter plot, one plasma AEA concentration and three plasma concentrations of PEA appeared to be outliers, despite the Grubb's test indicating that they were not. Nevertheless, further analysis of the data with the single AEA data point omitted from the plasma AEA analysis and the three PEA concentrations omitted from the PEA analysis (**Figure 2-3D**) showed that the plasma AEA ($p<0.05$) and PEA ($p=0.0219$) still showed statistical significant differences, when compared the control (atrophic) group. Furthermore sub-group analysis (**Figure 2-3E**) showed that the plasma AEA ($p<0.05$) and plasma PEA ($p<0.001$) levels in type 1 EC patients were significantly higher than in the control (atrophic) group whilst in type 2 EC, there was no significance. In addition, plasma AEA was analysed in all the three grades of type 1 EC (**Figure 2-3F**) and did not show any significance for type 1 but were significantly different for grade 2 and 3. Plasma PEA levels were significantly ($p<0.001$) higher in grade 1 type 1 when compared to control (atrophic) group (**Figure 2-3F**). Re-examination of the histological slides by the histopathologist of those patients thought to have isolated AEA or PEA values, revealed that these 4 patients presented with very early stage grade 1 type 1 EC.

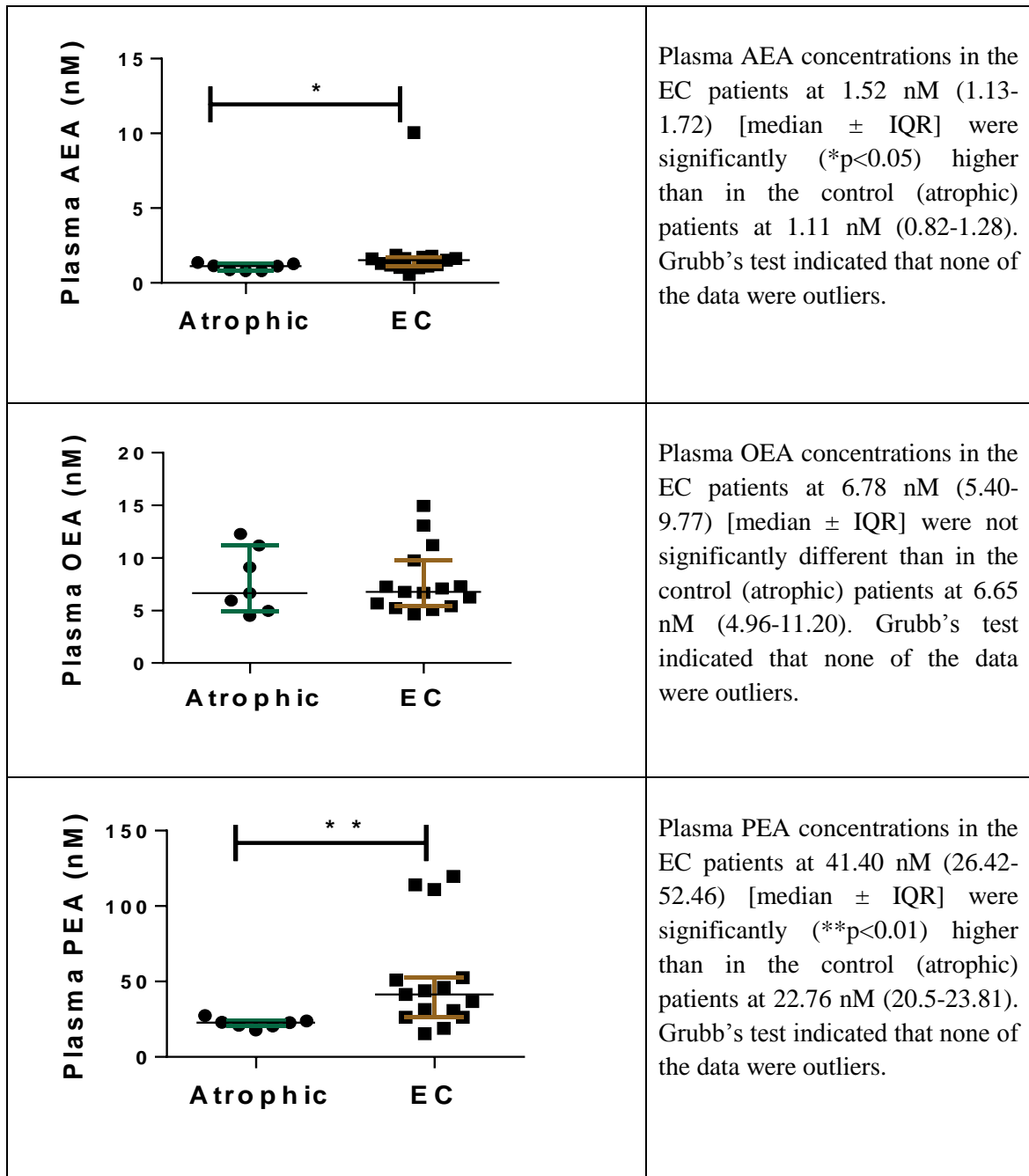


Figure 2-3A: Plasma NAEs in control (atrophic) patients and patients with endometrial cancer (EC).

Data are presented as median (IQR). Comparisons were made using Mann-Whitney U-test analysis. The number of samples were atrophic=7; EC=15.

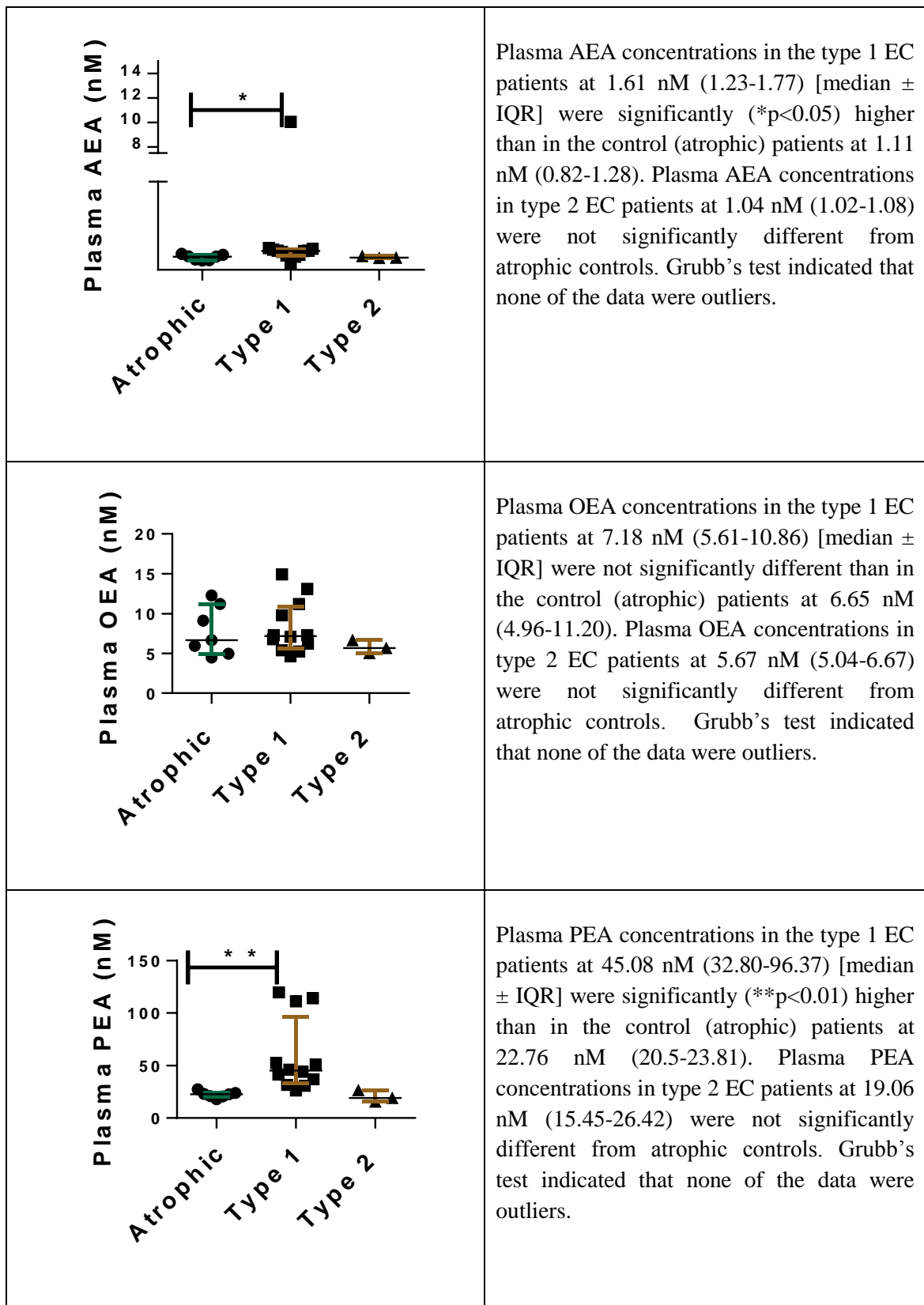


Figure 2-3B: Plasma NAEs in control (atrophic) patients and patients with type 1 and 2 EC.

Data are presented as median (IQR). Comparisons were made using Mann-Whitney U-test analysis. The number of samples were: atrophic=7; type 1=12; type 2=3.

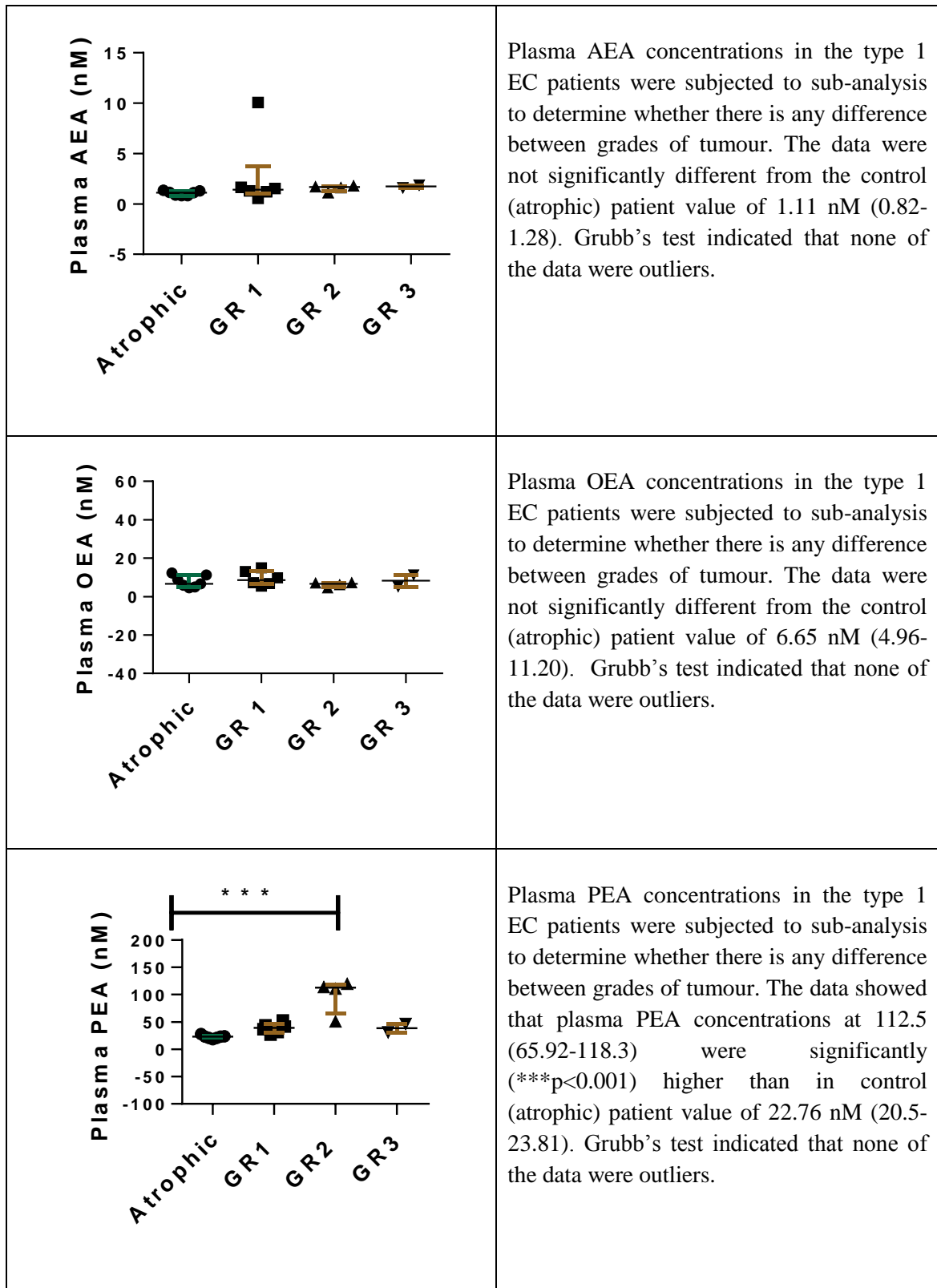


Figure 2-3C: Plasma NAEs in control (atrophic) and grade 1, 2 and 3 type 1 EC.

Data are presented as median (IQR) and *** $p < 0.001$. Comparisons were made with Kruskal-Wallis ANOVA with Dunn's ad hoc post -test analysis. The number of samples were: atrophic=7; type 1, grade 1=6; type 1, grade 1=4; type 1, grade 3=2.

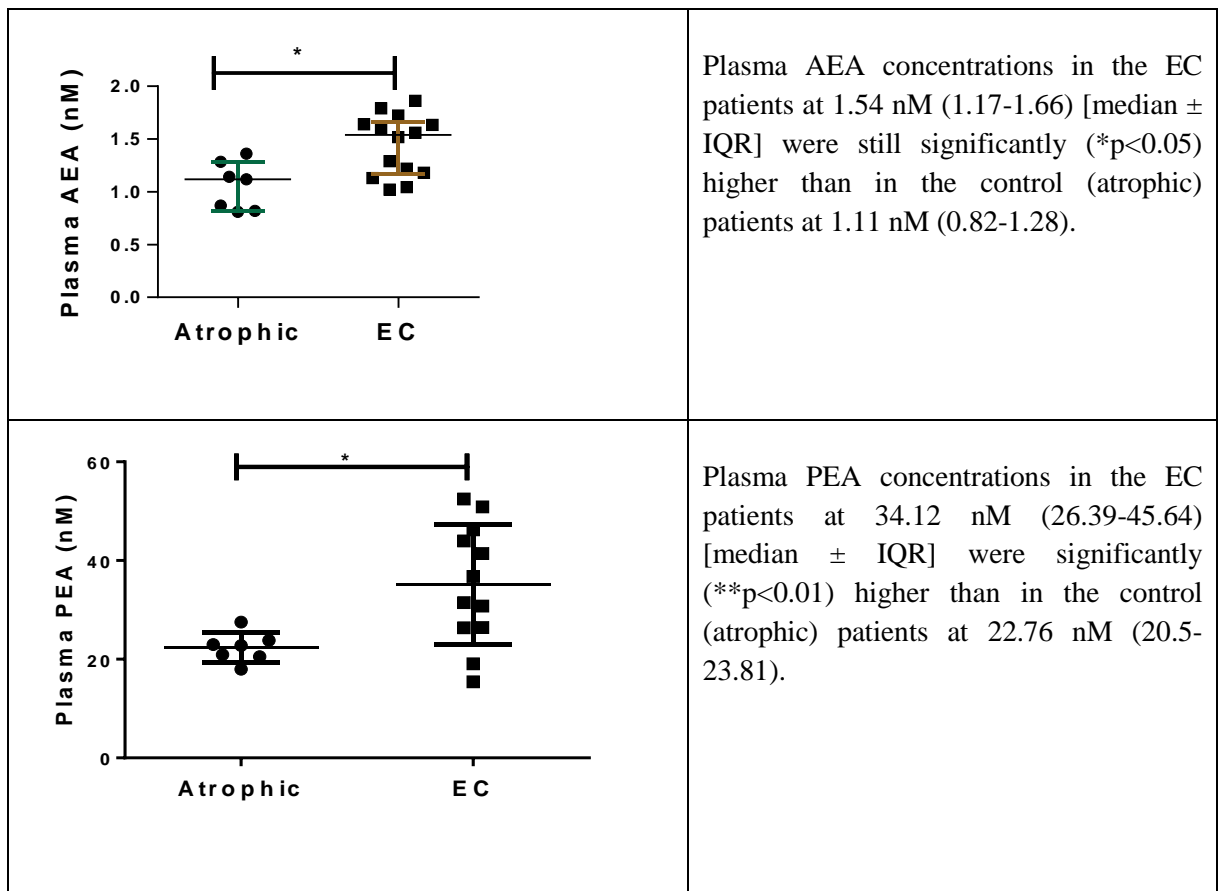


Figure 2-3D: A re-evaluation of plasma AEA (without one value) and PEA (without three values) in control (atrophic) patients and patients with endometrial cancer (EC).

Data are presented as median (IQR) * $p < 0.05$. Comparisons were with Mann-Whitney test analysis. The number of samples were atrophic=7; (AEA) EC=14; (PEA) EC=12.

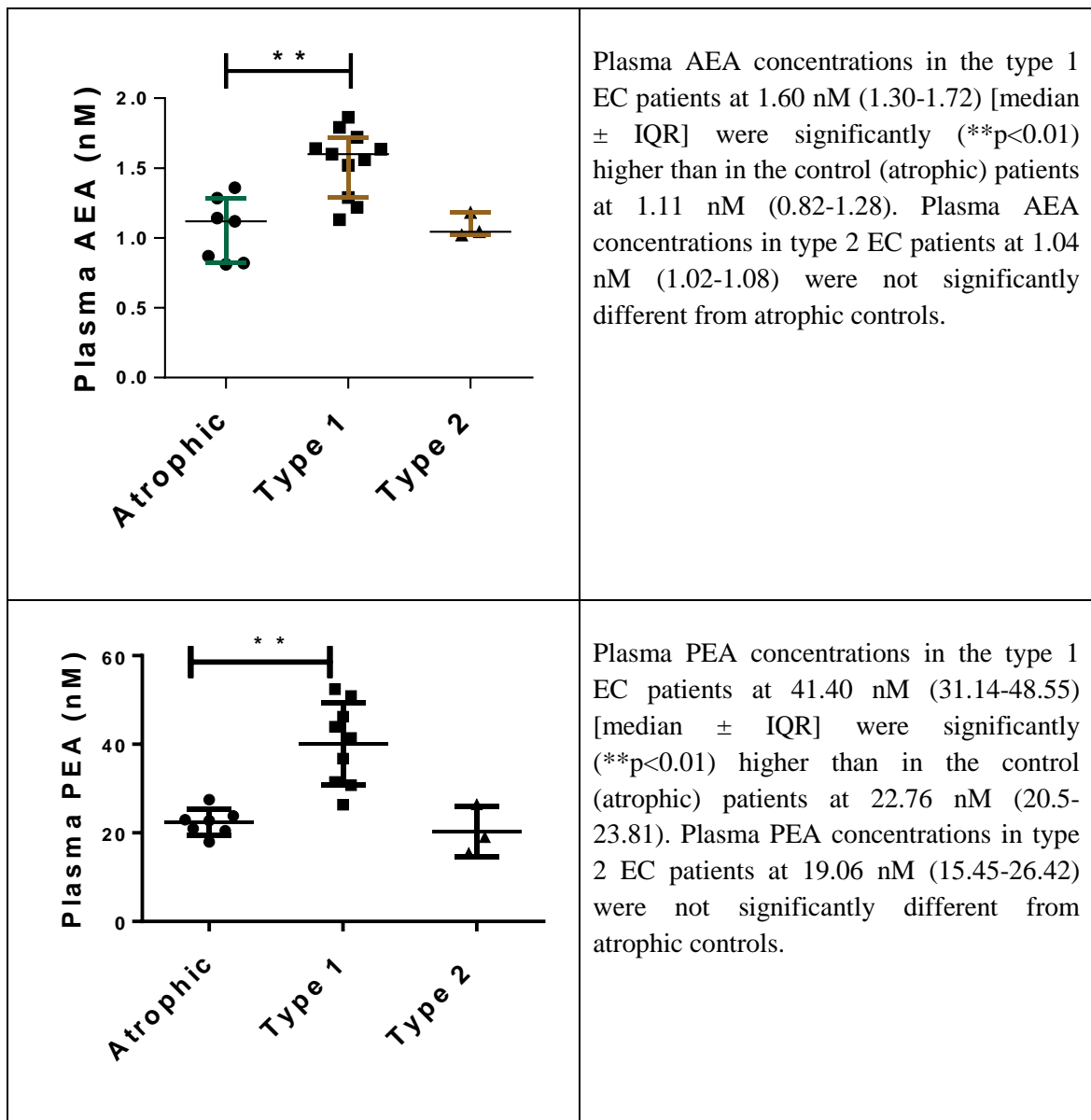


Figure 2-3E: A re-evaluation of plasma AEA (without one value) and PEA (without three values) in control (atrophic) patients and patients with type 1 and 2 EC.

Data are presented as median (IQR). Comparisons were made using Kruskal-Wallis ANOVA with Dunn's ad hoc post -test analysis. For AEA, the number of samples were: atrophic=7; type 1=11; type 2=3. For PEA, the number of samples were: atrophic=7; type 1=9; type 2=3.

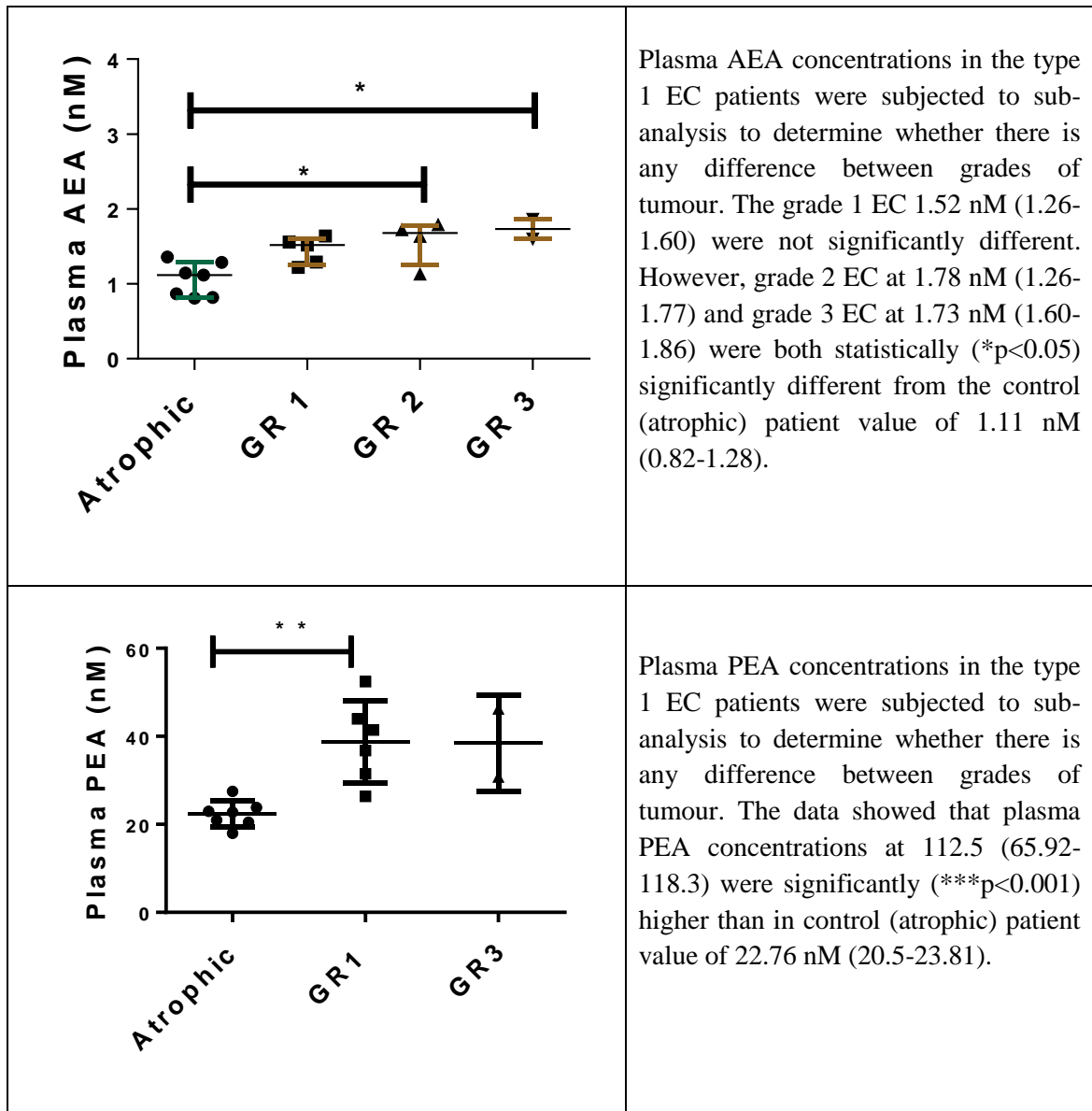


Figure 2-3F: A re-evaluation of plasma AEA (without one value) and PEA (without three values) concentrations in control (atrophic) and grade 1 and 3 type 1 EC patients.

Data are presented as median (IQR). Comparisons were made with Kruskal-Wallis ANOVA with Dunn's ad hoc post-test analysis. The number of samples were: atrophic=7; grade 1=5; grade 2=4; grade 3=2 for AEA and atrophic=7; grade 1=6 and grade 3=2. The three elevated PEA concentrations were within grade 2 category and removal resulted in only one data point and so not suitable for one-way ANOVA analysis.

2.7.5 Tissue Levels of *N*-acylethanolamines

Endometrial AEA and PEA tissue levels were significantly higher in women with EC than in atrophic controls ($p=0.046$ and $p=0.0313$, respectively), and tissue OEA levels were not significantly different ($p=0.0510$) (**Figure 2-4A**). AEA, OEA and PEA levels in type 1 EC tissues were significantly higher than in the control (atrophic) group ($p=0.0043$, $p=0.0269$ and $p=0.0002$), respectively, but all the NAEs failed to show any statistically significant differences between type 2 EC and normal atrophic endometrium (**Figure 2-4B**). Tissue OEA levels for all grades (1, 2 and 3) of type 1 EC were not statistically different from those of the control (atrophic) group, but those AEA and PEA in grade 1, type 1 EC were significantly higher ($p=0.0016$ and $p=0.0002$, respectively) (**Figure 2-4C**).

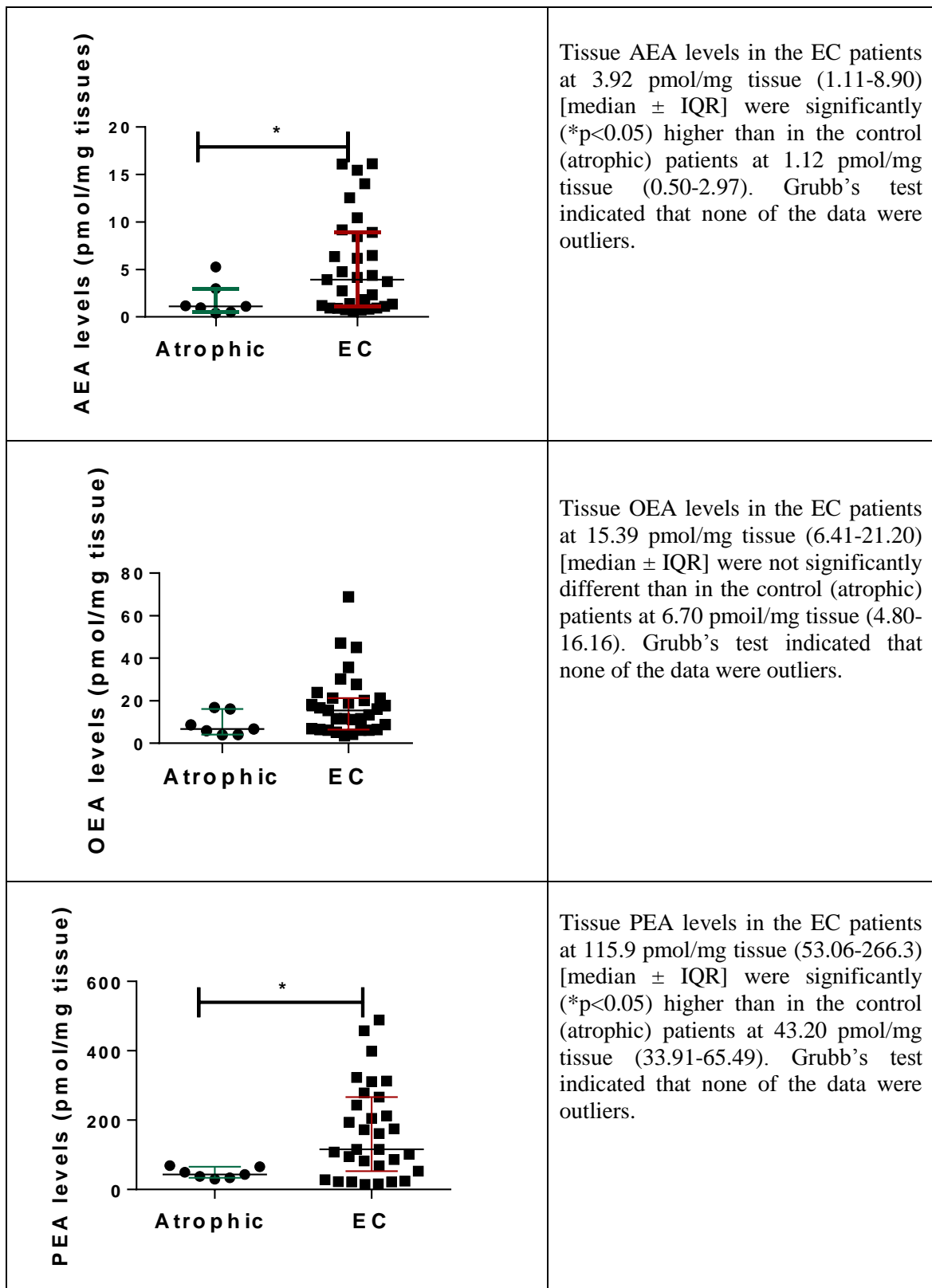


Figure 2-4A: Tissue NAEs in control (atrophic) patients and patients with endometrial cancer (EC).

Data are presented as median (IQR). Comparisons were made using Mann-Whitney U-test analysis. The number of samples were atrophic=7; EC=31.

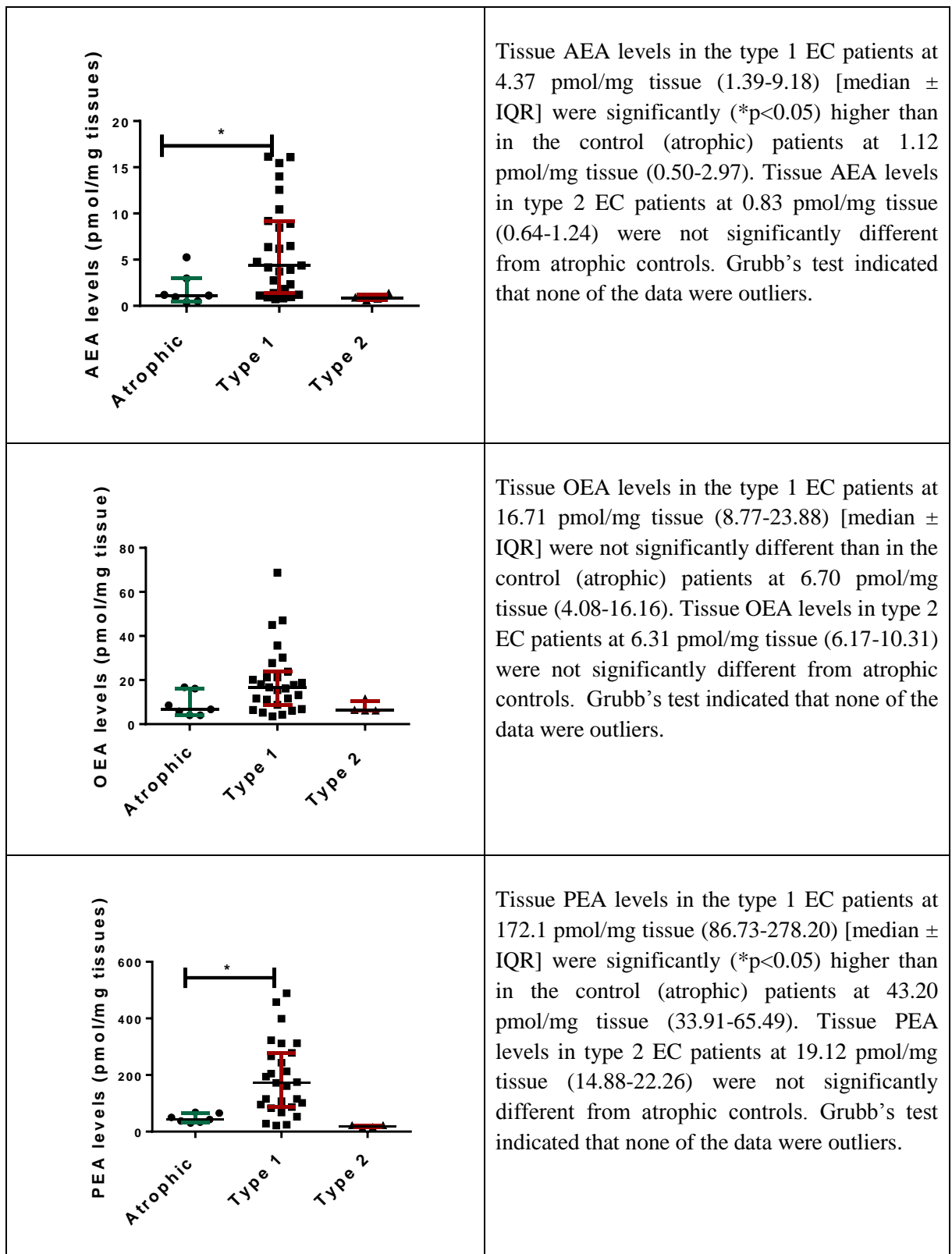


Figure 2-4B: Tissue NAEs in control (atrophic) patients and patients with type 1 and 2 EC.

Data are presented as median (IQR). Comparisons were made using Kruskal-Wallis ANOVA with Dunn's ad hoc post -test analysis. The numbers of samples were: atrophic=7; type 1=27; type 2=4.

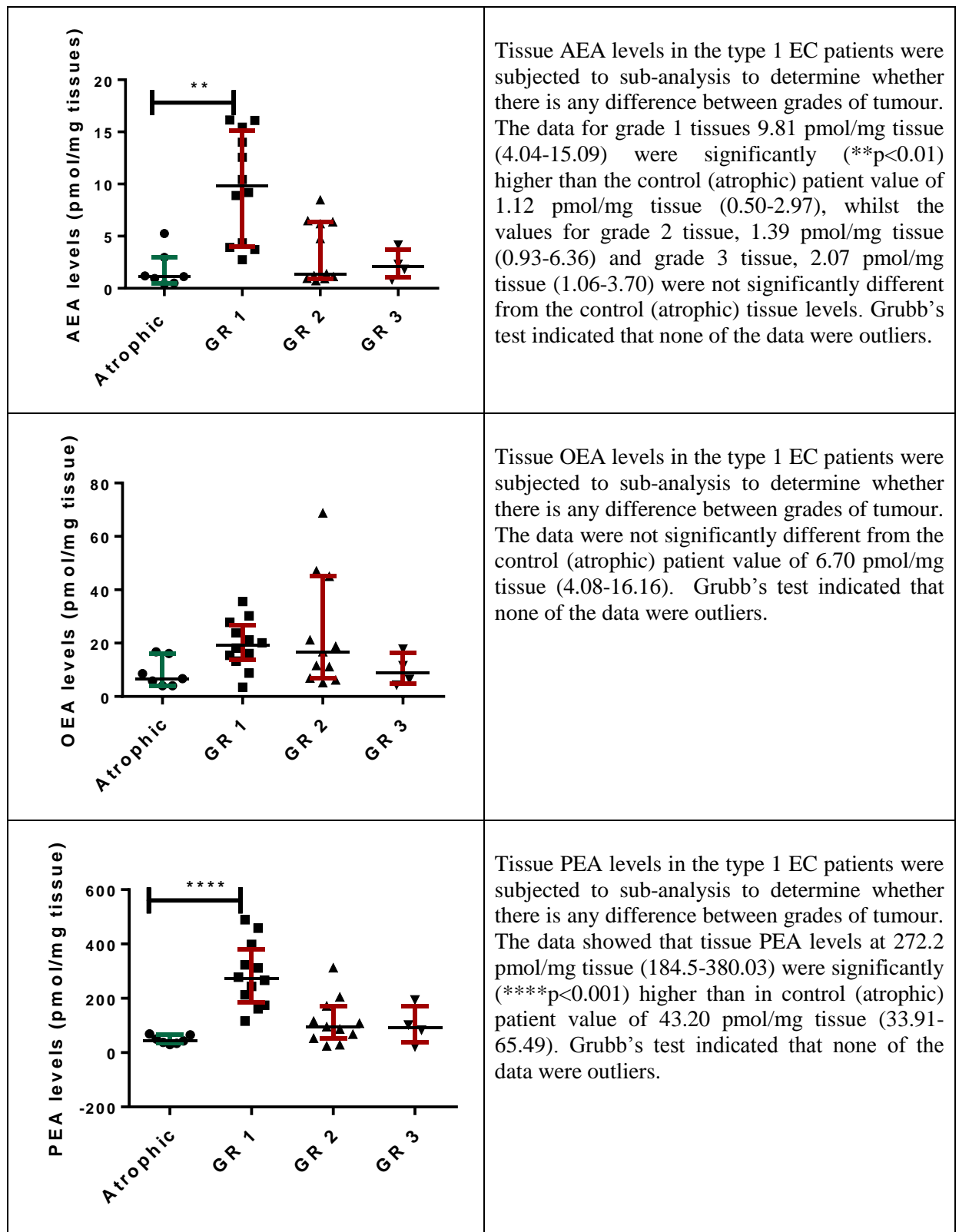


Figure 2-4C: Tissue NAEs in control (atrophic) and grade 1, 2 and 3 type 1 EC.

Data are presented as median (IQR). Comparisons were made with Kruskal-Wallis ANOVA with Dunn's ad hoc post -test analysis. The numbers of samples were: atrophic=7; type 1, grade 1=12; type 1, grade 2=11; type 1, grade 3=4.

2.7.6 The Relationship Between Plasma AEA, OEA and PEA Concentrations

Having determined the levels of NAEs in the endometrial tissues and the concentrations in the plasma, the next logical step was to determine if the plasma measurements of endocannabinoids are related with each other. Since AEA, OEA and PEA are thought to be produced in tandem in response to the same stimuli and because the same enzymes are thought to be responsible for their metabolism (synthesis and degradation), it was predicted that there would be a correlation between the concentrations of plasma AEA, OEA and PEA. Spearman's correlation was used to determine these relationships. This was possible only for 22 patients (atrophic and endometrial cancer) and it revealed a statistically significant positive correlation between plasma AEA and PEA ($r^2 = 0.424$; $p=0.001$) (**Figure 2-5A**), whilst there was no correlation between AEA and OEA ($r^2 = 0.093$; $p=0.169$) (**Figure 2-5B**) or OEA and PEA ($r^2 = 0.091$; $p=0.173$) (**Figure 2-5C**).

Because I was concerned that the single plasma AEA and three plasma PEA concentrations could have added bias to my analyses, I repeated the analyses in the absence of those 4 samples. A statistically significant positive correlation between plasma AEA and PEA ($r^2 = 0.299$; $p=0.015$) (**Figure 2-5D**), whilst again there was no correlation between AEA and OEA ($r^2 = 0.052$; $p=0.319$) (**Figure 2-5E**). However, removal of the 3 highest PEA plasma concentrations showed there to be a significant correlation between OEA and PEA ($r^2 = 0.218$; $p=0.044$) (**Figure 2-5F**).

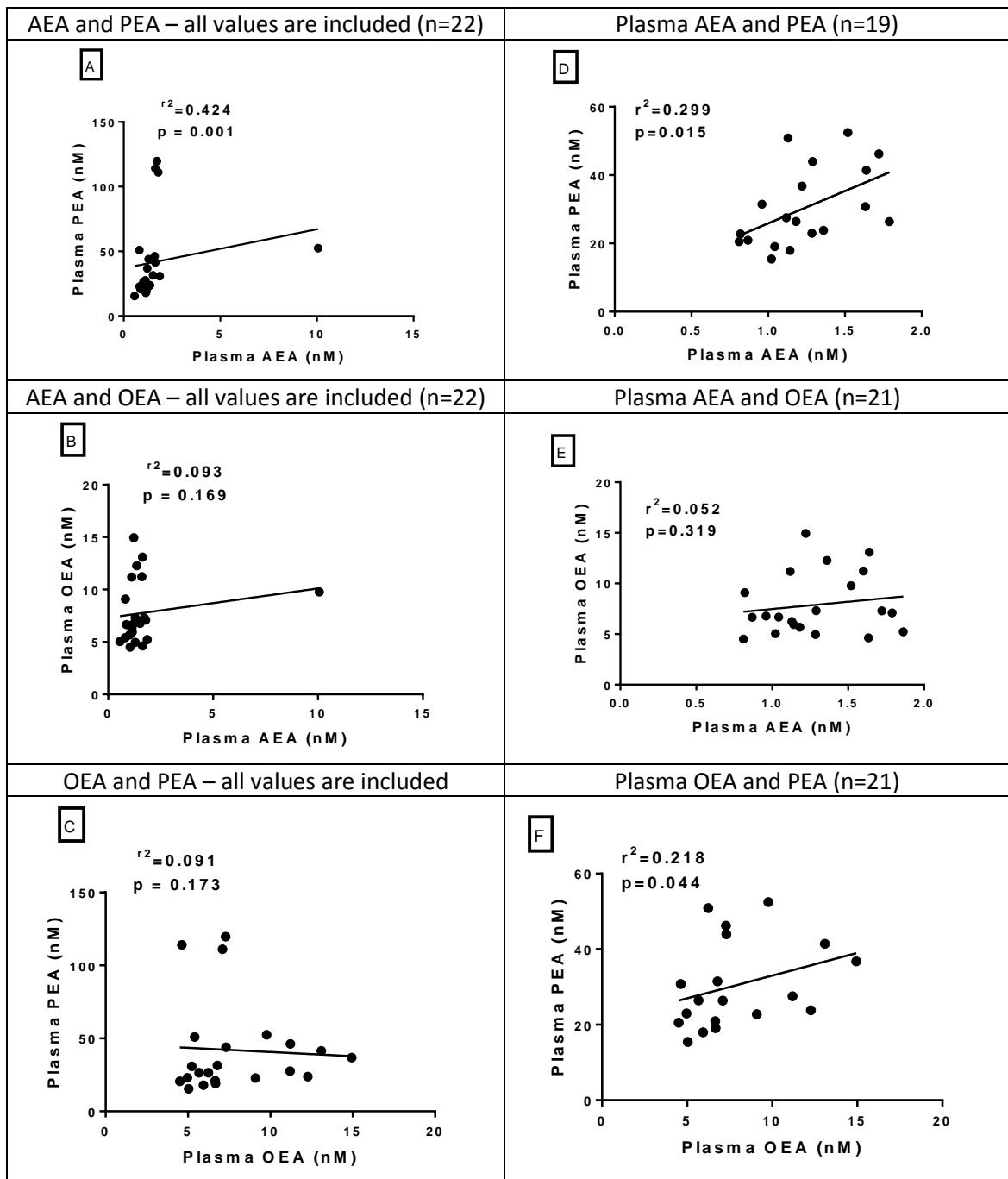


Figure 2-5A-F: Correlation curves showing the relationships between plasma levels of AEA, OEA and PEA.

The relationships between AEA and PEA (panel A), AEA and OEA (panel B) and OEA and PEA (panel C) are shown with all the values included in the analysis. Panels D, E and F show the same data, but with the highest plasma AEA and 3 highest PEA concentrations excluded from the analyses. The indicated r^2 and p -values were obtained using Spearman's correlation analysis.

2.7.7 The Relationship Between AEA, OEA and PEA Tissue Levels

Spearman correlation coefficients calculated from 38 tissue samples (atrophic and endometrial cancer) showed there was a statistically significant positive correlation between tissue AEA and PEA ($r^2 = 0.757$; $p < 0.0001$) (**Figure 2-6A**), AEA and OEA ($r^2 = 0.296$; $p = 0.0004$) (**Figure 2-6B**) and OEA and PEA ($r^2 = 0.201$; $p = 0.0048$) tissue levels (**Figure 2-6C**).

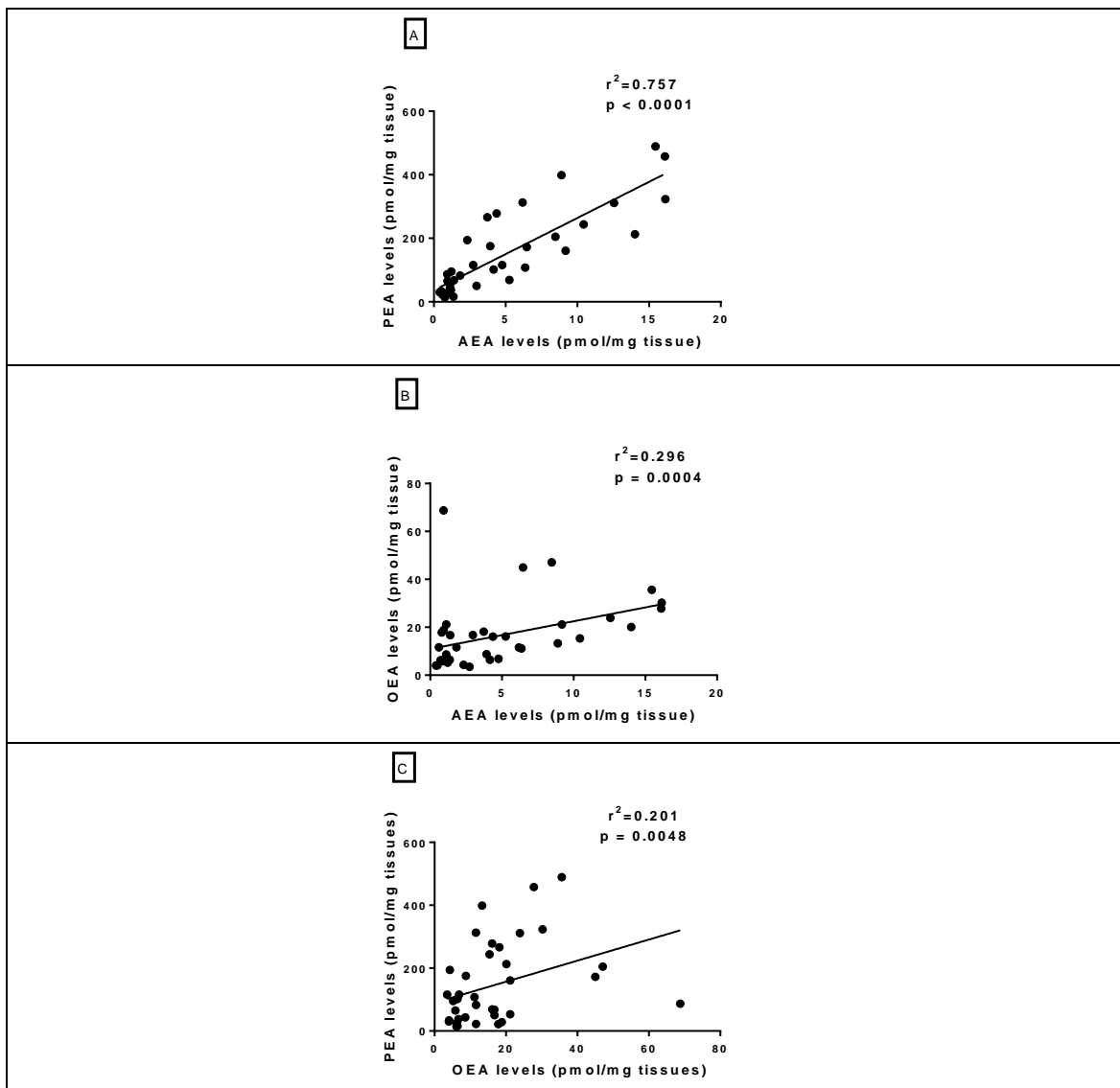


Figure 2-6A-C: Correlation curves showing the relationships between tissue levels of AEA, OEA and PEA.

Correlations curves between the tissue levels of AEA and PEA (panel A), AEA and OEA (panel B) and OEA and PEA (panel C). The relationships between AEA and PEA (panel A), AEA and OEA (panel B) and OEA and PEA (panel C) are shown. The indicated r^2 and p -values were obtained using Spearman's correlation analysis.

2.7.8 The Relationship Between Plasma Concentrations and Endometrial Tissue Levels of AEA, OEA and PEA

Having determined the levels of NAEs in plasma and tissues, the next logical analysis was to determine if these two parameters were related. Correlations between plasma and tissue levels of the NAEs (**Figure 2-7**) were determined in a subset of available samples (EC and atrophic). A statistically significant correlation was demonstrated between plasma and tissue AEA levels ($r^2 = 0.302$, $p=0.008$; $n=22$, (**Figure 2-7A**) and it was statistically similar even when the highest plasma AEA values was removed ($r^2 = 0.373$, $p=0.003$ and $n=21$) (**Figure 2-7B**). There was no statistically significant correlation between plasma and tissue OEA levels ($r^2 = 0.022$, $p=0.5063$, $n=22$) (**Figure 2-7C**), whilst a statistically significant correlation was demonstrated between plasma and tissue PEA levels ($r^2 = 0.182$, $p=0.048$, $n=22$) (**Figure 2-7D**). Furthermore, when the three highest plasma PEA values were removed from the analysis the relationship continued to be significant ($r^2 = 0.345$, $p=0.008$, $n=19$) (**Figure 2-7E**).

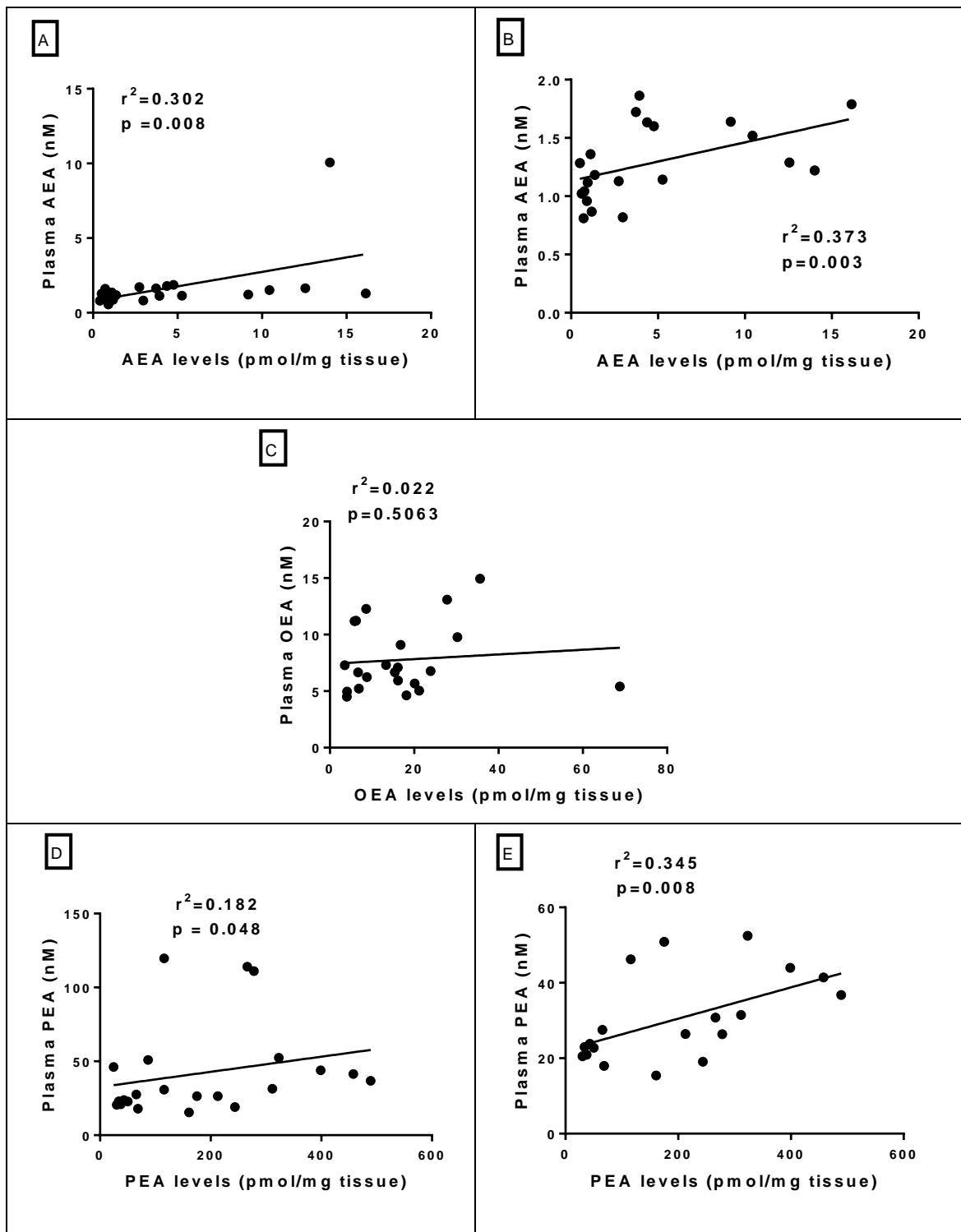


Figure 2-7A-E: Relationship between plasma and endometrial tissue concentrations of AEA, OEA or PEA in EC.

Correlations curves between the tissue levels and plasma concentrations of AEA including the highest plasma concentration (panel A) and without the highest plasma concentration (panel B) are shown together with the OEA analysis (panel C) and the PEA analysis with the 3 highest plasma concentrations (D) and without the 3 highest PEA plasma concentrations (panel E). The indicated r^2 and p -values were obtained using Spearman's correlation analysis.

2.7.9 Receiver-operator Characteristic (ROC) Analyses

To determine the diagnostic performance of NAEs in women with endometrial cancer, receiver-operator characteristic (ROC) curves were constructed using the patient's (controls and cancer patient) plasma concentrations. Each biomarker will be examined in turn.

2.7.9.1 Diagnostic Significance of Plasma AEA

Plasma AEA showed its best diagnostic capability with an area under the curve (AUC) of 0.781. At a cut-off value of 1.36 nM, plasma AEA had a sensitivity of 53.3% and specificity of 100% for the diagnosis of EC. The calculated p-value was 0.0734 and the likelihood ratio 5.250 (**Figure 2-8**). This means that a plasma concentration of >1.36 nM indicates that individual is ~5-times more likely to have endometrial cancer.

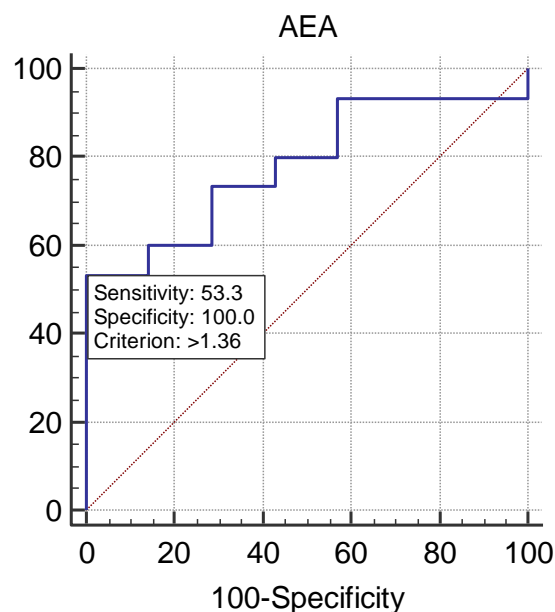


Figure 2-8: Diagnostic test in plasma AEA in atrophic and EC.

ROC analysis was performed using MEDCALC software and the graph is directly from the software.

When the ROC analysis was limited to the plasma concentrations of control and type 1 EC patients alone, the diagnostic capability of plasma AEA for EC was improved with AUC of 0.845. At the same cut-off value of 1.36 nM, plasma AEA had a sensitivity of 66.7% and specificity of 100% for the diagnosis of type 1 EC. The p-value was now significant ($p=0.0246$) and the likelihood ratio was 4.500 (**Figure 2-9**), suggesting a good biomarker for type 1 EC.

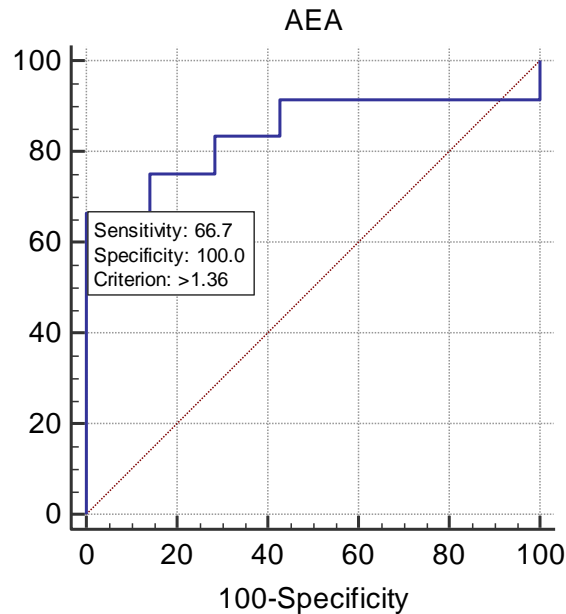


Figure 2-9: Diagnostic test in plasma AEA in atrophic and type 1 EC. ROC analysis was performed using MEDCALC software and the graph is directly from the software.

2.7.9.2 Diagnostic Significance of Plasma OEA

Plasma OEA ($n = 22$), showed its best diagnostic capability with an AUC of 0.543. At a cut-off value of 4.965 nM, plasma OEA had a sensitivity of 93.3% and specificity of 28.6% for the diagnosis of EC. It was not statistically significant and the likelihood ratio of correctly diagnosing EC was only slightly elevated at 1.307 (**Figure 2-10**).

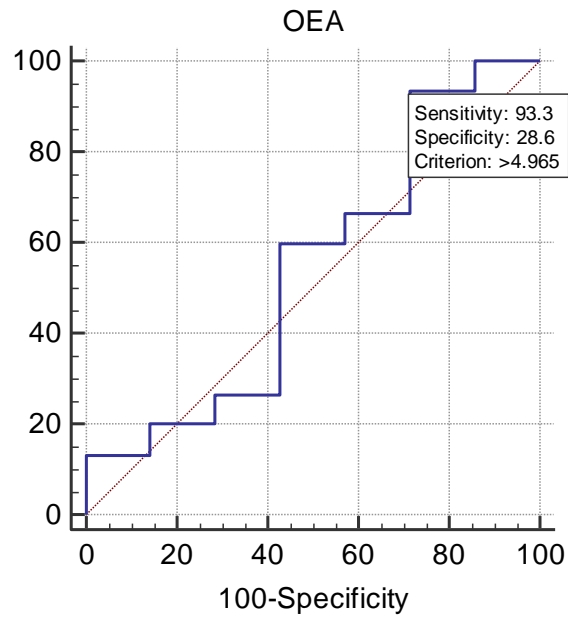


Figure 2-10: Diagnostic test in plasma OEA in atrophic and EC. ROC analysis was performed using MEDCALC software and the graph is directly from the software.

When ROC analysis was limited to the plasma concentrations of control and type 1 EC samples alone ($n = 19$), the diagnostic capability of plasma OEA improved with an AUC of 0.583. At a cut-off value of 6.655 nM, plasma OEA had a sensitivity of 66.7% and specificity of 57.1% for the diagnosis of type 1 EC. The calculated p- value was significant ($p=0.0026$) with a likelihood ratio of 1.56 for the correct diagnosis of type 1 EC (**Figure 2-11**).

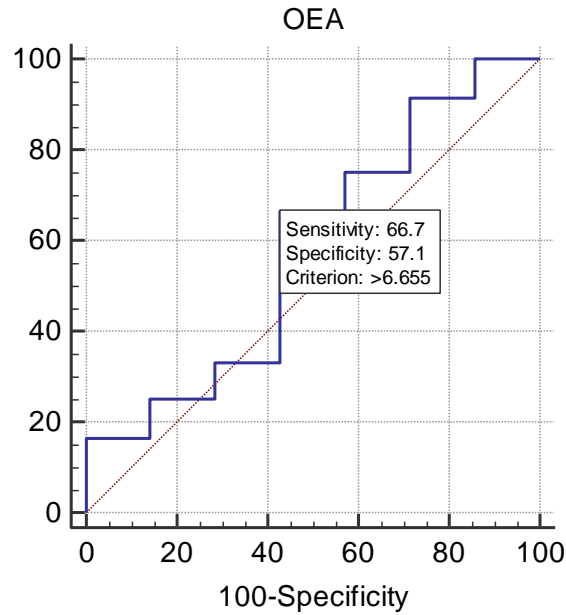


Figure 2-11: Diagnostic test in plasma OEA in atrophic and type 1 EC. ROC analysis was performed using MEDCALC software and the graph is directly from the software.

2.7.9.3 Diagnostic Significance of Plasma PEA

ROC analysis of plasma PEA using atrophic and EC samples (n = 22), showed its best diagnostic capability with an AUC of 0.857 (Figure 2-10). At a cut-off value of 27.5 nM, plasma PEA had a sensitivity of 73.3% and specificity of 100.0% for the diagnosis of EC. The calculated p-value was highly significant ($p < 0.0001$) with a likelihood ratio of 6.067 (Figure 2-12).

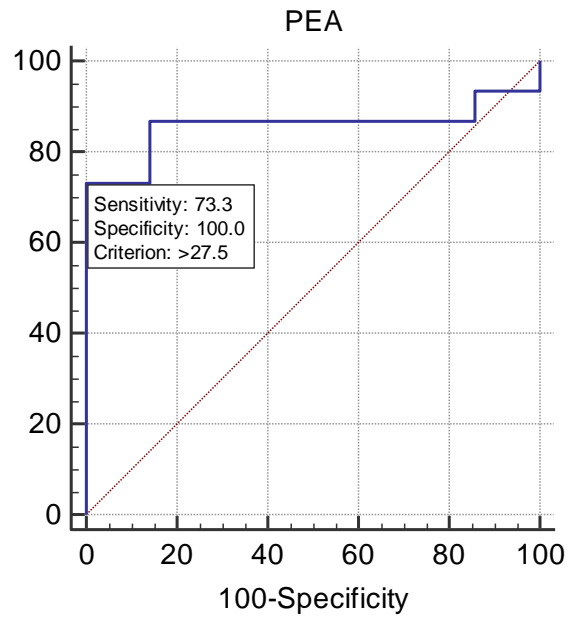


Figure 2-12: Diagnostic test in plasma PEA in atrophic and EC.

ROC analysis was performed using MEDCALC software and the graph is directly from the software.

When ROC analysis was limited to the plasma concentrations of control atrophic and type 1 EC patients ($n = 19$), plasma PEA was improved with an AUC of 0.821. At a cut-off value of 23.8 nM, plasma PEA had a sensitivity of 83.3% and specificity of 85.7% for the diagnosis of type 1 EC. The p-value was now significant ($p=0.0026$) and the likelihood ratio was 5.833 (**Figure 2-13**), suggesting a good biomarker for type 1 EC.

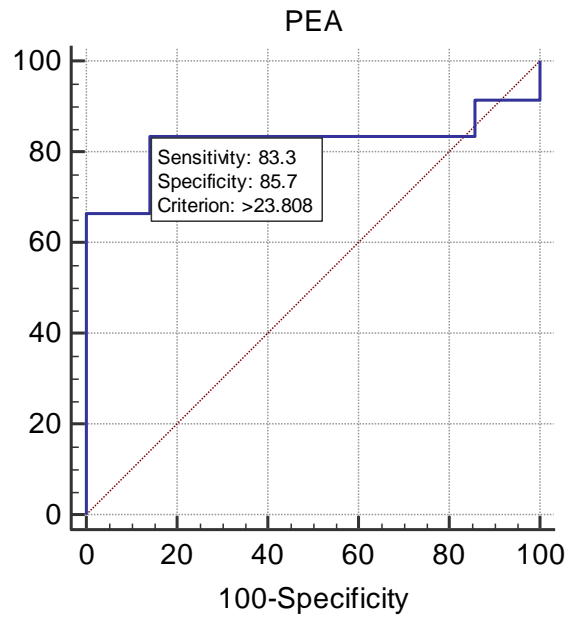


Figure 2-13: Diagnostic test in plasma PEA in atrophic and Type 1 EC. ROC analysis using the MEDCALC.

2.7.9.4 Combining the Best Two AUC Values - Plasma AEA and PEA

The probability of diagnosing EC was further evaluated in combinations of plasma AEA and PEA concentrations using logistic regression. According to the logistic regression statistical analysis, AUC values for ROC curve for the AEA and PEA combination was increased from 0.781 for AEA and from 0.857 for plasma PEA to 0.924 for both. The sensitivity achieved following the combination of these two markers was 93.3% and the specificity 85.7%. Limiting the analysis just to control and type 1 EC patients did not improve the diagnostic capabilities of these tests, because the AUC remained unchanged at 0.92 with a sensitivity of 91.7% and specificity of 85.7%.

2.7.9.5 Combining All Three Biomarkers - Plasma AEA, PEA and OEA

The probability of diagnosing EC was further evaluated by combination plasma AEA, PEA and OEA concentrations using logistic regression. The calculated AUC of the ROC curve of the three combined plasma markers (AEA, PEA and OEA) increased from 0.781 for AEA, 0.857 for PEA and 0.543 for OEA to 0.933 when all three were combined, resulting in a sensitivity of 93.3% and specificity of 85.7%. When the analysis was limited to control and type 1 EC patients, the AUC value decreased slightly to 0.92 but was similar to combining AEA and PEA with a sensitivity of 91.7% and specificity of 85.7%. From these data it can be concluded that adding plasma OEA to the calculation of diagnosis of EC or type 1 EC does not improve the diagnostic capability of plasma AEA and PEA.

2.8 Discussion

Quantification of NAEs in endometrial cancer tissues has only been previously investigated in small numbers and with conflicting results (Schmid et al. 2002, Guida et al. 2010). The first study performed by Schmid et al., measured AEA in endometrial sarcoma and demonstrated that levels were elevated compared with those in non-malignant (normal) endometrial tissue. A second study, by Guida et al., measured AEA, 2AG and PEA and found statistically significant increased 2AG levels but in contrast to the finding of Schmid et al found no statistical significance increase in AEA levels. Furthermore PEA levels were also not significantly different. Neither of these grouped examined the levels of the other NAEs in endometrial cancer tissues.

The endocannabinoids (AEA, OEA and PEA) were all present in measurable quantities in plasma and solid tissues (endometrial cancer) and the atrophic endometrium in the women, reported on in this chapter.

The plasma and tissue levels varied and these differences were depended upon the nature of the patient (cancer or control) and the type and grade of cancers. There was also a correlation noted between plasma NAEs and endometrial tissues levels.

Higher levels of AEA (plasma and tissues) have been associated with various pathological conditions such as miscarriage in early pregnancy (Maccarrone et al. 2002,

Wang et al. 2004) and malignancies (De Petrocellis et al. 1998, Maccarrone et al. 2000, Contassot et al. 2004, Bifulco et al. 2006). In this study there was a trend towards higher levels of AEA in earlier grades and the well differentiated endometrial cancers, such as type 1 endometrioid endometrial cancer. Furthermore there was a possible statistical correlation between the plasma and tissue AEA levels (endometrial cancer and atrophic; n=22) ($r = 0.55$, $P = 0.008$). These data suggest that plasma AEA could be considered as a surrogate of the tissue levels of AEA and this may potentially be used as a plasma biomarker for detecting early EC.

Although OEA levels in the plasma of endometrial cancer patients were higher they were not statistically different from those of the atrophic endometrium group. The tissue levels of OEA were only significantly higher ($p < 0.05$) when the type 1 grade 1 tumour tissues were compared with the atrophic endometrium. OEA has not been previously quantified in EC to the best of my knowledge.

Finally, the anti-inflammatory AEA analogue, palmitoylethanolamine (PEA) was investigated. Plasma PEA levels in the endometrial cancer patients were significantly higher ($P = 0.0066$) when compared with atrophic control group. When plasma PEA levels of type 1 and type 2 endometrial cancers were individually compared to plasma level from the control group, only the type 1 levels were statistically elevated ($P < 0.01$). Sub-analysis of the type 1 EC levels showed that only patients with grade 2 cancers had significantly elevated plasma PEA levels. Similarly, PEA levels in the endometrial cancer tissue were significantly higher ($P < 0.05$) than in the atrophic controls, but in contrast to the plasma levels it was significantly higher in those with grade 1, type 1 endometrial cancer. Correlation study between tissue and plasma PEA concentrations revealed a significant positive correlation. These data suggests that plasma could be considered as a surrogate of the tissue levels of PEA and thus may possibly be used as a plasma biomarker for diagnosing early endometrial cancers. In addition, PEA has been recently suggested to act as modulator of the endocannabinoid system in various cancer types, where it has been identified that PEA may mediate the antiproliferative and apoptotic effects via both cannabinoid receptor-dependent and -independent pathways. Interestingly, PEA a fatty-acid amide that does not bind to cannabinoid receptors, enhances the anti-proliferative effects of AEA, arvanil, olvanil and HU-210 (Di Marzo et al., 2001; De Petrocellis et al., 2002), which is suggestive of synergism or an entourage effect (Ben-Shabat et al., 1998; De Petrocellis et al., 2002), and this may

explain the differences in the plasma and tissue PEA levels for the different grades of type 1 endometrial cancer. Moreover, compounds like PEA might act as ‘entourage’ substance for AEA, enhancing its cannabinoid biological actions. Di Marzo et al. (2001) reported that chronic treatment with PEA enhance AEA-induced inhibition of cell proliferation through decreased expression of fatty acid amide hydrolase (FAAH), the enzyme chiefly responsible for AEA degradation.

The potential to use levels of AEA and PEA in plasma as biomarkers for diagnostic purpose in clinical practice to speed up the waiting lists and outcome of patient care, are supported, by the ROC analysis curve for diagnosis of EC. These findings may have both pathophysiological as well as diagnostic consequences for EC, but need further investigations, to clarify the role of endocannabinoids in the aetiopathogenesis of EC at the intracellular level, growth, apoptosis, invasion and metastasis and determine whether these *N*-acylethanolamines may be targeted for specific biological or cytotoxic therapies.

Furthermore, the specific strengths of my cohort were the pure sample of EC without any medical comorbidity, all were postmenopausal, and non-smokers gives the true effect of the endocannabinoid system in EC. Limited number of samples and patient represented here were the minority group and are not representing a true pool of EC. Therefore, in order to use the endocannabinoids in our daily clinical practice as a diagnostic tool, it need further large multicentre-trial from various country to validate my pilot study results.

2.9 Conclusions

The data presented in this Chapter showed elevated levels of AEA and PEA in plasma and endometrial tissues of cancer patients. Whether these differences are part of difference in the whole endocannabinoid system such as enzymes and receptors, will be examined in the next chapters.



Chapter 3

Activity, Expression and Location of the Endocannabinoid Regulating Enzymes FAAH and NAPE-PLD

3.1 Introduction

In Chapter 2, the presence of the endocannabinoid ligands AEA, OEA and PEA were confirmed and then quantified in the plasma and endometrial tissues of postmenopausal women with and without endometrial carcinoma. Although concentrations of the ligands AEA and PEA were elevated in the women with endometrial carcinoma, both in plasma and malignant endometrial tissues, the reasons for those elevations were not obvious. Since the main regulators of these NAEs in other tissues are the relative expression and actions of the synthesising enzyme NAPE-PLD (Matias et al. 2006) and the degradation enzyme FAAH (Matias et al. 2006), exploring the expression and action of these two enzymes in the two patient groups could offer possible explanations. The expression and actions of these two enzymes could be performed using basic biochemical techniques, such as enzyme activity assays, immunohistochemistry and from the measurement of transcript levels using PCR of reverse transcribed messenger RNA (RT-PCR).

Quantitative real time PCR (qRT-PCR) is a very sensitive tool applied to the study of molecular factors involved in initiation of endometrial cancer and its progression (Burns et al. 2006) and it has been used to evaluate and identify several molecular markers associated with the stage of the cancer, its metastatic potential and prognosis (Wong et al. 2008, Porichi et al. 2009).

Before examining the transcript levels of FAAH and NAPE-PLD, the selection of an appropriate endogenous control reference gene (the paramount step in relation to measuring the relative expression of genes at the transcript level) was performed to ensure consistency and reproducibility of published data. The “Minimum Information for publication of Quantitative real time PCR Experiments” (MIQE) guidelines recommend that the justification of choice and number of reference genes should be an essential part of all qRT-PCR studies guaranteeing normalization of resulting data. The reference gene (“endogenous control gene”) should be one whose expression is stable in all samples, regardless of tissue type, disease state, progression and/or treatment (Dheda et al. 2005, Bonefeld et al. 2008). This normalization step compensates for any variations in experimental conditions, reagents or technique. A single “best” reference gene is therefore unlikely to be found in practice because almost all genes are modified under some conditions (Kubista et al. 2006). In previous qRT-PCR studies of

endometrial cancer, normalization was mostly performed with arbitrarily chosen reference genes, such as β -actin (ACTB) (Papageorgiou et al. 2009, Guida et al. 2010), glyceraldehyde-3-phosphate dehydrogenase (GAPDH) (Du et al. 2009, Kashima et al. 2009), or 18S RNA ribosomal unit 1 (18S rRNA) (Baldinu et al. 2007). Only a few studies (von Wolff et al. 2000, Walker et al. 2009, Vestergaard et al. 2011, Gebeh et al. 2012, Jursza et al. 2014) have evaluated the stability and suitability of some genes in this study environment, and certainly no studies have evaluated the stability of the genes presented here (32 panel of genes from TaqMan) as possible reference genes in qRT-PCR studies on endometrial cancer, despite the recommendation from the MIQE guidelines (Bustin et al. 2009). The aim of this part of the Chapter was therefore to robustly evaluate and identify the best reference genes for qRT-PCR amongst a comprehensive panel of 32 potential genes and then use them as controls for the measurement of the transcript levels for FAAH and NAPE-PLD.

Such qRT-PCR data will often indicate that a protein can be made by the cells from whence it was isolated, but will not confirm that the protein exists. Immunolocalisation of FAAH and NAPE PLD protein was performed as previously described (Brighton et al. 2009), allowing precise localisation of the enzymes in the tissue. Histomorphometric analyses of the tissue staining patterns (unbiased histoscore) allows the semi-quantitative analysis of protein distribution the different tissue components (stroma and epithelial cell), adding an additional layer of data for interpretation. Such methods have been validated and previously published on normal human endometrium (Taylor et al. 2010, Mehaseb et al. 2011, Nassar et al. 2011, Taylor et al. 2011, Gebeh et al. 2013) but not on endometrial carcinoma tissue.

3.1.1 Hypothesis

Since plasma NAE levels are elevated in endometrial cancer patients (Chapter 2) it is hypothesized that FAAH activity in the lymphocytes will be lower in patients with endometrial cancers compared to controls. Additionally, the expression of FAAH will be lower and NAPE-PLD expression increased in cancerous tissue when compared to that of atrophic endometrium. These differences will be more marked at the protein level for NAPE-PLD and FAAH in both groups.

3.1.2 Aims

- (A) To quantify FAAH enzyme activity in lymphocytes (whole blood sample) from patients with endometrial cancer and controls.
- (B) To determine the most stable validated endogenous control reference genes for qRT-PCR investigations
- (C) To find the relative levels of transcripts for the regulating enzymes FAAH and NAPE-PLD in normal and malignant endometrium.
- (D) To identify, localise and semi-quantitatively measure FAAH and NAPE-PLD immunoreactivity in the two types of tissue using histomorphometric measurements.

3.2 Materials and Methods

3.2.1 Recruitment and Subjects

All the volunteers gave written informed consent to take part in the study, which was approved and conducted according to the guidelines of Leicestershire and Rutland Research Ethics Committee (reference number 06/Q2501/49). Volunteers were post-menopausal women undergoing hysterectomy for endometrial carcinoma (study group) or a benign gynaecological condition, uterine prolapse (control group). Exclusion criteria were those women with concurrent or previous hormonal treatment, (such as hormone replacement therapy or the levonorgestrel intrauterine system) or currently on prescription or recreational drugs. Women with chronic medical conditions or any other type of cancer were also excluded.

This Chapter comprises four studies that examine the four aims stated in **section 3.1.2**. The numbers of samples used for each study are not identical and are shown in **Table 3-1**.

Table 3-1: Individual studies and the number of subjects/samples used

Individual studies	Controls (n)	Endometrial Cancers (n)	
		EC Type 1	EC Type 2
FAAH enzyme activity measurement in blood	Atrophic = 6	15	-
Endogenous control reference gene selection	Atrophic = 3 Proliferative = 3 Secretory = 3	Grade 1 = 3 Grade 2 = 3 Grade 3 = 3	Carcinosarcoma = 3 Serous = 3
Relative expression of NAPE-PLD and FAAH transcripts	Atrophic = 6	Grade 1 = 6 Grade 2 = 6 Grade 3 = 3	Carcinosarcoma = 3 Serous = 3
Immunohistochemistry & histomorphometric analysis of NAPE-PLD and FAAH proteins	Atrophic = 6	Grade 1 = 6 Grade 2 = 6 Grade 3 = 6	Carcinosarcoma = 6 Serous = 4

3.2.2 Quantification of the FAAH Enzyme Activity in Lymphocytes by Reverse Phase High Performance Liquid Chromatography (HPLC)

Venous blood (2.7 ml) was collected into pre-filled monovettes with acid citrate dextrose (ACD: blood ratio 1:10) anticoagulant. Samples were transported to the laboratory on ice and stored at -80°C for later investigation. FAAH activity in peripheral lymphocytes was kindly performed by Professor Mauro Maccarrone's team, (Department of Biomedical Sciences, Faculty of Veterinary Medicine, University of Teramo, and Teramo, Italy).

Lymphocyte membranes were prepared by the ice-cold hypotonic lysis method and by pelleting of resultant membranes at 11000 x g at 4°C for 20 mins (Maccarrone et al. 2000). The membranes were resuspended at a concentration of 1 mg/ml and 50 µg of membrane protein incubated with 10µM AEA-ethanolamine-1-[³H] (60 Ci/mmol; NEN DuPont de Nemours, Wilmington, DE, USA) for 15 min at 37°C. The reaction was stopped by the addition of 800 µl of ice-cold chloroform/methanol (1:2 v/v) and mixed thoroughly by vortex mixing. At this point, 240 µl of chloroform and 240 µl of dH₂O were added and the mixture vortexed again. After incubation at room temperature for 10 mins, the mixture was centrifuged at 3000 x g for 5 min and the aqueous layer discarded. The lower organic layer was dried by centrifugation in a DNA mini speedvac

at 100mbar at 30°C for 30 min. The dried lipids were dissolved in 50 µl of methanol and analysed by reverse phase HPLC. FAAH activity was expressed as pmol of product ($[^3\text{H}]\text{-AA}$) formed per min per mg of protein. HPLC was performed using a Nelson model 1022 Plus chromatograph equipped with a series 200 LC pump, an LC295 UV/VIS detector, and a Canberra Packard flow scintillation analyser (500 TR series) (Perkin-Elmer). The separations were carried out on a C18 (5 µm, 3.0 mm x 150 mm) column (Waters, Milford, MA, USA) with a mobile phase of methanol-water-acetic acid (85:15:0.1, v/v/v) at a flow rate of 0.8 ml/min. UltimaFlo M liquid scintillation cocktail (Perkin-Elmer) was mixed with the eluent at a 2:1 (v/v) ratio post column. The linearity and sensitivity of the online scintillation counting was determined from the peak areas of known amounts of $[^3\text{H}]\text{-AEA}$, with the limit of detection (signal-to-noise ratio > 4) being 0.5 fmol $[^3\text{H}]\text{-AEA}$ (0.12 nCi). The amounts of $[^3\text{H}]\text{-AEA}$ and $[^3\text{H}]\text{-AA}$ formed were calculated from the corresponding peak areas. The identity of the peaks was also assessed by UV detection of cold (unlabelled) standards at 204 nm (Maccarrone et al. 1998, Fezza et al. 2006, Gattinoni et al. 2010).

3.2.3 Identification of Endogenous Control Reference Genes for Normalizing Gene Expression Studies

In order to identify the correct endogenous reference genes, the gene primers and probes are conveniently supplied as a kit system. The system uniquely uses TaqMan® Chemistry.

3.2.3.1 Taqman® Chemistry

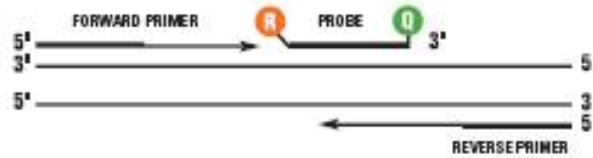
TaqMan® Chemistry, also known as fluorogenic 5' nuclease chemistry has many advantages (Table 3-2) and the steps involved are detailed in Figure 3-1.

Table 3-2: Advantages of TaqMan® Chemistry

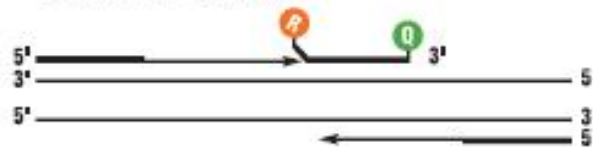
Features	TaqMan® Chemistry
Specificity	High
Sensitivity-Low Copies	1-10 copies
Reproducibility	High
Multiplexing	Yes
Pre-designed Assays	Yes
Gene Expression	High level of quantification

TAQMAN® PROBE-BASED ASSAY CHEMISTRY

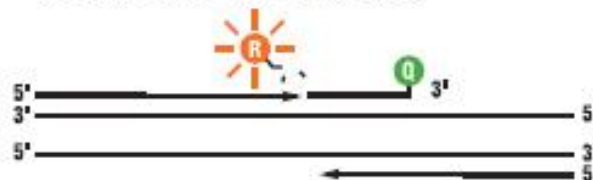
1. **Polymerization:** A fluorescent reporter (R) dye and a quencher (Q) are attached to the 5' and 3' ends of a TaqMan® probe, respectively.



2. **Strand displacement:** When the probe is intact, the reporter dye emission is quenched.



3. **Cleavage:** During each extension cycle, the DNA polymerase cleaves the reporter dye from the probe.



4. **Polymerization completed:** Once separated from the quencher, the reporter dye emits its characteristic fluorescence.

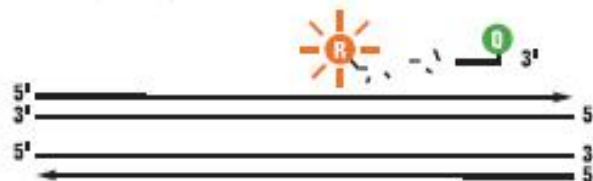


Figure 3-1: The steps involved in TaqMan® Chemistry. Adapted from applied Biosystems.

1. An oligonucleotide probe is constructed that contains a reporter fluorescent dye on the 5' end and a quencher dye on the 3' end. The proximity of the quencher dye greatly reduces the fluorescence emitted by the reporter dye by fluorescence resonance energy transfer (FRET), while the probes are still intact.
2. Once the target sequence is found, the probe anneals downstream from one of the primer sites and is cleaved by the 5' nuclease activity of Taq DNA polymerase as this primer is extended.
3. This cleavage of the probe results in two further important steps:

- a. It results in separation of the reporter dye from the quencher dye, thereby increasing the reporter dye signals
 - b. Removes the probe from the target strand, allowing the primer extension to continue to the end of the template strand. Therefore, the inclusion of the probe does not inhibit the overall PCR process.
4. With each cycle, additional reporter dye molecules are cleaved from their respective probes. This results in an increase in fluorescence intensity proportional to the amount of amplicon formed and the amount of DNA template present in the PCR (Clegg 1992, Heid et al. 1996).

In the initial cycles of PCR, there is little change in fluorescence signal and this defines the baseline for the amplification plot. An increase in fluorescence above the baseline indicates the detection of accumulated target. A fixed fluorescence threshold can be set above the baseline called the C_T (threshold cycle) and is this intersection between an amplification curve and a threshold line that provides a relative measure of the concentration of target in the PCR.

3.2.3.2 Taqman® Array 96-Well Fast Plates

The TaqMan® Array 96-Well Fast Plates Plus Candidate Endogenous Control Genes were purchased from Life Technologies, (Paisley, UK). Quantitative Real-Time PCR experiments were performed using validated human endogenous control assay TaqMan® Array 96-Well Plates consisting of 32 reference genes (see **Table 3-3**); (Bustin et al. 2009). Each TaqMan® Gene Expression Assay consisted of a fluorogenic carboxyfluorescein (FAM™) dye-labelled minor groove binder (MGB) probe and two amplification primers (forward and reverse) provided in a pre-formulated 20x mix; 1x final concentrations were 250 nM for the probe and 900 nM for each primer. Each assay had an amplification efficiency of $100 \pm 10\%$ (Technologies). The 96 well plates were Format 32, i.e. each plate contains *three sets* of one manufacturing control (18S rRNA) and 31 expression assays. The TaqMan® Array 96-Well Fast Plates Assay ID and the Gene names and accession numbers are shown in **Table 3-3**.

Table 3-3: TaqMan® Endogenous Control Genes Assay ID, gene names and accession numbers

Gene ID	Gene name	Accession number	Life Technologies assay ID
RPLPO	Ribosomal protein, large, PO	NM_001002	Hs99999902_m1
ACTB	Actin, beta	NM_001101	Hs99999903_m1
PPIA	Peptidylpropyl isomerase A (cyclophilin A)	NM_021330	Hs99999904_m1
PGK1	Phosphoglycerate kinase	NM_000291	Hs99999906_m1
B2M	Beta-2-microglobulin	NM_004048	Hs99999907_m1
GUSB	Glucuronidase, beta	NM_000181	Hs99999908_m1
HPRT1	Hypoxanthine phosphoribosyl transferase	NM_000194	Hs99999909_m1
TBP	TATA box-binding protein	M34960	Hs99999910_m1
18S	Eukaryotic 18S ribosomal RNA	X03205	Hs99999901_s1
GAPDH	Glyceraldehyde-3-phosphate dehydrogenase	NM_002046	Hs99999905_m1
TFRC	Transferrin receptor (P90, CD71)	NM_003234	Hs99999911_m1
IPO8	Importin 8	NM_006390	Hs00183533_m1
POLR2A	Polymerase (RNA) II (DNA-directed) polypeptide A	NM_000937	Hs00172178_m1
UBC	Ubiquitin C	NM_021009	Hs00824723_m1
YWHAZ	Tyrosine 3-monooxygenase/tryptophan 5-monooxygenase activation protein, zeta polypeptide	NM_003406	Hs00237047_m1
HMBS	Hydroxymethylbilane synthase	NM_000190	Hs00609297_m1
CASC3	Cancer susceptibility Candidate 3	NM_007359	Hs00201226_m1
CDKN1A	Cyclin-dependent kinase Inhibitor 1A (p21, Cip1)	NM_000389	Hs00355782_m1
CDKN1B	Cyclin-dependent kinase Inhibitor 1B (p27, Kip1)	NM_004064	Hs00153277_m1
GADD45A	Growth arrest and DNA- damage- include, alpha	NM_001199741	Hs00169255_m1

<i>PUM1</i>	Pumilio homolog 1(Drosophila)	NM_001020658	Hs00206469_m1
<i>PSMC4</i>	Proteasome (prosome, Macropain) 26S subunit, ATPase, 4	NM_006503	Hs00197826_m1
<i>EIF2B1</i>	Eukaryotic translation initiation factor 2B, subunit 1 alpha, 26 kDa	NM_001414	Hs00426752_m1
<i>PES1</i>	Pescadillo homolog 1, containing BRCT domain (zebra fish)	NM_001243225	Hs00362795_g1
<i>ABL1</i>	V-abl Abelson murine leukemia viral oncogene homolog 1	NM_005157	Hs00245445_m1
<i>ELF1</i>	E74-like factor 1 (ets domain transcription factor)	NM_001145353	Hs00152844_m1
<i>MT-ATP6</i>	Mitochondrially encoded ATP synthase 6	NC_012920	Hs02596862_g1
<i>MRPL19</i>	Mitochondrial ribosomal protein L19	NM_014763	Hs00608519_m1
<i>POP4</i>	Processing of precursor 4, ribonuclease P/MRP subunit (<i>S. cerevisiae</i>)	NM_006627	Hs00198357_m1
<i>RPL37A</i>	Ribosomal protein L37a	NM_000998	Hs01102345_m1
<i>RPL30</i>	Ribosomal protein L30	NM_000989	Hs00265497_m1
<i>RPS17</i>	Ribosomal protein S17	NM_001021	Hs00734303_g1

3.2.3.3 Reagents, Buffers and Solutions

The RNAlater®, High Capacity cDNA Reverse Transcriptase Kit with RNase Inhibitor, TaqMan Gene Expression Master Mix, Turbo-DNA *free* Kit, *mirVana* miRNA Isolation Kit, PCR graded water and MicroAmp® Optical Adhesive Film were all purchased from Life Technologies, (Paisley, UK). The TaqMan® genes Expression Assay FAAH (Hs01038660_m1), NAPE-PLD (Hs00419593_m1) and CB1 (Hs00275634_m1) were purchased from Applied Biosystem (Life Technologies), as FAM/MGB dye-labelled probes. The ‘in-house’ validated Taqman endogenous control reference genes used for normalization of the above genes of interest during qRT-PCR were all 4,7,2'-trichloro-7'-phenyl-6-carboxyfluorescein (VIC)/6-carboxytetramethylrhodamine (TAMRA) dye-labelled assays purchased from Applied Biosystem (Life Technologies). They were MRPL19 (Hs00608519_m1), PPIA (Hs99999904_m1) and IPO8 (Hs00183533_m1).

3.2.3.4 Preparation and Storage of Endometrial Tissues

Fresh uteri were transported on ice to the hospital Histopathology Department where endometrial biopsies were obtained and a consultant gynaecological histopathologist divided the biopsies into two; one for this study and the other for histological confirmation of diagnosis. The biopsy for study was washed with phosphate buffered saline (PBS) to remove excess blood and stored in RNAlater® (Life Technologies, Paisley, UK) at -80°C for further processing.

3.2.3.5 RNA Extraction and cDNA Synthesis

Endometrial tissues (100 mg) were disrupted and homogenised using a TissueRuptor homogeniser (Qiagen Crawley, UK) in lysis/binding buffer (1ml lysis/binding buffer solution per 100 mg of tissues (miRNA Isolation Kit) at medium speed for 60 seconds on ice. The tissue was homogenised until all visible 'clumps' were dispersed and total RNA extracted using the *mirVana*TM miRNA Isolation Kit (Life Technologies, Paisley, UK) according to the manufacturer's protocol. Total RNA was quantified and its purity determined using a NanoDrop 2000c spectrophotometer (Thermo Scientific, Detroit, MI, USA) and genomic DNA digested by treating with a TURBO-DNase free kit (Life Technologies, Paisley, UK). At this point, the RNA concentration was standardised to 10 µg/100 µl, incubated at 37°C for 30 min, the reaction inactivated with 10µl of inactivation buffer (supplied in the TURBO-DNase free kit) and the solution centrifuged for 90 seconds at 10,000 x g. The supernatants containing total cellular RNA (1 µg) were subjected to first strand complementary DNA (cDNA) synthesis using the high capacity cDNA MultiScribeTM Reverse Transcriptase Kit (Life Technologies, Paisley, UK) according to the manufacturer's protocol; the contents of the reverse transcription reaction are shown in **Table 3-3**. Incubation occurred with oligo-dT₁₆ as the primer at 25°C for 10 min, 37°C for 120 min, 85°C for 5 min and then cooled to 4°C. The cDNA was stored at -20°C. The contents of the reverse transcription reactions are shown in **Table 3-4**.

3.2.3.6 Quantitative Real-Time PCR

All the reactions for the endogenous control study were performed in a final volume reaction of 20µl consisting of 2 µl of cDNA, 8 µl of DNase-free water and 10 µl of TaqMan® Universal PCR Master Mix. For the PCR reaction of individual genes of interest, the PCR sample reaction consisted of: TaqMan® universal PCR Master Mix (10µl), endogenous control reference gene (1 µl), gene of interest (1 µl), PCR graded water (6 µl) and sample (cDNA) (2 µl) making a total volume of 20 µl. RT-(minus) and no template controls (NTC), containing DNase-free water instead of template mRNA, were included in each run. No product was synthesized in the NTC and RT-(minus) controls, confirming the absence of contamination with exogenous DNA. The plates were run on an Applied Biosystem's StepOne Plus instrument (Life Technologies, Paisley, UK) and the thermal cycler profile was as follows: 2 min at 50°C, 10 min at 95°C, 40 cycles of 15 seconds at 95°C and 1 min at 60°C. All the reactions for the reference genes were performed in triplicate (both biological and technical).

Table 3-4: The contents of the reverse transcription reactions, reagents and volumes needed to create cDNA from the total RNA samples.

	RT (+VE) sample	RT (-VE) sample
10 x RT Buffer	4µl	4µl
dNTP Mix	1.6µl	1.6µl
10 x Random Primers	4µl	4µl
Multiscribe Reverse Transcriptase Enzyme	2µl	-
RNase Inhibitor	2µl	2µl
PCR Graded Water	6.4µl	8.4µl
Sample - cDNA	20µl	20µl
Total	40µl	40µl

3.2.3.7 Software Determination of Reference Gene Stability

Gene expression stability was evaluated using three universally available mathematical software packages: geNorm^{PLUS} version 2.2. incorporating the updated version of qbase^{PLUS2} (available from <https://www.biogazelle.com/qbaseplus>) (Biogazelle,

Zwijnaarde, Belgium) (Hellemans et al. 2007), NormFinder version 0.953 (*NormFinder* 2005) (available from Aarhus University, Denmark; <http://moma.dk/normfinder-software>) and BestKeeper (Pfaffl et al. 2004) (available from <http://www.gene-quantification.com/bestkeeper.html>; accumulated standard deviation data obtained from the NormFinder algorithm were incorporated into GenEx software version 5.3.6.170 (2011) (available from <http://www.multid.se/contact.php>). Details of the statistical methods used by both qbase^{PLUS2} and NormFinder have been described elsewhere (Andersen et al. 2004, Beekman et al. 2011, Pinto et al. 2012).

3.2.3.8 Stability of the Chosen Reference Gene

The mRNA gene expression stability analysis for the 32 endogenous reference control genes was obtained using the mean qRT-PCR threshold cycle (Ct) value, defined as the number of cycles required for the fluorescent signal to cross the threshold (i.e. 0.5SD above background levels). The Ct values obtained were converted into quantitative relative expression values using the $2^{-\Delta\Delta Ct}$ method (Penna et al. 2011).

3.2.3.9 Expression and Relative Quantification of FAAH and NAPE-PLD

The expression of FAAH and NAPE-PLD was determined relative to the geometric mean of the expression of three endogenous control reference genes (MRPL19, PPIA and IPO8) identified in the studies outlined above. The relative expression for each gene of interest was calculated using the following formula:

1. Endogenous Control Reference Gene = (geometric mean of MRPL19, PPIA and IPO8 Ct values).
2. ΔCt value: Gene of interest – Endogenous Control Reference Gene.
3. Average ΔCt values between experiments.
4. $\Delta\Delta Ct$ values: Delta Ct experiment – Delta Ct control.
5. Relative expression of the gene of interest using the equation: $2^{(-\Delta\Delta Ct)}$.

3.2.4 Identification, Localisation and Histomorphometric Analysis of FAAH and NAPE-PLD Protein

Immunolocalisation of the FAAH and NAPE-PLD immunoreactivity was performed using commercially available antibodies against FAAH and NAPE-PLD proteins, and with standard immunohistochemistry protocols as described previously (Brighton et al. 2009).

3.2.4.1 Reagents and Solutions for Immunohistochemistry (IHC)

Table 3.5 shows the reagents used in the experiments and their sources together with the concentration of the primary antibody supplied for NAPE-PLD.

Table 3-5: Chemicals used for the IHC studies and their sources.

Product	Sources
Xylene and industrial methylated spirit (IMS)	Genta Medical, York, UK.
Mayer's haematoxylin	Sigma-Aldrich Ltd, Dorset, UK.
Hydrogen peroxide	Fisher Scientific, Loughborough, UK.
Methanol	Fisher Scientific, Loughborough, UK.
Normal goat serum	Vectorlabs, Peterborough, UK.
Avidin-biotin kit	Vectorlabs, Peterborough, UK.
ABC detection system	Vectorlabs, Peterborough, UK.
3,3'-diaminobenzidine (DAB)	Vectorlabs, Peterborough, UK.
XAM mounting medium	BDH, Dorset, UK.
Primary antibodies Anti-NAPE-PLD (Rabbit Polyclonal - HPA024338- (concentration – 0.05 mg/ml)	SIGMA Life Science. Stockholm, Sweden
Anti-FAAH (antiserum) rabbit polyclonal antibody (FAAH11-S)	Alpha Diagnostics International, San Antonio, TX, USA.
Biotinylated secondary anti-rabbit antibody	Vectorlabs, Peterborough, UK.

3.2.4.2 Tissue Preparation

Tissue blocks (endometrial carcinoma and control) were obtained from the hospital Histopathology Department. The samples for IHC were provided as 4 µm thick sections cut on a microtome and placed onto saline-coated slides. After drying, representative sections were first subjected to haematoxylin and eosin (H & E) staining for histological confirmation of disease or normality. This was kindly performed by the gynaecological pathology consultant.

3.2.4.3 FAAH Immunohistochemistry

Paraffin embedded tissues slides were dewaxed in xylene and re-hydrated through graded alcohols by placing in 100% industrial methylated spirits (IMS), then 95%, then 90%, then 80%, then 70% and then 50% IMS and finally placed into dH₂O. This was performed for 4 minutes for each solution. To suppress endogenous peroxidase activity, slides were then incubated in 6% hydrogen peroxide (H₂O₂) (51 ml H₂O₂ and 249 ml of iced cold water) for 10 min. Following that, sections were washed in running tap water for 5 min and then placed in tris-buffered saline (TBS) /1% bovine serum albumin (BSA) for 5 min. Non-specific binding sites were blocked by applying 100µl of normal goat serum (NGS) 1:10 (diluted in TBS/1%BSA) to each slide at room temperature (RT) for 20 min. Slides were then drained and avidin blocking solution (4 drops/ml avidin in 10% NGS/TBS/1% BSA) applied for 15 min at RT. The avidin blocking solution was washed away in TBS for 20 min and a biotin blocking solution (4 drops/ml biotin in 10% NGS/TBS/1% BSA) applied for 15 min. Following that, excess liquid was drained from each slide and 100µl of FAAH antibody (1:2000 dilution in 10% NGS/TBS/1% BSA) applied to test slides and rabbit IgG 1:2000 (diluted in 10% NGS/TBS/1% BSA) applied to control slides and incubated overnight at 4 °C in a humid chamber.

The next day, the slides were washed in TBS/1% BSA for 20 min in a sandwich box on a magnetic stirrer set at a moderate mixing rate ensuring that the rabbit IgG slides (negative controls) and the positive FAAH slides were washed separately. After wiping around the tissue section, 100µl of the biotinylated goat anti-rabbit secondary antibody (diluted 1:400 in TBS), was applied to each slide and incubated for 30 min at RT. To remove unreacted secondary antibody, slides were washed in TBS/1% BSA for 20 min,

before horseradish-peroxidase conjugated avidin-biotin complex (ABC Elite, Vector Labs, Peterborough, UK.) was applied for 30 min (made up in TBS at least 30 min before use: 2.5ml TBS, 1 drop A, 1 drop B; then mixed). Again, the slides were washed in TBS/1% BSA for 20 min and incubated with 100 μ l/section of 3,3'-diaminobenzidine (DAB) (2.5 ml dH₂O, 1 drop buffer, 1 drop H₂O₂) and vortexed, and 2 drops DAB added and mixed by inversion) for 5 min. Excess DAB was removed from the racked slides by washing them in tap water for 5 min. Sections were counterstained by immersion in Mayer's haematoxylin for 1 min and rinsed in tap water until the "blue" water ran clear. Finally, the slides were dehydrated through the graded alcohols, cleared in xylene (3 min/step) and mounted in XAM mounting medium.

3.2.4.4 NAPE-PLD Immunohistochemistry

The immunohistochemistry protocol for NAPE-PLD was similar to that for FAAH, but contained some important differences. After the slides were dewaxed in xylene and re-hydrated through the different concentrations of alcohol to water (4 min per step) they were transferred to 500 ml of citrate buffer (10 mM citric acid pH6.0) in a plastic container and microwaved at 700 Watts for 20 min. After cooling for exactly 20 min in the microwave, the racked slides were placed in de-ionised water for 5 min and endogenous peroxidase activity blocked with 0.3% H₂O₂ in ice cold-ethanol (95%) for 5 min. Following that, the racked slides were transferred to TBS-Tween₂₀ for 5 min, the sections wiped around with paper tissue, placed in a humidity chamber and then blocked with 100 μ l/section of NGS (5%) in TBS for 30 min at room temperature. Avidin solution (100 μ l/section) was then added (4 drops/ml of 1:20 NGS/TBS) for 15 min and the slides re-racked and washed in TBS-Tween₂₀ for 5 min twice before the addition of 100 μ l/section of biotin solution (4 drops/ml of 1:20 NGS/TBS) for 15 min. Finally, the slides were drained and incubated with 100 μ l/section of primary antibody (anti-NAPE-PLD) that was diluted at 1:50 in blocking solution (1:20 NGS/TBS), whilst 100 μ l/section of rabbit IgG, (1:50 in 1:20 NGS/TBS) was added to IgG control slides and then all were incubated at RT overnight.

The following day, the slides were washed in TBS/Tween₂₀ in a sandwich box on a magnetic stirrer set at a moderate mixing rate for 20 min, the sections were wiped around with paper tissue and incubated with 100 μ l/section of biotinylated goat anti-rabbit antibodies diluted 1:400 in TBS for 30 min. The slides were then washed in

TBS/Tween₂₀ for 20 min and then incubated with 100 µl/section of ABC Elite complex (1 drop A and 1 drop B, added to 2.5 ml TBS, vortexed and made up 30 min before use). After 30 min, slides were washed in TBS/Tween₂₀ for 20 min, then incubated with 100 µl/section of DAB (2.5 ml dH₂O, 1 drop buffer, 1 drop H₂O₂ and vortexed, then 2 drops DAB added) for 5 min. The slides were racked again and washed in tap water for 5 min, counterstained by immersion in Mayer's haematoxylin for 1 min and rinsed in tap water until the "blue" water ran clear. Finally, the slides were dehydrated through graded alcohols, cleared in xylene (3 min/step) and mounted in XAM mounting medium.

3.2.4.5 Image Capture and Evaluation of Immunohistochemical Staining

Images were taken on an Axioplan transmission microscope equipped with a Sony DXC-151P analogue camera (Sony Corp., Japan). The camera was connected to a computer running image capture and processing software (Axiovision version 4.4; Carl Zeiss Ltd., Hertfordshire, UK). All images were captured at a 200X magnification using daylight and medium neutral density filters with the lamp set at 6400K (Taylor et al. 2010). Percentage positivity and immunoreactive histoscore (H-score) was evaluated by taking 10 random fields per slide. These images were analysed using the image analysis software, ImageScope version 10.2.2.2319 (Aperio Technologies, Inc, USA). This software has been shown to be substantively equivalent to using other manual light microscopy methods by an experienced pathologist (Nassar et al. 2011). The areas of interest, e.g. epithelium and the glands were outlined using the positive pen tool within ImageScope and thus selected for subsequent analysis (**Figure 3-2**). Artefacts were excluded from analysis using the negative pen tool. The positive pixel count algorithm version 9.1 was used for quantitative evaluation of immunohistochemical staining. Default settings provided by the software were used and pixel counts automatically calculated and displayed as brown for strong positive, red for normal positivity, yellow for weak positivity and blue for negative staining (**Figure 3-2**). Positivity was measured as a fraction of the total stained area. This image analysis software has been validated by previous studies (Taylor et al. 2010, Taylor et al. 2011, Gebeh et al. 2012).

The following parameters were used to generate the H-score:

N_{wp} = total number of weak positives

N_{sp} = total number of strong positives

N_{np} = total number of normal positives

N_p = total number of positives = $N_{wp} + N_{sp} + N_{np}$

N_n = total number of negatives

NT = total count ($N_{sp} + N_{wp} + N_{np} + N_n$)

Immunoreactivity was assessed semi-quantitatively by assigning scores as 0 (no staining), 1 (weak staining), 2 (moderate staining) and 3 (strong staining) as determined by the software for the image analysis. Therefore, the immunohistochemical score (histoscore or H-score) was calculated using the formula: $H\text{-score} = [300 \times (N_{sp}/NT)] + [200 \times (N_{np}/NT)] + [100 \times (N_{wp}/NT)] + [0 \times (N_n/NT)]$

The maximum possible score is 300, where 100% of the tissue section is strongly stained (N_{sp}) for the protein of interest.

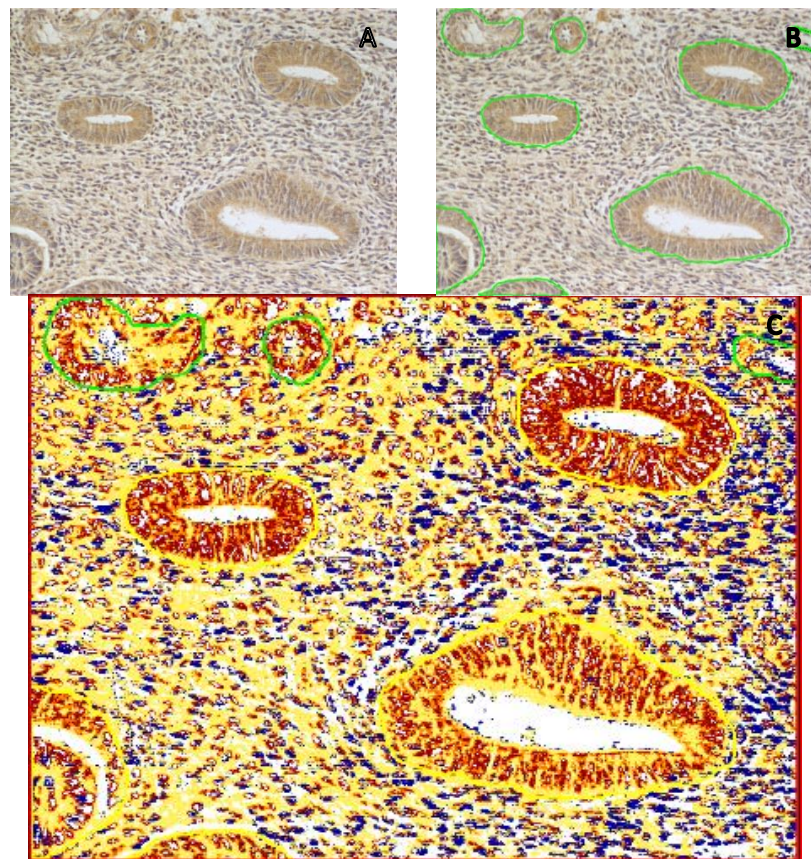


Figure 3-2: Illustration of FAAH immunohistochemical staining of atrophic tissues and how the Imagescope software image analysis system was used.

Panel A shows the original FAAH IHC image as loaded into the software. Panel B shows where the glands were selected using the positive analysis pen tool (solid green lines), and the

capillaries were de-selected using the negative analysis pen tool (dotted green lines – upper part of image). Panel C shows the software mark-up of the image, with the brown colour indicating strongly stained tissue, the orange colour indicating stained tissue, the yellow colour indicating weakly stained tissue, the blue colour indicating unstained tissue and white areas indicating parts of the slide where there was no tissue detected. Note, the solid green lines (in panel B) have turned yellow (in panel C) and the boundary of entire image red. These allow the ‘switching’ between glands and stroma to determine the final histoscore. The lines surrounding blood vessels remain green, showing that they have been omitted from the analyses.

3.2.5 Statistical Analysis

Statistical analysis of the stability of putative reference genes and ranking was provided by geNorm qBasePLUS, NormFinder and BestKeeper. Statistical analysis for the relative expression of mRNA and protein level data, the detection of outliers (Grubb’s test) and correlation analyses were performed using Prism version 6.00 for windows (GraphPad Software, San Diego CA, USA, www.graphpad.com). Data that did not follow a Gaussian distribution were expressed as medians and inter-quartile range (IQR) and comparison between groups performed using one-way analysis of variance (ANOVA) followed by the appropriate ad hoc post analysis or Mann-Whitney U-test. Conversely, if the data that were consistent with a normal distribution they were analysed by the parametric one-way ANOVA with Dunnett’s ad hoc post analysis or Student’s unpaired t-test. In all cases, $P < 0.05$ was considered to be significant.

3.3 Results

3.3.1 Selection of Endogenous Control Reference Genes

Arbitrary selection of endogenous control reference genes for normalization in qRT-PCR studies of EC, without validation, risks the production of inaccurate data and should therefore be discouraged. The first aim in the PCR study was therefore to identify and evaluate from the 32 possible reference genes from the TaqMan array panel those suitable to be used as internal control reference genes for this cohort of subjects.

3.3.1.1 Patient Characteristics

Table 3-6 shows some of the characteristics of the volunteers. There were no statistically significant differences in age and BMI between the controls (atrophic endometrium) and cancer patients.

3.3.1.2 RNA Concentration and Purity

The purity of the extracted RNA, as measured with a Nanodrop spectrophotometer, indicated good quality RNA with a mean ratio (\pm SD) absorbance of 2.10 ± 0.31 (OD A_{260}/A_{280} ratio), indicating that all the samples were free from proteins potentially accruing during the RNA extraction step. The mean absorbance ratio (\pm SD) at 260nm and 230nm was 2.19 ± 0.43 (OD A_{260}/A_{230} ratio) indicating that samples were free from reagent contaminants. The average yield of RNA after the extraction was 1.17 ± 0.61 $\mu\text{g}/\mu\text{l}$ (mean \pm SD), and ranged between 0.125 and 3.038 $\mu\text{g}/\mu\text{l}$.

Table 3-6. Patient Characteristics

Patient Group	Age in years (Mean \pm SD)	BMI in Kg/m ² (Mean \pm SD)
Normal (n=3)		
Atrophic Endometrium	62.33 \pm 4.61	26.67 \pm 6.42
Secretory Phase	46.00 \pm 4.35	26.00 \pm 1.00
Proliferative Phase	47.33 \pm 0.57	26.00 \pm 1.73
Endometrial Carcinoma Type 1 (n=3)		
Grade 1	78.00 \pm 13.23	31.33 \pm 6.65
Grade 2	67.67 \pm 11.06	30.67 \pm 1.52
Grade 3	72.67 \pm 12.06	35.33 \pm 6.11
Endometrial Carcinoma Type 2 (n=3)		
Serous	59.00 \pm 3.46	37.67 \pm 2.51
Carcinosarcoma	50.00 \pm 5.00	36.67 \pm 6.42

Age and BMI of women were analysed using one-way analysis of variance with Dunnett's multiple comparisons test with women with atrophic endometrium used as the control. None of the data show statistically significant differences among groups.

3.3.1.3 Analysis of Reference Gene Stabilities via the GeNorm PLUS Algorithm

The geNorm^{PLUS} (q base^{PLUS2}) algorithm determines the medium reference target stability measure (M), as the average pair-wise variation of each reference gene in relation to all the other reference genes enabling the elimination of the least stable gene. This is followed by recalculation of the M values resulting in ranking of the most stable genes, i.e. the lower the M value, the higher the gene stability. The software indicates that a good stable reference gene should have an average geNorm M value ≤ 1.0 in a heterogeneous set of samples (Hellemans et al. 2007). Using geNorm^{PLUS} (q base^{PLUS2})

the rank order of the reference genes evaluated (from least stable to most stable) is shown in **(Figure 3-3)**. Analysis of the rank order indicated that *MRPL19* and *PPIA* ($M \leq 1.0$) were the two most stable genes in normal and malignant endometrial samples, and the two least stable genes were *RPL30* and *18S*. The commonly used β -actin (*ACTB*) and *GAPDH* reference genes were in the least stable ($M \geq 1.0$) category, with M-values of 1.387 and 1.150, respectively.

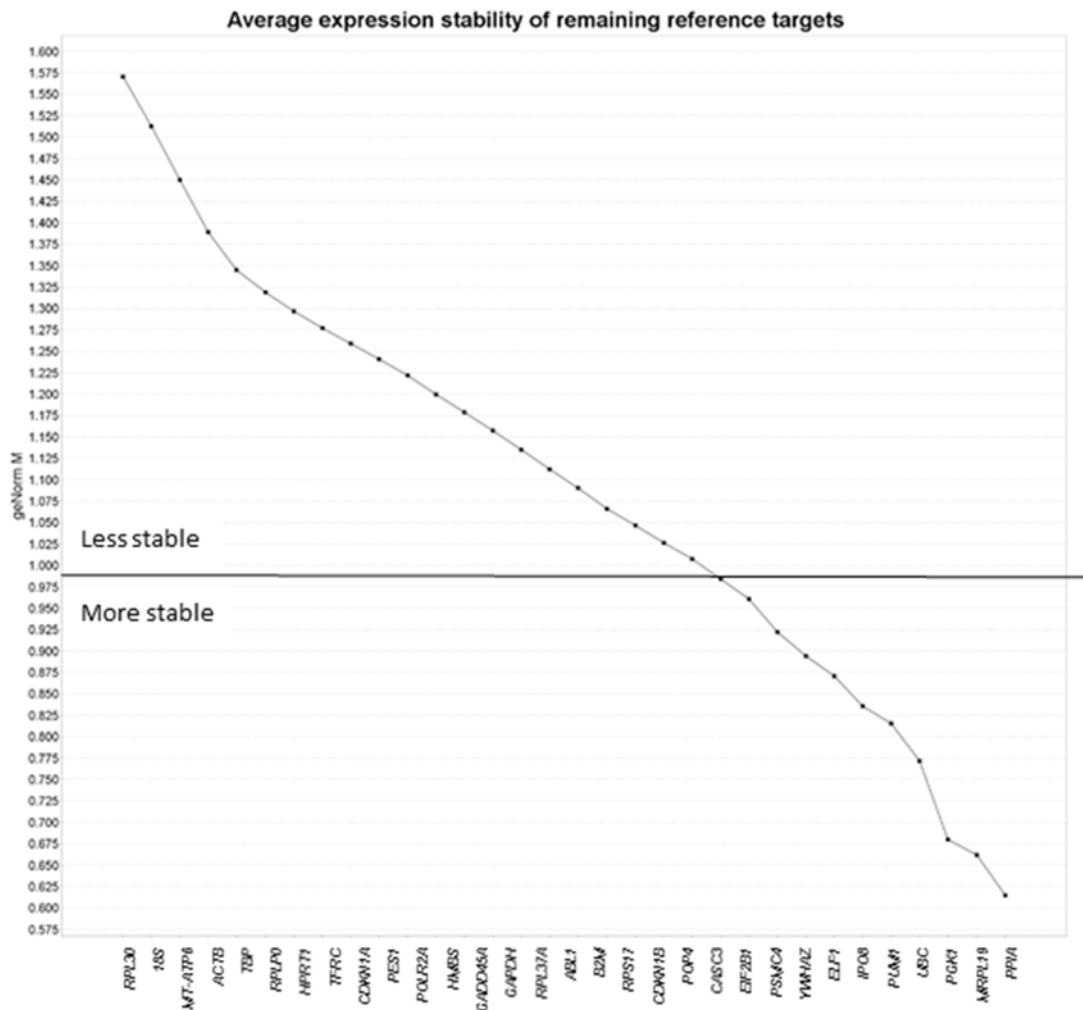


Figure 3-3: geNorm analyses of reference genes.

Medium reference target stability values (average geNorm $M \leq 1.0$) are shown. Average expression stability values (M, y-axis) of 32 reference genes (x-axis) and the associated ranking from least to most stable expression (left to right). Results are presented according to the output file obtained from qBasePLUS2 software. The $M \leq 1.0$ of average expression stability indicates more stable expression, using both normal (n=9) and malignant (n=15) endometrial samples. The gene names are: 18S RNA ribosomal unit 1 (*18S*), V-abl Abelson murine leukemia viral oncogene homolog 1 (*ABL1*), beta actin (*ACTB*), beta 2-macroglobulin (*B2M*), cancer susceptibility candidate 3 (*CASC3*), cyclin-dependent kinase inhibitor 1A (*CDKN1A*), cyclin-dependent kinase inhibitor 1B (*CDKN1B*), eukaryotic translation initiator factor 2B, subunit 1

alpha (*EIF2B1*), E74-like factor 1 (*ELF1*), alpha growth arrest and DNA-damage include (*GADD45A*), glyceraldehyde-3-phosphate dehydrogenase (*GAPDH*), beta glucuronidase (*GUSB*), hydroxymethylbilane synthase (*HMBS*), hypoxanthine phosphoribosyl transferase (*HPRT1*), importin 8 (*IPO8*), mitochondrial ribosomal protein L19 (*MRPL19*), mitochondrially encoded ATP synthase 6 (*MT-ATP6*), Pescadillo homolog 1 (*PESI*), phosphoglycerate kinase (*PGK1*), Polymerase (RNA) II (DNA-directed) polypeptide A (*POLR2A*), processing of precursor 4 (*POP4*), peptidylpropyl isomerase A (cyclophilin A) (*PPIA*), proteasome 26S subunit, ATPase, 4 (*PSMC4*), Pumilio homolog 1 (Drosophila) (*PUM1*), ribosomal protein L30 (*RPL30*), ribosomal protein 37A (*RPL37A*), ribosomal protein, large, P0 (*RPLP0*), ribosomal protein S17 (*RPS17*), TATA box-binding protein (*TBP*), transferrin receptor (*TFRC*), ubiquitin C (*UBC*) and tyrosine 3-monooxygenase (*YWHAZ*).

Furthermore, the $\text{geNorm}^{\text{PLUS}}$ ($\text{q base}^{\text{PLUS}^2}$) algorithm was used to calculate the minimum number of genes required for a reliable normalization factor, using the pairwise variation V_n / V_{n+1} between two sequential normalization factors (NF), NF_n and NF_{n+1} . In addition, this software defines a pairwise variation of 0.15 as the optimal cut off value, below which the inclusion of an additional reference genes is unnecessary (**Figure 3-4**) (Hellemans et al. 2007). Gene stability analysis revealed that the optimal number of reference targets was 5 genes ($\text{geNorm } V < 0.15$ when comparing a normalization factor based on the 5 or 6 most stable targets). $\text{geNorm}^{\text{PLUS}}$ ($\text{qbase}^{\text{PLUS}^2}$) thus predicted that the optimal normalization factor would be the geometric mean of the reference targets *PUM1*, *UBC*, *PGK1*, *MRPL19* and *PPIA* when based on the 5 most stable genes, or *IPO8*, *PUM1*, *UBC*, *PGK1*, *MRPL19* and *PPIA* when based on the 6 most stable reference gene targets.

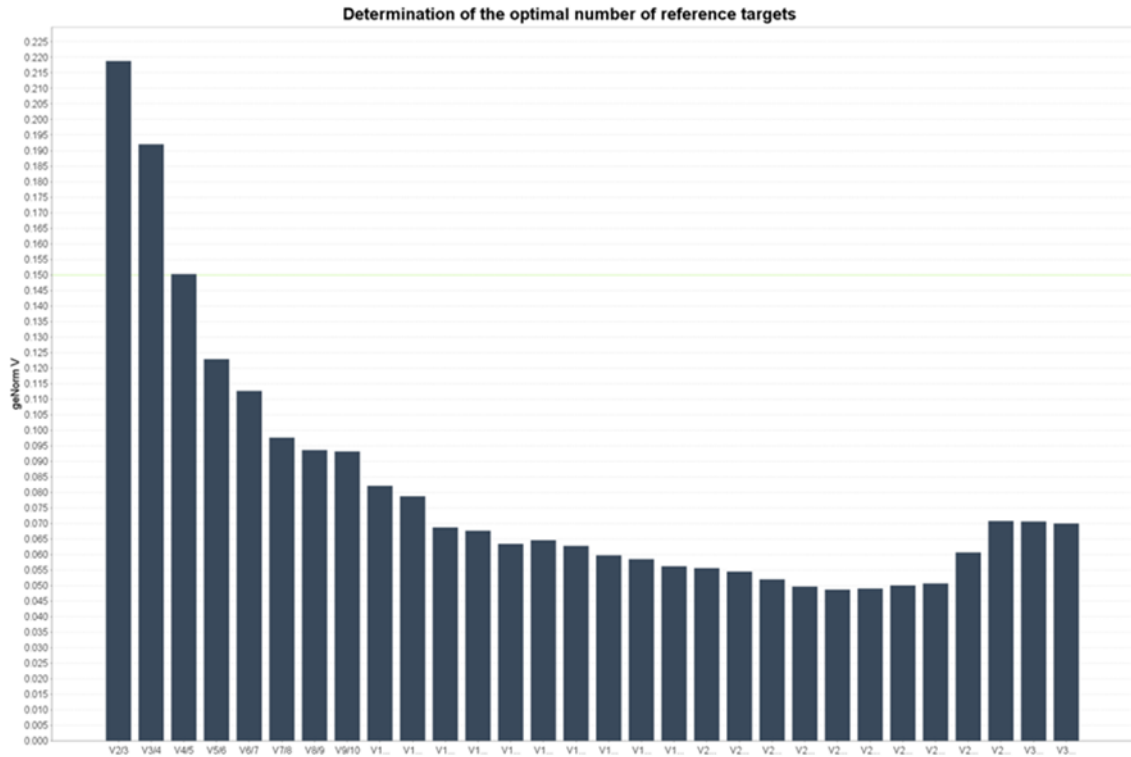


Figure 3-4: geNorm^{PLUS} analysis of 32 reference genes.

Results are presented according to the output file obtained from qBase^{PLUS2}. Determination of the optimal number of reference genes for normalization depends on pair-wise variation (V) analyses, using both normal (n=9) and malignant (n=15) endometrial samples. The x-axis represents the incremental combination of reference genes from V2/3 to V31/32. The most stable combination with the least number of genes is V4/5 and V5/6. The threshold is noted at 0.15 geNorm V by a horizontal line.

3.3.1.4 Analysis of Reference Gene Stability via the NormFinder Algorithm

NormFinder uses a mathematical model (Andersen et al. 2004, *NormFinder* 2005), which takes into consideration the intergroup and intragroup expression variations (stability) and then ranks them in order such that the lower the stability value is, the better the reference gene or reference gene combination. NormFinder selected mitochondrial ribosomal protein L19 (*MRPL19*) with a stability value of 0.5353 as the single most stable gene and indicated that the best combination of two genes was importin 8 (*IPO8*) and cyclophilin A (*PPIA*) with a stability value of 0.3824 (**Figure 3-5**).

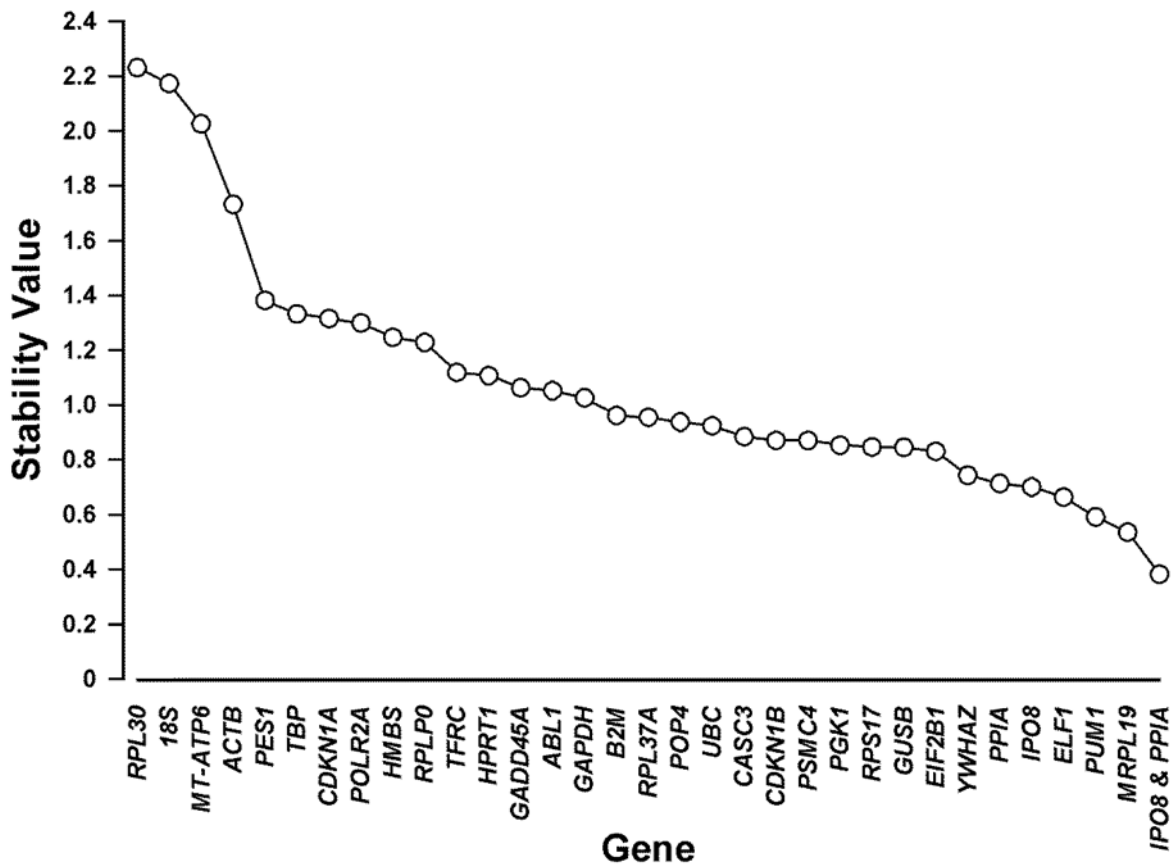


Figure 3-5: Stability values for the 32 endogenous ‘housekeeping genes’ as ranked by NormFinder.

High expression stability is shown by a low stability value as an evaluation of the combined intergroup and intragroup variations of the individual reference genes, thus the most stable genes are to the right. NormFinder also calculated that most stable gene combination was IPO8 and PPIA. Both normal (n=9) and malignant (n=15) endometrial samples were used.

3.3.1.5 Analysis of Reference Gene Stability via the BestKeeper Algorithm

BestKeeper is a widely available software package used to generate the best stable reference genes, but has a limitation in that it can only work with a maximum of 10 genes. Therefore, following the geNorm and NormFinder analyses for the most stable gene expression, the best 10 candidate reference control genes (*MRPL19*, *ELF1*, *PPIA*, *PUM1*, *YWHAZ*, *PGK1*, *GUSB*, *IPO8*, *UBC* and *EIF2B1*) were chosen for assessment using the BestKeeper algorithm. Since BestKeeper calculates SD and the coefficient of variance (CV) based on raw Ct values, the average Ct values for each gene were calculated and imported to the Microsoft Excel-based BestKeeper application (Pfaffl et al. 2004), where a SD < 1 indicates putative stably expressed genes. The software

estimates the BestKeeper index (BI) as the geometric mean of the stable control genes' Ct values and then creates pair-wise correlations between each gene and the BI. Reference genes with the highest Pearson correlation coefficient ($r \sim 1$) and probability (p) < 0.05 (**Table 3-7**) are then considered to be most stable.

The best correlation between one endogenous reference control gene and the BI was obtained for *MRPL19* ($r=0.98$), followed by *ELF1*, *PPIA*, *PUM1* and *YWHAZ*, *PGK1*, *GUSB*, *IPO8*, *UBC* and *EIF2B1*. BestKeeper analyses revealed that *MRPL19* (SD 1.66) was the gene with the lowest overall variation, followed by *PUM1* (SD 1.73), *IPO8* (SD 1.79) and *PPIA* (SD 1.81), whereas *GUSB* was the highest (SD 2.21) (**Table 3-7**).

3.3.1.6 Expression Stability of Putative Reference Genes Recommended by the Three Software Packages

In order to test the effects of using combinations of reference genes on the gene expression profiles, the relative expression of *CBI* mRNA in the endometrial cancer tissues and the normal endometrium was calculated using the recommended combinations of genes from the three software packages, geNorm, NormFinder and BestKeeper. The relative expression of *CBI* using *PUM1*, *UBC*, *PGK1*, *MRPL19* and *PPIA* as the best reference gene combinations recommended by geNorm-qBasePLUS, revealed statistically significant ($p=0.0067$) down-regulation of *CBI* in malignant tissue (**Figure 3-6A**).

Table 3-7: BestKeeper output

Measurements	MRPL19	PPIA	PUM1	ELF1	IPO8	YWHAZ	EIF2B1	GUSB	PGK1	UBC
N	24	24	24	24	24	24	24	24	24	24
Geo Mean Ct	27.57	23.08	26.46	26.47	27.57	29.07	28.30	28.10	24.93	23.69
Ar Mean Ct	27.64	23.18	26.55	26.60	27.66	29.18	28.39	28.22	25.04	23.79
Min Ct	24.96	19.79	22.85	22.92	24.19	25.53	24.87	23.64	21.54	19.47
Max Ct	32.44	27.95	31.90	33.42	33.92	34.36	34.93	33.94	30.81	28.59
SD Ct	1.66	1.81	1.73	2.11	1.79	2.15	1.80	2.21	1.88	1.83
CV % Ct	6.02	7.81	6.53	7.95	6.49	7.36	6.34	7.82	7.53	7.71
Coeff. of corr (r)	0.979	0.972	0.970	0.978	0.962	0.970	0.933	0.963	0.965	0.959
p-value	0.001	0.001	0.001	0.001	0.001	0.001	0.001	0.001	0.001	0.001

N = number of samples; Geo Mean Ct = geometric mean of Ct values; Ar Mean Ct = arithmetic mean of the Ct values; Min and Max Ct = extreme values of the Ct; SD Ct = standard deviation of the Ct values; CV % Ct = coefficient of variance expressed as percentage on the Ct level; Coeff. of corr (r) = coefficient of correlation (r).

CBI expression was also significantly ($P=0.0027$) down-regulated in malignancy when normalized against the single best gene (*MRPL19*), as recommended by NormFinder and BestKeeper (**Figure 3-6B**). Furthermore, using the best two-gene combination recommended by NormFinder (*IPO8* and *PPIA*), *CBI* expression was also significantly ($P=0.0067$) down-regulated in the malignant samples (**Figure 3-6C**). Interestingly, the p-values following the normalization recommended by geNorm and Normfinder (two best combination genes) were similar. The normalized *CBI* expression data using the genes recommended by the three software packages are displayed in (**Figure 3-6**).

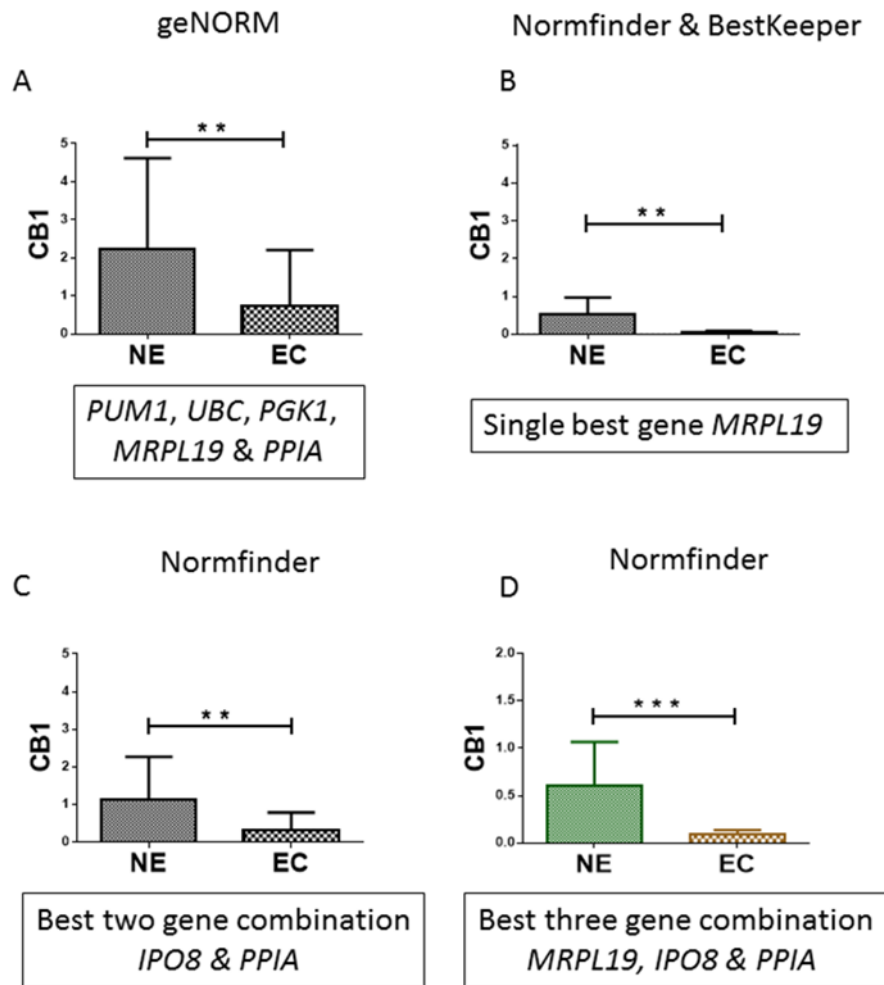


Figure 3-6: Relative *CBI* expressions in endometrial carcinoma using the indicated combinations of genes for normalization from the three software packages.

Samples from the endometrial carcinoma group (EC; Type 1 and 2) were compared to the normal endometrium group (NE; atrophic, secretory and proliferative phases) (n=3 in all cases). Data are presented as the mean \pm SD; **p<0.001; ***p<0.0001, unpaired Student's t-test. The data above each graph indicates the software used and the box below each graph indicates the predicted best gene or gene combinations.

3.3.1.7 The Effect of Using Three Endogenous Reference Genes (MRPL19, IPO8 and PPIA) for Normalization

When the expression levels of *MRPL19*, *PPIA* and *IPO8* were combined and evaluated as the endogenous control for normalization of *CBI* transcript levels (**Figure 3-6D**), the data showed that there was a statistically significant ($p=0.0004$) decrease in *CBI* expression in the endometrial cancer tissues when compared with the normal endometrium (control group). This is further illustrated in (**Figure 3-6 (A-D)**) where the P-values for the difference in *CBI* expression depended on the number of endogenous control genes and type of endogenous control used, with the expression of *CBI* transcripts being most significantly ($p<0.0001$) down-regulated when normalized against the geometric mean of *MRPL19*, *IPO8* and *PPIA*. The p-value of this normalization manipulation was lower than any other combination of endogenous control genes, suggesting that these 3 genes provide the best normalizer of gene expression for studies of human endometrial cancer, when normal endometrial tissue is used as the control.

3.3.2 FAAH Activity and Expression

Since FAAH is considered as the “gate keeper” of endocannabinoid levels it was anticipated that lymphocytic FAAH activity would be the main controller of plasma endocannabinoid concentrations in the plasma of the endometrial cancer patients. By examining its lymphocyte activity, expression and location, a role for this enzyme in endometrial cancer might be revealed.

3.3.2.1 Patient Characteristics - FAAH Activity

For the measurement of FAAH lymphocyte activity in endometrial cancer, only type 1 EC patients were included because these were the patients with increased plasma AEA concentrations (Chapter 2). There was no statistical difference in either the age or BMI of type 1 EC patients when compared to the atrophic (control) group (Table **3-8**).

Table 3-8: Patient characteristics of blood samples sent for FAAH activity analysis

Groups (n)	Age (years)	BMI (Kg/m ²)
Control (6)	60.67 ± 4.27	26.67 ± 6.50
Endometrial Carcinoma Type 1 (15)	63.87 ± 11.11 ^{ns}	33.13 ± 6.64 ^{ns}

The EC group only consisted of only type 1 EC patients. All data are presented as the mean ± SD. Student's t-test was used to determine statistical differences; n.s. = not significantly different.

3.3.2.2 FAAH Enzyme Activity Measurement in Peripheral Lymphocytes

Figure 3.7 shows the median (IQR) FAAH enzyme activity in lymphocytes from EC patients at 136.0 (125.0 – 165.0) pmol/min/mg protein and in the lymphocytes from control group at 131.0 (125.0 – 149.3 pmol/min/mg protein). These values were not statistically different ($p=0.635$, Mann Whitney U-test) (Figure 3-7).

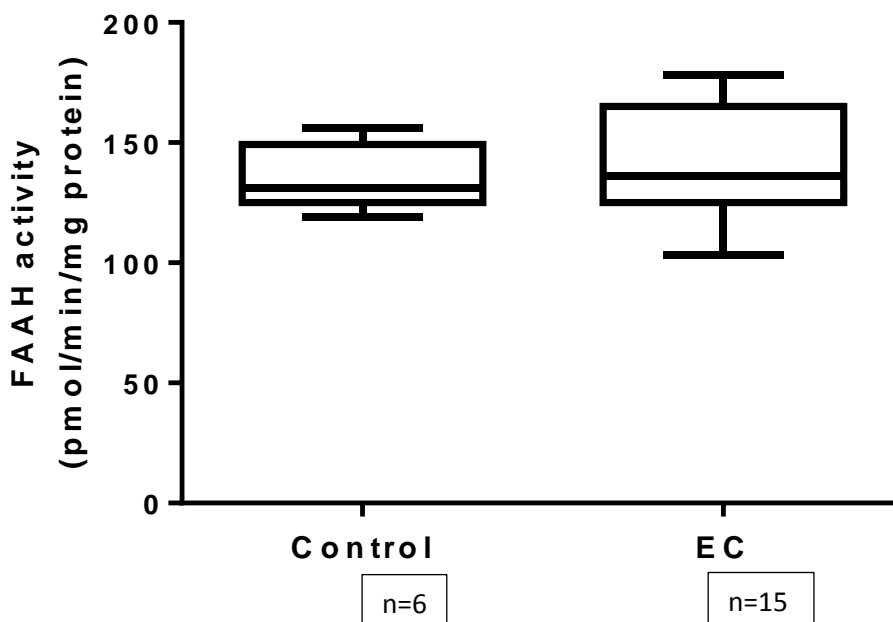


Figure 3-7: FAAH activity in peripheral blood lymphocytes in EC.

FAAH activity in EC was elevated when compared to the control group but it failed to reach statistical significance. FAAH activity data are presented as median (IQR and range), with the number of samples assessed shown under each group.

Sub-analysis of lymphocytic FAAH enzyme activity [median (IQR)] from patients in the various grades of type 1 EC showed the following atrophic, 131.0 pmol/min/mg protein (125.0 – 149.3), grade 1 EC, 150.0 pmol/min/mg protein (120.0 – 170.5), grade 2 EC, 135 pmol/min/mg protein (126.3 – 159.5) and grade 3 EC 118 pmol/min/mg protein (103.0 – 133.0) (**Figure 3-8**). The data were not statistically significantly different ($p=0.519$, Kruskal-Wallis ANOVA with Dunn's ad hoc post-test analysis) between the groups, even though FAAH activity was higher in the grade 1 and 2 EC groups when compared to that observed in grade 3 EC (**Figure 3-8**).

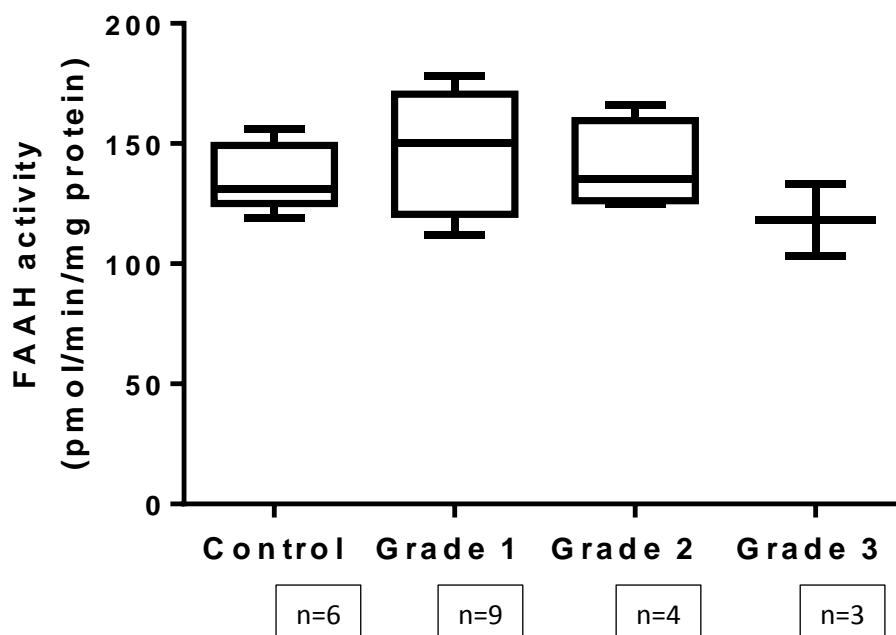


Figure 3-8: FAAH activity in peripheral blood lymphocytes in different grades of type 1 EC.

FAAH data are presented as median (IQR) and range, with the number of samples assessed shown under each group.

3.3.2.3 FAAH Enzyme Activity and its Correlation with Plasma AEA Concentrations

Figure 3-9 shows that there was a significant inverse correlation between plasma AEA concentrations and lymphocytic FAAH activity ($r=-0.5088$; $p=0.018$), however, one of the plasma AEA concentrations appeared to be much higher than all the others (see Panel A). A Grubb's test for the identification of outliers indicated that this data point was not an outlier. Nevertheless, re-analysis of the data with this data point omitted (panel B) showed that a significant inverse correlation between plasma AEA concentrations and lymphocytic FAAH activity ($r = -0.577$; $p=0.007$) remained. A re-examination of the patient's notes associated with the 'high plasma AEA' data point, revealed that she differed from the other patient's in her group in that she had a very early stage grade 1 type 1 endometrial EC.

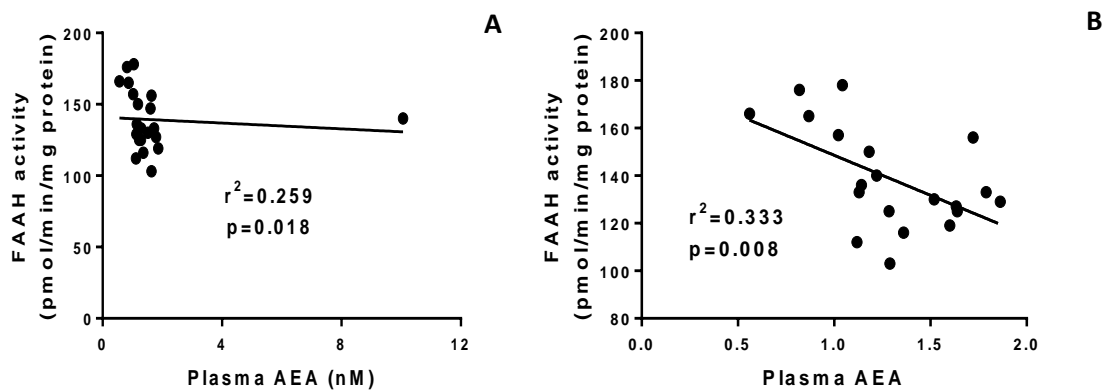
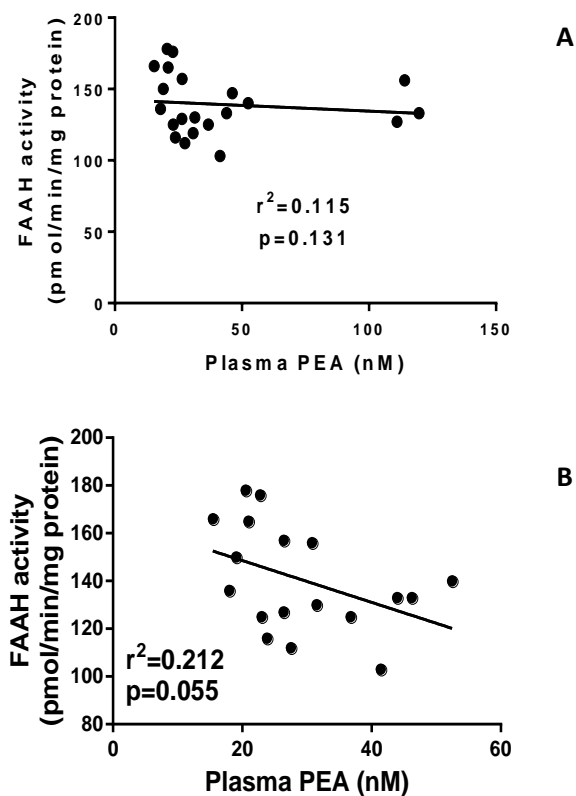


Figure 3-9: Spearman correlation analysis of lymphocytic FAAH activity and plasma AEA concentrations.

Panel A shows the correlation between levels of lymphocytic FAAH activities and plasma AEA concentrations for the type 1 EC patients and the atrophic endometria controls ($n = 21$). Panel B shows the same data with the data point from the extreme right of panel A omitted from the analysis ($n = 20$). The data indicate a significant inverse correlation between FAAH activities and plasma AEA concentrations in both analyses.

3.3.2.4 FAAH Enzyme Activity and its Correlation with Plasma PEA Concentrations

Figure 3-10 shows the relationship between lymphocytic FAAH activities and plasma PEA concentrations. The data revealed that there was no correlation ($r=-0.3405$; $p=0.131$), however, three plasma PEA values appeared to be potentially much higher than the other samples (see panel A). Even though these three samples were not outliers in a Grubb's test, exclusion of those three values in a re-evaluation of the remaining samples, revealed a statistically insignificant ($r=-0.4605$; $p=0.055$) inverse correlation between FAAH activity and PEA concentration (see panel B).



3.3.2.5 FAAH Enzyme Activity and its Correlation with Plasma OEA Concentrations

Figure 3-11 shows that there was a significant inverse correlation between plasma OEA concentrations and lymphocytic FAAH activity ($r = -0.4685$; $p = 0.032$).

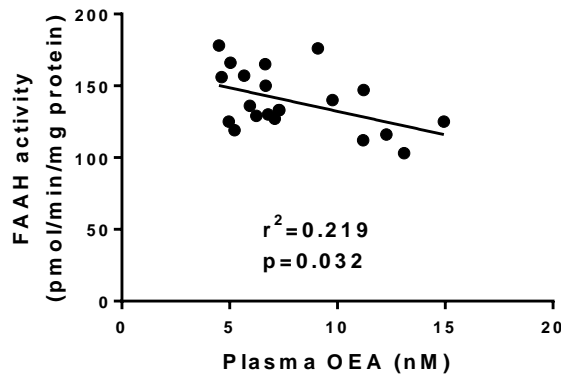


Figure 3-11: Spearman correlation analysis of lymphocytic FAAH enzyme activities and plasma OEA concentrations ($n=21$).

3.3.3 FAAH Transcript Levels

Following the interesting finding that plasma AEA and OEA concentrations were inversely related to lymphocytic FAAH activity, it was decided to examine FAAH activity at the level of the transcript level using the PCR technique and to correlate this with lymphocytic FAAH activity.

3.3.3.1 Patient Characteristics - FAAH Transcript Levels

The ages of women in all the individual groups (Table 3-9) showed there to be no statistical significant difference. The BMI of the control group was $26.67 \pm 6.50 \text{ Kg/m}^2$ whilst that of type 1 EC was $33.27 \pm 6.93 \text{ Kg/m}^2$, and that of type 2 EC was $37.17 \pm 4.40 \text{ Kg/m}^2$. The BMI of the type 1 EC group was not significantly different to that of the atrophic control, but that of the type 2 EC group was significantly larger ($p < 0.05$). When the BMI of the control group was compared against the entire EC group, the BMI of EC group was significantly larger ($p = 0.0163$), indicating that the increased BMI is primarily due to the BMI of the type 2 EC group.

Table 3-9: Patient characteristics for the expression of FAAH mRNAs in endometrial cancer

Patient Groups	Age in years (Mean \pm SD)	BMI in Kg/m ² (Mean \pm SD)
Normal		
Atrophic (n=6)	60.67 \pm 4.27	26.67 \pm 6.50
Endometrial Carcinoma Type 1		
Grade 1 (n=6)	66.17 \pm 16.14	33.50 \pm 8.92
Grade 2 (n=6)	66.50 \pm 10.25	32.00 \pm 5.97
Grade 3 (n=3)	72.67 \pm 12.06	35.33 \pm 6.11
Endometrial Carcinoma Type 2		
Serous (n=3)	59.00 \pm 3.46	37.67 \pm 2.52
Carcinosarcoma (n=3)	50.00 \pm 5.00	36.67 \pm 6.43

Age and BMI of women were analysed using one-way analysis of variance with Dunnett's multiple comparisons test with atrophic used as the control.

3.3.3.2 Relative Expression of FAAH mRNA

The relative transcript levels for FAAH as determined by qRT-PCR are shown in **Figure 3-12**.

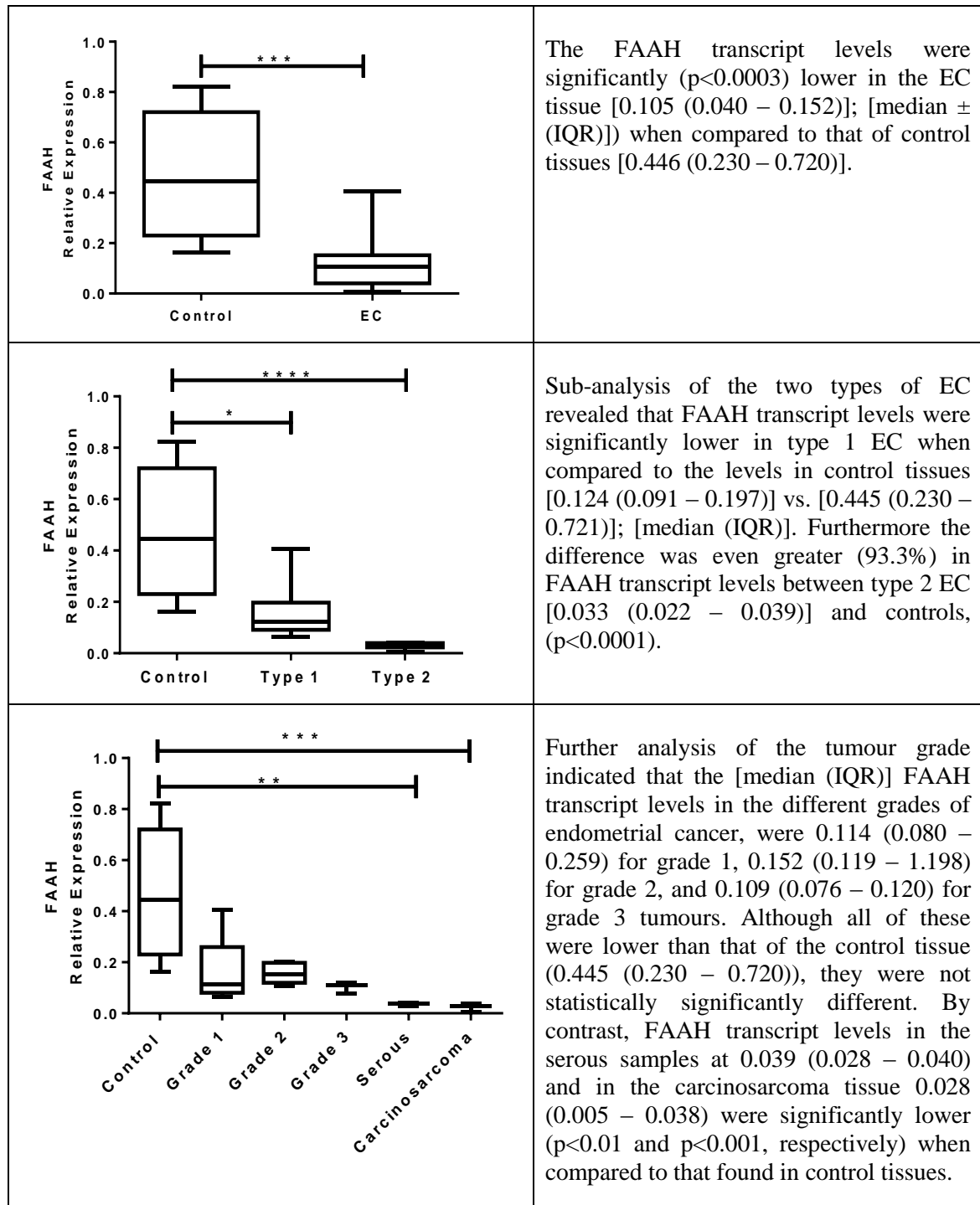


Figure 3-12: Relative expression of FAAH mRNAs via qRT-PCR.

P values were obtained using Mann-Whitney analysis and Kruskal Wallis ANOVA with Dunn's ad hoc post-test analysis. Data are presented as [median (IQR)].

3.3.4 FAAH Protein Levels

Following the identification of differences in the levels of FAAH transcript in the various groups EC, the next step was to determine where in the tissue FAAH was being expressed and confirm that these transcript changes were reflected at the protein level, by using immunohistochemistry (IHC).

3.3.4.1 Patient Characteristics-FAAH Protein Levels

The ages of women in all the individual groups (**Table 3-10**) were not statistically significantly different. Although the BMI of the control group at $26.67 \pm 6.50 \text{ Kg/m}^2$ was not significantly different to that of the type 1 EC group ($33.11 \pm 6.04 \text{ Kg/m}^2$), it was significantly smaller to that of type 2 EC group ($p < 0.05$; $34.50 \pm 6.10 \text{ Kg/m}^2$). When the BMI of the control group was compared against the entire EC group, the BMI of EC group was significantly larger ($p = 0.016$) indicating that the increased BMI is primarily due to the BMI of the type 2 EC group (**Table 3-10**).

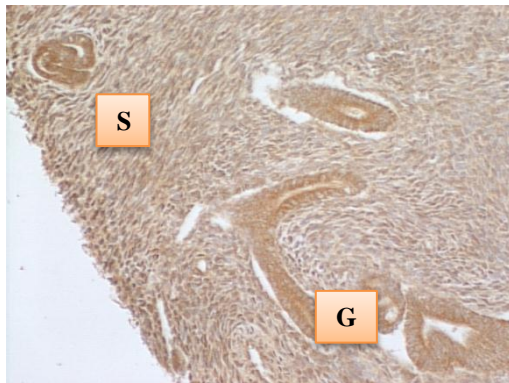
Table 3-10: Age and BMI characteristics of the patients who provided samples for the FAAH IHC experiment

Patient Groups	Age in years (Mean \pm SD)	BMI in Kg/m ² (Mean \pm SD)
Normal		
Atrophic (n=6)	60.67 \pm 4.27	26.67 \pm 6.50
Endometrial Carcinoma Type 1		
Grade 1 (n=6)	62.50 \pm 13.90	33.00 \pm 8.76
Grade 2 (n=6)	65.17 \pm 9.86	34.83 \pm 5.56
Grade 3 (n=6)	66.83 \pm 7.88	31.50 \pm 3.08
Endometrial Carcinoma Type 2		
Serous (n=4)	70.25 \pm 10.97	33.00 \pm 6.83
Carcinosarcoma (n=6)	58.33 \pm 7.42	35.50 \pm 5.99

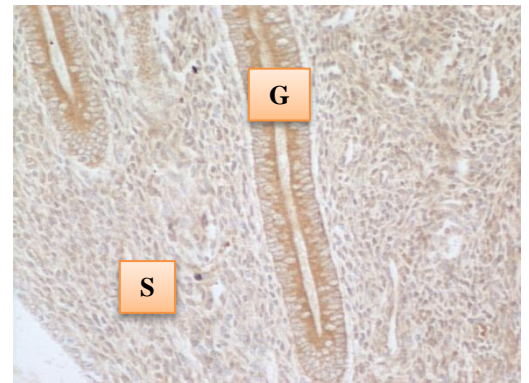
Age and BMI of women were analysed using one-way analysis of variance with Dunnett's multiple comparisons test with atrophic used as the control.

3.3.4.2 Optimisation and Validation of FAAH Immunohistochemical Methods

The optimal primary antibody dilution for FAAH was obtained using different dilutions, as follows: (1:1000, 1:2000, 1: 3000 and 1:4000). An example of the staining intensities obtained using these dilutions are shown in **Figure 3-13**. From these images, the best dilution used was determined to be 1:2000.



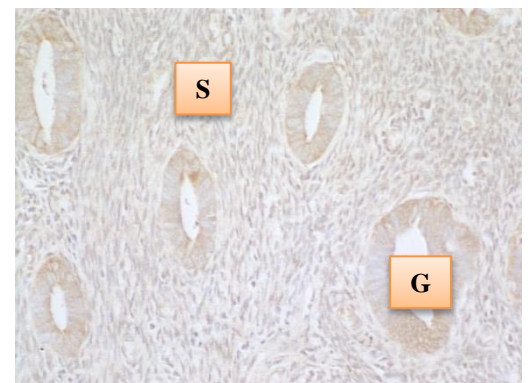
FAAH 1:1000



FAAH 1:2000



FAAH 1:3000

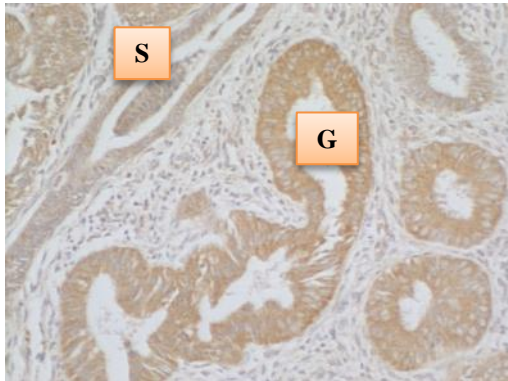


FAAH 1:4000

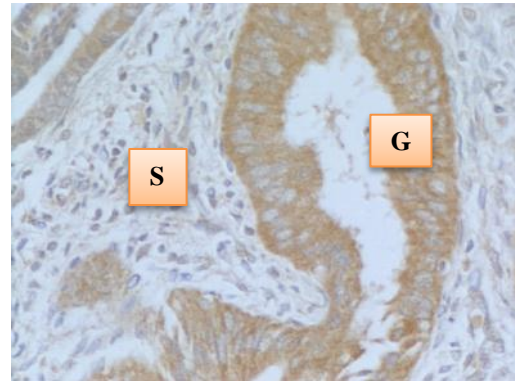
Figure 3-13: Staining intensities for FAAH at different antibody dilutions (S=stroma, G=glands).

Very strong staining was obtained with 1:1000 and very light staining with 1:3000 and 1:4000. The 1:2000 dilutions provided the optimal staining pattern.

Antibody specificity was determined using equivalent concentrations of non-immune IgG (**Figure 3-14**). The lack of 3, 3'-diaminobenzidine (DAB) staining in the IgG controls indicates that the antibodies are specific for FAAH.



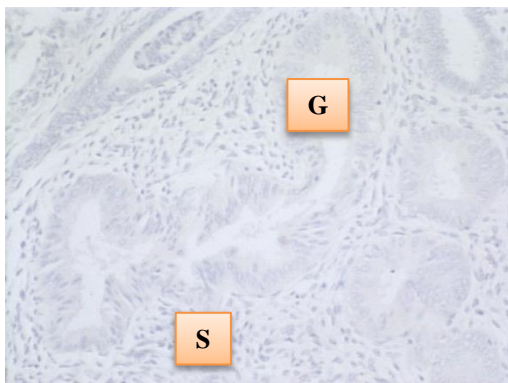
(A) FAAH primary antibody (X 20)



(B) FAAH primary antibody (X 40)

Positive control

Positive control



(C) diluted rabbit serum (X 20)

Negative control



(D) diluted rabbit serum (X 40)

Negative control

Figure 3-14: An example of a control experiment demonstrating the specificity of the primary antibody FAAH.

Images A and B show positive staining of the primary FAAH antibody with more intense staining in the glands (G) than in the stoma (S), whilst images C and D show no staining for the non-immune rabbit serum control. All the slides are uterine samples.

3.3.4.3 Identification and Localisation of FAAH Protein

Figure 3-15 illustrates the staining pattern of FAAH in atrophic and EC samples. Following the optimisation of FAAH antibody, all the studies were undertaken as a single run to minimise variations.

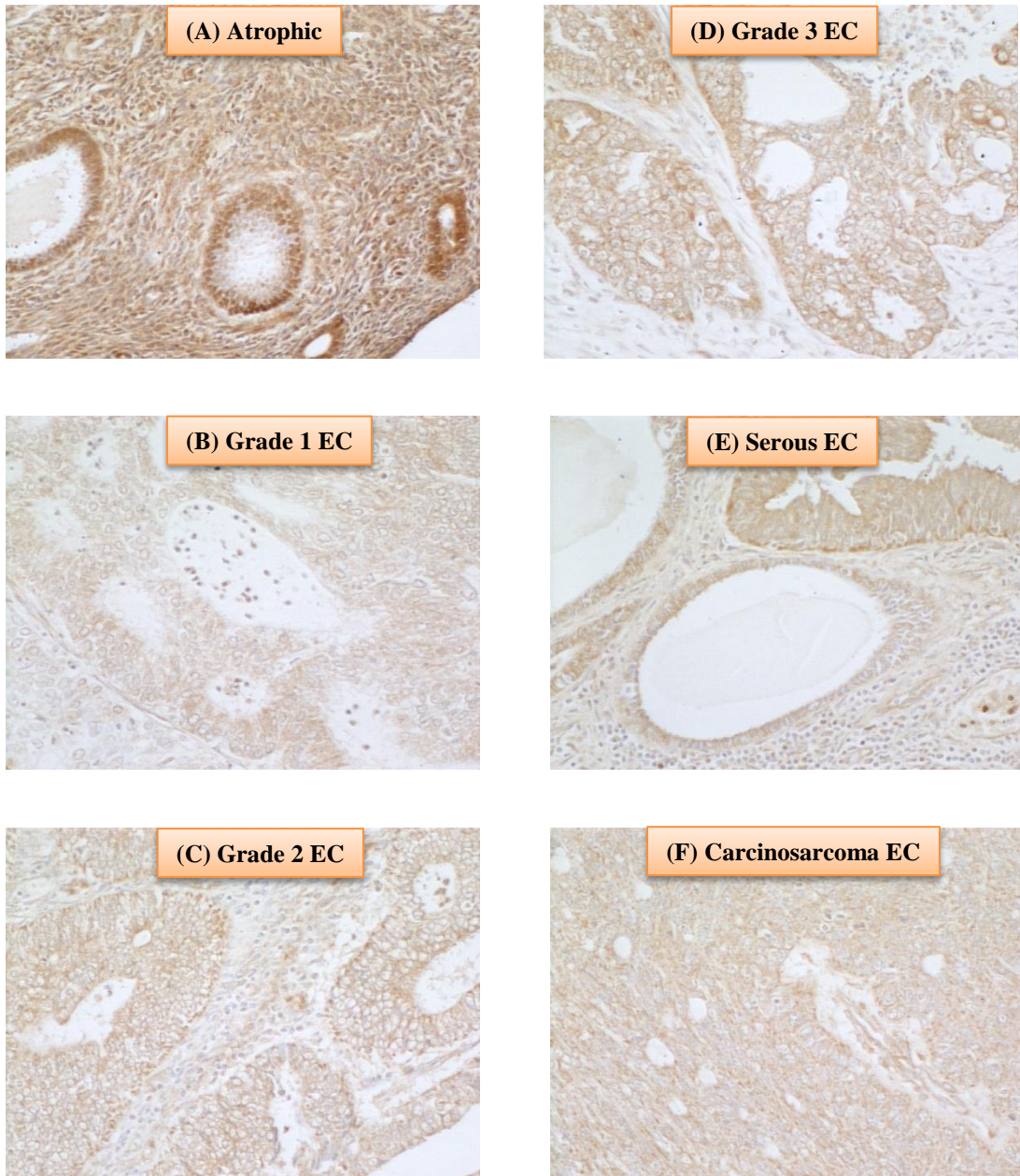


Figure 3-15: Localisation and expression of FAAH protein in various tissues (G = glands, S = stroma, EC = endometrial cancers).

The immunoreactive FAAH staining intensity was strong to very strong in atrophic endometrium, covering both the stroma and the glands. In atrophic endometria, immunoreactive FAAH protein was expressed at higher levels in the glands when compared to the stroma with a stronger intensity of immunoreactivity along the basal region of the glands compared to the apical region. Furthermore, the number and size of glands were markedly reduced in the atrophic endometrium when compared to all the other tissues. In comparison to other tissues, the stroma of atrophic endometria was stronger than in the stroma of other tissues and weaker than that observed in the glands of all tissues (see panel A) (**Figure 3-15**). FAAH staining was also primarily localised to the plasma membrane of cells, with some staining demonstrated in the cytoplasm and the nucleus whereas in other tissues, it was absent from the nuclei, but visibly attached to the nuclear membranes (see panels B, C, D and E). FAAH staining intensity in grade 2 EC was very low when compared to the control (atrophic) group, with weaker staining in both the glands and stroma. In the glands, FAAH staining was localised more in the cytoplasm and with more intensity towards the apical region of the glands and the nuclear envelope was only slightly stained. FAAH staining in carcinosarcoma (panel F) showed very low intensity when compared to that observed in the control (atrophic) group, but involved both the glands and stroma. It was difficult to see the glandular structure in the carcinosarcoma, because the glands had broken down and the epithelial cells dispersed throughout the tissue, but in those epithelial cells, FAAH staining is more cytoplasmic and focussed to the apical region of the cells. Consistent with the staining in other tissues, the nuclear envelope and the nucleus have taken some staining. This was observed in both the glands and stroma.

3.3.4.4 Histomorphometric Quantification of FAAH Proteins

Figure 3-16A shows the data from the histomorphometric analysis of glands and stroma (G+S). The data indicate that the amount of immunoreactive FAAH in the entire tissue (G+S) was always lower in the EC when compared to the atrophic endometria. Sub-analysis of the H-score for the endometrial cancer showed that the EC tissue was always lower than that found in the atrophic tissue. **Figures 3-16B and 3-16C** show comparable data from the glandular tissue and stromal tissue, respectively. The data show that the staining patterns occur throughout the tissue with significant reductions in FAAH immunoreactivity in both the glands and stroma of EC tissue when compared to that of atrophic tissue.

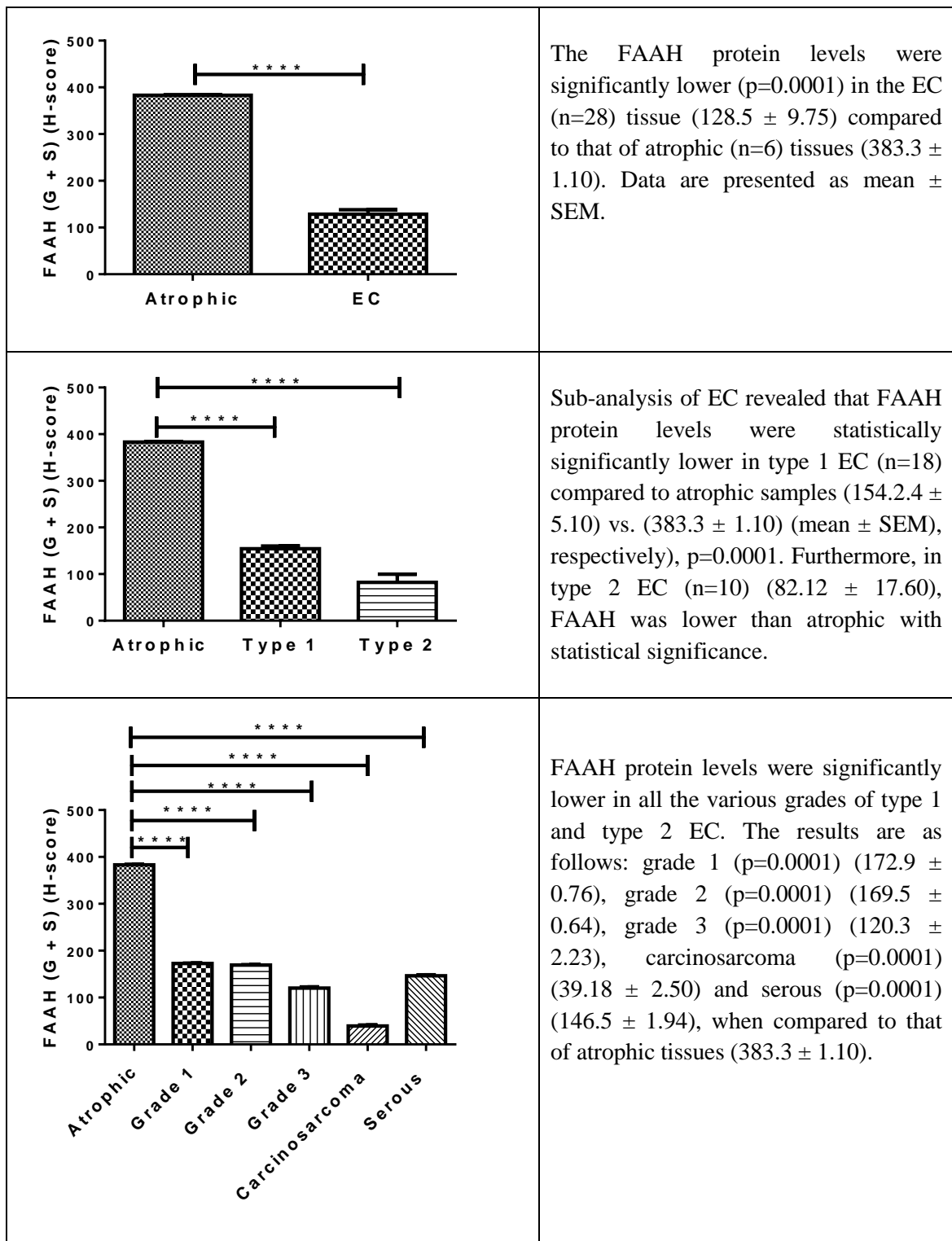


Figure 3-16A: Histomorphometric analysis (H-Score) of FAAH (G + S) immunoreactivity.

P values were obtained using Student's t-test and one way ANOVA with Dunnett's ad hoc post-test analysis of both components of the tissues, and the glands and stoma separately. Data are presented as mean \pm SEM. Collectively, FAAH protein levels are reduced in EC (G+S) when compared to the control (atrophic) group.

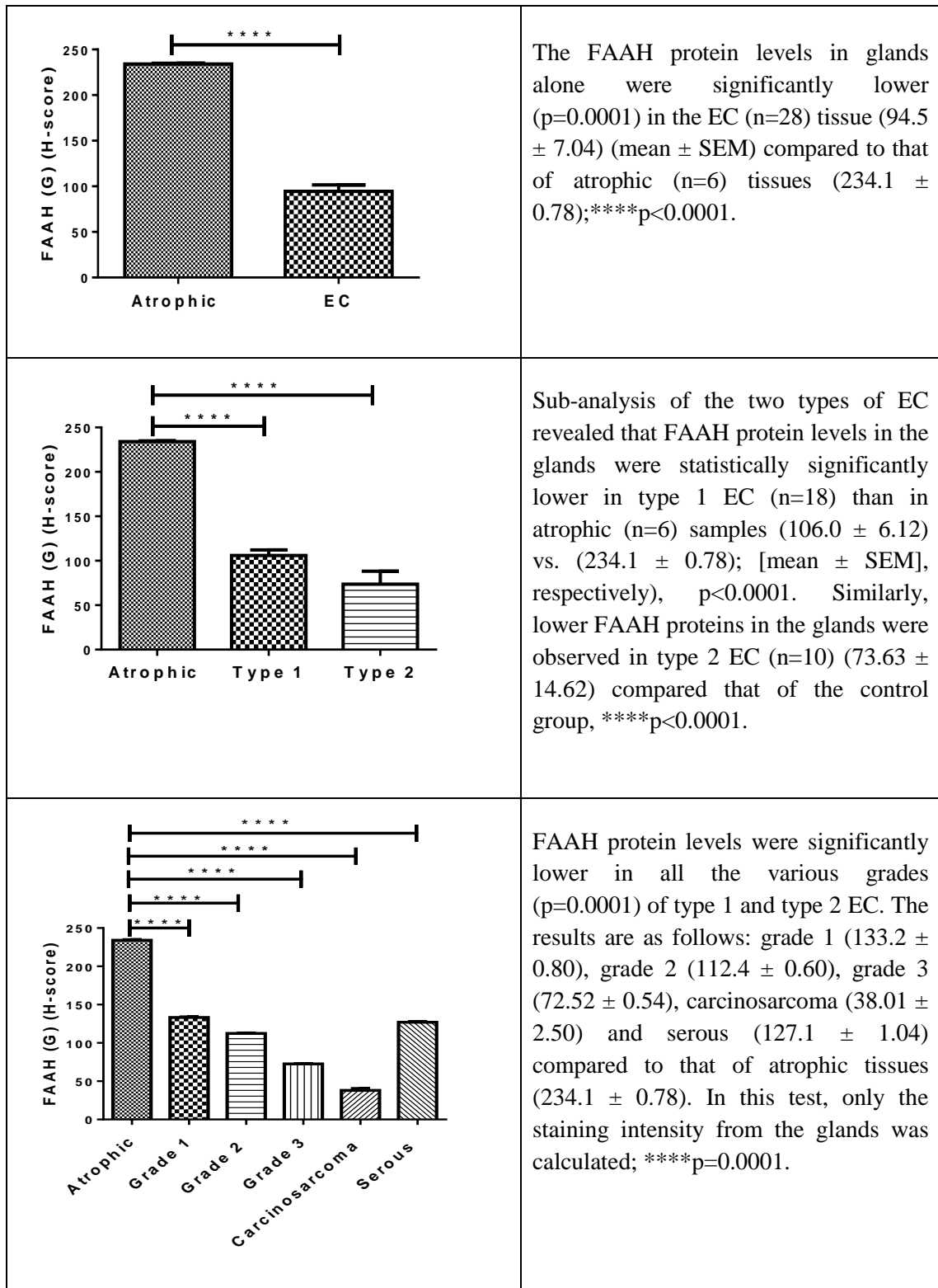


Figure 3-16B: Histomorphometric analysis of FAAH immunoreactivity (H-score) in the glandular tissue (G).

P values were obtained using Student's t-test and one way ANOVA with Dunnett's ad hoc post-test analysis of the gland components of the tissues (luminal epithelial cells and glandular epithelial cells). Data are presented as mean \pm SEM. Collectively, FAAH protein levels are reduced in EC (G) when compared to the control (atrophic) group.

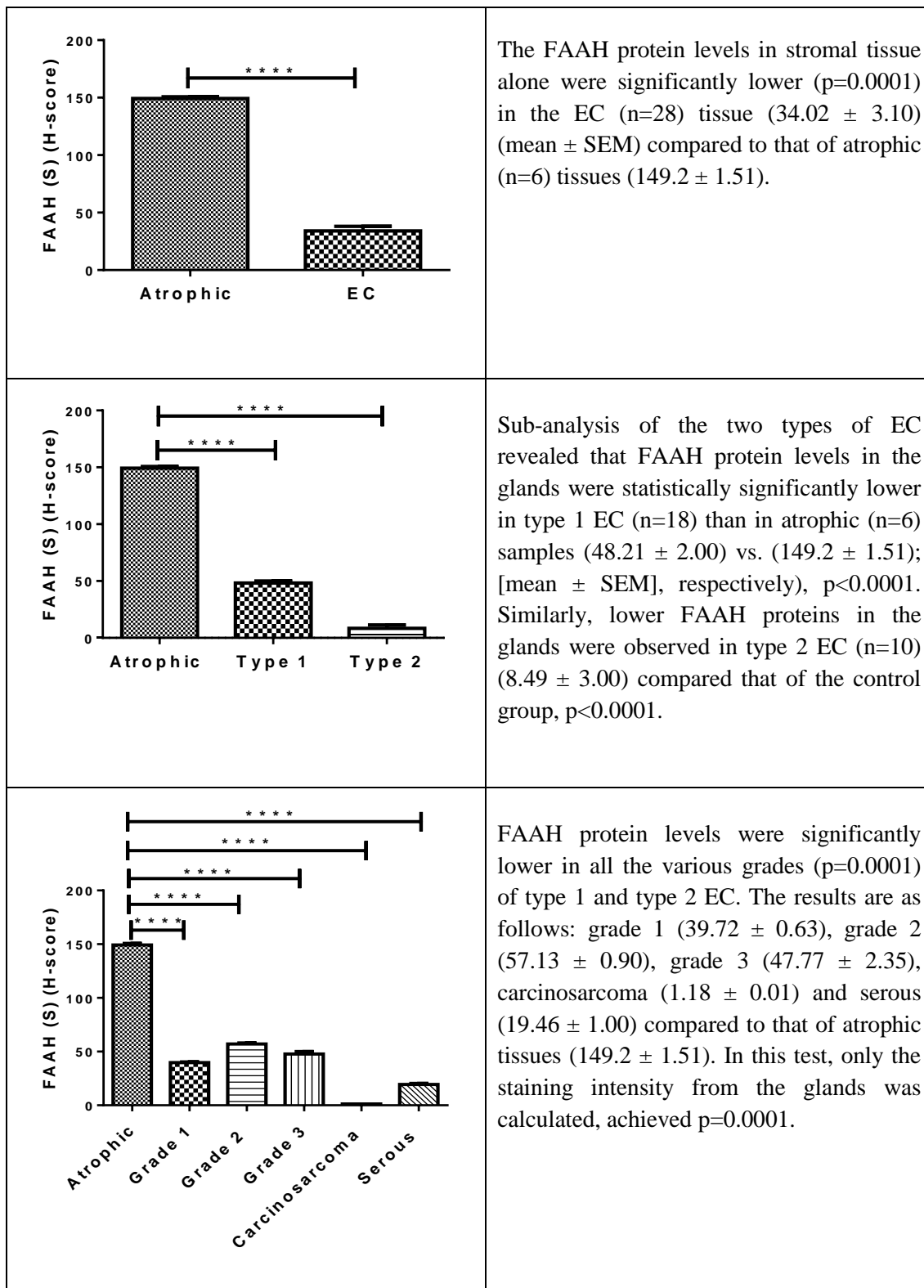


Figure 3-16C: Histomorphometric analysis of FAAH immunoreactivity (H-score) in stromal (S) tissues.

P values were obtained using Student's t-test and one way ANOVA with Dunnett's ad hoc post-test analysis of the stromal component. Data presented as mean \pm SEM. Collectively, FAAH protein levels are reduced in EC (S) in grade 1 and 2, while raised in grade 3, carcinosarcoma and serous, when compared to control (atrophic) group.

3.3.5 NAPE-PLD Transcript Levels

In this section data on the expression and location of the second key endocannabinoid metabolising enzyme, NAPE-PLD, which is considered to be the main synthesizing enzyme for endocannabinoids are presented.

3.3.5.1 Patient Characteristics – NAPE-PLD Transcript Levels

Patient characteristics for this part of the study are the same as for the FAAH transcript level study, and are presented in **Table 3-9**.

3.3.5.2 Relative Expression of NAPE-PLD mRNA

The levels of NAPE-PLD transcripts, as studied via qRT-PCR, are shown in **Figure 3-17**. Unlike the expression of FAAH transcript levels in the EC samples, NAPE-PLD transcript levels were not significantly different in the endometrial cancer and control groups (**Figure 3-17**). Because there was a larger than expected variation in the NAPE-PLD transcript levels, a sub-analysis of the types of EC was performed. The data revealed that there was no statistical difference in NAPE-PLD transcript levels across the groups, although the type 1 EC group continued to show a large variation. To resolve this issue, an additional analysis based on tumour grade was performed and showed that grade 2 and 3, type 1 EC had higher NAPE-PLD transcript levels when compared to the atrophic (control) endometria or grade 1 type 1 EC tissues, but that difference did not reach statistical significance (**Figure 3-17**).

3.3.6 NAPE-PLD Protein Levels

To confirm that NAPE-PLD transcript levels were also affected by disease at the protein levels IHC was performed.

3.3.6.1 Patient Characteristics - NAPE-PLD Protein Levels

The same tissue sections as for the FAAH IHC study (**Section 3.3.2.3**) were used for this study and so the patient characteristics are the same (**Table 3-10**).

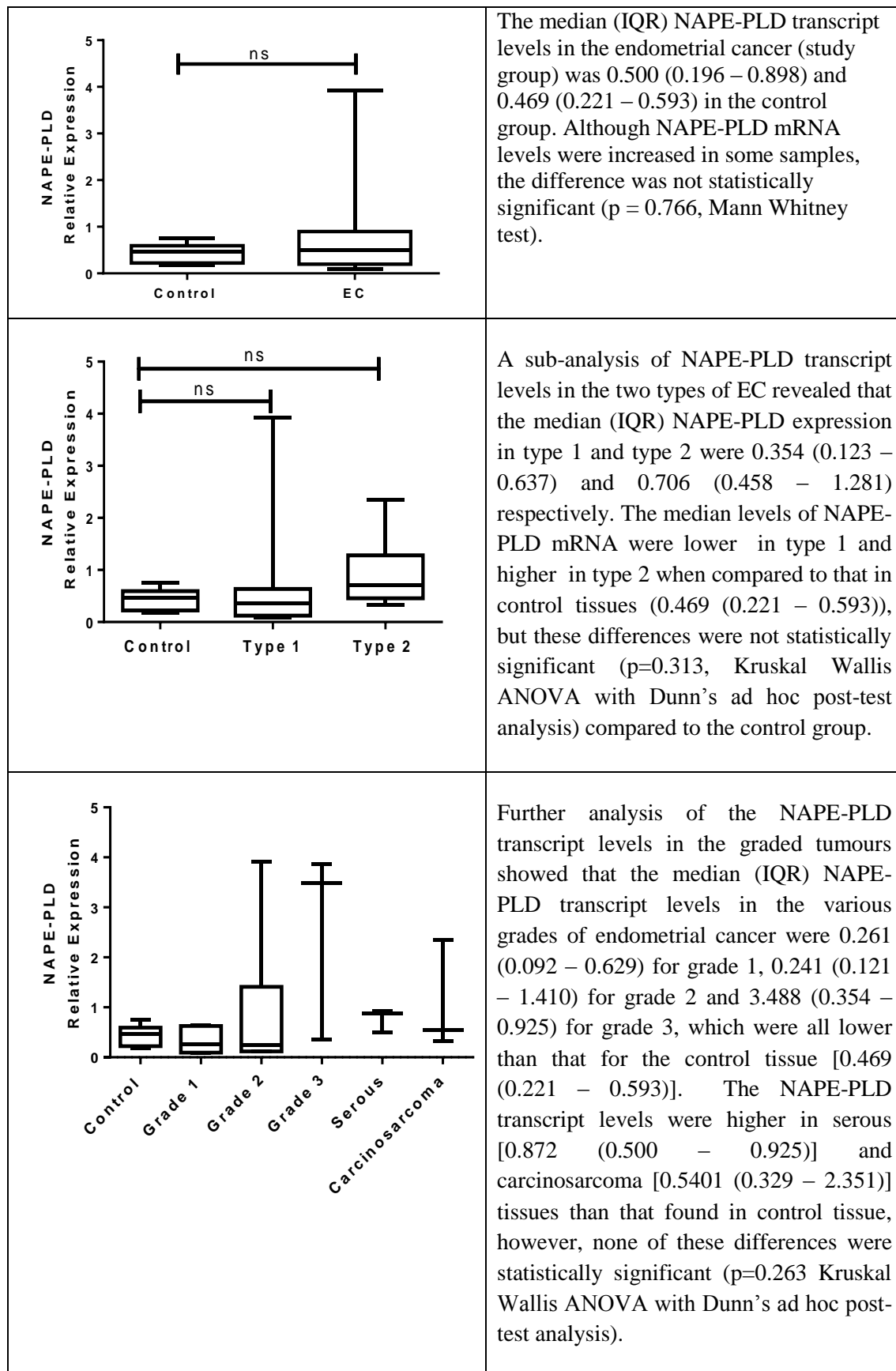


Figure 3-17: Relative expression of NAPE-PLD mRNAs as determined by qRT-PCR.

3.3.6.2 Optimisation and Validation of the NAPE-PLD Immunohistochemical Methods

The optimal primary antibody dilution for NAPE-PLD was obtained by using different dilutions, as follows: (1:25, 1:50, 1: 100 and 1:200). An example of the staining intensities obtained using these dilutions are shown in **Figure 3-18**. From these images, the best dilution was determined to be 1:50.

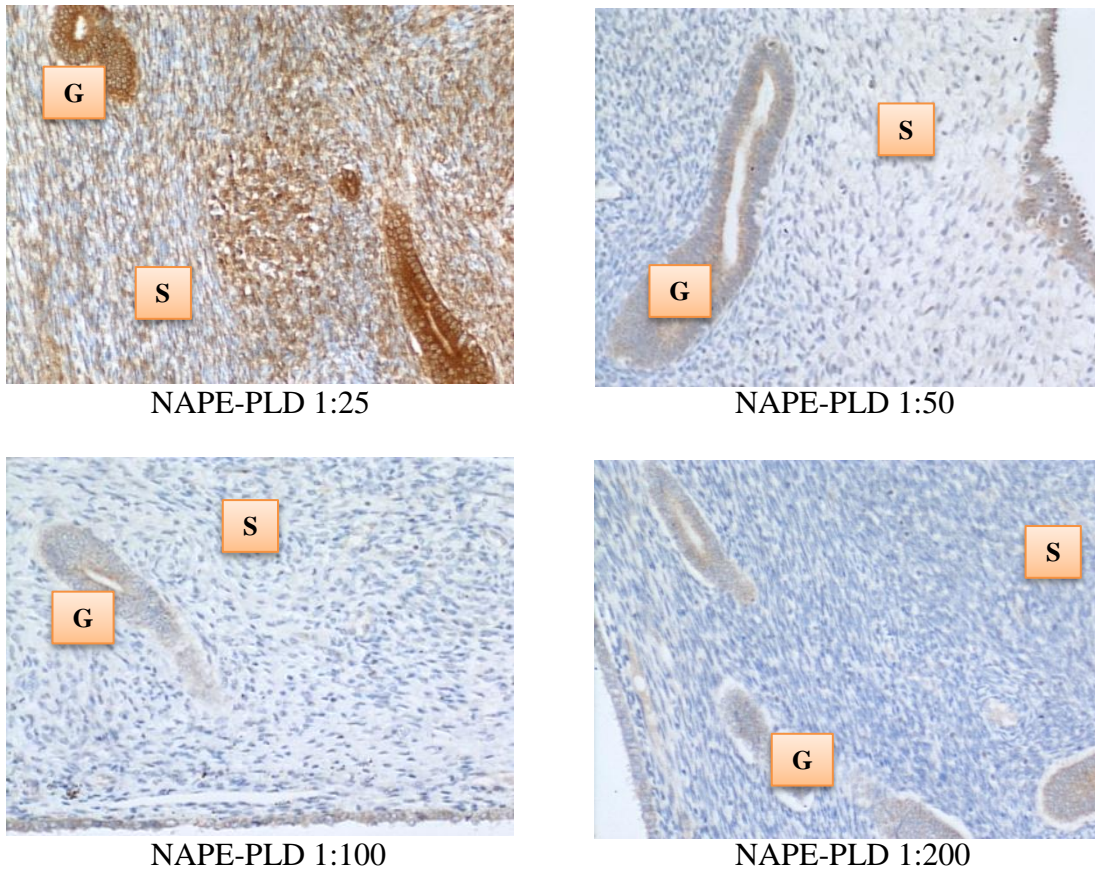


Figure 3-18: Staining intensities for NAPE-PLD at different antibody dilutions (S=stroma, G=glands).

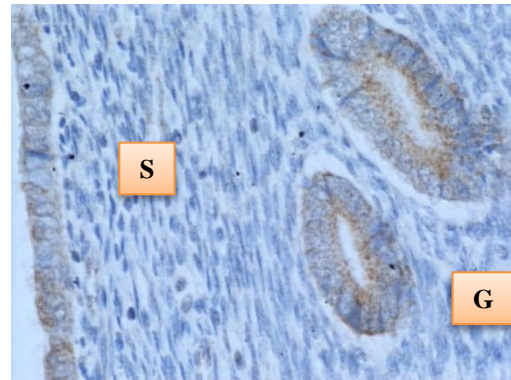
Very strong staining was obtained with 1:25 and very light staining with 1:100 and 1:200. The 1:50 dilutions provided the optimal staining pattern.

Antibody specificity was determined using equivalent concentrations of non-immune IgG (**Figure 3-19**). The lack of DAB staining in the IgG controls indicates that the antibodies are specific for CB2.



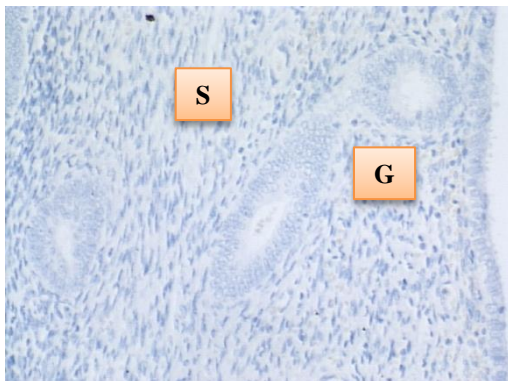
(A) NAPE-PLD primary antibody (X20)

Positive control



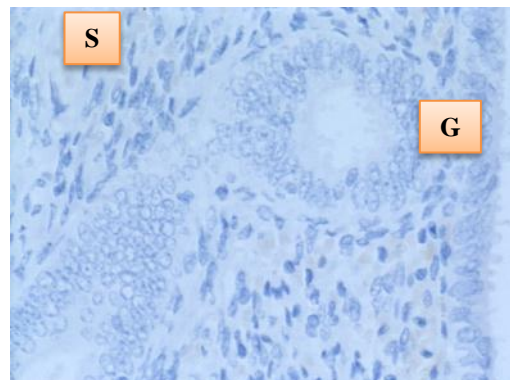
(B) NAPE-PLD primary antibody (X40)

Positive control



(C) IgG antibody (X20 magnification)

Negative control



(D) IgG antibody (X40 magnification)

Negative control

Figure 3-19: Negative control demonstrating the specificity of the primary antibody NAPE-PLD.

Images (A) and (B) show positive staining of the primary antibody NAPE-PLD (more in the glands than the stoma), whilst images (C) and (D) show no staining for the IgG controls.

3.3.6.3 Identification and Localisation of NAPE-PLD Protein

Figure 3-20 illustrates the staining pattern of NAPE-PLD antibodies for atrophic and EC tissues. Following the optimisation of NAPE-PLD antibody, all subsequent studies were undertaken as a single run to minimise variations.

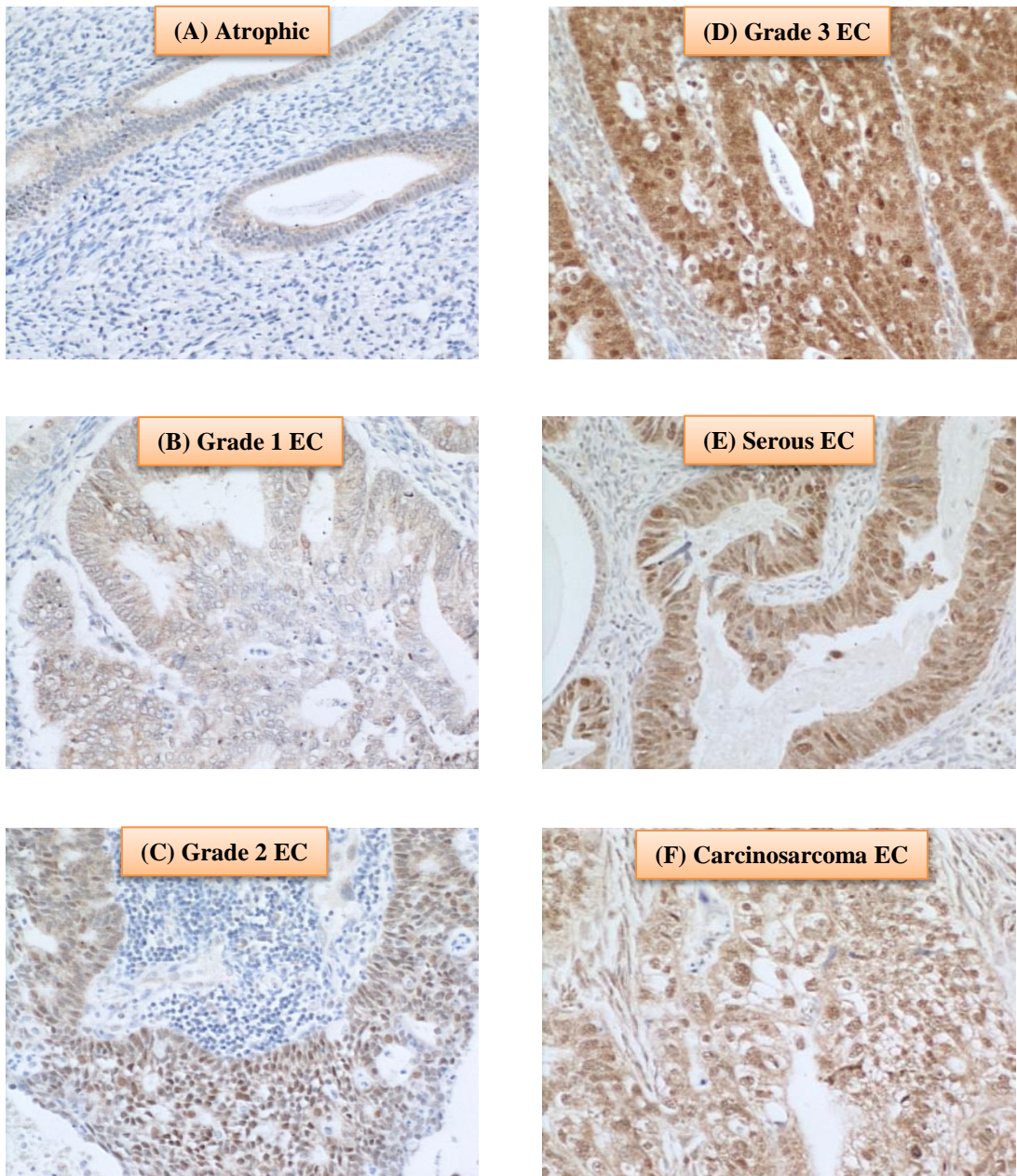


Figure 3-20: Localisation and expression of the NAPE-PLD protein in various tissues (G=gland, S=stroma, EC=endometrial cancer).

In atrophic endometrium, NAPE-PLD immunoreactivity was found in the glandular epithelium with the most intense staining observed in the basal region of the glands away from the lumen. No significant immunoreactivity was demonstrated in the stroma. Although NAPE-PLD staining was demonstrated in the cell cytoplasm, no staining was found in the cell nucleus (**Figure 3-20A**).

The NAPE-PLD staining intensity in grade 1 EC was slightly increased when compared to the atrophic tissue. The staining clearly shows that it was not present in the stroma but like the atrophic tissue involved the glands, staining mainly in the cytoplasm with most nuclei non-stained (**Figure 3-20B**).

The NAPE-PLD staining intensity in grade 2 EC was more intense, being greater than that of both the atrophic and grade 1 EC. The stroma again was devoid of any staining and clearly shows it may be confined to the glands, where it was denser in the cytoplasm but unlike the atrophic and grade 1 EC involved the nucleus (**Figure 3-20C**).

The NAPE-PLD staining intensity in grade 3 EC was most intense and was dramatically higher when compared to the previously described groups. There was mild staining of the stroma, and very dense staining in the glands; staining was found in both the cytoplasm and nucleus. In addition, some staining was observed in the nuclei of stromal cells (**Figure 3-20D**).

NAPE-PLD staining in serous EC was also greater when compared to the atrophic, grade 1 and grade 2 EC samples, but slightly less than in the grade 3 EC samples, primarily because of lesser staining in the stroma. The staining involved both the glands and the stroma, and as the glands are notably bigger compared to any other groups, they stained intensely to NAPE-PLD. In the glands, the staining was denser in the cytoplasm but also present in the nucleus. Wherever the glands appeared 'stretched' with a very big cyst-like appearance, the glandular epithelium were stretched and very thin and had comparably lower NAPE-PLD immunoreactivity. In addition, NAPE-PLD was also found in the nuclei of these glandular epithelial cells with surrounding stromal cells showing both nuclear staining and light staining in the cytoplasm (**Figure 3-20E**).

The NAPE-PLD staining intensity in carcinosarcoma EC was increased dramatically when compared to all the other categories, especially when compared to the control (atrophic) group. The staining involved both the glands and the stroma, with staining being denser in the epithelial cytoplasm and nucleus. In addition, NAPE-PLD staining was observed in the stromal cell nucleus (**Figure 3-20F**).

3.3.6.4 Histomorphometric Quantification of NAPE-PLD Proteins

Figure 3-21A shows the data from the histomorphometric analysis of the glands and stroma (G + S). The data indicate that the amount of immunoreactive NAPE-PLD in the entire tissue (G+S) was always higher in the EC when compared to the atrophic endometria. Sub-analysis of the H-score for the endometrial cancer showed that the EC tissue was always higher than that found in the atrophic tissue. **Figures 3-21B and 3-21C** show comparable data from the glandular tissue and stromal tissue, respectively. The data show that the staining patterns occur throughout the tissue with significant increases in NAPE-PLD immunoreactivity in both the glands and stroma of EC tissue when compared to that of atrophic tissue.

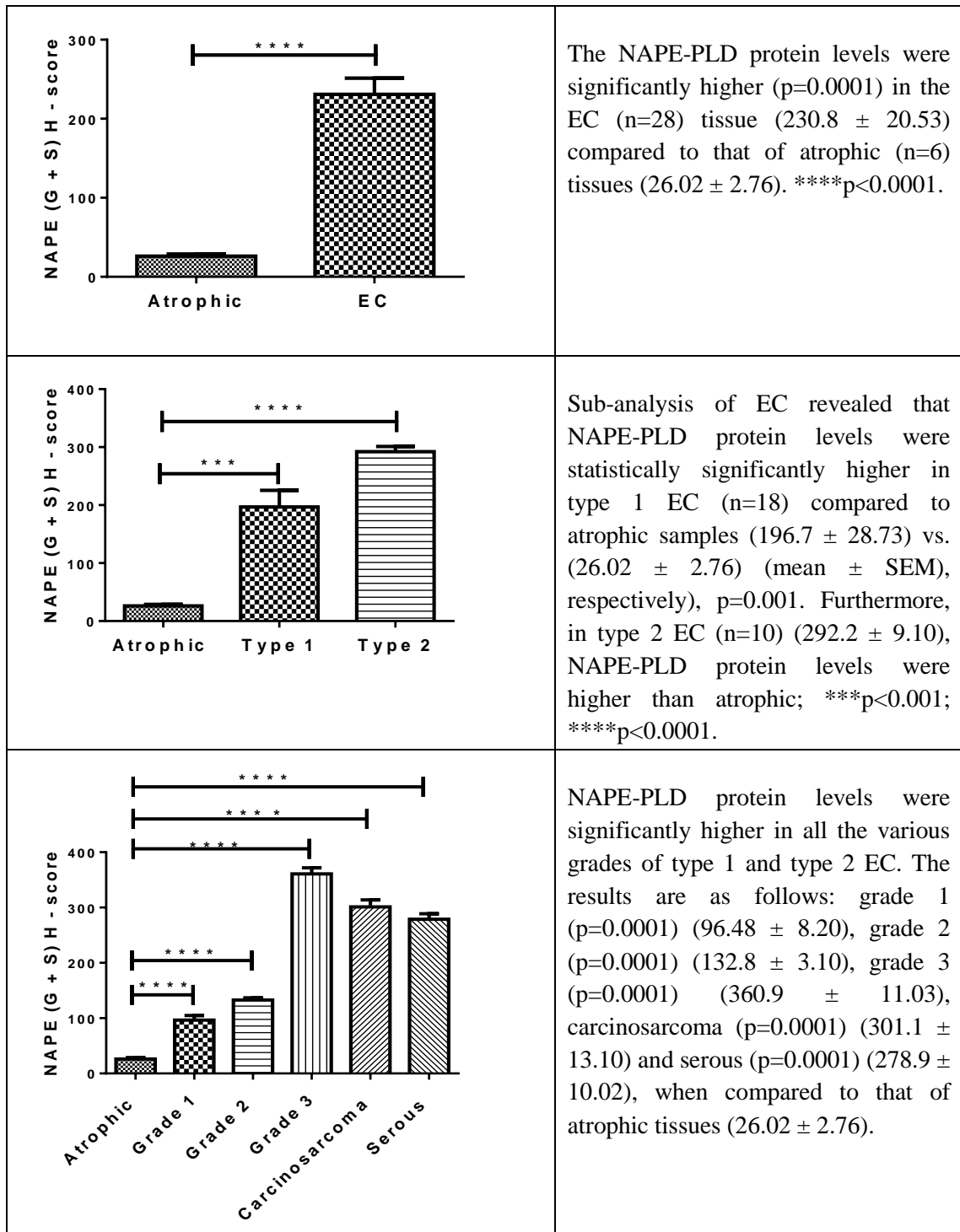


Figure 3-21A: Histomorphometric analysis (H-Score) of NAPE-PLD (G + S) immunoreactivity.

P values were obtained using Student's t-test and one way ANOVA with Dunnett's ad hoc post-test analysis of both components of the tissues, and the glands and stoma separately. Data are presented as mean \pm SEM. Collectively; NAPE-PLD protein levels are higher in EC (G+S) when compared to that found in the control (atrophic) group.

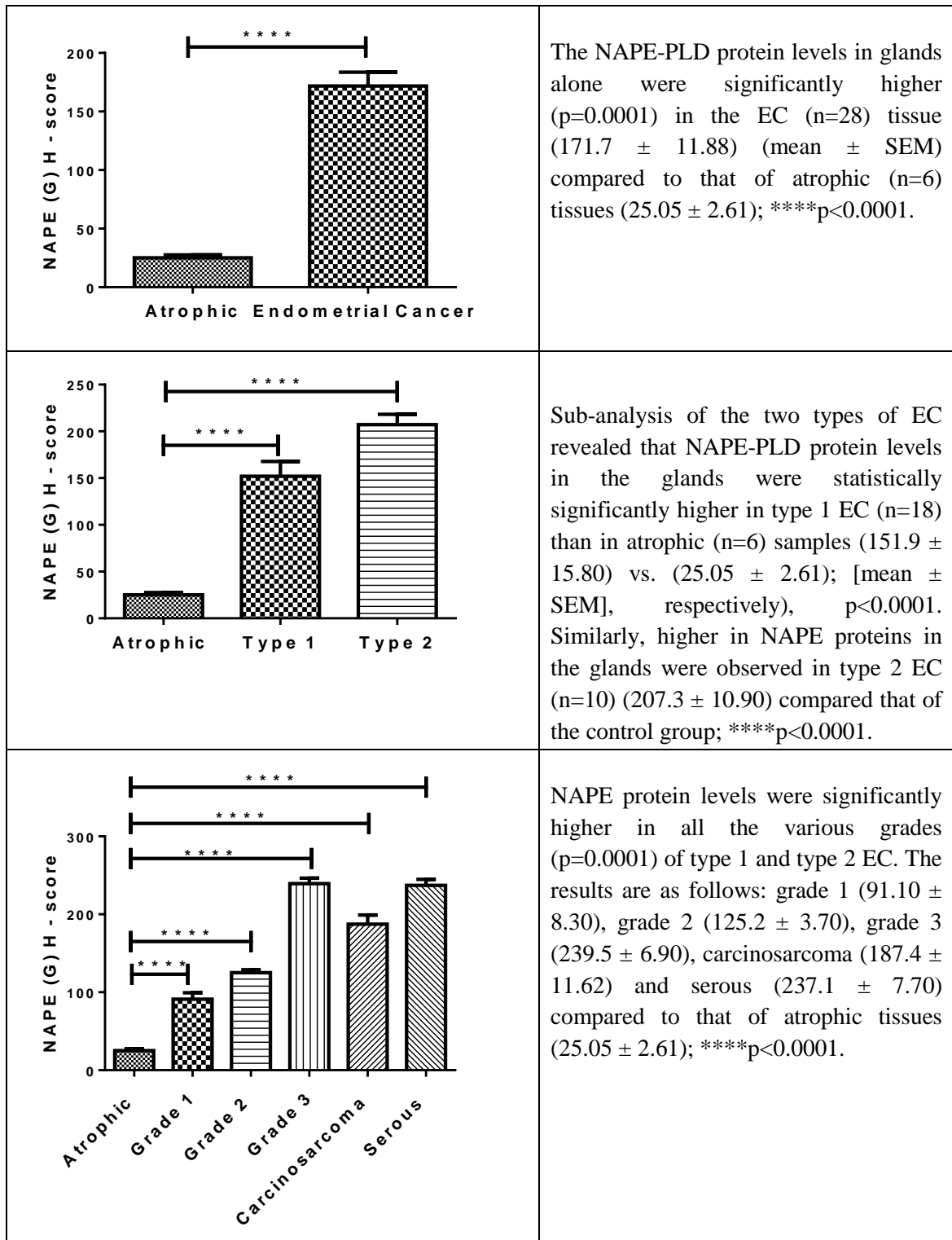


Figure 3-21B: Histomorphometric analysis of NAPE-PLD immunoreactivity (H-score) in the glandular tissue (G).

P values were obtained using Student's t-test and one way ANOVA with Dunnett's ad hoc post-test analysis of the gland components of the tissues. Data are presented as mean \pm SEM. Collectively, NAPE-PLD protein levels are increased in EC (G) when compared to the control (atrophic) group.

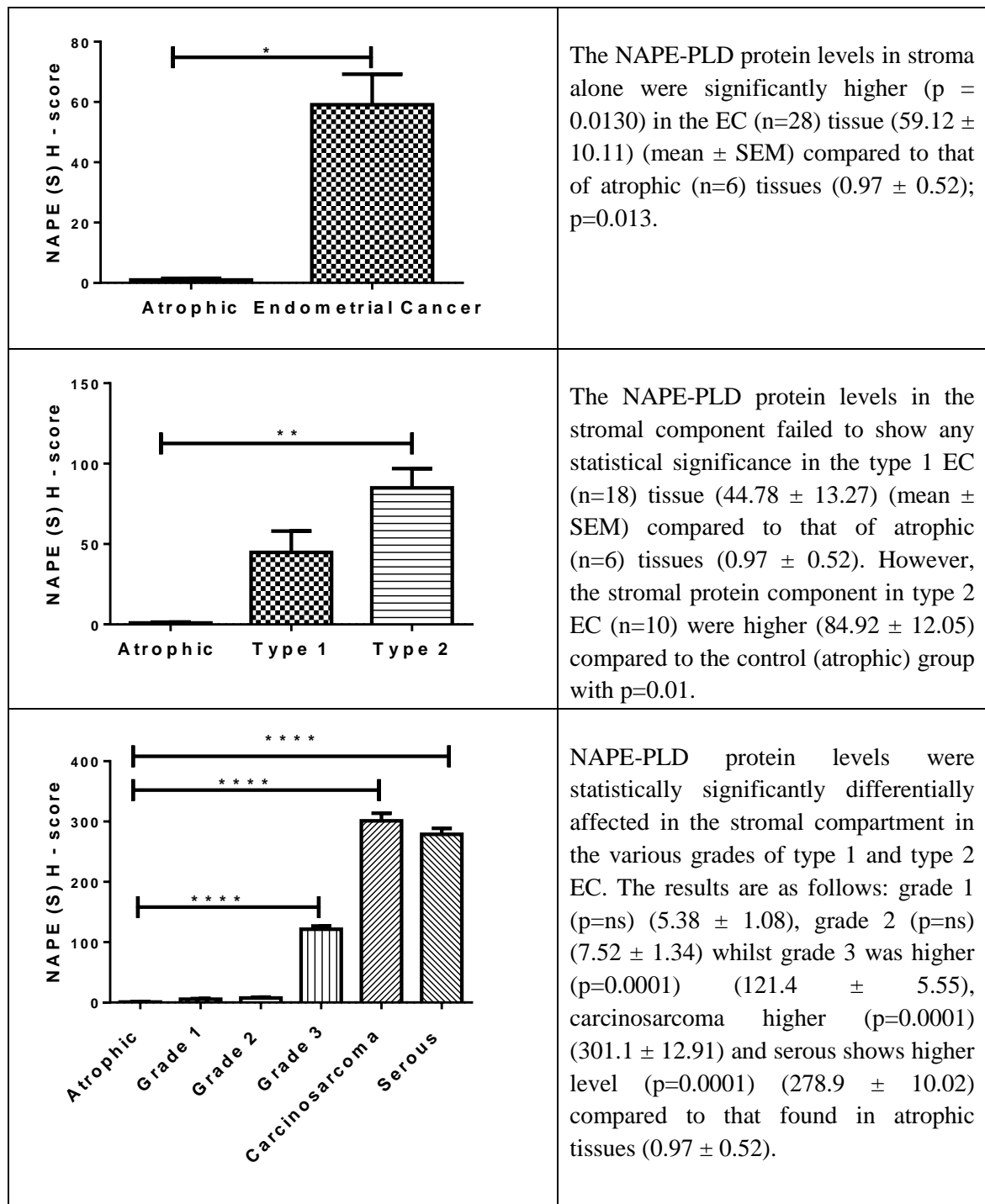


Figure 3-21C: Histomorphometric analysis of NAPE-PLD immunoreactivity (H-score) in stromal tissue (S).

P values were obtained using Student's t-test and one way ANOVA with Dunnett's ad hoc post-test analysis of the stromal component. Data presented as mean \pm SEM. Collectively, NAPE-PLD protein levels were raised in grade 3, carcinosarcoma and serous, when compared to control (atrophic) group.

3.3.7 The Relationship Between the NAPE-PLD and FAAH Expression Levels

As there was a lack of congruence between plasma endocannabinoid concentrations and the levels of the enzymes in the tissue, further analysis of the transcript and protein expression data was required. In this section, the relationships between the transcript and protein expression values were examined. Furthermore, evidence from placental studies has demonstrated that a stronger conclusion about the relative merits of enzyme activities could be generated using the NAPE-PLD: FAAH expression ratios (Karasu et al. 2014), so this was also examined.

3.3.7.1 Examination of the Relationship Between FAAH Transcript and Protein Levels

Figure 3-22 shows the relationship between FAAH transcripts and protein levels. The graphs in clearly show that both FAAH transcript level and FAAH protein levels are decreased in EC. These data go some way towards explaining the observed increased concentrations of AEA and PEA in EC (Chapter 2).

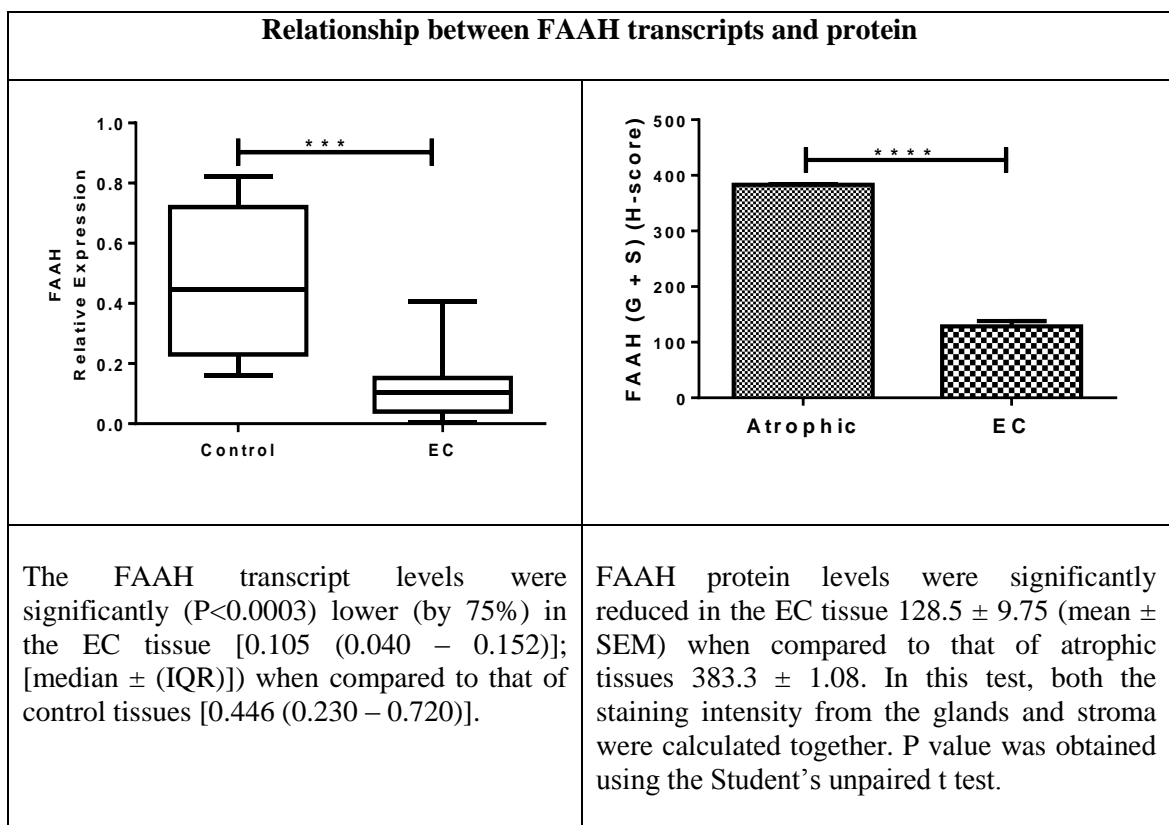


Figure 3-22: Graphs comparing FAAH transcripts and FAAH H-scores.

3.3.7.2 Examination of the Relationship Between NAPE-PLD Transcript and Protein Levels

Figure 3-23 shows the relationship between NAPE-PLD transcript and protein levels. The data indicate that although NAPE-PLD transcript levels were higher in EC, this did not reach statistical significance, yet the higher NAPE-PLD protein level did reach statistical significance. These data suggest that both FAAH and NAPE-PLD in the endometrial tissue may contribute to the observed increases in AEA and PEA found in plasma. Which of these two enzymes is the key one could be determined using correlation analyses.

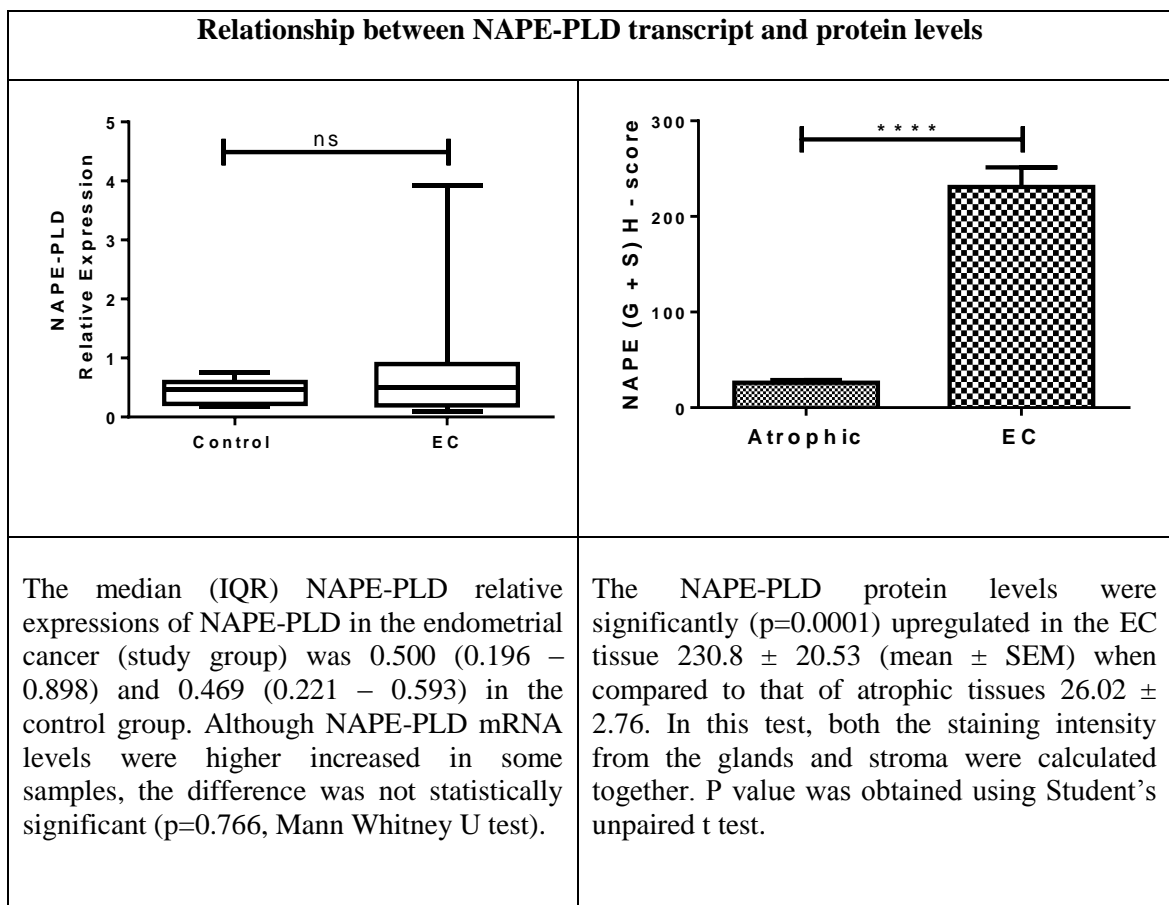


Figure 3-23: Graphs comparing NAPE-PLD transcripts and NAPE-PLD H-scores.

3.3.7.3 Correlation of NAPE-PLD and FAAH Expression at the Transcript Level

Figure 3-24 shows the correlation between NAPE and FAAH at transcript level. There was no significant relationship between the two transcripts, suggesting that the expression of these two enzymes may not controlled by similar factors.

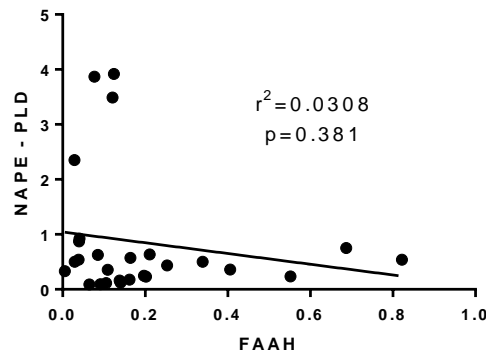


Figure 3-24: Correlation between NAPE-PLD and FAAH at the transcript level.

The graph shows the relative expression values of NAPE and FAAH transcripts for the same sample. The data were analysed using Spearman correlation.

3.3.7.4 Correlation of NAPE-PLD and FAAH Expression at the Protein Level

The correlation between NAPE-PLD and FAAH protein in the endometrial tissue are shown in **Figure 3-25**. There was a significant inverse correlation between the expression of the two proteins, suggesting that whatever regulates FAAH likely inversely affects NAPE-PLD protein expression and *vice versa*.

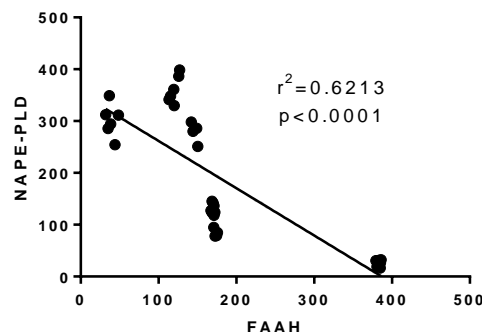


Figure 3-25: Correlation between NAPE-PLD and FAAH protein in the endometrium.

H-score values for NAPE-PLD and FAAH from the same samples were analysed using Spearman correlation.

3.3.7.5 NAPE-PLD: FAAH Transcript Ratios

NAPE-PLD: FAAH ratios at the transcript and protein level are compared in **Figure 3-26**. In both cases, the NAPE-PLD: FAAH ratios were increased in the EC group, suggesting that this is a good indicator of what is happening the endometrial cancer tissue, with NAPE-PLD being perhaps more important than FAAH in the regulation of plasma AEA and PEA levels.

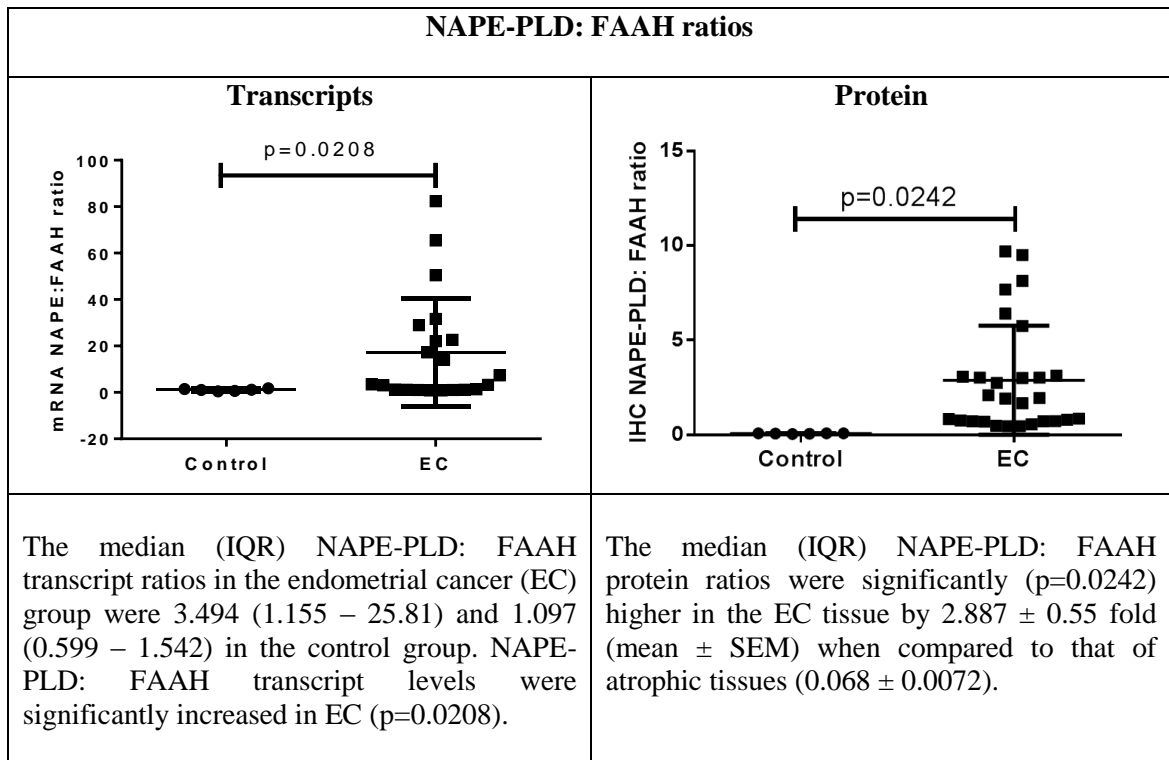


Figure 3-26: NAPE-PLD: FAAH transcript and protein ratios in control and EC endometria.

The NAPE-PLD: FAAH transcript and protein ratios were statistically significantly increased in EC group ($n = 28$), when compared to the atrophic (control) group ($n = 6$).

3.4 Discussion

In Chapter 2, I showed that AEA and PEA levels were higher in the plasma and endometrial tissues of patients with endometrial carcinoma. This prompted the question, “What could account for these observations?” The answer probably comes from the observation that the main regulators of these endocannabinoids in other tissues are the synthesising enzyme NAPE-PLD (Matias et al. 2006) and the degradation enzyme FAAH (Matias et al. 2006). Thus, I came to the hypothesis that the expression or activities of these two metabolising enzymes were probably perturbed in women with endometrial cancer and that this would be evident in the enzyme activities of peripheral lymphocytes, and/or the expression of the enzymes in the malignant tissue.

NAPE-PLD and FAAH are considered to be the “gate-keepers” in the production and degradation of several endocannabinoids, especially AEA and OEA, and through the entourage effect, PEA (Fezza et al. 2008). Although these enzymes could therefore play a vital role in influencing plasma and tissue endocannabinoids levels, there have been no published studies that have investigated the activity of FAAH and NAPE-PLD in endometrial cancers. However, there have been studies of these enzyme activities in early pregnancy complications, such as miscarriage (Maccarrone et al. 2000), in which they showed that low FAAH activity and high AEA tissue/plasma levels, were related to miscarriage but could not show an effect in NAPE-PLD expression or activity (Karasu et al. 2011, Taylor et al. 2011). What is interesting is that FAAH activity was reduced in ectopic pregnancy with no effect on NAPE-PLD expression (Gebeh et al. 2013). These data suggest that in non-malignant states, the main controlling factor for plasma endocannabinoid concentrations is FAAH expression and activity.

The data presented in this Chapter indicate that in patients with endometrial cancer peripheral lymphocytic FAAH activity is lower when compared to that of the controls. However, this lower activity failed to reach statistical significance, probably due to the small number of samples assessed. Although the number of blood samples collected should have been sufficient, the collaborators in Italy was unable to process all samples due to financial constraints and so the results are based on a smaller number of samples. Nevertheless, the lower FAAH activity in whole blood from EC patients goes a small way to explain the previously observed elevated AEA plasma concentrations (Chapter 2), since the expression of lower FAAH activity in patients with tumour probably

controls plasma AEA levels, as shown by the strong statistically significant inverse correlations between plasma AEA and OEA concentrations and lymphocytic FAAH activities. The statistically significant inverse correlation with plasma OEA concentrations may be explained by the “entourage effects” of FAAH (Lambert et al. 2002, Rodriguez de Fonseca et al. 2005), whereby one or two endocannabinoids are preferentially degraded, thereby potentiating the levels and actions of AEA in the local milieu. Interestingly, the inverse correlation between plasma PEA concentrations and FAAH, suggest that PEA is the endocannabinoid that is preferentially degraded by lymphocytic FAAH activity, although others suggest that PEA is not a substrate for FAAH (Maccarrone et al. 2002). Whether that is the same for tissue FAAH activities is impossible to conclude because that was not examined in this study, nor were peripheral and tissue NAPE-PLD activities examined, again because of the collaborator’s financial restraints. This is a drawback on this study, because these extra data could have allowed for a more robust interpretation of the results and thus is helpful in understanding the mechanism whereby plasma AEA and PEA concentrations are higher in patients with EC. There is some evidence that FAAH and NAPE-PLD enzyme activities are directly linked to their mRNA and protein expression (Maccarrone et al. 2000, Bari et al. 2006, Fonseca et al. 2014). In the light of the lack of enzyme activity data, the expression of the enzymes at the transcript and protein levels were used as surrogates for the enzyme activity data. Before the transcript study was undertaken, it was important to determine the optimal ‘endogenous control genes’, as per the MIQE guidelines (Bustin et al. 2009).

3.4.1 Identifying and Validating Endogenous Control Reference Genes for the Transcript Studies

Using a TaqMan® gene Expression Assay panel of 32 endogenous control reference genes, which represent different gene families and functional classes for use as reference genes to normalize qRT-PCR data, and using three commonly available software packages (geNorm, NormFinder and BestKeeper) to ascertain the best endogenous control reference genes, it was shown that the NormFinder software package was the most robust method of evaluating reference gene stability because it takes into consideration both the inter- and intra-variability during stabilisation assessment. Using NormFinder, MRPL19 was revealed to be the best single reference

gene and that PPIA and IPO8 to be the best two gene combination. To validate the best stable endogenous control to use here, MRPL19, PPIA and IPO8 were combined and used to normalize the expression of a gene of interest (CB1) and that pilot study showed that CB1 expression is reduced in endometrial cancer (this will be discussed further in Chapter 4). CB1 was chosen because the expression of CB1 transcripts in the menstrual cycle was already known (Taylor et al. 2010). From this normalization study, it was concluded that when comparing gene expression in normal and malignant endometrial tissues by qRT-PCR, the most reliable normalization is achieved with a combination of MRPL19, PPIA and IPO8 as the endogenous reference gene. This was then applied to the study evaluating the expression of FAAH and NAPE-PLD transcripts.

FAAH transcript levels were significantly lower by 75% in the malignant tissue when compared to that of control tissues. Sub-analysis of the two types of EC revealed that FAAH transcript levels were statistically significantly 73.3% lower in type 1 EC than in atrophic samples. Furthermore, a greater (93.3%) lower difference in FAAH transcript was observed in type 2 EC when compared that of the control group. When the EC was evaluated in various grades of tumour FAAH expression was lower in grade 1, 2 and 3 but it was higher in serous and carcinosarcoma EC when compared to the control group, but these results failed to show any statistical significance. Nevertheless, the data overall suggest that the higher plasma AEA and PEA concentrations could be controlled by the lower expression of FAAH transcript in the endometrium. Similar studies in prostate adenocarcinoma have shown that there was a higher FAAH expression in prostate cancers when compared to normal prostate tissues (Endsley et al. 2008), suggesting that not all cancers behave in the same way.

On the other hand, NAPE-PLD transcript levels were higher in EC but did not reach statistical significance compared to control (atrophic) group. When analysing the various grades, the relative expression of NAPE-PLD was lower in grade 1, 2 and 3, whilst it was higher in serous and carcinosarcoma EC, but however, all these results failed to reach any statistical significance. The interesting observation is that the expression of NAPE-PLD and FAAH transcripts appears to be inversely related; where FAAH is higher, NAPE-PLD is lower, suggesting that these two enzymes have a common regulator, albeit in different directions.

3.4.2 Localisation and Histomorphometric Analysis of NAPE-PLD and FAAH Expression

The data presented for NAPE-PLD and FAAH protein expression followed a similar pattern to that of the transcripts, only this time the differences observed had strong statistical significance, with the immunohistochemical scores for FAAH being all lower in EC and regardless of grade of tumour. These data suggest that protein measurements of enzyme expression are better than transcript measurements in providing support for the idea that plasma AEA and PEA concentrations are possibly regulated at the tissue level, if the relationship between protein expression and enzyme activity (Maccarrone et al. 2000, Maccarrone et al. 2002, Maccarrone et al. 2002, Maccarrone 2009) holds true for the endometrium. What is clear is that both enzymes show a difference of expression within the tissue cells that was related to disease.

The localisation of FAAH protein in the stroma and glands coupled with the reduction in FAAH histoscore is a novel finding as it implicates a possible role for this enzyme in regulating the local concentrations of the endocannabinoids (AEA and PEA) in the endometrium. The intensity of the staining pattern was lower in EC and various grades of EC tissues when compared to a strong staining intensity detected in the atrophic tissues.

On the other hand, the NAPE-PLD expression was localised both in the stroma and the glands of the EC with strong staining intensity, furthermore the intensity increased as the higher the histological grade of EC, when compared to very faintly stained NAPE-PLD in atrophic tissues. Again, this evidence was further strongly supported by a strong statistical significance in the high levels of histoscore in NAPE-PLD in EC and also in the various grades of EC, when compared to the control control (atrophic) group.

In summary, the observations presented in this Chapter indicate that there is an apparent perturbation in the regulation of the enzymes that possibly control local tissue and plasma concentrations of AEA and PEA (and perhaps OEA) in EC. If the effect is confined only to the endometrium, and the plasma concentrations are only a marker of what is happening in endometrium, then it might be more important to know how these changes affect “endocannabinoid signalling” in the local tissue milieu in endometrial cancer.

Therefore, working on the principle that expression (mRNA and protein) is related to function, the effect of local endocannabinoid production and stability can be assessed by localising the proteins of the receptors that endocannabinoids bind to, with the idea that knowing that information may help in understanding the role of endocannabinoid signalling in the development of EC.



Chapter 4

Expression and Localisation of the Classical and Non-Classical Endocannabinoid Receptors

4.1 Introduction

In previous chapters, the endocannabinoid ligands AEA, OEA and PEA were confirmed and quantified in plasma and endometrial tissues of both atrophic (control) and endometrial carcinoma (study) tissues. Plasma AEA and PEA concentrations and tissue levels were higher in endometrial carcinoma when compared to that in atrophic endometrium. Furthermore, it was shown that the metabolising enzymes NAPE-PLD and FAAH are present in the endometria of both groups of women and that the FAAH enzyme was active and different in the blood of these two groups. Following these observations, it was therefore thought now vital to further assess in detail the receptors involved in the endocannabinoid signalling and the mechanisms of action in EC.

AEA, the first endogenous ligand identified for cannabinoid receptors (Devane et al. 1992), is known to induce apoptotic cell death and to inhibit cell proliferation and migration in numerous murine and human tumour cell lines, including those derived from breast, prostate and uterine cervix cancer via CB1/CB2 receptor and TRPV1 receptor-dependent or -independent mechanisms (De Petrocellis et al. 1998, Maccarrone et al. 2000, Sanchez et al. 2003, Contassot et al. 2004). Higher AEA and 2AG tissue levels have been found in glioblastoma, pituitary adenoma, colon carcinoma and prostate carcinoma compared to normal tissues (Pagotto et al. 2001, Schmid et al. 2002, Ligresti et al. 2003, Nithipatikom et al. 2004, Petersen et al. 2005, Flygare et al. 2008) and in precancerous colon polyps than in colon carcinoma (Ligresti et al. 2003) and now in endometrial cancer tissues (Chapter 2). How this higher tissue level of AEA results in the reduced cell proliferation in murine and human tumour cell lines, but not in the tissue itself was the basis of the next stage of the work in this thesis.

Pharmacological studies have indicated the existence of other cannabinoid receptor subtypes (Mackie et al. 2006) and recently the orphan G protein coupled receptor, GPR55 has been characterised as a cannabinoid receptor (Okuno et al. 2011). GPR55 has been identified in the brain and several peripheral tissues, such as the gut, spleen, adrenals and the reproductive tract and two endocannabinoid ligands, 2-AG and PEA seem to have the greatest affinity for this receptor. In a recent study, it was reported that, 2-arachidonolyl lysophosphatidyl-inositol (LPI), may also be a ligand for GPR55

(Okuno et al. 2011). Since PEA is also elevated in endometrial cancer, it seemed prudent to include this receptor in the studies presented here.

The non-cannabinoid receptor known as the transient receptor potential vanilloid subtype 1 (TRPV1), a ligand-gated, Ca²⁺ permeable ion channel that has an almost ubiquitous distribution is thought to be involved in the ion-mediated actions of some cannabinoids including AEA (Huang et al. 2002) and *N*-arachidonoyldopamine (NADA), which bind to this receptor. For this reason, the endocannabinoids that act on the endovanilloid receptor, TRPV1, have also been referred to as endovanilloids (Huang et al. 2002).

In addition to cannabinoid receptor-mediated effects, it has been proposed that AEA also instigates cytotoxic effects in a cannabinoid-receptor-independent mechanism (Gustafsson et al. 2009), whereby it acts as an agonist at TRPV1 or GPR55 receptors. Although these receptors have been less widely investigated when compared to the classical cannabinoid receptors, CB1 and CB2, it is known that TRPV1 is overexpressed in human prostate cancer (Czifra et al. 2009) and squamous cell carcinoma of the tongue (Marincsak et al. 2009) and that lysophospholipids, recently identified as potent ligands for GPR55 (Okuno et al. 2011), are markedly elevated in ascites fluid of ovarian cancer patients (Xiao et al. 2001).

In this chapter, therefore, data from studies on the expression and distribution of the endocannabinoid and the non-endocannabinoid receptors CB1, CB2, GPR55 and TRPV1 are presented using RT-PCR Taqman chemistry technology to study transcript levels and immunohistochemistry to identify and locate the receptors at the protein level.

4.1.1 Aims

- (1) To determine the relative transcript levels of the receptors, CB1, CB2, GPR55 and TRPV1 in the normal and malignant endometrium.
- (2) To determine whether the transcript levels of CB1, CB2, GPR55 and TRPV1 differ in the normal and malignant endometrium using quantitative methods.
- (3) To localise and determine distribution patterns of the proteins for CB1, CB2, GPR55 and TRPV1 in the normal and malignant endometrium using IHC.

4.2 Subjects and Methods

4.2.1 Participants

The details of the subjects are as provided in Chapter 3 (**section 3.3.3.1**).

4.2.2 Transcript Levels for CB1, CB2, GPR55 and TRPV1

The techniques for the preparation of mRNA, conversion to cDNA and qRT-PCR are all described in Chapter 3 (**sections 3.2.3.5 and 3.2.3.6**). CB1, CB2, GPR55 and TRPV1 transcript levels were measured in triplicate and normalized against the geometric means of the housekeeping genes PPIA, MRPL19, and IPO8 (these based on the experiments in chapter 3), using the TaqMan real-time PCR technique.

The TaqMan® genes Expression Assay Kit, CNR1 (Hs00275634_m1), CNR2 (Hs00275635_m1), GPR55 (Hs00995276_m1) and TRPV1 (Hs00218912_m1) were purchased from Applied Biosystem's, Life Technologies, (Paisley, UK), as FAM/MGB dye-labelled probe. The validated TaqMan® endogenous control reference genes used for normalization were all VIC/TAMARA dye labelled assays purchased from Applied Biosystem's, Life Technologies, (Paisley, UK), and were, MRPL19 (Hs00608519_m1), PPIA (Hs99999904_m1) and IPO8 (Hs00183533_m1) and were chosen based on the data presented in chapter 3.

4.2.3 Localisation and Determination of Distribution Patterns of CB1, CB2, GPR55 and TRPV1 Receptor Proteins Using Immunohistochemistry

The expression and localisation patterns of CB1, CB2, GPR55 and TRPV1 proteins were obtained using the primary and secondary antibodies shown in **Table 4-1**.

Table 4-1: The antibodies used for IHC studies (with their sources and suppliers)

Antibodies	Source (Manufacturer)
<p style="text-align: center;">Primary</p> <ul style="list-style-type: none"> ❖ CB1 Rabbit Polyclonal Anti-Cannabinoid Receptor 1 (Sigma C1108) (Concentration 83.6 µg/ml) ❖ CB2 Rabbit Polyclonal Anti-Cannabinoid Receptor 2 (Sigma C1358) ❖ GPR55 Rabbit Polyclonal Anti-GPR55 Receptor (NB110-55498) (Concentration 1.0 mg/ml) ❖ TRPV1 Rabbit Polyclonal Anti-TRPV1 Receptor (Alomone labs ACC-030) (Concentrations 0.8 mg/ml) 	<p>SIGMA Life Science. Stockholm, Sweden</p> <p>Spruce Street Saint Louis, Missouri, USA</p> <p>Novus Biologicals Europe, Cambridge Science Park, UK</p> <p>Har Hotzvim Hi-Tech Park, Jerusalem, Israel</p>
<p style="text-align: center;">Secondary</p> <ul style="list-style-type: none"> ❖ Goat anti-rabbit Biotinylated antibody (secondary antibody 1:400 for CB1, CB2, GPR55 and TRPV1). 	<p>Vectorlabs, Peterborough, UK</p>

4.2.3.1 Immunohistochemistry for CB1

The techniques for IHC were similar to those for NAPE-PLD IHC (described in Chapter 3, section 3.2.4.4) except for the fact that on day 1, the washes were with TBS/0.1% BSA and 100 µl of CB1 1:500 and Rabbit IgG 1:10000 (both diluted in 10%NGS/TBS/0.1%BSA) and on day 2, sections were washed with TBS/0.1% BSA. Incubation of these reagents was performed overnight at 4°C in a humid chamber.

4.2.3.2 Immunohistochemistry for CB2

The methods were identical to one for CB1, except the primary CB2 antibody was used at a 1:150 dilution and the Rabbit IgG at a 1:5000 dilution. On the second day, the biotinylated goat anti-rabbit was used at the same dilution (1:400) but diluted in TBS.

4.2.3.3 Immunohistochemistry for GPR55

Slides were dewaxed in xylene and re-hydrated through graded alcohols (99% IMS to 70% IMS) and then to water (5 min each step) and then incubated in 6% H₂O₂ [51ml H₂O₂ + 249ml ice-cold dH₂O] for 10 min. The slides were next washed in dH₂O for 5 min and PBA [1% BSA in PBS (pH 7.4)] for 5 min. After wiping around the sections with tissue paper, 100 µl of normal goat serum (NGS) diluted to 1:20 in PBA was applied. These were placed in a humidity chamber for 30 min at room temperature and after the 30 minutes, drained and avidin blocking solution (4 drops/ml in 5% NGS/PBA) applied for 15 min. Following that, slides were racked and washed with PBA for 5 min before a biotin blocking solution (4 drops/mL in 5% NGS/PBA) was applied for 15 min. The slides were then completely drained before being incubated with 100 µl/section of the primary antibody (GPR55) diluted to 1:200 in NGS/PBA overnight at 4°C.

On day 2, the slides were washed in PBA (with magnetic stirring) for 20 min and incubated with 100 µl/section of biotinylated goat anti-rabbit antibodies diluted to 1:400 in PBS for 30 minutes. Thereafter, they were washed in PBA for 20 min. The avidin-biotin complexes, DAB staining and haematoxylin counterstaining were performed exactly as described for FAAH IHC (chapter 3, **section 3.2.4.3**) except PBA was used for the washing steps.

4.2.3.4 Immunohistochemistry for TRPV1

This was the same as that for NAPE-PLD (Chapter 3, **section 3.2.4.4**) except there was no antigen retrieval step (slides were not microwaved) and the TRPV1 primary antibody was diluted to 1:200 in TBA [1g BSA/100ml TBS].

On the second day, the only difference was that the racked slides were taken out of the refrigerator and placed on the bench and allowed to warm to room temperature for 1 hour before washing with TBA and exposure to secondary antibody.

4.3 Statistics

Statistical analysis of the data was performed using GraphPad Prism version 6.00 for Windows (GraphPad Software, San Diego CA, USA, www.graphpad.com). Data that did not follow a Gaussian distribution were expressed as medians and inter-quartile

range (IQR) and comparison between groups was performed using a one-way analysis of variance (ANOVA) followed by an appropriate ad hoc post analysis. On the other hand, data that was consistent with a normal distribution were analysed by the parametric one-way ANOVA with Dunnett's ad hoc post-test. In all cases, a $p < 0.05$ was considered significant.

4.4 Results

4.4.1 Patient Characteristics

These were presented in Chapter 3 (Results **section 3.3.4.1**).

4.4.2 CB1 Expression

4.4.2.1 CB1 Transcript Levels

The relative levels of CB1 transcript identified via qRT-PCR are shown and described in **Figure 4-1**. The data indicate that CB1 transcript levels were lower in malignant endometrium when compared to that of atrophic endometrium. Furthermore, sub analysis revealed that CB1 transcript levels were consistently lower across all grades and types of endometrial cancers.

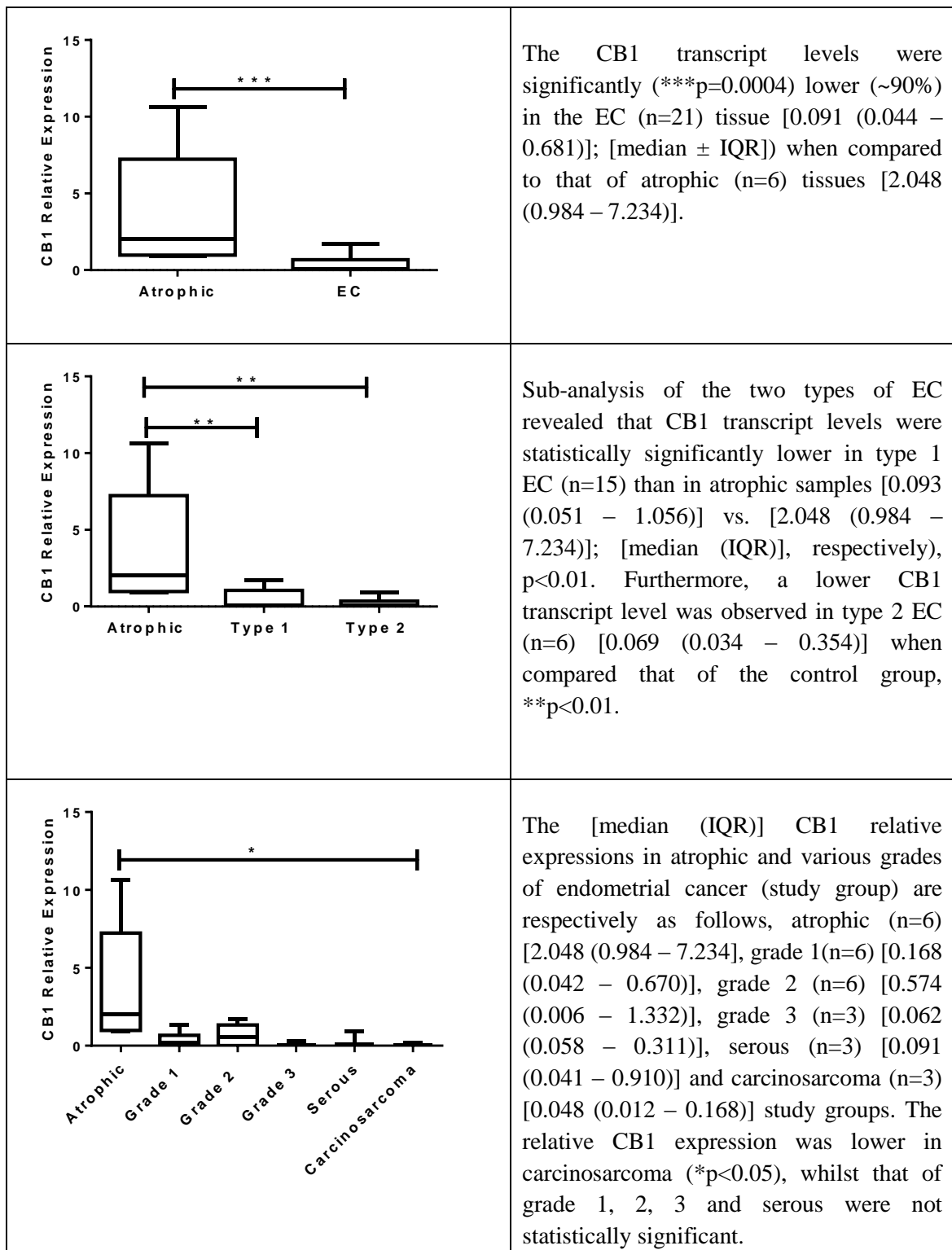


Figure 4-1: Relative expression of tissue CB1 transcript levels.

Data are presented as [median (IQR)]. P values were obtained using Mann-Whitney analysis and Kruskal-Wallis ANOVA with Dunn's ad hoc post-test analysis.

4.4.2.2 CB1 Protein Expression

4.4.2.2.1 Optimisation and Validation of Immunohistochemical Methods for CB1

The optimal primary antibody dilution for CB1 was obtained by using different dilutions, as follows: (1:400, 1:500, 1:600 and 1:700). An example of the staining intensities obtained using these dilutions are shown in **Figure 4-2**. From these images, the best dilution used was determined to be 1:500.

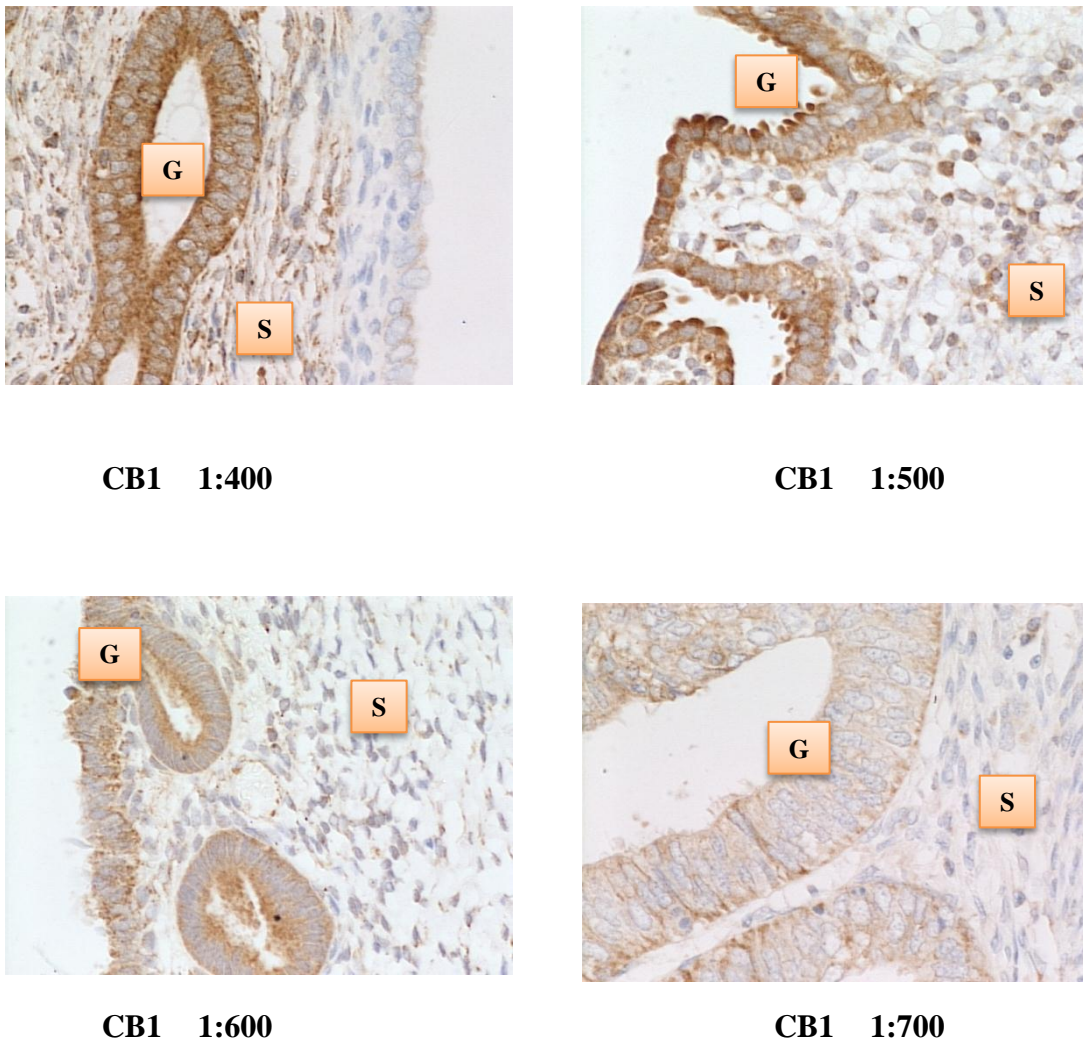


Figure 4-2: Staining intensities for CB1 at different antibody dilutions (S=stroma, G=glands).

Very strong staining was obtained with 1:400 and very light staining with 1:600 and 1:700 dilutions. The 1:500 dilutions provided the optimal staining pattern.

Antibody specificity was determined using equivalent concentrations of non-immune IgG (**Figure 4-3**). The lack of 3, 3'-diaminobenzidine (DAB) staining in the IgG (negative) controls indicates that the antibodies are specific for CB1.

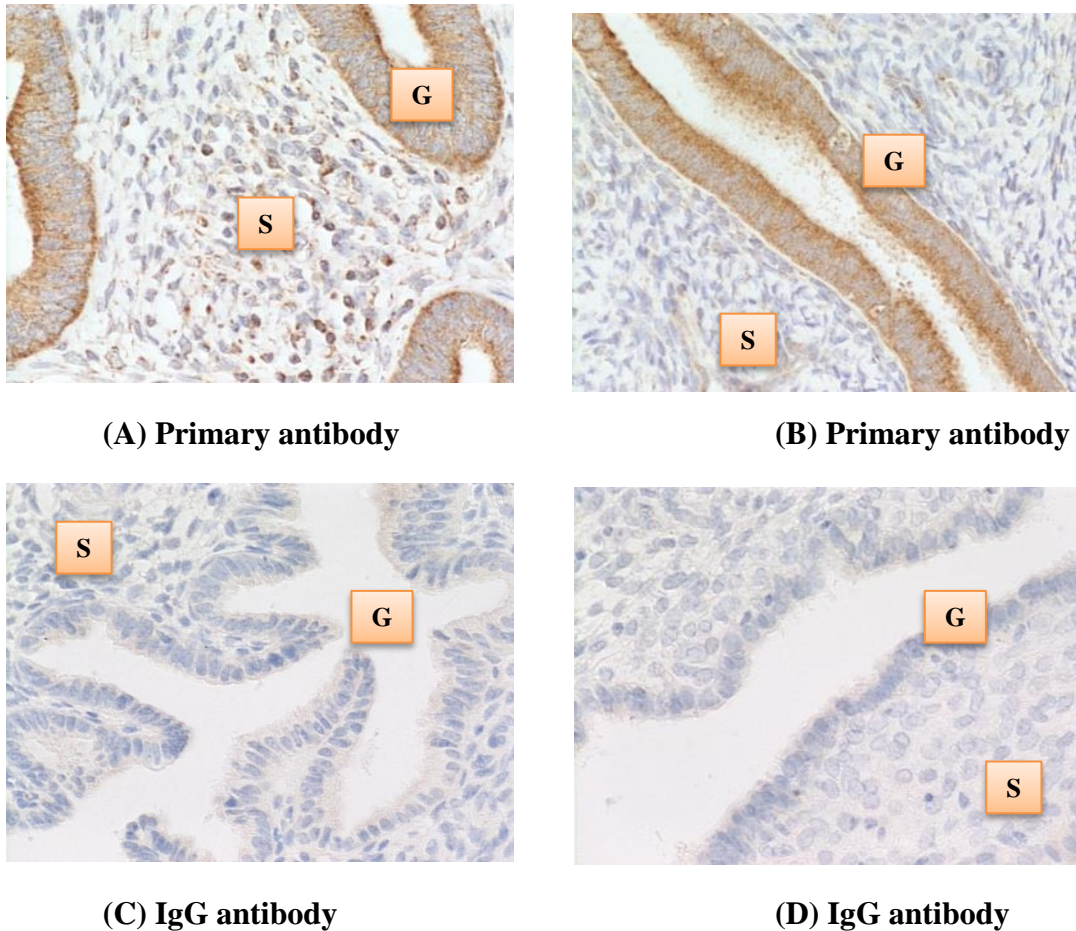


Figure 4-3: Specificity of the primary CB1 antibody.

Images (A) and (B) show positive DAB staining of the tissue with the primary CB1 antibody (more in the glands than the stroma), whilst images (C) and (D) show no DAB staining of the tissue for the IgG (negative) controls. All the slides used were uterine samples, (S=stroma, G=glands).

4.4.2.2 Identification and Location of CB1 Protein Expression

Figure 4-4 illustrates the staining pattern of CB1 in atrophic and EC samples. Following the optimisation of CB1 antibody, all the studies were undertaken as a single run to minimise variations.

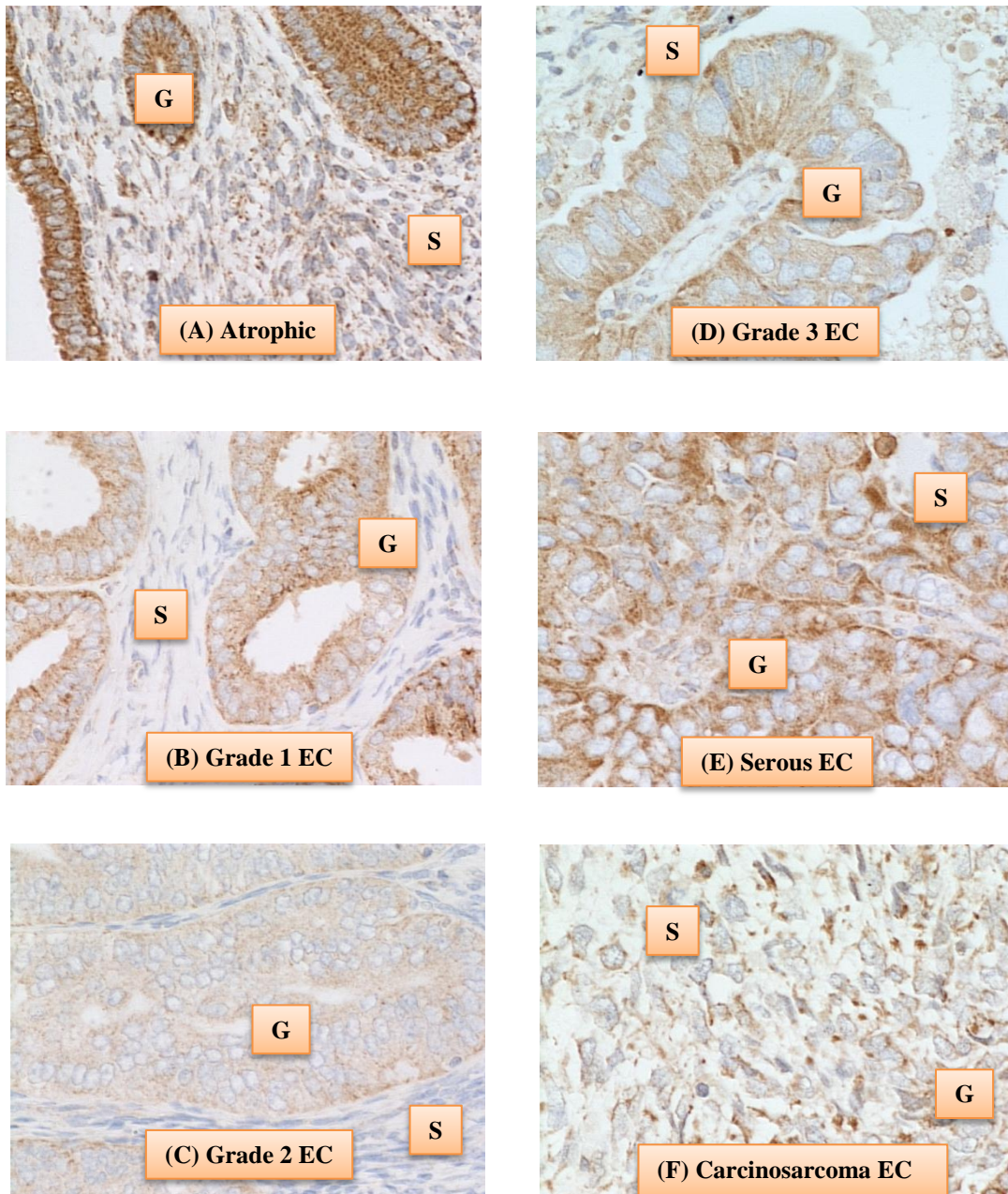


Figure 4-4: Localisation and expression of the CB1 protein in various tissues (G=glands, S=stroma, EC=endometrial cancer).

Staining was found in both the glands and stroma and differed between tissue samples. In atrophic tissue, immunoreactive CB1 protein was expressed very strongly in the glands, particularly along the apical region of the epithelial cells when compared to the basal region of the cells. As expected, the number of glands was markedly reduced in the atrophic endometrium compared to cancer tissue. Furthermore, the stromal component of the atrophic endometrium also showed evidence of immunoreactivity. CB1 was demonstrated in the cytoplasm of the glands and concentrated more to the apical region but not in the nucleus (**Figure 4-4A**).

The CB1 staining intensity in grade 1 EC was lower compared to that observed in the atrophic endometrium. The staining involved both the stroma and the glands; more prevalent in the epithelial cell cytoplasm. The nuclei were not stained (**Figure 4-4B**).

The CB1 staining intensity in grade 2 EC tissues was very low compared to atrophic endometrium. This staining clearly involved both the glands and the stroma. In the glands, the staining was more cytoplasmic and also concentrated towards the apical region of the cells. The nuclear envelope was only slightly stained (**Figure 4-4C**).

The CB1 staining intensity in grade 3 EC was very low compared to atrophic tissue. It clearly showed involvement of the glands with a very low intensity in the stroma. In the glands, the staining was also cytoplasmic and concentrated towards the apical region of the cells. The nuclear envelope was slightly stained but the nucleus itself was negative (**Figure 4-4D**).

The CB1 staining intensity in serous carcinoma was of low intensity compared to atrophic endometrium. It involved the glands (very mild intensity) in the stroma. In the glands, staining was cytoplasmic, and more diffuse in both at the apical and basal regions of the cells. The nuclear envelope and the nucleus showed staining both in the glands and the stroma (**Figure 4-4E**).

The CB1 staining intensity in carcinosarcoma was very low compared to the atrophic endometrium. It involved both the glands and the stroma. In the carcinosarcoma tissue the glandular structure was completely 'broken down' and the epithelial cells scattered throughout the tissue making it very difficult to differentiate the glands. Nevertheless, the staining was cytoplasmic with more towards the apical region of the cells. The

nuclear envelope and the nucleus showed staining both in the glands and the stroma (**Figure 4-4F**).

4.4.2.2.3 Histomorphometric Quantification of CB1 Protein

Figure 4-5A, shows the data from the histomorphometric analysis of glands and stroma (G+S), whilst **Figures 4-5B** and **4-5C** show the analysis for the glands (G) and stroma (S) alone, respectively. The data show that CB1 protein levels are lower in the endometrial cancer tissue in line with the data shown in **Figure 4-4**. The lowest levels were observed in type 1 EC tissues (grades 1, 2 and 3), but also significantly lower in the type 2 EC tissues (carcinosarcoma and serous).

When the H-score for the glands alone were examined (**Figure 4-5B**), all of the EC tissues showed lower CB1 protein intensities compared to atrophic endometria. By contrast, the H-scores for the stromal tissue alone (**Figure 4-5C**) showed a significant higher staining intensity in the type 2 EC tissues (carcinosarcoma and serous) and no effect in the type 1 EC tissue, because there was significantly lower stromal H-score for grade 1 and grade 2 tissues compared to atrophic tissue, but a significantly higher stromal H-score for the grade 3 tissue (**Figure 4-5C, lower panel**).

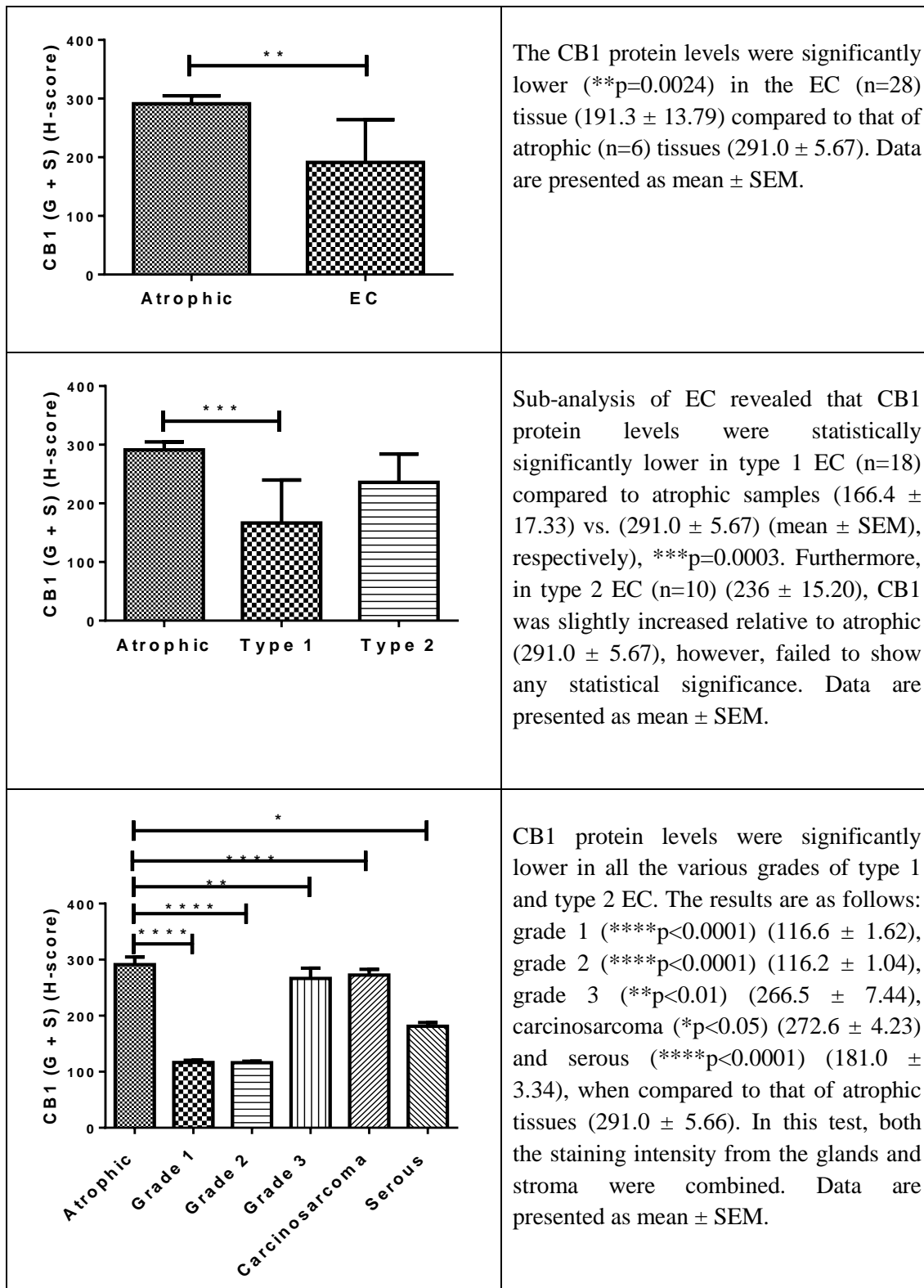


Figure 4-5A: Histomorphometric (H-score) analysis of immunoreactive CB1 (G + S) proteins.

P values were obtained using Student's t-test and one way ANOVA with Dunnett's ad hoc post-test analysis of both components of the tissues, and the glands and stoma separately. Data are presented as mean \pm SEM. Collectively, CB1 protein levels are reduced in EC (G+S) tissue when compared to the atrophic endometrium.

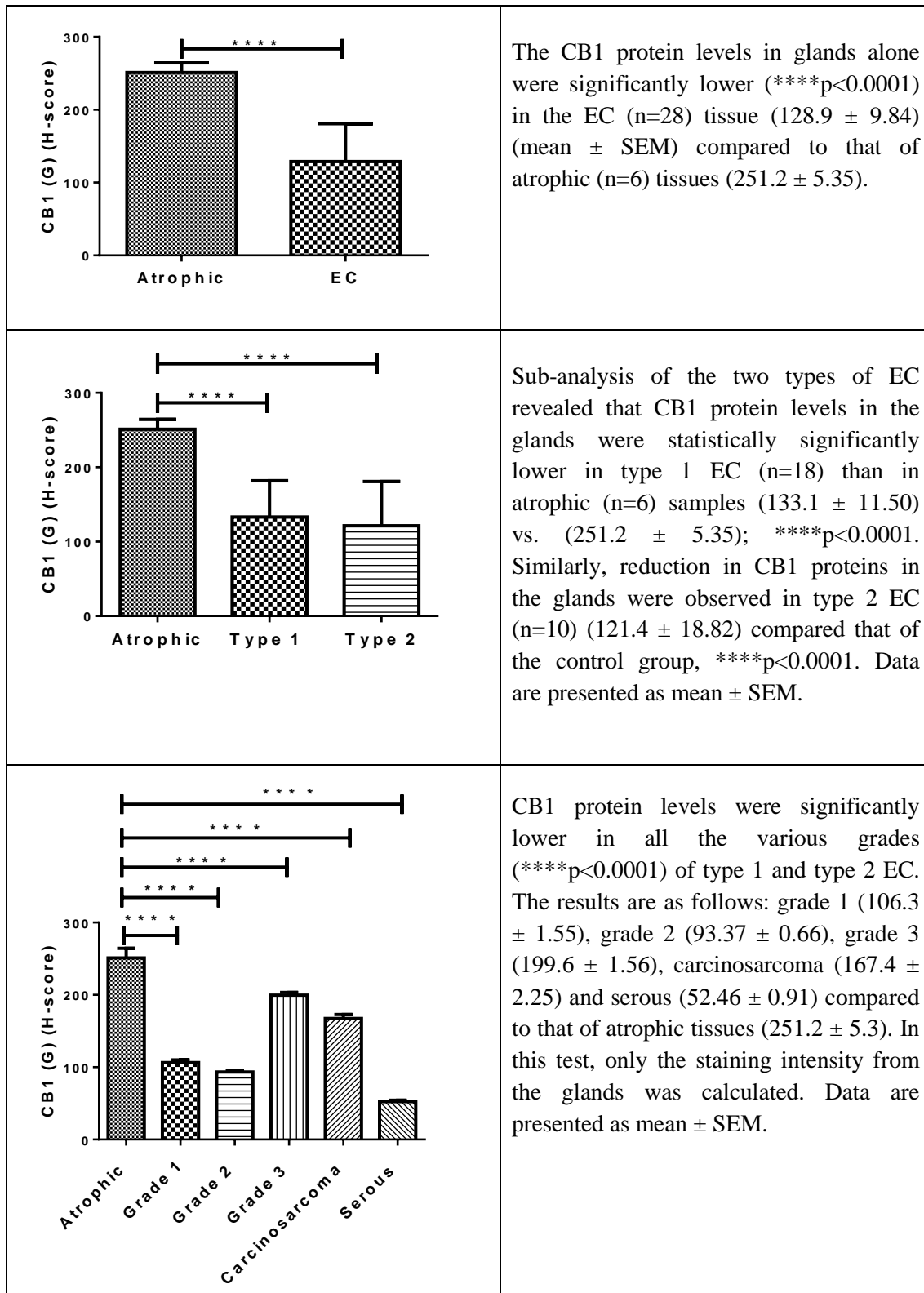


Figure 4-5B: Histomorphometric (H-score) analysis of immunoreactive CB1 (G) proteins.

P values were obtained using Student's t-test and one way ANOVA with Dunnett's ad hoc post-test analysis of the gland components of the tissues. Data are presented as mean \pm SEM. Collectively; CB1 protein levels are lower in EC (G) when compared to the atrophic endometrium.

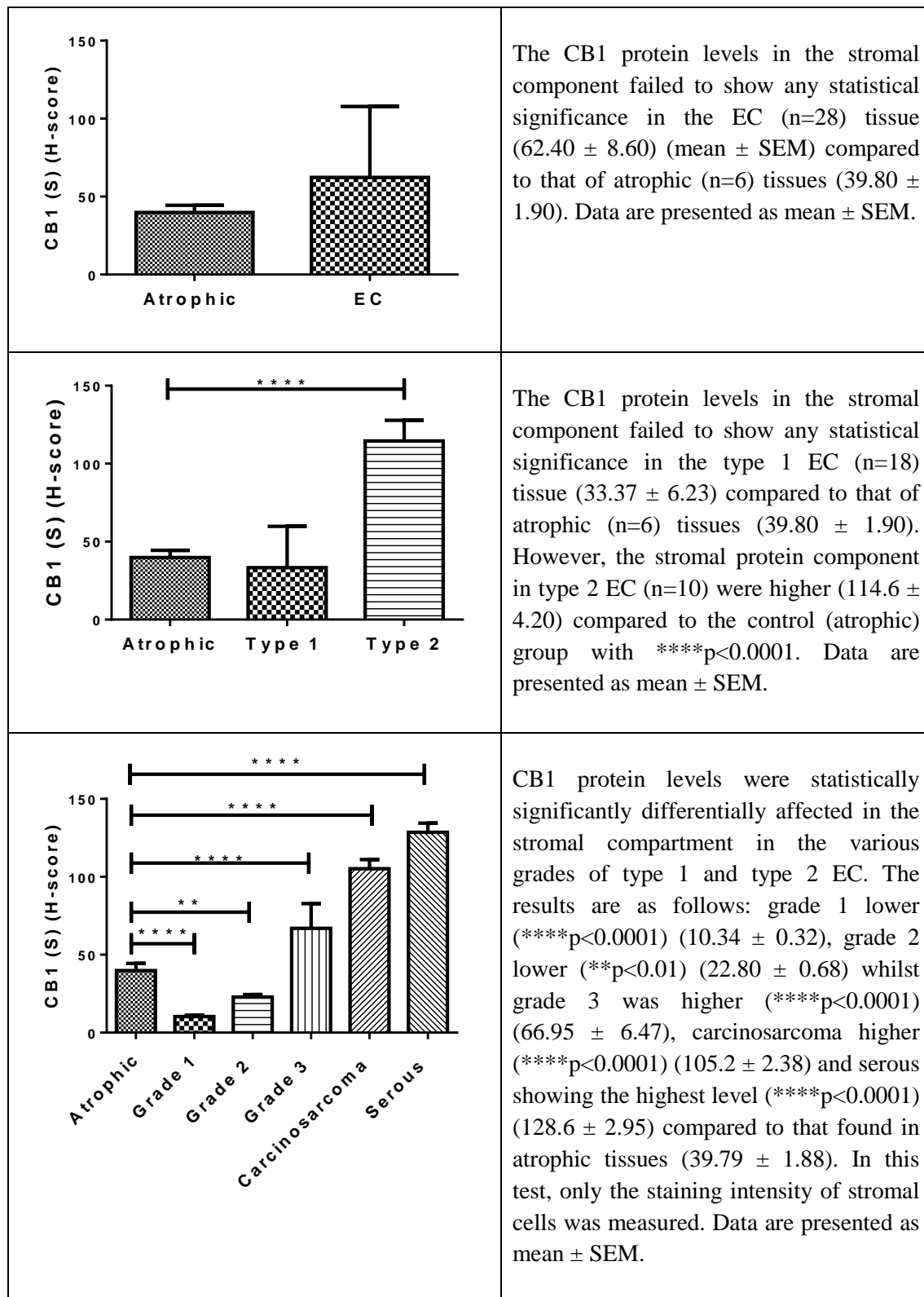


Figure 4-5C: Histomorphometric (H-score) analysis of immunoreactive CB1 (S) proteins.

P values were obtained using Student's t-test and one way ANOVA with Dunnett's ad hoc post-test analysis of the stromal component. Data presented as mean \pm SEM. Collectively, CB1 protein levels are reduced in the stroma (S) of grade 1 and 2 EC, while raised in grade 3, carcinosarcoma and serous, when compared to the atrophic endometrium.

4.4.3 CB2 Expression

4.4.3.1 CB2 Transcript Levels

The relative CB2 transcript levels expressed in atrophic and malignant endometrium, as determined by qRT-PCR, are shown in **Figure 4-6**. The data show that like CB1, the transcript levels for CB2 were lower in endometrial cancer. Furthermore, sub-analysis of CB1 transcript levels showed that they were lower in both type 1 and type 2 EC compared to atrophic endometrium. When the analysis was performed on the various grades, it was evident that CB2 transcript levels were lower in the high grade EC (grade 3, carcinosarcoma and serous).

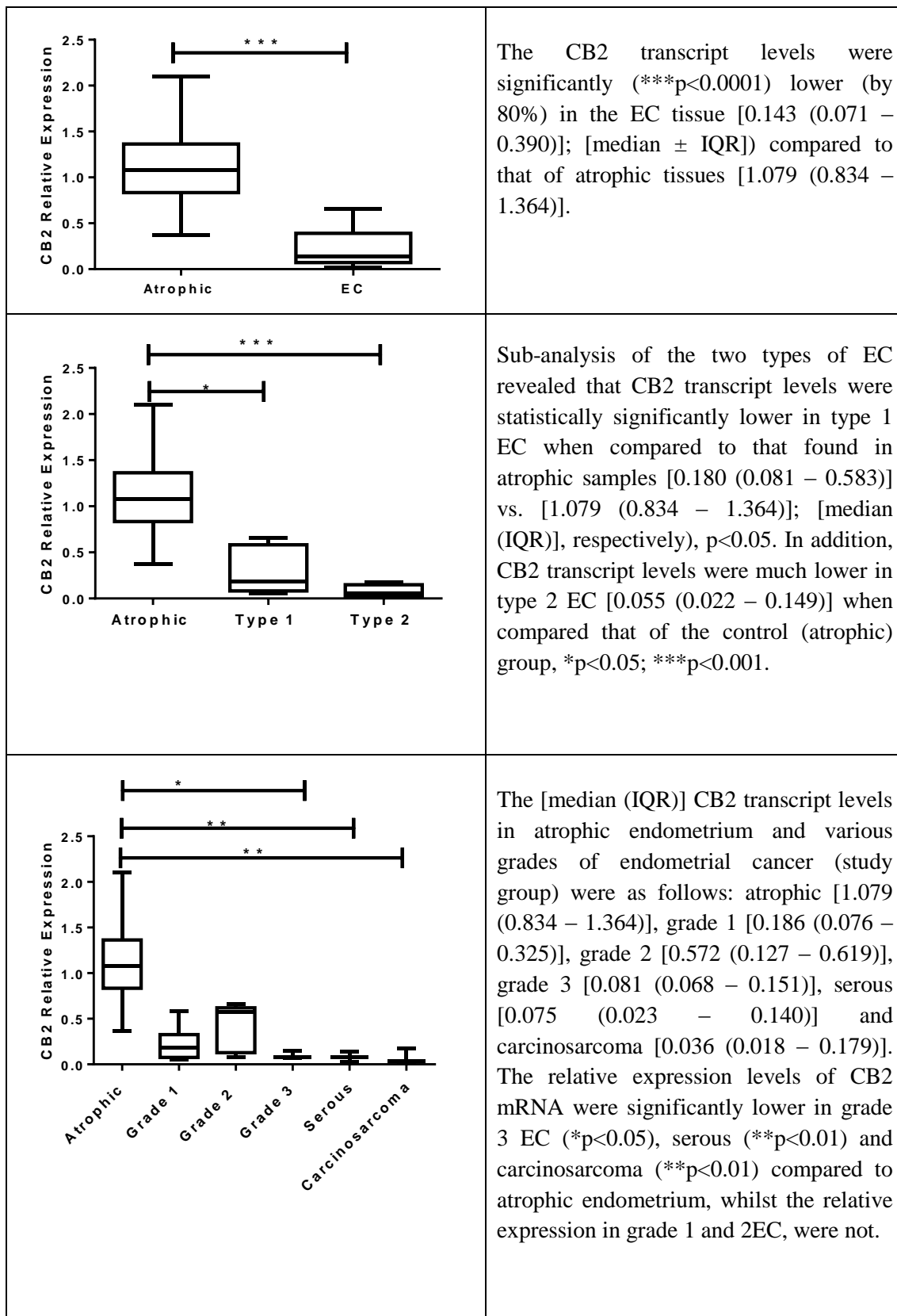


Figure 4-6: Relative expression of CB2 transcript levels.

Data are presented as [median (IQR)]. P values were obtained using Mann-Whitney U-test and Kruskal-Wallis ANOVA with Dunn's ad hoc post-test analysis.

4.4.3.2 CB2 Protein Expression

4.4.3.2.1 Optimisation and Validation of Immunohistochemical Methods for CB2

The optimal primary antibody dilution for CB2 was obtained by using different dilutions, as follows: (1:100, 1:150, 1: 200 and 1:300). An example of the staining intensities obtained using these dilutions are shown in **Figure 4-7**. From these images, the best dilution was determined to be 1:150.

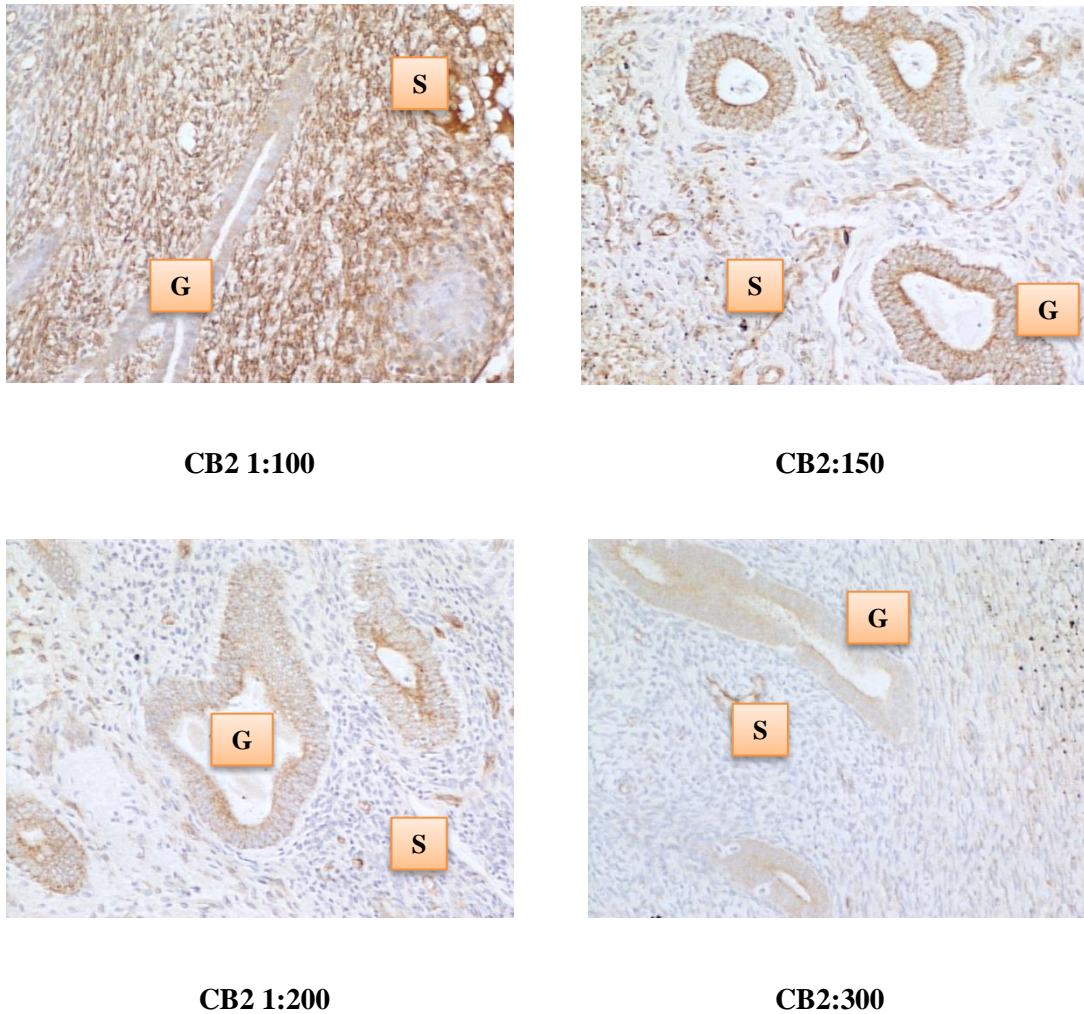
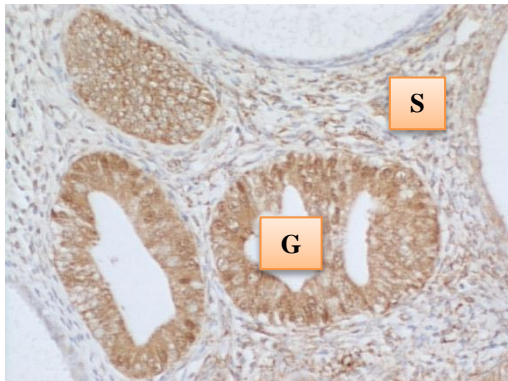


Figure 4-7: Staining intensities for CB2 at different antibody dilutions (S=stroma, G=glands).

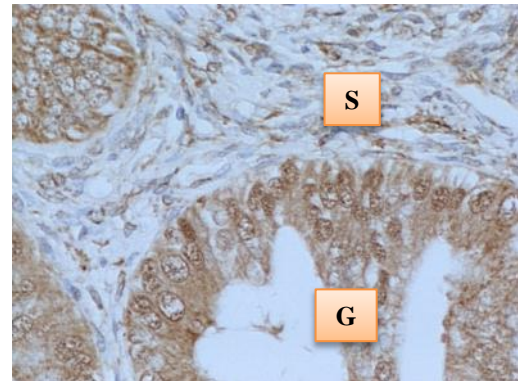
Very strong staining of the entire tissue was obtained with the 1:100 antibody dilution and very light staining with 1:200 and 1:300. The 1:150 antibody dilutions provided the optimal staining pattern.

Antibody specificity was determined using equivalent concentrations of non-immune IgG (**Figure 4-8**). The lack of DAB staining in the IgG controls indicates that the antibodies are specific for CB2.



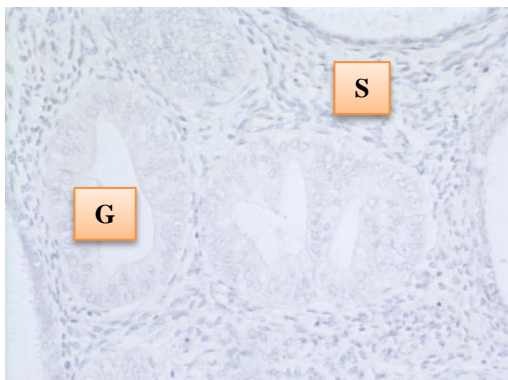
(A) CB2 primary antibody

Positive control



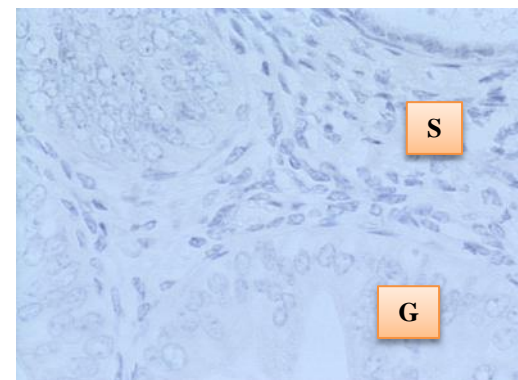
(B) CB2 primary antibody

Positive control



(C) IgG antibody

Negative control



(D) IgG antibody

Negative control

Figure 4-8: Negative control experiment demonstrating the specificity of the primary CB2 antibody.

Images (A) and (B) show positive staining of the primary antibody CB2 (more staining was observed in the glands than in the stoma), whilst images (C) and (D) show no staining for the IgG controls. Images on the left were taken at 200x magnification, and those on the right at 400x magnification.

4.4.3.2.2 Identification and Locations of CB2 Protein

Figure 4-9 illustrates the staining pattern for CB2 antibodies in atrophic and EC tissues. Following the optimisation of CB2 antibody, all the studies were undertaken as a single run to minimise variations.

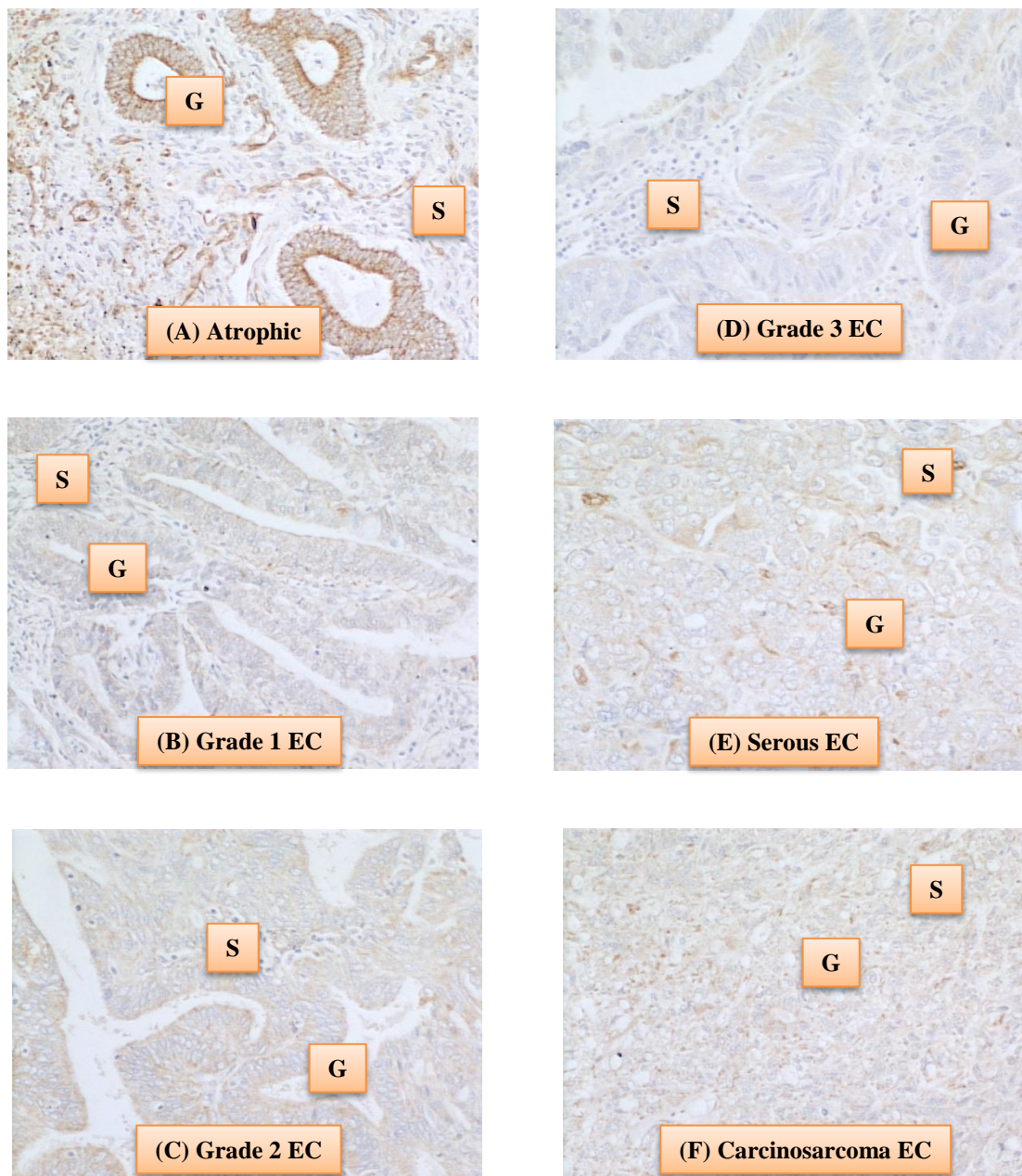


Figure 4-9: Localisation and expression of the CB2 protein in various tissues (G=gland, S=stroma, EC=endometrial cancers).

The data in **Figure 4-9** show that CB2 staining intensity was very strong in the atrophic glands, with additional staining in the stroma. In the atrophic tissue, CB2 immunoreactive protein was observed at a strong intensity of immunoreactivity along the luminal and basal surfaces of the glands compared to the remaining cell membranes. It was evident that the stroma was highly stained with strong immunoreactivity in and around the smaller blood vessels, but the staining was not as strong as that observed in the glands. The slightly lower staining intensity might be related to cellularity since the stromal cells cover a larger area especially when the numbers of glands are reduced in atrophic endometrium. CB2 was demonstrated in the cytoplasm of the both glandular epithelial and stromal cells with some staining observed over the nucleus in both cell types.

In type 1 EC (**Figure 4-9**), the glands were stained more when compared to the stromal component and this was true for grade 1 (panel B), grade 2 (panel C) and grade 3 (panel D), with generally more staining in the cytoplasm than in the nucleus of type 1 EC. Furthermore, in serous tissue, the CB2 staining was more easily observed in the glands especially in the apical region. Staining in the stromal cell was minimal, whilst in carcinosarcoma, it seems that CB2 staining involved the nucleus of the gland and spared its cytoplasm, whilst stromal involvement was very minimal.

4.4.3.2.3 *Histomorphometric Quantification of CB2 Protein*

Figure 4-10A shows the data from the histomorphometric analysis of the glands and stroma (G + S) combined, while **Figures 4-10B** and **4-10C** show the analysis for the glands (G) and stroma (S) alone, respectively. The data show that immunoreactive CB2 protein levels are lower in the endometrial cancer tissue in line with the transcript data shown in **Figure 4-6**. The levels observed in type 1 EC tissues were just as low as that in type 2 EC tissue.

When the H-score for the glands alone were examined (**Figure 4-10B**), all of the EC tissues showed lower CB2 protein intensities compared to atrophic endometria. Similarly, the H-scores for the stromal tissue alone (**Figure 4-10C**) showed a significant lower staining intensity in the type 1 and 2 EC tissues compared to the atrophic endometrium.

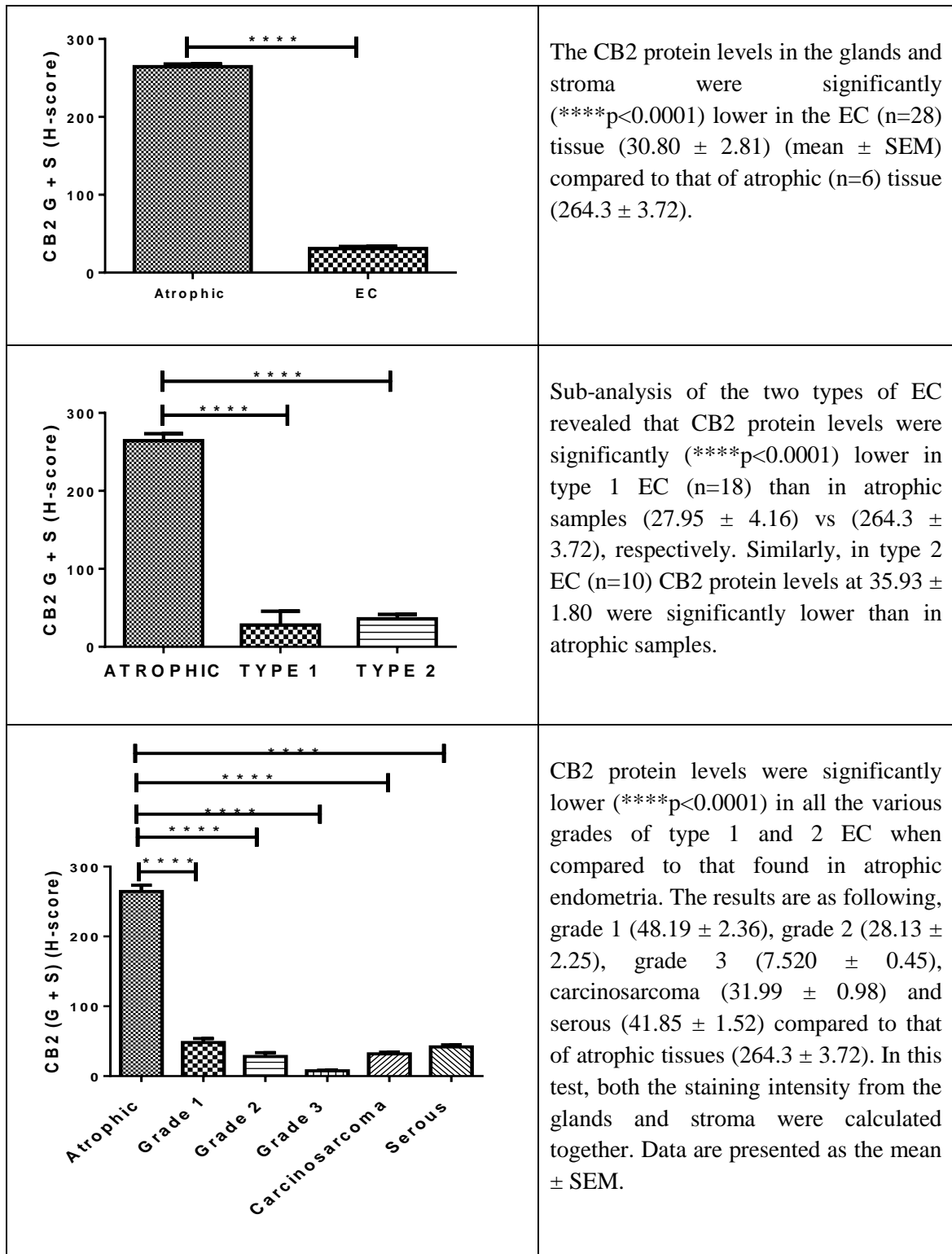


Figure 4-10A: Histomorphometric (H-score) analysis of immunoreactive CB2 (G + S) protein.

P values were obtained using Student's t-test and one way ANOVA with Dunnett's ad hoc post-test analysis of both the entire tissue, and the glands and stroma alone. Data are presented as mean \pm SEM. Collectively, CB2 protein levels are reduced in EC (G+S) when compared to the atrophic endometrium.

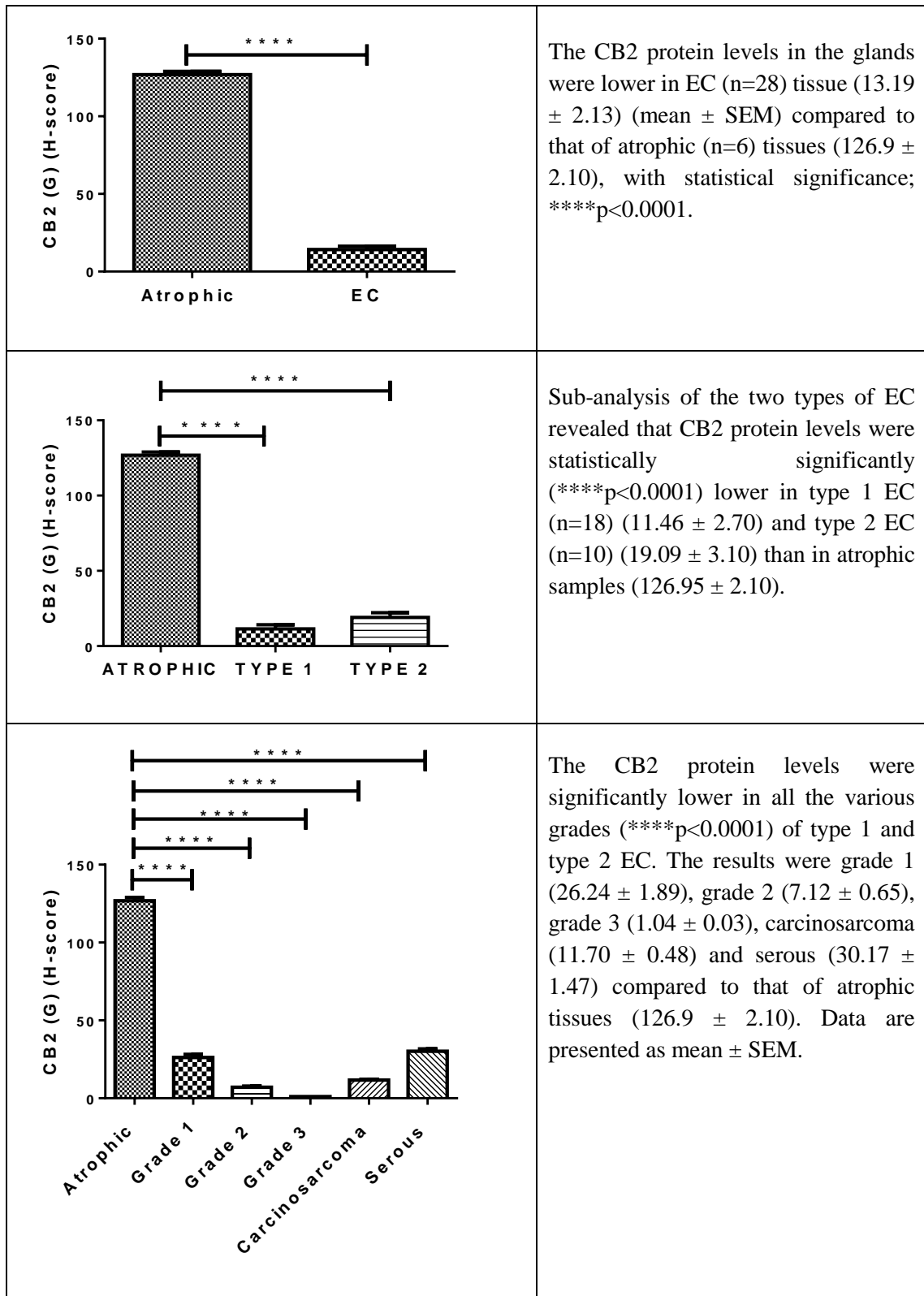


Figure 4-10B: Histomorphometric (H-score) analysis of immunoreactive CB2 (G) protein.

P values were obtained using Student's t-test and one way ANOVA with Dunnett's ad hoc post-test analysis of the glands. Data are presented as the mean \pm SEM. Collectively, CB2 protein levels are reduced in EC (G) when compared to atrophic endometrium.

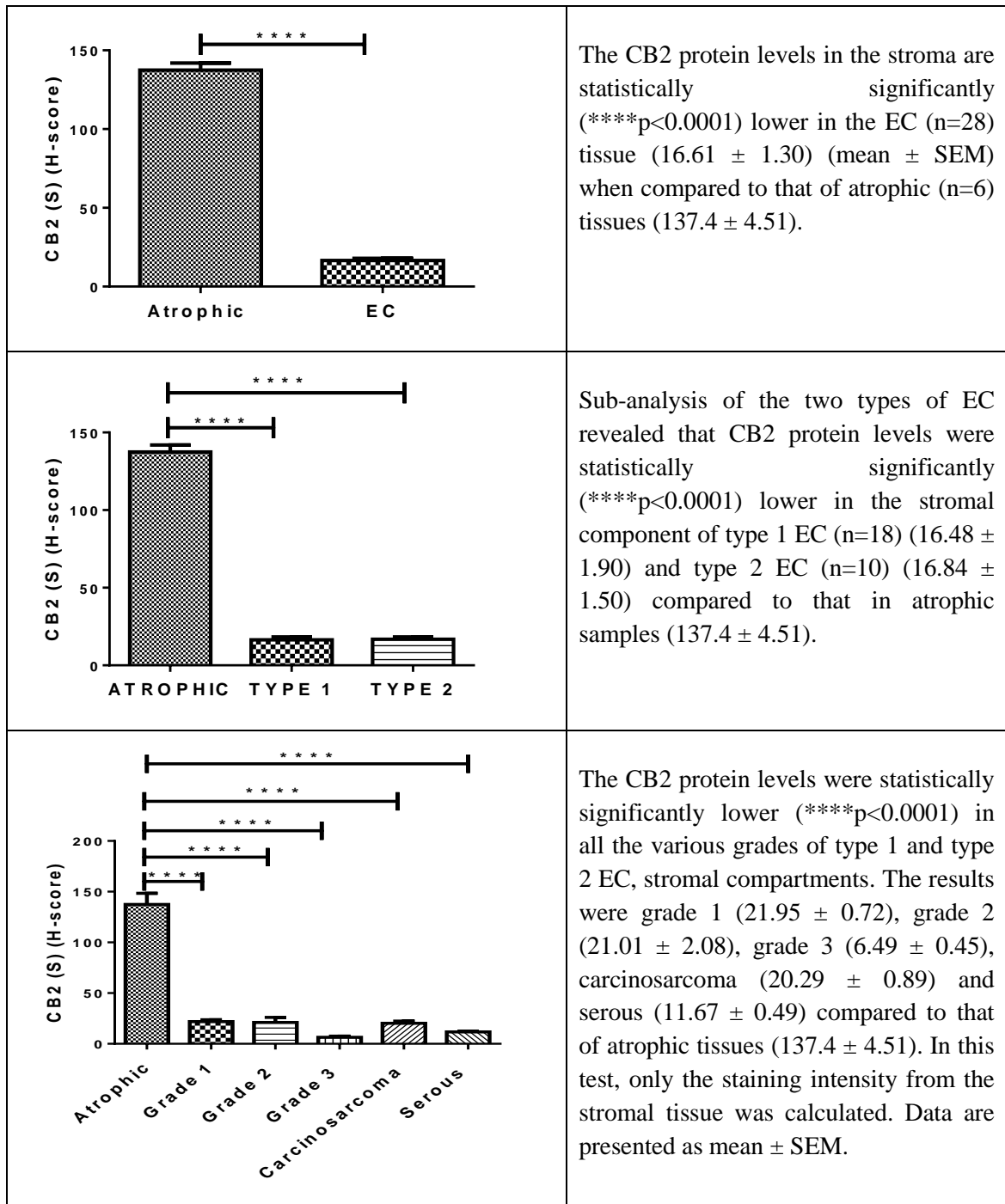


Figure 4-10C: Histomorphometric (H-score) analysis of immunoreactive CB2 (S) protein.

P values were obtained using Student's t-test and one way ANOVA with Dunnett's ad hoc post-test analysis of the stromal tissue. Data presented as mean \pm SEM. Collectively, CB2 protein levels are reduced in the EC (S) when compared to that of the atrophic endometrium.

4.4.4 GPR55 Expression

4.4.4.1 GPR55 Transcript Levels

The transcript levels for GPR55 were the exact opposite of those for CB1 and CB2 with significantly higher levels in the malignant tissue (**Figure 4-11**). Furthermore, sub-analysis showed that only the levels in the type 1 EC tumour was responsible for this increased expression (**Figure 4-11**). More detailed analysis showed that this was confined primarily to grade 1, type 1 EC, and although the GPR55 transcript levels in grades 2 and 3, and type 2 EC were also higher, they did not reach statistical significance. These data suggest that the GPR55 receptor may be a key molecule in the early stages of EC development.

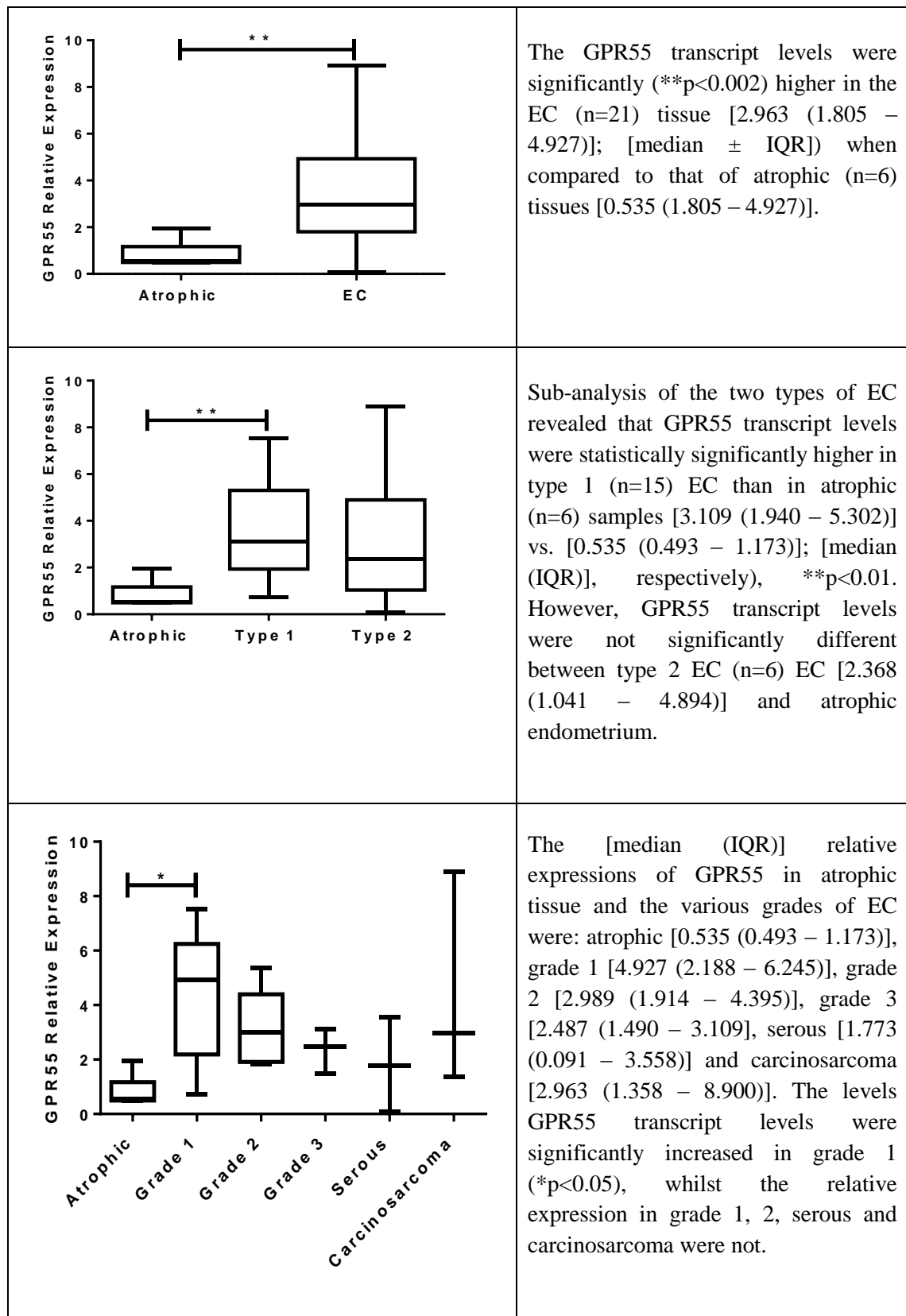


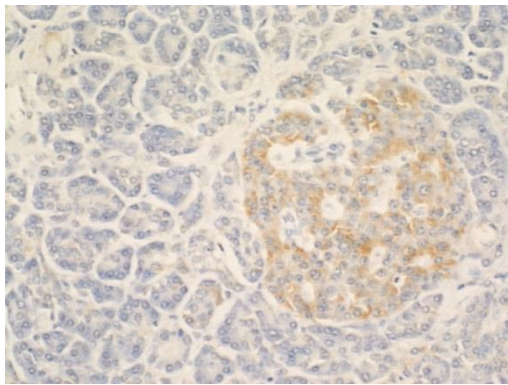
Figure 4-11: Relative expression of GPR55 transcript levels.

Data are presented as [median (IQR)]. P values were obtained using Mann-Whitney analysis and Kruskal-Wallis ANOVA with Dunn's ad hoc post-test analysis.

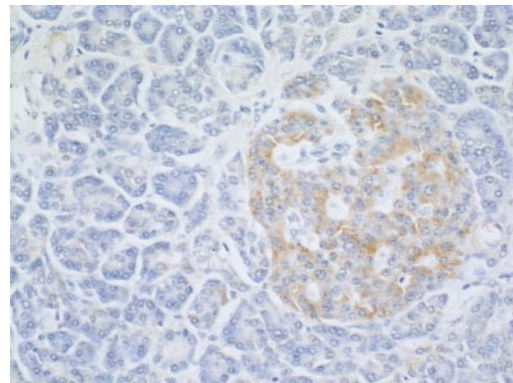
4.4.4.2 GPR55 Protein Expression

4.4.4.2.1 *Optimisation and Validation of Immunohistochemical Methods for GPR55*

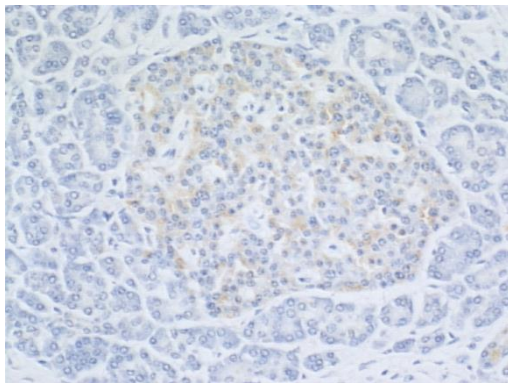
The optimal primary antibody dilution for GPR55 was obtained by using different dilutions, as follows: (1:100, 1:200, 1: 300 and 1:350). An example of the staining intensities obtained using these dilutions are shown in **Figure 4-12**. From these images, the best antibody dilution was determined to be 1:200.



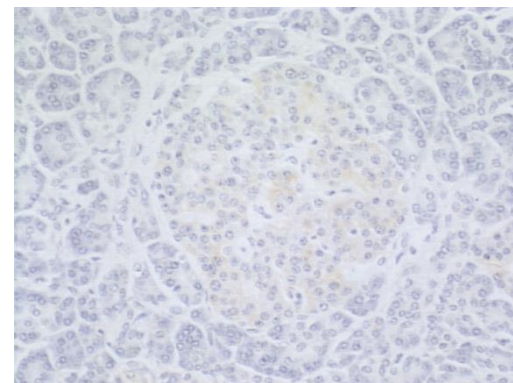
GPR55 1:100



GPR55 1:200



GPR55 1:300

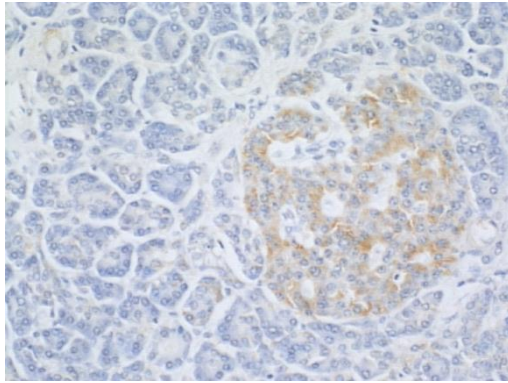


GPR55 1:350

Figure 4-12: Staining intensities for GPR55 at different antibody dilutions using human pancreas as the control tissue.

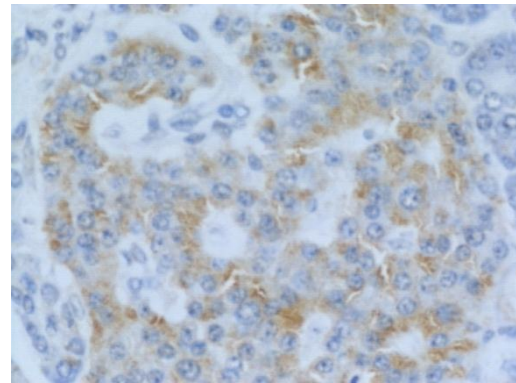
Very strong staining was obtained within Islets of Langerhans's with the 1:100 GPR55 antibody dilutions, together with some non-specific staining of the acinar cells. A very light staining with 1:300 and 1:350 antibody dilutions. The 1:200 antibody dilutions provided the optimal staining pattern (lightly stained acinar cells, but positive stained Islets of Langerhans's).

Antibody specificity was determined using equivalent concentrations of non-immune IgG (**Figure 4-13**). The lack of DAB staining in the IgG controls indicates that the antibodies are specific for GPR55.



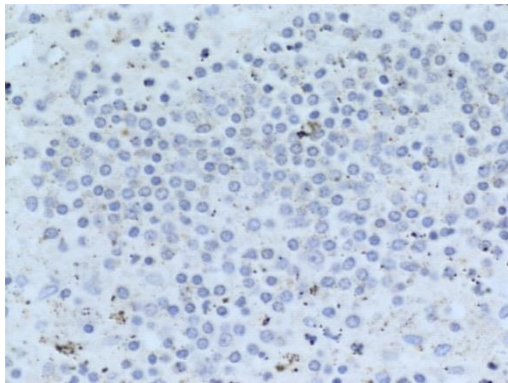
(A) GPR55 primary antibody

Positive control



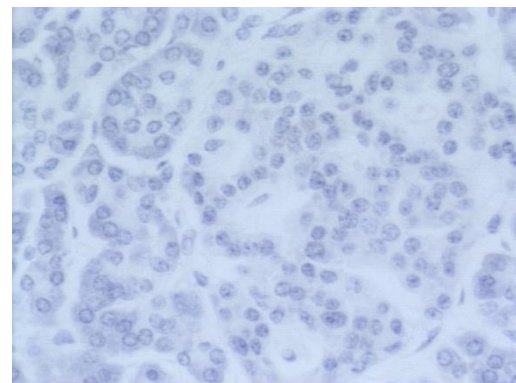
(B) GPR55 primary antibody

Positive control



(C) IgG antibody

Negative control



(D) IgG antibody

Negative control

Figure 4-13: Negative control experiment demonstrating the specificity of the primary GPR55 antibody in pancreatic tissue.

Images (A) and (B) show positive staining of the primary antibody GPR55, whilst images (C) and (D) shows no staining for the IgG controls. Images on the left were taken at 200x magnification, and those on the right at 400x magnification.

4.4.4.2.2 Identification and Locations of GPR55 Protein

Figure 4-14 illustrates the staining pattern of GPR55 antibodies in atrophic and EC tissues. Following the optimisation of GPR55 antibody, all the studies were undertaken in a single run to minimise variations.

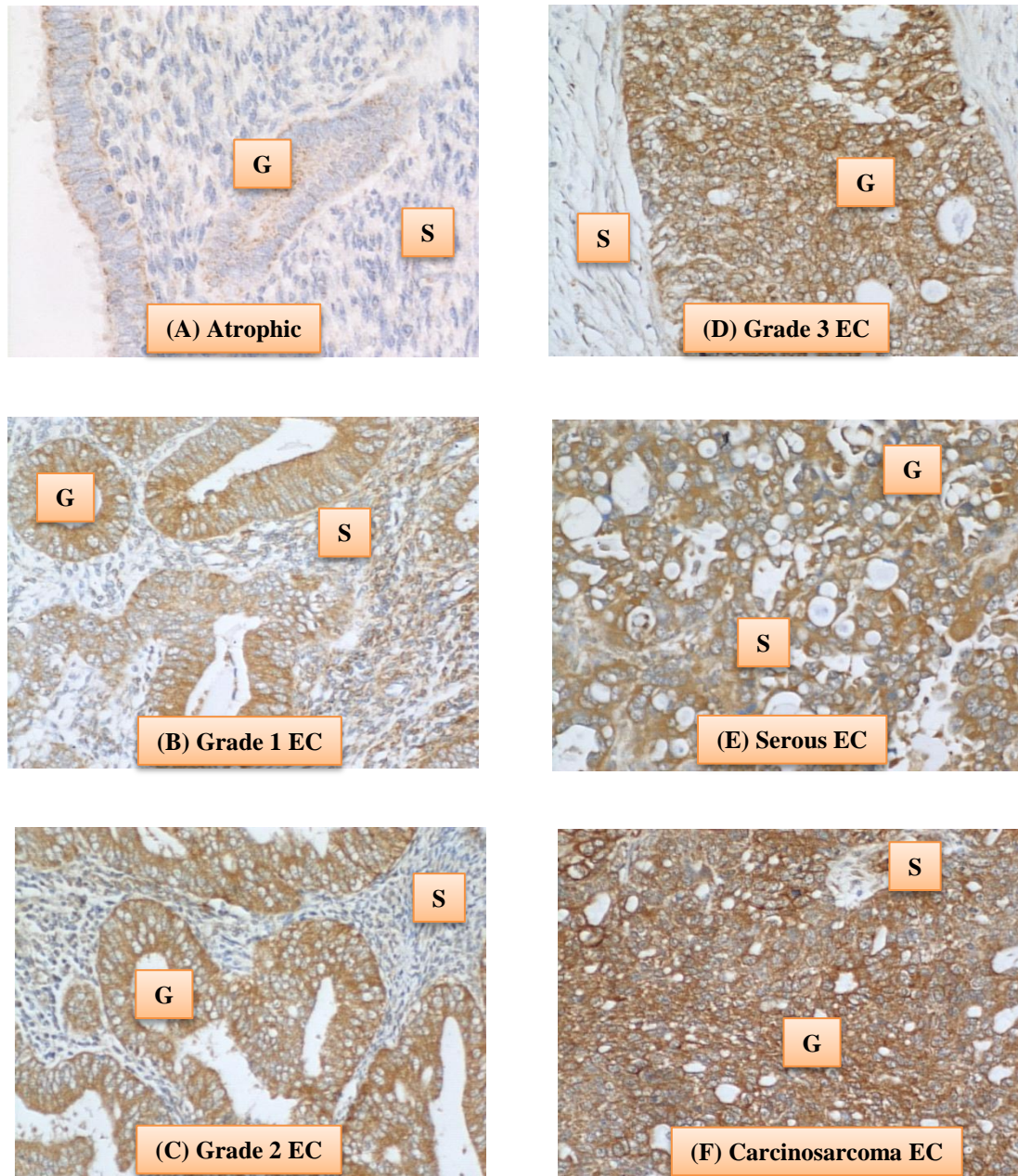


Figure 4-14: Localisation and expression of the GPR55 protein in various tissues (G=glands, S=stroma, EC=endometrial cancer).

The data on GPR55 staining indicated that very light staining was observed in atrophic endometrium and involved both the stroma and the glands. GPR55 protein was expressed at a relatively stronger intensity in the glands compared to the stroma, with the strongest immunoreactivity along the luminal and basal surfaces of the glands. It was evident that the stromal staining was very light and not uniform.

The type 1 EC tissue showed not only cell membrane staining but also strong cytoplasmic immunoreactivity in glandular epithelial and stromal cells, with stronger staining in the glands than in the stroma. Similar data were obtained for grade 1 (panel B), grade 2 (panel C) and grade 3 (panel D) cancers. Generally, in type 1 EC, GPR55 staining was confined to the cell cytoplasm with no staining observed in the nucleus. Furthermore, in serous EC, GPR55 staining was more concentrated in the glands than the stroma, whilst in carcinosarcoma, staining seems to encompass the entire tissue and was very intense in all cell types.

4.4.4.2.3 Histomorphometric Quantification of GPR55

Figure 4-15 show the data from the histomorphometric analysis of glands and stroma (G + S). GPR55 protein expression appeared to increase from the lowest level in the atrophic tissues, gradually to the more advanced malignancies.

Figure 4-15A shows the data from the histomorphometric analysis of the glands and stroma (G + S) combined, while **Figures 4-15B** and **4-15C** show the analysis for the glands (G) and stroma (S) alone, respectively. The data show that immunoreactive GPR55 protein levels are higher in the endometrial cancer tissue in line with the transcript data shown in **Figure 4-11**. The levels observed in type 1 EC tissues were just as high as that in type 2 EC tissue.

When the H-score for the glands alone were examined (**Figure 4-15B**), all of the EC tissues showed higher GPR55 protein intensities compared to atrophic endometria. Similarly, the H-scores for the stromal tissue alone (**Figure 4-15C**) showed a significant higher staining intensity in the type 1 and 2 EC tissues compared to the atrophic endometrium.

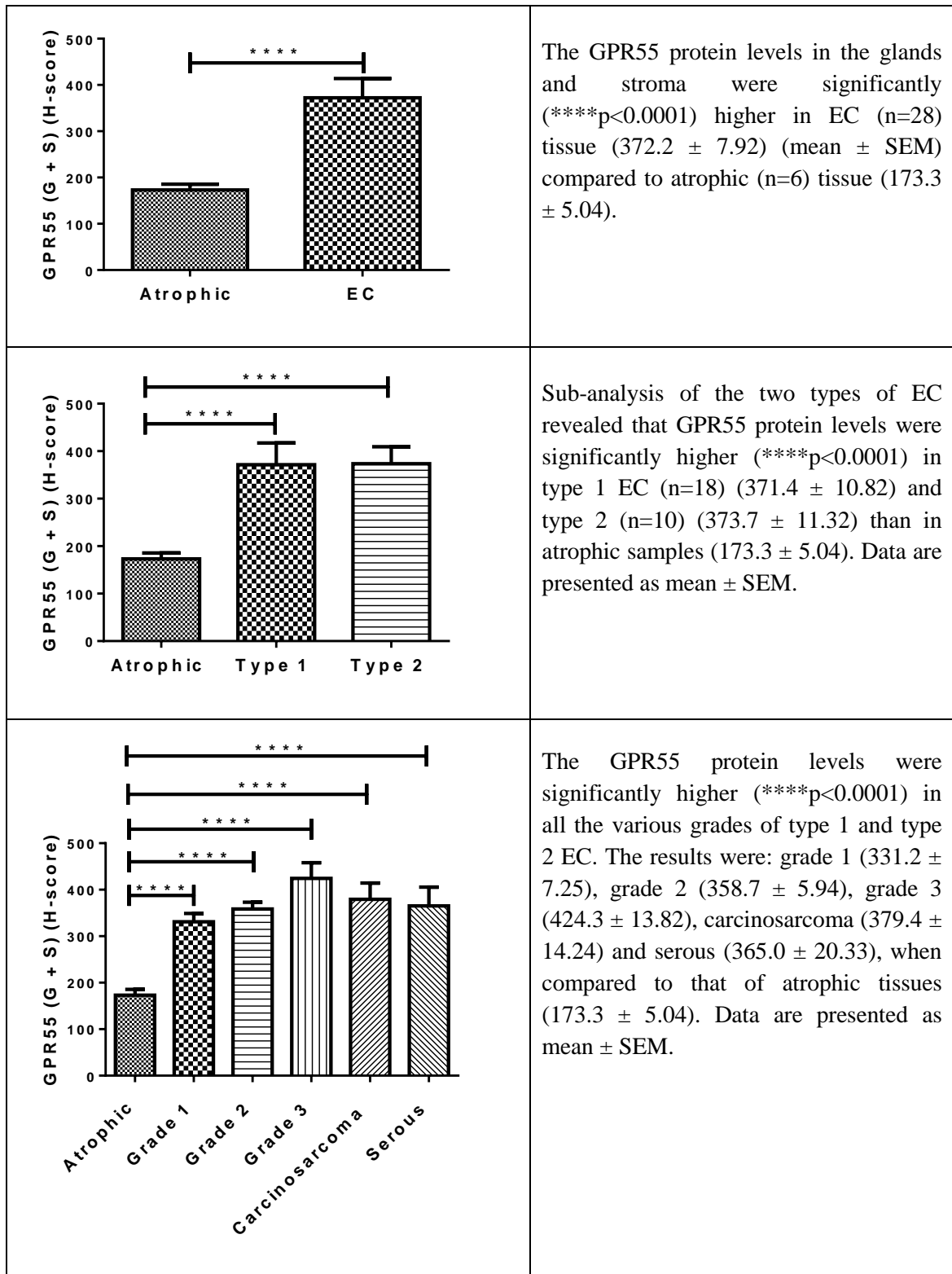


Figure 4-15A: Histomorphometric (H-score) analysis of immunoreactive GPR55 (G + S) protein.

P values were obtained using Student's t-tests and one way ANOVA with Dunnett's ad hoc post-test analysis of both the components of the tissues, the glands and stomas. Data are presented as the mean \pm SEM. Collectively, GPR55 protein levels are increased in EC tissue (G+S) when compared to that of the atrophic endometrium.

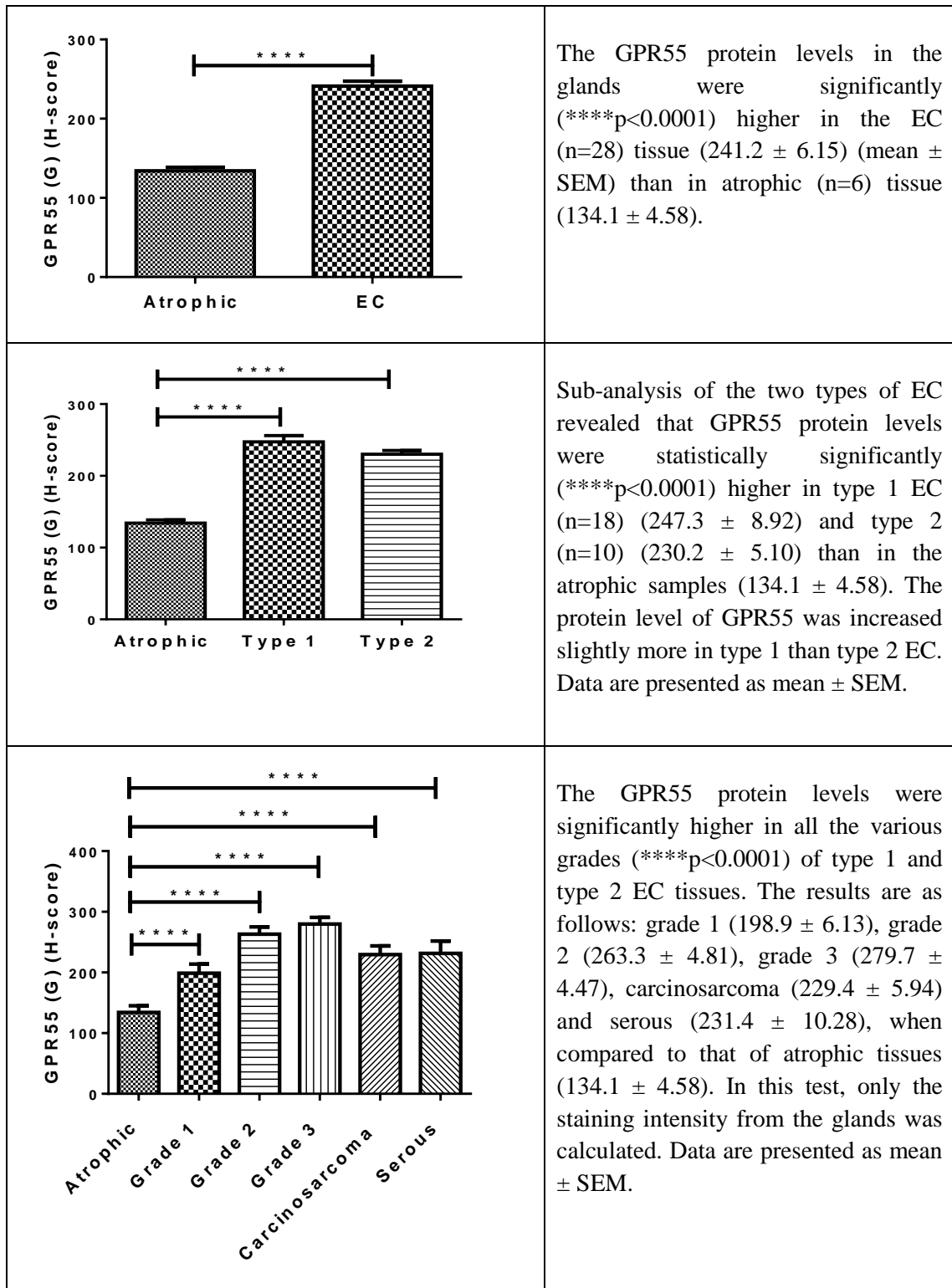


Figure 4-15B: Histomorphometric (H-score) analysis of immunoreactivity GPR55 (G) protein.

P values were obtained using Student's t-test and one way ANOVA with Dunnett's ad hoc post-test analysis of the glands. Data are presented as the mean \pm SEM. Collectively, GPR55 protein levels are increased in EC (G) when compared to atrophic endometrium.

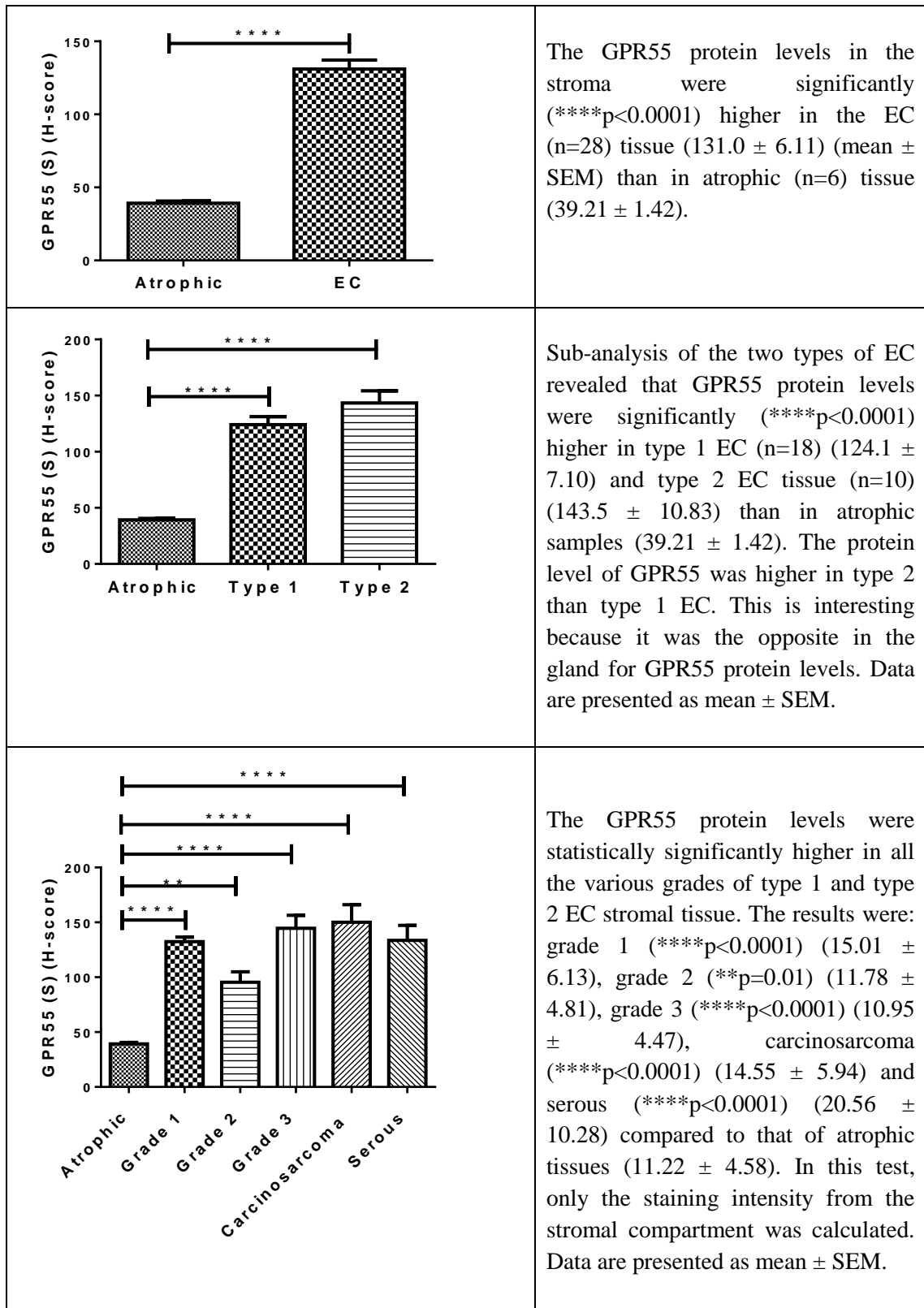


Figure 4-15C: Histomorphometric (H-score) analysis of immunoreactive GPR55 (S) protein.

P values were obtained using Student's t-test and one way ANOVA with Dunnett's ad hoc post-test analysis of the glands. Data are presented as the mean \pm SEM. Collectively, GPR55 protein levels are increased more in type 2 EC of the stromal component (S) when compared to that of the atrophic endometrium.

4.4.5 TRPV1 Expression

4.4.5.1 TRPV1 Transcript Levels

The relative transcript levels for TRPV1 in atrophic and malignant endometrium are shown in **Figure 4-16**. The data show that like CB1 and CB2, the transcript levels for TRPV1 were lower in endometrial cancer. Furthermore, sub-analysis showed that the levels of TRPV1 transcript levels were lower in both type 1 and 2 EC compared to atrophic endometrium. More detailed analysis showed that the lower transcript levels of TRPV1 in the various tumour grades, did not reach statistical significance for any of the individual groups.

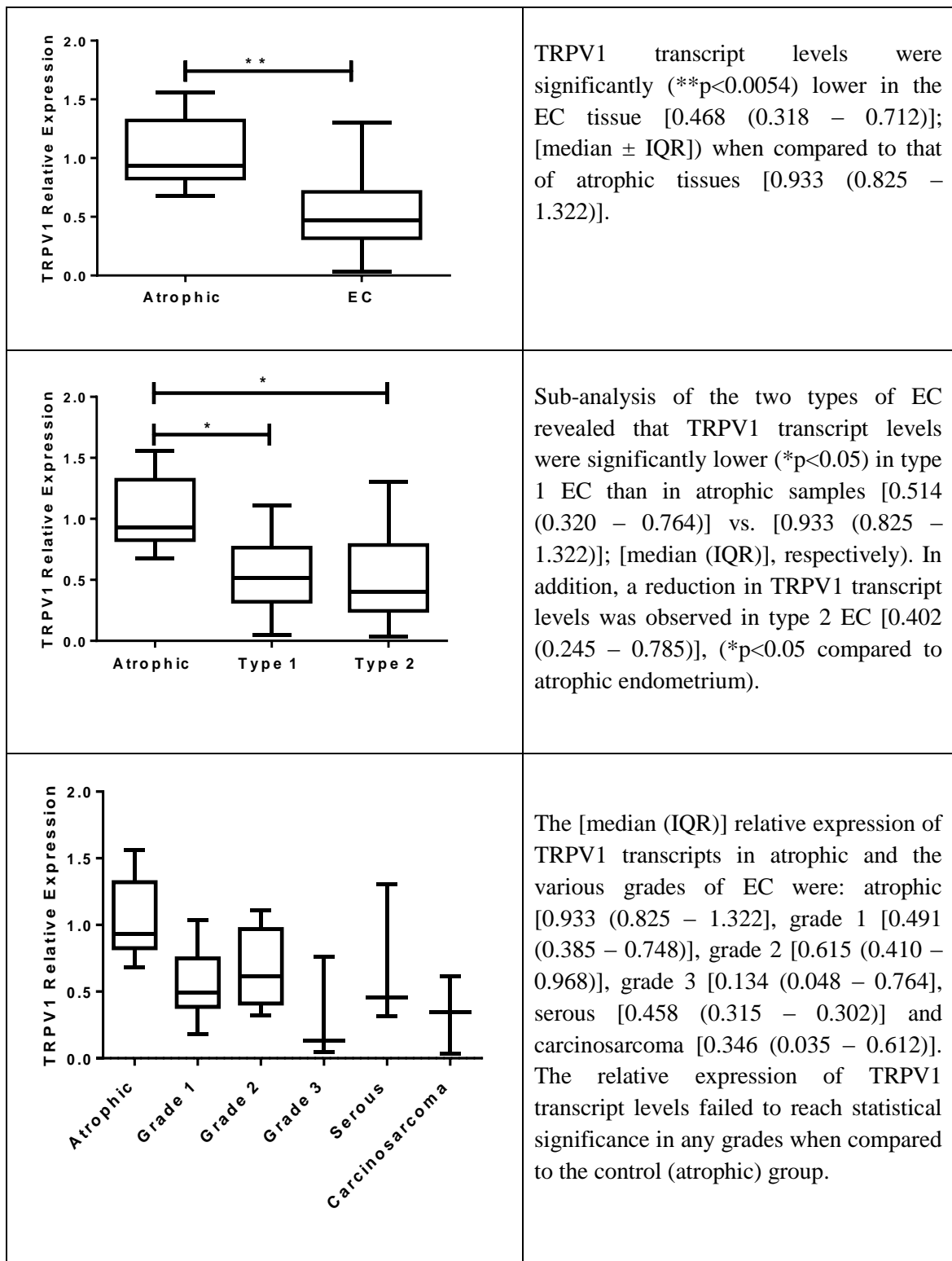


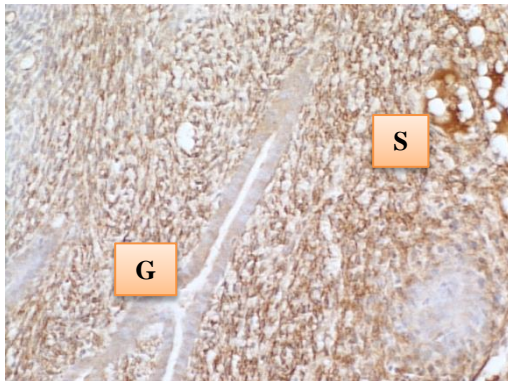
Figure 4-16: Relative expression of TRPV1 transcript levels.

Data are presented as [median (IQR)]. P values were obtained using Mann-Whitney analysis and Kruskal-Wallis ANOVA with Dunn's ad hoc post-test analysis.

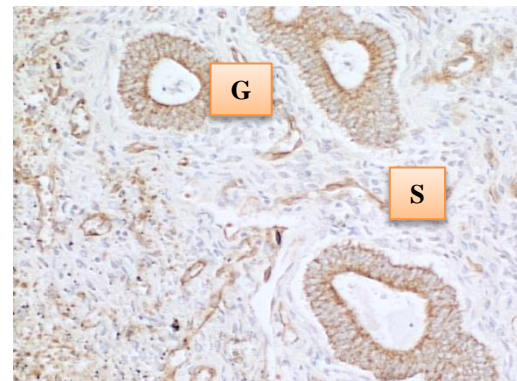
4.4.5.2 TRPV1 Protein Expression

4.4.5.2.1 Optimisation and Validation of Immunohistochemical Methods for TRPV1

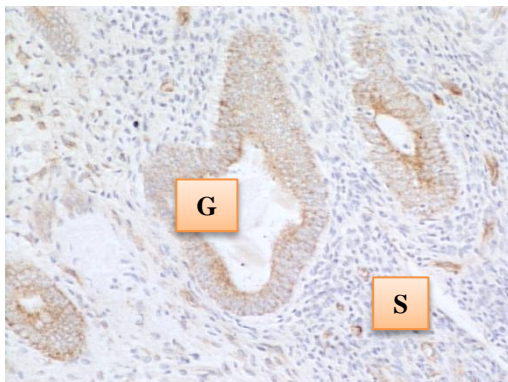
The optimal primary antibody dilution for TRPV1 was obtained by using different dilutions, as follows: (1:100, 1:200, 1: 300 and 1:400). An example of the staining intensities obtained using these dilutions are shown in **Figure 4-17**. From these images, the best dilution was 1:200.



TRPV1 1:100



TRPV1 1:150



TRPV1 1:200

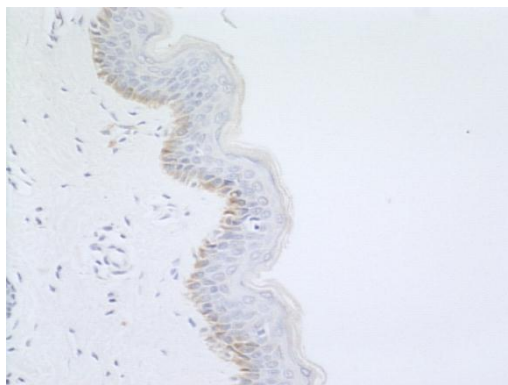


TRPV1 1:300

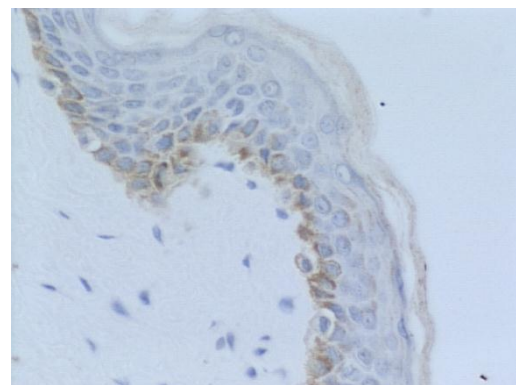
Figure 4-17: Staining intensities for TRPV1 at different antibody dilution (S=stroma, G=glands).

Very strong staining was obtained with the 1:100 antibody dilution and very light staining with the 1:300 and 1:400 dilutions. The 1:200 dilutions provided the optimal staining pattern.

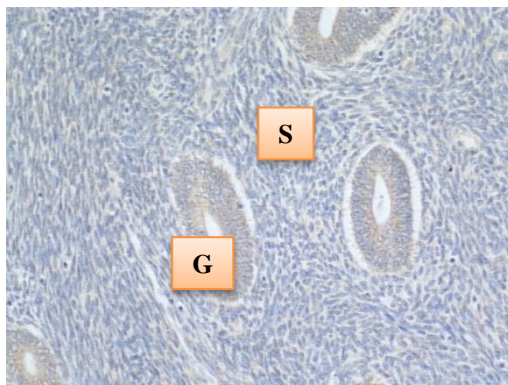
Antibody specificity was determined using equivalent concentrations of non-immune IgG (**Figure 4-18**). The lack of DAB staining in the IgG controls indicates that the antibodies are specific for TRPV1.



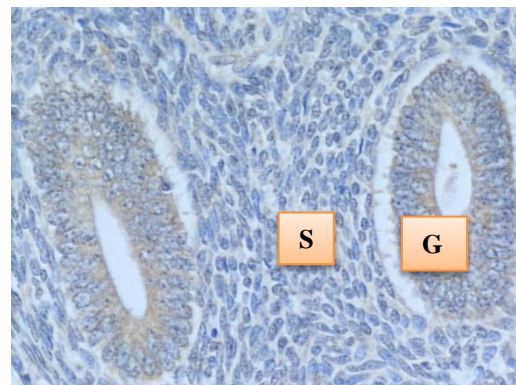
(A) TRPV1 primary antibody
Positive control



(B) TRPV1 primary antibody
Positive control



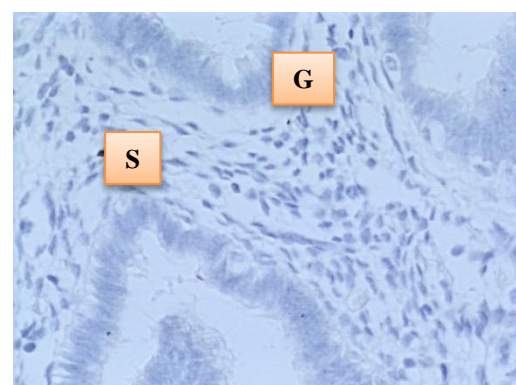
(C) TRPV1 primary antibody
Positive control



(D) TRPV1 primary antibody
Positive control



(E) IgG antibody
Negative control



(F) IgG antibody
Negative control

Figure 4-18: Negative control experiment demonstrating the specificity of the TRPV1 primary antibody (S=stroma, G=glands).

Images (A) and (B) show positive staining pattern of TRPV1 antibody in skin tissue. Skin slides were selected because TRPV1 has previously been shown to present in that tissue and so acted as a positive control. TRPV1 antibody was also evaluated in atrophic uterine tissues (panel C)

and (panel D) and with equivalent concentrations of IgG, (panel C) and (panel D), which showed no staining (the negative control). Images on the left were taken at 200x magnification, and those on the right at 400x magnification.

4.4.5.2.2 Identification and Locations of TRPV1 Protein

Figure 4-19 illustrates the staining pattern of TRPV1 antibodies in atrophic and the EC tissues. Following the optimisation of TRPV1 antibody, all the studies were undertaken in single run to minimise variations.

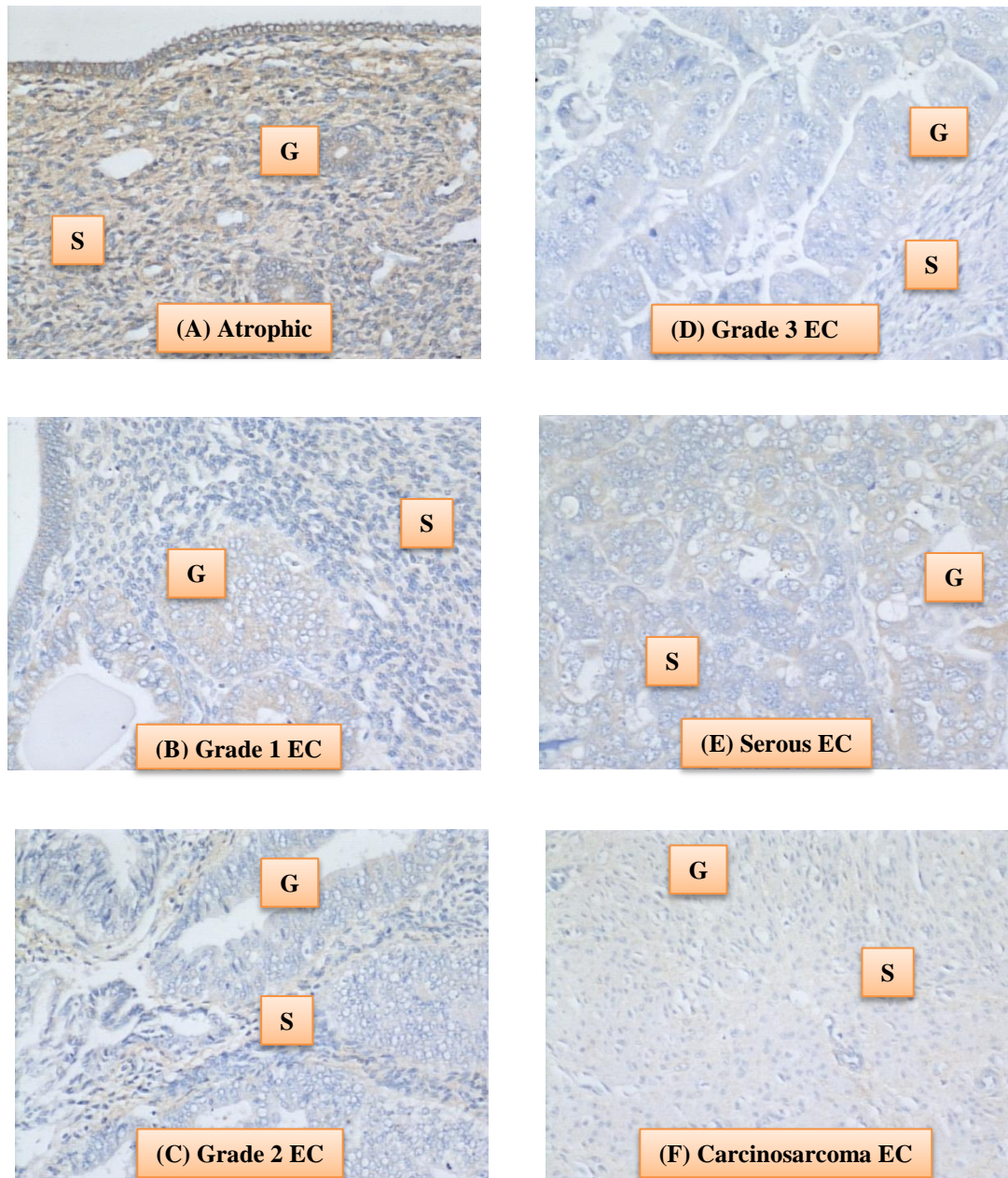


Figure 4-19: Localisation and expression of the TRPV1 protein in various tissues (G=glands, S=stroma, EC=endometrial cancer).

In comparison to the other cannabinoid binding receptors, TRPV1 staining in the tissue was less intense. Within the group, TRPV1 staining was more intense in atrophic than the malignant endometrium and was observed in both the stroma and the glands. In atrophic tissue, although the number of glands was small, TRPV1 protein was expressed strongly in the glands with the strongest staining on the luminal surface of the glands. It was evident that the stroma was also strongly stained. TRPV1 was demonstrated in the cytoplasm of both glandular epithelial and stroma cells.

In grade 1 EC, the staining was more concentrated in the glands rather than the stroma, with the stroma of grade 1 EC tissue being almost devoid of staining. However, in grade 2 EC, it is the opposite, with staining noted in the stroma more than the glands. In grade 3 EC, the staining was very light in both the glands and the stroma. In serous carcinoma, staining was more cytoplasmic and in the glands that were scattered throughout the section; staining in stromal cells was very light. In carcinosarcoma tissues, staining spread all over the stroma but the nucleus component was spared.

4.4.5.2.3 *Histomorphometric Quantification of TRPV1*

Figure 4-20A shows the data from the histomorphometric analysis of the glands and stroma (G + S) combined, while **Figures 4-20B** and **4-20C** show the analysis for the glands (G) and stroma (S) alone, respectively. TRPV1 staining was markedly lower in all malignant tissues compared to that in the atrophic tissues. The data show that immunoreactive TRPV1 protein levels are lower in the endometrial cancer tissue in line with the transcript data shown in **Figure 4-16**. The levels observed in type 1 EC tissues were just as low as that in type 2 EC tissue.

When the H-score for the glands alone were examined (**Figure 4-20B**), all of the EC tissues showed very low TRPV1 protein intensities compared to atrophic endometria. Similarly, the H-scores for the stromal tissue alone (**Figure 4-20C**) showed a significant lower staining intensity in the type 1 and 2 EC tissues compared to the atrophic endometrium. In all EC tissues, immunoreactive TRPV1 protein was essentially absent.

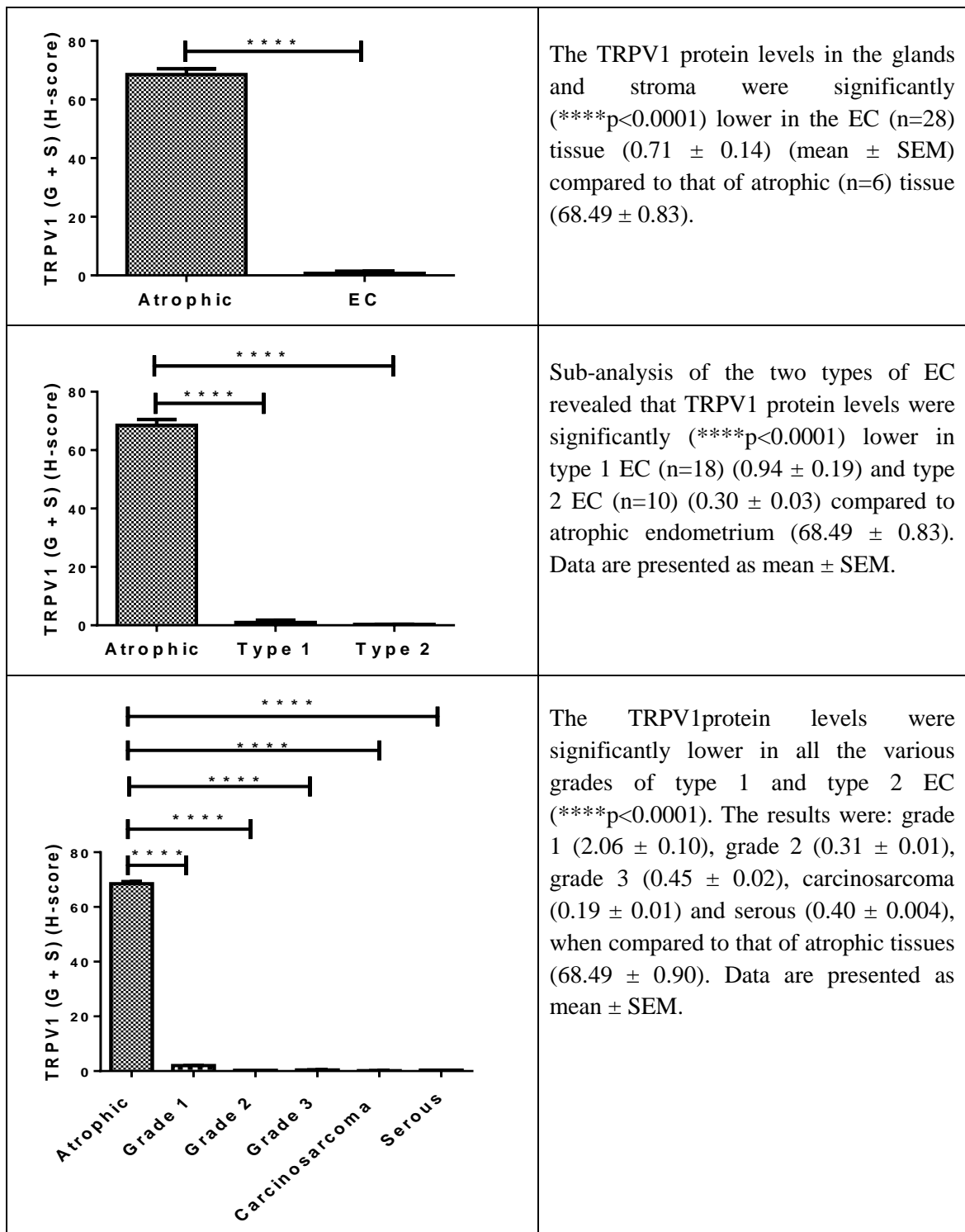


Figure 4-20A: Histomorphometric (H-score) analysis of immunoreactive TRPV1 (G + S) protein.

P values were obtained using Student's t-test and one way ANOVA with Dunnett's ad hoc post-test analysis of both the components of the tissues, the glands and stomas. Data are presented as the mean \pm SEM. Collectively, TRPV1 protein levels are reduced in EC (G+S) when compared to that observed in the atrophic endometrium.

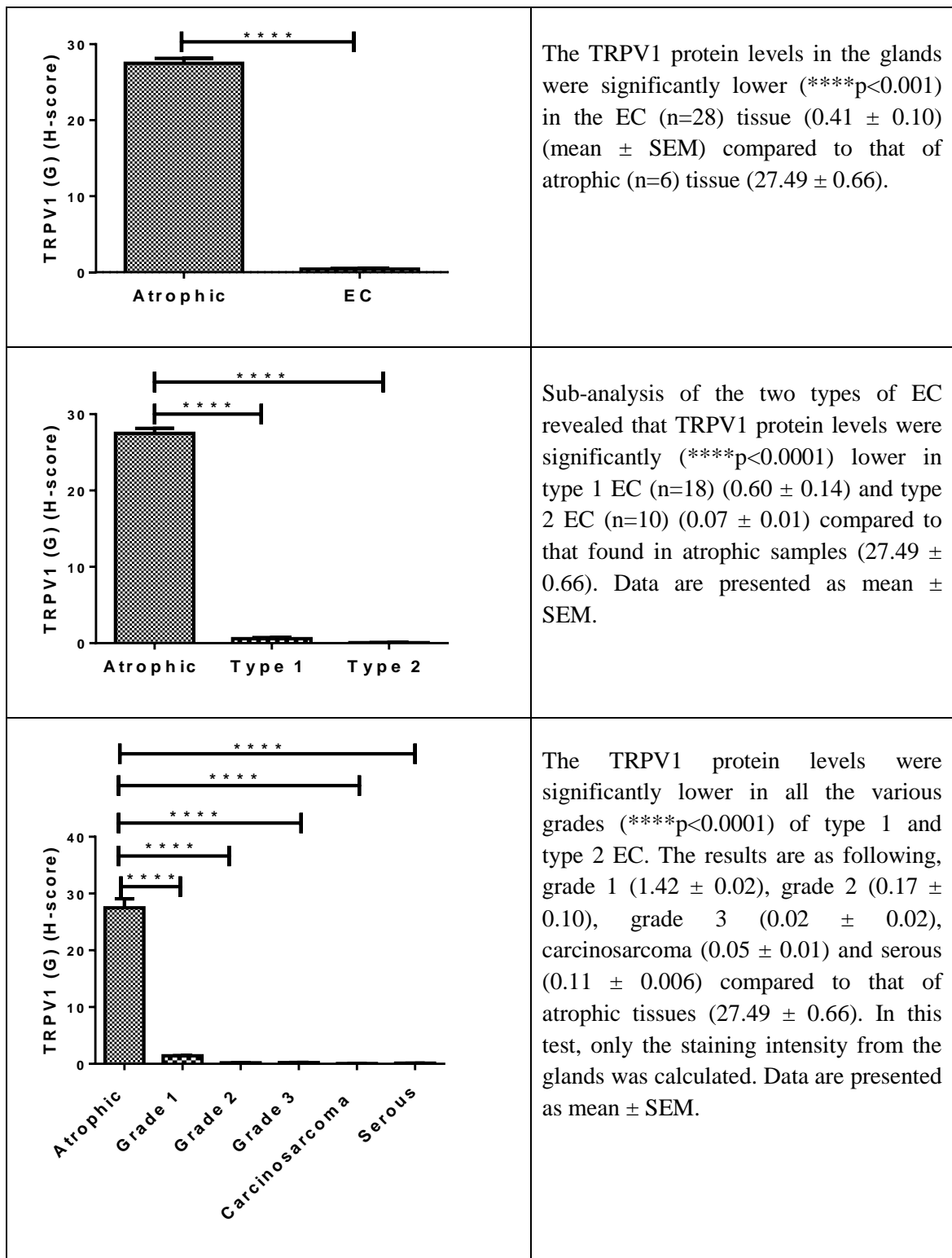


Figure 4-20B: Histomorphometric (H-score) analysis of immunoreactive TRPV1 (G) protein.

P values were obtained using Student's t-test and one way ANOVA with Dunnett's ad hoc post-test analysis of the glands alone. Data are presented as the mean \pm SEM. Collectively, TRPV1 protein levels are reduced in EC (G) tissue when compared to that observed in the atrophic endometrium.

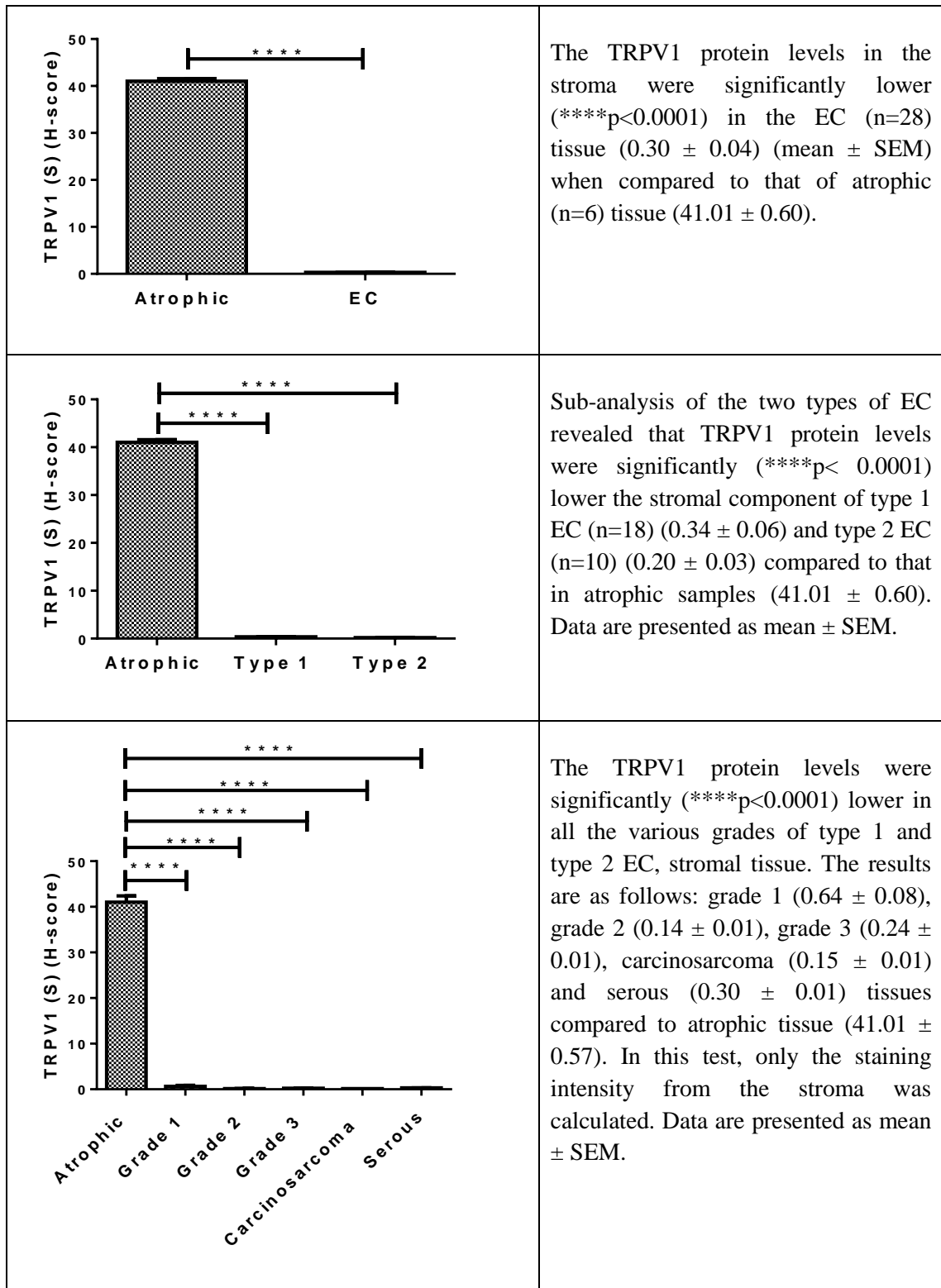


Figure 4-20C: Histomorphometric (H-score) analysis of immunoreactive TRPV1 (S) protein.

P values were obtained using Student's t-test and one way ANOVA with Dunnett's ad hoc post-test analysis of the stromal compartment. Data are presented as the mean \pm SEM. Collectively, TRPV1 protein levels are reduced in EC (S) when compared to that observed in atrophic endometrium.

4.5 Discussion

Several studies suggested that the classical cannabinoid receptors (CB1 and CB2) (Michalski et al. 2008, Wang et al. 2008, Cudaback et al. 2010, Larrinaga et al. 2013) and the non-classical receptors (GPR55 and TRPV1) (Domotor et al. 2005, Hartel et al. 2006, Kalogris et al. 2010, Andradas et al. 2011, Hu et al. 2011, Pineiro et al. 2011) are altered during carcinogenesis of several cancers. Following on from these observations, it was reasoned that similar changes may also exist in endometrial cancers. Hence, the transcript and the protein expression levels of CB1, CB2, GPR55 and TRPV1 were compared between atrophic and endometrial cancer tissues.

In the endometrial cancer tissues, transcripts for CB1 and CB2 were significantly lower compared to that found in atrophic tissues. Similarly, CB1 and CB2 protein expression was reduced in the endometrial cancer suggesting that there is a tight link between CB1/CB2 transcription and translation in the endometrium. The CB1 and CB2 proteins demonstrated differential localisation patterns within the stromal and glandular components of the endometrial tissues, with a clear loss of CB1 immunoreactive protein from the luminal epithelial cell and stronger staining in the deeper glands. The results from this study support the hypotheses that loss of CB1 and CB2 receptors may be involved in the aetiopathology of endometrial cancer.

The variability of cannabinoid effects in different tumour models is highly contradictory, which may be a consequence of the differential cannabinoid receptor expression. It has been hypothesised that cannabinoids are more effective in killing tumours that abundantly express cannabinoid receptors, such as gliomas, but may increase the growth and metastasis or at least inhibit cytotoxicity in other types of tumours, such as breast cancer, that show no or low expression of cannabinoid receptors, possibly by suppression of the anti-tumour immune response (McKallip et al. 2005). Several malignancies, such as prostate and non-Hodgkin lymphoma (Gustafsson et al. 2008, Czifra et al. 2009), have been shown to express elevated levels of cannabinoid receptors and higher CB1 expression has been associated with increased disease severity and poor prognosis in prostate and pancreatic cancer (Michalski et al. 2008, Chung et al. 2009), suggesting that CB receptor expression and tumour response are likely to be tumour specific. In contrast, low level cannabinoid receptor expression is associated with an increase in apoptosis in astrocytoma, whereas no apoptosis occurs

in astrocytoma cells with high receptor expression (Cudaback et al.) and CB1 knockout, but not CB2 knockout APCmin mice (a model of colorectal cancer), that have an increase in intestinal polyp that can be replicated by treatment with CB1 antagonists (Wang et al. 2008). Similar effects are observed in human colorectal tumours where reduced levels of CB1 mRNA relate to increased tumour growth (Wang et al. 2008). In addition, it has been proposed that AEA also exhibits cytotoxic effects in a cannabinoid-receptor-independent mechanism (Gustafsson et al. 2009).

CB2 receptor control is likely to be dysregulated in endometrial cancer, as CB2 levels have been shown to be significantly higher in the AN3CA human endometrial carcinoma cell line compared to control cells when transfected with a plasmid containing the cDNA for the endocannabinoid receptor CB2 (Guida et al. 2010). From these data, it has been concluded that CB2 receptors might play a vital role in the growth of endometrial cancer (Guzman et al. 2002).

Recent research showed that the complete endogenous pathway for CB2 was altered significantly in endometrial adenocarcinoma, with the marked elevation of CB2 receptor expression and 2-AG in endometrial cancer tissues possibly due to the underlying imbalance in the estrogen/progesterone ratio, which is one of the aetiological factors for the development of endometrial cancer (Guida et al. 2010), but this has not been fully tested. What has been tested is the effect of CB2 elevation in the transfected AN3CA cells where CB2 caused a 40% reduction of cell mitochondrial function compared the control cells (Guzman et al. 2002). This effect was not improved by the CB2 receptor agonist, JWH133, but was fully prevented by the CB2 receptor antagonist SR144528.

Both receptors are widely distributed in human tissues including the brain, testis, sperm, leucocytes, placenta, fetal membranes, endothelial cells, anterior eye, pituitary gland, breast and reproductive tissues (Gerard et al. 1991, Bouaboula et al. 1993, Liu et al. 2000, Porcella et al. 2000, Pagotto et al. 2001, Pertwee 2005, Bifulco et al. 2006, El-Talatini et al. 2009, Taylor et al. 2010, Gebeh et al. 2013) and now shown to be reduced in endometrial cancer tissue.

GPR55 transcript levels were significantly raised ($p < 0.002$) in the endometrial cancer tissue compared with atrophic tissues and this was further supported by the IHC studies shown by the strong staining intensities. Importantly, patients with type 1 disease had

GPR55 levels that were significantly ($p < 0.0007$) higher compared to that in atrophic tissue, but in patients with type 2 disease this was not significant ($p = 0.1320$). Furthermore, GPR55 transcript levels in both grade 1 and 2 EC type 1 were statistically significantly elevated, but grade 3 type 1 EC and type 2 EC (serous carcinoma and carcinosarcoma) did not show any statistical difference. These data were confirmed by the immunohistochemistry data, indicating a tight link between GPR55 transcription and translation in the endometrium. It was evident that GPR55 protein staining was more markedly intense in the endometrial cancer tissues, suggesting that GPR55 may play a possible role in the aetiopathogenesis of EC and could be used as a novel cancer biomarker and a potential therapeutic target.

TRPV1 receptor transcript levels were significantly reduced in the EC tissue compared with atrophic tissues. Sub-analyses revealed that TRPV1 receptor transcript levels in patients both with type 1 and type 2 EC were significantly lower compared to control tissue and that TRPV1 receptor transcript levels in patients with grade 3 type 1 EC were also significantly lower. Although transcript levels were lower in patients with grade 1 and 2 EC type 1, the difference was not statistically significant and levels in type 2 (serous carcinoma and carcinosarcoma) samples were not altered. IHC showed TRPV1 receptor immunoreactivity to be markedly lower in all but type 2 EC samples, correlating with the observed transcript levels. This pilot study showed the presence of TRPV1 receptor at both the transcript and protein level in human endometrium, with lower TRPV1 expression in EC compared to normal atrophic endometrium.

Both GPR55 and TRPV1 have been less widely investigated than the classical cannabinoid receptors CB1 and CB2, but TRPV1 has been shown to be increased in both human prostate cancer (Czifra et al. 2009) and squamous cell carcinoma of the tongue (Marincsak et al. 2009). Furthermore, lysophospholipids, recently identified as potent ligands for GPR55 (Okuno et al. 2011), are markedly elevated in ascites fluid from ovarian cancer patients compared with non-malignant controls (Xiao et al. 2001), suggesting a role for GPR55 in ovarian cancer. GPR55 is also a good marker of tumour grade and prognosis in glioma, breast, pancreas, prostate and ovarian cancers (Andradas et al. 2011, Hu et al. 2011, Pineiro et al. 2011).

Pharmacological studies have strongly suggested the existence of novel cannabinoid receptor subtypes (Begg et al. 2005), with GPR55 having been proposed to be a

cannabinoid receptor. GPR55 has been identified in the brain and in the gut, spleen and adrenals (Sawzdargo et al. 1999, Ryberg et al. 2007, Oka et al. 2010). Of the endocannabinoids, *N*-palmitoylethanolamide (PEA) has the greatest affinity for this receptor, although other endocannabinoids also bind to GPR55 (Ryberg et al. 2007), as does lysophosphatidylinositol (Oka et al. 2007). Recent evidence suggests that GPR55 is an essential player at the molecular level in the regulation of the modulation of the signalling pathways involved in malignant transformation, tumour growth and progression (Dorsam et al. 2007) since it is expressed by a large number of human cancer cell lines and human tumours and, most importantly, its expression correlates in the “aggressiveness” of such tumours (Andradas et al. 2011). The novel data shown in this chapter suggests that GPR55 plays a key role in endometrial cancer, something that had not been studied before.

The expression of TRPV1 in other estrogen-stimulated neoplastic tissues, such as carcinoma of the human prostate, colon and breast, suggest it might also be expressed in endometrial carcinoma. However, in this study, TRPV1 receptor was found to be expressed only in the atrophic endometrium, and not in the endometrial cancer tissue. The knowledge that TRPV1 is a ligand-gated Ca^{2+} -permeable ion channel, which is usually activated by noxious stimuli such as acidity and heat, and is involved in transmission and modulation of pain (Huang et al. 2002), may explain why uterine pain is not detected in early endometrial cancer. Moreover, both AEA and acyl-dopamine are now considered to be endovanilloids because they bind to this receptor (Huang et al. 2002) and a concomitant increase in tissue AEA production may be a reflection of the loss of the receptor in the diseased tissue. Although evidence exists to support a role for TRPV1 activation by the vanilloid capsaicin and AEA, with this association known to regulate cancer cell growth and disease progression (Contassot et al. 2004), similar studies in endometrial cancer are lacking in the literature. The data presented here suggest a possible role for the endocannabinoids and/or endovanilloids in the pathogenesis of endometrial cancer. How these activated receptors affect endometrial cell growth and survival will be the subject of the next Chapter.



Chapter 5

***In-Vitro* Modelling - Effect of Endocannabinoids on Endometrial Carcinoma Cell Growth and Survival**

5.1 Introduction

In chapters 2, 3 and 4, it was established that all components of the endocannabinoid system are present in endometrial cancer (EC) and that most components are dysregulated with the levels of AEA, OEA and PEA clearly perturbed. Additionally, it was shown in Chapter 4 that the non-classical cannabinoid receptor, TRPV1, is also dysregulated suggesting that loss of this receptor may also be important in the pathogenesis of EC. The natural ligand for this receptor, capsaicin, is a key component in red and chilli peppers (Cortright et al. 2004, Sawynok 2005).

The potential roles of AEA, OEA, PEA and capsaicin in EC is far from clear with only two publications, that were not extensive in the investigations undertaken, suggesting a role for the ECS in endometrial carcinogenesis (Schmid et al. 2002, Guida et al. 2010). The observed changes in AEA, OEA and PEA tissue levels of EC patients reported in chapter 2, raises the question “what effect does AEA, OEA, PEA and capsaicin, if any, have on the proliferation (growth) and cell death of endometrial epithelial cells; the main cell type affected by EC?”. Previous work by others (Kerr et al. 1972, Bhargava et al. 1994, Kounelis et al. 2000, Cong et al. 2007), suggests that apoptosis may play an important role in cancer pathogenesis with dysregulation of apoptosis responsible for the ensuing growth potential of glandular epithelial cells, especially in the post-menopausal endometrium exposed to exogenous estrogens or tamoxifen (Habiba et al. 1998, Reed 1999, Lewis-Wambi et al. 2009).

Recent studies by McHugh *et al.* using the HEC-1B endometrial epithelial cell line showed that AEA, Δ^9 -THC and *N*-arachidonoyl glycine (NAGLy) induced cellular migration through CB2 and GPR18 receptor activation (McHugh et al. 2012). By contrast, Gentilini *et al.* showed that primary human endometrial stromal cells migrated following administration of R1-metAEA, suggesting that CB1 is the main signalling pathway involved in the cell migration process (Gentilini et al. 2010), however, McHugh *et al.* suggested it is a CB1-receptor independent mechanism (McHugh et al. 2012). One reason for the differences in these studies could be due to the use of different cell types (primary cultures vs. cell lines), however this may not be the only reason. This is supported by the studies of Leconte *et al.* who examined the role of cannabinoids in the proliferation of endometrial cells (Leconte et al. 2010) using the agonist WIN 55212-2 and showed that it had an anti-proliferative effect. In contrast, a

study by Resuehr *et al.*, speculated that reduced cannabinoid signalling might underlie the enhanced proliferative capacity of endometriotic lesions (Resuehr et al. 2012).

5.1.1 Aim

The aim in this section of the thesis was to investigate the effects of the NAEs (AEA, OEA and PEA) and the natural TRPV1 receptor ligand capsaicin, on survival, death and proliferation indices of an EC model, the Ishikawa cell line.

5.2 Materials and Methods

5.2.1 The Materials Used for the Cell Culture Studies

The various agents used in the experiment are listed in **Table 5-1** with their sources.

Table 5-1. The agents used in the cell culture experiments and their sources

Product	Sources
Ishikawa cell line	Dr A.H. Taylor, University of Leicester
Heat Inactivated Fetal Bovine Serum	Gibco
Phosphate buffered saline	Oxoid Limited
Trypsin	Invitrogen
GlutaMAX™ Supplement	Gibco
Dulbecco's Modified Eagle Medium (DMEM): F12	Gibco
Cell Proliferation Kit II assay XTT	Roche
Stripette	Costar, Corning Incorporated
Tissue Culture Plastic	Greiner Bio-One
Falcon Tube (50 ml)	Becton Dickinson Labware
Haemocytometer	Weber Scientific International Ltd
Anandamide (AEA)	Sigma-Aldrich
<i>N</i> - Palmitoylethanolamide (PEA)	Sigma-Aldrich
<i>N</i> - Oleoylethanolamine (OEA)	Sigma-Aldrich
Capsaicin	Sigma-Aldrich
Antibiotics (Penicillin/Streptomycin)	Gibco

5.2.2 Cell Culture

Ishikawa cells were cultured in DMEM: F12 medium containing 10% fetal bovine serum (FBS) with antibiotics (1% streptomycin and 1U/ml penicillin). Cells were maintained at 37°C in a humid atmosphere of 5% CO₂ in air. Cells were fed with fresh medium every 2 days.

5.2.2.1 Subculture

When the cells reached approximately 80-90% confluence, they were sub-cultured to allow continued growth and proliferation. Using an aseptic technique, the medium in one T-75 flask was aspirated and the flask washed with 10 ml of phosphate buffered saline (PBS), the PBS aspirated and 2 ml of trypsin/ ethylenediaminetetraacetic acid (EDTA) was added and gently swirled around to cover the cell growth surface. The flask was then placed in the incubator for five minutes for the trypsin/EDTA to catabolise fibronectin and other adherence proteins, allowing the cells to lift away from the plastic-ware. Ten ml of new normal growth medium was used to disperse any clumps of cells. The cells were then aliquoted into three new T-75 flasks and 16 ml of growth medium added and the cells re-incubated.

5.2.2.2 Cryopreservation and Recovery

These cells were then cryopreserved allowing for a steady supply of cells for growth studies. To cryopreserve the cells, confluent cultures were treated with trypsin/EDTA, neutralised with 10 ml of growth medium as described in **section 5.2.2.1** and transferred to a Falcon tube (12 ml in total). After centrifugation at 14,000 rpm for 5 minutes at 4° C, the entire medium was carefully aspirated so as to not disturb the cell pellet. The cells were re-suspended in 1.5 ml of fresh growth medium and then mixed with 1.5 ml of freezing solution (60% DMEM: F12, 20%FBS and 20% dimethyl sulphoxide). After thorough mixing, 1 ml of this mixture was pipetted into small cryotubes (three in total), closed tightly and labelled, then placed in a polystyrene sandwich box, taped tightly and placed at -80° C overnight before storage in liquid nitrogen.

When it was necessary to place the cells back into culture, the cryotubes were removed from the liquid nitrogen, semi-thawed in warm water (37°C) and their external surfaces

sterilised with 70% IMS. The cells were then transferred into a T-75 flask with 20 ml of pre-equilibrated medium and the cells re-incubated.

5.2.2.3 Cell Count

Cells were counted using an improved Neubauer haemocytometer (**Figure 5-1**). To count the cells, cultured were treated with 3 ml of trypsin/EDTA and neutralised with 10 ml of normal new growth medium as described (**section 5.2.2.1**).

Before counting the cells, the haemocytometer was set up by firmly applying the coverslip over the two counting chambers with the aid of a small amount of liquid at the edges. A 20 μ l sample of the cell suspension was introduced at the interface between the coverslip and the counting chambers, with the cells drawn into the chamber under the coverslip via capillary action. The haemocytometer was placed under a light microscope and the counting grid visualised. The cells within the large central square were counted on both sides of the haemocytometer to give two cell counts and the average used to estimate the number of cells present. This was then multiplied by 10^4 (the counting volume = 0.1 μ l) to give the number of cells per ml. An accurate cell count allowed the cells to be plated to different plastic trays at specific densities, as required for the experiment.

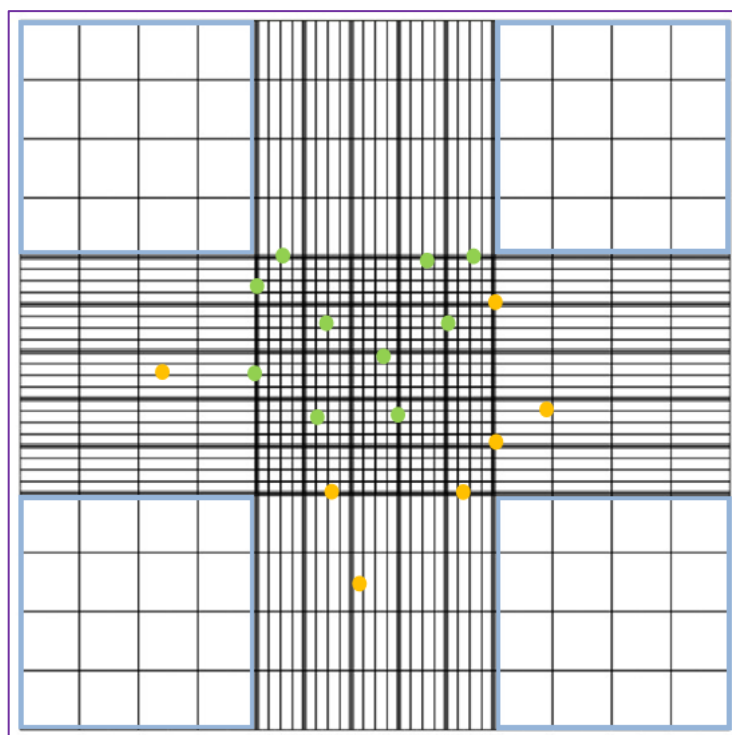


Figure 5-1: A diagrammatic representation of a grid on the Neubauer haemocytometer.

When counting cells the two grids on the haemocytometer separated by the midline groove are used. In each grid (shown above), cells in the central square and four grids (lined with blue colour) in the corners of the image were counted. Cells in the upper and left borders were included in the cell count (as shown in green spots) and cells in the lower and the right border were not (as shown in the yellow spots). After counting both grids on the haemocytometer, the average number of cells was calculated.

5.2.3 Ishikawa Cell Dose-Response Curve Model

To evaluate the effect of the endocannabinoids on the Ishikawa cell lines, a full, confluent, flask of Ishikawa cells was sub-cultured into a single 96-well tissue culture plate at a cell density of 4×10^3 cells per well in 200 μl of normal cell culture medium and the cells allowed to grow in the incubator for 24 hours. The medium was then changed to serum-free DMEM: F12 containing antibiotics/anti-mycotic and the cells allowed to grow for 24 hours. At this point, fresh growth medium (without serum) was prepared containing 1.0 nM to 10 μM of, AEA, OEA, PEA or capsaicin (**section 5.2.4**). Sufficient media containing each of the compounds (enough for 5 wells) was made. Once prepared, the existing serum-free medium was aspirated and 200 μl of each of the prepared compounds used in quadruplicate according to the scheme shown in **Figure 5-2**.

No drug	1nM	10nM	100nM	1µM	10µM	
○ ○	○ ○	○ ○	○ ○	○ ○	○ ○	AEA
○ ○	○ ○	○ ○	○ ○	○ ○	○ ○	
○ ○	○ ○	○ ○	○ ○	○ ○	○ ○	OEA
○ ○	○ ○	○ ○	○ ○	○ ○	○ ○	
○ ○	○ ○	○ ○	○ ○	○ ○	○ ○	PEA
○ ○	○ ○	○ ○	○ ○	○ ○	○ ○	
○ ○	○ ○	○ ○	○ ○	○ ○	○ ○	Capsaicin
○ ○	○ ○	○ ○	○ ○	○ ○	○ ○	

Figure 5-2: A graphical representation of the Ishikawa modelling experiments.

The concentration of each compound is indicated above the plate (shown in blue with the individual wells depicted in circles). The order in which the drugs (listed to the right) were added to cultured cells was always from lowest to highest concentration.

After 20 hours, 50 µl of XTT reagent (prepared just before use; details in **(section 5.2.5)**) was added and the cells re-incubated for 4 hours. The absorbance at 450nm and 620nm was read on a Multiskan Ascent ELISA (MTX Lab Systems Inc, Bradenton, FL, USA) plate reader. The cells were re-incubated for an additional 44 hours and re-read on the plate reader at 18, 24 and 48 hours. Output data were copied to an Excel file and the absorbance changes relative to the untreated controls calculated.

5.2.4 Production of Endocannabinoid/ Endovanilloid Containing Media

A master stock solution of each of the compounds (endocannabinoids and endovanilloid) at 1000x the highest concentration required (i.e. 10 mM of each) were created. To make the correct amount of growth medium with compounds or control (0.1% Ethanol), the stock solutions were then serially diluted (10 µl of the master stock added to 90 µl of ethanol to create 1 mM, 100 µM, 10 µM and 1 µM working stock solutions). The final growth solutions were made by diluting 3 µl of each of the working stock solutions with 2997 µl of cell growth medium, i.e. 1000th dilutions. The control in each case was made using 9µl of ethanol diluted with 8991µl of cell growth medium.

This was then added to the cells and the experiments allowed proceed as shown in **Figure 5-3**.

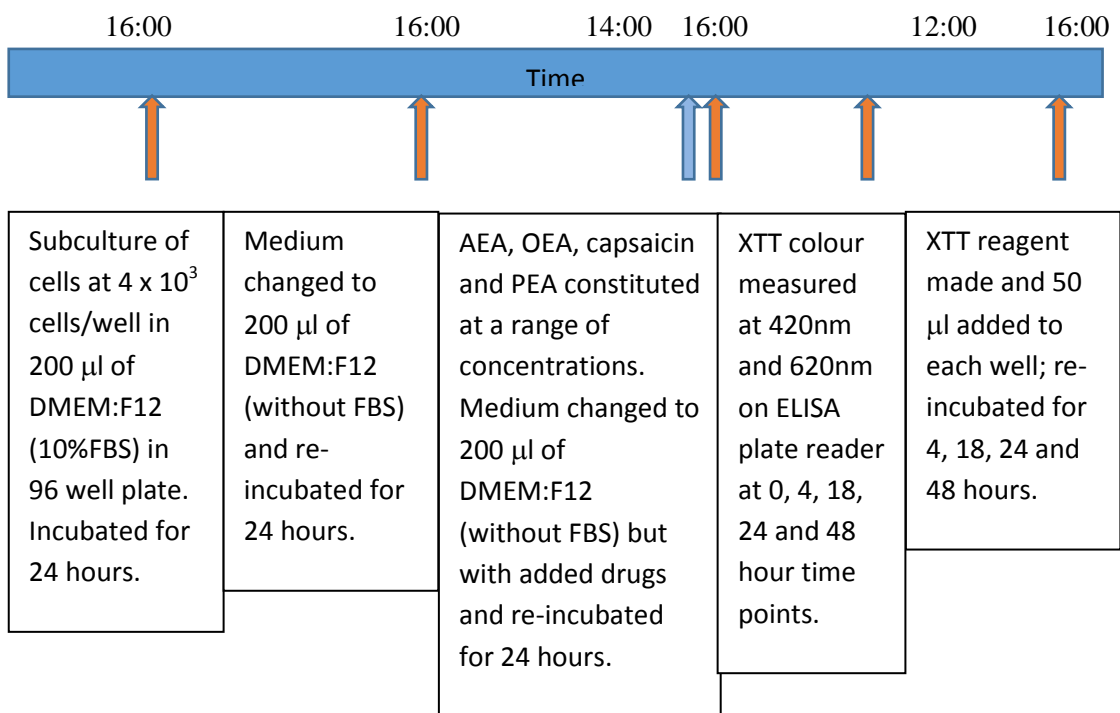


Figure 5-3: Visual representation of the Ishikawa cell modelling experiment.

The time lines shows the points when cells were taken from the incubator (brown arrows) and when the different changes in media additions (including compound containing media – Blue arrow) were made.

5.2.5 Cell Proliferation (XTT) Assay

The colorimetric assay (XTT based) kit from Roche diagnostics was used for the non-radioactive quantification of cell proliferation and viability, by estimating the number of cells present post- treatment using a Multiskan Ascent ELISA plate reader. The principle behind the assay is that mitochondrial dehydrogenase enzymes in viable cells are able to metabolise the XTT into formazan dye, which is proportional to the number of viable cells, enabling the rate of proliferation to be assessed. The reaction can be seen as change in colour of the solution from yellow to orange-brown.

XTT labelling mixture was prepared by thoroughly mixing 15 ml of the XTT reagent with 300 μ l of electron coupling reagent to form a clear solution at 37°C. After treatment in the presence of XTT for 4, 18, 24 and 48 hours, the absorbance at 450nm with a reference wavelength of 620nm were recorded. The corrected absorbance values

calculated by subtracting the absorbance at 620nm from that of 450nm, were used to calculate the mean and standard deviation of four absorbance readings for each compound concentrations. These values were then used to construct dose-time curves for each compound. Each experiment was performed three times.

5.2.6 Statistical Analysis

GraphPad Prism 7.0 software was used for statistical analysis. The mean and standard error of mean (SEM) were calculated and one-way analysis of variance (ANOVA) with appropriate ad hoc post-tests. A p value of < 0.05 was taken to be statistically significant.

5.3 Results

5.3.1 Dose-response Curve for AEA, OEA, PEA and Capsaicin

Dose-response curves for AEA, OEA, PEA and capsaicin when measured after 18 hours of XTT (the recommended time point by the manufacturer) are shown in **Figure 5-4**. The data for AEA showed a significant ($p < 0.05$) decrease in cell number at 1 nM, 100 nM and 10,000 nM but not at 10 nM or 1,000 nM where the cell number was similar to untreated cultures. OEA, PEA and capsaicin all showed variable responses, with only the highest doses (10,000 nM) being consistently effective in decreasing cell numbers. However, the only statistically significant ($p < 0.05$) effect at this high dose was observed with OEA. PEA and capsaicin failed to show any statistical dose response.

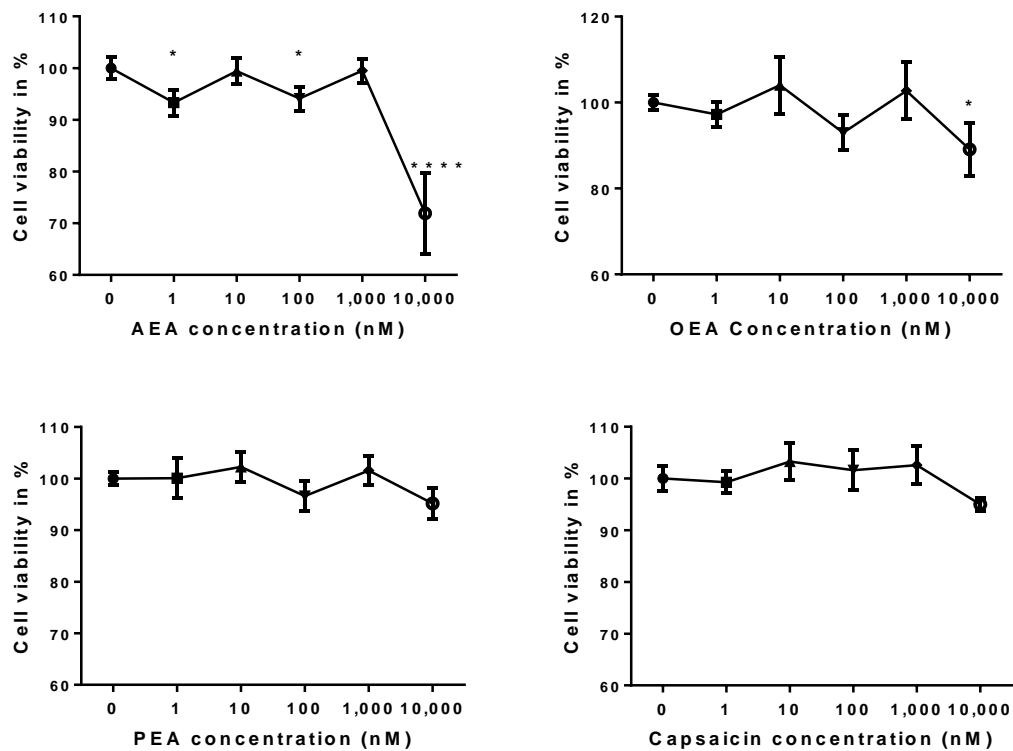


Figure 5-4: Dose-response curves for the indicated endocannabinoid and capsaicin ligands.

The graphs were created from the data collected after 18 hours of XTT addition to the Ishikawa cell cultures. The dose response curve shows statistical significance following AEA and OEA administration in the Ishikawa cells. The data were analysed using one-way ANOVA with Dunnett's ad hoc post test; *p<0.05; ****p<0.0001 when compared to the untreated controls.

5.3.2 Time Dependent Effect of Endocannabinoids/ Endovanilloids on Cell Viability

As the manufacturer's recommended XTT measurement time-point of 18 hours was used here, it was possible that any effect of the NAEs or capsaicin on Ishikawa cell viability could either have already occurred or not happened yet. In order to investigate these possibilities, Ishikawa cells were grown in the presence of different concentrations of NAEs or capsaicin (1 nM, 10 nM, 100 nM, 1,000 nM and 10,000 nM) for 0, 4, 18, 24 and 48 hours. Because the data are complex, the data for each of these compounds will be presented individually; first at the highest dose and then at lower doses. This is because the highest dose in each case appeared to have an effect on Ishikawa cell viability at 18 hours of XTT exposure (even if it was not significantly different from the untreated cells for PEA and capsaicin, see **Figure 5-4**).

5.3.3 Effect of AEA on Ishikawa Cell Viability

The effect of AEA on Ishikawa cell numbers at the different time points is shown in **Figure 5-5**, with the highest effective dose shown in **Figure 5-4** (10,000 nM of AEA); this was used as the benchmark. A 10,000 nM dose caused a gradual decrease in cell viability with time, reaching a nadir at 18 hours (as was shown in **Figure 5-4**), which then returned back to normal (100% cell viability) at 48 hours. At 1 nM AEA, there was a significant reduction in cell numbers at 18 hours that was also significantly lower than that found at 4 hours, but then the number of viable cells also returned to the 100% level at 24 and 48 hours. At 10 nM of AEA, there was no effect at any time point. At 100 nM AEA, there was a significant effect at 18 hours that was significantly different to all other time points, with the cell viability returning to 100% at 48 hours. Strangely, 1,000 nM AEA had no effect at any time point. These data suggest that AEA acts in a pseudo dose-dependent manner with a threshold effect occurring only at the highest dose.

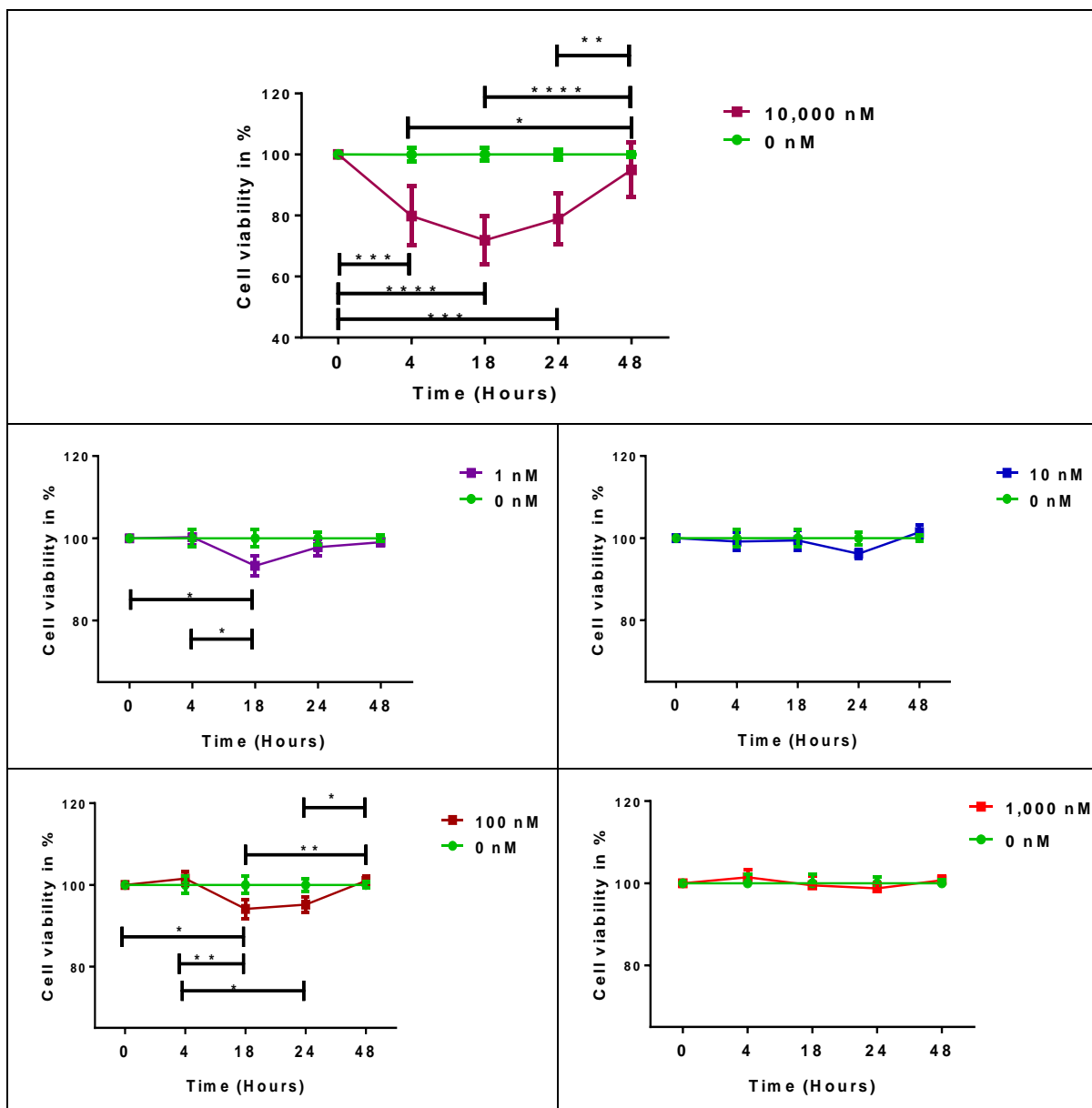


Figure 5-5: Effect of time on the treatment of Ishikawa cells with different AEA concentrations.

XTT values were normalized against the corrected XTT values at time 0 and then multiplied by 100% to create the % Cell Viability at time 0. This was then set at 100% and consequently all other data were relative to that value. The data are expressed as the mean \pm SEM of three independent experiments performed in quadruplicate (n=12); *p<0.05, **p<0.01, ***p<0.001 and ****p<0.0001 versus untreated Ishikawa cells (0 nM – green line in all graphs) at the corresponding time (0, 4, 18, 24 and 48 hours) points; P values were obtained using one-way ANOVA with Tukey’s multiple comparison ad hoc post-tests.

5.3.4 Effect of OEA on Ishikawa Cell Viability

The effect of OEA on Ishikawa cell numbers at the different time points is shown in **Figure 5-6**, with the highest effective dose shown in **Figure 5-4** (10,000 nM of OEA), this was used as the benchmark for the other doses. The 10,000 nM dose caused a gradual decrease in cell viability with time, reaching a low point at 4 hours and remaining at that level and becoming significantly different from the zero time point at 18 hours (as was shown in **Figure 5-4**). At 24 hours the number of cells had returned back to normal (100% cell viability) and that was maintained (if slightly elevated) at 48 hours.

The different doses of OEA produced variable effects on the cell numbers. Although a maximal decrease in cell numbers at 18 hours was observed with 1 nM, 100 nM and 10,000 nM OEA, (similar to AEA, see **Figure 5-4**), an effect at 4 hours was also observed in which cell numbers increased with all doses, except for the 10,000 nM OEA dose. However, the effects on Ishikawa cell number of the maximum dose of OEA at 18 hours was negated at 24 hours post XTT addition, which reveals that this may not be a true dose dependent reduction in cell number; rather it may be a pseudo-dose dependent effect, probably through the inhibition of cell proliferation rather than cell death because the cells recover in long-term culture (see **Figure 5.6**). In contrast, there were no statistically significant changes in the cell viability with OEA at doses of 10 nM and 1,000 nM in any time point.

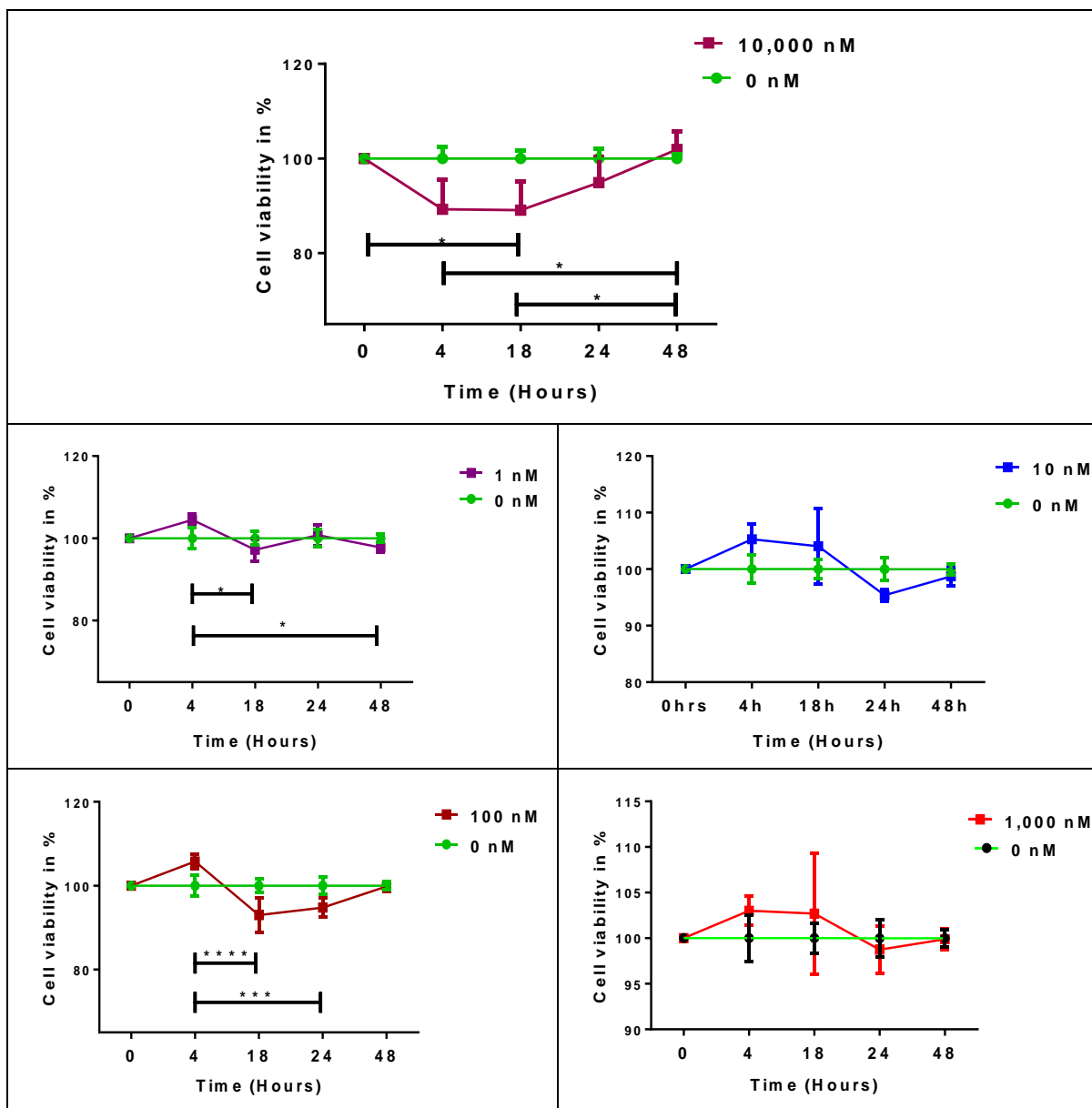


Figure 5-6: Effect of time on the treatment of Ishikawa cells with different OEA concentrations.

XTT values were normalized against the corrected XTT values at time 0 and then multiplied by 100% to create the % Cell Viability at time 0. This was then set at 100% and consequently all other data were relative to that value. The data are expressed as the mean \pm SEM of three independent experiments performed in quadruplicate ($n=12$); data point denoted with * $p<0.05$, *** $p<0.001$ and **** $p<0.0001$ versus untreated Ishikawa cells in various timeline (0, 4, 18, 24 and 48 hours) with three treatment doses of OEA which showed statistical significance (1 nM, 100 nM and 10,000 nM), whilst, the 10 nM and 1000 nM doses, failed to show any statistically significant effect at any timeline. P value obtained by one-way ANOVA with Tukey's multiple comparison post hoc test.

5.3.5 Effect of PEA on Ishikawa Cell Viability

The effect of PEA on Ishikawa cell numbers at the different time points is shown in **Figure 5-7**, with the highest effective dose shown in **Figure 5-4** (10,000 nM of PEA). The 10,000 nM dose caused an immediate decrease in cell viability with time, reaching a low point at 4 hours that was maintained until 24 hours, which then exceeded the normal (>100% cell viability) at 48 hours.

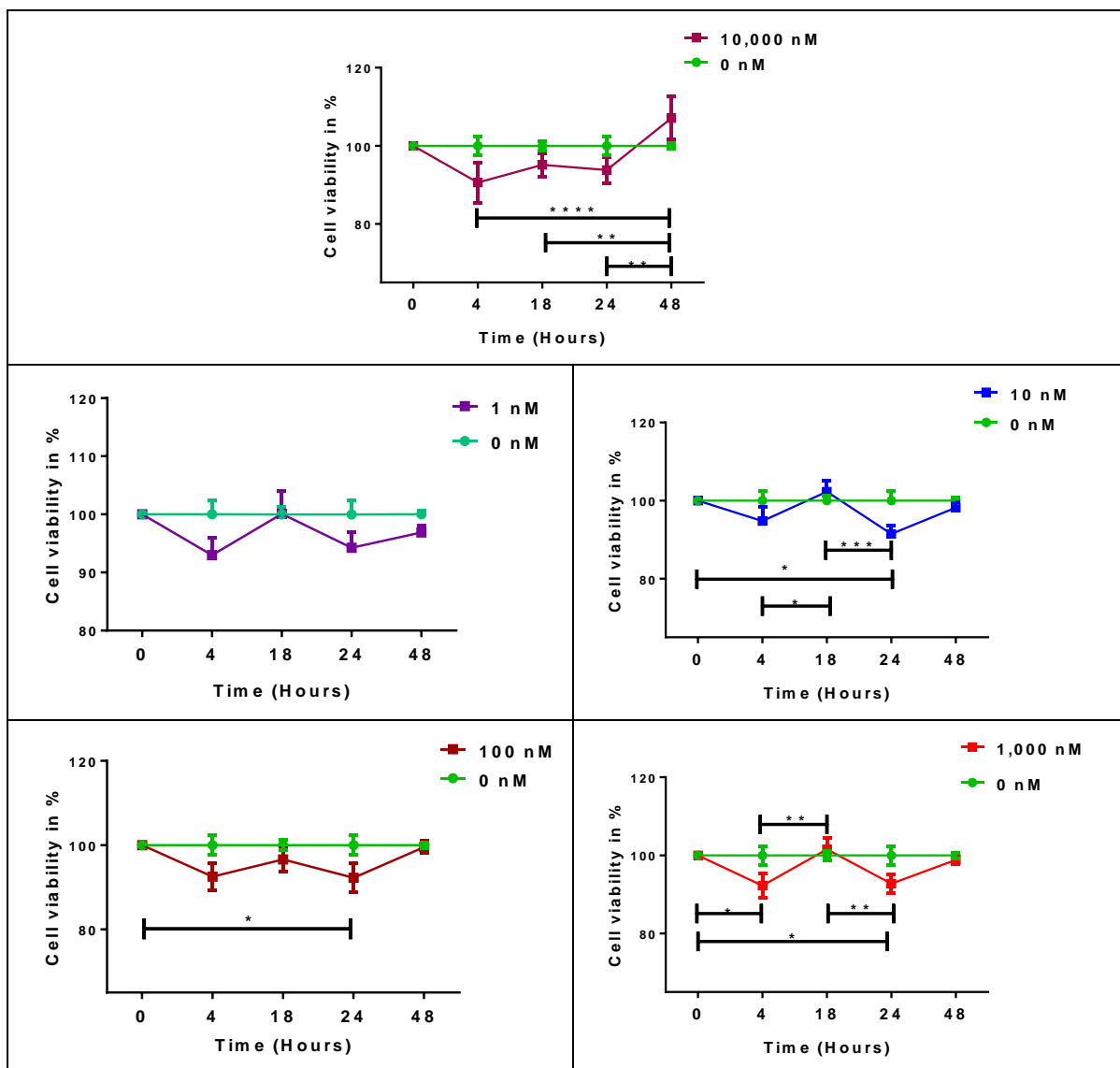


Figure 5-7: Effect of time on the treatment of Ishikawa cells with different PEA concentrations.

XTT values were normalized against the corrected XTT values at time 0 and then multiplied by 100% to create the % Cell Viability at time 0. This was then set at 100% and consequently all other data were relative to that value. The data are expressed as the mean \pm SEM of three independent experiments performed in quadruplicate ($n=12$); data point denoted with * $p<0.05$, ** $p<0.01$, *** $p<0.001$ and **** $p<0.0001$ versus untreated Ishikawa cells in various timeline (0, 4, 18, 24 and 48 hours) with four treatment doses of PEA which showed statistical significance (10 nM, 100 nM, 1000 nM and 10,000 nM), whilst, the 1 nM doses, failed to show any statistically significant effect at any timeline. P value obtained by one-way ANOVA with Tukey's multiple comparison post hoc tests.

5.3.6 Effect of Capsaicin on Ishikawa Cell Viability

The effect of capsaicin on Ishikawa cell numbers at the different time points is shown in **Figure 5-8**, with the highest effective dose shown in **Figure 5-4** (10,000 nM of capsaicin). The 10,000 nM dose caused a gradual decrease in cell viability with time, reaching a low point at 18 hours (as was shown in **Figure 5-4**), and then returning back to normal at 24 hours and then significantly ($*p < 0.05$ compared to the 4 hour data and $*p < 0.0001$ compared to the 18 hour data) exceeding this value ($>100\%$ cell viability) at 48 hours, suggesting that increased cell proliferation had occurred during the 2 days of culture in the presence of this TRPV1 agonist.

The lowest dose of capsaicin (1 nM) appeared to have no effect at any time point, whilst 10 nM, 100 nM and 1,000 nM capsaicin showed a similar pattern with a slight increase in cell numbers at 4 hours; a decrease at 18 hours, another increase at 24 hours followed by a return to normal levels at the end of the experiment (**Figure 5-8**), however the only significant effect was recorded using 10 nM capsaicin between 18 and 24 hours of treatment. These effects may be due to the entourage effects of the endocannabinoids or capsaicin may have an effect on other non-classical endocannabinoid receptors.

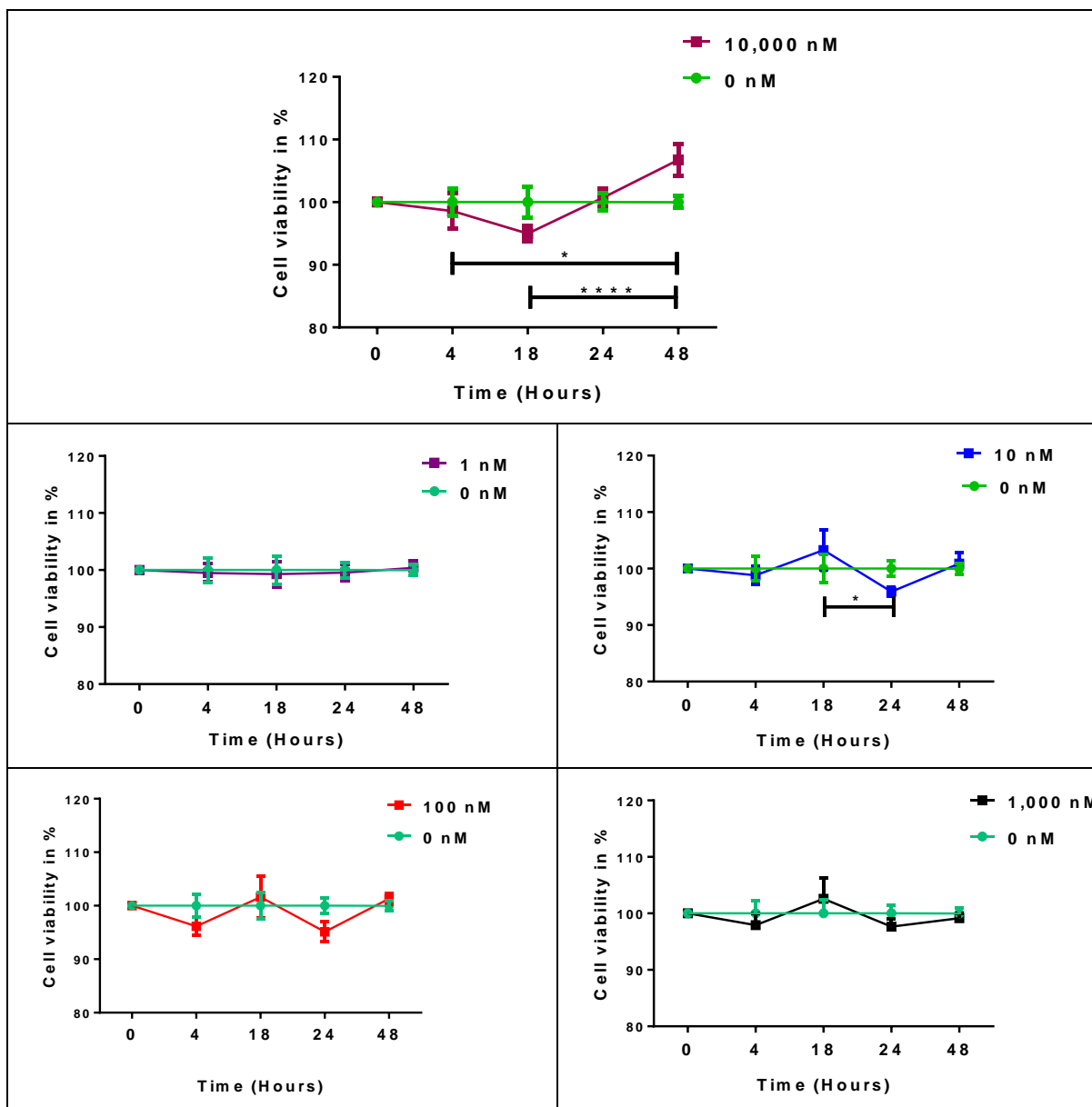


Figure 5-8: Effect of time on the treatment of Ishikawa cells with different capsaicin concentrations.

XTT values were normalized against the corrected XTT values at time 0 and then multiplied by 100% to create the % Cell Viability at time 0. This was then set at 100% and consequently all other data were relative to that value. The data are expressed as the mean \pm SEM of three independent experiments performed in quadruplicate (n=12); data point denoted with *p<0.05 and ****p<0.0001 versus untreated Ishikawa cells in various timeline (0, 4, 18, 24 and 48 hours) with two treatment doses of capsaicin which showed statistical significance (10 nM and 10,000 nM), whilst, the 1 nM, 10 nM and 1,000 nM doses, failed to show any statistically significant effect at any timeline. P value obtained by one-way ANOVA with Tukey's multiple comparison post hoc tests.

5.4 Discussion

Ishikawa cells were used because they are known to express the endocannabinoid receptors (Dr Sarah Melford, personal communication) including TRPV1 (Dr Tim Marczylo, ERG, University of Leicester, unpublished observation).

All four compounds, AEA, OEA, PEA and capsaicin (CAP), caused a reduction in cell number, but only the highest dose (10,000 nM) of AEA induced a maximal reduction (from 100% to 71.9%) after 18 hours, whilst OEA reduced cell numbers from 100% to 89.1% at the same time point. PEA was quicker and reduced cell numbers to 90.5% after 4 hours and CAP was the least effective producing only a 5% (from 100% to 95%) reduction in cell numbers after 18 hours. Each compound had a variable effect on Ishikawa cell numbers at different time points with maximal effect of AEA after 18 hours, being reversed at 48 hours following the addition of XTT. Similarly, Ishikawa cells treated with OEA and CAP recovered 24 hours after the addition of XTT, while PEA treated cells recovered earlier by 18 hours. These four compounds (AEA, OEA, PEA and CAP) reduced the number of Ishikawa cells in a time-dependent and dose-dependent manner. These effects are probably through inhibition of cell proliferation rather than cell death, because the cultures were not full of dead floating cells and furthermore they recovered in long-term culture.

This conclusion is not supported by other studies that have shown that endocannabinoids 'kill' numerous cancer cell types, primarily through apoptosis (Maccarrone et al. 2000, Carracedo et al. 2006, Giuliano et al. 2009, Sreevalsan et al. 2011, Pellerito et al. 2014, McAllister et al. 2015). Mimeault *et al.* reported that AEA inhibits cell proliferation and induced apoptosis in the prostate cancer cell lines LNCaP, DU145 and PC3 by activating CB1 receptors on the cancer cell surface resulting in decreased expression of epidermal growth factor (EGFR) and therefore AEA cut-off a significant source of fuel for the cancer cells (Mimeault et al. 2003). By contrast, data presented by Linsalata *et al.* showed that AEA treatment for 24 to 48 hours affected the growth of colon cancer cell lines HT-29, SW620 and DLD-1 by decreasing cell proliferation in a dose-dependent manner due to AEA's ability to reduce polyamine levels (Linsalata et al. 2010). In addition, it has been shown that AEA inhibits breast cancer cell proliferation through a decrease in prolactin receptor expression (Melck et al. 1999) and to induce neuroblastoma, lymphoma and uterine cervix carcinoma cell

death through their vanilloid receptors (Maccarrone et al. 2000, Contassot et al. 2004). Moreover, it has also been proposed that in cholangiocarcinoma, the anti-proliferative and pro-apoptotic action of AEA is facilitated by lipid rafts (DeMorrow et al. 2007) and the apoptosis induced by AEA in human neuroglioma cells is COX-2 mediated (Hinz et al. 2004). Thus, the exact mechanism of cancer cell senescence is most probably cell-specific and ligand-specific.

When the Ishikawa cells were cultured with the structural relatives of AEA, OEA and PEA, a pseudo time-dependent and dose-dependent response curve was obtained. OEA caused a reduction in cell numbers after 18 hours that recovered by 24 hours. On the other hand, PEA was quicker in causing a distinct reduction in cell numbers after only 4 hours and interestingly the recovery was also quick reaching normal cell numbers by 18 hours. Similar observations have been demonstrated in NIE-115 neuroblastoma cells exposed to AEA, OEA and PEA (Hamtiaux et al. 2011). While a reduction in cell viability often leads to apoptosis, Hamtiaux *et al.* found that OEA and PEA reduced the number of viable cells without inducing apoptosis (Hamtiaux et al. 2011). Furthermore, OEA has been shown to inhibit cell proliferation and to induce apoptosis in the ovarian cancer cell line OV2008 independently of the PPAR- α signalling pathway that OEA normally activates (Kisgeropoulos 2013), whilst PEA exerts an anti-proliferative and anti-angiogenic effect on cultured human colon carcinoma Caco-2 cells through a PPAR- α -dependent inhibition of the Akt/mTOR pathway, achieved in a concentration-dependent manner (Sarnelli et al. 2016). Interestingly, PEA inhibits the expression of FAAH and enhances the anti-proliferative effect of AEA in breast cancer cells (Di Marzo et al. 2001), suggesting that the expression of FAAH could be critical for the control of cell growth for some cancers.

The Ishikawa cells treated with the highest dose of CAP (10,000 nM) showed maximal reduced cell viability effect after 18 hours. Thereafter, the cells started to recover and grow. Unlike all the other experiments with the NAEs, by 48 hours there was marked proliferation of the cancer cell line beyond the starting point. Some investigators have documented that CAP is a carcinogen, a co-carcinogen and a cancer cell growth promoter (Bode et al. 2011), while others have shown that it has chemo-preventive and chemotherapeutic effects (Surh et al. 1995, Surh et al. 1996, Surh et al. 1998, Surh 1999, Surh 2002). However, capsaicin has been found to repress the growth of some transformed cancer tumours of human and mouse origin (Morre et al. 1995, Morre et al.

1996). Moreover, some studies have shown anti-proliferative and apoptotic effects on human cancer cell lines derived from gastric cancer (Kim et al. 1997), colon carcinoma (Lu et al. 2010), breast cancer (Thoennissen et al. 2010) and the human KB cancer cell line (Lin et al. 2013). The molecular mechanisms whereby capsaicin induces programmed cell death in these cells remains unknown (Macho et al. 1998, Macho et al. 1999, Macho et al. 2000). Since capsaicin is known to have two actions: inhibiting tumour and promoting tumour growth (Bode et al. 2011), then it may have a dual role in EC that is dependent on an initial anti-proliferative CAP response that then supports EC cell recovery that extends beyond the starting point and supports extended EC pathogenesis. The mechanism involved here remains unknown.

In this chapter, evidence has been provided to suggest that the NAEs and capsaicin reduces Ishikawa endometrial cancer cell viability probably through the inhibition of proliferation or induction of apoptosis, with unexpected increased cell viability (increased proliferation) with CAP. In all cases, the growth of the cultures recovered, suggesting that either the ligands have been degraded with time, or that some of the cells in culture do not express the appropriate receptors to respond to the ligands. Since the exact mechanism involved remains unclear, it would be useful to evaluate whether the effect demonstrated on Ishikawa cells (a model of EC) is replicated happens *in vivo*. This is not ethically possible, but could be examined on biopsies already collected, because AEA, OEA and PEA were all increased in the endometria of EC patients (Chapter 2). Thus, any relationship or association between the tissue AEA, OEA or PEA levels and cell proliferation markers or cell death by apoptotic markers in those biopsies can be examined. This will be presented in the next Chapter.



Chapter 6

Cellular Apoptosis and Proliferation Markers in Endometrial Cancer and their Relationship with the Endocannabinoid System

6.1 Introduction

In chapters 2, 3 and 4 it was established that all components of the endocannabinoid system are present in endometrial cancer (EC) tissue and most were dysregulated with AEA, OEA and PEA levels clearly higher than those found in atrophic endometrium. Additionally, it was shown that the non-classical receptor TRPV1 is also dysregulated suggesting that loss of this receptor may also be important in the pathogenesis of EC. Capsaicin, the natural ligand for TRPV1 is a key component of red and chilli peppers (Cortright et al. 2004, Sawynok 2005). In Chapter 5, it was shown that all 4 ligands, AEA, OEA, PEA and capsaicin affected Ishikawa cell numbers, with the highest doses of AEA and OEA reducing cell numbers within 18 hours of treatment, whilst PEA and capsaicin had similar effects at earlier and later time points, respectively. These data suggest that, these four ligands may alter endometrial epithelial cell number in EC by either inhibiting cell proliferation or affecting the cell/tissue's ability to undergo apoptosis.

BAX and Bcl-2 are members of a gene family involved in the regulation of apoptosis (Craig 1995). Previous studies involving BAX and Bcl-2 in cultured cells have established that Bcl-2 protein can be functionally characterised as an apoptosis-suppressing factor whereas BAX protein can be characterised as an apoptosis-promoting factor (Oltvai et al. 1993). These two proteins have been described as a cellular 'rheostat' of apoptosis sensitivity (Oltvai et al. 1993, Yang et al. 1996, Perlman et al. 1999). Moreover, the intracellular BAX/Bcl-2 protein ratio can profoundly influence the ability of a cell to respond to an apoptotic signal (Yang et al. 1996). Accordingly, a cell with a high BAX/Bcl-2 ratio will be more sensitive to a given apoptotic stimuli when compared to a similar cell type with a comparatively low BAX/Bcl-2 ratio.

To test this idea in the cohort of patients here, these two proteins were examined by immunohistochemistry (IHC) so as to enable localisation and quantification of their levels. Many studies examining the expression of BAX and Bcl-2 in endometrial cancer (Bozdogan et al. 2002, Sakuragi et al. 2002, Porichi et al. 2009, Banno et al. 2012), have been contradictory and furthermore, to my knowledge, there have been no studies that have examined the potential relationship between these proteins and the ECS in endometrial cancer.

Dysregulated abnormal proliferation in endometrial cancer cells may be associated with numerous regulatory mechanisms that could be related to non-apoptotic processes. To examine this possibility, the expression of Ki-67, one of the key cell cycle regulatory proteins in endometrial tissue proliferation was examined, using a quantitative IHC method, thus allowing for the assessment of its relationship to the NAEs and other components of the ECS.

6.1.1 Hypothesis

Increased BAX expression and decreased Bcl-2 expression, which leads to an increase in the BAX/Bcl-2 ratio, may promote apoptosis and this imbalance may be associated with endometrial carcinogenesis.

6.1.2 Aims

- (A) To localise and determine the distribution patterns for the proteins BAX (a promoter of apoptosis), Bcl-2 (an inhibitor of apoptosis) and Ki-67 (a cell proliferation marker) in normal and malignant endometrium using IHC.
- (B) To identify the relationships between the above markers and components of the endocannabinoid system.

6.2 Subjects and Methods

6.2.1 Patient Characteristics

The samples used for the IHC of the BAX, Bcl-2 and Ki-67 studies were identical to those used in Chapter 3 (section 3.3.4.1; table 3-10). Consequently, the patient characteristics are the same as those listed in Table 3-10.

6.2.2 Localisation and Determination of Distribution Patterns of BAX, Bcl-2 and Ki-67 Proteins Using Immunohistochemistry

The expression and locations of the BAX, Bcl-2 and Ki-67 proteins were identified using the primary and secondary antibodies shown in **Table 6-1**.

Table 6-1: The antibodies (and their sources and their suppliers) used for BAX, Bcl-2 and Ki-67 IHC studies

Antibodies	Source (manufacturer)
Primary	
❖ BAX Rabbit Polyclonal IgG (Concentration 200 µg/ml)	Santa Cruz Biotechnology (N-20) Catalogue number SC-493
❖ Bcl-2 Mouse Monoclonal IgG (Concentration 200 µg/ml)	Santa Cruz Biotechnology (Clone C-2) Catalogue number SC-7382
❖ Ki-67 Mouse Monoclonal	Novocastra-Clone MM1 (NCL-Ki-67-MM1)
Secondary	
❖ Goat anti Rabbit Biotinylated antibody) (Secondary antibody 1:400 for BAX)	DAKO
❖ Rabbit anti Mouse Biotinylated antibody (Secondary antibody 1:400 for Bcl-2)	DAKO
❖ Goat anti Mouse Biotinylated antibody) (Secondary antibody 1:400 for Ki-67)	VECTOR (I-2000)

6.2.3 Immunohistochemistry for BAX

The slides were dewaxed in xylene and re-hydrated through graded alcohol to water (4 min each step), moved into 500 mls of citrate buffer (10 mM, pH6) in a plastic container and then subjected to microwave energy at 750 Watts for exactly 30 minutes. The slides were then allowed to cool for exactly 20 minutes. Next, these were placed in dH₂O for 5 minutes and then incubated in 6% H₂O₂ [51ml H₂O₂ + 249ml ice-cold dH₂O] for 10 min. The slides were next washed in dH₂O for 5 min, placed in a rack and transferred to PBS-T₂₀ for 5 minutes. Excess liquid was removed from around the tissue section using a folded paper tissue and placed in a humidity chamber and blocked with 100µl/section of 1:10 normal goat serum (NGS) in TBS, for 10 minutes at room temperature. After draining, the slides were incubated with 100µl/section of primary antibody (BAX) diluted at 1:200 in blocking solution (NGS/TBA), at 4°C overnight. On day 2, the racked slides were washed in PBS in a sandwich box on a magnetic stirrer set at a moderate mixing rate for 20 minutes. After wiping around the sections with paper tissue, they were incubated with 100µl/section of biotinylated goat anti-rabbit antibodies diluted by 1:400 in PBS for 30 minutes. After washing again in PBS for another 20 minutes, sections were incubated with ABC Elite complex (100µl/section) for 30 minutes. After washing again in PBS for 20 minutes the section were incubate with DAB (100µl/section) for 5 minutes before being washed in tap water for 5 minutes. These were then counterstained by immersion in Mayer's haematoxylin for 1-2 min and rinsed in tap water until the "blue" ran clear. Finally, the slides were dehydrated through graded alcohol, cleared in xylene and mounted in XAM mounting medium (BDH, Poole, UK).

6.2.4 Immunohistochemistry for Bcl-2

The methods were identical to those for BAX, except the sections were blocked with 100µl/section of 1:20 normal rabbit serum in PBS for 20 minutes at room temperature. The slides were then drained and incubated with 100ul/section of primary antibody (Bcl-2) diluted 1:25 in PBS before being incubate at 4°C overnight. On the second day, the detection of primary antibody was made using biotinylated rabbit anti mouse antibodies (1:400) dilution in PBS.

6.2.5 Immunohistochemistry for Ki-67

The methods were identical to one for those Bcl-2, except the sections were blocked with 100 µl/section of 1:20 normal goat serum in TBS/3% BSA for 20 minutes at room temperature. The slides were then drained and incubated with 100 µl/section of primary antibody (Ki-67) diluted at 1:150 in blocking solution (1:20NGS/TBS/BSA) and incubate at 4°C overnight. On the second day, biotinylated goat anti-rabbit antibodies were used at a 1:400 dilution in PBS. All washes on the second day were performed using the PBS/Tween₂₀ whilst the rest of the methods were the same.

6.2.6 Statistical Analysis

GraphPad Prism 7.0 software was used for statistical analysis. The data are presented as the mean and standard error of the mean (SEM) and significance determined using one-way analysis of variance (ANOVA) with appropriate post hoc tests. A p-value of <0.05 was taken to represent statistical significance.

6.3 Results

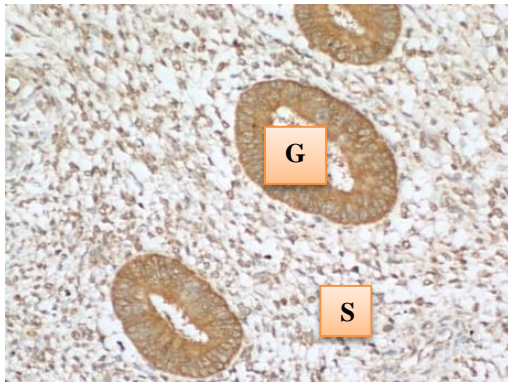
6.3.1 Patient Characteristics for IHC

These were as presented in Chapter 3 (section 3.3.4.1; table 3-10).

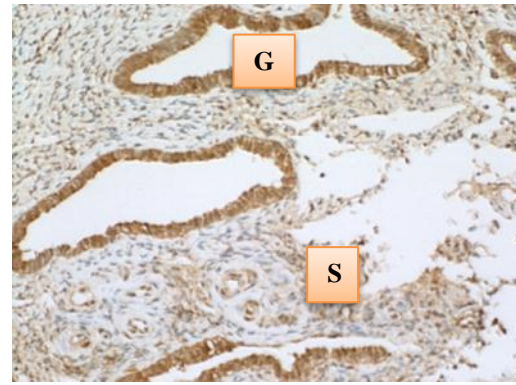
6.3.2 BAX Protein Expression

6.3.2.1 Optimisation of Immunohistochemical Methods for BAX

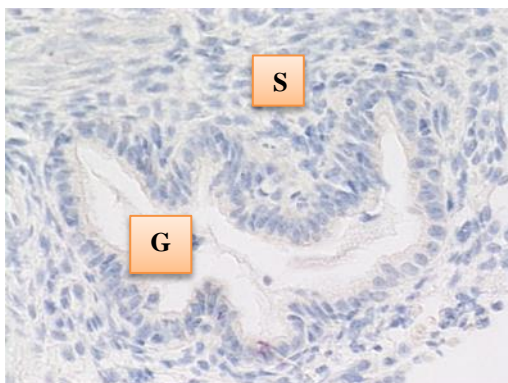
The optimal primary antibody dilution for the BAX studies had previously been standardized in the endometrium at 1 in 200. Antibody specificity was determined using equivalent concentrations of non-immune IgG (**Figure 6-1**). The lack of 3, 3'-diaminobenzidine (DAB) staining in the IgG controls indicates that the antibodies are specific for BAX.



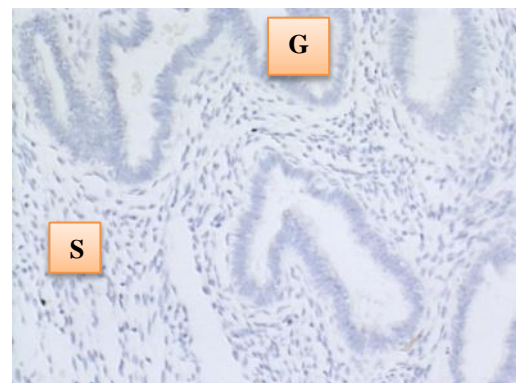
(A) Primary antibody



(B) Primary antibody



(C) IgG antibody



(D) IgG antibody

Figure 6-1: Negative control demonstrating the specificity of the primary antibody BAX.

Images (A) and (B) proliferative endometrium showing very strong positive staining of the primary BAX antibody; more in the glands especially on the apical region and basal region also enveloping the nuclear membrane with strong stain and furthermore involving the stroma: (C) and (D) show no staining for the IgG controls. All the slides are from the proliferative phase of the menstrual cycle.

6.3.2.2 Identification and Locations of BAX Proteins

Figure 6-2 illustrates the staining pattern of BAX in atrophic and EC samples. Following the optimisation of BAX antibody, all the studies were undertaken as a single run to minimise variations.

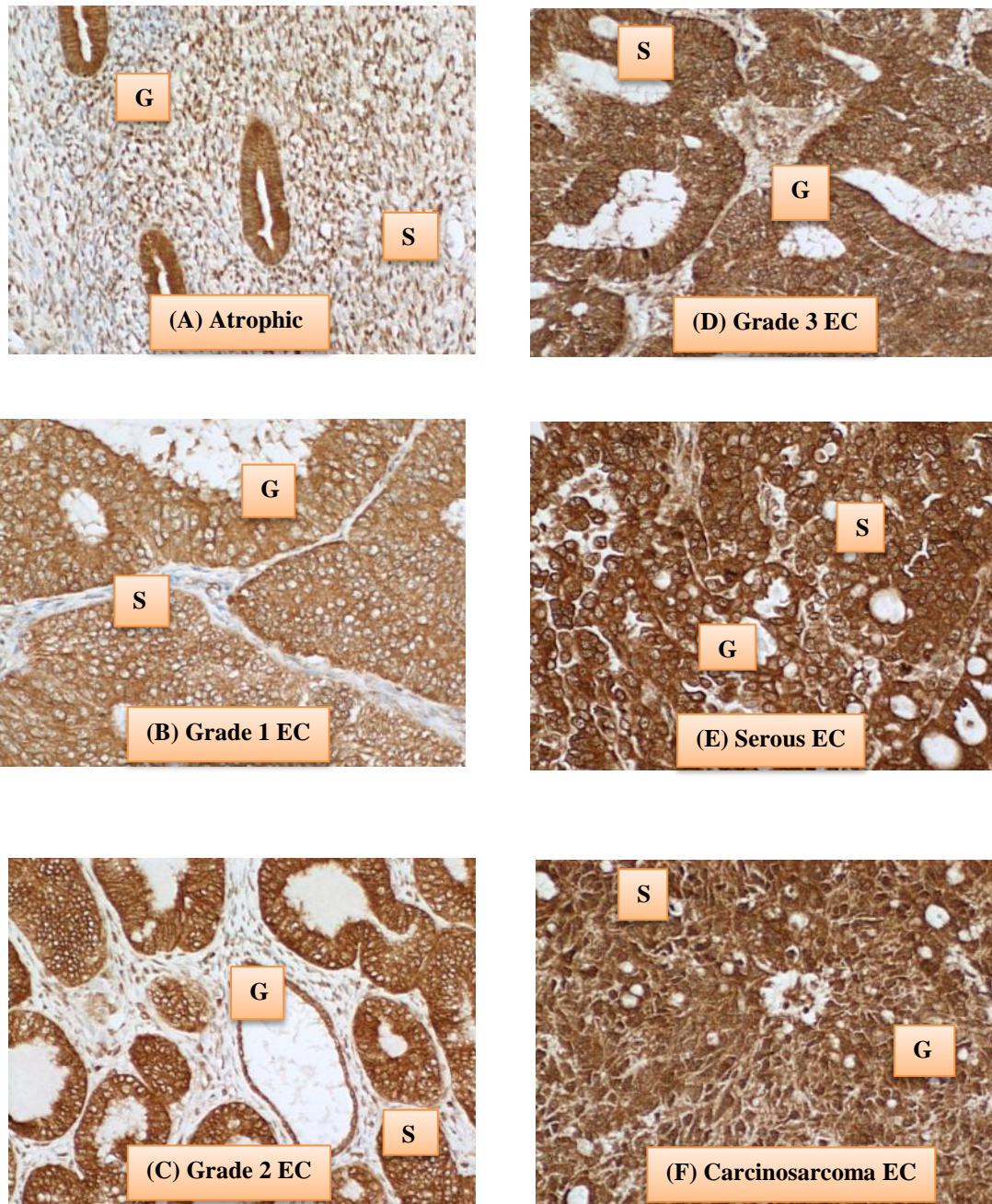


Figure 6-2: Localisation and expression of the BAX protein (G = glands, S = stroma, EC = endometrial cancers).

In atrophic tissue, immunoreactive BAX protein was expressed very strongly in the glands involving the cytoplasm and nucleus. The numbers of glands were markedly reduced in the atrophic endometrium compared to cancer tissue. Furthermore, the stromal component of the atrophic endometrium also showed strong evidence of immunoreactivity. BAX staining was demonstrated in the cytoplasm and the nucleus of the glandular cells and also in the stromal cells where it was sparingly stained with moderate brown intensity (**Figure 6-2A**).

The BAX staining intensity in grade 1 EC was higher compared to that in the atrophic endometrium. The staining involved both the stroma and the glands and was more prevalent in the glandular cells. The nuclei were also stained (**Figure 6-2B**).

The BAX staining intensity in grade 2 EC tissues was very high when compared to that of the atrophic endometrium. This staining clearly involved both the glands and the stroma. In the glands, the staining was more cytoplasmic and also concentrated towards the apical region of the cells. The nucleus and its envelope were also stained (**Figure 6-2C**).

The BAX staining intensity in grade 3 EC was very high compared to atrophic tissue. It clearly showed involvement of the glands with a very high intensity in the glands and stroma. In the glands, the staining was also cytoplasmic and all over the cells. The nuclear envelope and the nucleus was stained very strongly (**Figure 6-2D**).

The BAX staining in serous carcinoma was of very high intensity compared to atrophic endometrium. It involved the glands and the stroma. In the glands, staining was cytoplasmic, and more diffuse over the cells. The nuclear envelope and the nucleus stained strongly (**Figure 6-2E**).

The BAX staining intensity in carcinosarcoma was again very high compared to the atrophic endometrium. It involved both the glands and the stroma. In carcinosarcoma tissue, the glandular structure was completely 'broken down' and the epithelial cells scattered throughout the tissue making it very difficult to differentiate the glands from the stroma. Nevertheless, the staining was cytoplasmic with involvement of the whole cells. The nuclear envelope and the nucleus also showed strong staining both in the glands and the stroma (**Figure 6-2F**).

6.3.2.3 Histomorphometric Quantification of BAX Proteins

Figure 6-3A shows the data from the histomorphometric analysis of glands and stroma (G+S) combined. The data clearly shows that BAX expression was statistically significantly higher in the EC tissue and that it reached statistical significance in the both type 1 and 2 EC when compared to the levels observed in the atrophic endometrium. Furthermore, when the glands alone were examined, higher BAX levels were again observed in both types of EC (**Figure 6-3B**) with BAX levels being higher in the stromal compartment of both types of EC (**Figure 6-3C**).

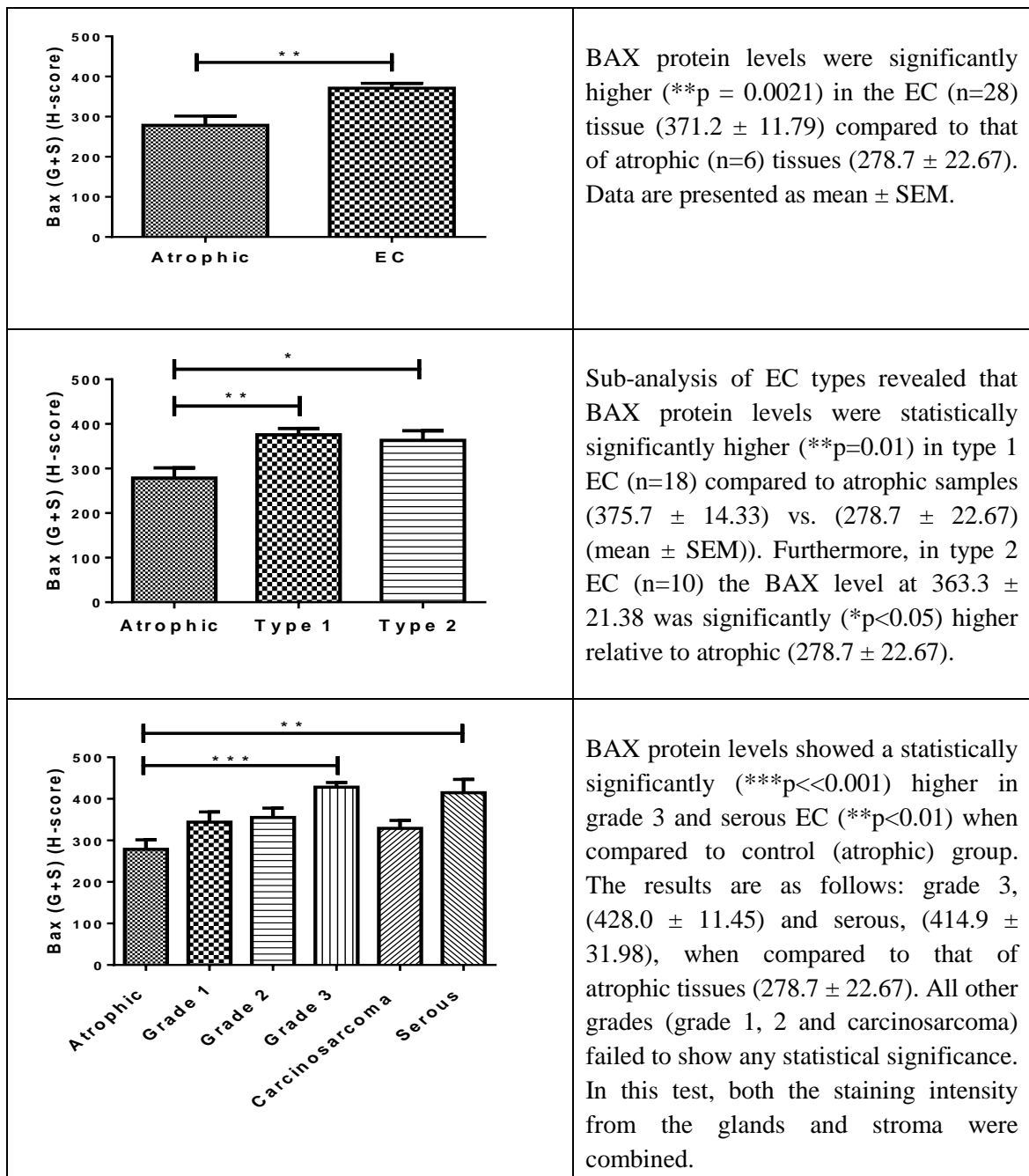


Figure 6-3A: Histomorphometric analysis of BAX (G + S) (H-score) proteins immunoreactivity.

P values were obtained using Student's t-test or one way ANOVA with Dunnett's ad hoc post-test analysis of both tissue components. Data are presented as mean \pm SEM. Collectively, BAX protein levels are increased in EC (G+S) when compared to the control (atrophic) group.

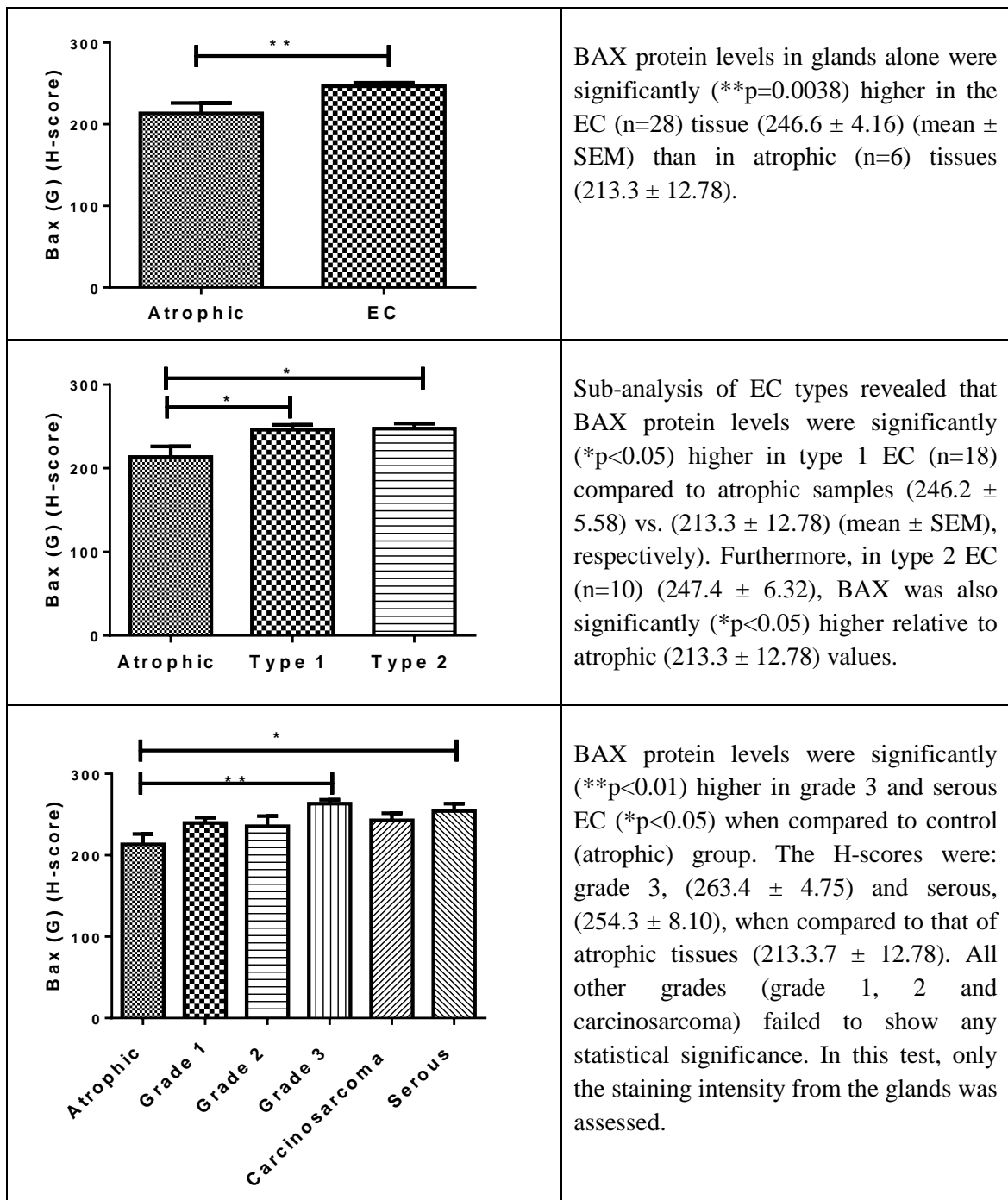


Figure 6-3B: Histomorphometric analysis of BAX (G) (H-score) immunoreactivity.

P values were obtained using Student's t-test and one way ANOVA with Dunnett's ad hoc post-test analysis of the gland components of the tissues. Data are presented as mean \pm SEM. Collectively, BAX protein levels are reduced in EC (G) when compared to the control (atrophic) group.

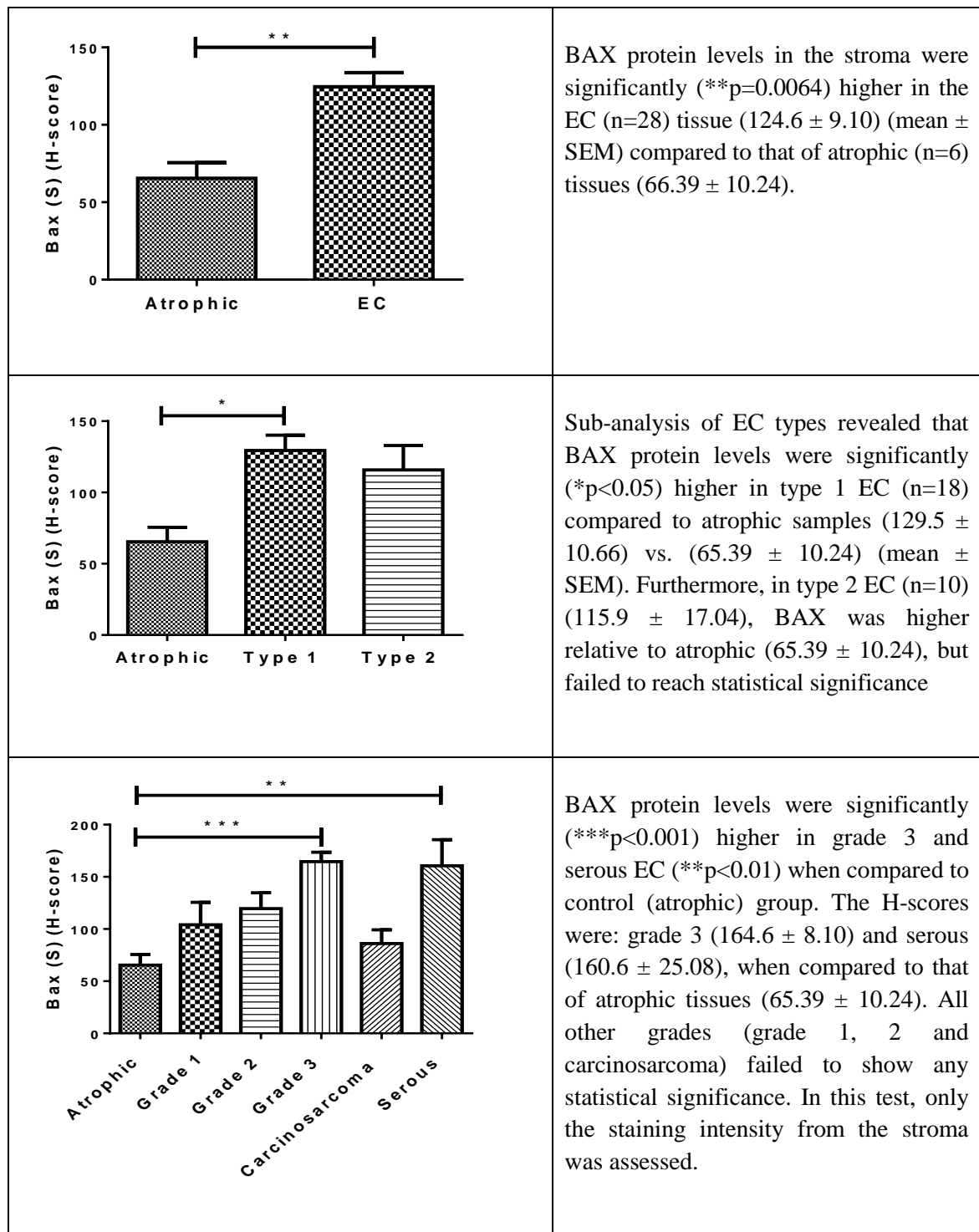


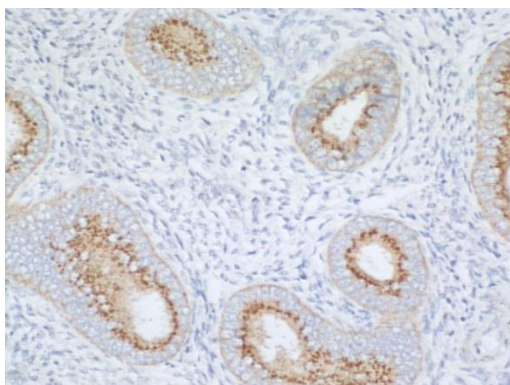
Figure 6-3C: Histomorphometric analysis of BAX (S) (H-score) proteins immunoreactivity.

P values were obtained using Student's t-test and one way ANOVA with Dunnett's ad hoc post-test analysis of the stromal component. Data presented as mean \pm SEM. Collectively, BAX protein levels are increased in EC (S) in grades 1, 2, and 3, and in carcinosarcoma and serous, when compared to the control (atrophic) group.

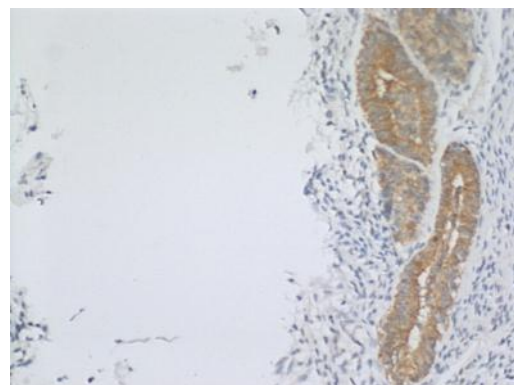
6.3.3 Bcl-2 Protein Expression

6.3.3.1 Optimisation of Immunohistochemical Methods for Bcl-2

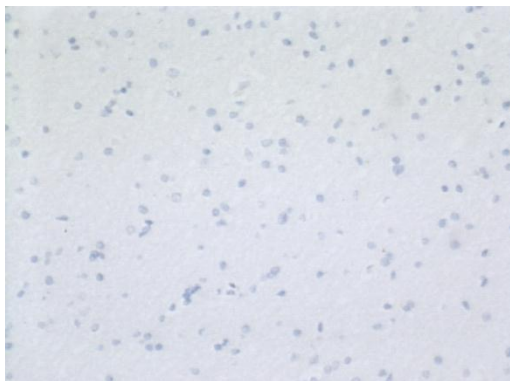
The optimal primary antibody dilution for Bcl-2 had already been standardized in the endometrium; the best dilution was found to be 1:25. Antibody specificity was determined using equivalent concentrations of non-immune IgG (**Figure 6-4**). The lack of 3, 3'-diaminobenzidine (DAB) staining in the IgG controls indicates that the antibodies are specific for Bcl-2.



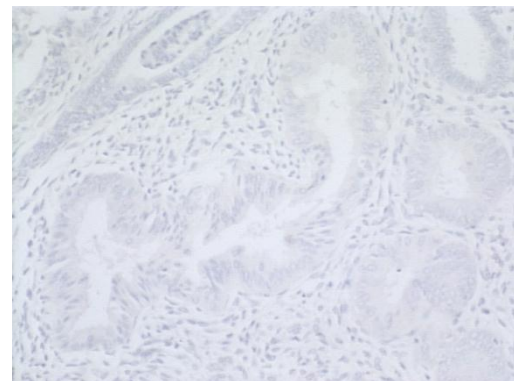
(A) Primary antibody



(B) Primary antibody



(C) IgG antibody



(D) IgG antibody

Figure 6-4: Negative control demonstrating the specificity of the primary antibody Bcl-2.

Images (A) and (B) show positive staining of the primary antibody Bcl-2, which is confined to the apical region on the glands and slight staining of the gland envelope and spares the stroma, whilst images (C) cerebrum and (D), proliferative endometrium show no staining for the IgG controls.

6.3.3.2 Identification and Locations of Bcl-2 Proteins

Figure 6-5 illustrates the staining pattern of Bcl-2 in atrophic and EC samples. Following the optimisation of the Bcl-2 antibody, all the studies were undertaken as a single run to minimise variations.

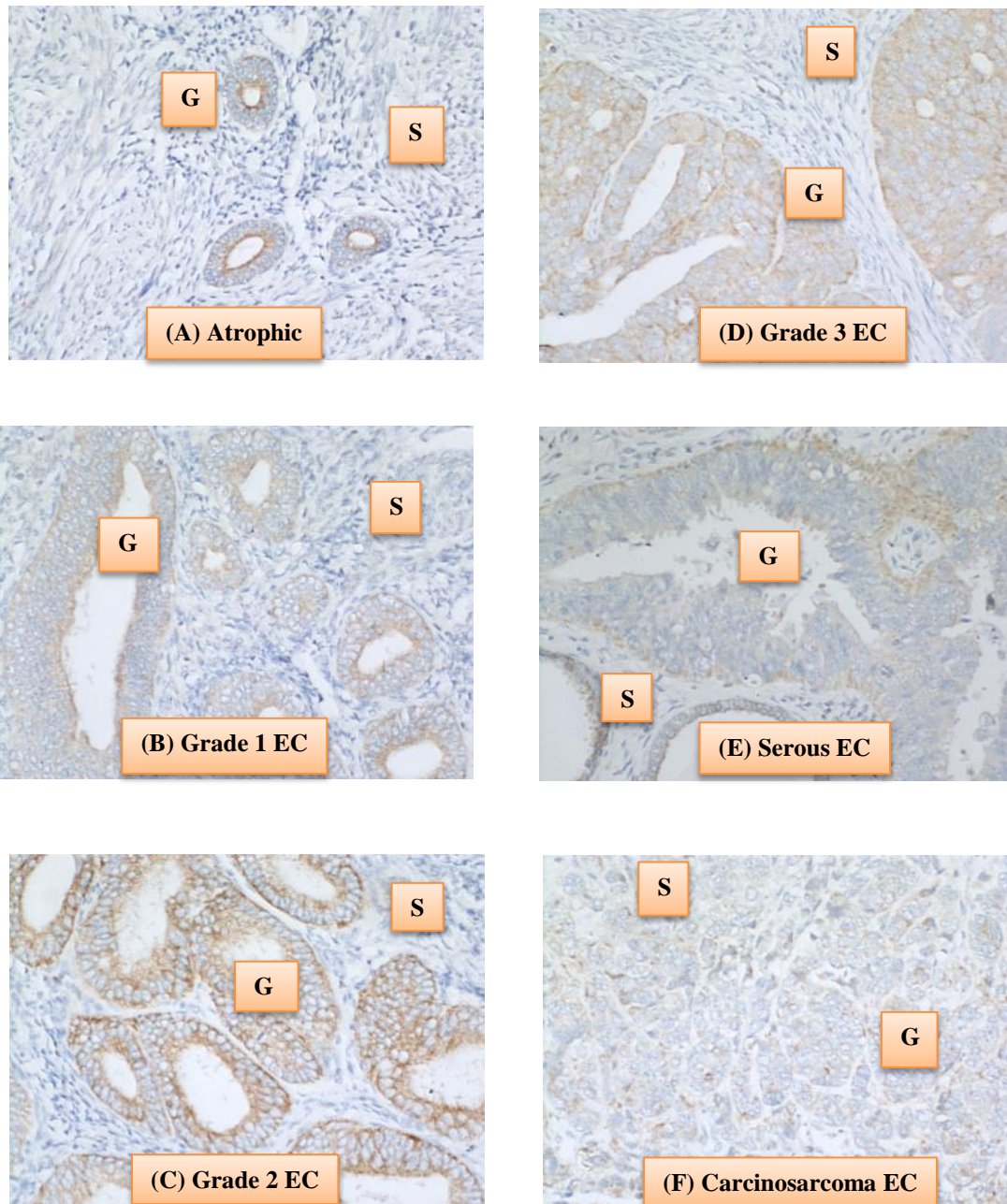


Figure 6-5: Localisation and expression of the Bcl-2 protein (G = glands, S = stroma, EC = endometrial cancers).

In atrophic tissue, immunoreactive Bcl-2 protein was strongly expressed in the glands, particularly along the apical region of the epithelial cells. The number of glands were reduced in the atrophic endometrium compared to the numbers present in cancer tissues. In contrast to the glands, the stromal component of the atrophic endometrium failed to show any evidence of immunoreactivity. Bcl-2 was demonstrated minimally in the cytoplasm of the glands and concentrated more to the apical region and was absent from the nucleus (**Figure 6-5A**).

The Bcl-2 staining intensity in grade 1 EC was lower than that observed in the atrophic endometrium. The staining involved both the apical and basal regions of the glands and was more prevalent in the apical region of the epithelial cell cytoplasm. The nuclei and the stroma were not stained (**Figure 6-5B**).

The Bcl-2 staining intensity in grade 2 EC tissues was more than that seen in atrophic endometrium. This staining clearly involved both the apical and basal regions of the glands and the stroma was not stained. In the glands, the staining was more cytoplasmic and also concentrated towards the apical region of the cells. The nuclear envelope was strongly stained (**Figure 6-5C**).

The Bcl-2 staining intensity in grade 3 EC was slightly more than that seen in atrophic tissue. It clearly showed involvement of the glands with a moderate intensity in the apical and basal part of the cells, whilst the stroma was not stained. In the glands, the staining was cytoplasmic and concentrated towards the apical region of the cells. The nuclear envelope was stained most but the nucleus itself was negative (**Figure 6-5D**).

The Bcl-2 staining intensity in serous carcinoma was of low intensity compared to atrophic endometrium. It involved the glands (very mild intensity) and the stroma was not stained. In the glands, staining was cytoplasmic and more diffuse at the apical compared to the basal regions of the cells. The nuclear envelope was very mildly stained in the glands (**Figure 6-5E**).

The Bcl-2 staining intensity in carcinosarcoma was at a very low intensity compared to the atrophic endometrium and involved both the glands and the stroma (probably all the glands are degraded and may show a false involvement of the stomas). In the carcinosarcoma tissue, the glandular structure was completely 'broken down' and the epithelial cells scattered throughout the tissue making it very difficult to differentiate

the glands. Nevertheless, the staining was cytoplasmic with more towards the apical region of the cells. The nuclear envelope and very occasionally the nucleus in the glandular epithelial cells showed staining with some sparse staining in the stroma (**Figure 6-5F**).

6.3.3.3 Histomorphometric Quantification of Bcl-2 Proteins

Figure 6-6A shows the data from the histomorphometric analysis of glands and stroma (G+S) combined. The data clearly show that Bcl-2 expression is lower in the EC tissue and that it reaches statistical significance in type 2 EC when compared to the levels observed in atrophic endometria. Furthermore, when the glands alone were examined, the lower Bcl-2 levels observed in the tissue were due to the lower levels in Type 2 EC glands (**Figure 6-6B**) and not due to a lower level in Type 2 stroma (**Figure 6-6C**) because the Bcl-2 levels in the type 2 EC stromal compartment were not significantly affected by disease and in carcinosarcoma Bcl-2 staining was undetectable in any of the samples.

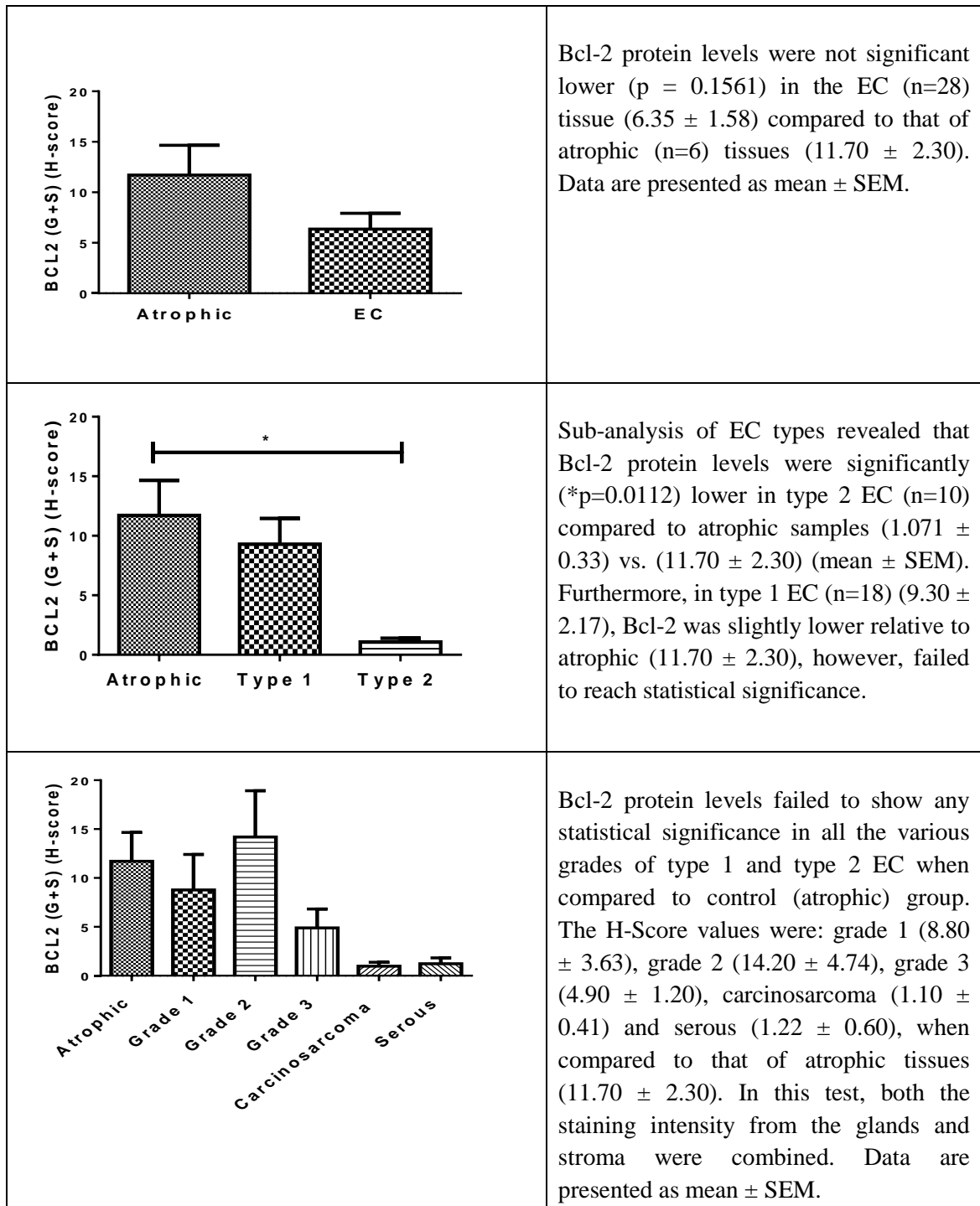


Figure 6-6A: Histomorphometric analysis of Bcl-2 (G + S) (H-score) proteins immunoreactivity.

P values were obtained using Student's t-test and one way ANOVA with Dunnett's ad hoc post-test analysis of both components of the tissues, i.e. glands and stoma separately. Data are presented as mean \pm SEM. Collectively, Bcl-2 protein levels are reduced in EC (G+S) when compared to the control (atrophic) group.

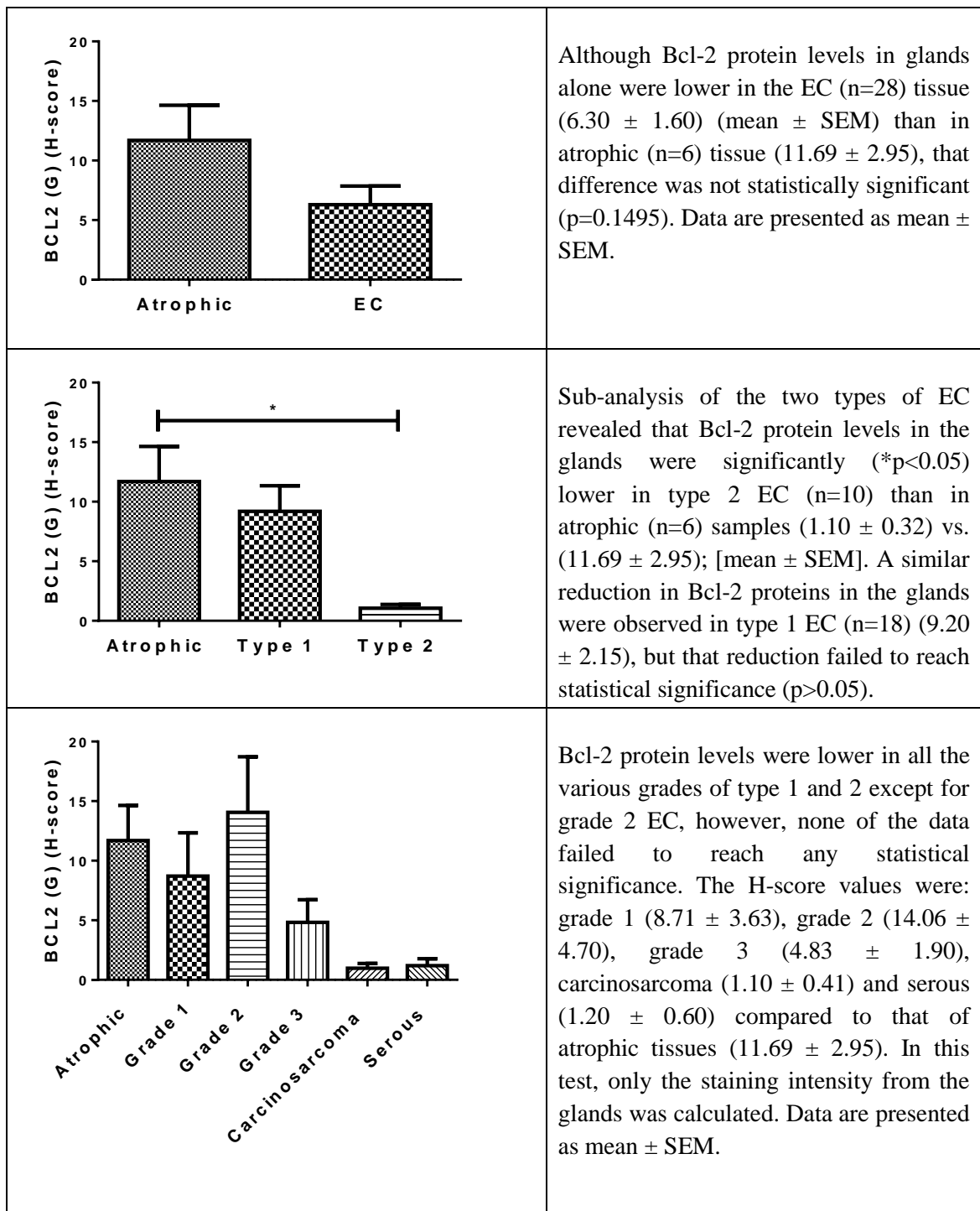


Figure 6-6B: Histomorphometric analysis of Bcl-2 (G) (H-score) immunoreactivity.

P values were obtained using Student's t-test and one way ANOVA with Dunnett's ad hoc post-test analysis of the gland components of the tissues. Data are presented as mean \pm SEM. Collectively, Bcl-2 protein levels are reduced in EC (G) when compared to the control (atrophic) group.

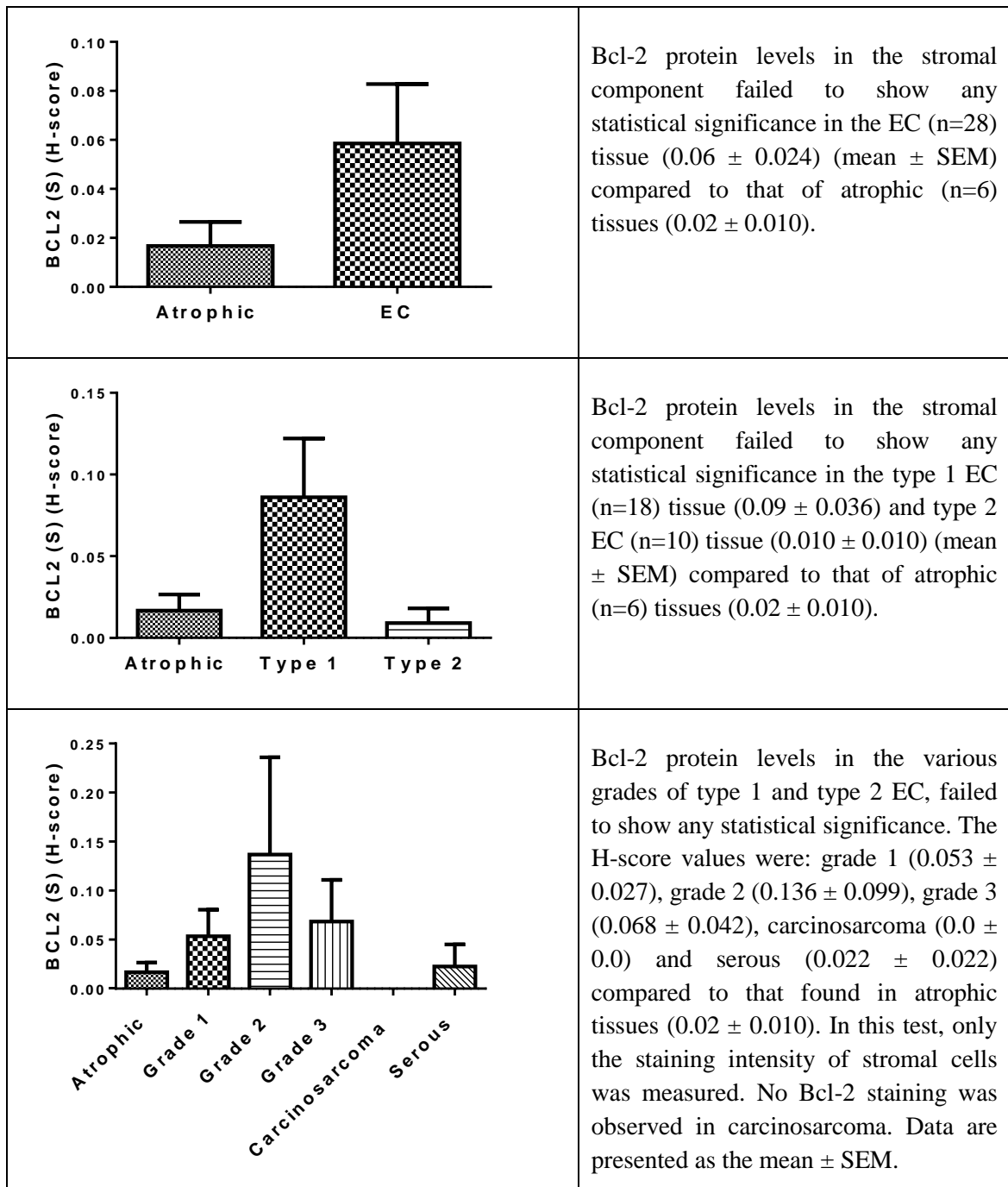


Figure 6-6C: Histomorphometric analysis of Bcl-2 (S) (H-score) proteins immunoreactivity.

P values were obtained using Student's t-test and one way ANOVA with Dunnett's ad hoc post-test analysis of the stromal component. Data presented as mean \pm SEM. Collectively, Bcl-2 protein levels are reduced in EC (S) in grades 1 and 3 and serous, while raised in grade 2 when compared to control (atrophic) group and absent from carcinosarcoma stroma.

6.3.4 Ki-67 Protein Expression

6.3.4.1 Optimisation of Immunohistochemical Methods for Ki-67

The optimum primary antibody dilution for Ki-67 has already been standardized for the endometrium and is 1:150. Antibody specificity was determined using equivalent concentrations of non-immune IgG (**Figure 6-7**). The lack of 3, 3'-diaminobenzidine (DAB) staining in the IgG controls indicates that the antibodies are specific for Ki-67.

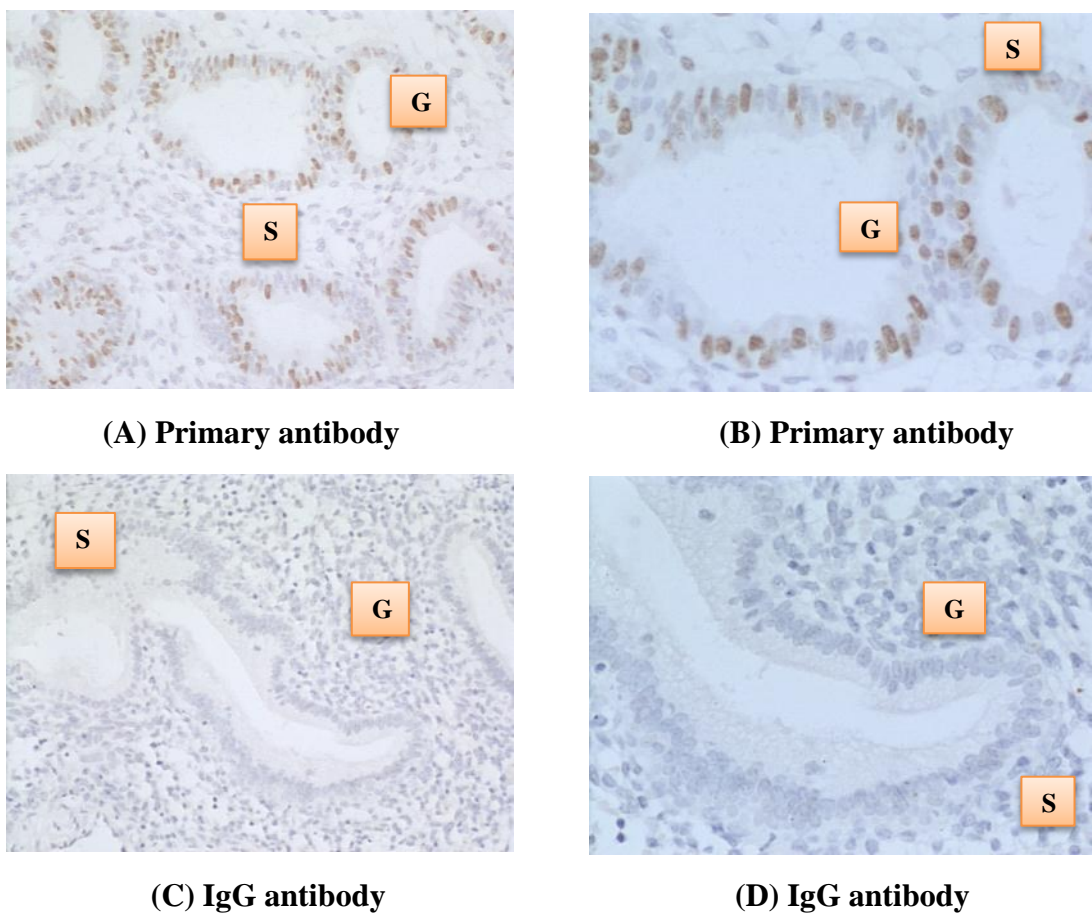


Figure 6-7: Negative control demonstrating the specificity of the primary antibody Ki-67.

Images (A) and (B) show positive staining of the primary antibody Ki-67, which is confined to the nucleus, with more cells in the glands being positive than cells in the stroma, whilst images (C) and (D) show no staining for the IgG controls. All the slides are from the proliferative phase of the menstrual cycle.

6.3.4.2 Identification and Locations of Ki-67 Proteins

Figure 6-8 illustrates the staining pattern of Ki-67 in atrophic and EC samples. Following the optimisation of Ki-67 antibody, all the studies were undertaken as a single run to minimise variations.

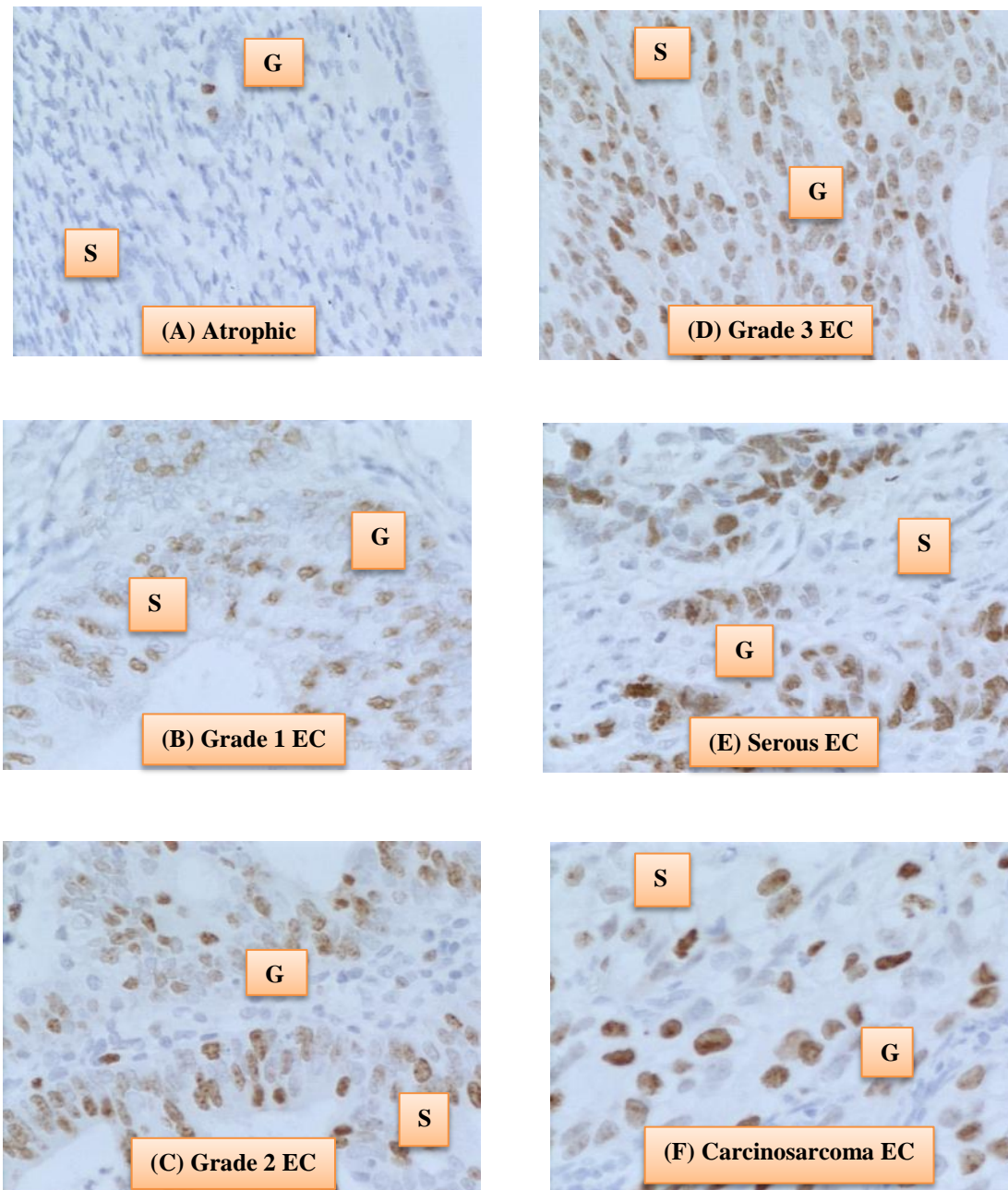


Figure 6-8: Localisation and expression of the Ki-67 protein (G = glands, S = stroma, EC = endometrial cancer).

In atrophic tissue, immunoreactive Ki-67 protein was expressed very minimally in the nuclei of the glandular epithelium. Occasionally, there was evidence of brown staining in nuclei of some stromal cells. The numbers of glands were markedly reduced in

atrophic endometrium when compared to cancer tissue. Furthermore, the lack of brown staining in atrophic endometrial tissues supports the inactive nature of this endometrium (**Figure 6-8A**). The Ki-67 staining intensity in grade 1 EC was higher compared to that observed in the atrophic endometrium. The staining involved the glands; more prevalent in the nucleus of the cell (**Figure 6-8B**). The Ki-67 staining intensity in grade 2 EC tissue was higher compared to that of the atrophic endometrium. This staining clearly involved both the glands and the stroma. In the glands, only the nucleus was stained (**Figure 6-8C**). The Ki-67 staining intensity in grade 3 EC was higher when compared to atrophic tissue. It clearly showed a high intensity of staining in the glands. The nucleus was strongly stained in the glands (**Figure 6-8D**). The Ki-67 staining intensity in serous carcinoma was of high intensity compared to atrophic endometrium. It involved the glands and very rarely cells within in the stroma. In the glands, staining was cytoplasmic and nuclear. The nuclear envelope and the nucleus showed staining both in the glands (**Figure 6-8E**). The Ki-67 staining intensity in carcinosarcoma was at a very high intensity compared to the atrophic endometrium and was present in both the glands and stroma. In the carcinosarcoma tissue the glandular structure was completely 'broken down' and the epithelial cells scattered throughout the tissue making it very difficult to differentiate the glands. Nevertheless, the staining was only nuclear (**Figure 6-8F**).

6.3.4.3 Quantification of Ki-67 Proteins

Figure 6-9A shows the data from the histomorphometric analysis of glands and stroma (G+S) combined. The data clearly shows that Ki-67 expression was higher in the EC tissue and it reached statistical significance in both types 1 and 2 ECs when compared to the levels observed in the atrophic endometrium. Furthermore, when the glands alone were examined, higher Ki-67 levels were noted in almost all the grades of ECs except grade 1 and carcinosarcoma (**Figure 6-9B**). In stroma alone, in generally, the levels were high in EC but failed to show any statistical significance (**Figure 6-9C**) but when looking into the subtypes, Ki-67 levels were statistically significantly higher in type 2 EC when compared to atrophic endometrium. In the stromal compartment, Ki-67 expression was only statistically significantly higher in the carcinosarcoma and serous tissues.

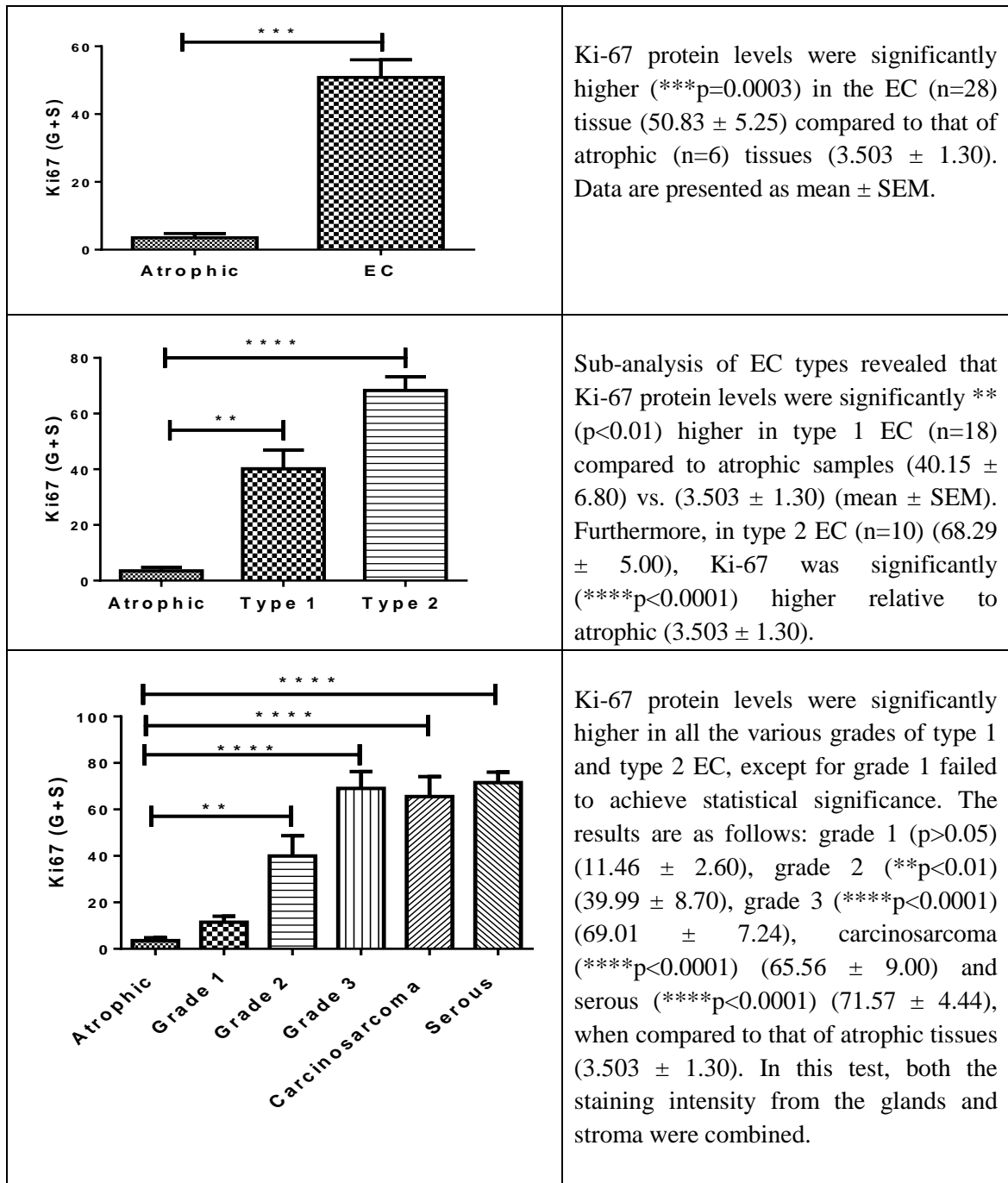


Figure 6-9A: Histomorphometric analysis of Ki-67 (G + S) (H-score) proteins immunoreactivity.

P values were obtained using Student's t-test and one way ANOVA with Dunnett's ad hoc post-test analysis of both the glands and stoma combined. Data are presented as mean \pm SEM. Collectively, Ki-67 protein levels are increased in EC (G+S) when compared to the control (atrophic) group.

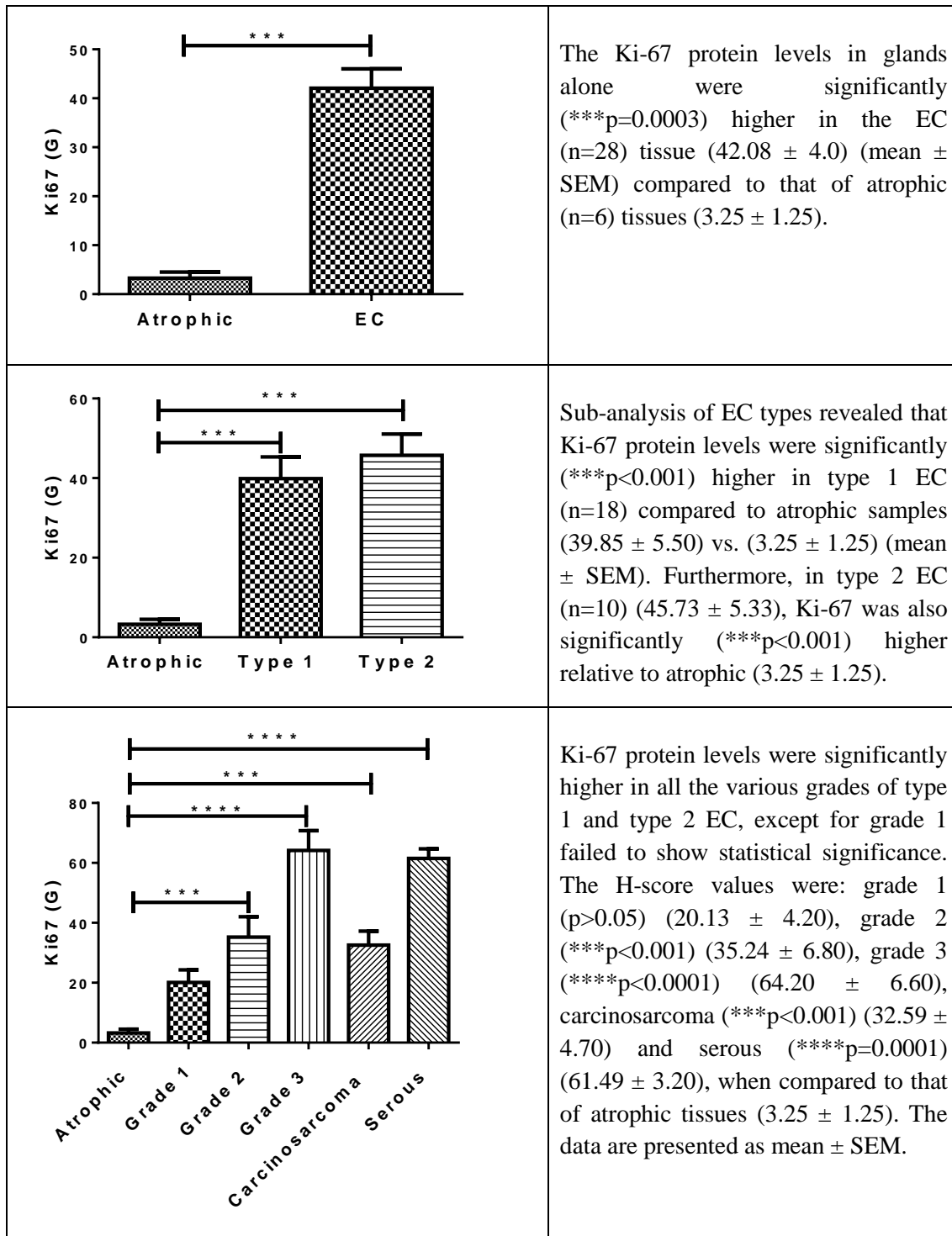


Figure 6-9B: Histomorphometric analysis of Ki-67 (G) (H-score) immunoreactivity.

P values were obtained using Student's t-test and one way ANOVA with Dunnett's ad hoc post-test analysis of the gland components of the tissues. Data are presented as mean ± SEM. Collectively, Ki-67 protein levels are increased in EC (G) when compared to the control (atrophic) group.

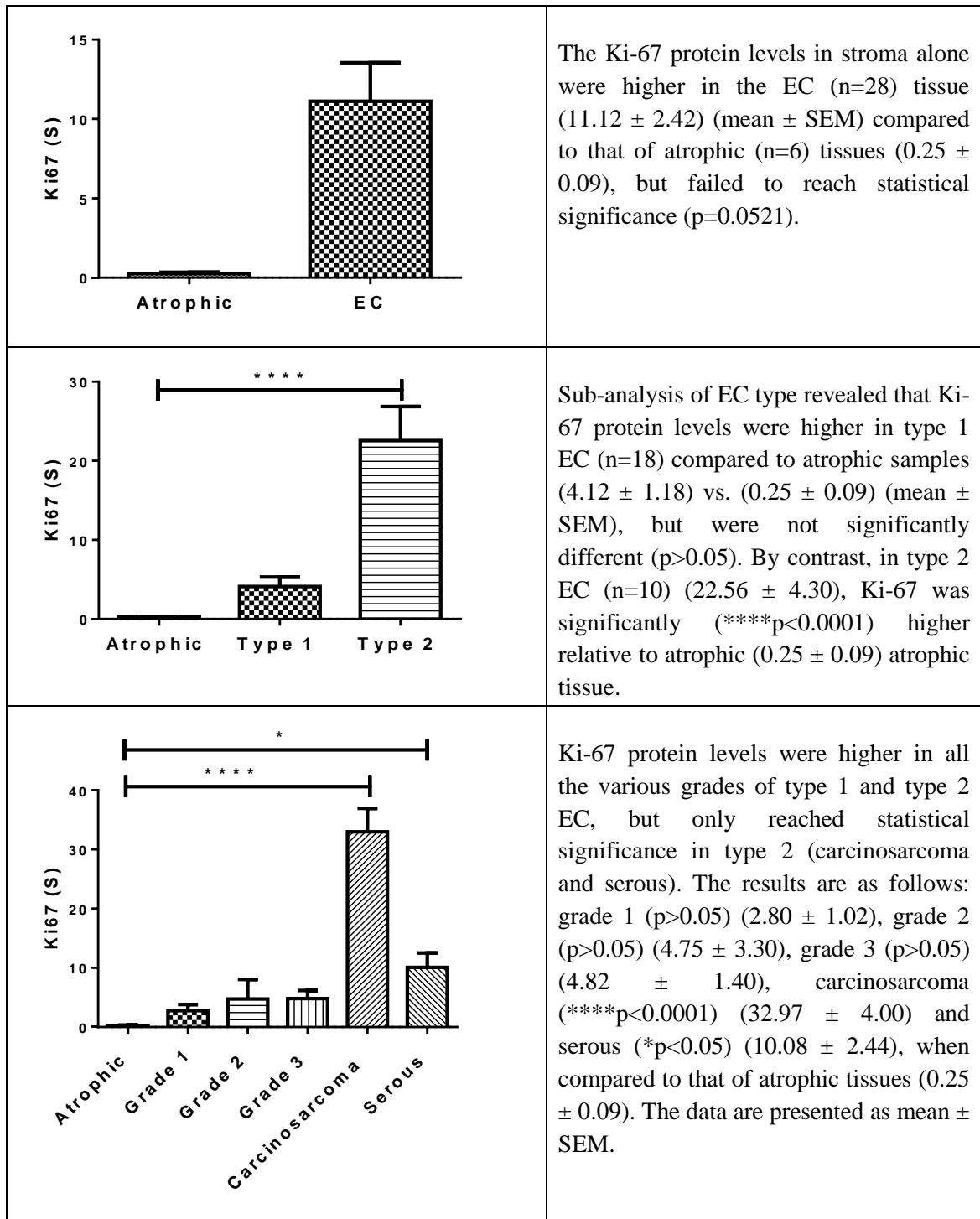


Figure 6-9C: Histo-morphometric analysis of Ki-67 (S) (H-score) proteins immunoreactivity.

P values were obtained using Student's t-test and one way ANOVA with Dunnett's ad hoc post-test analysis of the stromal component. Data presented as mean \pm SEM. Collectively, Ki-67 protein levels are increased in EC (S) in all types of EC, but only significantly higher in the type 2 EC when compared to control (atrophic) group.

6.3.5 The BAX/Bcl-2 Ratio

The BAX/Bcl-2 ratio is a good indicator of the quality of the apoptotic 'rheostat' within a tissue. Therefore, the BAX/Bcl-2 ratio was calculated for EC and atrophic endometrium. **Figure 6-10A** shows these BAX/Bcl-2 ratios from the analysis of glands and stroma (G+S) combined. The data clearly show that the BAX/Bcl-2 ratio was higher in EC tissue and reached statistical significance and furthermore when the subtypes were analysed the BAX/Bcl-2 ratio was high and reached statistical significance in type 2 EC but failed to show any statistical significance in type 1 EC when compared to the ratio from atrophic endometrium. While looking at various grades, the BAX/Bcl-2 ratio was statistically significantly higher in carcinosarcoma and serous tissues. Interestingly, when the BAX/Bcl-2 ratio was analysed for the glands alone, it was similar to the combined ratios (**Figure 6-10B**). When the BAX/Bcl-2 ratio was analysed for the stromal compartment only, it failed to show any statistically significant difference between types and grades of EC (**Figure 6-10C**).

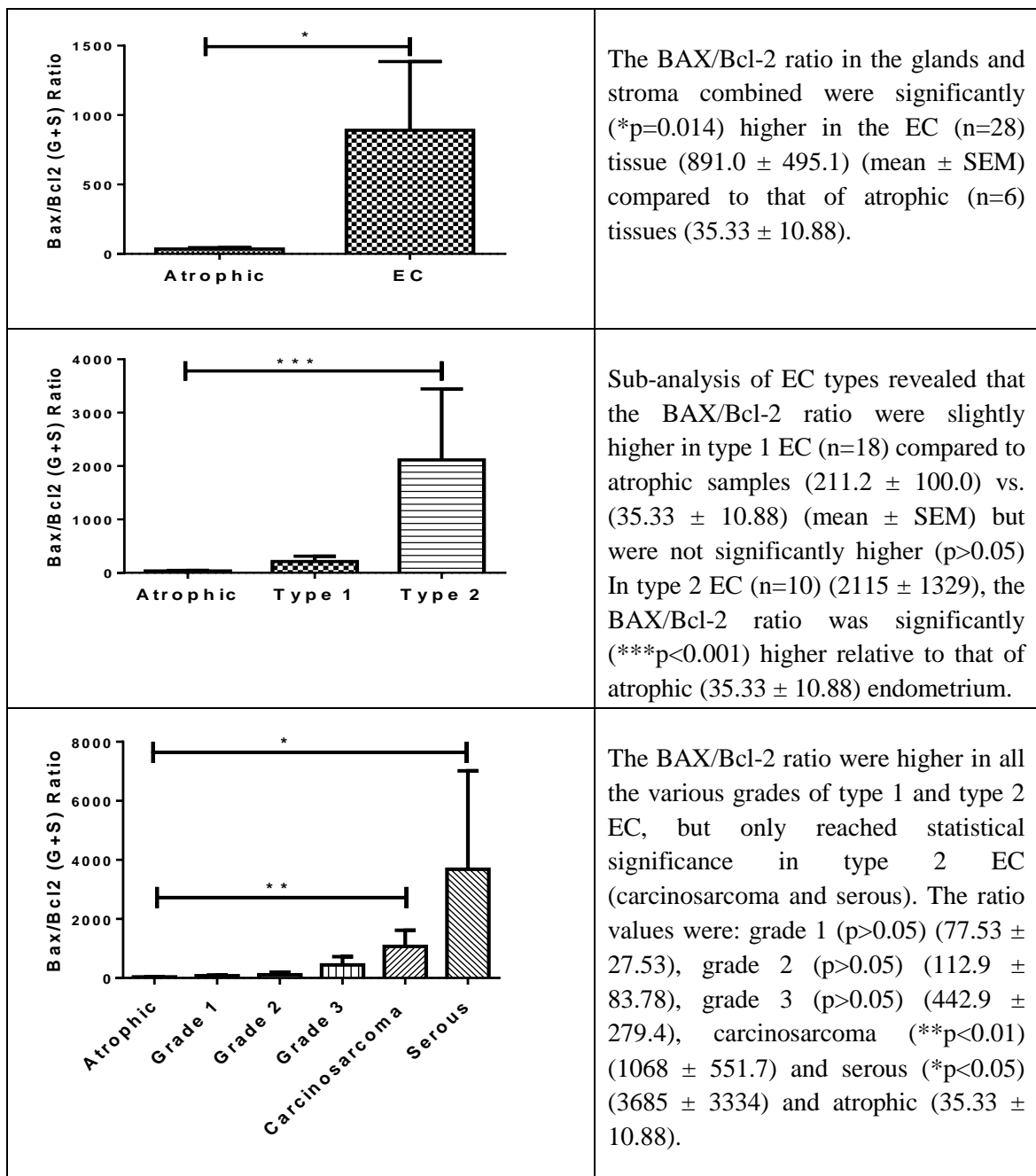


Figure 6-10A: BAX/Bcl-2 ratio analysis of (G+S).

P values were obtained using Mann Whitney U test and Kruskal-Wallis test one way ANOVA with Dunn's ad hoc post-test analysis of the glands and stromal components combined. Data are presented as mean \pm SEM. Collectively; BAX/Bcl-2 ratio were increased in all EC (G+S) types but only reached statistical significance in type 2 EC endometria when compared to that of the control (atrophic) group.

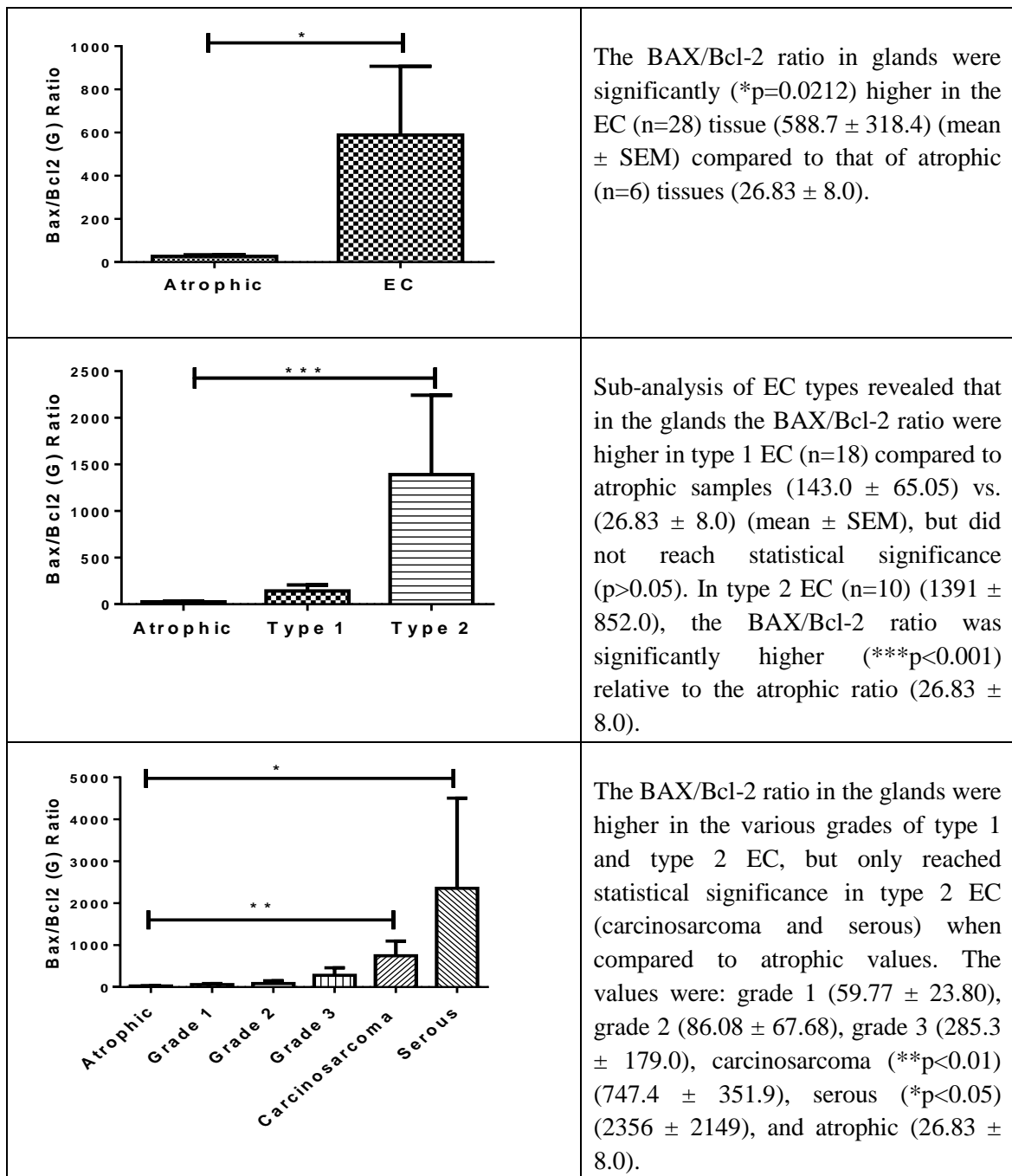


Figure 6-10B: BAX/Bcl-2 ratio analysis in glands only (G).

P values were obtained using Mann Whitney U test and Kruskal-Wallis test one way ANOVA with Dunn's ad hoc post-test analysis of the glandular epithelial cell component. Data are presented as mean \pm SEM. Collectively; the BAX/Bcl-2 ratio in the glands are increased in all EC types, but only reached statistical significance in type 2 EC endometria when compared to that of the control (atrophic) group.

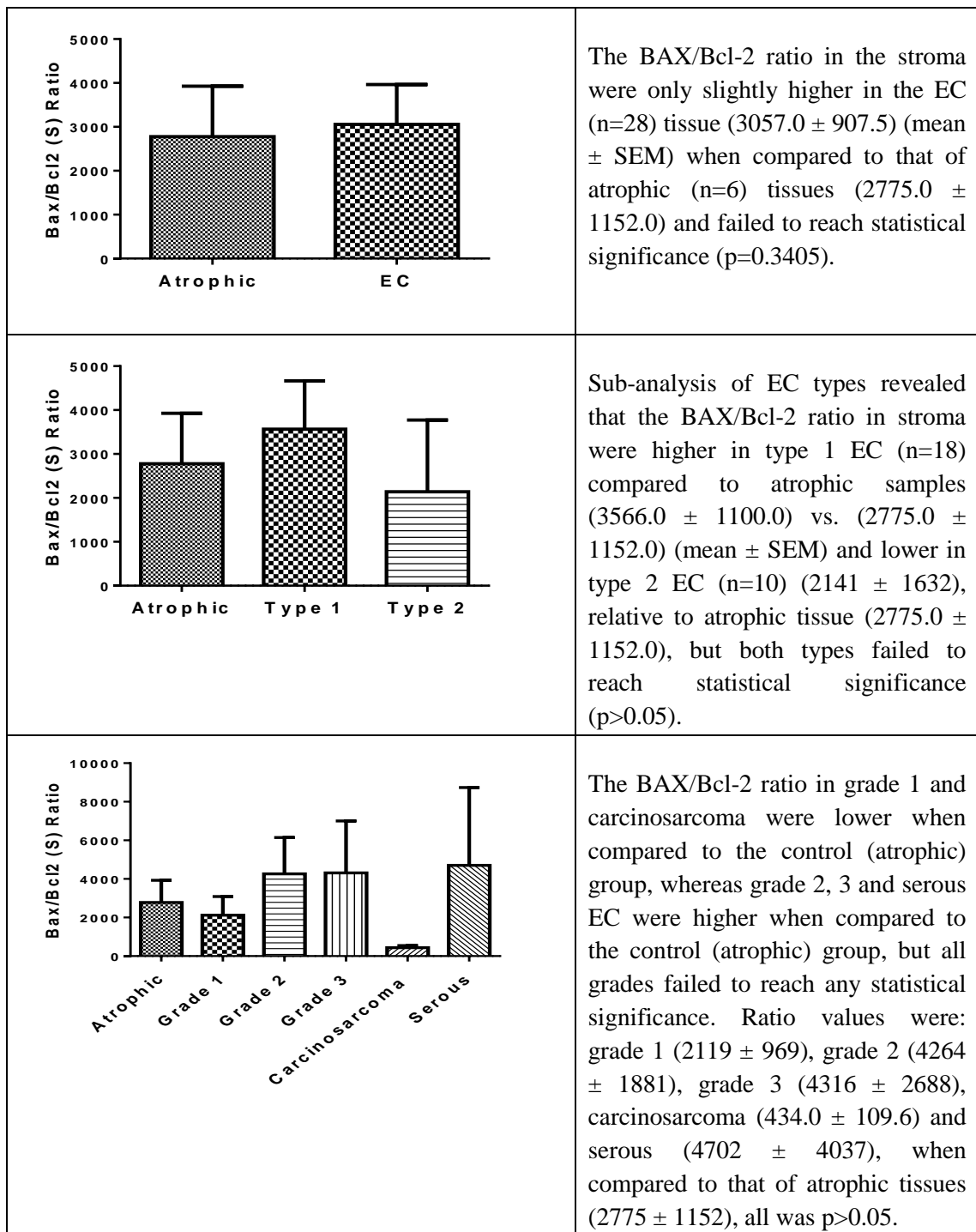


Figure 6-10C: BAX/Bcl-2 ratio analysis in the stromal compartment alone (S).

P values were obtained using Mann Whitney U test and Kruskal-Wallis test one way ANOVA with Dunn's ad hoc post-test analysis of the stromal (S) compartment. Data are presented as mean \pm SEM. The BAX/Bcl-2 ratio show no clear variation and were not statistically significant when compared to ratio of the control (atrophic) group.

6.3.6 Relationship Between Proliferation and Apoptosis Markers

This section examines the possible relationship between the proliferation and apoptotic markers in the tissue samples.

6.3.6.1 Ki-67 and BAX

Spearman's statistical analysis was used to evaluate the relationship between the cellular proliferation markers (Ki-67) and the cellular apoptotic promoter marker (BAX). **Figure 6-13**, show that there was a strong relationship between the Ki-67 and BAX tissue levels, supporting previous findings of high levels of abnormal proliferation in EC.

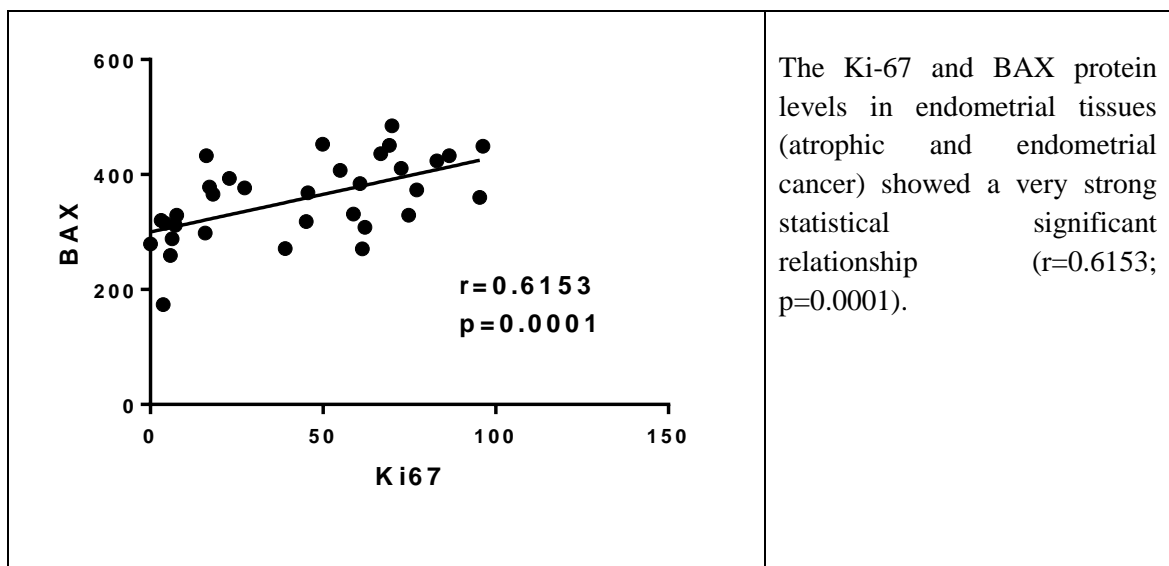


Figure 6-11: Correlation between Ki-67 and BAX tissue protein levels.

The indicated r and p-values were obtained using Spearman's correlation analysis.

6.3.6.2 Ki-67 and Bcl-2

Figure 6-14 shows an inverse relationship between Ki-67 and Bcl-2 protein levels.

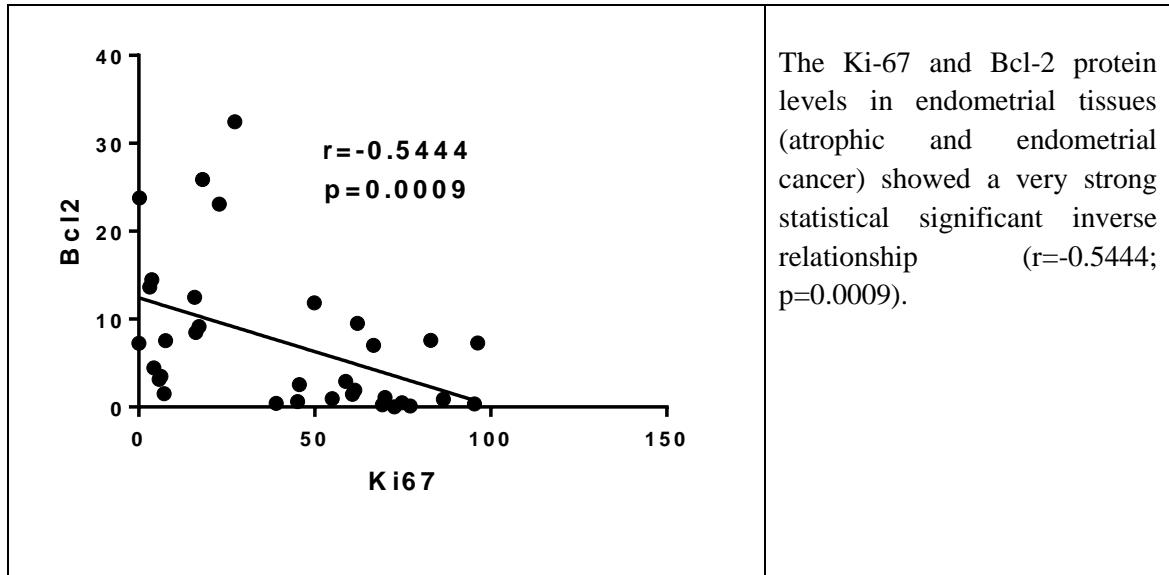


Figure 6-12: Correlation between Ki-67 and Bcl-2 tissue protein levels.

The indicated r and p -values were obtained using Spearman's correlation analysis.

6.3.6.3 Ki-67 and BAX/Bcl-2 Ratio

Figure 6-15 shows a strong relationship between the Ki-67 and BAX/Bcl-2 protein ratio levels in the tissues.

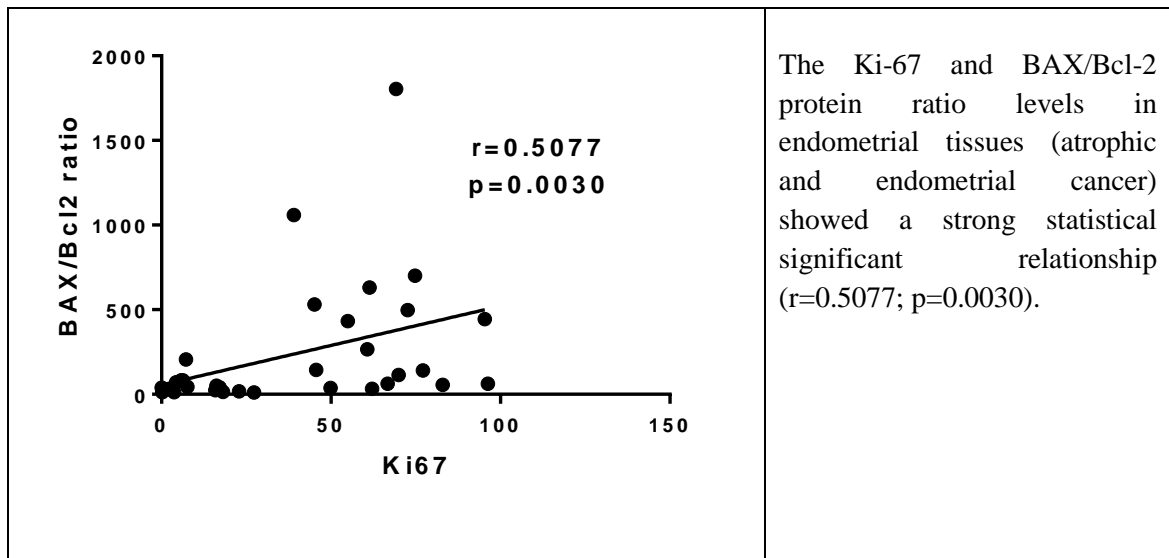


Figure 6-13: Correlation between Ki-67 and BAX/Bcl-2 protein ratio tissue levels.

The indicated r and p -values were obtained using Spearman's correlation analysis.

6.3.7 Relationship Between BAX/Bcl-2 Ratio or Ki-67 Expression with Components of the ECS

After establishing the presence of the proteins involved in cellular apoptosis (BAX, an apoptosis-promoting factor), (Bcl-2, an apoptosis-suppressing factor) and their ratios, and the expression of a proliferation marker (Ki-67), it was important to examine whether these parameters had any relationship with the expression of components of the ECS, including the tissue levels of the endocannabinoid ligands. The tissue levels of the receptors and ECS metabolising enzymes and the H-score values obtained from the IHC studies were presented in Chapters 3 and 4.

Initially, the endocannabinoid ligands were investigated to establish whether they have any relationship with the BAX/Bcl-2 ratio. Spearman correlation analysis was used to determine this. There were no relationships between the BAX/Bcl-2 ratio and AEA, OEA and PEA at tissue level (**Figure 6-16**), or between BAX/Bcl-2 ratio and the classical cannabinoid receptors CB1 and CB2 (**Figure 6-17**). The next step was to examine the relationship between BAX/Bcl-2 ratio and the non-classical cannabinoid receptors GPR55 and TRPV1. **Figure 6-18**, shows strong relationships between BAX/Bcl-2 ratio and these receptors. The relationship between the metabolising enzymes of the ECS and BAX/Bcl-2 ratio was next examined and there was a strong relationship between BAX/Bcl-2 ratio and both FAAH and NAPE-PLD (**Figure 6-19**).

In addition, the endocannabinoid ligands were investigated to establish whether they have any relationship with Ki-67. Similar to the apoptotic markers, AEA, OEA and PEA failed to show any significant relationship with the cellular proliferation marker, Ki-67 (**Figure 6-20**). The relationship between Ki-67 and the classical cannabinoid receptors is shown in **Figure 6-21**. There was no significant relationship exists between Ki-67 and CB1 but interestingly there was a positive significant relationship between Ki-67 and CB2 ($r=-0.6141$; $p=0.0001$). Equally, there was a positive correlation between Ki-67 and both GPR55 and TRPV1 (**Figure 6-22**). The metabolising enzymes of the ECS, FAAH and NAPE-PLD, had a strong relationship with Ki-67 ($r=-0.8038$; $p<0.0001$ and $r=0.7928$; $p=0.00001$, respectively) (**Figure 6-23**).

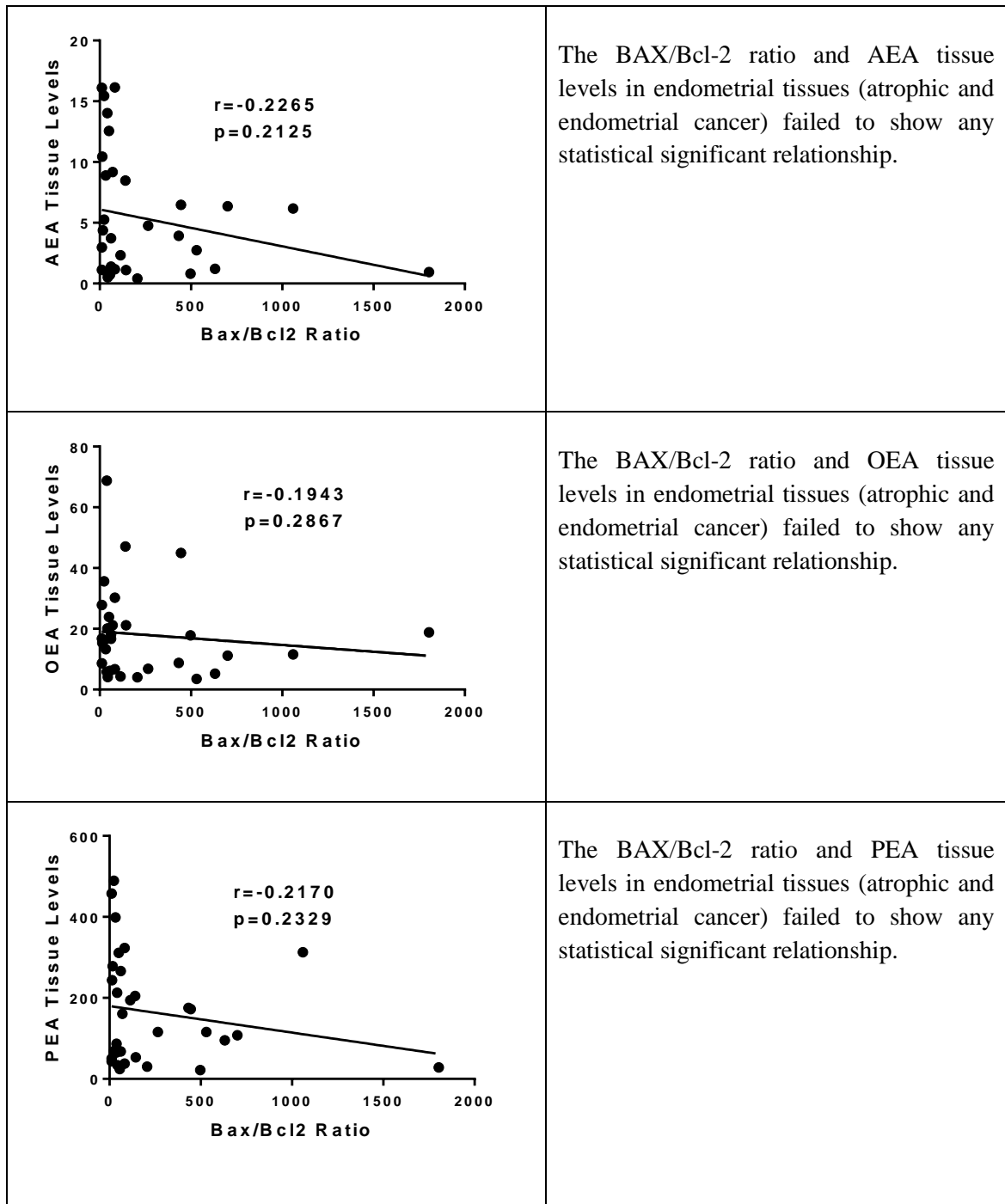


Figure 6-14: Analysis of the relationship between BAX/Bcl-2 ratio and the endocannabinoid ligands.

The indicated r and p values were obtained using Spearman's correlation analysis.

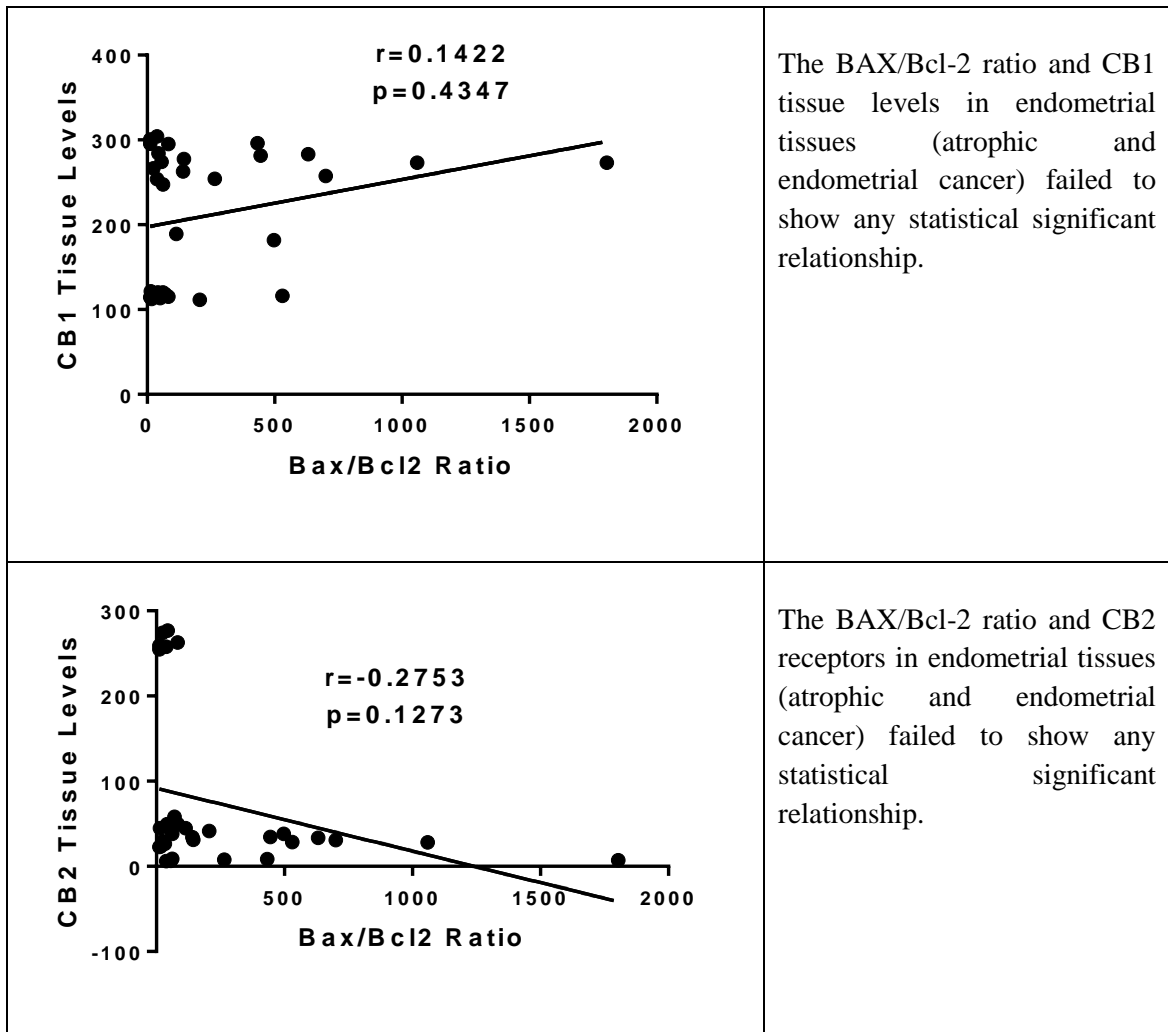


Figure 6-15: Analysis of the relationship between BAX/Bcl-2 ratio and the classical cannabinoid receptors CB1 and CB2.

The indicated r and p values were obtained using Spearman's correlation analysis.

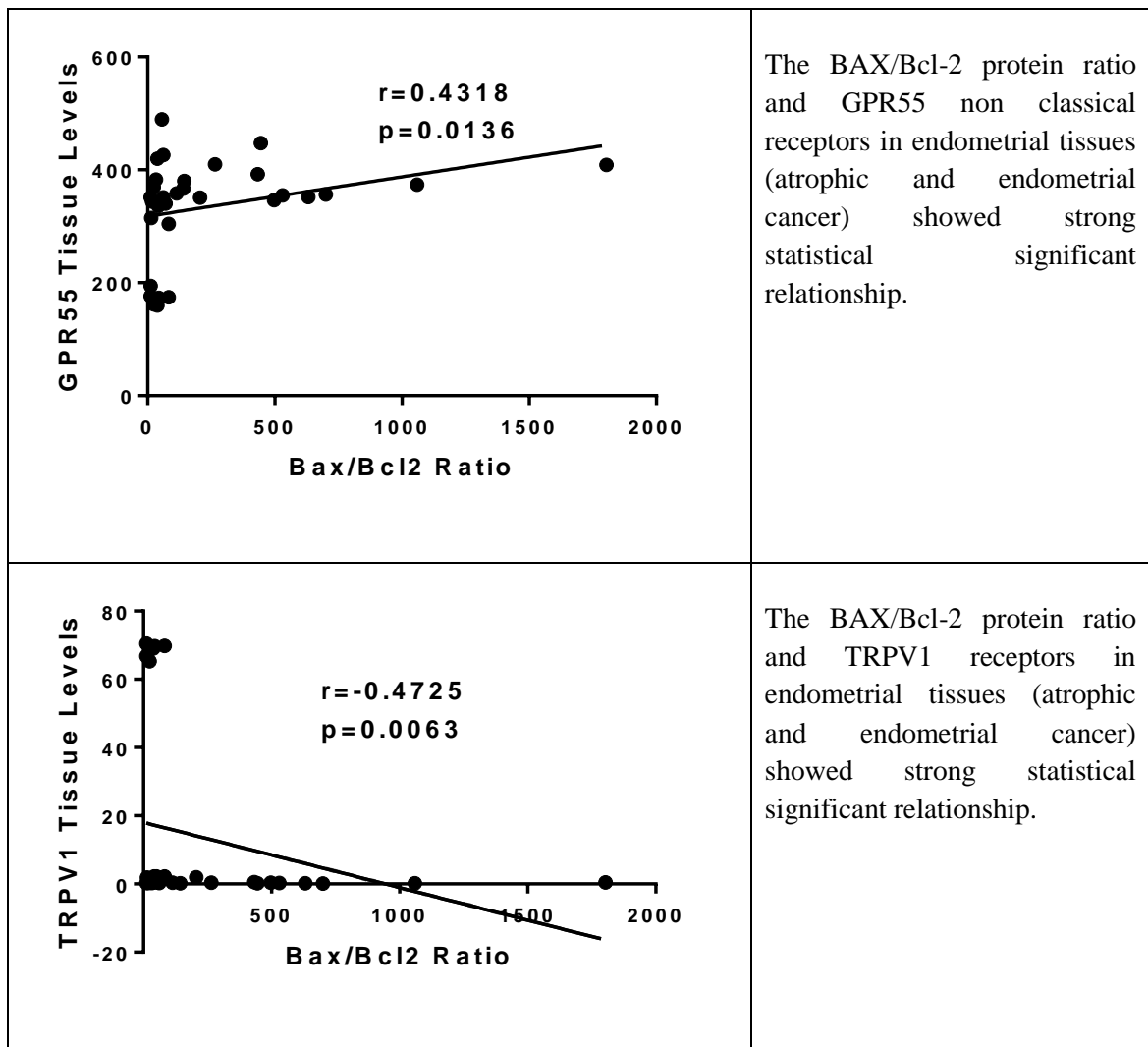


Figure 6-16: Analysis of the relationship between BAX/Bcl-2 ratio and the non-classical receptors, GPR55 and TRPV1.

The indicated r and p values were obtained using Spearman's correlation analysis.

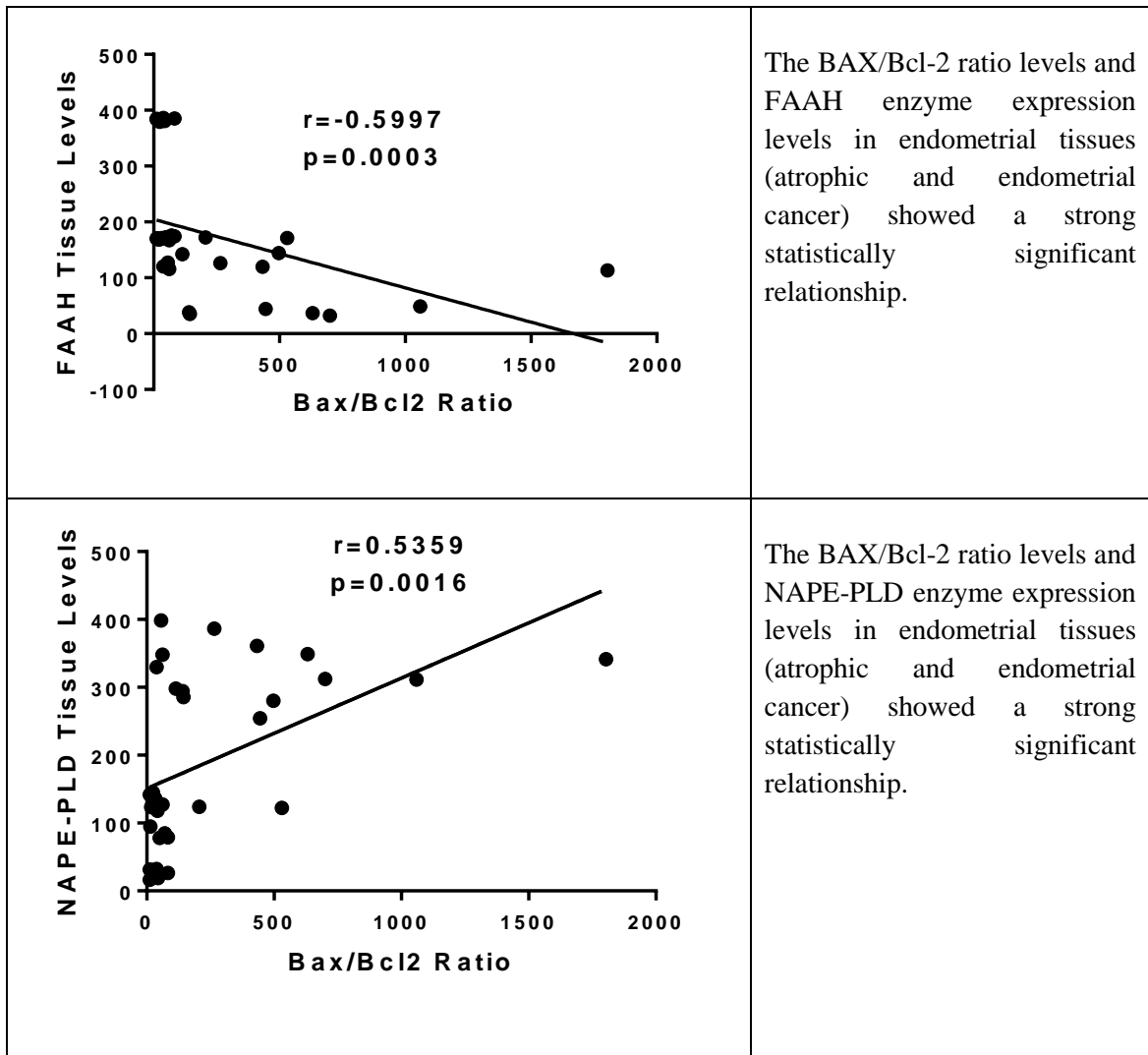


Figure 6-17: Analysis of the relationship between BAX/Bcl-2 ratio and the metabolising enzymes FAAH and NAPE-PLD.

The indicated r and p values were obtained using Spearman's correlation analysis.

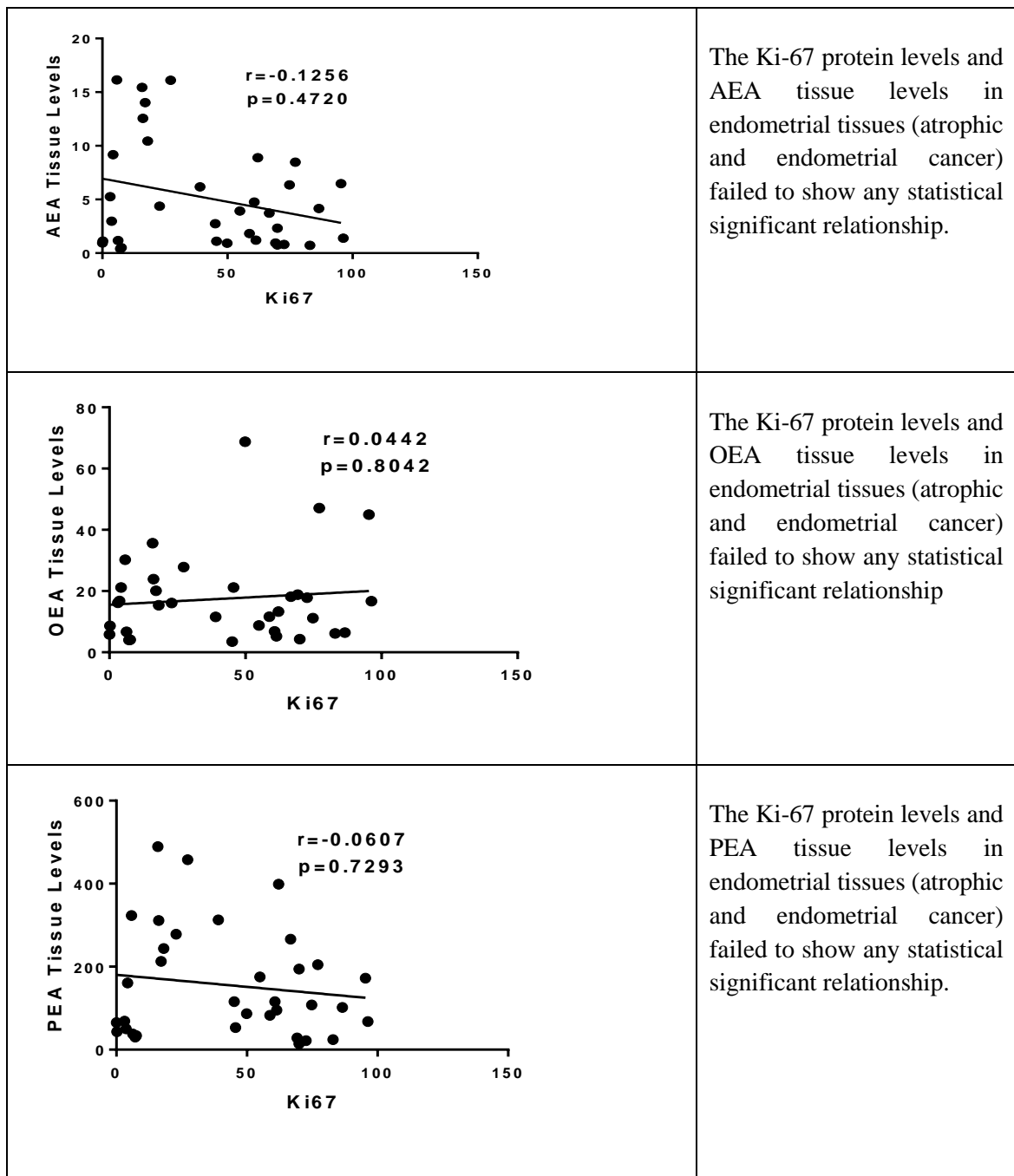


Figure 6-18: Analysis of the relationship between Ki-67 and the endocannabinoid ligands.

The indicated r and p values were obtained using Spearman's correlation analysis.

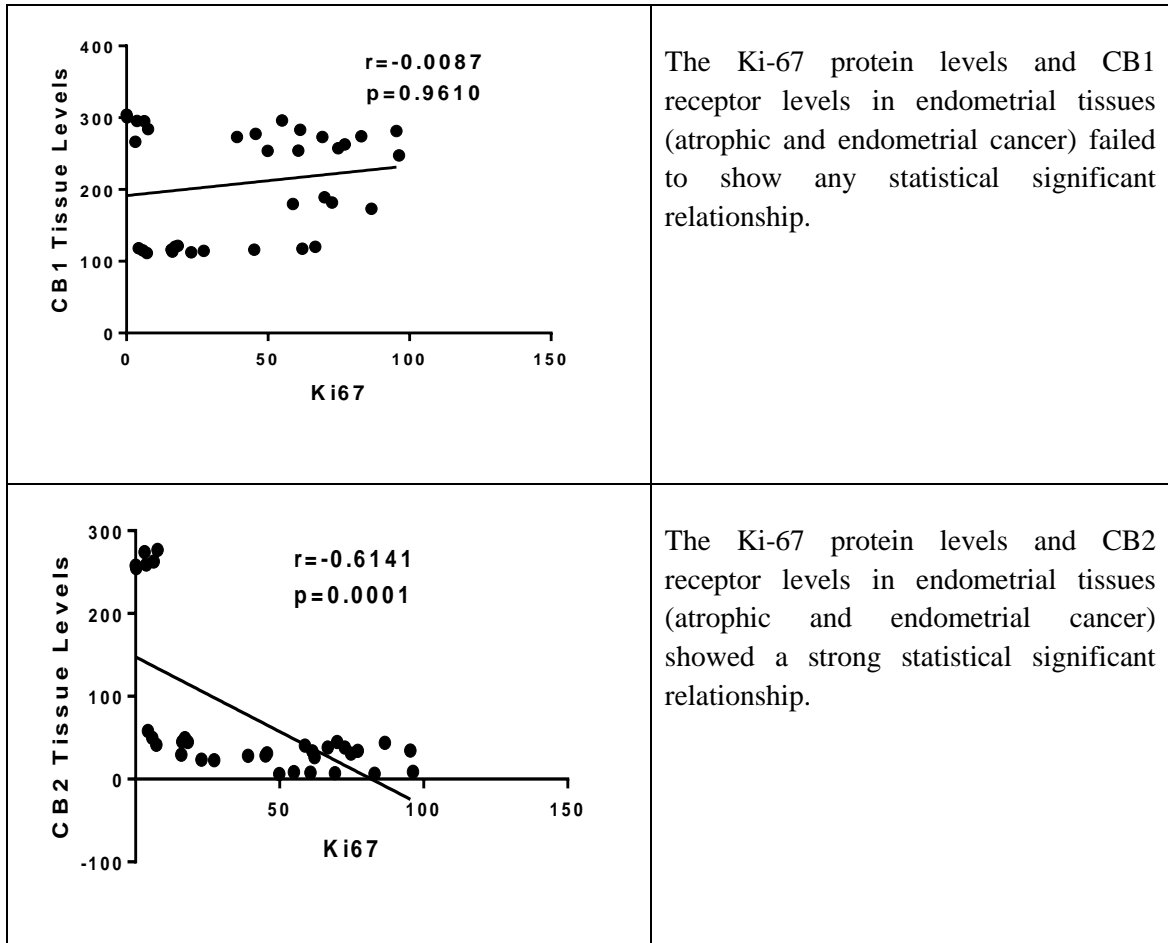


Figure 6-19: Analysis of the relationship between Ki-67 and the classical cannabinoid receptors CB1 and CB2.

The indicated r and p values were obtained using Spearman's correlation analysis.

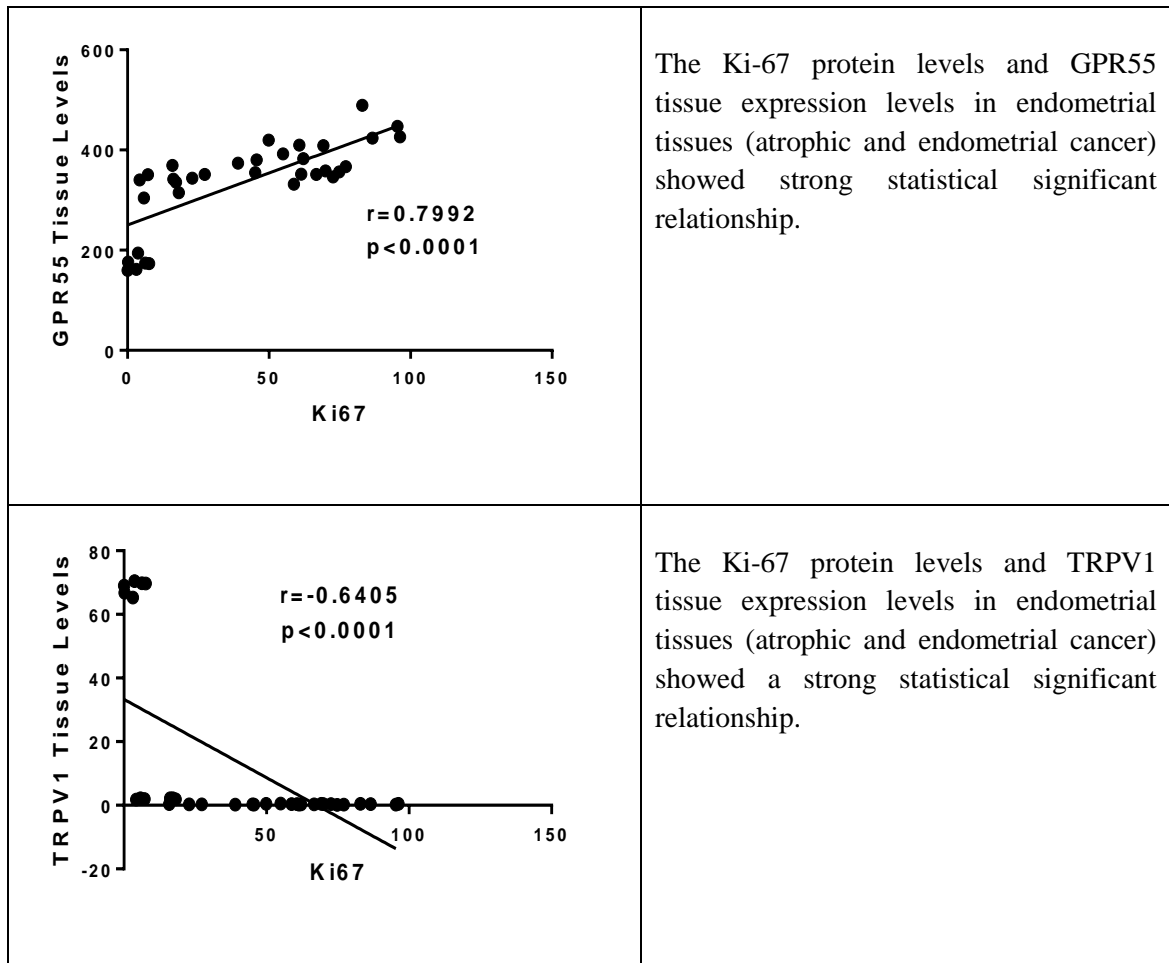


Figure 6-20: Analysis of the relationship between Ki-67 and the non-classical receptors GPR55 and TRPV1.

The indicated r and p values were obtained using Spearman's correlation analysis.

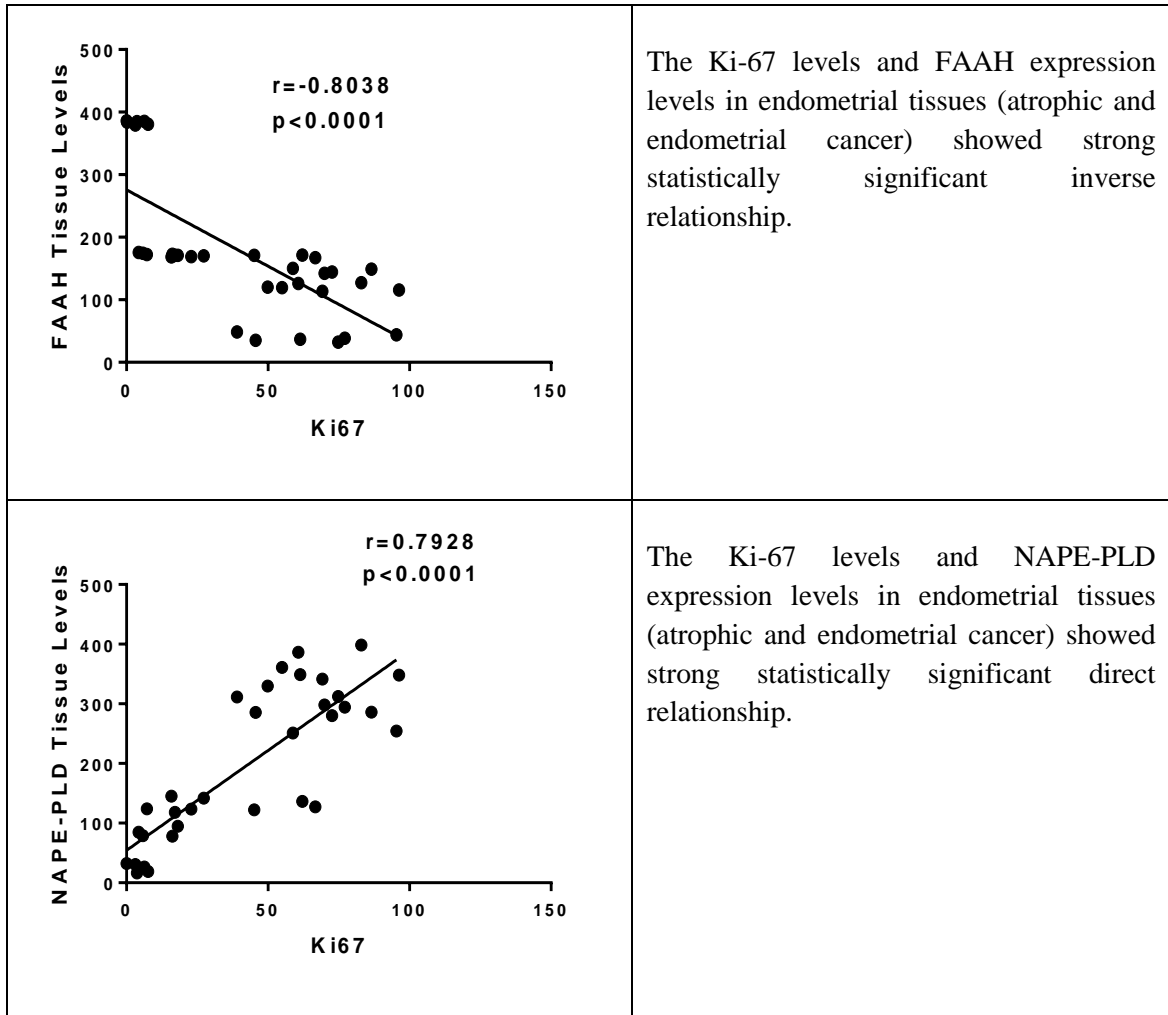


Figure 6-21: Analysis of the relationship between BAX/Bcl-2 ratio and the metabolising enzymes FAAH and NAPE-PLD.

The indicated r and p values were obtained using Spearman's correlation analysis.

6.4 Discussion

In this study, cellular apoptosis (BAX, Bcl-2 and the BAX/Bcl-2 ratio) and cellular proliferation (Ki-67) were examined in endometrial carcinoma and related to the expression of the ECS in these tissues. This had not been previously studied. The study showed a high BAX protein expression and reduced Bcl-2 levels in EC when compared to atrophic endometrium. The BAX protein levels were higher in both types of EC (1 and 2) with more immunohistochemical staining in the glands compared to the stroma. These higher expressions were further supported by a higher H-score in the all the grades of EC. These findings suggest that apoptosis may be potentially active in EC tissue because BAX is a pro-apoptotic marker. In addition, Bcl-2 expression was weak in EC tissue when compared to atrophic endometrium. The Bcl-2 protein functionally counteracts the process of apoptosis (Reed 1994), by binding to BAX protein. Finally, the cellular proliferation marker Ki-67 was strongly expressed in all types of EC within both the glands and the stroma when assessed by immunohistochemistry and subsequent H-score.

Although there are many studies detailing the expression of Bcl-2 (Henderson et al. 1996, Saegusa et al. 1996), how it plays a role in the carcinogenesis of EC, especially in the various grades, remains unclear. For example, Kokawa et al. (Kokawa et al. 2001) showed that BAX expression was increased in EC whilst Bcl-2 was lower when compared to their postmenopausal endometrium (which is similar to the data from the studies presented here), whereas Sakuragi et al (Sakuragi et al. 2002) documented decreased BAX expression leading to an increased Bcl-2/BAX ratio (which is the opposite to the data presented by Kokawa et al., and presented here). The reason for this discrepancy is unclear, but may either be due to a difference in materials (primary antibodies or primer sequences) or a difference in the parts of the BAX molecule being detected in the different studies. For example, it is now known that specific mutations in the BAX gene occur in both type 1 and type 2 EC, with codon 58 being the preferred target of BAX gene mutations in EC (Burks et al. 1994, Sakuragi et al. 2002). The BAX gene frameshift mutation appears to cause high levels of BAX expression in EC (Catusus et al. 1998) supporting the observations made here. These authors suggested that the gene mutations result in a lack of apoptosis occurring in a specific population of cells in the different grades of EC and that highly deranged BAX expression might

cause histological differentiation in EC types. This is supported by the data presented here, with high BAX and low Bcl-2 expression in EC compared to atrophic endometrium. A similar study also showed the same effect (Kokawa et al. 2001). Therefore, it is highly likely that an imbalance in apoptotic homeostasis leads to the high BAX/Bcl-2 ratio, in which the mutated BAX protein cannot function as a pro-apoptotic protein, resulting in dysregulation of the cellular “rheostat” of apoptosis that allows cell survival and proliferation. It has been suggested that the sustained high BAX and low Bcl-2 protein concentrations (and a consequential high BAX/Bcl-2 ratio) may make such cells more sensitive to a given apoptotic stimuli and cause marked apoptosis imbalance leading to endometrial carcinogenesis (Buttayan et al. 1999, Perlman et al. 1999, Kokawa et al. 2001, Vaskivuo et al. 2002). Because the above phenomenon was not observed here, then the antibody being used probably detects both wild-type and mutated BAX proteins, explaining the very high levels of BAX expression, but low apoptosis in the EC tissue. Thus, dysfunction of the BAX/Bcl-2 apoptosis signalling pathway has been suggested to play a role in tumorigenesis and tumour progression.

A hypothetical relationship of these apoptosis-related genes in endometrial cells is shown in **Figure 6.24**. Apoptotic stimuli cause DNA damage and activate the p53 tumour suppressor gene, which then decreases Bcl-2 expression (Miyashita et al. 1994) and increases BAX expression (Miyashita et al. 1994) causing the BAX/Bcl-2 ratio increase observed in this study. It is known that unopposed estrogen stimulation is associated with or acts as a stimulatory factor in the development of EC. Reduced Bcl-2 expression synergistically enhances estradiol-induced apoptosis in estrogen receptor positive breast cancers (Song et al. 2005), whilst Bcl-2 is also regulated by both ER and PR receptors in breast cancer tissue (Park et al. 2002). In the human endometrium, Bcl-2 expression is regulated by estrogen in the opposite way to that of breast cancer; Bcl-2 is increased in the estrogen-dominant proliferative phase and reduced in the progesterone-dominant secretory phase (Otsuki et al. 1994). Therefore, unopposed estrogen may induce an increase in Bcl-2 expression leading to a high BAX/Bcl-2 ratio, which may disrupt the normal apoptotic process and hence promote cell proliferation. Such effects support the reduced Bcl-2 expression and BAX/Bcl-2 ratio in EC shown in this chapter and also documented by others (Chan et al. 1995, Niemann et al. 1996), suggesting that sustained low Bcl-2 expression and a high BAX/Bcl-2 ratio in

endometrial glands may play a pivotal role in the genesis of estrogen-dependent (endometrioid) endometrial cancers.

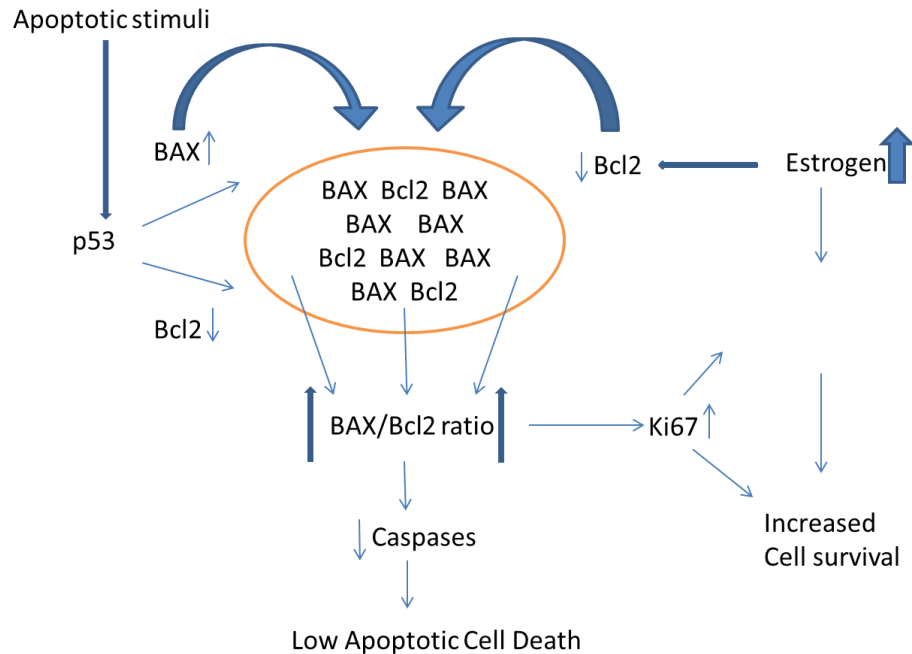


Figure 6-22: A hypothetical pathway of endometrial cell apoptosis and cellular proliferation.

Although the above provides an attractive mechanism for the pathogenesis of estrogen-dependent EC, other studies suggest a non-estrogen receptor mediated mechanism in relation to BAX and Bcl-2 expression. It is known that BAX, Bcl-2 and Ki-67 are all regulated by estrogen (Zhang et al. 2012), but the lack of immunohistochemical evidence showing a relationship between BAX and Bcl-2 with ER expression (Kounelis et al. 2000), led to the suggestion of a non-receptor mediated mechanism. These data emphasise the paucity of evidence on the exact involvement of BAX, Bcl-2 and estrogen in EC, although, when there is an imbalance in the “rheostat” of apoptosis, the high BAX/Bcl-2 ratio and high Ki-67 may directly or indirectly cause EC (Risberg et al. 2002).

By contrast, Ki-67 a proliferation marker that is tightly regulated in the menstrual cycle (Konstantinos et al. 2013), was strongly expressed in the nuclei of all EC grades and higher in EC compared to the atrophic endometrium, where none was observed. This is

to be expected because an atrophic endometrium by definition is non-proliferating and by definition a cancer shows uncontrolled proliferation and Ki-67 is only produced in a cell that is traversing the cell cycle. What was an interesting finding was that Ki-67 expression appeared to be stronger and more significant with advancing EC type and tumour severity, i.e. more proliferation in the more advanced tumours. This was related to the high BAX expression as noted above.

The strong statistical associations between Ki-67 and BAX ($p=0.0001$), and Ki-67 and the BAX/Bcl-2 ratio ($p=0.0030$), with a strong inverse relationship between Ki-67 and Bcl-2 ($p=0.0099$) indicate that an imbalance between proliferation and apoptosis may be an additional important factor in the development of different endometrial grades of endometrial carcinoma, as suggested by Risberg et al. (Risberg et al. 2002).

To the best of my knowledge, no studies have evaluated the relationship between BAX, Bcl-2, the BAX/Bcl-2 ratio or Ki-67 and the endocannabinoid system in endometrial carcinoma. The data presented here showed that there were no statistically significant relationships between BAX, Bcl-2, the BAX/Bcl-2 ratio or Ki-67 with the tissue concentrations of NAEs, AEA, OEA and PEA. Furthermore, there appeared to be no association between BAX, Bcl-2, the BAX/Bcl-2 ratio or Ki-67 and the classical endocannabinoid receptors CB1 and no association between BAX, Bcl-2, the BAX/Bcl-2 ratio and, CB2, but there was a statistically significant relationship between Ki-67 and CB2, suggesting that the main stimulator of Ki-67 expression and hence endometrial epithelial cell proliferation could be *via* the CB2 receptor. Interestingly, there was a significant relationship between the BAX/Bcl-2 ratio and Ki-67 expression, the non-classical receptors GPR55 and TRPV1 and the metabolising enzymes of ECS (FAAH and NAPE-PLD).

Previous studies have documented that activation of either CB1 or CB2 receptors triggers the ceramide ERK signalling pathways to promote apoptosis (Kogan 2005, Sarfaraz et al. 2006, Sarfaraz et al. 2008). This may be a possible activated pathway in EC development, but will need to be examined in future studies.

In human neuroblastoma and C6 glioma cells AEA induces apoptosis through vanilloid receptor-mediated increases in intracellular calcium concentrations, which activates COX-2, releases cytochrome c and activates caspase 3 (Contassot et al. 2004). This mechanism may be active in EC, because a strong relationship between TRPV1 and

BAX was observed. On the other hand, capsazepine, a TRPV1 antagonist, increased BAX expression (Sung et al. 2012) and several authors have shown that capsaicin-treated cells have increased BAX coupled to decreased Bcl-2 (Hetz 2007). This decrease in Bcl-2 expression caused by capsaicin has been noted in other studies (Pacak et al. 2012, Krizanova et al. 2014), suggesting that TRPV1 activation is characterised by reduced Bcl-2 expression and it is that change that causes cellular apoptosis.

Several other studies documented pro-apoptotic effects of cannabinoids in different cells (Freimuth et al. 2010). In hepatocellular carcinoma-2 cells, CB1 receptor agonists induced apoptosis and that was accompanied by up regulation of the death signalling factor BAX and down regulation of the survival factors Bcl-2 (Giuliano et al. 2009). These observations support the results presented in this chapter.



Chapter 7

General Discussion and Future Directions

This thesis provides evidence that the major components of the endocannabinoid system, i.e. the ligands (AEA, OEA and PEA), the metabolising enzymes (NAPE-PLD and FAAH) for these ligands, the classical cannabinoid receptors (CB1 and CB2) and two of the non-classical cannabinoid receptors (GPR55 and TRPV1) that these ligands bind to, are all altered in women with endometrial carcinoma (EC). The key observation was that the ligands were all elevated in the EC tissue, but only AEA and PEA were elevated in plasma, probably due to a tumour specific entourage effect. Once it was established that all components of the endocannabinoid system are different in EC, it was important to determine what effect these alterations might have on endometrial cell growth and survival and so, an *in vitro* study was undertaken to investigate the effects of AEA, OEA, PEA and capsaicin on the growth and survival of Ishikawa cells (a endometrial cancer cell line). It showed that the highest dose of all compounds caused a reduction in cell number. This led to a re-examination of the endometrial biopsies to determine what effect the increased NAE concentrations might be having on cell number (i.e. were they decreasing cell proliferation or increasing apoptosis ?). These parameters were measured using markers of cellular proliferation (Ki-67) and apoptosis (BAX and Bcl-2) and the data indicated that reduced cell numbers in the culture experiment was probably due to an increase in apoptosis with an associated reduced anti-apoptosis. It would have been ideal to have investigated this further, but time and financial constraints prevented this. From the studies presented in this thesis, it is clear that there is a complex (and at times puzzling) interplay between the various components of the ECS in endometrial cells of patients with EC and that the ECS probably plays a vital role in the carcinogenesis of EC.

7.1 Discussion

Prior to the commencement of this project, very little was known about the expression or function of the ECS in endometrial cancer. What was known was that AEA, CB1, CB2, FAAH and NAPE-PLD are produced in and function in the normal human endometrium and were regulated by the sex steroid hormones, E2 and P4, and the gonadotrophins LH and FSH (El-Talatini et al. 2010). The lack of studies on the endocannabinoid system in EC was probably not because there was no relationship between the ECS and EC, but simply because either the data very limited or there had been yet no specific studies looking at the ECS in EC. After starting the studies reported

here, a pilot investigation on Italian women was published and the authors found that EC biopsies contained picomole concentrations, normalized per mg of wet tissues of AEA and PEA that were not significantly different to those of non-malignant endometrium, but levels of 2-AG were significantly elevated in the tumour when compared with age-matched controls. They also found that CB1 expression was unchanged but CB2 expression increased in malignant endometrial tissues (Guida et al. 2010). These findings are different to those reported here for the three NAEs (AEA, OEA and PEA), which were elevated in EC tissues and with only AEA and PEA being significantly elevated in plasma. Here, 2-AG was not measured because previous experience in the endocannabinoid research group showed that its measurement is inaccurate (2-AG is rapidly converted to 1-AG and so any measurements would be erroneous [Tim Marczylo, personal communication]).

The possible reason for the discrepancy in the plasma measurements of AEA and PEA in this study and that of the Italian group is not readily apparent, but could be related to patient selection. The patients in this study were from different ethnic groups, whilst those in Italy were all Caucasian. It has already been demonstrated that the plasma NAEs may be affected by ethnicity (Karasu 2012). Similarly, the difference between CB1 and CB2 receptor expression in this present study and the study by Guida et al. could be due to patient selection; patients here had different types and grades of EC, whereas the patients in the Italian cohort were from a more confined group, mainly type 1 (endometrioid) grade 1 and 2. An alternative explanation for the differences in CB1 and CB2 receptor expression in these two studies could be due to the different sources of antibody used. It is well known that there are some problems with antibodies used in endocannabinoid research (Grimsey et al. 2008) and to overcome this, a lot of time was spent characterising antibodies from different companies and optimising those antibodies using positive control tissues, (brain for CB1, spleen for CB2, pancreas for GPR55 and skin for TRPV1), a step which had not been performed by the Italian group. This, coupled with the use of menstrual cycle samples as additional controls (data not shown – but the results were the same as those described by other members of the endocannabinoid research group (Taylor et al. 2010), together with corroborating transcript levels for these receptors (Chapter 4) suggest that data produced here valid.

The data on plasma NAE concentrations (Chapter 2) suggest a vital role for AEA and PEA in the pathogenesis of endometrial cancer. The close correlation between plasma

and tissue AEA and PEA levels, but not OEA suggest that both former molecules could be used as biomarkers for disease. Indeed, the high sensitivity and specificity values obtained from the ROC analyses indicated that the two NAE values when combined generated a very good diagnostic tool. The area under the curve (AUC) was 0.933 (with OEA included) and 0.917 (with OEA omitted), which in diagnostic terms, is excellent. An AUC of 1.0 is considered perfect and an AUC of 0.5 is considered to be no better than ‘tossing a coin’, so a diagnostic test this good is unprecedented in the diagnosis of EC. The next best known diagnostic test with serum samples of HE4 (WFDC2) and CA-125 produced an AUC of 0.629 (Sun et al; 2015) and so the data here are very encouraging. The only limitation of this study (and that of Guida et al.) is the relatively small number of patients studied and so these observations would need to be examined with much larger numbers.

The failure of OEA to achieve significantly different levels between the EC and controls could be explained by the ‘entourage effect’, where the degradation of one NAE leads to an elevation of other NAEs (Ben-Shabat et al. 1998). The lower FAAH and high NAPE-PLD expression in tumour and lower plasma FAAH activity in the lymphocytes of patients with type 1 EC when compared to controls may explain the elevated AEA and PEA tissue and plasma concentrations, especially as the expression of FAAH in tumours (Chapter 3) probably controls both tissue and plasma AEA and PEA levels. For this to also work for OEA, then the tissue must preferentially degrade OEA sparing AEA and PEA. Although much is known about the regulation of FAAH expression, little is known about other isoforms. For example, human FAAH differs from that of other species in that there are two isoforms, FAAH-1 and FAAH-2 (Cravatt et al. 1996). The data presented in this thesis concentrate on FAAH-1 expression and activity, and so measures only that isoform. Recent evidence points to FAAH-2 being present in the endometrium (Scotchie et al. 2015). It is therefore possible that the expression of FAAH-2 is altered in the EC tissues and that could explain the observed differences in AEA and PEA levels compared to that of OEA here. It is also unclear whether there a preferential ligand specificity for FAAH-2, when compared to FAAH-1. In hindsight, these additional experiments should have been performed, but they had not been planned. Such experiments though should be performed in the future.

The novel data shown in this thesis support the original hypothesis (Chapter 1) and demonstrate that all parts of the ECS studied may have a role to play in the pathogenesis of EC. The ECS is thus probably a good target for future therapeutic intervention.

Endocannabinoids are increasingly implicated for their role in the regulation of key processes involved in the development of cancer. For example, the endocannabinoid system is reported to induce apoptosis (Galve-Roperh et al. 2000, Sanchez et al. 2001, Gomez del Pulgar et al. 2002), cell cycle arrest (De Petrocellis et al. 1998, Melck et al. 1999, Melck et al. 2000), and the inhibition of angiogenesis and metastasis for some (Blazquez et al. 2003, Casanova et al. 2003, Portella et al. 2003), but not all tumours (Molina-Holgado et al. 2002). Furthermore, there is a suggestion that endocannabinoid signalling in the tumorigenic cell differs to that of its 'normal' counterpart (Bifulco et al. 2001, McAllister et al. 2005, Blazquez et al. 2006). The problem with all the aforementioned studies is that they have not linked what is happening in the tissue with what is happening in the plasma of patients with disease. In Chapter 2, the experiments performed addressed this shortfall and to the best of my knowledge, this is the first time where all the three NAEs have been investigated together in the plasma and endometrial tissues of all types of EC. Some researchers have tried to explain elevated levels of AEA and PEA in the tumour microenvironment and in plasma, by suggesting that this is most likely as a result of the growing tumour displacing normal cells that produce the metabolising enzymes and destroying the sensory neuronal fibres that innervate the tumour (Constantin et al. 2008). The authors suggest that these terminals are a major source of AEA (and its analogue PEA) in the tumour microenvironment and as long as these terminals secrete AEA and PEA the tumour itself may develop an aberrant metabolising enzyme or that because AEA and PEA concentrations are highly elevated, they directly or indirectly override the metabolising enzymes in the EC *via* negative feed-back loops. Furthermore, this would suggest that high AEA and PEA plasma concentrations may potentially arise from the tumour secreting high levels of these ligands into the blood stream *via* various mechanisms. The latter explanation is more logical because of the observed expression patterns of NAPE-PLD and FAAH in the cancerous tissue and the near perfect relationship between the plasma concentrations and tissue levels of AEA and PEA with the NAPE-PLD/FAAH ratio. Additionally, there was a good correlation between OEA and the NAPE-PLD/FAAH expression ratio indicating that although this endocannabinoid was not directly related to the

pathogenesis of endometrial cancer (Chapter 2), its production is regulated by the relevant expression ratio of NAPE-PLD and FAAH in the different endometrial tissues. Although, plasma OEA concentrations were not significantly elevated in cancer tissue, they were still elevated compared to normal tissues, suggesting that these data may need to be confirmed in a much larger patient cohort. Sailler et al. (Sailler et al. 2014) reported that OEA concentration in plasma of cancer patients were reduced initially but increased once the cancers became more advanced to metastatic disease. This shows that OEA is raised in poorly differentiated carcinoma or in metastatic disease, which is similar to that presented here where the type 2 EC patients (who often have more advanced disease) had raised plasma OEA concentrations. The results reported by Sailler et al (2014), were thought to be directly associated with the number of metastases, particularly liver metastasis. A low OEA level has been shown to enhance cancer cell proliferation and migration, suggesting the loss of OEA in the local tumour micro-environment. Furthermore, the study by Schmid et al (2002) using GC-MS showed that AEA levels in EC (endometrial sarcoma and adenocarcinoma tissue biopsies) were higher and so were similar to the data presented in Chapter 2 (Schmid et al., 2002).

Since the consensus appears to be that the tissue levels of the NAEs appears to increase in EC, then it follows that something must regulate those levels. Initially, the plan was to investigate the enzyme activities of both NAPE-PLD and FAAH in blood samples obtained from the patients because the activities of these enzymes either within peripheral lymphocyte membranes or the malignant endometrial tissue could point to a major control point in the regulation of AEA or PEA concentrations. However, there were problems with the assessment of the NAPE-PLD activity assay in the collaborators group in Rome. This was disappointing because the expression of these two enzymes are known to be present and regulated in the normal endometrium (Maccarrone et al. 2002, Taylor et al. 2010) suggesting that they could be present in the endometrium of women with endometrial cancer, but to the best of my knowledge this had not been examined before the start of this project. It is also well documented that the activities of these enzymes are closely related to their expression. Since there could be no reliance on the NAPE-PLD activities, their expression profiles were used instead. The increased AEA and PEA levels in EC could therefore be due to either a reduction in FAAH

expression, or an increase in NAPE-PLD expression, or from both events occurring simultaneously.

The data in Chapter 3 shows that although FAAH enzyme activity levels were higher in the lymphocytes of the EC group than that of the control group, the difference was not statistically significant, even when the data were sub-divided by the different grades and types of tumour. There was however significant inverse correlations between plasma AEA and OEA concentrations and lymphocytic FAAH activities, but not between lymphocytic FAAH activities and plasma PEA. To the best of my knowledge, this is the first time that FAAH enzyme activity in the lymphocytic membranes of post-menopausal women with EC have been compared and the data presented adds to the generalised knowledge on the functions of these two important regulatory enzymes (NAPE-PLD and FAAH) considered to be the “gate-keepers” in the production and degradation of AEA, PEA and OEA. Drawing inferences these interesting data is difficult. It had been anticipated that AEA and PEA would show significant inverse correlations with FAAH activity, but not OEA. As suggested above, OEA activity could be related to FAAH-2 expression in the EC, but not in the lymphocytes, where FAAH-1 expression is supposed to dominate (Giang et al. 1997), and thus provide the only differential that explains these differences. Again, this would require further studies comparing endometrial tissue FAAH activities with lymphocytic FAAH activities in the EC population.

The relative expression of FAAH and NAPE-PLD at the transcript level in the endometrium was also examined. Prior to doing this, it was determined that the best ‘housekeeping’ gene for qRT-PCR had not yet been established. Steps were then taken to do this in keeping with the MIQE recommendation. The three best housekeeping genes identified using Taqman technologies were MRPL19, IPO8 and PPIA (Ayakannu et al. 2015) and these were used to normalize all qRT-PCR studies.

Analysis of FAAH transcript levels relative to the geometric mean of the three housekeeping genes (Ayakannu et al. 2015) indicated a gradual decrease in levels of FAAH transcript as tumour type and grade increased. Unlike the expression of FAAH transcripts in the EC samples, NAPE-PLD transcript levels were not different in any of the endometrial cancer types or grades when compared to that of the control atrophic tissue, even though there was a general increase in NAPE-PLD transcript levels. These

changes were also mirrored at the protein level using immunohistochemistry (IHC) and histomorphometric analyses.

The immunoreactive FAAH staining intensity was very strong in atrophic endometria, covering both stroma and glands, whilst FAAH staining intensity in EC was overall very low. FAAH protein levels in the glands and stroma combined were significantly lower in all the various grades of type 1 (grade, grade 2 and grade 3) and type 2 EC (serous and carcinosarcoma) when compared to the atrophic control tissue. This was interesting because it could immediately explain the increased AEA, OEA and PEA tissue levels in EC, as less degradative enzyme in the tissue would result in increased ligand concentrations.

Similar studies were performed using a commercial NAPE-PLD antibody. This took a considerable amount of time to achieve, because the antibodies that others in our research group (El-Talatini et al. 2009, Gebeh et al. 2012) had used previously were no longer available. This necessitated an arduous work-up of the antibody and correlation with previous observations, so there could be confidence in what was observed with this new antibody. As slightly better staining with the antibody was obtained compared to that of others hence there was confidence in the observations made here.

NAPE-PLD staining in grade 2 EC was more intense, being greater than that of both the atrophic and grade 1 EC. NAPE-PLD staining intensity in carcinosarcoma EC was higher than in all the other EC grades, especially when compared to the control (atrophic) group. NAPE-PLD staining in serous EC was also higher compared to that in atrophic, grade 1 and grade 2 EC tissues, but slightly lower than in grade 3 EC tissues, primarily because of reduced staining in the stroma. Furthermore, histomorphometric analysis of these data confirmed the visual staining patterns in the glands and stroma alone, and when the glands and stroma were combined. The amount of immunoreactive NAPE-PLD in the entire tissue (G+S) was always higher in the EC when compared to the atrophic endometria. These data could also explain the observed AEA, OEA and PEA levels in EC tissue because increased NAPE-PLD activity would result in increased ligand production in the tissue.

Furthermore, evidence from placental studies (Karasu et al. 2014) suggest that investigating NAPE-PLD/FAAH expression ratios could provide possible explanation to some of the above observations. This was therefore undertaken as reported in Chapter

3. The data showed very strong relationships between NAPE-PLD and FAAH transcript as well as their respective protein levels (H-score where G and S were combined) when all the EC samples were combined suggesting that both NAPE-PLD and FAAH in the endometrial tissue may contribute to the observed increases in AEA and PEA found in plasma. Correlation analyses indicated that there was no relationship between the levels of NAPE-PLD and FAAH transcript, but there was a strong inverse correlation between the H-scores for NAPE-PLD and FAAH protein levels, suggesting that the expression of these two enzymes at the transcript level are not controlled by a common factor, but reciprocal regulation of NAPE-PLD and FAAH protein expression is controlled by a single regulator or system (at least in the human endometrium). The examination of the NAPE-PLD/FAAH ratios for the transcripts and proteins indicated that both transcript and protein were significantly increased in EC tissue, suggesting that this is a good indicator of what is happening at the EC tissue level, with NAPE-PLD being perhaps more important than FAAH in the regulation of plasma AEA and PEA concentrations. Both enzymes (NAPE-PLD and FAAH) were expressed in the endometrial tumour tissue and differentially regulated with regards to the type of tumour present, with the main regulator of plasma AEA and PEA concentrations probably not being lymphocytic FAAH activity as might have been anticipated from other endocannabinoid regulatory studies (Maccarrone et al. 2001, Gasperi et al. 2014), but by endometrial tumour cell FAAH and NAPE-PLD protein expression levels. These data suggest that modulation of the expression of these two enzymes may result in the prevention of endometrial cancer in susceptible individuals, but this requires further investigation and a better understanding of the factors that regulate the expression of these two enzymes.

A literature review to evaluate studies that have examined the activity of FAAH and NAPE-PLD in cancers revealed that there were none that specifically examined their respective lymphocytic or endothelial cell activities in relation to cancer. In contrast, there is some evidence that these enzyme activities have been studied in early pregnancy complications, such as miscarriage (Maccarrone et al. 2000), in which low FAAH activity and high AEA tissue/plasma levels were associated with miscarriage; NAPE-PLD expression or activity was however not studied (Karasu et al. 2011, Taylor et al. 2011). What is interesting is that FAAH activity was also reduced in ectopic pregnancy with no effect on NAPE-PLD expression (Gebeh et al. 2013). These data

suggest that in non-malignant states, the main controlling factor for plasma endocannabinoid concentrations is most likely FAAH expression and activity. However, the data presented in this thesis indicate that although peripheral lymphocytic FAAH activity is non-significantly reduced in EC compared to atrophic controls as reported from studies on non-malignant disease (Maccarrone et al. 2002, Wang et al. 2006), that decrease failed to reach statistical significance, probably due to the small sample size.

Finally these data suggest that evaluating enzyme expression and protein measurement is better than transcript measurements as this provides more support for the idea that plasma AEA and PEA concentrations are possibly regulated at the tissue level, if the relationship between protein expression and enzyme activity (Maccarrone et al. 2000, Maccarrone et al. 2002, Maccarrone et al. 2002, Maccarrone 2009), holds true for the endometrium. The data for NAPE-PLD and FAAH protein expression followed a similar pattern to that of the transcripts indicating that protein expression is related to transcript levels. Whilst FAAH immunoreactivity was distributed throughout the tissue, NAPE-PLD expression was primarily localised both in the glandular epithelial cells of EC tissue with intensity increasingly correlating with more advanced disease.

As there is a lot of information about aberrant cannabinoid receptor expression in the female reproductive tract, with some evidence that CB1 and CB2 are regulated by the actions of estrogens (El-Talatini et al. 2009, Ribeiro et al. 2009), it was considered prudent to examine the expression of these receptors in EC, especially as the endometrioid (type 1) is thought to be estrogen-dependent (Doherty et al. 2007). Because all three NAEs were elevated in EC tissue (Chapter 2), it was felt that this could affect the expression of both cannabinoid and non-cannabinoid receptors, as has been observed in other tissues and tumours (Jones et al. 2003, Alexander et al. 2009, Pertwee et al. 2010, Ayakannu et al. 2013, Ayakannu et al. 2015). The expression of classical (CB1 and CB2) and non-classical (GPR55 and TRPV1) cannabinoid receptors with two different methods (qRT-PCR and IHC) were thus examined and reported in chapter 4.

The data (Chapter 4) showed that CB1 and CB2 transcript levels in EC were significantly decreased when compared to that in atrophic tissues. The main reduction in CB1 transcript levels were primarily due to the reduction observed in carcinosarcoma, whilst the levels in grade 1, 2, 3 (type 1 EC) and serous EC were not statistically

significantly different from those in atrophic tissues. By contrast, the CB2 mRNA was decreased in grade 3, serous and carcinosarcoma, whilst the relative expression in grade 1 and 2, was not. A link between decreased CB1 and CB2 transcript levels and increasingly advanced EC stage was thus established. These observations were supported by the IHC and histomorphometric studies where CB1 staining intensity was decreased in all types of EC with the intensity decreasing in line with the EC severity. Similarly, CB2 staining intensity was very strong in atrophic tissue with CB2 protein levels statistically significantly lower in type 1 EC and type 2 EC. This is at odds with the finding of Guida et al (2010), where there was increased CB2 protein expression but no difference in CB1 expression. The reason for this is not obvious, but it could be related to patient group selection. An alternative and probably more tenable explanation is that a different set of antibodies were used here. There are some questions raised about the specificity of the CB1 antibodies used for endocannabinoid research (Grimsey et al. 2008), suggesting that optimisation of antibodies and careful selection of controls is important. Having said that the fact that the transcript and protein levels for both CB1 and CB2 decreased in EC, provides some confidence that the data presented here are correct, with regards to the non-classical cannabinoid receptors, GPR55 transcript levels were significantly higher in the EC with this being confined to grade 1 and 2 EC type 1 sample. These data were again backed by the H-score which showed that GPR55 protein levels in the glands and stroma were higher with statistical significance in EC tissue compared to that of atrophic tissues. This time though, the protein expression pattern did not exactly match the transcript pattern, with GPR55 protein levels being significantly higher in all the various grades of type 1 and type 2 EC. The discrepancy between protein and transcript levels is not easy to explain, but is probably a reflection of the small sample size. Since there are no reported studies GPR55 regulations in EC, there are therefore no comparable data. However, recent evidence suggests that GPR55 is an essential key player at the molecular level in the modulation of the signalling pathways involved in malignant transformation, tumour growth and progression (Dorsam et al. 2007) since it is expressed by a large number of human cancer cell lines and human tumours and most importantly its expression correlates in an “aggressiveness”-related manner (Andradas et al. 2011). Similarly, a link between GPR55 levels and increasingly advanced stages of human pancreatic ductal adenocarcinoma has been reported (Andradas et al. 2011), and GPR55 is increased in human skin tumours and other squamous cell carcinomas (Perez-Gomez et al. 2013), in

a highly metastatic MDA-MB-231 human breast cancer cell line (Ford et al. 2010), in prostate (PC-3 and DU145) cancer cell lines and human ovarian cells (OVCAR3 and A2780) (Pineiro et al. 2011). An interesting observation is that GPR55 is also markedly elevated in ascites fluid of ovarian cancer patients making GPR55 a good marker of tumour grade and prognosis in this and other tumours such as glioma, breast, pancreas and prostate (Andradas et al. 2011, Hu et al. 2011, Pineiro et al. 2011).

TRPV1 receptor transcript levels were shown to significantly lower in EC when compared with atrophic tissues. This was supported by the IHC data showing the intensity of TRPV1 staining getting gradually lower as the severity of the disease increased. In grade 1 EC the staining was focused on the glands rather than the stroma, with the stroma being nearly devoid of staining. However, in grade 2 EC staining, it was opposite as it occurred with more intensity in stromal region than in the glands. Overall, TRPV1 protein levels were significantly lower in all the various grades of type 1 and type 2 EC.

These alterations in classical and non-classical receptor expression in EC may go some way in explaining the variable effects of endocannabinoids in different tumour models. It has been stated that cannabinoids are more effective in killing tumours that abundantly express cannabinoid receptors, such as gliomas, but may increase the growth and metastasis or at least inhibit cytotoxicity in other types of tumours, such as breast cancer, with no or low expression of cannabinoid receptors, possibly by suppression of the anti-tumour immune response (McKallip et al. 2005). This would fit with what was observed here in that CB1, CB2 and TRPV1 receptors were reduced in EC, suggesting that suppression of an anti-tumour immune response occurs in such individuals (McKallip et al. 2005). This could be a general phenomenon. For example, human colorectal tumours have lower CB1 mRNA and increased tumour growth (Wang et al. 2008); reduced cannabinoid receptor expression is associated with an increase in apoptosis in astrocytoma whereas no apoptosis occurs in astrocytoma cells with high receptor expression (Cudaback et al. 2010). Similarly, CB1 knockout, but not CB2 knockout APC^{min} mice (a model of colorectal cancer) have an increased risk of intestinal polyp development that can be replicated by treatment with CB1 antagonists (Wang et al. 2008). These reductions are similar to the findings shown here where the CB1 and CB2 expression was reduced in the malignant compared to the benign tissues, suggesting that increased apoptosis may be present in EC. By contrast, several

malignancies, including prostate and non-Hodgkin lymphoma (Gustafsson et al. 2008, Czifra et al. 2009), have been shown to express elevated cannabinoid receptor levels, with higher CB1 expression being associated with increased disease severity and poor prognosis in prostate and pancreatic cancer (Michalski et al. 2008, Chung et al. 2009). From these data, it is clear that there are no consistent receptor patterns in cancer and that receptor expression is probably tumour dependent.

In addition to cannabinoid receptor-mediated effect, it has been proposed that AEA also instigates a cytotoxic effects through a cannabinoid-receptor-independent mechanism (Gustafsson et al. 2009), with AEA acting as an agonist on TRPV1 or GPR55 receptors. These receptors have been less widely investigated than the classical cannabinoid receptors (CB1 and CB2) but it is known that TRPV1 is also overexpressed in both human prostate cancer (Czifra et al. 2009) and squamous cell carcinoma of the tongue (Marincsak et al. 2009) and the lysophospholipids, recently identified as potent ligands for GPR55 (Okuno et al. 2011), are markedly elevated in ascites fluid of ovarian cancer patients compared with non-malignant controls (Xiao et al. 2001).

These data support the hypothesis that reduced expression of CB1 and CB2 receptors and the concomitant increase in GPR55 expression and loss of TRPV1 receptor may be involved in the pathogenesis of EC. It is hoped that innovative targeting of these receptors may contribute to a novel tumour-suppressive treatment strategy for EC. For example, over-expression of CB1 may restore cell cycle function in the malignant cell. Of course, such experiments would need to be conducted. As a preliminary step to better understand how the endocannabinoid system might affect the cell cycle, a pilot study using an *in vitro* model of EC was performed.

The cell line chosen was the Ishikawa cell line, because it was generated from an adenocarcinoma of the endometrium, is known to express receptors for estrogen and progesterone (Lessey et al. 1988), and in a preliminary study performed by the endocannabinoid research group, it was shown to express CB1, CB2, FAAH, NAPE-PLD, GPR55 and TRPV1 at the transcript level (Tim Marczyklo personal communication).

This pilot showed that AEA, OEA, PEA and capsaicin (a direct activator of TRPV1) on the Ishikawa cell proliferation and viability and found that AEA, OEA, PEA and capsaicin all caused a time- and pseudo dose-dependent reduction in cell viability

(Chapter 5) with the cells recovering in long-term culture, suggesting that the effect of all four compounds is probably through inhibition of cell proliferation rather than cell death, because the cells recovered with time. The reason why the cells recovered may be due to the actions of FAAH. As stated above, Ishikawa cells make FAAH transcripts and so with time the cells would be able to metabolise the NAEs and so reduce the cell selection pressure. However, that does not explain the capsaicin result, because this molecule is not degraded by FAAH. Hamtiaux et al. postulated that receptor density is responsible here (Hamtiaux et al. 2011) especially in neuroblastoma cancer cell lines or this effect could be indirectly dependent upon CB1, CB2, GPR55 or TRPV1 receptor density (Movsesyan et al. 2004). Whatever the mechanism, the reduction in cell number may be partly because of inhibition of AEA hydrolysis and consequent increase in the concentration of endocannabinoids, especially AEA and PEA, i.e. the entourage effect. Whether this operates in Ishikawa cells is unknown, but would be a useful adjunct for future investigation. It is likely that the combination of these molecules might synergistically increase cell proliferation after 48 hours without inducing cell apoptosis or necrosis. These data also suggest that the increased plasma and tissue AEA/PEA concentrations observed in EC patients (Chapter 2) are probably a 'counter mechanism' against further cancer growth.

The molecular mechanism(s) underlying the effects of endocannabinoids in EC is (are) still largely unknown. A proposed mechanism, is that of growth inhibition, which may involve induction of apoptosis in tumour cells, or an anti-proliferative action and an anti-metastatic effect through inhibition of angiogenesis and tumour cell migration (Bifulco et al. 2002, Guzman et al. 2002, Parolaro et al. 2002, Guzman 2003, Jones et al. 2003, Velasco et al. 2004, Patsos et al. 2005). Indeed, in other cell systems, cannabinoids produce their effects by modulating several important intracellular pathways such as inhibiting regulators of the cell cycle, where AEA has been shown to arrest human MDA-MB-231 breast cancer cells in the S phase of the cell cycle as a consequence of the loss in Cdk2 activity, up-regulation of p21waf and a reduced formation of the active cyclin E/Cdk2 kinase complex (Laezza et al. 2006). Similarly, cell cycle arrest at G0/G1 can result in stimulation of apoptosis *via* a change in the BAX/Bcl-2 ratio and the activation of caspases (Sarfaraz et al. 2006). Data from other tumours makes correlations to EC difficult because inhibition of cancer cell proliferation by endocannabinoids can be confusing and is probably incomplete. For

example, breast cancer cell proliferation is inhibited by AEA *via* down-regulation of the prolactin receptor, the BRCA 1 gene product and the high affinity neurotrophin receptor *trk* (Melck et al. 1999, Melck et al. 2000). In these cases, the anti-proliferative effect of AEA is proportional to the hormone-dependency of the cell lines used, with the mechanism relying on the inhibition of the phospho-kinase A (PKA) pathway (Melck et al. 2000). Furthermore, inhibition of cancer cell invasion by endocannabinoids may involve inhibition of the endogenous tissue inhibitor of metalloproteinase TIMP-1 (Ramer et al. 2008), inhibition of FAK/Src signalling (Grimaldi et al. 2006) and inhibition of matrix metalloproteinase-2 (MMP-2) (Blazquez et al. 2008) expression. In SW480 colon carcinoma cells, AEA inhibited cell migration *via* activation of CB1 receptors (Joseph et al. 2004) and inhibition of migration in lung cancer cells was reported for both AEA and Δ -9-THC (Ramer et al. 2008). Whether similar effects occur in EC, is unknown.

Inhibition of cancer angiogenesis by endocannabinoids can affect tumour growth by lowering vascular tissue concentrations, decreased production of pro-angiogenic factors and/or by direct modulation of endothelial cell function (Freimuth et al. 2010). It has been reported that AEA induces both neuroblastoma and lymphoma cell death *via* vanilloid receptor-mediated mechanisms (Maccarrone et al. 2000). Inhibition of cancer cell invasion through TIMP-1 by methanandamide is also mediated through TRPV1 (Ramer et al. 2008) and some cannabinoids including cannabidiol interfere with the ability of lysophosphatidylinositol (LPI) to bind to GPR55 (Pineiro et al. 2011). LPI induces cancer cell proliferation *via* GPR55 stimulation by the triggering of ERK, AKT and calcium mobilization cascades. Furthermore, pre-treatment of breast and prostate cancer cells with cannabidiol or rimonabant, blocks LPI to induce cell proliferation *via* GPR55 (Pineiro et al. 2011). These data support the previous statement that the effect of endocannabinoids on a particular part of the pathogenesis of a particular tumour are likely to be tumour-specific. What is interesting is the observation that cell cycle arrest at G0/G1 can result in stimulation of apoptosis *via* a change in the BAX/Bcl-2 ratio (Sarfaraz et al. 2006). This was the rationale for the studies presented in the final chapter of this thesis.

The key finding was that there were no statistically significant associations between BAX, Bcl-2, the BAX/Bcl-2 ratio or Ki-67 (a marker of proliferation) with tissue concentrations of AEA, OEA or PEA. Furthermore, there appeared to be no association

between BAX, Bcl-2, the BAX/Bcl-2 ratio or Ki-67 and the classical endocannabinoid receptor CB1 expression, but there was a statistically significant association between Ki-67 and CB2, suggesting that the main stimulator of Ki-67 expression and hence endometrial epithelial cell proliferation could be *via* the CB2 receptor. This supports Guida et al.'s data, where the expression of CB2 was higher in EC (Guida et al. 2010). Interestingly, there was a strong association between the BAX/Bcl-2 ratio and Ki-67 expression, the non-classical receptors GPR55 and TRPV1 and the metabolising enzymes of ECS (FAAH and NAPE-PLD).

Previous studies have documented that activation of either CB1 or CB2 receptors triggers the ceramide ERK signalling pathways to promote apoptosis (Kogan 2005, Sarfaraz et al. 2006, Sarfaraz et al. 2008). This may be a possible activated pathway in EC development, but will need to be examined in future studies.

In human neuroblastoma and C6 glioma cells, AEA induces apoptosis through vanilloid receptor-mediated increases in intracellular calcium concentrations, which activates cyclo-oxygenase 2 (COX-2), releases cytochrome c and activates caspase 3 (Contassot et al. 2004). This mechanism may be active in EC, because a strong relationship between TRPV1 and BAX was observed. On the other hand, capsazepine, a TRPV1 antagonist, increased BAX expression (Sung et al. 2012) and several authors have shown that capsaicin-treated cells have increased BAX coupled to decreased Bcl-2 (Hetz 2007). This decrease in Bcl-2 expression caused by capsaicin has been noted in other studies (Pacak et al. 2012, Krizanova et al. 2014), suggesting that TRPV1 activation is characterised by reduced Bcl-2 expression and it is that change that causes cellular apoptosis.

Several other studies have documented pro-apoptotic effects of cannabinoids in different cells (Freimuth et al. 2010). In hepatocellular carcinoma (Hep-G2) cells, CB1 receptor agonists induced apoptosis and that was accompanied by up regulation of the death signalling factor BAX and down regulation of the survival factors Bcl-2 (Giuliano et al. 2009).

7.2 Future Work

- 1) To gain a world-wide acceptance of plasma AEA, OEA and PEA as clinical biomarkers for EC, a multi-centre trial using a much larger cohort of patients would be ideal.
2. Guida *et al.*, showed the expression of CB2 and measured 2-AG in endometrial cancer. However, in this thesis CB2 expression was different to that reported by Guida *et al.* It would thus be interesting to re-examine this data and fully understand the mechanism of the 2-AG pathway in EC.
- 3) The expression of FAAH-2 would be useful to study in EC. These experiments should examine the differential expression of the FAAH-1 enzyme and FAAH-2 and their abilities to regulate the degradation of AEA, OEA and PEA and to see if they can support a tissue-specific ‘entourage’ effect in EC. This would require the use of an endometrial epithelial cell line that already expresses FAAH-1 (such as the Ishikawa cell). To prevent FAAH-1 activity, enzyme specific inhibitors such as UB-273 could be used.
- 4) Although the effect of AEA, OEA, PEA and capsaicin on Ishikawa cell viability was established here, the receptor responsible for that activity was not examined. Further studies should be undertaken using CB1, CB2, GPR55 and TRPV1 receptor antagonists and agonists to determine receptor specific effects. The work could be expanded to include markers of cell proliferation and apoptosis (such as the caspases and annexin V) and PTEN and/or cyclins/cdks/ ERK-signalling. The second messengers and their pathways (as have been assessed in other tumour models) could also be examined.
- 5) Examine the changes induced by AEA or PEA signalling in endometrial gene expression of endometrial carcinoma. Microarray (mRNA and miRNA) analyses have identified differentially expressed genes and their associated pathways in endometrial carcinoma providing insight into the characterisation of molecules involved in endometrial carcinogenesis. Microarrays (mRNA and miRNA, in house) will be performed on RNA extracted from normal and malignant primary cells before and after challenging with metAEA to examine the change in gene expressions. Significant changes in expression will be verified by qRT-PCR analysis of selected up and down

regulated genes. Pathways analyses will be undertaken to highlight the major pathways modified by endocannabinoids treatments.

7.3 Conclusions

The work presented in this thesis reveals that the endocannabinoid system is deranged in the EC tissue, and is particularly more deranged in the tissues from advanced disease. These tissue changes are mirrored by higher plasma AEA and PEA concentration. This thesis also provides evidence that when endocannabinoids were administered to an endometrial cancer cell line model, cell viability was reduced. This suggests that *in vivo*, the endocannabinoids also cause reduced cell viability through CB-dependent pathways, but later, as the tumour converts from an estrogen-dependent tissue to a non-estrogen-dependent tissue, it also converts to a non-endocannabinoid tissue and starts using GPR55 instead of CB1 and CB2, which have disappeared along with TRPV1.

The data generated from this thesis also support the postulated theory that endometrial cancer cells initially go through a cellular apoptotic phase (cell death/necrosis), which were supported by increases in the BAX: Bcl-2 ratio and also cellular proliferation with increased levels of Ki-67 in the endometrial cancer cells suggesting that these factors play an important role in the carcinogenesis of EC. Moreover, plasma and ECS profiles in the various stages of EC pathogenesis may eventually become useful for assessing the individual course of the disease and possibly, that correction of some of the deranged ECS components may be used as supportive interventions for the prevention or reversal of EC.



Chapter 8

Appendices

8.1 Letter of Ethical Approval

Below is a PDF image of the letter of approval from the local research ethics committee relating to the studies presented herein.



Leicestershire, Northamptonshire & Rutland Research Ethics Committee 1
 1 Standard Court
 Park Row
 Nottingham
 NG1 6GN
 Telephone: 01159123344
 Facsimile: 01159123300

13 June 2006

Professor J Konje
 Professor of Obstetrics & Gynaecology
 University of Leicester
 Robert Kilpatrick Clinical Sciences Building,
 Leicester Royal Infirmary
 Leicester, LE2 7LX

Dear Professor Konje,

Full title of study: **The Role of Endogenous Cannabinoids (chemicals similar to cannabis but produced naturally in the human body) in Reproduction**

REC reference number: **06/G2501/49**

Thank you for your letter of 02 June 2006, responding to the Committee's request for further information on the above research and submitting revised documentation.

The further information has been considered on behalf of the Committee by the Chair.

Confirmation of ethical opinion

On behalf of the Committee, I am pleased to confirm a favourable ethical opinion for the above research on the basis described in the application form, protocol and supporting documentation as revised.

Conditions of approval

The favourable opinion is given provided that you comply with the conditions set out in the attached document. You are advised to study the conditions carefully.

Approved documents

The final list of documents reviewed and approved by the Committee is as follows:

Document	Version	Date
Application	1	24 February 2006
Investigator CV	1	23 February 2006
Protocol	2	23 May 2006
Peer Review		
Letter of invitation to participant – V menstrual cycle studies	2	23 May 2006
Letter of invitation to participant – V undergoing gynae surgery	2	23 May 2006
Letter of invitation to participant – Non-P V with non-surgical gynae problem	2	23 May 2006
Letter of invitation to participant - STOP V	2	23 May 2006

An advisory committee to Leicestershire, Northamptonshire and Rutland Strategic Health Authority

Leicestershire, Northamptonshire & Rutland Research Ethics Committee 1

LIST OF SITES WITH A FAVOURABLE ETHICAL OPINION

For all studies requiring site-specific assessment, this form is issued by the main REC to the Chief Investigator and sponsor with the favourable opinion letter and following subsequent notifications from site assessors. For issue 2 onwards, all sites with a favourable opinion are listed, adding the new sites approved.

REC reference number:	06/G2501/49	Issue number:	1	Date of issue:	13 June 2006
Chief Investigator:	Professor J C Konje				
Full title of study:	The Role of Endogenous Cannabinoids (chemicals similar to cannabis but produced naturally in the human body) in Reproduction				
This study was given a favourable ethical opinion by Leicestershire, Northamptonshire & Rutland Research Ethics Committee 1 on 12 June 2006. The favourable opinion is extended to each of the sites listed below. The research may commence at each NHS site when management approval from the relevant NHS care organisation has been confirmed.					
Principal Investigator	Post	Research site	Site assessor	Date of favourable opinion for this site	Notes ⁽¹⁾
Professor J C Konje	Professor of Obstetrics and Gynaecology and Honorary Consultant	University Hospitals of Leicester NHS Trust, Leicester Royal Infirmary	Leicestershire, Northamptonshire & Rutland Research Ethics Committee 1	13/06/2006	
Approved by the Chair on behalf of the REC:					
..... (Signature of Chair/Administrator)					
(Delete as applicable)					
..... (Name)					

(1) The notes column may be used by the main REC to record the early closure or withdrawal of a site (where notified by the Chief Investigator or sponsor), the suspension or termination of the favourable opinion for an individual site, or any other relevant development. The date should be recorded.

8.2 Published Works

The following are PDF copies of the papers arising from this thesis.



Chapter 9

Bibliography

9.1 References

(2009). *GraphPad Prism*. G. Software. San Diego, CA, USA.

(2011). *GenEx software*. M. A. AB. Göteborg, Sweden.

Ahn, K., M. K. McKinney and B. F. Cravatt (2008). "Enzymatic pathways that regulate endocannabinoid signaling in the nervous system." *Chem Rev* **108**(5): 1687-1707.

Alexander, A., P. F. Smith and R. J. Rosengren (2009). "Cannabinoids in the treatment of cancer." *Cancer Lett* **285**(1): 6-12.

Aloe, L., A. Leon and R. Levi-Montalcini (1993). "A proposed autacoid mechanism controlling mastocyte behaviour." *Agents Actions* **39 Spec No**: C145-147.

Amoako, A. A., T. H. Marczylo, P. M. Lam, J. M. Willets, A. Derry, J. Elson and J. C. Konje (2010). "Quantitative analysis of anandamide and related acylethanolamides in human seminal plasma by ultra performance liquid chromatography tandem mass spectrometry." *J Chromatogr B Analyt Technol Biomed Life Sci* **878**(31): 3231-3237.

Andersen, C. L., J. L. Jensen and T. F. Orntoft (2004). "Normalization of real-time quantitative reverse transcription-PCR data: a model-based variance estimation approach to identify genes suited for normalization, applied to bladder and colon cancer data sets." *Cancer Res* **64**(15): 5245-5250.

Andradas, C., M. Caffarel, E. Perez-Gomez, M. Salazar, M. Lorente, G. Velasco, M. Guzman and C. Sanchez (2011). "The orphan G protein-coupled receptor GPR55 promotes cancer cell proliferation via ERK." *Oncogene* **30**(2): 245-252.

Annuzzi, G., F. Piscitelli, L. Di Marino, L. Patti, R. Giacco, G. Costabile, L. Bozzetto, G. Riccardi, R. Verde, S. Petrosino, A. A. Rivellese and V. Di Marzo (2010). "Differential alterations of the concentrations of endocannabinoids and related lipids in the subcutaneous adipose tissue of obese diabetic patients." *Lipids Health Dis* **9**: 43.

Ayakannu, T., A. H. Taylor, T. H. Marczylo, J. M. Willets and J. C. Konje (2013). "The endocannabinoid system and sex steroid hormone-dependent cancers." *Int J Endocrinol* **2013**: 259676.

Ayakannu, T., A. H. Taylor, J. M. Willets, L. Brown, D. G. Lambert, J. McDonald, Q. Davies, E. L. Moss and J. C. Konje (2015). "Validation of endogenous control reference genes for normalizing gene expression studies in endometrial carcinoma." *Mol Hum Reprod* **21**(9): 723-735.

Ayakannu, T., A. H. Taylor, J. M. Willets and J. C. Konje (2015). "The evolving role of the endocannabinoid system in gynaecological cancer." Hum Reprod Update **21**(4): 517-535.

Baekelandt, M. M., M. Castiglione and E. G. W. Group (2009). "Endometrial carcinoma: ESMO clinical recommendations for diagnosis, treatment and follow-up." Ann Oncol **20 Suppl 4**: 29-31.

Baldinu, P., A. Cossu, A. Manca, M. P. Satta, M. C. Sini, G. Palomba, S. Dessole, P. Cherchi, L. Mara, F. Tanda and G. Palmieri (2007). "CASC2a gene is down-regulated in endometrial cancer." Anticancer Res **27**(1A): 235-243.

Banno, K., I. Kisu, M. Yanokura, K. Tsuji, K. Masuda, A. Ueki, Y. Kobayashi, W. Yamagami, H. Nomura, E. Tominaga, N. Susumu and D. Aoki (2012). "Biomarkers in endometrial cancer: Possible clinical applications (Review)." Oncol Lett **3**(6): 1175-1180.

Bansal, N., V. Yendluri and R. M. Wenham (2009). "The molecular biology of endometrial cancers and the implications for pathogenesis, classification, and targeted therapies." Cancer Control **16**(1): 8-13.

Bari, M., N. Battista, F. Fezza, A. Finazzi-Agro and M. Maccarrone (2005). "Lipid rafts control signaling of type-1 cannabinoid receptors in neuronal cells. Implications for anandamide-induced apoptosis." J Biol Chem **280**(13): 12212-12220.

Bari, M., N. Battista, F. Fezza, V. Gasperi and M. Maccarrone (2006). "New insights into endocannabinoid degradation and its therapeutic potential." Mini Rev Med Chem **6**(3): 257-268.

Basavarajappa, B. S. (2007). "Neuropharmacology of the endocannabinoid signaling system-molecular mechanisms, biological actions and synaptic plasticity." Curr Neuropharmacol **5**(2): 81-97.

Basil, J. B., P. J. Goodfellow, J. S. Rader, D. G. Mutch and T. J. Herzog (2000). "Clinical significance of microsatellite instability in endometrial carcinoma." Cancer **89**(8): 1758-1764.

Beekman, L., T. Tohver, R. Dardari and R. Leguillette (2011). "Evaluation of suitable reference genes for gene expression studies in bronchoalveolar lavage cells from horses with inflammatory airway disease." BMC Mol Biol **12**: 5.

Begg, M., P. Pacher, S. Batkai, D. Osei-Hyiaman, L. Offertaler, F. M. Mo, J. Liu and G. Kunos (2005). "Evidence for novel cannabinoid receptors." Pharmacol Ther **106**(2): 133-145.

Ben-Shabat, S., E. Fride, T. Sheskin, T. Tamiri, M. H. Rhee, Z. Vogel, T. Bisogno, L. De Petrocellis, V. Di Marzo and R. Mechoulam (1998). "An entourage effect: inactive endogenous fatty acid glycerol esters enhance 2-arachidonoyl-glycerol cannabinoid activity." Eur J Pharmacol **353**(1): 23-31.

Berchuck, A. and J. Boyd (1995). "Molecular basis of endometrial cancer." Cancer **76**(10 Suppl): 2034-2040.

Berdyshev, E. V. (2000). "Cannabinoid receptors and the regulation of immune response." Chem Phys Lipids **108**(1-2): 169-190.

Bethea, C. L. and A. A. Widmann (1998). "Differential expression of progesterin receptor isoforms in the hypothalamus, pituitary, and endometrium of rhesus macaques." Endocrinology **139**(2): 677-687.

Bhargava, V., D. L. Kell, M. van de Rijn and R. A. Warnke (1994). "Bcl-2 immunoreactivity in breast carcinoma correlates with hormone receptor positivity." Am J Pathol **145**(3): 535-540.

Bifulco, M. and V. Di Marzo (2002). "Targeting the endocannabinoid system in cancer therapy: a call for further research." Nat Med **8**(6): 547-550.

Bifulco, M., C. Laezza, S. Pisanti and P. Gazerro (2006). "Cannabinoids and cancer: pros and cons of an antitumour strategy." Br J Pharmacol **148**(2): 123-135.

Bifulco, M., C. Laezza, G. Portella, M. Vitale, P. Orlando, L. De Petrocellis and V. Di Marzo (2001). "Control by the endogenous cannabinoid system of ras oncogene-dependent tumor growth." FASEB J **15**(14): 2745-2747.

Bifulco, M., A. M. Malfitano, S. Pisanti and C. Laezza (2008). "Endocannabinoids in endocrine and related tumours." Endocr Relat Cancer **15**(2): 391-408.

Blazquez, C., A. Carracedo, L. Barrado, P. J. Real, J. L. Fernandez-Luna, G. Velasco, M. Malumbres and M. Guzman (2006). "Cannabinoid receptors as novel targets for the treatment of melanoma." FASEB J **20**(14): 2633-2635.

Blazquez, C., M. L. Casanova, A. Planas, T. Gomez Del Pulgar, C. Villanueva, M. J. Fernandez-Acenero, J. Aragonés, J. W. Huffman, J. L. Jorcano and M. Guzman (2003). "Inhibition of tumor angiogenesis by cannabinoids." FASEB J **17**(3): 529-531.

Blazquez, C., L. Gonzalez-Feria, L. Alvarez, A. Haro, M. L. Casanova and M. Guzman (2004). "Cannabinoids inhibit the vascular endothelial growth factor pathway in gliomas." Cancer Res **64**(16): 5617-5623.

- Blazquez, C., M. Salazar, A. Carracedo, M. Lorente, A. Egia, L. Gonzalez-Feria, A. Haro, G. Velasco and M. Guzman (2008). "Cannabinoids inhibit glioma cell invasion by down-regulating matrix metalloproteinase-2 expression." Cancer Res **68**(6): 1945-1952.
- Bode, A. M. and Z. Dong (2011). "The two faces of capsaicin." Cancer Res **71**(8): 2809-2814.
- Bokhman, J. V. (1983). "Two pathogenetic types of endometrial carcinoma." Gynecol Oncol **15**(1): 10-17.
- Bonefeld, B. E., B. Elfving and G. Wegener (2008). "Reference genes for normalization: a study of rat brain tissue." Synapse **62**(4): 302-309.
- Bornheim, L. M., E. T. Everhart, J. Li and M. A. Correia (1993). "Characterization of cannabidiol-mediated cytochrome P450 inactivation." Biochem Pharmacol **45**(6): 1323-1331.
- Bornheim, L. M., K. Y. Kim, B. Chen and M. A. Correia (1995). "Microsomal cytochrome P450-mediated liver and brain anandamide metabolism." Biochem Pharmacol **50**(5): 677-686.
- Bouaboula, M., M. Rinaldi, P. Carayon, C. Carillon, B. Delpech, D. Shire, G. Le Fur and P. Casellas (1993). "Cannabinoid-receptor expression in human leukocytes." Eur J Biochem **214**(1): 173-180.
- Bozdogan, O., P. Atasoy, S. Erekul, N. Bozdogan and M. Bayram (2002). "Apoptosis-related proteins and steroid hormone receptors in normal, hyperplastic, and neoplastic endometrium." Int J Gynecol Pathol **21**(4): 375-382.
- Bray, F., I. Dos Santos Silva, H. Moller and E. Weiderpass (2005). "Endometrial cancer incidence trends in Europe: underlying determinants and prospects for prevention." Cancer Epidemiol Biomarkers Prev **14**(5): 1132-1142.
- Bray, F., A. Jemal, N. Grey, J. Ferlay and D. Forman (2012). "Global cancer transitions according to the Human Development Index (2008-2030): a population-based study." Lancet Oncol **13**(8): 790-801.
- Bray, F., J. S. Ren, E. Masuyer and J. Ferlay (2013). "Global estimates of cancer prevalence for 27 sites in the adult population in 2008." Int J Cancer **132**(5): 1133-1145.
- Brighton, P. J., J. McDonald, A. H. Taylor, R. A. Challiss, D. G. Lambert, J. C. Konje and J. M. Willets (2009). "Characterization of anandamide-stimulated cannabinoid

receptor signaling in human ULTR myometrial smooth muscle cells." Mol Endocrinol **23**(9): 1415-1427.

Brinton, L. A., M. L. Berman, R. Mortel, L. B. Twiggs, R. J. Barrett, G. D. Wilbanks, L. Lannom and R. N. Hoover (1992). "Reproductive, menstrual, and medical risk factors for endometrial cancer: results from a case-control study." Am J Obstet Gynecol **167**(5): 1317-1325.

Brown, A. J. (2007). "Novel cannabinoid receptors." Br J Pharmacol **152**(5): 567-575.

Buczynski, M. and L. Parsons (2010). "Quantification of brain endocannabinoid levels: methods, interpretations and pitfalls." British Journal of Pharmacology: 423-442.

Burks, R. T., T. D. Kessis, K. R. Cho and L. Hedrick (1994). "Microsatellite instability in endometrial carcinoma." Oncogene **9**(4): 1163-1166.

Burns, J. M., B. C. Summers, Y. Wang, A. Melikian, R. Berahovich, Z. Miao, M. E. Penfold, M. J. Sunshine, D. R. Littman, C. J. Kuo, K. Wei, B. E. McMaster, K. Wright, M. C. Howard and T. J. Schall (2006). "A novel chemokine receptor for SDF-1 and I-TAC involved in cell survival, cell adhesion, and tumor development." J Exp Med **203**(9): 2201-2213.

Bustin, S. A., V. Benes, J. A. Garson, J. Hellemans, J. Huggett, M. Kubista, R. Mueller, T. Nolan, M. W. Pfaffl, G. L. Shipley, J. Vandesompele and C. T. Wittwer (2009). "The MIQE guidelines: minimum information for publication of quantitative real-time PCR experiments." Clin Chem **55**(4): 611-622.

Buttayan, R., A. Shabsigh, H. Perlman and M. Colombel (1999). "Regulation of apoptosis in the prostate gland by androgenic steroids." Trends in Endocrinology and Metabolism **10**(2): 47-54.

Caduff, R. F., C. M. Johnston and T. S. Frank (1995). "Mutations of the Ki-ras oncogene in carcinoma of the endometrium." Am J Pathol **146**(1): 182-188.

Caffarel, M. M., D. Sarrio, J. Palacios, M. Guzman and C. Sanchez (2006). "Delta9-tetrahydrocannabinol inhibits cell cycle progression in human breast cancer cells through Cdc2 regulation." Cancer Res **66**(13): 6615-6621.

Calignano, A., G. La Rana, A. Giuffrida and D. Piomelli (1998). "Control of pain initiation by endogenous cannabinoids." Nature **394**(6690): 277-281.

Calle, E. E., C. Rodriguez, K. Walker-Thurmond and M. J. Thun (2003). "Overweight, obesity, and mortality from cancer in a prospectively studied cohort of U.S. adults." N Engl J Med **348**(17): 1625-1638.

Cancer Research UK. (September 2014). "Cancer Research Statistics, Cancer Incidence and Mortality in the UK."

Capasso, R. and A. A. Izzo (2008). "Gastrointestinal regulation of food intake: general aspects and focus on anandamide and oleoylethanolamide." J Neuroendocrinol **20 Suppl 1**: 39-46.

Carracedo, A., M. Lorente, A. Egia, C. Blazquez, S. Garcia, V. Giroux, C. Malicet, R. Villuendas, M. Gironella, L. Gonzalez-Feria, M. A. Piris, J. L. Iovanna, M. Guzman and G. Velasco (2006). "The stress-regulated protein p8 mediates cannabinoid-induced apoptosis of tumor cells." Cancer Cell **9**(4): 301-312.

Casanova, M. L., C. Blazquez, J. Martinez-Palacio, C. Villanueva, M. J. Fernandez-Acenero, J. W. Huffman, J. L. Jorcano and M. Guzman (2003). "Inhibition of skin tumor growth and angiogenesis in vivo by activation of cannabinoid receptors." J Clin Invest **111**(1): 43-50.

Catusus, L., X. Matias-Guiu, P. Machin, J. Munoz and J. Prat (1998). "BAX somatic frameshift mutations in endometrioid adenocarcinomas of the endometrium: evidence for a tumor progression role in endometrial carcinomas with microsatellite instability." Lab Invest **78**(11): 1439-1444.

Chakravarti, B., J. Ravi and R. K. Ganju (2014). "Cannabinoids as therapeutic agents in cancer: current status and future implications." Oncotarget **5**(15): 5852-5872.

Chan, W. K., M. M. Mole, D. A. Levison, R. Y. Ball, Q. L. Lu, K. Patel and A. M. Hanby (1995). "Nuclear and cytoplasmic bcl-2 expression in endometrial hyperplasia and adenocarcinoma." J Pathol **177**(3): 241-246.

Chung, S. C., P. Hammarsten, A. Josefsson, P. Stattin, T. Granfors, L. Egevad, G. Mancini, B. Lutz, A. Bergh and C. J. Fowler (2009). "A high cannabinoid CB1 receptor immunoreactivity is associated with disease severity and outcome in prostate cancer." European Journal of Cancer **45**(1): 174-182.

Cianchi, F., L. Papucci, N. Schiavone, M. Lulli, L. Magnelli, M. C. Vinci, L. Messerini, C. Manera, E. Ronconi, P. Romagnani, M. Donnini, G. Perigli, G. Trallori, E. Tanganelli, S. Capaccioli and E. Masini (2008). "Cannabinoid receptor activation induces apoptosis through tumor necrosis factor alpha-mediated ceramide de novo synthesis in colon cancer cells." Clin Cancer Res **14**(23): 7691-7700.

Clegg, R. M. (1992). "Fluorescence resonance energy transfer and nucleic acids." Methods Enzymol **211**: 353-388.

- Cleland, W. H., C. R. Mendelson and E. R. Simpson (1985). "Effects of aging and obesity on aromatase activity of human adipose cells." J Clin Endocrinol Metab **60**(1): 174-177.
- Clement, P. B. and R. H. Young (2002). "Endometrioid carcinoma of the uterine corpus: a review of its pathology with emphasis on recent advances and problematic aspects." Adv Anat Pathol **9**(3): 145-184.
- Cong, L., J. Gasser, J. Zhao, B. Yang, F. Li and A. Z. Zhao (2007). "Human adiponectin inhibits cell growth and induces apoptosis in human endometrial carcinoma cells, HEC-1-A and RL95 2." Endocr Relat Cancer **14**(3): 713-720.
- Constantin, C. E., N. Mair, C. A. Sailer, M. Andratsch, Z. Z. Xu, M. J. Blumer, N. Scherbakov, J. B. Davis, H. Bluethmann, R. R. Ji and M. Kress (2008). "Endogenous tumor necrosis factor alpha (TNFalpha) requires TNF receptor type 2 to generate heat hyperalgesia in a mouse cancer model." J Neurosci **28**(19): 5072-5081.
- Contassot, E., M. Tenan, V. Schnuriger, M. F. Pelte and P. Y. Dietrich (2004). "Arachidonyl ethanolamide induces apoptosis of uterine cervix cancer cells via aberrantly expressed vanilloid receptor-1." Gynecol Oncol **93**(1): 182-188.
- Conti, S., B. Costa, M. Colleoni, D. Parolaro and G. Giagnoni (2002). "Antiinflammatory action of endocannabinoid palmitoylethanolamide and the synthetic cannabinoid nabilone in a model of acute inflammation in the rat." Br J Pharmacol **135**(1): 181-187.
- Cornillie, F. J., J. M. Lauweryns and I. A. Brosens (1985). "Normal human endometrium. An ultrastructural survey." Gynecol Obstet Invest **20**(3): 113-129.
- Cortright, D. N. and A. Szallasi (2004). "Biochemical pharmacology of the vanilloid receptor TRPV1. An update." Eur J Biochem **271**(10): 1814-1819.
- Costa, B., S. Conti, G. Giagnoni and M. Colleoni (2002). "Therapeutic effect of the endogenous fatty acid amide, palmitoylethanolamide, in rat acute inflammation: inhibition of nitric oxide and cyclo-oxygenase systems." Br J Pharmacol **137**(4): 413-420.
- Craig, R. W. (1995). "The bcl-2 gene family." Semin Cancer Biol **6**(1): 35-43.
- Cravatt, B. F., D. K. Giang, S. P. Mayfield, D. L. Boger, R. A. Lerner and N. B. Gilula (1996). "Molecular characterization of an enzyme that degrades neuromodulatory fatty-acid amides." Nature **384**(6604): 83-87.

- Critchley, H. O. D., Drudy, T.A., Millar, M., MacPherson, S., Saunders, P.T.K. (2000). "Is estrogen receptor β (ER β) responsible for steroid mediated effects on the endometrial vasculature. ." J Soc Gynecol Investig **7**(Suppl:220A).
- Cudaback, E., W. Marrs, T. Moeller and N. Stella (2010). "The expression level of CB1 and CB2 receptors determines their efficacy at inducing apoptosis in astrocytomas." PLoS One **5**(1): e8702.
- Curran, S. and G. I. Murray (2000). "Matrix metalloproteinases: molecular aspects of their roles in tumour invasion and metastasis." Eur J Cancer **36**(13 Spec No): 1621-1630.
- Czifra, G., A. Varga, K. Nyeste, R. Marincsak, B. I. Toth, I. Kovacs, L. Kovacs and T. Biro (2009). "Increased expressions of cannabinoid receptor-1 and transient receptor potential vanilloid-1 in human prostate carcinoma." J Cancer Res Clin Oncol **135**(4): 507-514.
- Day, T. A., F. Rakhshan, D. G. Deutsch and E. L. Barker (2001). "Role of fatty acid amide hydrolase in the transport of the endogenous cannabinoid anandamide." Mol Pharmacol **59**(6): 1369-1375.
- De Petrocellis, L., M. G. Cascio and V. Di Marzo (2004). "The endocannabinoid system: a general view and latest additions." Br J Pharmacol **141**(5): 765-774.
- De Petrocellis, L., D. Melck, T. Bisogno and V. Di Marzo (2000). "Endocannabinoids and fatty acid amides in cancer, inflammation and related disorders." Chem Phys Lipids **108**(1-2): 191-209.
- De Petrocellis, L., D. Melck, A. Palmisano, T. Bisogno, C. Laezza, M. Bifulco and V. Di Marzo (1998). "The endogenous cannabinoid anandamide inhibits human breast cancer cell proliferation." Proc Natl Acad Sci U S A **95**(14): 8375-8380.
- DeMorrow, S., S. Glaser, H. Francis, J. Venter, B. Vaculin, S. Vaculin and G. Alpini (2007). "Opposing actions of endocannabinoids on cholangiocarcinoma growth: recruitment of Fas and Fas ligand to lipid rafts." J Biol Chem **282**(17): 13098-13113.
- Devane, W. A., L. Hanus, A. Breuer, R. G. Pertwee, L. A. Stevenson, G. Griffin, D. Gibson, A. Mandelbaum, A. Etinger and R. Mechoulam (1992). "Isolation and structure of a brain constituent that binds to the cannabinoid receptor." Science **258**(5090): 1946-1949.
- DeVita, V. T., Jr. and S. A. Rosenberg (2012). "Two hundred years of cancer research." N Engl J Med **366**(23): 2207-2214.

Dheda, K., J. F. Huggett, J. S. Chang, L. U. Kim, S. A. Bustin, M. A. Johnson, G. A. Rook and A. Zumla (2005). "The implications of using an inappropriate reference gene for real-time reverse transcription PCR data normalization." Anal Biochem **344**(1): 141-143.

Di Marzo, V. (1998). "'Endocannabinoids' and other fatty acid derivatives with cannabimimetic properties: biochemistry and possible physiopathological relevance." Biochim Biophys Acta **1392**(2-3): 153-175.

Di Marzo, V. (2008). "Endocannabinoids: synthesis and degradation." Rev Physiol Biochem Pharmacol **160**: 1-24.

Di Marzo, V., T. Bisogno, T. Sugiura, D. Melck and L. De Petrocellis (1998). "The novel endogenous cannabinoid 2-arachidonoylglycerol is inactivated by neuronal- and basophil-like cells: connections with anandamide." Biochem J **331** (Pt 1): 15-19.

Di Marzo, V., A. Fontana, H. Cadas, S. Schinelli, G. Cimino, J. C. Schwartz and D. Piomelli (1994). "Formation and inactivation of endogenous cannabinoid anandamide in central neurons." Nature **372**(6507): 686-691.

Di Marzo, V., D. Melck, P. Orlando, T. Bisogno, O. Zagoory, M. Bifulco, Z. Vogel and L. De Petrocellis (2001). "Palmitoylethanolamide inhibits the expression of fatty acid amide hydrolase and enhances the anti-proliferative effect of anandamide in human breast cancer cells." Biochem J **358**(Pt 1): 249-255.

Doherty, J. A., K. L. Cushing-Haugen, B. S. Saltzman, L. F. Voigt, D. A. Hill, S. A. Beresford, C. Chen and N. S. Weiss (2007). "Long-term use of postmenopausal estrogen and progestin hormone therapies and the risk of endometrial cancer." Am J Obstet Gynecol **197**(2): 139 e131-137.

Doll, A., M. Abal, M. Rigau, M. Monge, M. Gonzalez, S. Demajo, E. Colas, M. Llauro, H. Alazzouzi, J. Planaguma, M. A. Lohmann, J. Garcia, S. Castellvi, J. Ramon y Cajal, A. Gil-Moreno, J. Xercavins, F. Alameda and J. Reventos (2008). "Novel molecular profiles of endometrial cancer-new light through old windows." J Steroid Biochem Mol Biol **108**(3-5): 221-229.

Domotor, A., Z. Peidl, A. Vincze, B. Hunyady, J. Szolcsanyi, L. Kereskay, G. Szekeres and G. Mozsik (2005). "Immunohistochemical distribution of vanilloid receptor, calcitonin-gene related peptide and substance P in gastrointestinal mucosa of patients with different gastrointestinal disorders." Inflammopharmacology **13**(1-3): 161-177.

Dorsam, R. T. and J. S. Gutkind (2007). "G-protein-coupled receptors and cancer." Nat Rev Cancer **7**(2): 79-94.

Du, X. L., T. Jiang, X. G. Sheng, R. Gao and Q. S. Li (2009). "Inhibition of osteopontin suppresses in vitro and in vivo angiogenesis in endometrial cancer." Gynecol Oncol **115**(3): 371-376.

Edgemon, W. S., C. J. Hillard, J. R. Falck, C. S. Kearn and W. B. Campbell (1998). "Human platelets and polymorphonuclear leukocytes synthesize oxygenated derivatives of arachidonylethanolamide (anandamide): their affinities for cannabinoid receptors and pathways of inactivation." Mol Pharmacol **54**(1): 180-188.

El-Talatini, M. R., A. H. Taylor, J. C. Elson, L. Brown, A. C. Davidson and J. C. Konje (2009). "Localisation and function of the endocannabinoid system in the human ovary." PLoS One **4**(2): e4579.

El-Talatini, M. R., A. H. Taylor and J. C. Konje (2010). "The relationship between plasma levels of the endocannabinoid, anandamide, sex steroids, and gonadotrophins during the menstrual cycle." Fertil Steril **93**(6): 1989-1996.

Ellert-Miklaszewska, A., B. Kaminska and L. Konarska (2005). "Cannabinoids down-regulate PI3K/Akt and Erk signalling pathways and activate proapoptotic function of Bad protein." Cell Signal **17**(1): 25-37.

Endsley, M. P., R. Thill, I. Choudhry, C. L. Williams, A. Kajdacsy-Balla, W. B. Campbell and K. Nithipatikom (2008). "Expression and function of fatty acid amide hydrolase in prostate cancer." Int J Cancer **123**(6): 1318-1326.

Fegley, D., S. Kathuria, R. Mercier, C. Li, A. Goutopoulos, A. Makriyannis and D. Piomelli (2004). "Anandamide transport is independent of fatty-acid amide hydrolase activity and is blocked by the hydrolysis-resistant inhibitor AM1172." Proc Natl Acad Sci U S A **101**(23): 8756-8761.

Ferenczy, A., G. Bertrand and M. M. Gelfand (1979). "Proliferation kinetics of human endometrium during the normal menstrual cycle." Am J Obstet Gynecol **133**(8): 859-867.

Ferlay J, S. H., Bray F, Forman D, Mathers C, Parkin DM (2008) "Cancer Incidence and Mortality Worldwide.GLOBOCAN 2008 v1.2. Cancer Incidence and Mortality Worldwide: IARC CancerBase No. 10 [Internet]. Lyon, France: International Agency for Research on Cancer, 2010. Available from: <http://globocan.iarc.fr>. Accessed May 2011."

Fezza, F., N. Battista, M. Bari and M. Maccarrone (2006). "Methods to assay anandamide hydrolysis and transport in synaptosomes." Methods Mol Med **123**: 163-168.

- Fezza, F., C. De Simone, D. Amadio and M. Maccarrone (2008). "Fatty acid amide hydrolase: a gate-keeper of the endocannabinoid system." Subcell Biochem **49**: 101-132.
- Flygare, J. and B. Sander (2008). "The endocannabinoid system in cancer - Potential therapeutic target?" Seminars in Cancer Biology **18**(3): 176-189.
- Fonseca, B. M., N. Battista, G. Correia-da-Silva, C. Rapino, M. Maccarrone and N. A. Teixeira (2014). "Activity of anandamide (AEA) metabolic enzymes in rat placental bed." Reprod Toxicol **49**: 74-77.
- Ford, L. A., A. J. Roelofs, S. Anavi-Goffer, L. Mowat, D. G. Simpson, A. J. Irving, M. J. Rogers, A. M. Rajnicek and R. A. Ross (2010). "A role for L-alpha-lysophosphatidylinositol and GPR55 in the modulation of migration, orientation and polarization of human breast cancer cells." Br J Pharmacol **160**(3): 762-771.
- Fowler, C. J. (2013). "Transport of endocannabinoids across the plasma membrane and within the cell." FEBS J **280**(9): 1895-1904.
- Fox, H. and D. K. Sen (1970). "A controlled study of the constitutional stigmata of endometrial adenocarcinoma." Br J Cancer **24**(1): 30-36.
- Freimuth, N., R. Ramer and B. Hinz (2010). "Antitumorigenic effects of cannabinoids beyond apoptosis." J Pharmacol Exp Ther **332**(2): 336-344.
- Friberg, E., N. Orsini, C. S. Mantzoros and A. Wolk (2007). "Diabetes mellitus and risk of endometrial cancer: a meta-analysis." Diabetologia **50**(7): 1365-1374.
- Fride, E., T. Bregman and T. C. Kirkham (2005). "Endocannabinoids and food intake: newborn suckling and appetite regulation in adulthood." Exp Biol Med (Maywood) **230**(4): 225-234.
- Fu, J., G. Bottegoni, O. Sasso, R. Bertorelli, W. Rocchia, M. Masetti, A. Guijarro, A. Lodola, A. Armirotti, G. Garau, T. Bandiera, A. Reggiani, M. Mor, A. Cavalli and D. Piomelli (2012). "A catalytically silent FAAH-1 variant drives anandamide transport in neurons." Nat Neurosci **15**(1): 64-69.
- Furberg, A. S. and I. Thune (2003). "Metabolic abnormalities (hypertension, hyperglycemia and overweight), lifestyle (high energy intake and physical inactivity) and endometrial cancer risk in a Norwegian cohort." Int J Cancer **104**(6): 669-676.
- Galve-Roperh, I., C. Sanchez, M. L. Cortes, T. Gomez del Pulgar, M. Izquierdo and M. Guzman (2000). "Anti-tumoral action of cannabinoids: involvement of sustained

ceramide accumulation and extracellular signal-regulated kinase activation." Nat Med **6**(3): 313-319.

Garcia, E., P. Bouchard, J. De Brux, J. Berdah, R. Frydman, G. Schaison, E. Milgrom and M. Perrot-Applanat (1988). "Use of immunocytochemistry of progesterone and estrogen receptors for endometrial dating." J Clin Endocrinol Metab **67**(1): 80-87.

Gasperi, V., R. Ceci, M. Tantimonaco, E. Talamonti, N. Battista, A. Parisi, R. Florio, S. Sabatini, A. Rossi and M. Maccarrone (2014). "The fatty acid amide hydrolase in lymphocytes from sedentary and active subjects." Med Sci Sports Exerc **46**(1): 24-32.

Gattinoni, S., C. De Simone, S. Dallavalle, F. Fezza, R. Nannei, D. Amadio, P. Minetti, G. Quattrociochi, A. Caprioli, F. Borsini, W. Cabri, S. Penco, L. Merlini and M. Maccarrone (2010). "Enol carbamates as inhibitors of fatty acid amide hydrolase (FAAH) endowed with high selectivity for FAAH over the other targets of the endocannabinoid system." ChemMedChem **5**(3): 357-360.

Gebeh, A. K., E. L. Marczylo, A. A. Amoako, J. M. Willets and J. C. Konje (2012). "Variation in stability of endogenous reference genes in fallopian tubes and endometrium from healthy and ectopic pregnant women." Int J Mol Sci **13**(3): 2810-2826.

Gebeh, A. K., J. M. Willets, M. Bari, R. A. Hirst, T. H. Marczylo, A. H. Taylor, M. Maccarrone and J. C. Konje (2013). "Elevated anandamide and related N-acylethanolamine levels occur in the peripheral blood of women with ectopic pregnancy and are mirrored by changes in peripheral fatty acid amide hydrolase activity." J Clin Endocrinol Metab **98**(3): 1226-1234.

Gebeh, A. K., J. M. Willets, E. L. Marczylo, A. H. Taylor and J. C. Konje (2012). "Ectopic pregnancy is associated with high anandamide levels and aberrant expression of FAAH and CB1 in fallopian tubes." J Clin Endocrinol Metab **97**(8): 2827-2835.

Gentilini, D., A. Besana, P. Vigano, P. Dalino, M. Vignali, M. Melandri, M. Busacca and A. M. Di Blasio (2010). "Endocannabinoid system regulates migration of endometrial stromal cells via cannabinoid receptor 1 through the activation of PI3K and ERK1/2 pathways." Fertil Steril **93**(8): 2588-2593.

Gerard, C. M., C. Mollereau, G. Vassart and M. Parmentier (1991). "Molecular cloning of a human cannabinoid receptor which is also expressed in testis." Biochem J **279** (Pt 1): 129-134.

Giang, D. K. and B. F. Cravatt (1997). "Molecular characterization of human and mouse fatty acid amide hydrolases." Proc Natl Acad Sci U S A **94**(6): 2238-2242.

Giuliano, M., O. Pellerito, P. Portanova, G. Calvaruso, A. Santulli, A. De Blasio, R. Vento and G. Tesoriere (2009). "Apoptosis induced in HepG2 cells by the synthetic cannabinoid WIN: involvement of the transcription factor PPARgamma." Biochimie **91**(4): 457-465.

Glass, M., M. Dragunow and R. L. Faull (1997). "Cannabinoid receptors in the human brain: a detailed anatomical and quantitative autoradiographic study in the fetal, neonatal and adult human brain." Neuroscience **77**(2): 299-318.

GLOBOCAN. (2012). "International Agency for Research (IARC)."

Godlewski, G., L. Offertaler, J. A. Wagner and G. Kunos (2009). "Receptors for acylethanolamides-GPR55 and GPR119." Prostaglandins Other Lipid Mediat **89**(3-4): 105-111.

Gomez del Pulgar, T., G. Velasco, C. Sanchez, A. Haro and M. Guzman (2002). "De novo-synthesized ceramide is involved in cannabinoid-induced apoptosis." Biochem J **363**(Pt 1): 183-188.

Gong, J. P., E. S. Onaivi, H. Ishiguro, Q. R. Liu, P. A. Tagliaferro, A. Brusco and G. R. Uhl (2006). "Cannabinoid CB2 receptors: immunohistochemical localization in rat brain." Brain Res **1071**(1): 10-23.

Goparaju, S. K., N. Ueda, K. Taniguchi and S. Yamamoto (1999). "Enzymes of porcine brain hydrolyzing 2-arachidonoylglycerol, an endogenous ligand of cannabinoid receptors." Biochem Pharmacol **57**(4): 417-423.

Goparaju, S. K., N. Ueda, H. Yamaguchi and S. Yamamoto (1998). "Anandamide amidohydrolase reacting with 2-arachidonoylglycerol, another cannabinoid receptor ligand." FEBS Lett **422**(1): 69-73.

Green, S., P. Walter, V. Kumar, A. Krust, J. M. Bornert, P. Argos and P. Chambon (1986). "Human oestrogen receptor cDNA: sequence, expression and homology to v-erb-A." Nature **320**(6058): 134-139.

Grimaldi, C., S. Pisanti, C. Laezza, A. M. Malfitano, A. Santoro, M. Vitale, M. G. Caruso, M. Notarnicola, I. Iacuzzo, G. Portella, V. Di Marzo and M. Bifulco (2006). "Anandamide inhibits adhesion and migration of breast cancer cells." Exp Cell Res **312**(4): 363-373.

Grimsey, N. L., C. E. Goodfellow, E. L. Scotter, M. J. Dowie, M. Glass and E. S. Graham (2008). "Specific detection of CB1 receptors; cannabinoid CB1 receptor antibodies are not all created equal!" J Neurosci Methods **171**(1): 78-86.

Guida, M., A. Ligresti, D. De Filippis, A. D'Amico, S. Petrosino, M. Cipriano, G. Bifulco, S. Simonetti, P. Orlando, L. Insabato, C. Nappi, A. Di Spiezio Sardo, V. Di Marzo and T. Iuvone (2010). "The levels of the endocannabinoid receptor CB2 and its ligand 2-arachidonoylglycerol are elevated in endometrial carcinoma." Endocrinology **151**(3): 921-928.

Guo, Y., H. Wang, Y. Okamoto, N. Ueda, P. J. Kingsley, L. J. Marnett, H. H. Schmid, S. K. Das and S. K. Dey (2005). "N-acylphosphatidylethanolamine-hydrolyzing phospholipase D is an important determinant of uterine anandamide levels during implantation." J Biol Chem **280**(25): 23429-23432.

Gustafsson, K., X. Wang, D. Severa, M. Eriksson, E. Kimby, M. Merup, B. Christensson, J. Flygare and B. Sander (2008). "Expression of cannabinoid receptors type 1 and type 2 in non-Hodgkin lymphoma: growth inhibition by receptor activation." Int J Cancer **123**(5): 1025-1033.

Gustafsson, S. B., T. Lindgren, M. Jonsson and S. O. P. Jacobsson (2009). "Cannabinoid receptor-independent cytotoxic effects of cannabinoids in human colorectal carcinoma cells: synergism with 5-fluorouracil." Cancer Chemotherapy and Pharmacology **63**(4): 691-701.

Guzman, M. (2003). "Cannabinoids: potential anticancer agents." Nat Rev Cancer **3**(10): 745-755.

Guzman, M., C. Sanchez and I. Galve-Roperh (2002). "Cannabinoids and cell fate." Pharmacol Ther **95**(2): 175-184.

Habayeb, O. M., A. H. Taylor, M. D. Evans, M. S. Cooke, D. J. Taylor, S. C. Bell and J. C. Konje (2004). "Plasma levels of the endocannabinoid anandamide in women--a potential role in pregnancy maintenance and labor?" J Clin Endocrinol Metab **89**(11): 5482-5487.

Habayeb, O. M., A. H. Taylor, M. Finney, M. D. Evans and J. C. Konje (2008). "Plasma anandamide concentration and pregnancy outcome in women with threatened miscarriage." JAMA **299**(10): 1135-1136.

Habiba, M. A., S. C. Bell and F. Al-Azzawi (1998). "Endometrial responses to hormone replacement therapy: histological features compared with those of late luteal phase endometrium." Hum Reprod **13**(6): 1674-1682.

Hamtaux, L., L. Hansoulle, N. Dauguet, G. G. Muccioli, B. Gallez and D. M. Lambert (2011). "Increasing antiproliferative properties of endocannabinoids in N1E-115 neuroblastoma cells through inhibition of their metabolism." PLoS One **6**(10): e26823.

- Hansen, H. S. (2010). "Palmitoylethanolamide and other anandamide congeners. Proposed role in the diseased brain." Exp Neurol **224**(1): 48-55.
- Hartel, M., F. F. di Mola, F. Selvaggi, G. Mascetta, M. N. Wenthe, K. Felix, N. A. Giese, U. Hinz, P. Di Sebastiano, M. W. Buchler and H. Friess (2006). "Vanilloids in pancreatic cancer: potential for chemotherapy and pain management." Gut **55**(4): 519-528.
- Hecht, J. L. and G. L. Mutter (2006). "Molecular and pathologic aspects of endometrial carcinogenesis." J Clin Oncol **24**(29): 4783-4791.
- Heid, C. A., J. Stevens, K. J. Livak and P. M. Williams (1996). "Real time quantitative PCR." Genome Res **6**(10): 986-994.
- Hellemans, J., G. Mortier, A. De Paepe, F. Speleman and J. Vandesompele (2007). "qBase relative quantification framework and software for management and automated analysis of real-time quantitative PCR data." Genome Biol **8**(2): R19.
- Henderson, G. S., K. A. Brown, S. L. Perkins, T. M. Abbott and F. Clayton (1996). "bcl-2 is down-regulated in atypical endometrial hyperplasia and adenocarcinoma." Modern Pathology **9**(4): 430-438.
- Hetz, C. A. (2007). "ER stress signaling and the BCL-2 family of proteins: from adaptation to irreversible cellular damage." Antioxid Redox Signal **9**(12): 2345-2355.
- Hillard, C. J., W. S. Edgmond, A. Jarrahan and W. B. Campbell (1997). "Accumulation of N-arachidonylethanolamine (anandamide) into cerebellar granule cells occurs via facilitated diffusion." J Neurochem **69**(2): 631-638.
- Hillard, C. J. and A. Jarrahan (2003). "Cellular accumulation of anandamide: consensus and controversy." Br J Pharmacol **140**(5): 802-808.
- Hinz, B., R. Ramer, K. Eichele, U. Weinzierl and K. Brune (2004). "Up-regulation of cyclooxygenase-2 expression is involved in R(+)-methanandamide-induced apoptotic death of human neuroglioma cells." Mol Pharmacol **66**(6): 1643-1651.
- Ho, W. S., D. A. Barrett and M. D. Randall (2008). "'Entourage' effects of N-palmitoylethanolamide and N-oleoylethanolamide on vasorelaxation to anandamide occur through TRPV1 receptors." Br J Pharmacol **155**(6): 837-846.
- Hu, G., G. Ren and Y. Shi (2011). "The putative cannabinoid receptor GPR55 promotes cancer cell proliferation." Oncogene **30**(2): 139-141.

Huang, S. M., T. Bisogno, M. Trevisani, A. Al-Hayani, L. De Petrocellis, F. Fezza, M. Tognetto, T. J. Petros, J. F. Krey, C. J. Chu, J. D. Miller, S. N. Davies, P. Geppetti, J. M. Walker and V. Di Marzo (2002). "An endogenous capsaicin-like substance with high potency at recombinant and native vanilloid VR1 receptors." Proc Natl Acad Sci U S A **99**(12): 8400-8405.

Jabbour, H. N., R. W. Kelly, H. M. Fraser and H. O. Critchley (2006). "Endocrine regulation of menstruation." Endocr Rev **27**(1): 17-46.

Jacobs, I., A. Gentry-Maharaj, M. Burnell, R. Manchanda, N. Singh, A. Sharma, A. Ryan, M. W Seif, N. N Amso, G. Turner, C. Brunell, G. Fletcher, R. Rangar, K. Ford, K. Godfrey, A. Lopes, D. Oram, J. Herod, K. Williamson, I. Scott, H. Jenkins, T. Mould, R. Woolas, J. Murdoch, S. Dobbs, S. Leeson, D. Cruickshank, S. J Skates, L. Fallowfi eld, M. Parmar, S. Campbell and U.Menon (2011). "Sensitivity of transvaginal ultrasound screening for endometrial cancer in postmenopausal women: a case-control study within the UKCTOCS cohort." Lancet Oncol; 12 (1): 38–48.

Jia, W., V. L. Hegde, N. P. Singh, D. Sisco, S. Grant, M. Nagarkatti and P. S. Nagarkatti (2006). "Delta9-tetrahydrocannabinol-induced apoptosis in Jurkat leukemia T cells is regulated by translocation of Bad to mitochondria." Mol Cancer Res **4**(8): 549-562.

Jick, S. S., A. M. Walker and H. Jick (1993). "Estrogens, progesterone, and endometrial cancer." Epidemiology **4**(1): 20-24.

Jones, S. and J. Howl (2003). "Cannabinoid receptor systems: therapeutic targets for tumour intervention." Expert Opin Ther Targets **7**(6): 749-758.

Joseph, J., B. Niggemann, K. S. Zaenker and F. Entschladen (2004). "Anandamide is an endogenous inhibitor for the migration of tumor cells and T lymphocytes." Cancer Immunol Immunother **53**(8): 723-728.

Judd, H. L. (1976). "Hormonal dynamics associated with the menopause." Clin Obstet Gynecol **19**(4): 775-788.

Jursza, E., D. J. Skarzynski and M. J. Siemieniuch (2014). "Validation of reference genes in the feline endometrium." Reprod Biol **14**(4): 302-306.

Kaaks, R., A. Lukanova and M. S. Kurzer (2002). "Obesity, endogenous hormones, and endometrial cancer risk: a synthetic review." Cancer Epidemiol Biomarkers Prev **11**(12): 1531-1543.

Kaczocha, M., S. T. Glaser, J. Chae, D. A. Brown and D. G. Deutsch (2010). "Lipid droplets are novel sites of N-acylethanolamine inactivation by fatty acid amide hydrolase-2." J Biol Chem **285**(4): 2796-2806.

Kaczocha, M., S. T. Glaser and D. G. Deutsch (2009). "Identification of intracellular carriers for the endocannabinoid anandamide." Proc Natl Acad Sci U S A **106**(15): 6375-6380.

Kalogris, C., S. Caprodossi, C. Amantini, F. Lambertucci, M. Nabissi, M. B. Morelli, V. Farfariello, A. Filosa, M. C. Emiliozzi, G. Mammana and G. Santoni (2010). "Expression of transient receptor potential vanilloid-1 (TRPV1) in urothelial cancers of human bladder: relation to clinicopathological and molecular parameters." Histopathology **57**(5): 744-752.

Karasu, T. (2012). "The Role of the Endocannabinoid System in the Fertility Control". PhD Thesis, University of Leicester, UK.

Karasu, T., T. H. Marczylo, M. Maccarrone and J. C. Konje (2011). "The role of sex steroid hormones, cytokines and the endocannabinoid system in female fertility." Hum Reprod Update **17**(3): 347-361.

Karasu, T., T. H. Marczylo, E. L. Marczylo, A. H. Taylor, E. Oloto and J. C. Konje (2014). "The effect of mifepristone (RU486) on the endocannabinoid system in human plasma and first-trimester trophoblast of women undergoing termination of pregnancy." J Clin Endocrinol Metab **99**(3): 871-880.

Kashima, H., T. Shiozawa, T. Miyamoto, A. Suzuki, J. Uchikawa, M. Kurai and I. Konishi (2009). "Autocrine stimulation of IGF1 in estrogen-induced growth of endometrial carcinoma cells: involvement of the mitogen-activated protein kinase pathway followed by up-regulation of cyclin D1 and cyclin E." Endocr Relat Cancer **16**(1): 113-122.

Katayama, K., N. Ueda, Y. Kurahashi, H. Suzuki, S. Yamamoto and I. Kato (1997). "Distribution of anandamide amidohydrolase in rat tissues with special reference to small intestine." Biochimica Et Biophysica Acta-Lipids and Lipid Metabolism: 212-218.

Kerr, J. F., A. H. Wyllie and A. R. Currie (1972). "Apoptosis: a basic biological phenomenon with wide-ranging implications in tissue kinetics." Br J Cancer **26**(4): 239-257.

Khandekar, M. J., P. Cohen and B. M. Spiegelman (2011). "Molecular mechanisms of cancer development in obesity." Nat Rev Cancer **11**(12): 886-895.

Kim, J. D., J. M. Kim, J. O. Pyo, S. Y. Kim, B. S. Kim, R. Yu and I. S. Han (1997). "Capsaicin can alter the expression of tumor forming-related genes which might be

followed by induction of apoptosis of a Korean stomach cancer cell line, SNU-1." Cancer Lett **120**(2): 235-241.

Kisgeropoulos, E. (2013). Inhibition of ovarian cancer cell proliferation by oleoylethanolamide and its metabolically stable analog AM3102, Kent State University Honors College.

Knab, D. R. (1977). "Estrogen and endometrial carcinoma." Obstet Gynecol Surv **32**(5): 267-281.

Kogan, N. M. (2005). "Cannabinoids and cancer." Mini Rev Med Chem **5**(10): 941-952.

Kohno, M., H. Hasegawa, A. Inoue, M. Muraoka, T. Miyazaki, K. Oka and M. Yasukawa (2006). "Identification of N-arachidonylglycine as the endogenous ligand for orphan G-protein-coupled receptor GPR18." Biochem Biophys Res Commun **347**(3): 827-832.

Kokawa, K., T. Shikone, T. Otani, R. Nishiyama, Y. Ishii, S. Yagi and M. Yamoto (2001). "Apoptosis and the expression of Bax and Bcl-2 in hyperplasia and adenocarcinoma of the uterine endometrium." Hum Reprod **16**(10): 2211-2218.

Kokawa, K., T. Shikone, T. Otani, R. Nishiyama, Y. Ishii, S. Yagi and M. Yamoto (2001). "Apoptosis and the expression of Bcl-2 and Bax in patients with endometrioid, clear cell, and serous carcinomas of the uterine endometrium." Gynecologic Oncology **81**(2): 178-183.

Kondo, S., H. Kondo, S. Nakane, T. Kodaka, A. Tokumura, K. Waku and T. Sugiura (1998). "2-Arachidonoylglycerol, an endogenous cannabinoid receptor agonist: identification as one of the major species of monoacylglycerols in various rat tissues, and evidence for its generation through CA²⁺-dependent and -independent mechanisms." FEBS Lett **429**(2): 152-156.

Konstantinos, K., S. Marios, M. Anna, K. Nikolaos, P. Efstratios and A. Paulina (2013). "Expression of ki-67 as proliferation biomarker in imprint smears of endometrial carcinoma." Diagnostic Cytopathology **41**(3): 212-217.

Kounelis, S., N. Kapranos, E. Kouri, D. Coppola, H. Papadaki and M. W. Jones (2000). "Immunohistochemical profile of endometrial adenocarcinoma: A study of 61 cases and review of the literature." Modern Pathology **13**(4): 379-388.

Kozak, K. R. and L. J. Marnett (2002). "Oxidative metabolism of endocannabinoids." Prostaglandins Leukot Essent Fatty Acids **66**(2-3): 211-220.

- Kozak, K. R., S. W. Rowlinson and L. J. Marnett (2000). "Oxygenation of the endocannabinoid, 2-arachidonylglycerol, to glyceryl prostaglandins by cyclooxygenase-2." J Biol Chem **275**(43): 33744-33749.
- Krizanova, O., I. Steliarova, L. Csaderova, M. Pastorek and S. Hudecova (2014). "Capsaicin induces apoptosis in PC12 cells through ER stress." Oncol Rep **31**(2): 581-588.
- Kubista, M., J. M. Andrade, M. Bengtsson, A. Forootan, J. Jonak, K. Lind, R. Sindelka, R. Sjoback, B. Sjogreen, L. Strombom, A. Stahlberg and N. Zoric (2006). "The real-time polymerase chain reaction." Mol Aspects Med **27**(2-3): 95-125.
- Laezza, C., S. Pisanti, E. Crescenzi and M. Bifulco (2006). "Anandamide inhibits Cdk2 and activates Chk1 leading to cell cycle arrest in human breast cancer cells." FEBS Lett **580**(26): 6076-6082.
- Lam, P. M., T. H. Marczylo, M. El-Talatini, M. Finney, V. Nallendran, A. H. Taylor and J. C. Konje (2008). "Ultra performance liquid chromatography tandem mass spectrometry method for the measurement of anandamide in human plasma." Anal Biochem **380**(2): 195-201.
- Lam, P. M., T. H. Marczylo and J. C. Konje (2010). "Simultaneous measurement of three N-acylethanolamides in human bio-matrices using ultra performance liquid chromatography-tandem mass spectrometry." Anal Bioanal Chem **398**(5): 2089-2097.
- Lambert, D. M. and C. J. Fowler (2005). "The endocannabinoid system: drug targets, lead compounds, and potential therapeutic applications." J Med Chem **48**(16): 5059-5087.
- Lambert, D. M., S. Vandevoorde, K. O. Jonsson and C. J. Fowler (2002). "The palmitoylethanolamide family: a new class of anti-inflammatory agents?" Curr Med Chem **9**(6): 663-674.
- Larrinaga, G., B. Sanz, L. Blanco, I. Perez, M. L. Candenias, F. M. Pinto, A. Irazusta, J. Gil and J. I. Lopez (2013). "Cannabinoid CB1 receptor is expressed in chromophobe renal cell carcinoma and renal oncocytoma." Clin Biochem **46**(7-8): 638-641.
- Lax, S. F., B. Kendall, H. Tashiro, R. J. Slebos and L. Hedrick (2000). "The frequency of p53, K-ras mutations, and microsatellite instability differs in uterine endometrioid and serous carcinoma: evidence of distinct molecular genetic pathways." Cancer **88**(4): 814-824.

Leconte, M., C. Nicco, C. Ngo, S. Arkwright, C. Chereau, J. Guibourdenche, B. Weill, C. Chapron, B. Dousset and F. Batteux (2010). "Antiproliferative effects of cannabinoid agonists on deep infiltrating endometriosis." Am J Pathol **177**(6): 2963-2970.

Lessey, B. A., A. P. Killam, D. A. Metzger, A. F. Haney, G. L. Greene and K. S. McCarty, Jr. (1988). "Immunohistochemical analysis of human uterine estrogen and progesterone receptors throughout the menstrual cycle." J Clin Endocrinol Metab **67**(2): 334-340.

Lewis-Wambi, J. S. and V. C. Jordan (2009). "Estrogen regulation of apoptosis: how can one hormone stimulate and inhibit?" Breast Cancer Res **11**(3): 206.

Ligresti, A., T. Bisogno, I. Matias, L. De Petrocellis, M. Cascio, V. Cosenza, G. D'Argenio, G. Scaglione, M. Bifulco, I. Sorrentini and V. Di Marzo (2003). "Possible endocannabinoid control of colorectal cancer growth." Gastroenterology **125**(3): 677-687.

Ligresti, A., E. Morera, M. Van Der Stelt, K. Monory, B. Lutz, G. Ortar and V. Di Marzo (2004). "Further evidence for the existence of a specific process for the membrane transport of anandamide." Biochem J **380**(Pt 1): 265-272.

Ligresti, A., A. S. Moriello, K. Starowicz, I. Matias, S. Pisanti, L. De Petrocellis, C. Laezza, G. Portella, M. Bifulco and V. Di Marzo (2006). "Antitumor activity of plant cannabinoids with emphasis on the effect of cannabidiol on human breast carcinoma." J Pharmacol Exp Ther **318**(3): 1375-1387.

Lin, C. H., W. C. Lu, C. W. Wang, Y. C. Chan and M. K. Chen (2013). "Capsaicin induces cell cycle arrest and apoptosis in human KB cancer cells." Bmc Complementary and Alternative Medicine **13**.

Linsalata, M., M. Notarnicola, V. Tutino, M. Bifulco, A. Santoro, C. Laezza, C. Messa, A. Orlando and M. G. Caruso (2010). "Effects of anandamide on polyamine levels and cell growth in human colon cancer cells." Anticancer Res **30**(7): 2583-2589.

Liu, J., B. Gao, F. Mirshahi, A. J. Sanyal, A. D. Khanolkar, A. Makriyannis and G. Kunos (2000). "Functional CB1 cannabinoid receptors in human vascular endothelial cells." Biochem J **346 Pt 3**: 835-840.

Liu, J., L. Wang, J. Harvey-White, B. X. Huang, H. Y. Kim, S. Luquet, R. D. Palmiter, G. Krystal, R. Rai, A. Mahadevan, R. K. Razdan and G. Kunos (2008). "Multiple pathways involved in the biosynthesis of anandamide." Neuropharmacology **54**(1): 1-7.

Liu, J., L. Wang, J. Harvey-White, D. Osei-Hyiaman, R. Razdan, Q. Gong, A. C. Chan, Z. Zhou, B. X. Huang, H. Y. Kim and G. Kunos (2006). "A biosynthetic pathway for anandamide." Proc Natl Acad Sci U S A **103**(36): 13345-13350.

LoVerme, J., G. La Rana, R. Russo, A. Calignano and D. Piomelli (2005). "The search for the palmitoylethanolamide receptor." Life Sci **77**(14): 1685-1698.

LoVerme, J., R. Russo, G. La Rana, J. Fu, J. Farthing, G. Mattace-Raso, R. Meli, A. Hohmann, A. Calignano and D. Piomelli (2006). "Rapid broad-spectrum analgesia through activation of peroxisome proliferator-activated receptor-alpha." J Pharmacol Exp Ther **319**(3): 1051-1061.

Lu, H. F., Y. L. Chen, J. S. Yang, Y. Y. Yang, J. Y. Liu, S. C. Hsu, K. C. Lai and J. G. Chung (2010). "Antitumor activity of capsaicin on human colon cancer cells in vitro and colo 205 tumor xenografts in vivo." J Agric Food Chem **58**(24): 12999-13005.

Lutz, B. (2002). "Molecular biology of cannabinoid receptors." Prostaglandins Leukot Essent Fatty Acids **66**(2-3): 123-142.

Maccarrone, M. (2009). "Endocannabinoids: friends and foes of reproduction." Prog Lipid Res **48**(6): 344-354.

Maccarrone, M., M. Bari, T. Lorenzon, T. Bisogno, V. Di Marzo and A. Finazzi-Agro (2000). "Anandamide uptake by human endothelial cells and its regulation by nitric oxide." J Biol Chem **275**(18): 13484-13492.

Maccarrone, M., T. Bisogno, H. Valensise, N. Lazzarin, F. Fezza, C. Manna, V. Di Marzo and A. Finazzi-Agro (2002). "Low fatty acid amide hydrolase and high anandamide levels are associated with failure to achieve an ongoing pregnancy after IVF and embryo transfer." Mol Hum Reprod **8**(2): 188-195.

Maccarrone, M., E. Dainese and S. Oddi (2010). "Intracellular trafficking of anandamide: new concepts for signaling." Trends Biochem Sci **35**(11): 601-608.

Maccarrone, M. and A. Finazzi-Agro (2002). "Endocannabinoids and their actions." Vitam Horm **65**: 225-255.

Maccarrone, M., T. Lorenzon, M. Bari, G. Melino and A. Finazzi-Agro (2000). "Anandamide induces apoptosis in human cells via vanilloid receptors. Evidence for a protective role of cannabinoid receptors." J Biol Chem **275**(41): 31938-31945.

Maccarrone, M., M. Ranalli, L. Bellincampi, M. L. Salucci, S. Sabatini, G. Melino and A. Finazzi-Agro (2000). "Activation of different lipoxygenase isozymes induces apoptosis in human erythroleukemia and neuroblastoma cells." Biochem Biophys Res Commun **272**(2): 345-350.

Maccarrone, M., H. Valensise, M. Bari, N. Lazzarin, C. Romanini and A. Finazzi-Agro (2000). "Relation between decreased anandamide hydrolase concentrations in human lymphocytes and miscarriage." Lancet **355**(9212): 1326-1329.

Maccarrone, M., H. Valensise, M. Bari, N. Lazzarin, C. Romanini and A. Finazzi-Agro (2001). "Progesterone up-regulates anandamide hydrolase in human lymphocytes: role of cytokines and implications for fertility." J Immunol **166**(12): 7183-7189.

Maccarrone, M., M. van der Stelt, A. Rossi, G. A. Veldink, J. F. Vliegthart and A. F. Agro (1998). "Anandamide hydrolysis by human cells in culture and brain." J Biol Chem **273**(48): 32332-32339.

Macho, A., M. V. Blazquez, P. Navas and E. Munoz (1998). "Induction of apoptosis by vanilloid compounds does not require de novo gene transcription and activator protein 1 activity." Cell Growth Differ **9**(3): 277-286.

Macho, A., M. A. Calzado, J. Munoz-Blanco, C. Gomez-Diaz, C. Gajate, F. Mollinedo, P. Navas and E. Munoz (1999). "Selective induction of apoptosis by capsaicin in transformed cells: the role of reactive oxygen species and calcium." Cell Death Differ **6**(2): 155-165.

Macho, A., C. Lucena, M. A. Calzado, M. Blanco, I. Donnay, G. Appendino and E. Munoz (2000). "Phorboid 20-homovanillates induce apoptosis through a VR1-independent mechanism." Chem Biol **7**(7): 483-492.

Mackie, K. and N. Stella (2006). "Cannabinoid receptors and endocannabinoids: evidence for new players." AAPS J **8**(2): E298-306.

Mailleux, P., M. Parmentier and J. J. Vanderhaeghen (1992). "Distribution of cannabinoid receptor messenger RNA in the human brain: an in situ hybridization histochemistry with oligonucleotides." Neurosci Lett **143**(1-2): 200-204.

Marczylo, T. H., P. M. Lam, A. A. Amoako and J. C. Konje (2010). "Anandamide levels in human female reproductive tissues: solid-phase extraction and measurement by ultraperformance liquid chromatography tandem mass spectrometry." Anal Biochem **400**(2): 155-162.

Marczylo, T. H., P. M. Lam, V. Nallendran, A. H. Taylor and J. C. Konje (2009). "A solid-phase method for the extraction and measurement of anandamide from multiple human biomatrices." Anal Biochem **384**(1): 106-113.

Marincsak, R., B. I. Toth, G. Czifra, I. Marton, P. Redl, I. Tar, L. Toth, L. Kovacs and T. Biro (2009). "Increased expression of TRPV1 in squamous cell carcinoma of the human tongue." Oral Diseases **15**(5): 328-335.

Marincsak, R., B. I. Toth, G. Czifra, I. Marton, P. Redl, I. Tar, L. Toth, L. Kovacs and T. Biro (2009). "Increased expression of TRPV1 in squamous cell carcinoma of the human tongue." Oral Dis **15**(5): 328-335.

Matias, I. and V. Di Marzo (2006). "Endocannabinoid synthesis and degradation, and their regulation in the framework of energy balance." J Endocrinol Invest **29**(3 Suppl): 15-26.

Matias, I., M. P. Gonthier, S. Petrosino, L. Docimo, R. Capasso, L. Hoareau, P. Monteleone, R. Roche, A. A. Izzo and V. Di Marzo (2007). "Role and regulation of acylethanolamides in energy balance: focus on adipocytes and beta-cells." Br J Pharmacol **152**(5): 676-690.

Matsuda, L. A., S. J. Lolait, M. J. Brownstein, A. C. Young and T. I. Bonner (1990). "Structure of a cannabinoid receptor and functional expression of the cloned cDNA." Nature **346**(6284): 561-564.

Matsuzaki, S., T. Fukaya, T. Suzuki, T. Murakami, H. Sasano and A. Yajima (1999). "Oestrogen receptor alpha and beta mRNA expression in human endometrium throughout the menstrual cycle." Mol Hum Reprod **5**(6): 559-564.

McAllister, S. D., C. Chan, R. J. Taft, T. Luu, M. E. Abood, D. H. Moore, K. Aldape and G. Yount (2005). "Cannabinoids selectively inhibit proliferation and induce death of cultured human glioblastoma multiforme cells." J Neurooncol **74**(1): 31-40.

McAllister, S. D., L. Soroceanu and P. Y. Desprez (2015). "The Antitumor Activity of Plant-Derived Non-Psychoactive Cannabinoids." J Neuroimmune Pharmacol **10**(2): 255-267.

McFarland, M. J. and E. L. Barker (2004). "Anandamide transport." Pharmacol Ther **104**(2): 117-135.

McHugh, D., J. Page, E. Dunn and H. B. Bradshaw (2012). "Delta(9) - Tetrahydrocannabinol and N-arachidonyl glycine are full agonists at GPR18 receptors and induce migration in human endometrial HEC-1B cells." Br J Pharmacol **165**(8): 2414-2424.

McKallip, R. J., M. Nagarkatti and P. S. Nagarkatti (2005). "Delta-9-tetrahydrocannabinol enhances breast cancer growth and metastasis by suppression of the antitumor immune response." J Immunol **174**(6): 3281-3289.

McKinney, M. K. and B. F. Cravatt (2005). "Structure and function of fatty acid amide hydrolase." Annu Rev Biochem **74**: 411-432.

McPartland, J. M., I. Matias, V. Di Marzo and M. Glass (2006). "Evolutionary origins of the endocannabinoid system." Gene **370**: 64-74.

McPherson, C. P., T. A. Sellers, J. D. Potter, R. M. Bostick and A. R. Folsom (1996). "Reproductive factors and risk of endometrial cancer. The Iowa Women's Health Study." Am J Epidemiol **143**(12): 1195-1202.

Mechoulam, R., S. Ben-Shabat, L. Hanus, M. Ligumsky, N. E. Kaminski, A. R. Schatz, A. Gopher, S. Almog, B. R. Martin, D. R. Compton and et al. (1995). "Identification of an endogenous 2-monoglyceride, present in canine gut, that binds to cannabinoid receptors." Biochem Pharmacol **50**(1): 83-90.

Mehasseb, M. K., R. Panchal, A. H. Taylor, L. Brown, S. C. Bell and M. Habiba (2011). "Estrogen and progesterone receptor isoform distribution through the menstrual cycle in uteri with and without adenomyosis." Fertil Steril **95**(7): 2228-2235, 2235 e2221.

Melck, D., L. De Petrocellis, P. Orlando, T. Bisogno, C. Laezza, M. Bifulco and V. Di Marzo (2000). "Suppression of nerve growth factor Trk receptors and prolactin receptors by endocannabinoids leads to inhibition of human breast and prostate cancer cell proliferation." Endocrinology **141**(1): 118-126.

Melck, D., D. Rueda, I. Galve-Roperh, L. De Petrocellis, M. Guzman and V. Di Marzo (1999). "Involvement of the cAMP/protein kinase A pathway and of mitogen-activated protein kinase in the anti-proliferative effects of anandamide in human breast cancer cells." FEBS Lett **463**(3): 235-240.

Messeguer, A., R. Planells-Cases and A. Ferrer-Montiel (2006). "Physiology and pharmacology of the vanilloid receptor." Curr Neuropharmacol **4**(1): 1-15.

Michalski, C. W., F. E. Oti, M. Erkan, D. Saulitmaite, F. Bergmann, P. Pacher, S. Batkai, M. W. Muller, N. A. Giese, H. Friess and J. Kleeff (2008). "Cannabinoids in pancreatic cancer: Correlation with survival and pain." International Journal of Cancer **122**(4): 742-750.

Mills, A. M. and T. A. Longacre (2010). "Endometrial hyperplasia." Semin Diagn Pathol **27**(4): 199-214.

Mimeault, M., N. Pommery, N. Watez, C. Bailly and J. P. Henichart (2003). "Anti-proliferative and apoptotic effects of anandamide in human prostatic cancer cell lines: implication of epidermal growth factor receptor down-regulation and ceramide production." Prostate **56**(1): 1-12.

Miyashita, T., S. Krajewski, M. Krajewska, H. G. Wang, H. K. Lin, D. A. Liebermann, B. Hoffman and J. C. Reed (1994). "Tumor suppressor p53 is a regulator of bcl-2 and bax gene expression in vitro and in vivo." Oncogene **9**(6): 1799-1805.

- Molina-Holgado, E., J. M. Vela, A. Arevalo-Martin, G. Almazan, F. Molina-Holgado, J. Borrell and C. Guaza (2002). "Cannabinoids promote oligodendrocyte progenitor survival: involvement of cannabinoid receptors and phosphatidylinositol-3 kinase/Akt signaling." J Neurosci **22**(22): 9742-9753.
- Mollerstrom, G., K. Carlstrom, A. Lagrelorius and N. Einhorn (1993). "Is there an altered steroid profile in patients with endometrial carcinoma?" Cancer **72**(1): 173-181.
- Morre, D. J., P. J. Chueh and D. M. Morre (1995). "Capsaicin inhibits preferentially the NADH oxidase and growth of transformed cells in culture." Proc Natl Acad Sci U S A **92**(6): 1831-1835.
- Morre, D. J., E. Sun, C. Geilen, L. Y. Wu, R. de Cabo, K. Krasagakis, C. E. Orfanos and D. M. Morre (1996). "Capsaicin inhibits plasma membrane NADH oxidase and growth of human and mouse melanoma lines." Eur J Cancer **32A**(11): 1995-2003.
- Movahed, P., B. A. Jonsson, B. Birnir, J. A. Wingstrand, T. D. Jorgensen, A. Ermund, O. Sterner, P. M. Zygmunt and E. D. Hogestatt (2005). "Endogenous unsaturated C18 N-acyl ethanolamines are vanilloid receptor (TRPV1) agonists." J Biol Chem **280**(46): 38496-38504.
- Movsesyan, V. A., B. A. Stoica, A. G. Yakovlev, S. M. Knoblach, P. M. t. Lea, I. Cernak, R. Vink and A. I. Faden (2004). "Anandamide-induced cell death in primary neuronal cultures: role of calpain and caspase pathways." Cell Death Differ **11**(10): 1121-1132.
- Muccioli, G. G. (2010). "Endocannabinoid biosynthesis and inactivation, from simple to complex." Drug Discov Today **15**(11-12): 474-483.
- Munro, S., K. L. Thomas and M. Abu-Shaar (1993). "Molecular characterization of a peripheral receptor for cannabinoids." Nature **365**(6441): 61-65.
- Murataeva, N., A. Straiker and K. Mackie (2014). "Parsing the players: 2-arachidonoylglycerol synthesis and degradation in the CNS." Br J Pharmacol **171**(6): 1379-1391.
- Mutter, G. L., M. C. Lin, J. T. Fitzgerald, J. B. Kum, J. P. Baak, J. A. Lees, L. P. Weng and C. Eng (2000). "Altered PTEN expression as a diagnostic marker for the earliest endometrial precancers." J Natl Cancer Inst **92**(11): 924-930.
- Nabissi, M., M. B. Morelli, M. Santoni and G. Santoni (2013). "Triggering of the TRPV2 channel by cannabidiol sensitizes glioblastoma cells to cytotoxic chemotherapeutic agents." Carcinogenesis **34**(1): 48-57.

Naccarato, M., D. Pizzuti, S. Petrosino, M. Simonetto, L. Ferigo, F. C. Grandi, G. Pizzolato and V. Di Marzo (2010). "Possible Anandamide and Palmitoylethanolamide involvement in human stroke." Lipids Health Dis **9**: 47.

Nagamani, M., E. V. Hannigan, E. A. Dillard, Jr. and T. Van Dinh (1986). "Ovarian steroid secretion in postmenopausal women with and without endometrial cancer." J Clin Endocrinol Metab **62**(3): 508-512.

Nassar, A., C. Cohen, S. S. Agersborg, W. Zhou, K. A. Lynch, E. R. Heyman, A. Olson, H. Lange and M. T. Siddiqui (2011). "A new immunohistochemical ER/PR image analysis system: a multisite performance study." Appl Immunohistochem Mol Morphol **19**(3): 195-202.

NCI. (2014). "National Cancer Institute "Defining Cancer"." 2014.

Niemann, T. H., T. L. Trgovac, V. R. McGaughy and L. Vaccarello (1996). "bcl-2 expression in endometrial hyperplasia and carcinoma." Gynecol Oncol **63**(3): 318-322.

Nithipatikom, K., M. P. Endsley, M. A. Isbell, J. R. Falck, Y. Iwamoto, C. J. Hillard and W. B. Campbell (2004). "2-arachidonoylglycerol: A novel inhibitor of androgen-independent prostate cancer cell invasion." Cancer Research **64**(24): 8826-8830.

Nomura, D. K., J. Z. Long, S. Niessen, H. S. Hoover, S. W. Ng and B. F. Cravatt (2010). "Monoacylglycerol lipase regulates a fatty acid network that promotes cancer pathogenesis." Cell **140**(1): 49-61.

NormFinder (2005). *NormFinder*. Aarhus University Hospital: Aarhus, Denmark.

Noto, H., K. Osame, T. Sasazuki and M. Noda (2010). "Substantially increased risk of cancer in patients with diabetes mellitus: a systematic review and meta-analysis of epidemiologic evidence in Japan." J Diabetes Complications **24**(5): 345-353.

Oka, S., S. Kimura, T. Toshida, R. Ota, A. Yamashita and T. Sugiura (2010). "Lysophosphatidylinositol induces rapid phosphorylation of p38 mitogen-activated protein kinase and activating transcription factor 2 in HEK293 cells expressing GPR55 and IM-9 lymphoblastoid cells." J Biochem **147**(5): 671-678.

Oka, S., K. Nakajima, A. Yamashita, S. Kishimoto and T. Sugiura (2007). "Identification of GPR55 as a lysophosphatidylinositol receptor." Biochem Biophys Res Commun **362**(4): 928-934.

Okamoto, A., Y. Sameshima, Y. Yamada, S. Teshima, Y. Terashima, M. Terada and J. Yokota (1991). "Allelic loss on chromosome 17p and p53 mutations in human endometrial carcinoma of the uterus." Cancer Res **51**(20): 5632-5635.

Okamoto, Y., J. Morishita, K. Tsuboi, T. Tonai and N. Ueda (2004). "Molecular characterization of a phospholipase D generating anandamide and its congeners." J Biol Chem **279**(7): 5298-5305.

Okuda, T., A. Sekizawa, Y. Purwosunu, M. Nagatsuka, M. Morioka, M. Hayashi and T. Okai (2010). "Genetics of endometrial cancers." Obstet Gynecol Int **2010**: 984013.

Okulicz, W. C. (2002). Regeneration. London., Taylor and Francis.

Okuno, T. and T. Yokomizo (2011). "What is the natural ligand of GPR55?" Journal of Biochemistry **149**(5): 495-497.

Okuno, T. and T. Yokomizo (2011). "What is the natural ligand of GPR55?" J Biochem **149**(5): 495-497.

Oltvai, Z. N., C. L. Milliman and S. J. Korsmeyer (1993). "Bcl-2 heterodimerizes in vivo with a conserved homolog, Bax, that accelerates programmed cell death." Cell **74**(4): 609-619.

Ortega-Gutierrez, S., E. G. Hawkins, A. Viso, M. L. Lopez-Rodriguez and B. F. Cravatt (2004). "Comparison of anandamide transport in FAAH wild-type and knockout neurons: evidence for contributions by both FAAH and the CB1 receptor to anandamide uptake." Biochemistry **43**(25): 8184-8190.

Otsuki, Y., O. Misaki, O. Sugimoto, Y. Ito, Y. Tsujimoto and Y. Akao (1994). "Cyclic bcl-2 gene expression in human uterine endometrium during menstrual cycle." Lancet **344**(8914): 28-29.

Pacak, K., M. Sirova, A. Giubellino, L. Lencesova, L. Csaderova, M. Laukova, S. Hudecova and O. Krizanova (2012). "NF-kappaB inhibition significantly upregulates the norepinephrine transporter system, causes apoptosis in pheochromocytoma cell lines and prevents metastasis in an animal model." Int J Cancer **131**(10): 2445-2455.

Pacher, P., S. Batkai and G. Kunos (2006). "The endocannabinoid system as an emerging target of pharmacotherapy." Pharmacol Rev **58**(3): 389-462.

Padykula, H. A. (1989). Regeneration in the primate uterus: the role of stem cells. New York, Plenum Press.

Pagotto, U., G. Marsicano, F. Fezza, M. Theodoropoulou, Y. Grubler, J. Stalla, T. Arzberger, A. Milone, M. Losa, V. Di Marzo, B. Lutz and G. Stalla (2001). "Normal

human pituitary gland and pituitary adenomas express cannabinoid receptor type 1 and synthesize endogenous cannabinoids: First evidence for a direct role of cannabinoids on hormone modulation at the human pituitary level." Journal of Clinical Endocrinology & Metabolism **86**(6): 2687-2696.

Papageorgiou, I., P. K. Nicholls, F. Wang, M. Lackmann, Y. Makanji, L. A. Salamonsen, D. M. Robertson and C. A. Harrison (2009). "Expression of nodal signalling components in cycling human endometrium and in endometrial cancer." Reprod Biol Endocrinol **7**: 122.

Park, S. H., H. Kim and B. J. Song (2002). "Down regulation of bcl2 expression in invasive ductal carcinomas is both estrogen- and progesterone-receptor dependent and associated with poor prognostic factors." Pathol Oncol Res **8**(1): 26-30.

Parolaro, D., P. Massi, T. Rubino and E. Monti (2002). "Endocannabinoids in the immune system and cancer." Prostaglandins Leukot Essent Fatty Acids **66**(2-3): 319-332.

Patsos, H. A., D. J. Hicks, A. Greenhough, A. C. Williams and C. Paraskeva (2005). "Cannabinoids and cancer: potential for colorectal cancer therapy." Biochem Soc Trans **33**(Pt 4): 712-714.

Pecorelli, S. (2009). "Revised FIGO staging for carcinoma of the vulva, cervix, and endometrium." Int J Gynaecol Obstet **105**(2): 103-104.

Pellerito, O., A. Notaro, S. Sabella, A. De Blasio, R. Vento, G. Calvaruso and M. Giuliano (2014). "WIN induces apoptotic cell death in human colon cancer cells through a block of autophagic flux dependent on PPARgamma down-regulation." Apoptosis **19**(6): 1029-1042.

Penna, I., S. Vella, A. Gigoni, C. Russo, R. Cancedda and A. Pagano (2011). "Selection of candidate housekeeping genes for normalization in human postmortem brain samples." Int J Mol Sci **12**(9): 5461-5470.

Perez-Gomez, E., C. Andradas, J. M. Flores, M. Quintanilla, J. M. Paramio, M. Guzman and C. Sanchez (2013). "The orphan receptor GPR55 drives skin carcinogenesis and is upregulated in human squamous cell carcinomas." Oncogene **32**(20): 2534-2542.

Perlman, H., X. Zhang, M. W. Chen, K. Walsh and R. Buttyan (1999). "An elevated bax/bcl-2 ratio corresponds with the onset of prostate epithelial cell apoptosis." Cell Death Differ **6**(1): 48-54.

Pertwee, R. G. (2001). "Cannabinoid receptors and pain." Prog Neurobiol **63**(5): 569-611.

Pertwee, R. G. (2005). "Pharmacological actions of cannabinoids." Handb Exp Pharmacol(168): 1-51.

Pertwee, R. G., A. C. Howlett, M. E. Abood, S. P. Alexander, V. Di Marzo, M. R. Elphick, P. J. Greasley, H. S. Hansen, G. Kunos, K. Mackie, R. Mechoulam and R. A. Ross (2010). "International Union of Basic and Clinical Pharmacology. LXXIX. Cannabinoid receptors and their ligands: beyond CB(1) and CB(2)." Pharmacol Rev **62**(4): 588-631.

Petersen, G., B. Moesgaard, P. C. Schmid, H. H. O. Schmid, H. Broholm, M. Kosteljanetz and H. S. Hansen (2005). "Endocannabinoid metabolism in human glioblastomas and meningiomas compared to human non-tumour brain tissue." Journal of Neurochemistry **93**(2): 299-309.

Petrosino, S. and V. Di Marzo (2010). "FAAH and MAGL inhibitors: therapeutic opportunities from regulating endocannabinoid levels." Curr Opin Investig Drugs **11**(1): 51-62.

Pfaffl, M. W., A. Tichopad, C. Prgomet and T. P. Neuvians (2004). "Determination of stable housekeeping genes, differentially regulated target genes and sample integrity: BestKeeper--Excel-based tool using pair-wise correlations." Biotechnol Lett **26**(6): 509-515.

Pineiro, R., T. Maffucci and M. Falasca (2011). "The putative cannabinoid receptor GPR55 defines a novel autocrine loop in cancer cell proliferation." Oncogene **30**(2): 142-152.

Pinto, F., C. C. Pacheco, D. Ferreira, P. Moradas-Ferreira and P. Tamagnini (2012). "Selection of suitable reference genes for RT-qPCR analyses in cyanobacteria." PLoS One **7**(4): e34983.

Pisanti, S., P. Picardi, A. D'Alessandro, C. Laezza and M. Bifulco (2013). "The endocannabinoid signaling system in cancer." Trends Pharmacol Sci **34**(5): 273-282.

Pistis, M. and M. Melis (2010). "From surface to nuclear receptors: the endocannabinoid family extends its assets." Curr Med Chem **17**(14): 1450-1467.

Porcella, A., C. Maxia, G. L. Gessa and L. Pani (2000). "The human eye expresses high levels of CB1 cannabinoid receptor mRNA and protein." Eur J Neurosci **12**(3): 1123-1127.

Porichi, O., M. E. Nikolaidou, A. Apostolaki, A. Tserkezoglou, N. Arnogiannaki, D. Kassanos, L. Margaritis and E. Panotopoulou (2009). "BCL-2, BAX and P53 expression

profiles in endometrial carcinoma as studied by real-time PCR and immunohistochemistry." Anticancer Res **29**(10): 3977-3982.

Portella, G., C. Laezza, P. Laccetti, L. De Petrocellis, V. Di Marzo and M. Bifulco (2003). "Inhibitory effects of cannabinoid CB1 receptor stimulation on tumor growth and metastatic spreading: actions on signals involved in angiogenesis and metastasis." FASEB J **17**(12): 1771-1773.

Potischman, N., R. N. Hoover, L. A. Brinton, P. Siiteri, J. F. Dorgan, C. A. Swanson, M. L. Berman, R. Mortel, L. B. Twiggs, R. J. Barrett, G. D. Wilbanks, V. Persky and J. R. Lurain (1996). "Case-control study of endogenous steroid hormones and endometrial cancer." J Natl Cancer Inst **88**(16): 1127-1135.

Pradhan, M., V. M. Abeler, H. E. Danielsen, C. G. Trope and B. A. Risberg (2006). "Image cytometry DNA ploidy correlates with histological subtypes in endometrial carcinomas." Mod Pathol **19**(9): 1227-1235.

Prescott, S. M. and P. W. Majerus (1983). "Characterization of 1,2-diacylglycerol hydrolysis in human platelets. Demonstration of an arachidonoyl-monoacylglycerol intermediate." J Biol Chem **258**(2): 764-769.

Ramer, R. and B. Hinz (2008). "Inhibition of cancer cell invasion by cannabinoids via increased expression of tissue inhibitor of matrix metalloproteinases-1." J Natl Cancer Inst **100**(1): 59-69.

Rance, N. E. (2009). "Menopause and the human hypothalamus: evidence for the role of kisspeptin/neurokinin B neurons in the regulation of estrogen negative feedback." Peptides **30**(1): 111-122.

Reed, J. C. (1994). "Bcl-2 and the Regulation of Programmed Cell-Death." Journal of Cell Biology **124**(1-2): 1-6.

Reed, J. C. (1999). "Dysregulation of apoptosis in cancer." J Clin Oncol **17**(9): 2941-2953.

Reggio, P. H. (2010). "Endocannabinoid binding to the cannabinoid receptors: what is known and what remains unknown." Curr Med Chem **17**(14): 1468-1486.

Renahan, A. G., I. Soerjomataram, M. Tyson, M. Egger, M. Zwahlen, J. W. Coebergh and I. Buchan (2010). "Incident cancer burden attributable to excess body mass index in 30 European countries." Int J Cancer **126**(3): 692-702.

Resuehr, D., D. R. Glore, H. S. Taylor, K. L. Bruner-Tran and K. G. Osteen (2012). "Progesterone-dependent regulation of endometrial cannabinoid receptor type 1 (CB1-

R) expression is disrupted in women with endometriosis and in isolated stromal cells exposed to 2,3,7,8-tetrachlorodibenzo-p-dioxin (TCDD)." Fertil Steril **98**(4): 948-956 e941.

Reyes, F. I., J. S. Winter and C. Faiman (1977). "Pituitary-ovarian relationships preceding the menopause. I. A cross-sectional study of serum follicle-stimulating hormone, luteinizing hormone, prolactin, estradiol, and progesterone levels." Am J Obstet Gynecol **129**(5): 557-564.

Ribeiro, M. L., C. A. Vercelli, M. S. Sordelli, M. G. Farina, M. Cervini, S. Billi and A. M. Franchi (2009). "17beta-oestradiol and progesterone regulate anandamide synthesis in the rat uterus." Reprod Biomed Online **18**(2): 209-218.

Risberg, B., K. Karlsson, V. Abeler, A. Lagrelius, B. Davidson and M. G. Karlsson (2002). "Dissociated expression of Bcl-2 and Ki-67 in endometrial lesions: Diagnostic and histogenetic implications." International Journal of Gynecological Pathology **21**(2): 155-160.

Rodriguez de Fonseca, F., I. Del Arco, F. J. Bermudez-Silva, A. Bilbao, A. Cippitelli and M. Navarro (2005). "The endocannabinoid system: physiology and pharmacology." Alcohol Alcohol **40**(1): 2-14.

Rouzer, C. A., K. Ghebreselasie and L. J. Marnett (2002). "Chemical stability of 2-arachidonylglycerol under biological conditions." Chemistry and Physics of Lipids **119**(1-2): 69-82.

Rudolph, M. I., Y. Boza, R. Yefi, S. Luza, E. Andrews, A. Penissi, P. Garrido and I. G. Rojas (2008). "The influence of mast cell mediators on migration of SW756 cervical carcinoma cells." J Pharmacol Sci **106**(2): 208-218.

Ryan, A. J., B. Susil, T. W. Jobling and M. K. Oehler (2005). "Endometrial cancer." Cell Tissue Res **322**(1): 53-61.

Ryberg, E., N. Larsson, S. Sjogren, S. Hjorth, N. O. Hermansson, J. Leonova, T. Elebring, K. Nilsson, T. Drmota and P. J. Greasley (2007). "The orphan receptor GPR55 is a novel cannabinoid receptor." Br J Pharmacol **152**(7): 1092-1101.

Saegusa, M., Y. Kamata, M. Isono and I. Okayasu (1996). "Bcl-2 expression is correlated with a low apoptotic index and associated with progesterone receptor immunoreactivity in endometrial carcinomas." Journal of Pathology **180**(3): 275-282.

Sahdev, A. (2007). "Imaging the endometrium in postmenopausal bleeding." BMJ **334**(7594): 635-636.

Saia G, Z. M., Depalo V, Lautenschläger T & Chakravarti A (2007). "Molecular and genetic profiling of prostate cancer: implications for future therapy." Curr Cancer Ther Rev **3**: 25-36.

Sakuragi, N., A. E. Salah-eldin, H. Watari, T. Itoh, S. Inoue, T. Moriuchi and S. Fujimoto (2002). "Bax, Bcl-2, and p53 expression in endometrial cancer." Gynecol Oncol **86**(3): 288-296.

Sanchez, C., M. L. de Ceballos, T. Gomez del Pulgar, D. Rueda, C. Corbacho, G. Velasco, I. Galve-Roperh, J. W. Huffman, S. Ramon y Cajal and M. Guzman (2001). "Inhibition of glioma growth in vivo by selective activation of the CB(2) cannabinoid receptor." Cancer Res **61**(15): 5784-5789.

Sanchez, C., I. Galve-Roperh, D. Rueda and M. Guzman (1998). "Involvement of sphingomyelin hydrolysis and the mitogen-activated protein kinase cascade in the Delta9-tetrahydrocannabinol-induced stimulation of glucose metabolism in primary astrocytes." Mol Pharmacol **54**(5): 834-843.

Sanchez, M. G., L. Ruiz-Llorente, A. M. Sanchez and I. Diaz-Laviada (2003). "Activation of phosphoinositide 3-kinase/PKB pathway by CB(1) and CB(2) cannabinoid receptors expressed in prostate PC-3 cells. Involvement in Raf-1 stimulation and NGF induction." Cell Signal **15**(9): 851-859.

Santin, A. D. (2003). "HER2/neu overexpression: has the Achilles' heel of uterine serous papillary carcinoma been exposed?" Gynecol Oncol **88**(3): 263-265.

Sarfaraz, S., V. M. Adhami, D. N. Syed, F. Afaq and H. Mukhtar (2008). "Cannabinoids for cancer treatment: progress and promise." Cancer Res **68**(2): 339-342.

Sarfaraz, S., F. Afaq, V. M. Adhami, A. Malik and H. Mukhtar (2006). "Cannabinoid receptor agonist-induced apoptosis of human prostate cancer cells LNCaP proceeds through sustained activation of ERK1/2 leading to G1 cell cycle arrest." J Biol Chem **281**(51): 39480-39491.

Sarnelli, G., S. Gigli, E. Capoccia, T. Iuvone, C. Cirillo, L. Seguella, N. Nobile, A. D'Alessandro, M. Pesce, L. Steardo, R. Cuomo and G. Esposito (2016). "Palmitoylethanolamide Exerts Antiproliferative Effect and Downregulates VEGF Signaling in Caco-2 Human Colon Carcinoma Cell Line Through a Selective PPAR-alpha-Dependent Inhibition of Akt/mTOR Pathway." Phytother Res.

Sasano, H. and N. Harada (1998). "Intratumoral aromatase in human breast, endometrial, and ovarian malignancies." Endocr Rev **19**(5): 593-607.

Saso, S., J. Chatterjee, E. Georgiou, A. M. Ditri, J. R. Smith and S. Ghaem-Maghami (2011). "Endometrial cancer." BMJ **343**: d3954.

- Saturnino, C., S. Petrosino, A. Ligresti, C. Palladino, G. De Martino, T. Bisogno and V. Di Marzo (2010). "Synthesis and biological evaluation of new potential inhibitors of N-acylethanolamine hydrolyzing acid amidase." Bioorg Med Chem Lett **20**(3): 1210-1213.
- Saunders, P. T. (1998). "Oestrogen receptor beta (ER beta)." Rev Reprod **3**(3): 164-171.
- Sawynok, J. (2005). "Topical analgesics in neuropathic pain." Curr Pharm Des **11**(23): 2995-3004.
- Sawzdargo, M., T. Nguyen, D. K. Lee, K. R. Lynch, R. Cheng, H. H. Heng, S. R. George and B. F. O'Dowd (1999). "Identification and cloning of three novel human G protein-coupled receptor genes GPR52, PsiGPR53 and GPR55: GPR55 is extensively expressed in human brain." Brain Res Mol Brain Res **64**(2): 193-198.
- Schmid, H. H. (2000). "Pathways and mechanisms of N-acylethanolamine biosynthesis: can anandamide be generated selectively?" Chem Phys Lipids **108**(1-2): 71-87.
- Schmid, P., L. Wold, R. Krebsbach, E. Berdyshev and H. Schmid (2002). "Anandamide and other N-acylethanolamines in human tumors." Lipids **37**(9): 907-912.
- Schmid, P. C., L. E. Wold, R. J. Krebsbach, E. V. Berdyshev and H. H. Schmid (2002). "Anandamide and other N-acylethanolamines in human tumors." Lipids **37**(9): 907-912.
- Schuel, H., L. J. Burkman, J. Lippes, K. Crickard, E. Forester, D. Piomelli and A. Giuffrida (2002). "N-Acylethanolamines in human reproductive fluids." Chem Phys Lipids **121**(1-2): 211-227.
- Scotchie, J. G., R. F. Savaris, C. E. Martin and S. L. Young (2015). "Endocannabinoid regulation in human endometrium across the menstrual cycle." Reprod Sci **22**(1): 113-123.
- Sailler, S., K. Schmitz, E. Jager *et al.* (2014). "Regulation of circulating endocannabinoids associated with cancer and metastases in mice and human." Oncoscience **1**(4): 272-282.
- Sun, S.L.K., D. Zhang, R. Shrestha, Y. Zhao (2015). "Clinical Analysis of CA125, CA72-4, and Risk of Malignancy Index in Distinguishing Benign and Malignant Ovarian Masses." Hong Kong J Gynaecol Obstet Midwifery **2**(15): 159-165.
- Siiteri, P. K. (1978). "Steroid hormones and endometrial cancer." Cancer Res **38**(11 Pt 2): 4360-4366.
- Siiteri, P. K. (1987). "Adipose tissue as a source of hormones." Am J Clin Nutr **45**(1 Suppl): 277-282.

Simon, G. M. and B. F. Cravatt (2006). "Endocannabinoid biosynthesis proceeding through glycerophospho-N-acyl ethanolamine and a role for alpha/beta-hydrolase 4 in this pathway." J Biol Chem **281**(36): 26465-26472.

Sivridis, E. and A. Giatromanolaki (2004). "Proliferative activity in postmenopausal endometrium: the lurking potential for giving rise to an endometrial adenocarcinoma." J Clin Pathol **57**(8): 840-844.

Smith-Bindman, R., E. Weiss and V. Feldstein (2004). "How thick is too thick? When endometrial thickness should prompt biopsy in postmenopausal women without vaginal bleeding." Ultrasound Obstet Gynecol **24**(5): 558-565.

Smith, S.K. (2002). The menstrual cycle. Taylor and Francis, London.

Snijders, M. P., A. F. de Goeij, M. J. Debets-Te Baerts, M. J. Rousch, J. Koudstaal and F. T. Bosman (1992). "Immunocytochemical analysis of oestrogen receptors and progesterone receptors in the human uterus throughout the menstrual cycle and after the menopause." J Reprod Fertil **94**(2): 363-371.

Solorzano, C., C. Zhu, N. Battista, G. Astarita, A. Lodola, S. Rivara, M. Mor, R. Russo, M. Maccarrone, F. Antonietti, A. Duranti, A. Tontini, S. Cuzzocrea, G. Tarzia and D. Piomelli (2009). "Selective N-acylethanolamine-hydrolyzing acid amidase inhibition reveals a key role for endogenous palmitoylethanolamide in inflammation." Proc Natl Acad Sci U S A **106**(49): 20966-20971.

Song, R. X., Z. Zhang, G. Mor and R. J. Santen (2005). "Down-regulation of Bcl-2 enhances estrogen apoptotic action in long-term estradiol-depleted ER(+) breast cancer cells." Apoptosis **10**(3): 667-678.

Song, Z. H., C. A. Slowey, D. P. Hurst and P. H. Reggio (1999). "The difference between the CB(1) and CB(2) cannabinoid receptors at position 5.46 is crucial for the selectivity of WIN55212-2 for CB(2)." Mol Pharmacol **56**(4): 834-840.

Sreevalsan, S., S. Joseph, I. Jutooru, G. Chadalapaka and S. H. Safe (2011). "Induction of apoptosis by cannabinoids in prostate and colon cancer cells is phosphatase dependent." Anticancer Res **31**(11): 3799-3807.

Stamenkovic, I. (2000). "Matrix metalloproteinases in tumor invasion and metastasis." Semin Cancer Biol **10**(6): 415-433.

Staton, P. C., J. P. Hatcher, D. J. Walker, A. D. Morrison, E. M. Shapland, J. P. Hughes, E. Chong, P. K. Mander, P. J. Green, A. Billinton, M. Fulleylove, H. C. Lancaster, J. C. Smith, L. T. Bailey, A. Wise, A. J. Brown, J. C. Richardson and I. P. Chessell (2008).

"The putative cannabinoid receptor GPR55 plays a role in mechanical hyperalgesia associated with inflammatory and neuropathic pain." Pain **139**(1): 225-236.

Stefansson, I. M., H. B. Salvesen and L. A. Akslen (2004). "Prognostic impact of alterations in P-cadherin expression and related cell adhesion markers in endometrial cancer." J Clin Oncol **22**(7): 1242-1252.

Stella, N. (2009). "Endocannabinoid signaling in microglial cells." Neuropharmacology **56 Suppl 1**: 244-253.

Stella, N. and D. Piomelli (2001). "Receptor-dependent formation of endogenous cannabinoids in cortical neurons." Eur J Pharmacol **425**(3): 189-196.

Sugiura, T., T. Kodaka, S. Nakane, T. Miyashita, S. Kondo, Y. Suhara, H. Takayama, K. Waku, C. Seki, N. Baba and Y. Ishima (1999). "Evidence that the cannabinoid CB1 receptor is a 2-arachidonoylglycerol receptor. Structure-activity relationship of 2-arachidonoylglycerol, ether-linked analogues, and related compounds." J Biol Chem **274**(5): 2794-2801.

Sugiura, T., S. Nakane, S. Kishimoto, K. Waku, Y. Yoshioka, A. Tokumura and D. J. Hanahan (1999). "Occurrence of lysophosphatidic acid and its alkyl ether-linked analog in rat brain and comparison of their biological activities toward cultured neural cells." Biochim Biophys Acta **1440**(2-3): 194-204.

Sun, Y. X., K. Tsuboi, Y. Okamoto, T. Tonai, M. Murakami, I. Kudo and N. Ueda (2004). "Biosynthesis of anandamide and N-palmitoylethanolamine by sequential actions of phospholipase A2 and lysophospholipase D." Biochem J **380**(Pt 3): 749-756.

Sung, B., S. Prasad, J. Ravindran, V. R. Yadav and B. B. Aggarwal (2012). "Capsazepine, a TRPV1 antagonist, sensitizes colorectal cancer cells to apoptosis by TRAIL through ROS-JNK-CHOP-mediated upregulation of death receptors." Free Radic Biol Med **53**(10): 1977-1987.

Surh, Y. (1999). "Molecular mechanisms of chemopreventive effects of selected dietary and medicinal phenolic substances." Mutat Res **428**(1-2): 305-327.

Surh, Y. J. (2002). "Anti-tumor promoting potential of selected spice ingredients with antioxidative and anti-inflammatory activities: a short review." Food Chem Toxicol **40**(8): 1091-1097.

Surh, Y. J., E. Lee and J. M. Lee (1998). "Chemoprotective properties of some pungent ingredients present in red pepper and ginger." Mutat Res **402**(1-2): 259-267.

Surh, Y. J. and S. S. Lee (1995). "Capsaicin, a double-edged sword: toxicity, metabolism, and chemopreventive potential." Life Sci **56**(22): 1845-1855.

Surh, Y. J. and S. S. Lee (1996). "Capsaicin in hot chili pepper: carcinogen, co-carcinogen or anticarcinogen?" Food Chem Toxicol **34**(3): 313-316.

Szabo, B., U. Nordheim and N. Niederhoffer (2001). "Effects of cannabinoids on sympathetic and parasympathetic neuroeffector transmission in the rabbit heart." J Pharmacol Exp Ther **297**(2): 819-826.

Szallasi, A., D. N. Cortright, C. A. Blum and S. R. Eid (2007). "The vanilloid receptor TRPV1: 10 years from channel cloning to antagonist proof-of-concept." Nat Rev Drug Discov **6**(5): 357-372.

Tashiro, H., M. S. Blazes, R. Wu, K. R. Cho, S. Bose, S. I. Wang, J. Li, R. Parsons and L. H. Ellenson (1997). "Mutations in PTEN are frequent in endometrial carcinoma but rare in other common gynecological malignancies." Cancer Res **57**(18): 3935-3940.

Tashiro, H., C. Isacson, R. Levine, R. J. Kurman, K. R. Cho and L. Hedrick (1997). "p53 gene mutations are common in uterine serous carcinoma and occur early in their pathogenesis." Am J Pathol **150**(1): 177-185.

Tashiro, H., S. F. Lax, P. B. Gaudin, C. Isacson, K. R. Cho and L. Hedrick (1997). "Microsatellite instability is uncommon in uterine serous carcinoma." Am J Pathol **150**(1): 75-79.

Taylor, A. H., M. S. Abbas, M. A. Habiba and J. C. Konje (2010). "Histomorphometric evaluation of cannabinoid receptor and anandamide modulating enzyme expression in the human endometrium through the menstrual cycle." Histochem Cell Biol **133**(5): 557-565.

Taylor, A. H., M. Finney, P. M. Lam and J. C. Konje (2011). "Modulation of the endocannabinoid system in viable and non-viable first trimester pregnancies by pregnancy-related hormones." Reprod Biol Endocrinol **9**: 152.

Technologies, L. "Amplification Efficiency of TaqMan® Gene Expression Assays."

Thoennissen, N. H., J. O'Kelly, D. Lu, G. B. Iwanski, D. T. La, S. Abbassi, A. Leiter, B. Karlan, R. Mehta and H. P. Koeffler (2010). "Capsaicin causes cell-cycle arrest and apoptosis in ER-positive and -negative breast cancer cells by modulating the EGFR/HER-2 pathway." Oncogene **29**(2): 285-296.

- Tseng, L., J. Mazella, M. I. Funt, W. J. Mann and M. L. Stone (1984). "Preliminary studies of aromatase in human neoplastic endometrium." Obstet Gynecol **63**(2): 150-154.
- Tsuboi, K., Y. X. Sun, Y. Okamoto, N. Araki, T. Tonai and N. Ueda (2005). "Molecular characterization of N-acylethanolamine-hydrolyzing acid amidase, a novel member of the choloylglycine hydrolase family with structural and functional similarity to acid ceramidase." J Biol Chem **280**(12): 11082-11092.
- Tsuboi, K., L. Y. Zhao, Y. Okamoto, N. Araki, M. Ueno, H. Sakamoto and N. Ueda (2007). "Predominant expression of lysosomal N-acylethanolamine-hydrolyzing acid amidase in macrophages revealed by immunochemical studies." Biochim Biophys Acta **1771**(5): 623-632.
- Ueda, N., R. A. Puffenbarger, S. Yamamoto and D. G. Deutsch (2000). "The fatty acid amide hydrolase (FAAH)." Chem Phys Lipids **108**(1-2): 107-121.
- Vaccani, A., P. Massi, A. Colombo, T. Rubino and D. Parolaro (2005). "Cannabidiol inhibits human glioma cell migration through a cannabinoid receptor-independent mechanism." Br J Pharmacol **144**(8): 1032-1036.
- Vaskivuo, T. E., F. Stenback and J. S. Tapanainen (2002). "Apoptosis and apoptosis-related factors Bcl-2, Bax, tumor necrosis factor-alpha, and NF-kappa B in human endometrial hyperplasia and carcinoma." Cancer **95**(7): 1463-1471.
- Velasco, G., I. Galve-Roperh, C. Sanchez, C. Blazquez and M. Guzman (2004). "Hypothesis: cannabinoid therapy for the treatment of gliomas?" Neuropharmacology **47**(3): 315-323.
- Vestergaard, A. L., U. B. Knudsen, T. Munk, H. Rosbach and P. M. Martensen (2011). "Transcriptional expression of type-I interferon response genes and stability of housekeeping genes in the human endometrium and endometriosis." Mol Hum Reprod **17**(4): 243-254.
- von Wolff, M., C. J. Thaler, T. Strowitzki, J. Broome, W. Stolz and S. Tabibzadeh (2000). "Regulated expression of cytokines in human endometrium throughout the menstrual cycle: dysregulation in habitual abortion." Mol Hum Reprod **6**(7): 627-634.
- Wagner, J. A., Z. Jarai, S. Batkai and G. Kunos (2001). "Hemodynamic effects of cannabinoids: coronary and cerebral vasodilation mediated by cannabinoid CB(1) receptors." Eur J Pharmacol **423**(2-3): 203-210.

- Walker, C. G., S. Meier, M. D. Mitchell, J. R. Roche and M. Littlejohn (2009). "Evaluation of real-time PCR endogenous control genes for analysis of gene expression in bovine endometrium." BMC Mol Biol **10**: 100.
- Wang, D., H. Wang, W. Ning, M. G. Backlund, S. K. Dey and R. N. DuBois (2008). "Loss of cannabinoid receptor 1 accelerates intestinal tumor growth." Cancer Res **68**(15): 6468-6476.
- Wang, D. Z., H. B. Wang, W. Ning, M. G. Backlund, S. K. Dey and R. N. DuBois (2008). "Loss of cannabinoid receptor 1 accelerates intestinal tumor growth." Cancer Research **68**(15): 6468-6476.
- Wang, H., H. O. Critchley, R. W. Kelly, D. Shen and D. T. Baird (1998). "Progesterone receptor subtype B is differentially regulated in human endometrial stroma." Mol Hum Reprod **4**(4): 407-412.
- Wang, H., Y. Guo, D. Wang, P. J. Kingsley, L. J. Marnett, S. K. Das, R. N. DuBois and S. K. Dey (2004). "Aberrant cannabinoid signaling impairs oviductal transport of embryos." Nat Med **10**(10): 1074-1080.
- Wang, H., H. Xie, Y. Guo, H. Zhang, T. Takahashi, P. J. Kingsley, L. J. Marnett, S. K. Das, B. F. Cravatt and S. K. Dey (2006). "Fatty acid amide hydrolase deficiency limits early pregnancy events." J Clin Invest **116**(8): 2122-2131.
- Wang J, U. N. (2008). "Role of the endocannabinoid system in metabolic control." Curr Opin Nephrol Hypertens **17**: 1-10.
- Wei, B. Q., T. S. Mikkelsen, M. K. McKinney, E. S. Lander and B. F. Cravatt (2006). "A second fatty acid amide hydrolase with variable distribution among placental mammals." J Biol Chem **281**(48): 36569-36578.
- WHO. (February 2014). "Cancer Fact sheet N°297." 2014.
- Whyte, L. S., E. Ryberg, N. A. Sims, S. A. Ridge, K. Mackie, P. J. Greasley, R. A. Ross and M. J. Rogers (2009). "The putative cannabinoid receptor GPR55 affects osteoclast function in vitro and bone mass in vivo." Proc Natl Acad Sci U S A **106**(38): 16511-16516.
- Wise, P. M. (2005). Aging of the female reproductive system. Academic Press, Burlington.
- Wong, J. Y., G. S. Huggins, M. Debidia, N. C. Munshi and I. De Vivo (2008). "Dichloroacetate induces apoptosis in endometrial cancer cells." Gynecol Oncol **109**(3): 394-402.

Woodruff, J. D. and J. H. Pickar (1994). "Incidence of endometrial hyperplasia in postmenopausal women taking conjugated estrogens (Premarin) with medroxyprogesterone acetate or conjugated estrogens alone. The Menopause Study Group." Am J Obstet Gynecol **170**(5 Pt 1): 1213-1223.

Wynn, R. M. (1989). The human endometrium: cyclic and gestational changes. New York: Plenum Press.

Xiao, Y., B. Schwartz, M. Washington, A. Kennedy, K. Webster, J. Belinson and Y. Xu (2001). "Electrospray ionization mass spectrometry analysis of lysophospholipids in human ascitic fluids: Comparison of the lysophospholipid contents in malignant vs nonmalignant ascitic fluids." Analytical Biochemistry **290**(2): 302-313.

Yang, E. and S. J. Korsmeyer (1996). "Molecular thanatopsis: a discourse on the BCL2 family and cell death." Blood **88**(2): 386-401.

Yu, M., D. Ives and C. S. Ramesha (1997). "Synthesis of prostaglandin E2 ethanolamide from anandamide by cyclooxygenase-2." J Biol Chem **272**(34): 21181-21186.

Zeleniuch-Jacquotte, A., A. Akhmedkhanov, I. Kato, K. L. Koenig, R. E. Shore, M. Y. Kim, M. Levitz, K. R. Mittal, U. Raju, S. Banerjee and P. Toniolo (2001). "Postmenopausal endogenous oestrogens and risk of endometrial cancer: results of a prospective study." Br J Cancer **84**(7): 975-981.

Zhang, R., Y. F. He, X. L. Zhang, B. L. Xing, Y. H. Sheng, H. Lu and Z. H. Wei (2012). "Estrogen receptor-regulated microRNAs contribute to the BCL2/BAX imbalance in endometrial adenocarcinoma and precancerous lesions." Cancer Letters **314**(2): 155-165.

Zhao, L. Y., K. Tsuboi, Y. Okamoto, S. Nagahata and N. Ueda (2007). "Proteolytic activation and glycosylation of N-acylethanolamine-hydrolyzing acid amidase, a lysosomal enzyme involved in the endocannabinoid metabolism." Biochim Biophys Acta **1771**(11): 1397-1405.

Ziel, H. K. and W. D. Finkle (1975). "Increased risk of endometrial carcinoma among users of conjugated estrogens." N Engl J Med **293**(23): 1167-1170.